Agronomy Research

Established in 2003 by the Faculty of Agronomy, Estonian Agricultural University

Aims and Scope:

Agronomy Research is a peer-reviewed international Journal intended for publication of broad-spectrum original articles, reviews and short communications on actual problems of modern biosystems engineering incl. crop and animal science, genetics, economics, farm- and production engineering, environmental aspects, agro-ecology, renewable energy and bioenergy etc. in the temperate regions of the world.

Copyright:

Agronomy Research online:

Agronomy Research is available online at: http://agronomy.emu.ee/

Acknowledgement to Referees:

The Editors of *Agronomy Research* would like to thank the many scientists who gave so generously of their time and expertise to referee papers submitted to the Journal.

Abstracted and indexed:

SCOPUS, CABI Full Paper and Thompson Scientific database: (Zoological Records, Biological Abstracts and Biosis Previews, AGRIS, ISPI, CAB Abstracts, AGRICOLA (NAL; USA), VINITI, INIST-PASCAL.)

Subscription information:

Estonian Grassland Society
St. Teaduse 4, 75501 Saku, ESTONIA
E-mail: heli.meripold@eria.ee

Journal Policies:

Estonian University of Life Sciences, Estonian Research Institute of Agriculture, Latvia University of Agriculture, Aleksandras Stulginskis University, Lithuanian Institute of Agriculture and Lithuanian Institute of Horticulture and Editors of *Agronomy Research* assume no responsibility for views, statements and opinions expressed by contributors. Any reference to a pesticide, fertiliser, cultivar or other commercial or proprietary product does not constitute a recommendation or an endorsement of its use by the author(s), their institution or any person connected with preparation, publication or distribution of this Journal.

ISSN 1406-894X

CONTENTS

III BIOENERGY

Agronomy Research **13**(2), 277–286, 2015

Above ground and below ground biomass in grey alder *Alnus incana* (L.) Moench. young stands on agricultural land in central part of Latvia

A. Bārdulis*, D. Lazdiņa, M. Daugaviete, A. Bārdule, U. Daugavietis and G. Rozītis

Latvian State Forest Research Institute 'Silava', Rigas street 111, LV2169 Salaspils, Latvia; *Correspondence: andis.bardulis@silava.lv

Abstract. Young grey alder stands under 10 years of age that are growing on abandoned agricultural lands in Central Latvian lowlands were selected for this study. In the framework of the research the biomass of the trees was studied and an equation was developed for grey alder stands on abandoned agricultural lands. An allometric equation for the different biomass fractions of grey alder was developed. Tree biomass is characterised by a power model with a single independent variable (DBH), which also indirectly substitutes for the effect of the stand age. The model is adapted to each fraction by changing its ratio values. The determination coefficient of the model is high, varying from $R^2 = 0.89$ to $R^2 = 0.94$, and the confidence level of the model is 95%. The biomass of particular fractions is defined by a power regression, with the tree stem diameter at the height of 1.3 m used as an argument. In young grey alder stands on abandoned agricultural lands the majority, 64%, of root fractions is composed of coarse roots, followed by the stump fraction and fine roots, 28% and 8%, respectively. For aboveground biomass the largest fraction is stem, which constitutes 75% of the total aboveground biomass, while the share of branches is 25%.

Key words: allometric equations, coarse roots, fine roots, stump, stem, branches, power model.

INTRODUCTION

There is a growing interest in the evaluation of biomass in forest lands, as it plays an important role in the turnover cycle of carbon and nutrients. Easy-to-use and precise methods for biomass estimation concerning the aboveground components of the tree have been developed, but what is usually problematic and difficult to assess is the root biomass (Sanford & Cuevas, 1996). It is known that the aboveground tree characteristics, such as tree stem diameter and height, can be used to accurately predict the tree biomass fractions (Ruark & Bockheim, 1987; Lavigne & Krasowski, 2007), but our knowledge of the components of tree biomass and its division into the smallest fractions is incomplete. Biomass calculations are needed mainly for sustainable forest resource planning, as well as for studying energy and substance turnover cycles in ecosystems (Zianis et al., 2005). Biomass evaluation depends on the aboveground tree dimensions and that is why biomass equations are developed to predict it according to a fixed variable (Repola, 2009). To better understand the regularities and influencing factors of biomass division, we need to carry out research on stand structures, biogeochemical

cycles and many other aspects related to global climate change (Dixon et al., 1994; Sanford & Cuevas, 1996). A growth in biomass can be observed as the trees get older, but its decrease is observed in very old stands (Peet, 1981). The development of a tree is also affected by the density of the stand, access to nutrients and water, soil temperature, as well as changes in density and oxygen availability (Dobson & Moffat, 1993; Dobson, 1995; Makkonen & Helmissari, 1998; Dieter & Elsasse, 2002; Ehman et al., 2002; Finer et al., 2007). As different factors affect the formation of tree biomass, broad generalizations on tree biomass can be drawn, which means that extensive research is necessary to improve and develop on biomass calculation models (Zianis et al., 2005).

Differences in tree biomass fractions are based on the ability of the tree to adapt to various conditions (Melecis, 2011). On flooded, damp or dried out soils, where the growth of trees and roots is limited, roots may grow thin and reach several metres in depth (10 m or more), as long as there is a sufficient supply of oxygen, water and nutrients. In such areas the trees wither, become similar to shrubs; the roots are weakly developed and make up an insignificant part of the biomass production (Perry, 1982). It is known that the geographical location of woody plants affects their biomass structure and morphological parameters; in general, woody plants adapt to their respective conditions. Various environmental conditions, such as wet, dry or windy environment, low average temperature, soil fertility etc., significantly affect root morphology and the physiology of development as well as root biomass (Kramer & Kozlowski, 1960; Pyatt et al., 2001; Finer et al., 2007).

Biomass equations should be flexible and applicable to biomass calculations for young stands (Repola, 2008). Numerous studies on grey alder biomass equations have been published, but only few of them fulfil the above-mentioned criteria (Repola, 2009). The suitability and precision of biomass equations depend on the collected empirical material as well as the interpretation thereof. Most of the tree fraction biomass equations consist in a power equation (Zianis et al., 2005). In the framework of this study, a power equation suited to Latvian conditions was developed.

Over the past decade the economic situation has changed drastically in Latvia. Large areas of agricultural land have been left unmanaged, and at present more than 310,000.0 ha of these lands have been afforested or have become afforested naturally, mainly with birch and grey alder. The majority of these forest stands have reached the age of 5 to 15 years, and a significant amount of biomass and carbon has been accumulated both in the aboveground and underground tree parts. Grey alder is a wide-spread tree species throughout Latvia (Forestry-key indicators, 2013), and commercially important for Latvian forestry (Millers & Magaznieks, 2012). Ever since the inventory of forest resources, information concerning the aboveground part, including tree stem diameter and height, is widely accessible in Latvia. By using metrical values relating to the estimation of the aboveground part, it is possible to develop precise formulas for calculating tree biomass fractions as well as carbon accumulation models (Brassard et al., 2011). Tree biomass is an important part of forest ecosystems as it stimulates various economic and biological processes and performs an irreplaceable function in carbon attraction. To calculate the amount of the attracted carbon, a method for establishing the amount of the biomass is used, taking into account a number of recalculation factors (Jenkins et al., 2003). The aim of this study is to investigate the aboveground and root biomass of young grey alder stands on abandoned agricultural lands.

Studying the amount of biomass in young grey alder stands will allow to predict the amount of wood fuel, as well as to calculate the accumulation of carbon both in aboveground and underground biomass. Until now, little research has been conducted in Latvia on the development of grey alder biomass, especially root biomass (Gaitnieks et al., 2007; Daugaviete et al., 2008; Bardulis et al., 2009). This pilot study focused on the calculation of both root and aboveground biomass production in young grey alder stands. The results of the study are essential for a better understanding of grey alder biomass production on abandoned agricultural lands.

The aim of the study is to investigate root biomass and to develop equations for the calculation of different aboveground and underground biomass fractions. The study poses the following hypothesis: The relationship between the components of tree biomass is biologically determined, and the biomass can be calculated as a function of the dendrometric parameters of the tree.

MATHERIALS AND METHODS

The material was collected from 4 similar young grey alder *Alnus incana* (L.) Moench. stands (Table 1) in abandoned agricultural lands located in the central part of Latvia (Fig. 1). The empirical material was collected in 2011 and 2012 after the vegetation period (from September to October), when all the leaves had fallen. The average parameters and characteristics of the selected stands are given in Table 1.

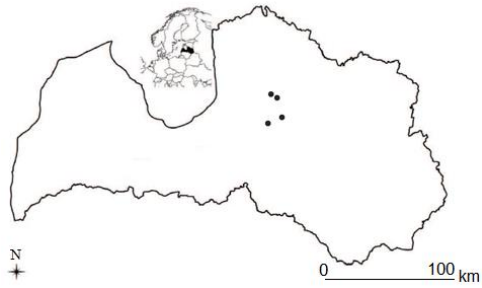

Figure 1. Locations of the studied stands.

The estimation methods for the aboveground part of the stand are based on dendrometric measurements carried out on circular sample plots with a horizontal radius of 12.62 m and area of 500 m^2. All types of tree measurements were carried out in the experiment and seven sample plots were established in each stand.

Table 1. Characteristics of grey alder experimental stands

No.	Coordinates		Age, years	Height, m
	N	E		
1	57°28.410	024°42.690	4	3.7
2	56°56.421	024°40.300	6	4.5
3	57°31.484	024°36.119	7	5.8
4	57°31.510	024°34.190	9	7.1
No.	Growing stock, m^3 ha^{-1}	Basal area, m^2 ha^{-1}	Stand density, stems ha^{-1}	Site class
1	17.8	5.6	7,700	1a
2	25.0	11.0	11,900	3
3	15.8	12.1	2,000	1
4	39.8	12.4	7,200	3

For the establishment and analysis of tree biomass, the sample trees were selected by considering their stem diameter at the height of 1.3 m (DBH) and the average height, including the average stand parameters where possible. Each sample tree was evaluated according to quality criteria – only healthy, vital sample trees with a single top were used in the study. Twenty sample trees from 4 stands were selected, representing a variety of different diameters (ranging from 1.9 cm to 6.8 cm) and heights (ranging from 3.1 m to 7.8 m), and felled for the measurement of aboveground and root biomass components.

For the calculation and analysis of the root biomass of the sample trees selected for this study, tree root system was divided into three fractions: coarse roots Ø > 5 mm; fine roots Ø < 5 mm, and stump. The stump fraction was included in the root biomass – in the aboveground (5–8 cm above the root neck) and underground fractions, the latter being a monolithic, non-differentiated part in some roots.

The grey alder tree stump and coarse root biomass was established for 20 sample trees by unearthing their root system, separating soil particles from the roots, washing the latter under a water jet and weighing them with the precision of ± 0.02 kg.

The soil core sampling method was used for collecting fine roots. Twenty soil cores (volumetric samples of 100 cm^3 and core diameter of 50 mm) per sampling were randomly taken from each sample plot for the determination of fine-root biomass. The soil cores were divided into four layers by depth: 0–10 cm, 10–20 cm, 20–30 cm and 30–40 cm of the mineral soil. The samples were placed in polyethylene bags, transported to the laboratory, and stored in a refrigerator at 4 °C prior to the analysis. In the laboratory, the roots were washed of soil and separated into grey alder roots and the roots of other plants. The separated fine roots were dried until they reached constant weight. They were then weighed to determine the dry biomass.

For the calculation and analysis of the aboveground biomass of the sample trees selected for this study, the aboveground parts were divided into two fractions: stem and branches. Two samples from the stem and branches of the living part were taken for the assessment of relative wood moisture. The stem of the tree was cut and weighed, while living branches from the living crown and dead branches were weighed separately. The dead branches were not included in the calculations. The dry biomass of the components was then calculated as weighted average from the relative humidity data using the measured weights of the respective parts of the tree.

To establish the specific weight of dry biomass (DM), tree fraction samples of an appropriate bark sector were collected for analysis and dried out at 105 °C until constant weight (Uri et al., 2002).

Allometric relationships between tree DBH, height and root biomass including the stump were tested. A frequently used model for such relationships is the following power model:

$$Y = \alpha \cdot X^{\beta} \quad (1)$$

where Y is the dependent variable (e.g., tree biomass fraction, kg dry mass), X is the independent variable (e.g., tree DBH, cm), and α and β are, respectively, the scaling coefficient (or allometric constant) and scaling exponent derived from the regression in accordance with empirical data.

The normality of the variables was verified with the Kolmogorov-Smirnov test. To analyse the effect of the qualitative factor on the response variables, One-Way ANOVA was applied. The LSD test was used for a multiple comparison of the mean values if the criteria were satisfied.

When the data did not follow a normal distribution pattern, or when inhomogeneity of group variance occurred, the nonparametric Mann-Whitney test was used for variance analysis. In all cases the level of significance $\alpha = 0.05$ was accepted. For data analyses the software SPSS Statistics 17.0 was used.

RESULTS AND DISCUSSION

As shown by scientific research, the growth of any tree species, including grey alder, is determined by soil fertility. The growth rate is established by examining the site index, which is expressed by the stand height at a given age. However, the site index shows the effect of lengthwise growth, but does not describe the stand biomass (Uri et al., 2007). The biomass of different parts of the twenty harvested sample trees ranges from 1.9 to 6.8 cm in diameter and from 3.1 to 7.8 m in height. The average tree height varies from 3.1 to 7.8 m, with the mean DBH ranging from 1.9 to 6.8. The average total dry biomass was 7.0 ± 0.4 kg, ranging from 2.2 ± 0.1 kg in a 4-year-old stand to 13.5 ± 0.5 kg in a 9-year-old stand (Fig. 2). As seen from Fig. 2, the average ratio of aboveground to root biomass is 3 : 1. Similar distribution patterns of aboveground and root biomass in grey alder plantations were found by scientists in Estonia on abandoned agricultural lands (Uri et al., 2002; Uri et al., 2007). In living plants, the root biomass plays an important part in carbon storage and makes up around 20% (Santantonio et al., 1977) to 26% (Cairns et al., 1997), or 19% to 28% according to Xiao & Ceulemans (2004), of the total tree biomass. The results of this study point to a similar proportion, 28% ± 1%.

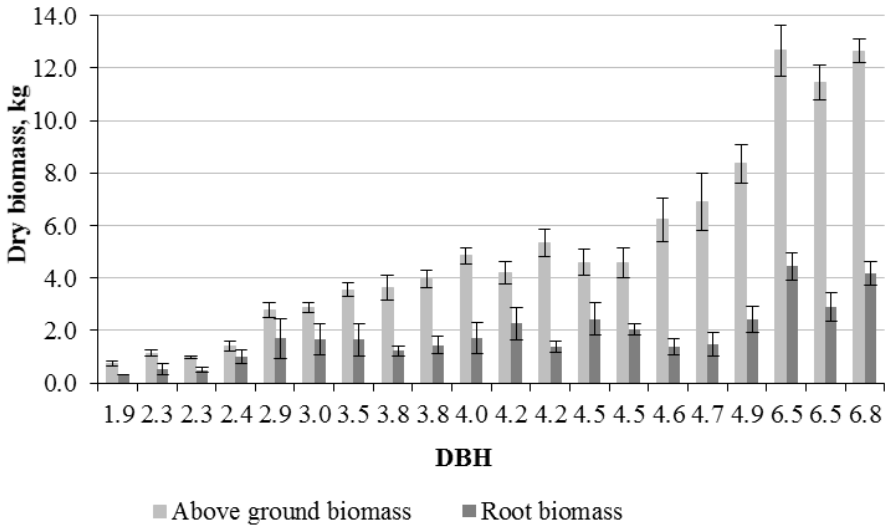

Figure 2. Dry aboveground and root biomass distribution ratio. Confidence interval ± 95% indicated in the error bars.

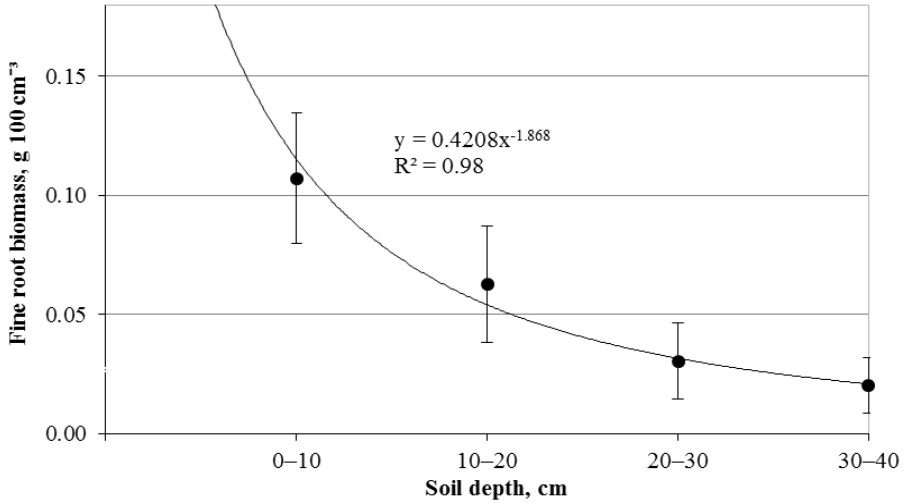

Figure 3. Average fine root biomass and its changes in the soil layer of young grey alder stands. Confidence interval ± 95% indicated in the error bars.

Scientists have developed a number of different biomass equations; however, new equations are needed that could be compared to the present ones, thus improving the biomass calculation models (Zianis et al., 2005). Scientific literature provides different equations for the calculation of root biomass fractions. The most common ones are regression equations with a single effective indicated value. In Europe, simple linear-type logarithmical equations are widely used for calculating root fraction biomass, although non-logarithmical power and straight-line equations are also employed – these use tree height, DBH or the product of squared diameter and height as an independent variable (Zianis et al., 2005). In the framework of this study, a common root biomass equation was developed. Several models were tested and the most precise one was the linear regression model (Formula 1), which included DBH as the single independent variable.

As shown in Fig. 4, tree height and DBH characterise the root biomass non-linearly. The determination ratios of the regression equation are high or moderately high. The data point to a high regression equation determination ratio with the total biomass values for the dependent variable – the tree DBH, or total predicted root biomass ($R^2 = 0.94$). Tree height also exhibits a high regression equation determination ratio with the parameter values, but less than the tree diameter at the height of 1.3 m, especially for total predicted root biomass ($R^2 = 0.66$). The determination ratio in the calculation and prediction of total grey alder root biomass is higher for tree diameter at the height of 1.3 m ($R^2 = 0.80$) than it is if for tree height ($R^2 = 0.31$), as well as for aboveground predictions, especially $R^2 = 0.89$ and $R^2 = 0.64$. Researchers point out that biomass equations should be flexible, multifunctional and applicable to biomass calculations for different tree stands (Repola, 2008).

Consequently, the relationship between tree diameter at the height of 1.3 m, tree height and total root biomass is characterised by a strength correlation, expressed by a correlation coefficient (r) equal to 0.97 ($\alpha = 0.05$) and 0.80 ($\alpha = 0.05$. Biomass is better

described by a regression, with tree diameter at the height of 1.3 m as an independent variable.

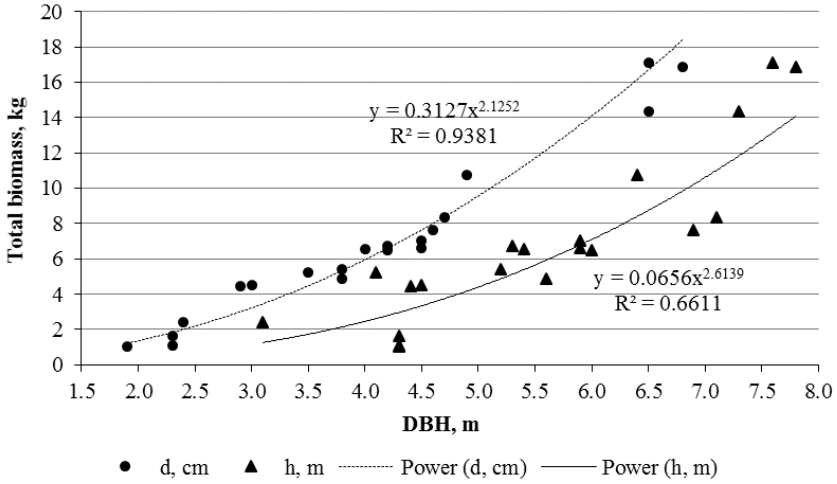

Figure 4. Relationship between the tree diameter and total root biomass.

Diameter at chest height was an effective predictor of all fractions of tree biomass in young grey alder stands, with the coefficient of determination R^2 values ranging from 0.89 to 0.94 ($p < 0.05$ for all models; Table 2). Therefore, the variation in total root biomass can be explained with a 94% model reliability by the developed non-linear regression model. Scientists point out that the developed tree biomass equations are of high value if the determination ratios are high or moderately high (R^2 = 0.63–0.99), allowing to predict the biomass with high precision (Zianis et al., 2005). We discovered that trees with a larger diameter exhibited greater error variance than smaller trees. However, plots of the residuals of coefficients demonstrated that there was no large or systematic bias toward over or underestimation of biomass at any DBH within the range used to develop the models.

Table 2. Allometric models for predicting root biomass in individual specimens taken from young grey alder stands

Biomass fraction	Equation parameter	Value of parameter	SE	p -value	R^2
Aboveground	α	0.163	0.009	0.041	0.92
	β	2.373	0.513	0.001	
Root biomass	α	0.418	0.005	0.009	0.89
	β	1.310	0.768	0.041	
Total biomass	α	0.241	0.002	0.032	0.94
	β	2.324	0.216	0.000	

Note: The models for all dependent variables follow the form $Y = \alpha * X^{\beta}$ where Y is the dependent variable (kg dry weight for root biomass fractions), X is the predictor variable (DBH, cm) and α and β are parameters of the equation. SE is the asymptotic standard error of the parameter estimate. All models were statistically significant ($p < 0.05$).

In conclusion, this study provides some of the first allometric biomass equations for grey alder stands in Latvia's conditions, and as expected, stem DBH was highly correlated with root biomass fractions.

CONCLUSIONS

An equation for calculating grey alder biomass was developed in the framework of this study. The equation remains the same for different tree fractions (coarse roots, stump, stem branches) and for trees of different age in abandoned agricultural lands. The amount of tree biomass in the above-mentioned fractions is characterised by a non-linear power model with one independent variable (DBH), which implicitly includes the effect of the stand age. The model is adapted to each fraction by modifying the numerical values of the ratio. The coefficient of determination of the model for total tree biomass is high at $R^2 = 0.94$.

In grey alder stands, the main part of the root fraction is made up of coarse roots (68% of the total root biomass), followed by the stump fraction (32%). The majority of the aboveground biomass fraction is made up of stem (75%), followed by branches (25%). The biomass of each of these tree fractions is established by a power regression with tree DBH used as an argument. The specific average value of dry biomass in grey alder stands in abandoned agricultural lands is 27.1 ± 2.3 t DM ha^{-1}.

The dry fine root biomass in young grey alder stands is 1.2 ± 0.4 DM t ha^{-1} in the mineral soil layer of 0–40 cm. Fine roots play a key role in tree ecosystems and make up 2.6 ± 0.8% of the total root system, but 8.6 ± 0.9% of the total tree biomass.

The study confirmed the hypothesis that the root fraction biomass can be calculated with high credibility as a function of easily measured tree parameters, i.e. tree DBH.

ACKNOWLEDGEMENTS. This study was funded by the European Regional Development Fund's project 'Developing the methods of plantation cultivation of fast-growing forest crops and evaluating the suitability of their wood for pelletizing' (contract number: No. 2013/0049/2DP/2.1.1.2.0/13/APIA/VIAA/031). The authors also express their gratitude to the staff of Latvian State Forest Research Institute 'Silava' for their assistance in the study.

REFERENCES

Bārdulis, A., Daugaviete, M., Komorovska, A., Liepiņš, K., Teliševa, G. 2009. Studies on the development of root systems in young forest stands of deciduous trees in naturally – afforested agricultural lands. *International Symposium 'Root Research and Applications'*, Vienna, Austria, p. 41.

Brassard, B.W., Chen, H.Y., Bergeron, Y., Pare, D. 2011. Differences in fine root productivity between mixed and single species stands. *Functional Ecology* **25**, 238–246.

Cairns, M.A., Brown, S., Helmer, E.H. 1997. Root biomass allocation in the world's upland forests. *Oecologia* **111**, 1–11.

Claus, A. & George, E. 2005. Effect of stand age on fine root biomass and biomass distribution in three European forest chronosequences. *Canadian Journal of Forest Research* **35**, 1617–1625.

Daugaviete, M., Gaitnieks, T., Kļaviņa, D., Teliševa, G. 2008 Oglekļa akumulācija virszemes un sakņu biomasā priedes, egles un bērza stādījumos lauksaimniecības zemēs. *Mežzinātne* **18**(51), 35–52. (in Latvian)

Dieter, M. & Elsasser, P. 2002. Carbon stocks and carbon stock changes in the tree biomass of Germany's forests. *Forstwissenschaftliches Centralblatt* **121** (4), 195–210.

Dixon, R.K., Brown, S., Houghton, R.A., Solomon, A.M., Trexler, M.C., Wisniewski, J. 1994. Carbon pools and flux of global forest ecosystems. *Science* **263**, 185–190.

Dobson, M. 1995. *Tree root systems*. Arboriculture Research and Information Note 130/95/ARB. Arboricultural Advisory and Information Service, Farnham.

Dobson, M.C. & Moffat, A.J. 1993 *The potential for woodland establishment on landfill sites*. HMSC London.

Ehman, J.L., Schmid, H.P., Grimmond, C.S.B., Randolph, J.C., Hanson, P.J., Wayson, C.A., Cropley, F.D. 2002 An initial intercomparison of micrometeorological and ecological inventory estimates of carbon exchange in a mid-latitude deciduous forest. *Global Change Biology* **8**, 575–589.

Finer, L., Helmisaari, H.S., Lohmus, K., Majdi, H., Brunner Borja, I., Eldhuset, T., Godbold, D., Grebenc, T, Konopka, B., Kraigher, H., Mottonen, M.R., Ohashi, M., Oleksyn, J., Ostonen, I., Uri, V., Vanguelova, E. 2007. Variation in fine root biomass of three European tree species: Beech (Fagus sylvatica L.), Norway spruce (*Picea abies* L. Karst.), and Scots pine (*Pinus sylvestris* L.). *Plant Biosystems* **141**(3), 394–405.

Forestry-key indicators 2013. Central Statistical Bureau of Latvia. [Online]. Available at: http://www.csb.gov.lv/en/statistikas-temas/forestry-key-indicators-30729.html [Accessed: 14 January 2015]

Fujii, S. & Kasuya, N. 2008. Fine root biomass and morphology of *Pinus densiflora* under competitive stress by Chameacyparis otusa. *Jornal of Forest Research* **13**, 185–189.

Gaitnieks, T., Kļaviņa, D., Arhipova, N. 2007. Comparison of development of spruce root system in the forest and agricultural lands. *LU 65. Scientific conference*, Jelgava, Latvia,

Gill, R.A. & Jackson, R.B. 2000. Global patterns of root turnover for terrestrial ecosystems. *New Phytologist* **147**, 13–31.

Helmisaari, H.S., Makkonen, K., Kellomaki, S., Valtonen, E., Malkonen, E. 2002. Below and above ground biomass, production and nitrogen use in Scots pine stands in eastern Finland. *Forest Ecology and Management* **165**, 317–326.

Jenkins, J.C., Chojnacky, D.C., Heath, L.S., Birdsey, R.A. 2003 National-scale biomass estimators for United States tree species. *Forest Science* **49**, 120–135.

Kramer, P.J. & Kozlowski, T.T. 1960. *Physiology of Trees*. New York: McGraw-Hill book company, Inc. 645 pp.

Lavigne, M.B. & Krasowski, M.J. 2007 Estimating coarse root biomass of balsam fir. *Canadian Journal of Forest Research* **37** (6), 8–991.

Makkonen, K. & Helmisaari, H.S. 1998 Seasonal and yearly variations of fine-root biomass and necromass in a Scots pine (*Pinus sylvestris* L.) stand. *Forest Ecology and Management* **102**, 283–290.

Melecis V. (2011) *Ekoloģija*. Rīga: LU Akadēmiskais apgāds, 352 pp (in Latvian).

Millers, M. & Magaznieks, J. 2012. Scots pine (*Pinus sylvestris* L.) stem wood and bark moisture and density influencing factors. In: Proceedings of the annual 18th International Scientific Conference „Research for Rural Development 2012". Jelgava, Latvia: Latvia University of Agriculture, 16-18 May 2012, **2**, 91–97.

Peet, R.K., 1981. *Changes in biomass and production during secondary forest succession. In Forest succession: concepts and applications.* Edited by D.C. West, H.H. Shugart, and D.B. Botkin. Springer, New York, 338 pp.

Perry, T.O. 1982. Tree roots. *Arboriculture* **8**(8), 197–211.

Pyatt, G., Ray, D., Fletcher, J. 2001. An ecological classification for forestry in Great Britain. Forestry Commission Bulletin, No.124. Forestry Commission, Edinburgh.

Repola, J. 2008. Biomass equations for birch in Finland. *Silva Fennica* **42**(4), 605–624.

Repola, J. 2009. Biomass equations for Scots pine and Norway spruce in Finland. *Silva Fennica*, **43** (4), 625–647.

Ruark, G.A. & Bockheim, J.G. 1987 Below-ground biomass of 10-, 20-, and 32-year-old *Populus tremuloides* in Wisconsin. *Pedobiologia* **30**, 17–207.

Sanford, R.L. & Cuevas, E. 1996. Root growth and rhizosphere interactions in tropical forests. In: Mulkey SS, Chazdon RL, Smith AP (eds) Tropical forest plant ecophysiology. Chapman and Hall, New York, 268–300.

Santantonio, D., Hermann, R.K., Overton, W.S. 1977. Root biomass studies in forest ecosystems. *Pedobiologia*, **17**, 1–31.

Trettin, C.C., Johnson, D.W., Todd, D.E. 1999. Forest nutrient and carbon pools at Walker Branch Watershed: Changes during a 21-year period. *Soil Sci. Soc. Am. J.*, **63**, 1436–1448.

Zianis, D., Muukkonen, P., Mäkipääand, R., Mencuccini, M. 2005. Biomass and Stem Volume Equations for Tree Species in Europe. *Silva Fennica Monographs* **4**, 63.

Uri, V., Lohmus, K., Ostonen, I., Tullus, H., Lastik, R., Vildo, M. 2007. Biomass production, foliar and root characteristics and nutrient accumulation in young silver birch (*Betula pendula* Roth.) stand growing on abandoned agricultural land. *European Journal of Forest Research* **126**, 495–506.

Uri, V., Tullus, H., Lohmus, K. 2002. Biomass production and nutrient accumulation in short-rotation grey alder (*Alnus incana* (L.) Moench) plantation on abandoned agricultural land. Forest Ecology and Management **169**, 161–179.

Xiao, C.W. & Ceulemans, R. 2004. Algometric relationships for below and aboveground biomass of young Scots pines. *Forest Ecology and Management* **203**, 177–186.

Agronomy Research **13**(2), 287–293, 2015

Production of fermentation feedstock from lignocellulosic biomass: applications of membrane separation

B. Dalecka*, M. Strods and L. Mezule

Riga Technical University, Faculty of Civil Engineering, Department of Water Science and Technology, Azenes 16/20-263, LV1048 Riga, Latvia;
*Correspondence: brigita.dalecka@gmail.com

Abstract. The development of cost-efficient, highly productive technologies for fermentation feed production from lignocellulose biomass is still a challenge. In this paper, the production of fermentable sugars from lignocellulosic biomass using hydrolysis techniques with membrane separation systems is studied. The research was conducted on both a laboratory and pilot level to evaluate and optimize the efficiency of the proposed technology. The results demonstrated that UF and NF permeate recovery increased efficiency, and the highest sugar recovery rates were obtained when secondary waste recirculation was introduced after NF and UF, reaching an almost 40% yield from all produced sugars.

Key words: fermentable sugars, lignocellulosic biomass, pre-treatment, membrane separation.

INTRODUCTION

Due to increasing energy demands and pollution problems caused by the use of non-renewable fossil fuels, it has become necessary to introduce alternative energy sources into the global energy turnover (Karmakar et al., 2010). Lignocellulosic biomass, such as wood, grass, agricultural and forest residues, has been regarded as a potential resource for the production of biofuels for many years (Sanchez & Cardona, 2007; Xu & Huang, 2014), since it is both renewable and available in large quantities all around the world. Large-scale processing technologies allowing to ferment biofuels from lignocellulose have been used for decades (Hamelinck et al., 2005). However, the extensive application of this resource is still linked to technological challenges and high production costs (Laser et al., 2001). Generally, the conversion of lignocellulosic biomass to biofuel consists of four major operations: pre-treatment, hydrolysis, fermentation, and product separation/purification (Moiser et al., 2005), where the effective conversion of biomass to fermentable sugars requires a combination of chemical, mechanical and/or enzymatic processes (Dhabhai et al., 2012).

The most commonly used pre-treatment methods are acid pre-treatment with high-pressure steam explosions, enzymatic hydrolysis, milling, etc. (Hamelinck et al., 2005; Hendriks & Zeeman, 2009; Alvira et al., 2010; Tutt et al., 2014). Nevertheless, cost-efficient, highly productive technologies for fermentation feed production from lignocellulose biomass still need to be developed. Membrane separation processes such as ultrafiltration (UF) and nanofiltration (NF) have gained much attention in the biotechnology industry due to their simplicity, high selectivity, low energy costs and

reduced chemical usage (Cho et al., 2012; Gryta et al., 2013). UF membranes can selectively remove not only large molecules such as proteins, viruses, and microorganisms from the biological environment through size sieving mechanisms but can also substantially reduce emulsion to improve the successive solvent extraction efficiency (Li et al., 2006; Yasan et al., 2009). However, after passing the UF membrane system the permeates are, in general, very diluted and great in volume. Therefore, NF membranes are suitable not only for the separation of small molecules like organic acids and salts but also for concentration (Bruggen et al., 1999; Yasan et al., 2009).

The aim of this study was to optimize and combine the available lignocellulosic biomass pre-treatment and hydrolysis techniques with UF–NF membrane separation systems to increase the product yields of enzymatic hydrolysis and decrease the production costs related to enzyme recovery as reported previously (Mezule et al., 2012). The research was conducted on both a laboratory and pilot level to evaluate the efficiency of the proposed technology.

MATERIALS AND METHODS

Lignocellulosic biomass

Hay mown in late June from lowland hay meadows located in Latvia was used as reference material. After drying, the lignocellulosic biomass was stored at room temperature until further processing. The dried biomass was ground (Retsch, GM200) to obtain the desired biomass particle size of < 0.5 cm (Hamelincik et al., 2005).

Batch scale substrate pre-treatment and hydrolysis

Batch scale tests were prepared to estimate the production yields of enzymatic hydrolysis with fungal enzymes. In brief, the biomass was diluted in a 0.05 M sodium citrate buffer (3% w v^{-1}) and boiled for 5 min to neutralize unnecessary microorganisms. After cooling, an enzyme (0.2 FPU ml^{-1}, 20 FPU g^{-1}, Mezule et al., 2012) was added to the diluted substrates and incubated on an orbital shaker for 24 hours at 30 °C. All tests were prepared in triplicate and sugar yields were estimated after hydrolysis.

Pilot tests

The tests were carried out in the pilot system developed by the Riga Technical University (Latvia). The main technological processes involved in this study are presented in Fig. 1. Hay biomass (3% w v^{-1}; with constant mixing) was boiled until the hydrolysis reactor temperature reached 120 °C (~ 1 h) and then cooled down to 40 °C. Subsequently, the substrate from the hydrolysis reactor was pumped through a rough water filter system (Geyser, Russia) to the UF ceramic tank. Then the substrate was filtered through the UF membrane system to the NF tank. Eventually the substrate was filtered through the NF membrane system to get the concentrated sugar solution into a collector tank. Sugar concentration was measured at all process stages. During all pilot tests enzymatic hydrolysis was omitted and sugars were either generated during grinding and heating or artificially added glucose (Bacteriological grade, Oxoid Ltd) was used.

Figure 1. Schematic diagram of the experimental set-up. 1: hydrolysis reactor (HR, working capacity 15 l), 2: rough filters (RF), 3: ultrafiltration (UF), 4: nanofiltration (NF), 5: collector (CC) for concentrated liquid.

Analysis of total reducing sugars

A reducing sugar analysis was performed for all the collected samples using the Dinitrosalicylic Acid (DNS) Method (Ghose, 1987). In brief, all samples were centrifuged (6,600 g, 10 min). Then 0.1 ml of the supernatant was mixed with 0.1 ml of the 0.05 M sodium citrate buffer and 0.6 ml of DNS. For blank control, distilled water was used instead of the sample. Then all samples were boiled for 5 min and transferred to cold water. Next, 4 ml of distilled water was added. Absorption was measured with the spectrophotometer M501 (Camspec, United Kingdom) at 540 nm. To obtain absolute concentrations, a standard curve against glucose was constructed.

RESULTS AND DISCUSSION

The effect pre-treatment has on lignocellulosic materials has been recognized for a long time (Ye & Cheng, 2002). Depending on the biomass source, different harvesting times and treatment methods used, sugar yields vary from 12% to 98% (Dhabhai et al., 2012; Tutt et al., 2012; Tutt et al., 2013). Enzymatic hydrolysis generally gives lower product yields than other hydrolysis methods, however, the technology is regarded as environmentally friendly and is less inhibitory to fermenting microorganisms (Ye & Cheng, 2002; Behera et al., 2014). Batch scale studies with hay and cellulolytic enzymes produced at laboratories generated 15% to 19% of sugar yields (45%–57% of the theoretical cellulose/hemicelluloses content), showing that the direct application of the technology in large-scale fermentation systems might not be productive enough. Thus, a combined UF–NF system for filtrating fermentation substrates (Yasan et al., 2009) was introduced as a technique to produce fermentation feed.

Initially the treatment involved the direct transfer of hydrolysis products through the filtration system. Heating to 120 °C prior to filtration did not produce more than a 15% increase in sugar; thus, the additional pre-treatment was accepted more as a step for substrate sterilization to remove indigenous microorganisms than a process for releasing sugar. Besides, previous studies have shown that pre-treatment at less than 150 °C does very little damage to plant cell walls, therefore, cellulose cannot be accessed for degrading it to glucose (Raud et al., 2014; Tutt et al., 2014). Sugars produced in the reactor after mixing and heating were regarded as a 100% sugar yield. The results of a direct hydrolysate transfer through the membrane showed that 46% of the generated sugar yield was lost in permeate-waste (Fig. 2, single) after UF. At the same time, rough filters and NF attributed to an 11% and 19% decrease respectively, thus producing only a 24% yield (6.55 g l^{-1}; initial yield 2.49 g l^{-1}) after sugar concentration. Generally, UF membranes can selectively remove large molecules such as proteins, viruses, and microorganisms through size sieving mechanisms and can substantially reduce emulsion to improve the successive solvent extraction efficiency (Li et al., 2006; Yasan et al.,

2009). However, the permeates after using the UF membrane system are, in general, very diluted and great in volume. To increase the product yields and subsequently decrease the sugars lost in the waste, a recirculation system was introduced into the pilot system where the UF permeate was transported back to the hydrolysis reactor. The collected UF permeate was mixed with 3 l of nanofiltred water to increase the product volume critical for the system. No improvements were observed when comparing these two setups, and the final sugar percentage yield in both attempts was less than 25% when compared to the initial yield (Fig. 2, double). At the same time, double recirculation generated more waste within the NF and required higher resource inputs (water, electricity). Thus, it was not considered to be potentially applicable.

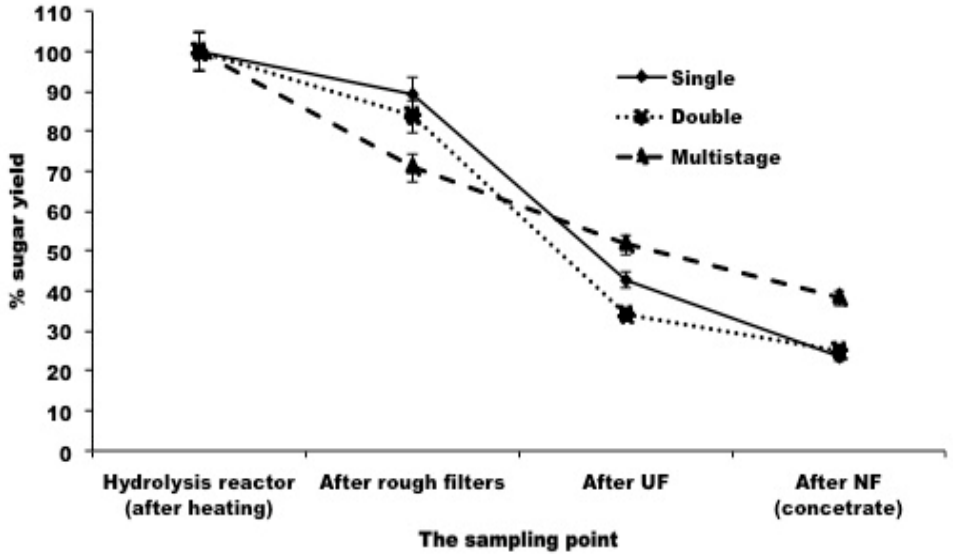

Figure 2. Sugar percentage yield changes in the pilot system with direct filtration (single), recirculation from the UF to a hydrolysis reactor (double) and multistage recirculation (multistage). Standard deviation represents the average from at least two repetitive measurements.

For the multistage setup (Fig. 2, multistage), sugar production was performed according to the method description with added UF and NF permeate recirculation. Retained large particles and molecules were initially separated from the substrate with RF and UF and then further filtered with NF, while permeates from UF and NF were retained and filtered once more. The results showed that UF and NF permeate recovery increased efficiency and the final sugar percentage yield reached almost 40% (7.01 g l^{-1}; initial yield 1.89 g l^{-1}) which was higher than with single and double filtration setups (Fig. 2). A certain decrease (up to 30%) in recovery was observed after RF. However, this was attributed to the potential shift in biomass size and mixing properties during hydrolysis. Thus there is a need for the further investigation of the process at this stage to minimize recovery fluctuations. At the same time, no significant difference ($p > 0.05$) in recovery was observed after NF for all three setups.

Since batch scale enzymatic hydrolysis produced 4.8–5.6 g l^{-1} of fermentable sugars on average, the multistage filtration treatment was tested on these concentrations on the pilot level. This was achieved by adding glucose to the hydrolysis reactor. The results showed that sugar recovery yields at multistage UF–NF separations do not differ significantly ($p > 0.05$) when the initial sugar concentration is changed (Fig. 3). Again, RF showed the highest decrease in recovery (around 30%) when compared to other process steps, and NF did not cause a more than 20% decrease.

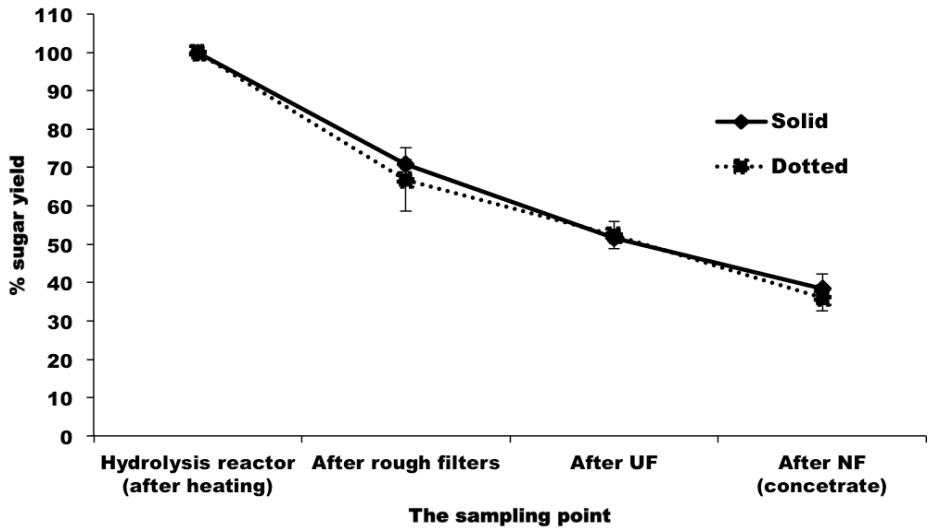

Figure 3. Sugar percentage yield changes during membrane multistage filtration processes in a system with added glucose (dotted) and without added glucose (solid). Standard deviation represents the average from two pilot runs.

The enzymatic hydrolysis of lignocellulosic biomass for biofuel production is a technology that has been thoroughly investigated over the years. Despite of its high potential, it is still not competitive enough due to low product yields when compared to production costs (Alvira et al., 2010). Effective fermentation feed production is closely linked to the separation of sugars from the generated waste. As suggested (Olofsson et al., 2008), the issue can be overcome by introducing simultaneous saccharification and fermentation techniques. However, the selection of the most favourable process conditions as well as enzyme and fermenting microorganism recovery are still challenging. In order to aid the separation of fermentation feed from waste, recover enzymes and decrease separation costs, multistage membrane separation can be introduced after enzymatic hydrolysis. Furthermore, when compared to the classical separation processes, membrane processes have several advantages as they work at low temperatures without phase change, and without the addition of chemicals (Karakulski & Morawski, 2002). The results of this research project showed that it is possible to apply membrane separation techniques to purify sugars produced during hydrolysis. Nevertheless, further research is still needed to increase the recovery rate and produce higher amounts of fermentation feed.

CONCLUSIONS

The results of this research project show that it is possible to introduce multistage separation techniques to generate fermentation feed for biofuel production from lignocellulosic biomass. The highest sugar recovery rates were obtained when secondary waste recirculation was introduced after NF and UF, and this yielded almost 40% of all produced sugars. Moreover, changing the initial sugar concentration did not significantly affect the efficiency of the process, which is more connected to various substrates and changing hydrolysis conditions.

ACKNOWLEDGEMENTS. This work has been partly supported by the Latvian National Research Programme 'LATENERGI' and EU LIFE+ Nature & Biodiversity program Project 'GRASSSERVICE' - Alternative use of biomass for maintenance of grassland biodiversity and ecosystem services (LIFE12 BIO/LV/001130).

REFERENCES

Alvira, P., Tomas–Pejo, E., Ballesteros, M., Negro, M.J. 2010. Pretreatment technologies for an efficient bioethanol production process based on enzymatic hydrolysis: A review. *Bioresource Technology* **101**, 4851–4861.

Behera, S., Arora, R., Nandhagopal, N., Kumar, S. 2014. Importance of chemical pretreatment for bioconversion of lignocellulosic biomass. *Renewable and Sustainable Energy Reviews* **36**, 91–106.

Bruggen, B., Scheap, J., Wilms, D., Vandecasteele, C. 1999. Influence of molecular size, polarity and charge on the retention of organic molecules by nanofiltration. *J. Membr. Sci.* **156**, 29–41.

Cho, Y.H., Lee, H.D., Park, H.B. 2012. Integrated membrane processes for separation and purification of organic acid from a biomass fermentation process. *Ind. Eng. Chem. Res.* **51**, 10207–12219.

Dhabhai, R., Jain, A., Chaurasia, S.P. 2012. Production of fermentable sugars by diluted acid pretreatment and enzymatic saccharification of three different lignocellulosic materials. *International Journal of ChemTech Research* **4**, 1497–1502.

Ghose, T.K. 1987. Measurement of cellulose activities. *Pure & Appl. Chem.* **59**, 257–268.

Gryta, M., Szczupak, M.A., Bastrzyk, J., Tomczak, W. 2013. The study of membrane distillation used for seperation of fermenting glycerol solution. *Journal of Membrane Science* **431**, 1–8.

Hamelincik, C.N., Hooijdonk, G., Faaij, A.P.C. 2005. Ethanol from lignocellulosic biomass: techno–economic performance in short–, middle– and long–term. *Biomass and Bioenergy* **28**, 384–410.

Hendriks, A.T.W.M. & Zeeman, G. 2009. Pretreatment to enhance the digestibility of lignocellulosic biomass. *Bioresource Technology* **100**, 10–18.

Karakulski, K. & Morawski, A.W. 2002. Treatment of spent emulsion from a cable factory by an integrated UF/NF membrane system. *Desalination* **149**, 163–167.

Karmakar, A., Karmakar, S., Mukherjee, S. 2010. Properties of various plants and animals feedstocks for biodiesel production. *Bioresource Technology* **101**, 7201–7210.

Laser, M., Schulman, D., Allen, S.G., Lichwa, J., Antal, Jr.M.J., Lynd, L.R. 2001. A comparison of liquid hot water and steam pretreatments of sugar cane bagasse for bioconversion to ethanol. *Bioresource Technology* **81**, 33–44.

Li, Y.B., Shahbazi, A., Kadzere, C.T. 2006. Separation of cells and proteins from fermentation broth using ultrafiltration. *J. Food Eng.* **75**, 574–580.

Mezule, L., Tihomirova, K., Nescerecka, A., Juhna, T. 2012. Biobutanol production from agricultural waste: A simple approach fro pre–treatment and hydrolysis. *Latv. J. Chem.* **4**, 407–414.

Moiser, N., Wyman, C., Dale, B., Elander, R., Lee, Y.Y., Holtzapple, M., Ladissch, M. 2005. Features of promising technologies for pretreatment of lignocellulosic biomass. *Bioresource Technology* **96**, 673–686.

Olofsson, K., Bertilsson, M., Liden, G. 2008. A short review of SSF–an interesting process option for ethanol production from lignocellulosic feedstocks. *Biotechnology for Biofuels* 1–7.

Raud, M., Kesperi, R., Oja, T., Olt, J., Kikas, T. 2014. Utilization of urban waste in bioethanol production: potential and technical solutions. *Agronomy Research* **12**, 397–406.

Sanchez, O.J. & Cardona, C.A. 2007. Trends in biotechnological production of fuel ethanol from different feedstocks. *Bioresource Technology* **99**, 5270–5295.

Tutt, M., Kikas, T., Kahr, H., Pointner, M., Kuttner, P., Olt, J. 2014. Using steam explosion pretreatment method for bioethanol production from floodplain meadow hay. *Agronomy Research* **12**, 417–424.

Tutt, M., Kikas, T., Olt, J. 2012. Influence of different pretreatment methods on bioethanol production from wheat straw. *Agronomy Research* **1**, 269–276.

Tutt, M., Kikas, T., Olt, J. 2013. Influence of harvesting time on biochemical composition and glucose yield from hemp. *Agronomy Research* **11**, 215–220.

Xu, Z. & Huang, F. 2014. Pretreatment Methods for Bioethanol Production. *Appl. Biochem. Biotechnol.* **62**, 143–174.

Yasan, H., Gang, C., Zhijuan, J., Shunxing, L. 2009. Combined UF–NF membrane system for filtering erythromycin fermentation broth and concentrating the filtrate to improve the downstream efficiency. *Seperation and Purification Technology* **66**, 390–396.

Ye, S. & Cheng, J. 2002. Hydrolysis of lignocellulosic materials for ethanol production: a review. *Bioresource Technology* **83**, 1–11.

Agronomy Research **13**(2), 294–302, 2015

Anaerobic digestion of vegetables processing wastes with catalyst metaferm

V. Dubrovskis* and I. Plume

Latvia University of Agriculture, Faculty of Engineering, Institute of Agriculture Energetics, 5, Cakstesblvd, LV3001 Jelgava, Latvia
*Correspondence: vilisd@inbox.lv

Abstract. There are 54 active biogas plants in Latvia today. It is necessary to investigate the suitability of various biomasses for energy production. Maize is the dominating crop for biogas production in Latvia. The cultivation of more varied crops with good economical characteristics and a low environmental impact is thus desirable. One of the ways for improving biogas yield in Latvian conditions is using biological catalysts. This paper explores the results of the anaerobic digestion of vegetables' processing wastes using the new biological catalyst Metaferm. The digestion process was investigated in view of biogas production in sixteen 0.7 l digesters operated in batch mode at the temperature of 38 ± 1.0 °C. The average methane yield per unit of dry organic matter added (DOM) from the digestion of onions was 0.433 l g_{DOM}^{-1}; with 1 ml of Metaferm: 0.396 l g_{DOM}^{-1}, and with 2 ml of Metaferm: 0.394 l g_{DOM}^{-1}. The average methane yield from the digestion of carrots was 0.325 l g_{DOM}^{-1}; with 1 ml of Metaferm: 0.498 l g_{DOM}^{-1}, and with 2 ml of Metaferm: 0.426 l g_{DOM}^{-1}. The average additional methane yield per unit of dry organic matter from the digestion of 50%:50% mixed onions and carrots was 0.382 l g_{DOM}^{-1} with 2 ml of Metaferm. The average additional methane yield per unit of dry organic matter from the digestion of cabbage leftovers was 0.325 l g_{DOM}^{-1}; with 1 ml of Metaferm: 0.375 l g_{DOM}^{-1}, and with 2 ml of Metaferm: 0.415 l g_{DOM}^{-1}. The average additional methane yield per unit of dry organic matter from the digestion of potato cuttings was 0.570 l g_{DOM}^{-1}; with 1 ml of Metaferm: 0.551 l g_{DOM}^{-1}, and with 2 ml of Metaferm:0.667 l g_{DOM}^{-1}. The average additional methane yield per unit of dry organic matter from the digestion of 50%:50% mixed cabbages and potatoes was 0.613 l g_{DOM}^{-1} with 2 ml of Metaferm. All investigated vegetable wastes can be successfully cultivated for energy production under agro-ecological conditions in Latvia. Adding the catalyst Metaferm increased methane yield, except for onions.

Key words: anaerobic digestion, onion, carrot, cabbage, potato, biogas, methane, biological catalyst.

INTRODUCTION

Energy production from renewable sources plays an important role in European energy policies. The share of renewable energy is expected to rise further to 21% by 2020 and 24% by 2030 (COM (2014) 15 final). According to calculations provided during the implementation of the Biomass Action Plan, 8% of Europe's energy needs covered by biomass can reduce greenhouse gas emissions equivalent to 209 million tonnes of CO_2 per year and create up to 300,000 new jobs in the agricultural and forestry sectors.

According to Directive 2009/28/EC, Annex I, Part A, the goal for Latvia is to increase the share of energy produced from renewable energy sources (RES) in gross final energy consumption from 32.6% in 2005 to 40% (1918 toe) in 2020 (Ministry of Economic, 2010).

One of the most promising renewable energy sources is biogas. Biogas production must be developed, as methane collection also helps to implement the Kyoto Protocol provisions. The Latvian Action Plan envisages the total electricity generation capacity of 92 MW for biogas plants in 2020. The number of working biogas cogeneration plants will increase up to 54 in Latvia in 2014 (Ministry of Economics, 2015). There is around 369,000 ha of available land suitable for growing energy crops and the production of biogas in Latvia (Dubrovskis, et al., 2011). However, many biogas plants are built in areas, e.g., in the subregion Zemgale, with little or no free additional land for growing biomass (mainly maize) for biogas plants. High cereals yields and increasing grain prices on the market can cause the further decreasing of maize areas, potentially limiting this traditional source for biogas production. Therefore, it is necessary to find new biomass sources to stabilise or increase biomethane production in biogas plants in Latvia.

An additional way for increasing biogas production is improving the anaerobic fermentation process itself. Currently, within some European countries, a variety of specific additives are being rapidly developed and their use is undergoing innovation (Feng, at al., 2010; Lemmer, at al., 2011; Irvan, 2012; Facchina, at al., 2013) with the aim of increasing biogas yield.

One available biomass source is vegetable and fruit waste from the food industry and/or households. Vegetable and fruit wastes have high initial moisture content in the range of 60–93%, and the wastes are easy degradable under anaerobic conditions.

The anaerobic processing of quickly degradable vegetable or fruit wastes can help avoid carbon dioxide emissions and runoff from biomass, facilitating biogas and fertilizer production in an environmentally friendly way. Research should be conducted on food industry waste processing to evaluate local or regional biogas potential. The aim of the research is to evaluate biogas and methane production from different vegetable residues, clarify whether the addition of biocatalyst Metaferm (made in Latvia) in substrates causes any positive effects, establish effective doses for optimised fermentation and determine the highest doses capable of inhibiting the anaerobic digestion process.

MATERIALS AND METHODS

In order to achieve greater statistical confidence, heated camera (Memmert incubator) and a number of small bioreactors were used. Small bioreactors were filled with substrate and placed in a heat chamber, and gas from each bioreactor was directed into a separate storage bag located outside the camera. Widely applied methods were used for obtaining results (Kaltschmitt, 2010).

The amount of dry matter was determined by investigating the initial biomass sample weight and dry weight with Shimazu scales at 105 °C and by investigating ash content with the help of a Nabertherm furnace, with which the samples were burnt at 550 °C. All mixtures were prepared, carefully mixed and all sealed bioreactors were put in heated camera within same time period before starting anaerobic digestion. The composition of the gas collected into the storage bags was measured with the gas

analyser GA 2000. With the help of this instrument, oxygen, carbon dioxide, methane and hydrogen sulphide were registered in the gas. Substrate pH value was measured before and after finishing the anaerobic fermentation process using a pH meter (PP–50) with accessories. Scales (Kern KFB 16KO2) were used for weighing the substrate before anaerobic processing and for weighing the digestate after finishing the fermentation process. Dry matter content and ash content were measured in the digestate originating from each of the bioreactors to determine dry organic matter (DOM) content.

Bioreactors with the volume of 0.7 l were filled with biomass samples of 20 ± 0.05 g and with 500.0 ± 0.2 g inoculum (fermented cattle manure from a 120 l bioreactor working in continuous mode). For calculation purposes control bioreactors were filled only with inoculum. All data were recorded in the journal of experiments and in a computer. All bioreactors were placed into an incubator with the operating temperature of 38 ± 0.5 °C, and every bioreactor had a flexible pipe connected to a gas storage bag positioned outside the heated camera. Every gas bag has a port normally closed with a tap for gas measurement. The quantity and composition of gases were measured every day. Bioreactors were also gently shaken to mix the floating layer regularly. The fermentation process was started with a single filling in batch mode until the biogas emission ceased. The final digestate was weighed; dry matter and ashes were investigated to evaluate organic dry matter content. The total biogas and methane production values were calculated using the normal biogas volumes and quality parameters obtained from the gas collected to the gas storage bags from each bioreactor. For statistical accuracy all final data values were calculated as averages on the basis of two identical substrates positioned in the heat camera.

In the **first study,** raw onion and carrot processing residues were studied. In the **second study,** cabbage leaves and potato processing wastes were used as raw material in the bioreactors. The methods of the experiments were the same for both projects.

RESULTS AND DISCUSSION

The results of analysing raw material samples in view of the anaerobic digestion of onion and carrot wastes in the **first study** are shown in Table 1.

The results of the digestate analysis after the anaerobic digestion process are shown in Table 2.

The production of biogas and methane from onion and carrot wastes and in control reactors is presented in Table 3.

Adding the biocatalyst Metaferm resulted in a considerably higher methane production compared to the control reactors (with onion or carrot substrates only) in all bioreactors except for reactors with onions. This indicates that onions contain substances that can facilitate active anaerobic fermentation processes on their own, or the substances may act as stimulants both with and without adding the biocatalyst MF.

It is necessary to research the subject further to clarify the biological impact of onions on anaerobic fermentation processes.

Table 1. Results of analysing raw material samples before anaerobic digestion

Bioreactor/Raw material	pH substr	TS %	TS g	ASH %	DOM %	DOM g	Weight g
R1, R16 IN	7.86	4.22	21.1	20.71	79.29	16.73	500
R2, R320 g ON		12.63	2.53	6.8	93.2	2.35	20
500g IN + 20 g ON	7.84	4.54	23.63	19.22	80.78	19.09	520
R4, R520gON		12.63	2.53	6.8	93.2	2.35	20
500gIN+20gON+1 ml MF	7.86	4.54	23.65	19.22	80.78	19.1	521
R6, R720gON		12.63	2.53	6.8	93.2	2.35	20
500gIN+20g ON+2ml MF	7.88	4.53	23.65	19.22	80.78	19.1	522
R8, R920g CR		10.64	2.128	9.74	90.26	1.92	20
500gIN+20g CR	7.82	4.47	23.24	19.69	80.31	18.66	520
R10, R1120g CR		10.64	2.128	9.74	90.26	1.92	20
500gIN+20g CR+1ml MF	7.85	4.47	23.28	19.69	80.31	18.7	521
R12, R1320 g CR		10.64	2.128	9.74	90.26	1.92	20
500gIN+20g CR+2ml MF	7.89	4.46	23.29	19.69	80.31	18.7	522
R14, R15		12.63	1.26	6.8	93.2	1.175	10*
10gON+10g CR+500gIN +2ml MF	7.91	10.64 4.44	1.064 23.41	9.74 19.49	90.26 80.51	0.96 18.85	10** 522

Abbreviations: IN – inoculum; ON – onions; CR – carrots; MF – biocatalyst Metaferm; TS – total solids; ASH – ashes; DOM – dry organic matter; *carrots – 10g; **onions – 10g.

Table 2. Results of digestate analysis for onion and carrot substrates

Bioreactor/Raw material	pH	TS %	TS g	ASH %	DOM %	DOM %	Weight g
R1 IN	7.21	4.48	22.19	14.57	85.43	18.96	495.4
R16 IN	7.20	4.44	21.71	24.55	75.45	16.38	488.9
R2 ON+IN	7.21	4.38	22.36	19.11	80.89	18.08	510.4
R3 ON+IN	7.21	4.64	23.74	21.87	78.13	18.55	511.6
R4 ON+IN +1ml MF	7.18	4.20	21.45	32.84	67.11	14.40	510.8
R5 ON+IN +1ml MF	7.20	3.97	20.29	28.36	71.64	14.54	511.2
R6 ON+IN +2ml MF	7.21	4.23	21.59	23.48	76.52	15.44	510.4
R7 ON+IN +2ml MF	7.14	4.06	20.72	26.20	73.80	15.29	515.4
R8 CR+IN	7.15	4.37	22.37	20.17	79.83	17.86	511.8
R9 CR+IN	7.23	4.24	21.73	27.87	72.13	15.67	512.6
R10 CR+IN+1ml MF	7.25	4.74	22.23	22.84	77.16	27.15	512.2
R11 CR+IN+1ml MF	7.16	4.31	22.09	23.21	76.79	16.96	512.6
R12 CR+IN+2ml MF	7.24	4.51	23.11	22.89	77.11	17.82	512.4
R13 CR+IN+2ml MF	7.21	4.57	23.36	22.96	77.04	17.99	511.2
R14 ON+CR+IN+2ml MF	7.25	4.61	23.66	22.61	77.39	18.31	513.4
R15 ON+CR+IN+2ml MF	7.22	4.67	23.98	23.30	76.70	18.39	513.6

Table 3. Production of biogas and methane from onion and carrot wastes in bioreactors

Bioreactor/Raw material	Biogas l	Biogas l g_{DOM}^{-1}	Methane aver.%	Methane l	Methane l g_{DOM}^{-1}
R1 IN	0.3	0.018	13.00	0.039	0.0023
R16 IN	0.3	0.018	14.00	0.042	0.0025
R2 ON+IN	2.3	0.978	43.87	1.009	0.429
R3 ON+IN	2.3	0.978	44.82	1.031	0.438
R4 ON+IN +1ml MF	2.1	0.894	45.47	0.959	0.408
R5 ON+IN +1ml MF	1.9	0.808	47.47	0.902	0.384
R6 ON+IN +2ml MF	2.1	0.894	43.81	0.920	0.391
R7 ON+IN +2ml MF	1.9	0.808	49.05	0.932	0.396
R8 CR+IN	1.5	0.781	47.13	0.707	0.368
R9 CR+IN	1.2	0.625	44.92	0.539	0.281
R10 CR+IN+1ml MF	2.0	1.041	47.75	0.955	0.497
R11 CR+IN+1ml MF	2.0	1.041	47.9	0.958	0.499
R12 CR+IN+2ml MF	1.7	0.885	42.00	0.714	0.372
R13 CR+IN+2ml MF	1.9	0.989	48.52	0.922	0.480
R14ON+CR+IN+2ml MF	1.5	0.703	44.13	0.662	0.310
R15 ON+CR+IN+2ml MF	1.6	0.749	60.50	0.968	0.453

Note: The average biogas and methane values obtained from reactors 1 and 16 have been already subtracted from the biogas and methane values for bioreactors 2–15 with fresh biomass.
Abbreviation: l g_{DOM}^{-1} – litres per 1 g of added dry organic matter (fresh organic matter added into inoculum)

Specific biogas and methane production volumes calculated for added onion and carrot biomass are shown in Fig. 1.

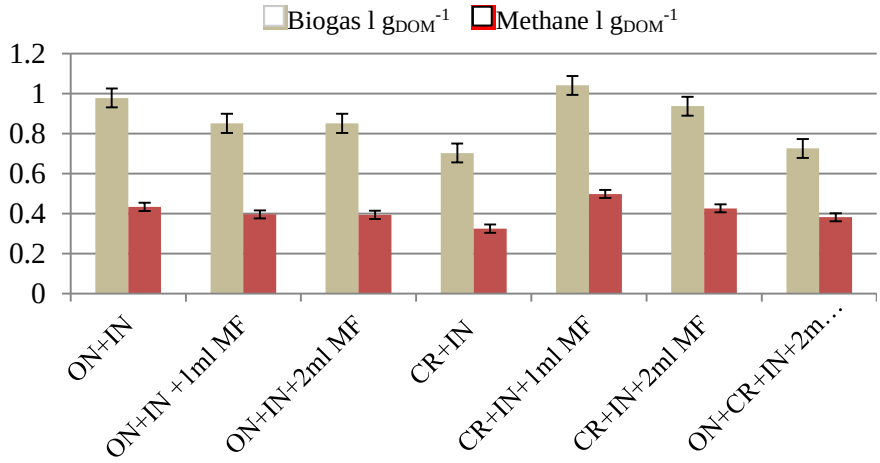

Figure 1. Specific production of biogas and methane from onion and carrot wastes with and without adding the biocatalyst MF.

A good biogas yield was obtained owing to the characteristics of the raw materials but also owing to the fact that the liquid fraction (also inoculum) still had a lot of utilizable substances for the bacteria (e.g., acetic acid) that was no reflected in the dry organic matter analysis.

Substrates with onion wastes provide relatively high methane yields, 0.433 l g_{DOM}^{-1} (litres per 1 g added dry organic matter) on average. Onion substrates with 1 ml or 2 ml of the biocatalyst Metaferm had a 0.396 l g_{DOM}^{-1} and 0.394 l g_{DOM}^{-1} specific methane production respectively. This may be explained by the bioreactors containing substances which inhibit the biocatalyst Metaferm. It is necessary to identify the precise reasons for such inhibition in further research.

Adding 1 ml of the biocatalyst Metaferm to substrates with carrots resulted in a very high average specific methane production of 0.498 l g_{DOM}^{-1} or more than the average methane yield of 0.325 l g_{DOM}^{-1} obtained from control bioreactors without the biocatalyst. Adding 2 ml of Metaferm to substrates with carrot wastes resulted in an average methane yield of 0.426 l g_{DOM}^{-1}. Adding 2 ml of the biocatalyst Metaferm to a carrot–onion 50%:50% mixture resulted in a bigger methane yield increase compared to that of the control bioreactors containing carrots, but smaller than that of control bioreactors with onions. This result also confirms the incompatibility or inhibitive interaction between onions and Metaferm in an anaerobic digestion process.

The results of analysing raw material samples in view of the anaerobic digestion of cabbage and potato wastes in the **second study** are shown in Table 4.

Table 4. Results of analysing raw material samples before anaerobic digestion

Bioreactor/Raw material	pH substr.	TS %	TS g	ASH %	DOM %	DOM g	Weight g
R1, R16 IN	7.54	3.98	19.9	27.72	72.28	14.38	500
R2, R320gCL	7.53	10.87	2.17	9.36	80.64	1.75	20
500g IN + 20gCL		4.24	22.57	25.68	74.32	16.41	520
R4, R520gCL	7.5	10.87	2.17	9.36	80.64	1.75	20
500gIN+20gCL+1mlMF		4.24	22.07	25.69	74.31	16.4	520
R6, R720gCL	7.5	10.87	2.1748	9.36	80.64	1.75	20
500gIN+20gCL+2mlMF		4.24	22	25.69	74.31	16.45	522
R8, R920gCL	7.48	19.36	3.87	5.45	94.55	3.66	20
500gIN + 20gPO		4.57	23.77	23.66	76.34	18.146	520
R10, R1120gPO	7.48	19.36	3.87	5.45	94.55	3.66	20
500gIN+20gPO+1mlMF		4.56	23.77	23.66	76.34	18.15	521
R12, R1320gPO	7.48	19.36	3.87	5.45	94.55	3.66	20
500gIN+20gPO+2mlMF		4.56	23.77	23.66	76.34	18.15	522
R14, R15	7.48	10.87	1.087	9.36	80.64	0.875	10
10gON+10gPO+500gIN +		19.36	1.98	5.45	94.55	1.83	10
2mlMF		4.39	22.92	24.64	75.36	17.27	522

Abbreviations: IN – inoculum; CL – cabbage leaves; PO – potato wastes; MF – biocatalyst Metaferm; TS – total solids; ASH – ashes; DOM – dry organic matter.

Results of the digestate analysis are shown in Table 5.

Table5. Results of the digestate analysis of substrates with cabbage and potato wastes

Bioreactor/Raw material	pH	TS %	TS g	ASH %	DOM %	DOM %	Weight g
R1 IN	7.25	3.58	17.78	22.72	77.28	13.74	496.6
R16 IN	7.27	3.5	17.26	20.64	79.36	13.7	293.2
R2 CL+IN	7.27	3.69	18.94	22.14	77.86	14.75	513.4
R3 CL+IN	7.25	3.58	18.29	20.16	79.84	14.6	510.8
R4 CL+IN +1ml MF	7.33	3.25	16.71	20.34	79.66	13.31	514.2
R5 CL+IN +1ml MF	7.35	3.27	16.83	22.92	77.08	12.98	514.8
R6 CL+IN +2ml MF	7.14	3.34	17.23	21.69	78.31	13.49	515.8
R7 CL+IN +2ml MF	7.19	3.63	18.53	21.34	78.66	14.58	510.5
R8 PO+IN	7.27	3.25	16.54	21.66	78.34	12.96	509
R9 PO+IN	7.31	3.38	17.16	22.18	77.82	13.36	507.8
R10 PO+IN+1 ml MF	7.21	3.29	16.92	20.13	79.87	13.51	514.2
R11 PO+IN+1 ml MF	7.16	3.49	17.88	23.68	76.32	13.64	512.2
R12 PO+IN+2 ml MF	7.25	3.38	17.35	24.53	75.47	13.09	513.2
R13 PO+IN+2 ml MF	7.21	3.23	16.53	22.95	77.05	12.74	512
R14 CL+PO+IN+2 ml MF	7.17	3.29	16.86	24.61	75.39	12.71	512.6
R15 CL+PO+IN+2 ml MF	7.25	3.22	16.54	26.56	73.44	12.15	513.8

The production of biogas and methane from cabbage and potato wastes is presented in Table 6 and Fig. 2.

Table 6. Production of biogas and methane from cabbage and potato wastes in bioreactors

Bioreactor/Raw material	Biogas l	Biogas l g_{DOM}^{-1}	Methane aver.%	Methane l	Methane l g_{DOM}^{-1}
R1 IN	0.3			0.039	
R16 IN	0.4			0.02	
R2 CL+IN*	1.2	0.685	50	0.597	0.341
R3 CL+IN	1.1	0.628	51	0.561	0.32
R4 CL+IN +1ml MF	1.3	0.742	51.92	0.675	0.385
R5 CL+IN +1ml MF	1.2	0.685	53.42	0.641	0.366
R6 CL+IN +2ml MF	1.5	0.857	49.4	0.741	0.423
R7 CL+IN +2ml MF	1.7	0.971	41.82	0.711	0.406
R8 PO+IN	4.1	1.12	52.71	2.161	0.59
R9 PO+IN	3.4	0.928	59.14	2.011	0.549
R10 PO+IN+1ml MF	4.1	1.12	53.68	2.201	0.601
R11 PO+IN+1ml MF	3.3	0.902	55.48	1.831	0.5*
R12 PO+IN+2ml MF	4.7	1.284	53.21	2.501	0.683
R13 PO+IN+2ml MF	4.7	1.284	50.66	2.381	0.651
R14 CL/PO+IN+2ml MF	3.1	1.034	49.39	1.531	0.565
R15 CL/PO+IN+2ml MF	3.7	1.367	48.41	1.791	0.662

*Reactor R11 had technical problems during fermentation; therefore, the data collected from it were replaced by data obtained from the reactor R10 (with the same substrate composition) in calculations.

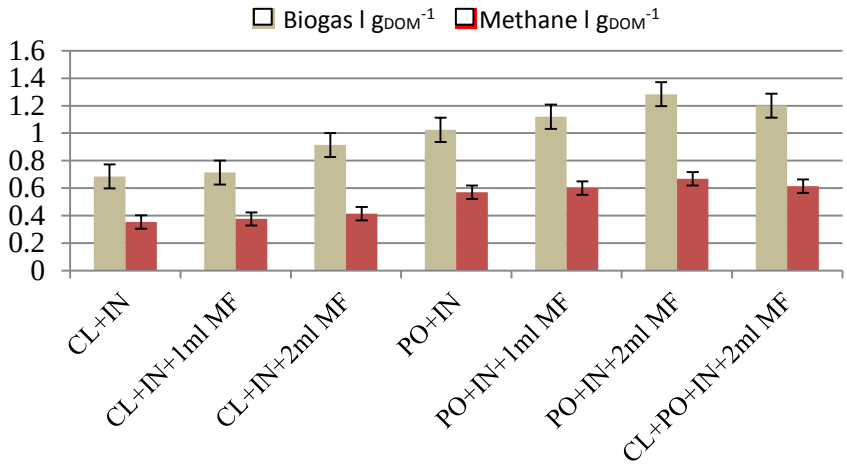

Figure 2. Specific production of biogas and methane from cabbages and potatoes with and without adding the biocatalyst Metaferm.

The main results obtained from the **second study** are the following:

Adding the biocatalyst Metaferm increased biogas and methane production for all reactors compared to the control reactors. Adding 1 ml of the biocatalyst Metaferm to substrates with cabbage leaves resulted in an average specific methane production of 0.376 l g_{DOM}^{-1}. Adding 2 ml of the biocatalyst MF to substrates with cabbage leaves resulted in a very high specific methane production (0.415 l g_{DOM}^{-1}). Adding 1 ml or 2 ml of the biocatalyst MF to substrates with potatoes increased the average specific methane production compared to the control bioreactors (potato without MF). Less methane was produced in the bioreactor R11 due to technical problems, therefore, data from this reactor were not included in calculations.

Adding 2 ml of the biocatalyst MF to substrates with cabbage leaves and potato cuttings (50 : 50) resulted in very high specific methane production (0.613 l g_{DOM}^{-1}).

CONCLUSIONS

Adding the biocatalyst Metaferm had an impact on the fermentation processes in all substrates compared to the control group without MF.

Adding 1 ml and 2 ml of the biocatalyst Metaferm to substrates with onions lowered methane production by 8.5% and 9% respectively compared to the control substrate. Interactions between inoculum, onion and biocatalyst should be investigated more thoroughly in further research.

Adding 1 ml of the biocatalyst Metaferm increased methane production by 5.5%, 13.6% and 53.2% in substrates with potato, cabbage and carrot wastes respectively compared to the control substrates.

Adding 2 ml of the biocatalyst Metaferm increased methane production by 17%, 25.2% and 31.1% in substrates with potato, cabbage, and carrot wastes respectively compared to the control substrates.

Adding 2 ml of the biocatalyst MF to substrates with cabbage and potato cuttings (50:50) caused the methane production to increase by 7.63% compared to the average methane production in cabbage and carrot substrates with 2 ml of MF.

Adding 2 ml of the biocatalyst Metaferm to a carrot–onion mixture (50%:50%) caused the methane yield to increase by 17.5% compared to the control bioreactors containing carrots, but the yield was 11.8% smaller than that of control bioreactors with onions. This result also confirms the inhibitive interaction between onions and Metaferm and/or inoculum in anaerobic digestion processes.

Adding 2 ml of the biocatalyst Metaferm to a cabbage–potato mixture (50%:50%) caused the methane yield to increase by 33% compared to the average value of control bioreactors containing cabbage and potato mixtures without MF. This result also confirms the positive effect of the biocatalyst Metaferm on cabbage or potato substrates undergoing anaerobic digestion processes.

REFERENCES

Ministry of Economics, 2010, Information Report: Republic of Latvia National Renewable Energy Action Plan for implementing Directive 2009/28/EC of the European Parliament and of the Council of 23 April 2009 on the promotion of the use of energy from renewable sources and amending and subsequently repealing Directives 2001/77/EC and 2003/30/EC by2020, p.103. online: http://www.ebbeu.org/legis/ActionPlanDirective2009_28/national_renewable_energy_action_plan_latvia_en.pdf

Communication from the commission to the European Parliament, the Council, the European Economic and Social Committee and the Committee of the Regions, A policy framework for climate and energy in the period from 2020 to 2030, COM(2014) 15 final, Brussels, 22.1.2014, pp.18, online: http://eurlex.europa.eu/legalcontent/EN/TXT/PDF/?uri=CELEX:52014DC0015&from=EN

Ministry of Economics, 2015, Register of subsidized electricity producers (in Latvian), online: https://www.em.gov.lv/files/energetika/SEN_reg_15012015.xls

Feng, XM., Karlsson, A., Svensson, BH., Bertilsson, S. 2010. Impact of trace element addition on biogas production from food industrial waste—linking process to microbial communities. FEMS Microbiol Ecol. 2010, Oct; 74(1), 226–40.

Lemmer, A, Vintiloiu, A., Preisler, D., Bauerle, L., Oechsner, H. 2011, Importance of mineral substances for anaerobic microorganisms and causes of concentrations differences in biogas digesters. Proceedings of International Congress Biogas in Progress 2 Hohenheim, Stuttgart, 2011, vol.1, pp. 216–222.

Dubrovskis, V., Plume, I., Kotelenecs, V., Zabarovskis, E. 2011. Biogas production and biogas potential from agricultural biomass and organic residues in Latvia. Proceedings of International Congress Biogas in Progress 2, Hohenheim, Stuttgart 2011, vol.2, pp. 80–83.

Irvan, I. 2012.Chemical Engineering Department, University of Sumatera Utara. Effect of Ni and Co as Trace Metals on Digestion Performance and Biogas Produced from The Fermentation of Palm Oil Mill Effluent. Internat. J. Waste Resources, Vol. 2(2), 2012, 16–19, p 4.

Facchina, V., Cavinatob, C., Pavanba, P., Bolzonella, D. 2013. Batch and Continuous Mesophilic Anaerobic Digestion of Food Waste: Effect of Trace Elements Supplementation. Chemical Engineering Transactions, vol 32, p.6.

Kaltschmitt, M. 2010. Methodenhandbuch Leipzig, p.93.

Agronomy Research **13**(2), 303–310, 2015

Comparison of technologic parameters of pellets and other solid fuels produced from various raw materials

T. Ivanova[1], M. Kaválek[1,*], B. Havrland[1], M. Kolaříková[1] and P. Skopec[2]

[1]Czech University of Life Sciences Prague, Faculty of Tropical AgriSciences, Kamycka 129, CZ16521 Prague 6 – Suchdol, Czech Republic
[2]Czech Technical University in Prague, Faculty of Mechanical Engineering, Zikova 1903/4, CZ16636 Prague 6, Czech Republic
[*]Correspondence: michal.kavalek@seznam.cz

Abstract. The article relates results of experiments and problem studies, the main goal of which was comparing four alternatives of solid biofuels suitable for heating private houses by low-power boilers. The results were obtained by burning of selected biofuels in an automatic pellet boiler specifically designed for combustion of pelletized fuels with high ash content. The emissions were set up related to the mass of burnt fuels and to the fuels' net calorific value (specific emissions), they were measured and analysed. Based on the emission concentration measurements and stoichiometric calculations, the fuel gas emissions' properties and boiler efficiency were compared at a range of power outputs of 7.5 kW, 12.5 kW and 18.5 kW. With regard to fuel properties and boiler outputs, the emissions of carbon monoxide (CO) were determined as well as emissions of nitrogen oxides (NO_x) and sulfur dioxide (SO_2) were measured and compared too. The results permitted to formulate conclusions that the wood pellets were having the lowest values of measured emissions, whereby Jatropha seed cakes showed several times higher emissions in comparison with emissions from wood pellets, oil palm shells and wheat straw pellets, where the last one is a typical representative of the agricultural biomass with relatively high nitrogen content and as was shown higher emissions of NOX as compared to wood pellets. Oil palm shells measured emissions were relatively similar to wood pellets emissions, especially concerning emissions of SO_2 and CO. All tested materials were having very low combustible sulphur contents and therefore the specific SO_2 emissions were negligible at all these fuels. A very important finding was that the amount of emissions was dependent on boiler output, where with the output decreasing the amount of emissions was growing. The other linkage – dependence of the boiler efficiency on power output was also proved in the present paper.

Key words: wood pellet, wheat straw, Jatropha seed cake, oil palm shell, emissions, biomass combustion.

INTRODUCTION

In view of approaching lack of fossil energy sources (particularly future shortage of crude oil and natural gas) which deposits are estimated to meet future needs some couple of decades only. Research of new energy sources gets high importance. Especially renewable energy sources seem being of very good prospects. The so called bioenergy produced from biomass (mainly waste biomass which is very abundant in both developed and developing regions) is one of renewable sources of energy. In some

regions it is the only one utilisable renewable energy source. For the above reasons much effort and many founds are yearly worldwide spent for researching new energy sources. In fact they have always been well known however their utilization is constrained by sometimes less economy (due to higher prices) or they feature some technological imperfections in comparison with fossil energy and generally have lower calorific values. On the other hand they have some properties which are superior to fossil fuels such as smaller amount of emissions or availability in distant areas.

As stated in the Abstract the present paper concerns results of testing solid biofuels made of four different raw materials in order to get more information useful for production process of biofuels as well as for their combustion.

MATERIALS AND METHODS

Two different kinds of pellets were used for experimental purposed: *wood pellets* and *wheat straw pellets*. As the substitutes to pellets *oil palm shells* and *Jatropha seed cake* were exanimated, too.

The pellets are commercialized in Czech Republic and they have a diameter of 6 mm. Jatropha seed cake is untreated waste material from mechanical oil extraction. Shape composition of Jatropha seed cake was: 86% shape of flakes from 1 to 8 cm in diameter and 3 mm thin and 14% of dusty material. Oil palm shells from Malaysian palm oil industry were used as untreated substitute for pellets; 95.9% of particles (shells) reach diameter 3.15–15 mm.

The basic properties of above mentioned tested biofuels, which encompasses calorific values and chemical composition were analysed according to European standard methods and they are presented in the Table 1.

Table 1. Biofuels chemical composition and calorific values

Chemical composition, w.b (%)	Wood pellets	Wheat straw pellets	Palm shells	Jatropha seed cake
C	46.23	43.04	39.41	44.72
H	6.29	6.51	4.81	6.07
N	0.24	0.72	0.08	3.80
S	0.0	0.05	0.06	0.0
O	39.45	43.28	48.18	37.44
Moisture content, w.b (%)	7.79	6.40	7.46	7.96
Ash content (%)	1.49	6.33	3.33	5.48
NCV (MJ kg^{-1})	16.35	17.60	17.35	17.56
GCV (MJ kg^{-1})	17.93	19.19	18.59	19.11
Ash deformation temperature, °C	1,300	800	1,345	1,110

The data of moisture content, ash content and its deformation temperature for oil palm shells were also published in our previous research (Kaválek et al., 2013a) and the parameters of Jatropha seed cake, except of chemical composition were presented at Kaválek et al., 2013b.

Commercially available automatic pellet boiler working with a range of 7.5–25 kW power output specifically designed for wood pellets burning was used for the experiments. The testes of the research materials were conducted at the power outputs 7.5 kW, 12.5 kW and 18.5 kW. The fuel was being loaded from a container attached to the furnace by a screw conveyer directly into the furnace. The boiler has separately distributed primary and secondary combustion air inputs. Capacity of the boiler can be controlled by adjustment of fuel loading intervals. Primary and secondary air flows are dependent on each other; because they are blown by a simple fan and cannot be controlled directly (i.e. control of the air flow by the speed of the fan is not possible). However the primary and secondary combustion air flows may be controlled by flaps. The boiler is also equipped with flue gas recirculation that is controlled by revolutions of the recirculation fan.

Fig. 1 shows schematic diagram of the boiler used for experiments, which consists of: fuel container having capacity of 25 kg and motor drive of the screw feeder to feed fuel into the combustion chamber, control panel (not shown in the figure) for controlling the feeding rate, then cyclically working grate to remove ash from the furnace, hot water heat exchanger to hand over the heat of combustion from the primary water circuit to the secondary one.

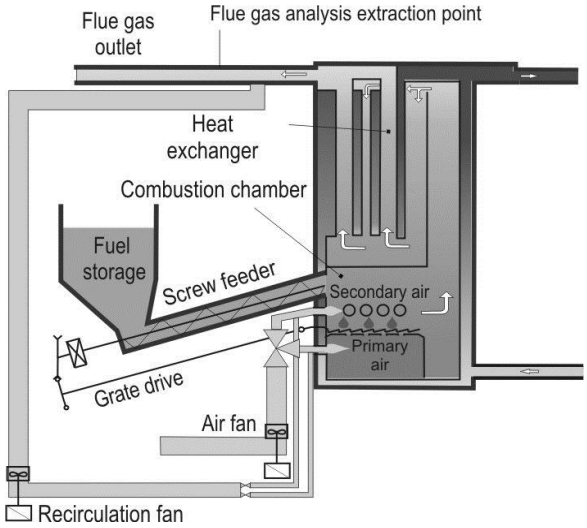

Figure 1. Schematic diagram of the boiler.

Gaseous compounds were measured continuously at the flue gas analysis extraction point (see Fig. 1) by Portable Emission Analyzer Testo 350 XL during all the experiment of the biomass combustion. CO_2, CO, NO_x, SO_2, O_2 and air excess where measured. Concentrations of O_2, CO, NO_x and SO_2 were evaluated and processed after the experiment. The concentration values were measured in volume fraction concentrations and then were converted into mass concentrations as related to dry flue gas at normal pressure and temperature and reference oxygen content, using the following equation (Dlouhý, 2007; Skopec et al., 2014):

$$C_m^X = C_V^X \cdot \frac{M_X \cdot p_{ref}}{R \cdot T_{ref}} \cdot \frac{(21 - O_{2,ref})}{(21 - O_{2,meas})} \quad (1)$$

where: C_V^X is measured volume concentration of given component X in volume ppm; M_X is molar mass in g mol^{-1}; p_{ref} is reference pressure of 101.325 kPa; R is universal gas constant equal to 8.3143 J K^{-1}mol^{-1}; T_{ref} is reference temperature of 273.15 K; $O_{2,ref}$ is reference oxygen content (for this purpose 10% given by law); $O_{2,means}$ is measured oxygen content in volume %. The final unit of mass concentration of the flue gas component is mg N^{-1}m^{-3}. Nitrogen oxides are calculated as NO_2 (Ibler et al., 2002).

RESULTS AND DISCUSSION

Average values of volume emission concentrations from the measurements were converted into mass concentrations at standard conditions and reference concentrations of oxygen. The results are presented in the Table 2 and Figs 2–4. These results show variability of boiler emissions in whole working range of boiler power output.

Specific emissions evidence strong influence of boiler power output. With increasing power output the emissions decrease. It means that the power output of the boiler significantly influence the amount of emissions.

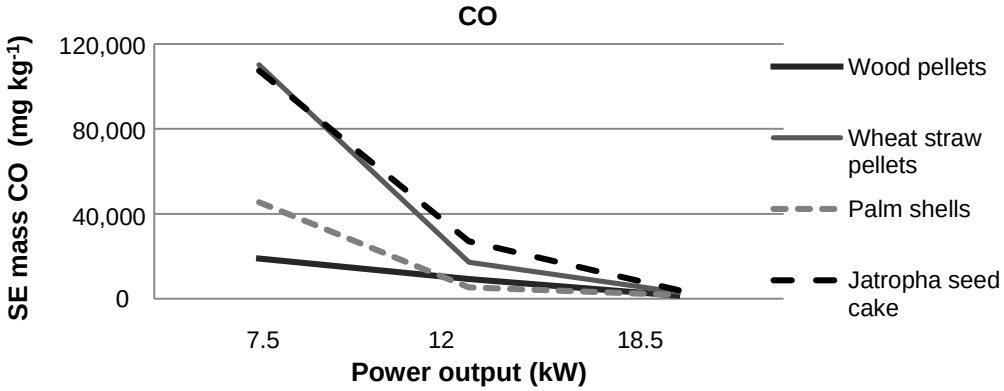

Figure 2. SE mass CO emissions.

Two kinds of specific emissions were evaluated and calculated on the basis of measured data. The specific emissions related to the fuel mass (SE mass) and the specific emissions related to the net calorific value (or low heating value) of the fuel (SE NCV). First the theoretical volume of the flue gas was calculated from the elemental composition of the fuel in order to obtain SE mass. Using oxygen concentration, the theoretical volume of the flue gas is converted to real volume of flue gas. The SE mass was obtained through multiplication by the recalculated emission mass concentration. SE NCV calculation is based on conversion of weight of the fuel to the recoverable energy stored in it. This provides an alternative way for comparison of different fuels.

In this case the differences are not fully apparent due to quite similar net calorific values of both groups of fuels.

The Fig. 2 demonstrates results of specific CO emissions' measurements from combustion of all four tested solid fuels.

CO emissions indicate the quality of the combustion process. Burning the wood pellets exhibited much better combustion stability and the boiler output was at the set up value. Burning the Jatropha seed cake showed the worse characteristics, but it was expected. In the course of the combustion of wheat straw pellets, palm shells as well as Jatropha seed cake the performance greatly fluctuated and it was necessary to set the shorter grating period especially due to the higher amount of ash content and in case of wheat straw pellets also due to the lower ash softening temperature and tendency to sintering.

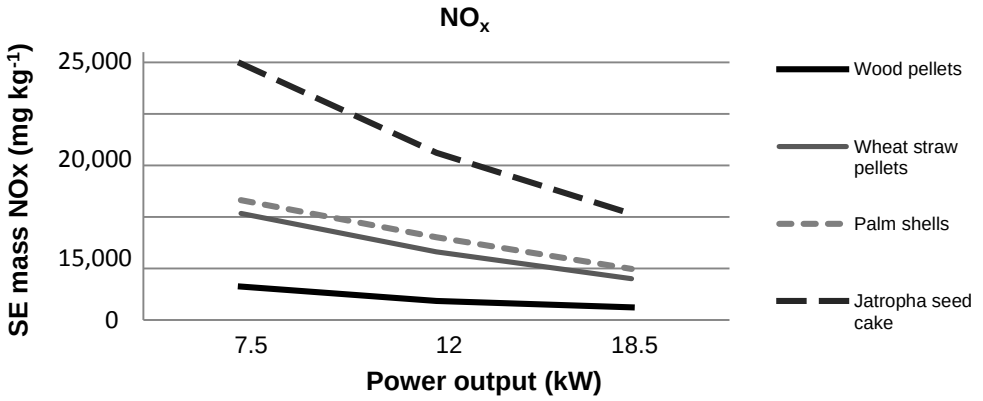

Figure 3. SE mass NOx emissions.

It is evident from Fig. 3, that the NO_x emissions from Jatropha seed cake combustion are almost ten times higher than the emissions released during the combustion of wood pellets. This finding corresponds to the nitrogen content in the fuels, as shown in the Table 1.

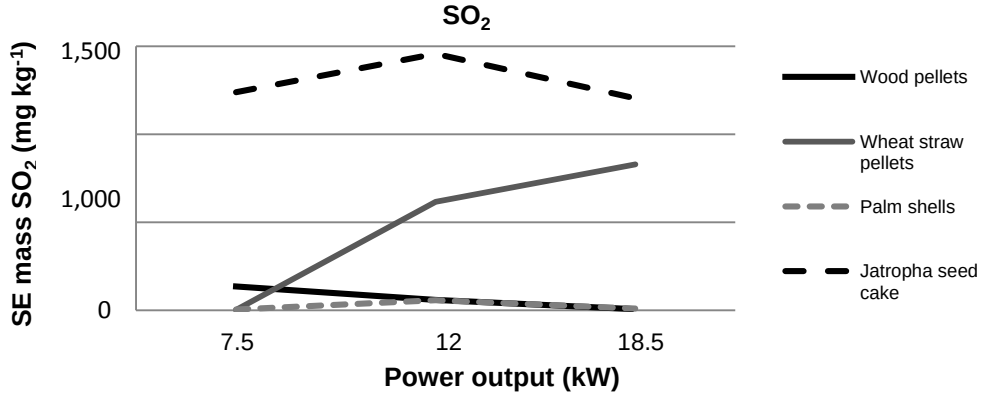

Figure 4. SE mass SO2 emissions.

SO_2 emissions for majority of tested biofuels are very low due to the low content of combustible sulphur (see Fig. 4). Only Jatropha seed cake shows increased SE mass due to its increased sulphur content.

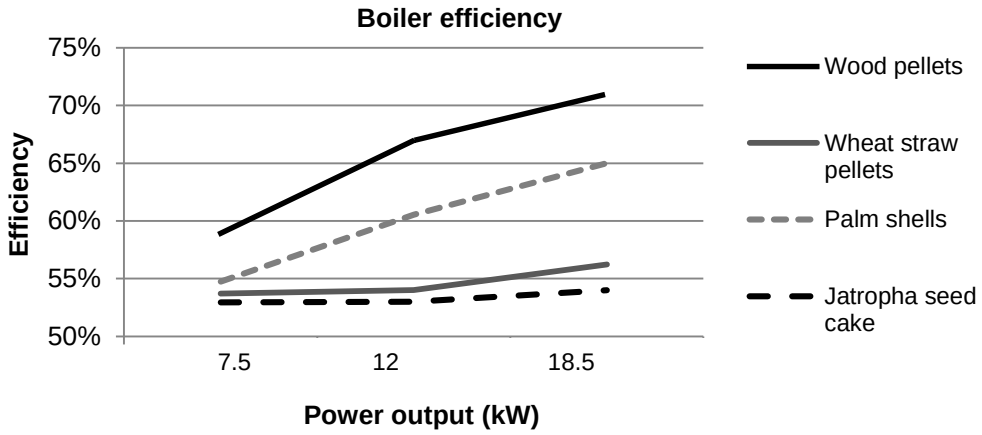

Figure 5. Boiler efficiency related to power output.

As demonstrated by Fig. 5 the boiler efficiency also shows dependence on the boiler power output. The strongest influence of power output on the boiler efficiency was found at combustion of wood pellets and the lowest one at Jatropha seed cake combustion. It can be seen, that in the case of wood pellets the boiler efficiency increased by 12% in comparison between 7.5 kW and 18.5 kW power outputs. In case of oil palm shells with increase of the boiler power output the efficiency has also increased significant (by 10%). In case of wheat straw and Jatropha seed cake the efficiency growing rate was confirmed as well, but the incensement itself was in both these cases not so rapid in comparison with two above mentioned materials.
The Table 2 gathers the overall results of specific emissions related to the fuel mass for all the biofuels tested within the present research.

Table 2. SE mass comparison

	Specific emissions CO ($mg\ kg^{-1}$)			Specific emissions NO_x ($mg\ kg^{-1}$)			Specific emissions SO_2 ($mg\ kg^{-1}$)		
Power output (kW)	7.5	12.0	18.5	7.5	12.0	18.5	7.5	12.0	18.5
Wood pellets	18,935	9,244	1,542	3,234	1,852	1,214	135	59	6
Wheat straw pellets	110,215	17,278	2,999	10,353	6,596	3,999	1	616	830
Palm shells	45,490	5,409	1,777	11,629	8,034	4,962	3	56	9
Jatropha seed cake	107,364	27,121	4,060	24,882	16,230	10,288	1,239	1,458	1,204

The results of specific emissions related to the net calorific value and their comparison with the other previously published data are presented in the Table 3. The SE NCV values measured at the nominal and minimal power output (18.5 kW and 7.5 kW, respectively) within this study were compared with specific emissions taken from the EMEP/EEA air pollutant emission inventory guidebook (Troozzi, 2006) and with specific emissions taken from Czech Hydrometeorological Institute (CHMI) (Horák, 2011). The values from EEA are related to small boilers with nominal capacity lower than 50 kW for burning wood and similar wooden waste. The values from CHMI are related to the combustion of wood. There is no published data found concerning the same parameter for biofuels made of agricultural biomass.

Table 3. Comparison of measured SE NCV with SE NCV available from EEA and CHMI

Pollutant	EEA	CHMI	Wood pellets		Wheat straw pellets		Palm shells		Jatropha seed cake	
Power output (kW)	-	-	18.5	7.5	18.5	7.5	18.5	7.5	18.5	7.5
CO (g GJ^{-1})	4,000	68.5	94	1,160	170	6,260	102	2,620	231	6,110
NO_x (g GJ^{-1})	120	205.5	74	198	227	588	277	670	586	1,420
SO_2 (g GJ^{-1})	30	68.5	0.4	8.3	0.5	47	0	0.7	70	70

Table 3 shows, that SE NCV of CO obtained by EEA for the same (wooden) material are extremely high in contrast with CHMI data and the results of this research. The EEA data seems to be unreliable since measured experimental data as well as the data from CHMI are much lower; even in comparison to the case of lower power outputs are EEA values four times higher. However, EEA emission values of CO are comparable to the values of Jatropha seed cake emissions and emissions from wheat straw pellets at minimal power output. Due to the lowers ash softening temperatures the burning process of wheat straw pellets could be assessed as difficult and highest CO concentrations are produced. CHMI values of CO emissions are close to emission values for wood pellets obtained in the present research at the boiler power output 18.5 kW.

On the other hand, the values of NO_x emissions published by EEA seem to be more accurate for nominal power output; the CHMI values are closer to our values measured at minimal power output. The measured NO_x values for wheat straw pellets, oil palm shell and especially Jatropha seed cake are much higher than EEA and CHMI values, mainly concerning to the minimal power output.

The values of SO_2 specific emissions are completely different from both the above information sources in comparison with our measured data. There is no reliable explanation for such a high discrepancy. The most probable problem resides in the applied measurement method for SO_2 concentration measuring, which is in the case of EEA and CHMI unknown. The SO_2 measurement methods/technique might be not enough precise and suitable for the low concentrations and might therefore be a source of errors. Unfortunatelyy, EEA and CHMI didn't mention any method used for their data meas

CONCLUSIONS

The specific emissions of CO, NO_x, CO_2, and SO_2 related to the mass of fuel burnt and the net calorific value of fuel was determined based on the emission concentration measurements and stoichiometric calculations done for four different types of solid biofuels at three different boiler power outputs. It was confirmed that wood pellets generally have much lower emission concentrations of harmful pollutants than other biofuels. Oppositely, Jatropha seed cake shows the highest concentrations of all tested pollutants. Oil palm shells showed similar values of CO emissions comparing to wood pellets. Wheat straw pellets are typical representative of agricultural biomass with relatively high nitrogen content. Therefore, their specific emissions of NO_x are several times higher in comparison to wood pellets and are comparable (similar) to NO_x emissions obtained from oil palm shells. All fuels have very low combustible sulphur content, except from Jatropha seed cake, while their SO_2 emissions are also quite negligible.

Comparison of calculated specific emissions with literature data provided different results. Specific emission of CO better corresponds to CHMI data, while NO_x values to EEA. However, there are uncertainties regarding experimental procedure and boiler used in these published references. According to Skopec et al. (2014), generally, a development and modernization of boiler construction should lead to their better efficiency and improved emission reflected in lower specific emissions. The boiler efficiency calculated in this study showed dependency of efficiency on the boiler power output.

ACKNOWLEDGEMENTS. The study was supported by Internal Grant Agency of the Faculty of Tropical AgriSciences, Czech University of Life Sciences Prague - grant number 20155015.

REFERENCES

Dlouhý, T. 2007. *Calculations of the boilers and combustion heat exchangers.* Czech technical university in Prague, Prague, 212 pp. (In Czech).

Ibler, Z., Ibler, Z., Karták, J., Mertlová, J. 2002. *Technical guide to power engineer*. BEN-technical literature, Prague, 616 pp. (In Czech).

Horák, J. 2011. Proposal of emission factors of the pollutants for solid fuels combustion in local furnaces. *Environment protection*: **3**, 7–11 (In Czech).

Kaválek, M., Havrland, B., Pecen, J., Ivanova T., & Hutla P. 2013[a]. Oil palm shell use as alternative biofuel. *Agronomy Research* **11**(1), 183–188.

Kaválek, M., Havrland, B., Ivanova, T., Hutla, P. & Skopec P. 2013[b]. Utilization of *Jatropha curcas* L. seed cake for production of solid biofuels. In *12th International Scientific Conference Engineering for Rural Development.* Latvia University of Agriculture, Jelgava, Latvia, pp. 536-540.

Skopec, J., Hrdlička, J., Kaválek, M. 2014. Specific emissions from biomass combustion. *Acta Polytechnica* **54**(1), 74–78.

Trozzi, C. 2009. *EMEP/EEA emission inventory guidebook 2009 – part B – 1.A.4. small combustion.* 119 pp. Available at <http://www.eea.europa.eu/publications/emep-eea-emission-inventory-guidebook-2009/part-b-sectoral-guidance-chapters/1-energy/1-a-combustion/1-a-4-small-combustion-tfeip-endorsed-draft.pdf/view>

Agronomy Research **13**(2), 311–317, 2015

Energy crops utilization as an alternative agricultural production

T. Ivanova[1], A. Muntean[2], V. Titei[3], B. Havrland[1] and M. Kolarikova[1,*]

[1]Czech University of Life Sciences Prague, Kamycka 129, CZ16521 Prague 6, Czech Republic; [*]Correspondence: kolarikova@ftz.czu.cz
[2]The State Agrarian University of Moldova, Mirceşti 42, Chişinău 2049, Republic of Moldova
[3]Botanical Garden of the Academy of Sciences of Moldova, Padurii 18, Chisinau 2002, Republic of Moldova

Abstract. Nowadays an increasing attention is given to the production and use of solid biofuels as an alternative to traditional fossil fuels. The common raw material for the production of solid biofuels is a biomass of vegetal origin, which is mainly represented by waste and secondary agricultural products as well as forest or wood residues. Unfortunately, these types of materials do not always meet the quality requirements for the production of biofuels in the form of pellets and briquettes. This is primarily due to the fact that much of the agricultural wastes have low calorific value, high ash content, low density, etc. and at the end all these facts also negatively affects the price of biofuels. In addition, an intensive use of agricultural waste as a raw material for the purpose of biofuels' production could have a negative impact on soil fertility. Based on abovementioned disadvantages of agricultural biomass, there is a big potential in utilization of alternative biomass such as energy crops. Several energy crops from the same biological family *Asteraceae* were selected for the research purposes. The main focus of this article is evaluation and comparison of the main solid biofuels' properties, which were measured according to European and International standards. Assessment of an energy potential of selected crops for the Republic of Moldova is presented here as well.

Key words: energy crops, solid biofuel, briquettes, gross calorific value, ash content.

INTRODUCTION

Supply of mankind with the food and energy remains the central topic of the XXI century. Economic growth and social development of society leads to increased consumption of energy resources, the cost of fossil types of fuels constantly rising and soon they may run short of reserves in general. According to the forecast developed by World Energy Council, consumption of energy in 2050 will double, which, in turn, will lead to increased CO_2 content in the atmosphere and to strengthening of greenhouse effect.

In regard to this, searches for new renewable sources of energy are actively conducted, including development of bioenergy, which gets increasing social demand and now it ranks among the main priorities of innovative development of world economy. The Republic of Moldova imports 95% of energy resources and energy costs

per unit of production are three times higher, than on average across Europe. According to Energy strategy of the Republic of Moldova (2013), the total amount of energy produced from renewable sources should be increased to 20% by the year 2020 and 3/4 of this amount will make energy from biomass. Taking into account that forests in Moldova cover less than 8% of the area, it becomes relevant to explore the suitability of using various types of phytoenergy plants (energy crops) as renewable energy sources, and also to develop technologies of their cultivation in order to obtain the maximum yield of technological raw materials for further processing into new types of fuels.

The brief description of selected crops, which seem to be perspective source of energy biomass for Moldova and were object of the present research, is as follow:

According to Shtar et al. (2006) and Teleuta et al. (2012) Jerusalem artichoke was introduced in Moldova at a turn of 17−18 centuries. Silage types of Jerusalem artichoke represent special interest for production of solid biofuel, because these taxa reach 4.2−4.5 m in height and 3.2−4.0 cm in diameter at the plant base.

More than half a century cup plant was studied in Moldova as fodder crop, but in recent years it also became interesting for development of bioenergy field. The plant is propagated by division of a bush, seedling and seeds. Seedling and seeds form only the socket in the first year. In the following years 12−20 shoots develop on one bush. Stem of the plants is straight, well leafy, thick, tetrahedral and by the end of growing season reaches 3.0−3.5 m (Teleuta & Titei, 2012).

By Titei & Teleuta (2011) New York aster was introduced as an ornamental flowering plant. It usually grows as a bush of back pyramidal form. Stems are up to 160 cm height, densely branched and leafy. The plant is propagated by division of a bush (spring), green stems and seeds. New York aster has high frost resistance and it can be used for development of abandoned and eroded lands.

Elecampane is cultivated for medicinal purposes, where rhizomes or leaves are applied, and stems can be used for energy. Propagation of the plant is done by division of a bush, seedling and seeds. In the first year plants form the socket and in the following years develop stems up to 2.3 m height, angular, thick, upright, and furrowed, at the top low-branchy, highly resistant to mechanical damages, steady against precipitations and strong wind during winter period (Halford & Karp, 2010).

The research problem was to evaluate the potential for the Republic of Moldova of solid biofuels produced from four promising energy crops on the basis of determination of their main parameters such as gross and net calorific values as well as ash content and due to calculation of the biomass energy yields.

MATERIALS AND METHODS

Material for research was perennial species of herbaceous plants from the family *Asteraceae*: Jerusalem artichoke (*Helianthus tuberosus* L.), cup plant (*Silphium perfoliatum* L.), New York aster (*Symphyotrichum novi-belgii* or syn. *Aster novi-belgii* L.) and elecampane (*Inula helenium* L.). The selected plants were grown under the same conditions in experimental plots of Chisinau Botanical Garden (Institute) of the Academy of Sciences of the Republic of Moldova (see Fig. 1).

Helianthus tuberosus L.

Silphium perfoliatum L.

Symphyotrichum novi-belgii L.

Inula helenium L.

Figure 1. Perennial energy crops from the family *Asteraceae.*

Aboveground biomass of the selected energy crops grown for research purposes was harvested in 2012 and the further measurements of biomass and biofuels properties were performed in the Laboratory of solid biofuel of the State Agrarian University of Moldova in accordance with European Union standards for solid biofuel, which were approved and came into force in the Republic of Moldova since 2012.

The gross calorific value (GCV) was determined by bomb calorimeter LAGET MS-10A for the totally dry materials (dry basis) and it was calculated by the following formula (Havrland et al., 2013):

$$GCV = \frac{dTk \cdot Tk - (c1+c2)}{m} \text{ J g}^{-1} \quad (1)$$

where: *dTk* – temperature jump, °C; Tk – heat capacity of calorimeter, J $^{o}C^{-1}$; c_1 –repair of benzoic acid, J; c_2 – repair of the heat released by burning spark fine wire, J; m – weight of material sample, g.

The net calorific value (NCV) was then defined as (Marian et al., 2013):

$$NCV = GCV - E_W \cdot (8.9 \cdot H + W),\ \text{J g}^{-1} \quad (2)$$

where: E_W – average value of heat of water evaporation, J g^{-1} (24.42 J g^{-1}); H – hydrogen content in a sample, %; W – moisture content in a sample, %.

Measurement of ash content (A_C) was performed in muffle furnace in accordance with the requirements of SMV EN14775:2012 standard and the following formula was used:

$$A_C = \frac{(m_3 - m_1)}{(m_2 - m_1)} \cdot 100, \% \quad (3)$$

where: m_1 – mass of an empty crucible, g; m_2 – mass of crucible with a sample, g; m_3 – mass of crucible with ash residue, g.

The maximum (theoretical) energy potential or biomass gross energy yield (BEY) of energy crops was found due to following calculation (Kolarikova et al., 2014):

$$BEY = GCV \cdot DM, \text{ GJ ha}^{-1} \quad (4)$$

where DM – productivity of the plant (dry matter yield), t ha^{-1}

RESULTS AND DISCUSSION

Table 1 (below) shows the results of laboratory measurements and calculations regarding to the main fuel properties of selected plants, such as calorific value and ash content. Sunflower like representative of the same family was taken for comparison.

It is evident from Table 1 that New York aster and Jerusalem artichoke have the highest values of gross and net calorific value and the lowest values from all the plants show elecampane. For more probability of the results standard deviations and confidence intervals were found.

Generally, the highest calorific values are typical for biofuels made of wood biomass. According to Jevič et al. (2008) net calorific value of wood ranges between 19.4–20.8 MJ kg^{-1}, which is much higher than net calorific value of presented crops. On the other hand, in accordance with EN 14961–3 the minimum net calorific value determined for the wood briquettes of A1 class should be 15.5 MJ kg^{-1}, which is reached by all the studied plants.

The same as calorific value the best results of ash content (the smallest amount) shows biomass of New York aster, followed by Jerusalem artichoke, and in contrast the highest amount of ash content after the biomass combustion has elecampane. The ash content in selected plants varies from 1.82–4.07%.

Table 1. Main characteristics of energy crops' biomass

Biomass	Parameters of calorific value				
	Calorific value (dry basis), J g^{-1}		Standard deviation	Confidence interval	Ash content, %
	Gross calorific value	Net calorific value			
Jerusalem artichoke (*Helianthus tuberosus* L.)	18,568.85	17,258.96	459.08	6.60	2.26
Cup plant (*Silphium perfoliatum* L.)	17,823.02	16,513.15	653.36	9.59	2.50
New York aster (*Symphyotrichum novi-belgii*)	18,726.84	17,416.95	481.71	6.89	1.82
Elecampane (*Inula helenium L.*)	17,653.07	16,343.18	498.75	7.35	4.07
Sunflower (*Helianthus annuus* L.)	18,437.85	17,127.96	332.17	4.79	2.73

According to the standard for a quality of wood briquettes EN 14961−1 ash content ranges between 0.5−3%. Chosen plants from *Asteraceae* family except from elecampane (including sunflower) fulfill this requirement. As reported by Kotlánová (2010) ash content of herbaceous biomass may reach values up to 10%. For example, ash content of hay (grass) measured by Hutla (2010) is 6.33%, which is much higher comparing to all selected plants. Kim et al. (2000) reported that the low ash content leads to better suitability of fuels for thermal utilization. High ash content causes high dust emission and negatively influences the combustion efficiency.

It is necessary to mention some other important notes and data from the field trials and laboratory measurements concerning the selected crops, e.g. biomass yield as well as bulk density of crushed biomass prepared for transportation and transformation to solid form of fuel.

It was found that stems of Jerusalem artichoke do not break and fall down and this contributes to high accumulation of aboveground dry biomass of about 26−28 t ha^{-1}. Bulk density of harvested and crushed dry biomass of the plant is 268−276 kg m^{-3}.

Cup plant biomass contains up to 25% of leaves that has impact on decrease of calorific value and bulk density. Bulk density of crushed biomass is 241 kg m^{-3}. But physical density of received briquettes made of cup plant is high (961 kg m^{-3}), this has positive impact on their storage and transportation. Biomass yield is about 16.4 t ha^{-1}.

Within establishing negative temperatures New York aster's shoots quickly dry up and at the beginning of December the moisture of harvested aboveground biomass drops below 10%. Biomass yield reaches 11.7 t ha^{-1}; leaves content is 10−18%. Bulk density of harvested and crushed dry biomass is about 248−256 kg m^{-3}.

Negative temperatures also quickly accelerate drying of elecampane's stems and by beginning of November it is possible to start collecting biomass. Harvested yield of aboveground dry biomass of this plant varies between 9−13 t ha^{-1}.

Very important indicator, which was calculated from the abovementioned results, is energy potential of the crop (see Fig. 2).

It is visible from the Fig. 2 that Jerusalem artichoke reaches almost double energy potential comparing to other crops. Energy potential of cup plant biomass is about 300 GJ ha^{-1} that is equal to about 10 t of fuel equivalent.

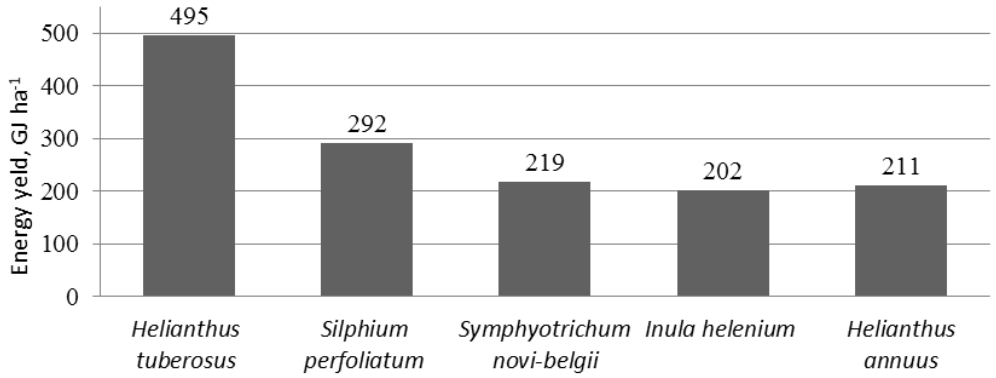

Figure 2. Maximum energy potential of studied plants from the family *Asteraceae*.

Theoretical energy yield of Jerusalem artichoke is approaching the maximum energy yield of *Miscanthus x giganteus*, which belongs to the top energy crop across the Europe. According to Havrland et al. (2013) the energy yield of *Miscanthus x giganteus* is around 531.9 GJ ha^{-1}. In comparison, the energy yield of Jerusalem artichoke is higher than the energy yield of some energy crops like giant reed (*Arundo donax* L.) – 451.6 GJ ha^{-1}, giant knotweed *(Reynoutria x bohemica)* – 387.7 GJ ha^{-1} and *Miscanthus sinensis* – 362.8 GJ ha^{-1}.

The values of energy potentials of New York aster, elecampane and sunflower are seminar and are close to energy yield of annual hemp (*Cannabis sativa* L.) – 213.6 GJ ha^{-1} (Havrland et al., 2013).

The energy potential presented in the study is theoretical maximum energy potential of the crops. It means that losses (post-harvest and combustion losses) were not taken into account; they can vary between 30–50% (Prade et al., 2011).

All of the above mentioned plants were grown under natural conditions without additional inputs in the form of fertilizers, irrigation, etc. It may be expected that some additional inputs will increase biomass yield and subsequently total energy potential of the plant.

CONCLUSIONS

Summarizing the results of calorific values, ash content and energy potential of selected crops, it can be concluded that crops from *Asteraceae* family have positive characteristics, which make them attractive raw materials for production of solid biofuels in the form of briquettes and pellets.

Conducted research demonstrated that Jerusalem artichoke is the most perspective energy crops among the tested plants due to the largest energy yield, followed by cup plant from the viewpoint of energy yield and New York aster with the highest calorific values and lowest ash content.

However for selection of energy crops it is also necessary to do calculations of energy and economical balances (inputs vs. outputs).

ACKNOWLEDGEMENTS. The study was supported by the Development project of Czech Republic Development Cooperation in Moldova (project SAUM) and by Internal Grant Agency of the Faculty of Tropical AgriSciences, Czech University of Life Sciences Prague (grant number 20155015).

REFERENCES

Energy strategy of the Republic of Moldova till 2030. 2013, MO N 27-30, st. N 146, 8.2.2013, pp. 32–62. (in Russian).

Halford, N.G. & Karp, A. 2010. *Energy Crops.* Royal Society of Chemistry. 442 pp.

Havrland, B., Ivanova, T., Lapczynska-Kordon, B. & Kolarikova, M. 2013. Comparative analysis of bio-raw materials and biofuels. *Engineering for Rural Development. 12th International Scientific Conference*, Latvia University of Agriculture, Jelgava, Latvia, pp. 541–544.

Hutla, P. 2010. Solid biofuels from local sources [online]. Available at www: http://biom.cz/cz/odborne-clanky/tuha-biopaliva-z-mistnich-zdroju (accessed 15 April 2013) (in Czech).

Jevič, P., Hutla, P. & Šedivá, Z. 2008. *Sustainable production and quality management of solid fuels based on agricultural bioproducts: Factors affecting the quality of solid biofuels and potential of biomass and biofuels.* VÚZT, Mze ČR, Praha, 124 pp. (in Czech).

Kim, H.J., Lu, G.Q., Naruse, I., Yuan, J. & Ohtake, K. 2000. Modeling on Combustion Characteristics of Biocoalbriquette. *Energy Resources and Technology* **123**(1), 27–31.

Kolarikova, M., Ivanova, T., Havrland, B. & Amonov, K. 2014. Evaluation of sustainability aspect – energy balance of briquettes made of hemp biomass cultivated in Moldova. *Agronomy Research* **12**(2), 519–3526.

Kotlánová, A. 2010. Methods of testing the physic-chemical properties of solid biofuels [online]. Available at http://biom.cz/cz/odborne-clanky/metody-zkouseni-fyzikalne-chemickych-vlastnosti-tuhych-biopaliv (accessed 7 March 2014) (in Czech).

Marian, Gr., Shirakawa, Y., Muntean, A., Gudima, A. & Druceoc, S. 2013. Estimating the calorific value of lignocellulosic biomass from different zones of the Republic of Moldova in the concept of solid fuel production. *Ştiinţa Agricolă* **1**, 97–104 (in Moldovan).

Prade, T., Svensson, S.E., Andersson, A. & Mattsson, J.E. 2011. Biomass and energy yield of industrial hemp grown for biogas and solid fuel. *Biomass and bioenergy* **35**(7), 3040–3049.

Shtar, D., Rakhmetov, D., Adam, A. (eds). 2006. *Renewable vegetable raw materials. Production and use.* Sankt-Peterburg-Pushkin, Book 1: 416 pp; Book 2: 382 pp. (In Russian).

Teleuta, A. & Titei, V. 2012. Species of Galega orientalis, Polygonum sachalinense, Silphium perfoliatum and their agrobiological pecularities in Republic Moldova's conditions. *Acta Horti Bot. Bucurest.* **39**, 95–100.

Teleuta, A., Titei, V. & Muntean, A. 2012. Species of new plants for producing biofuels in Moldova. *Conservation of plant diversity*. Ed. 2-a. Chisinau, pp. 396–403.

Titei, V., Teleuta, A. 2011. Introduction and cultivation perspective of energy plant in the Republic of Moldova. *Conservation of plant diversity in situ and ex situ*. Iaşi, pp. 56–57.

Agronomy Research **13**(2), 318–327, 2015

Lipid production from diverse oleaginous yeasts from steam exploded corn cobs

H. Kahr, M. Pointner, K. Krennhuber, B. Wallner and A. Jäger*

University of Applied Sciences Upper Austria, School of Engineering and Environmental Sciences, Stelzhamerstraße 23, 4600 Wels, Austria
*Correspondence: Heike.Kahr@fh-wels.at

Abstract. Corn cob hydrolysate was used as substrate for growth and lipid accumulation via oleaginous yeast species. A mass based suspension of 10 g 100 g^{-1} corn cob hydrolysate contained 26.0 g L^{-1} glucose, 8.5 g L^{-1} xylose. The inhibitor concentrations were 0.16 g L^{-1} acetic acid, 1.50 g L^{-1} formic acid, 0.48 g L^{-1} HMF and 0.06 g L^{-1} furfural. These conditions reduced the cell growth of non-adapted yeast. Successful adaptation of the tested yeasts over several generations in corn cob hydrolysate was performed. The adapted yeast *Candida lipolytica* produced 19.4 g 100 g^{-1} lipids in relation to the dry weight in 7.5 g 100 g^{-1} dry matter corn cob hydrolysate in fed batch mode. The scale up was done up to a volume of 2.5 litres – here lipid accumulation up to 17.5 g 100 g^{-1} was demonstrated with the quantitative GC/FID analyses. Predominantly oleic acid, palmitic acid, linoleic and palmitoleic acid were produced. This lipid spectrum is suitable for biodiesel production.

Key words: biodiesel, oleaginous yeast, corn cobs.

INTRODUCTION

Transportation is the largest energy consuming sector in Austria (BMWFW, 2014). Alternative to fossil fuels are needed because of climate change, energy security and the depletion of fossil fuels. Conventional biodiesel is produced from edible plant oils (mainly rapeseed in Austria), non-edible plants and waste oils and is therefore renewable and sustainable. The rising cost of the edible plant oils and the food versus fuel discussion intensify the development of alternative technologies.

Next generation biodiesel technology utilises lipid accumulating microorganisms like microalgae, bacteria, yeasts and fungi. These microorganisms produce and store lipids intracellular up to 70 g 100 g^{-1} of biomass. At specific culture conditions the oleaginous yeasts convert diverse competitive substrates like sugars from lignocellulose or glycerol to lipids. These lipids can be used as feedstock for biodiesel production. However the specific culture conditions (C/N ratio, temperature, pH value, aeration, cultivation mode) of each oleaginous yeast species vary and must be determined. The oleaginous yeasts have several advantages: yeast is a well-known organism, the cultivation is simple and low-cost, year-round production of yeasts respectively lipids (assumed available year-round substrate) on land unsuitable for agriculture is practicable. About 70 yeast species accumulated lipid efficiently under specific conditions - often an excess of carbon and nitrogen depletion (reviewed in Li et al., 2008;

Meng et al., 2009; Subramaniam et al., 2010; Huang et al., 2013a; Thevenieau & Nicaud; 2013, Sitepu et al., 2014a).

Several reports of conversion of various lignocellulosic hydrolysates to lipid via oleaginous yeasts exit. The ability for lipid accumulation of different *Trichosporon* species was tested mainly in acid corn cob hydrolysate. The lipid content in these studies ranged from 32% up to 47% and the biomass from 20 g L^{-1} up to 38 g L^{-1} (Chen et al., 2012; Huang et al., 2012a; Chang et al., 2013; Huang et al., 2013b; Huang et al., 2014).

One aspect particularly effects the lipid production via oleaginous yeasts – in dependency of the used pretreatment method diverse inhibitors at different concentrations are released during this process (reviewed in Kumar et al., 2009: Alvira et al., 2010). These substances inhibit the cell growth and subsequent lipid accumulation of oleaginous yeasts. Altogether few studies about the effects of inhibitors on cell growth and subsequent lipid accumulation are available (Chen et al., 2009; Huang et al., 2012b; Jönsson et al., 2013; Sitepu e et al., 2014b). The conditions for cell growth and subsequent lipid accumulation must be determined for each substrate and each yeast species. Often extensive detoxification methods were performed to reduce the inhibitor concentration or adapted or inhibitor resistant yeast species were used (Parawira & Tekere, 2011).

For the first time, the ability of two oleaginous yeast species *Candida lipolytica* and *Yarrowia lipolytica* to produced lipids in steam exploded, enzymatically hydrolysed corn cob hydrolysate was explored. No extra nitrogen source was added to reduce the cost of the lipid production. Furthermore the influence of the inhibitors on cell growth of non-adapted and adapted yeasts was tested. The practicability of an industrial lipid production via oleaginous yeast was tested with scaled up experiments.

MATERIALS AND METHODS

Corn cobs hydrolysate preparation

A mixture of air dried corn cobs (*Zea mays*) was collected from local producers in Austria and chopped up by a garden shredder (Viking GE 260, Kufstein, Austria) in pieces of 2–3 cm length. The pretreatment was performed with the steam explosion unit (Voest Alpine Montage, Wels, Austria) at optimal condition (200 °C, 10 minutes) to achieve high sugar and low inhibitor concentrations. The steam explosion pretreatment unit was already described (Eisenhuber et al., 2013). The pretreated corn cobs were dried at 40 °C to a moisture content of about 70 g 100 g^{-1}. Different dry matter contents were used for hydrolysis: 7.5 g 100 g^{-1} and 10 g 100 g^{-1} in citrate buffer (c = 50 mmol L^{-1}; pH 5; adjusted with NaOH, c = 4 mol L^{-1}). The enzyme mixture Accellerase 1500 from DuPont™Genencor® was used for hydrolysis at 30 FPU g^{-1} cellulose. Hydrolysis was performed at 50 °C for 96 hours in a shaking incubator (speed 2.5 s^{-1}). The corn cob hydrolysate was filtered with a Büchner funnel (filter paper MN 640 m). The sugar and inhibitor concentration of the liquid was determined with HPLC. The liquid was used for medium preparation.

Microorganism, media, precultivation, cultivation and scale up

The cell growth and lipid accumulation of two yeast species *Candida lipolytica* and *Yarrowia lipolytica* (kindly provided from the strain collection from the company Agrana (http://www.agrana.at/) were investigated in this study.

The precultivation was done with yeasts adapted over many generations in corn cobs hydrolysate medium (liquid filtered after hydrolysis plus 1.5 g L^{-1} yeast extract, 3 g L^{-1} peptone from casein, 2 g L^{-1} potassium dihydrogen phosphate, 1 g L^{-1} ammonium sulphate, 0.5 g L^{-1} magnesium sulphate heptahydrate, pH 6, sterile filtered) or YGC medium (5 g L^{-1} yeast extract, 20 g L^{-1} glucose, autoclaved at 121 °C for 20 minutes) with inhibitor (at different concentrations ranging 0.5 g L^{-1} up to 3.5 g L^{-1}). These yeasts were incubated for 12 hours at 25 °C or 30 °C in a shaking incubator (110 rpm). Ten percent preculture (v v^{-1}) was inoculated to corn cob hydrolysate medium without added chemicals. The samples were incubated at 25 °C or 30 °C for 7 days at 180 rpm in small scale (50 ml, no pH and no aeration control). The samples were centrifuged and resuspended in fresh corn cob hydrolysate medium without additional chemicals for fed batch mode. Samples were taken periodically for HPLC and GC analyses. The scale up was performed in Biostat C2 fermenter (Sartorius, Germany) with constant pH value 5.5, temperature 30 °C, 300 rpm, dragging air 2 litres min^{-1}) in batch or fed batch mode.

Testing the influence of inhibitors on cell growth

The precultivation was done in YPC medium with non-adapted or adapted yeasts. Ten percent preculture (v v^{-1}) was inoculated to YGC medium containing different inhibitors (acids and furans) at variable concentrations and incubated to a maximum of 48 hours at 30 °C at 110 rpm. Optical measurements at 600 nm with Spectrophotometer XION 500 (Hach Lange, Germany) were used to determine the cell growth and the influence of each inhibitor on cell growth.

Transmethylation and GC-FID analysis

For the analytical quantification of the fatty acid content and distribution, 5 mL yeast suspension was centrifuged at a rotational speed of 4,000 min^{-1}.The yeast pellet was washed once with 5 mL of deionized water and dried at 105 °C for 24 hours. The dry matter was resuspended and methylated with 5 mL of methanol/acetyl chloride with a volumetric dilution of 50:2 for 24 hours at 60 °C. Afterwards, the reaction was stopped by slowly adding 2.5 mL of a sodium carbonate solution with a concentration of 60 g L^{-1}. The resulting fatty acid methyl esters were extracted by adding 2 mL of hexane and shaking for 2 minutes. One mL of the upper phase, containing the methyl esters, was transferred in a 1.5 mL crimp vial and stored at -18 °C until measurement.

The hexane extract was injected in a Thermo Trace GC equipped with an autosampler AS 2000. The detection was carried out with a FID. The chromatographic conditions were the following: The injection volume was 2 µL, the injector temperature was set at 240 °C. Helium was used as carrier with 120 kPa constant pressure and a split flow at 30 mL min^{-1}. An Agilent J&W capillary column DB23 60 m, 0.25 mm ID and 0.25 µm film thickness was used for analytical separation. The oven temperature gradient was the following: 0–3 min 130 °C; 6.5 °C min^{-1} to 170 °C. 2.8 °C min^{-1} to 214 °C held 12 minutes. 3 °C min^{-1} to 240 °C held for 15 minutes. The FID was set at a temperature of 280 °C, 450 mL min^{-1} air flow, 45 mL min^{-1} hydrogen flow and nitrogen as make up gas at 40 mL min^{-1} were the torch conditions.

The data analysis was performed with the software Chrom Card Data System Ver. 2.8 from Thermo Finnigan. For calibration the external standard method has been used.

HPLC soluble contents

To determine the contents of sugars and inhibitors 1 mL of homogeneous yeast suspension was transferred into a 1.7 mL centrifugation tube and centrifuged for 5 minutes at an rotational speed of 13,000 min^{-1}. One mL clear supernant was transferred into a 1.7 mL screw cap vial and stored at -18 °C until measurement.

Saccharides and inhibitors were quantified by HPLC, using an Agilent Technologies 1200 Series equipped with a Varian Metacarb 87 H column (300 x 7.8 mm) at 65 °C, H_2SO_4 (c = 5 mmol L^{-1}) eluent and an isocratic flow rate of 0.8 mL min^{-1} was used. The data acquisition was performed per refractive index detection and UV–detection at 210 nm. For calibration the method of external standard was applied. Data analysis was performed per Agilent Chemstation 04.03 b.

Determination of nitrogen with Dumatherm

Nitrogen was determined according to the Dumas method with a Dumatherm analyzer 7700 (Gerhardt GmbH & Co. KG, Königswinter, Germany, Dumas, 1831).

Determination of acquired yeast biomass

One mL of homogeneous yeast suspension was transferred into a 1.7 mL centrifugation tube and centrifuged for 5 minutes at an rotational speed of 13,000 min^{-1}. The clear upper phase was dismissed and the pellet was washed twice with 1 mL deionized water. The pellet was spilled quantitatively on a weighed aluminum pan with about 2–3 mL deionized water and dried for 2 hours at 105 °C in a drying closet. The difference in weight is the biomass content of 1 mL suspension.

RESULTS AND DISCUSSION

Corn cobs hydrolysate at different temperatures

The corn cobs mixture was pretreated with steam explosion at 200 °C for 10 minutes to achieve the optimal sugar – inhibitors relationship, dried and hydrolysed via enzyme at 7.5 g 100 g^{-1} or 10 g 100 g^{-1} dry matter. HPLC analyses after hydrolysis were shown in Table 1. After hydrolysis 26.0 g L^{-1} glucose, 8.5 g L^{-1} xylose, 1.50 g L^{-1} acetic acid, 0.16 g L^{-1} formic acid, 0.48 g L^{-1} HMF (= 5-hydroxymethyl-2-furaldehyde) and 0.06 g L^{-1} furfural were detected within 10g 100g^{-1} corn cob hydrolysate (see Table 1). The hydrolysate at 7.5 10 g^{-1} dry matter contained lower concentration of each substances (see Table 1).

Table 1. HPLC results from steam exploded corn cobs after hydrolysis with 7.5 g 100 g^{-1} or 10 g 100 g^{-1} dry matter. Values of sugars and inhibitors in (g L^{-1}). Standard deviations varied between 0.01 and 0.04

Sample (g 100 g^{-1})	Glucose	Xylose	Formic acid	Acetic acid	HMF	Furfural
7.5	22	7.5	0.11	1.1	0.35	0.04
10	26	8.5	0.16	1.5	0.48	0.06

In other lipid production studies corn cobs were typically pretreated with acid – resulting in similar inhibitor concentrations but other sugar concentrations (Chen et al., 2012). No deeper study about steam exploded, enzymatically hydrolysed corn cobs exists and therefore no direct comparison is feasible.

Influence of the inhibitors on cell growth

The composition of the used corn cob hydrolysate was complex. Diverse substances within the corn cob hydrolysate inhibited the cell growth and lipid accumulation (Chen et al., 2009; Huang et al., 2012b; Jönsson et al., 2013; Sitepu et al., 2014b). Therefore the cell growth and the tolerance of the yeast to the different inhibitors were tested in synthetic medium. Different concentrations of acetic and formic acid were added alone or in combination to the YGC medium ranging from 1 up to 3 g L^{-1}. Purposely higher concentrations of the inhibitors were chosen to cover the higher inhibitor concentrations detected in hydrolysate from wet steam exploded corn cobs. The results were shown in Table 2.

Table 2. Optical density (= OD) at 600 nm from the non-adapted and adapted yeast *Candida lipolytica* after incubation in the presence of acetic and formic acid. Values of acids in (g L^{-1}). Standard deviations varied between 0.01 and 0.04.

	Acetic acid	Formic acid	$OD_{600\ nm}$
Non-adapted	-	-	17
	1	1	17
	2	2	0
		2	0
	3		13
Adapted	-	-	9
	1	1	8
	2	2	6
	3	3	0
	3		8
		3	6

The adapted *Candida lipolytica* grew slower than the non-adapted yeast. Non-adapted *Candida lipolytica* tolerated the combination of 1 g L^{-1} of acetic and formic acid. Two g L^{-1} formic acid inhibited total the cell growth whereas 3 g L^{-1} acetic acid slightly reduced the cell growth. Overall the adapted *Candida lipolytica* was more tolerant – only the combination of 3 g L^{-1} of acetic and formic acid prohibited the cell growth (see Table 2). The same approach with *Yarrowia lipolytica* revealed the same effects (data not shown).

The cell growth of non-adapted *Candida lipolytica* and *Yarrowia lipolytica* was tested in the presence of the inhibitors furfural and HMF. Unfortunately no furfural and/or HMF adapted yeast existed at the time. Furfural was investigated in the range of 0.5 to 1.4 g $L^{-1}$and 5-HMF 1 to 4 g L^{-1}. The optical density of the samples after 48 hours incubation was shown in Table 3.

Table 3. Optical density (= OD) at 600 nm from the non-adapted yeast *Candida lipolytica* after incubation in the presence of furfural and HMF. Values of furfural und HMF in (g L^{-1}). Standard deviations varied between 0.01 and 0.04

	Furfural	HMF	$OD_{600\ nm}$
Candida lipolytica	-	-	12
	1		0
		0.5	12
		1.6	17
	1	0.5	0

HMF did not inhibit the cell growth even at higher concentration but 1 g L^{-1} furfural together with 0.5 g L^{-1} HMF prohibited the cell growth. The same experiments with *Yarrowia lipolytica* revealed the same effect (data not shown).

Few studies exist about the effects of inhibitors on cell growth and subsequent lipid accumulation. These studies revealed similar effects – *Cryptococcus curvatus* was also more sensitive to furfural than HMF, another study with *Yarrowia lipolytica* reported similar results. For example, *Trichosporon fermentans* tolerated relative high concentrations acetic and formic acid (Chen et al., 2009; Yu et al., 2011; Huang et al., 2012b; Sitepu et al., 2014b). However each yeast species differs in tolerance of inhibitors and must be tested.

The cell growth of non-adapted and adapted yeasts was also tested at the inhibitor concentrations of the corn cob hydrolysates. The cell growth of non-adapted yeast was reduced at tested inhibitor concentrations. The adapted *Candida lipolytica* tolerated the inhibitors very well (data not shown). Adapted yeasts in corn cob hydrolysates were used in the subsequent approaches. The inhibitors were partially utilised via the yeast (data not shown).

Corn cob hydrolysate as substrate for lipid production

Initial experiments were performed unsuccessful in corn cob hydrolysate with additional nitrogen sources (yeast extract and peptone). Nitrogen determination was done from corn cob hydrolysate with Dumatherm – 10 g 100 g^{-1} dry matter corn cob hydrolysate contained 0.045 g total nitrogen per 100 g^{-1} biomass – enough nitrogen for cell growth. Therefore no external nitrogen was added to the corn cob hydrolysate in the subsequent experiments. Adapted yeast was tested in corn cob hydrolysate with fed batch mode. Fresh corn cob hydrolysate was added after seven days and fermentation was undertaken for further seven days. The lipid contents and cell biomass were shown in Table 4.

Candida lipolytica accumulated the highest lipid content (19.4 g 100 g^{-1}) in corn cob hydrolysate at 30 °C. *Yarrowia lipolytica* reached lipid contents similar to non-oleaginous yeasts. Fed batch experiment with 10 g 100 g^{-1} dry matter corn cob hydrolysate resulted in lipid content ranging from 4.5 g 100 g^{-1} to 8 g 100 g^{-1} (data not shown). Obviously the inhibitors within the corn cob hydrolysate did not interfere with the cell growth but with the lipid accumulation.

Table 4. Lipid content and cell biomass of the two yeast species in corn cob hydrolysate (fed batch mode, 7.5 g 100g^{-1} dry matter)

Yeast species	Dry matter (g 100 g^{-1})	Lipid content in medium (mg L^{-1})	Lipid content (g 100 g^{-1})
C. lipolytica 25 °C	1.3	1470	11.3
***C. lipolytica* 30 °C**	**0.83**	**1600**	**19.4**
Y. lipolytica 25 °C	1.27	1430	11.3
Y. lipolytica 30 °C	1.72	1600	9.3

Several studies about lipid accumulation were performed with corn cobs as substrate. The used yeast species produced higher lipid contents but in contrast to this study the total yeast lipids were extracted according the procedures described by Folch et al. (1957). The different extraction method or the use of other yeast species may explain the lower lipid content in this study. No studies about steam exploded corn cobs as substrate for lipid production via oleaginous yeasts existed. A direct comparison was therefore not possible.

Scale up experiments

Scale up to 2.5 litres in fermenter was done with the yeast *Candida lipolytica* to test the industrial scale of lipid production via yeast. The lipid content (gray bars) of the yeast *Candida lipolytica* in corn cob hydrolysate increased from 2.6 g 100 g^{-1} after 24 hours up to 17.5 g 100 g^{-1} after 168 hours incubation then the lipid content decreased due to depletion of the carbon source (black bars) (see Fig. 1). At the beginning 7.5 g 100 g^{-1} corn cob hydrolysate contained about 29 g L^{-1} total sugar (glucose plus xylose).

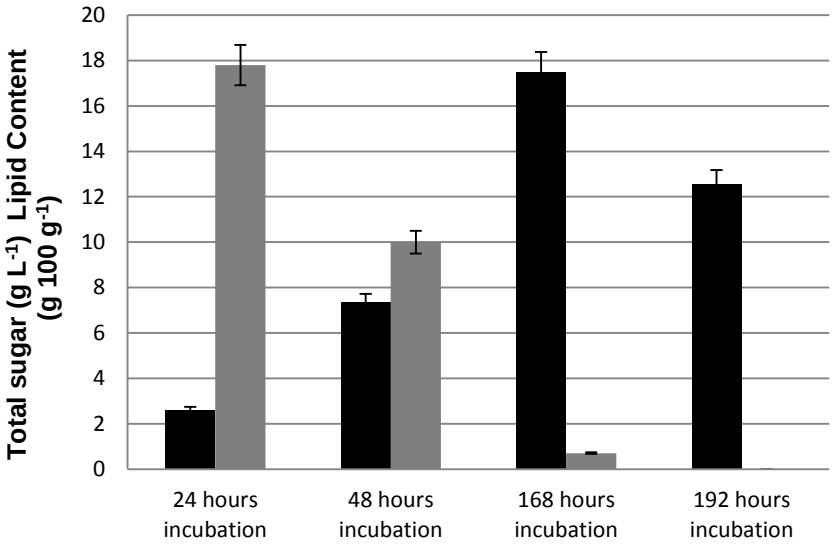

Figure 1. Lipid content (g 100 g^{-1}) and total sugar (g L^{-1}) of the yeast *Candida lipolytica* in corn cob hydrolysate during incubation time in fermenter.

More or less the same lipid content as before was achieved in fermenter with exact cultivation conditions – 17.5 g 100 g^{-1} lipid content in shorter time (7 days) in batch mode. Lower lipid content was reached with fed batch mode in fermenter (maximum 14.23 g 100 g^{-1}; data not shown). Other scale up experiments in corn cob hydrolysate were not reported in diverse studies (Chen et al., 2012; Huang et al., 2012a; Chang et al., 2013; Huang et al., 2013b; Huang et al., 2014).

The composition of the lipids produced in the scale up experiment was mainly palmitic acid, palmitoleic acid, stearic acid, oleic acid and linoleic acid which is suitable for biodiesel production. The values of these acids increased during the incubation time (see Table 5). The same acids were also detected in the other studies with corn cob hydrolysate (Chen et al., 2012; Huang et al., 2012a; Chang et al., 2013; Huang et al., 2013b; Huang et al., 2014).

Table 5. Values of the mainly produced acids in the scale up experiment during the incubation time. Values in (mg L^{-1})

Time	Palmitic acid	Palmitoleic acid	Stearic acid	Oleic acid	Linoleic acid
24 hours	39	12	0	113	51
48 hours	226	53	34	598	143
168 hours	624	188	81	1100	329
192 hours	708	279	120	1038	440

The lipid production increased during the incubation time however this experiment was discontinued due to the substrate depletion. In summary, steam exploded, enzymatically hydrolysed corn cobs will be a potential substrate for microbial lipid production due its availability.

CONCLUSIONS

Hydrolysate from steam exploded corn cobs was successfully used as substrate for lipid accumulation with specific oleaginous yeasts. Meanwhile hydrolysate from lignocellulose are produced competitive and is used as substrate for second generation bioethanol production replacing petrol (Forth International Conference on Lignocellulosic Ethanol, Straubing, 2014). Conventional biodiesel must be completed or replaced like bioethanol first generation production. Therefore my and several working group and companies worked worldwide with specific oleaginous microorganisms, often with yeasts due their numerous advantages.

Our results are lower than reported from other studies and differed probable due to the different extraction method or used yeast species. The corn cob hydrolysate mixture was complex, maybe further unknown inhibitors prevented higher lipid accumulation. Further studies concerning this issue will be done.

At the moment excessive costs prevent marketability of biodiesel from oleaginous yeast. However an economical process requires - an oleaginous yeast species which is tolerant to inhibitors and osmotolerant, grows fast and exhibits high oil accumulation; year-round available and competitive substrate; competitive extraction method and economic coproducts.

ACKNOWLEDGEMENTS. The project 'Next Generation Biodiesel' (Project-Code: DAABAA_00565) was financed within the scope of the European Union Program 'Regionale Wettbewerbsfahigkeit OO 2007–2013 (Regio 13)' from the purse of the European Funds for Regional Development (EFRE) and the Federal State of Upper Austria, Austria.

REFERENCES

Alvira, P., Tomás-Pejó, E., Ballesteros, M. & Negro, MJ. 2010. Pretreatment technologies for an efficient bioethanol production process based on enzymatic hydrolysis: A review. Bioresource Technology **101**, 4851–4861.

BMWFW, 2014. http://www.bmwfw.gv.at/EnergieUndBergbau/Energieeffizienz/ Publishing Images/Energiestatus%20%C3%96sterreich%202014_HP-Version.pdf. Accessed 19.1. 2015.

Chang, YH., Chang, KS., Hsu, CL., Chuang, LT., Chen, CY., Huang, FY. & Jang, HD. 2013. A comparative study on batch and fed-batch cultures of oleaginous yeast *Cryptococcus sp.* in glucose-based media and corncob hydrolysate for microbial oil production. Fuel **105**, 711–717.

Chen, X., Li, Z., Zhang, X., Hu, F., Ryu, DDY & Bao, J. 2009. Sreening of oleaginous yeast strains tolerant to lignocellulose degradation compounds. *Applied Biochemistry and Biotechnology* **159**, 591–604.

Chen, XF., Huang, C., Xiong, L., Chen, XD. & Ma, LL. 2012. Microbial oil production from corncob acid hydrolysate by *Trichosporon cutaneum*. Biotechnology Letters **34**, 1025–1028.

Dumas, JBA., 1831, Procedes de l'Analyse Organique, Annales de Chimie et de Physique **247**, 198–213.

Eisenhuber, K., Jäger, A., Kahr, H. & Wimberger, J. 2013. Comparison of different pretreatment methods for straw for lignocellulosic bioethanol production. *Agronomy Research* **11**, 173–182.

Folch, J., Lees, M. & Sloane-Stanley, GH. 1957. A simple method for the isolation and purification of total lipids from animal cells. *Journal Biological and Chemistry* **226**, 497–509.

Huang, C., Chen, XF., Xiong, L., Chen, XD. & Ma, LL. 2012a. Oil production by the yeast *Trichosporon dermatis* cultured in enzymatic hydrolysates of corncobs. Bioresource Technology **110**, 711–714.

Huang, C., Wu, H., Liu, ZJ., Cai, J., Lou, WY. & Zhong, MH. 2012b. Effect of organic acids on the growth and lipid accumulation of oleaginous yeast *Trichosporon fermentans*. Biotechnology for Biofuels **5**:4.

Huang, C., Chen, XF., Xiong, L., Chen, XD., Ma, LL. & Chen, Y. 2013a. Single cell oil production from low-cost substrates: The possibility and potential of its industrialization. Biotechnology Advances **31**, 129–139.

Huang, C., Chen, XF., Xiong, L., Yang, XY., Chen, XD., Ma, LL. & Chen, Y. 2013b. Microbial oil production from corncob acid hydrolysate by oleaginous yeast *Trichosporon coremiiforme*. Biomass and Bioenergy **49**, 273–278.

Huang, C., Chen, XF., Yang, XY., Xiong, L., Lin, XQ., Yang, J., Wang, B. & Chen, XD. 2014. Bioconversion of corncob hydrolysate into microbial oil by the oleaginous yeast *Lipomyces starkeyi*. Applied Biochemistry and Biotechnology **172**, 2197–2204.

Jönsson, LF. Alriksson, B. & Nilvebrant, NO. 2013. Bioconversion of lignocellulose: inhibitors and detoxification. Biotechnology for Biofuel **6**:16.

Kumar, P., Barrett, DM., Delwiche, MJ. & Stroeve, P. 2009. Methods for pretreatment biomass for efficient hydrolysis and biofuel production. Industrial & Engineering Chemistry Research **48**(8), 3713–3729.

Meng, X., Yang, J., Xu, X., Zhang, L., Nie, Q & Xian, M. 2009. Biodiesel production from oleaginous microorganisms. *Renewable Energy* **34**, 1–5.

Li, Q., Du, W. & Liu, D. 2008. Perspectives of microbial oils for biodiesel production. *Applied Microbiology and Biotechnology* **80**, 749–756.

Parawira, W. & Tekere, M. 2011. Biotechnological strategies to overcome inhibitors in lignocellulose hydrolysates for ethanol production: review. Critical Reviews in Biotechnology **31,** 20–31.

Sitepu, IR, Garay, LA., Sestric, R., Levin, D., Block, DE., German, JB. & Boundy-Mills, KL. 2014a. Oleaginous yeasts for biodiesel: Current and future trends in biology and production. Biotechnology Advances **32**, 1336–1360.

Sitepu, IR., Selby, T., Lin, T., Zhu, S. & Boundy-Mills, KL. 2014b. Carbon source utilization and inhibitor tolerance of 45 oleaginous yeast species. *Journal of Industrial Microbiology & Biotechnology* **41**, 1061–1070.

Subramaniam, R, Dufreche, MZ, Zappi, M. & Bajpai, R. 2010. Microbial lipids from renewable resources: production and characterization. *Journal of Industrial Microbiology & Biotechnology* **37**, 1271–1287.

Sun, Y. & Cheng, Y. 2002. Hydrolysis of lignocellulosic materials for ethanol production: a review. Bioresource Technology **83**, 1–11.

Thevenieau, F & Nicaud, JM. 2013. Microorganisms as sources of oils. **O**ilseeds & fats **C**rops and Lipids **20**(6) D603.

Yu, X, Zheng, Y., Dorgan, KM & Chen, S. 2011. Oil production by oleaginous yeasts using the hydrolysate from pretreatment of wheat straw with dilute sulfuric acid. Bioresource Technology **102**, 6134–6140.

Agronomy Research **13**(2), 328–336, 2015

Economic evaluation of hemp (Cannabis sativa) grown for energy purposes (briquettes) in the Czech Republic

M. Kolarikova[1,2], T. Ivanova[1,*], P. Hutla[2] and B. Havrland[1]

[1]Czech University of Life Sciences, Faculty of Tropics and Subtropics, Department of Sustainable Technologies, Kamycka 129, CZ16521 Prague 6, Czech Republic
[2]Research Institute of Agricultural Engineering, p.r.i., Drnovska 509, CZ16100 Prague 6, Czech Republic
[*]Correspondence: ivanova@ftz.czu.cz

Abstract. Depletion of fossil fuels and their environmental risks have brought to the foreground energy crops as a possible source of bioenergy. Industrial hemp (*Cannabis sativa* L.) has been suggested for production of solid biofuels (briquettes) due to good physic-mechanical properties as well as positive energy and combustion characteristics. This study determined economic potential of hemp briquettes production in the Czech Republic. A field trial was conducted in 2009–2014 in Prague in order to compare biomass yield (BY) of hemp varieties Bialobrzeskie (B) and Ferimon (F) harvested in autumn and spring period. Based on obtained results this study determined production costs of hemp briquettes (CZK t^{-1}), revenue (CZK t^{-1}) and rate of return (%) for four scenarios (B, F harvested in autumn and B, F harvested in spring). Briquettes production costs ranged from 4,015 CZK t^{-1} to 4,707 CZK t^{-1} for B in spring and B in autumn, respectively, due to 30% lower biomass yield in spring harvest. Results indicated that hemp briquettes production was not profitable if the selling price was the same as the price of wood briquettes and with BY obtained in experiment (7.18–10.7 t ha^{-1} of dry matter). Briquettes production in autumn made profit of 9% for B and 7% for F when subsidies for hemp cultivation were considered. In current conditions in the Czech Republic, utilization of hemp for briquettes production did not prove to be economically feasible.

Key words: hemp briquettes, economic analysis, production costs, revenue, rate of return.

INTRODUCTION

Energy is one of the most important commodities in today's world to ensure socio economic development of the country. Due to permanently decreasing reserves of conventional fossil fuels and their high environmental risks, countries have been looking for alternative sources of energy (Rehman et al., 2013). High potential lies in herbaceous biomass which has been on rise in recent years. To determine crops which are the most suitable for energy production, its energy characteristics, ecological impact and production economy must be investigated thoroughly.

Based on results of long term research and practical experience in the Czech Republic and foreign countries, industrial hemp (*Cannabis sativa* L.*)* has appeared to be promising energy crop in conditions of Central and Northern Europe (Honzík et al, 2012). Industrial hemp has been suggested by various researchers for production of biodiesel (Rehman et al., 2013), bioethanol (Tutt, 2011), biogas (Prade et al., 2011) and

also briquettes (Mankowski & Kolodzej, 2008) for household heating. Uniqueness of hemp consists in its ability to yield about 10–15 t ha^{-1} in 100–120 days which is more than other energy crops (Kolarikova et al., 2014). Hemp has proved positive energy balance (Prade et al., 2011) and combustion properties which are comparable to woody materials (Mankowski & Kolodzej, 2013). Furthermore, it showed to be suitable for crop rotation due to its phytoremediation characteristics.

Since various energy crops with very similar or even better characteristics exist, production costs may play significant role in decision of producer which crop to cultivate. Until now many publications regarding hemp cultivation for various purposes have been published, however, any of them included detailed manual for evaluation of economy of hemp briquettes production.

The main objective of this contribution is to calculate production costs, revenues and profitability of hemp briquettes comparing two varieties of *Cannabis sativa* L. (Bialobrzeskie, Ferimon) harvested in autumn and spring seasons in conditions of the Czech Republic.

MATERIALS AND METHODS

Biomass yield (BY)

A variety of hemp of Polish origin Bialobrzeskie and French Ferimon were cultivated in Prague in 2009–2013 (5 independent seasons) in order to obtain biomass for the energy yield evaluation from its autumn and spring harvests. Hemp was grown on a trial plot of 100 m^2 (50 m^2 each) with seed rate of 60 kg ha^{-1} and the biomass yields of the small-scale plots (determined by collecting and weighing all plants) were extrapolated to a biomass yield per hectare (BY). The average values over the observation period were considered for the calculation of economic balance.

Technological process of hemp briquette product

Economic analysis was calculated for large – scale utilization, therefore technological process included all necessary operations (fertilizing, tillage, hauling, soil preparation, sowing, mowing, compressing and transport and field treatment after harvest). For hemp processing into solid biofuel briquetting line comprised of separator RSM Turbo 180 and shredder STM 201 HL was considered. For pressing of the material briquetting device BrikStar 400 was used. Dry BY was recounted for moisture content (MC) 12% which was optimal for processing into solid biofuel. Loses during the separating and crushing were considered as 10%.

Economic inputs

Amount of material was taking into account as 60 kg of seeds per hectare for high biomass yield. For hemp grown for energy purposes it was considered 80 kg of pure nutrient of nitrogen, 45 kg of potassium chloride and 30 kg of phosphorus which was equal to 0.3 t of ammonium nitrate, 0.075 t of potassium salt and 0.17 t of superphosphate. Also 4.5 t of farmyard manure and 0.2t of limestone were considered. Hemp biomass was compressed into bales of 250 kg. For 1 bale 0.1 kg of string for fixing was considered. Briquettes were packed into 15 kg polyethylene (PE) bags. Prices of string and PE bags were assumed based on actual market prices.

Amount of labour and fuels was determined as a sum of labour requirements for component technological operations including hemp cultivation, harvesting and processing into briquettes. Work requirements and fuel consumption were based on average conditions of production. Average gross wage in agriculture accounted for 19,666 CZK per month of full time job. Average price per litre of diesel for final customer was 36.11 CZK l^{-1}. In compliance with regulation of Ministry of Agriculture 40% refund from consumer taxon diesel for farmers was in force for year 2013. Property insurance included natural disaster cover which was assumed to be 3% of total gross revenue.

To estimate depreciation of machines it was assumed that producer cultivated multiple crops not only hemp, thus machines were used in their full capacity. Machinery was bought in less than four years. It was supposed that producer cultivated hemp on rented land. Price represented average price for land in the Czech Republic in 2012. Costs for maintenance and reparation of machines and building as well as taxes and fees were assumed based on statistic of Czech Statistical Office. Producer owned all machines and performed all operations by himself, thus rent of machinery or services was not included. Overhead costs such as loan, leasing, etc. were not taken into consideration.

Total costs of briquettes production

Total costs (TC) of hemp briquettes production were calculated as a sum of fixed (FC) and variable costs (VC) (see formula 1, 2). Prices excluded value added tax (VAT 21%). Exchange rate of euro was taken into account as 25.97 CZK (average rate of Czech national bank for 2013).

$$TC = VC + FC \text{ (CZK ha}^{-1}\text{)} \quad (1)$$

where: TC – total costs; VC – variable costs; FC – fixed costs.

$$TC = (Cs + Cfe + Cst + Cbg + Cl + Cd + Ce + Cw + Ci) + (D + L + R + T) \text{ (CZK ha}^{-1}\text{)} \quad (2)$$

where: C – cost of: Cs – seeds; Cfe – fertilizers; Cst – string; Cbg – PE bags; Cl – human labour; Cd – diesel, Ce – electricity; Cw – water consumption; Ci – property insurance; D – depreciation of machines; L – land rent; R – reparation of machines and buildings; T – taxes and fees.

Price of labour per hour was determined from average month salary, increased by social insurance (25%) and health insurance (9%) divided by amount of working hours per month (160 hours). Price per litre of diesel was calculated from average price of fuel in 2013 decreased for refund of consumption tax (40% from 10.90 CZK).

Amount of string and PE bags was calculated based on formulas 3and 4:

$$Qs = \frac{\text{BY}}{\text{wtb}} \times \text{qs} \text{ (kg ha}^{-1}\text{)} \quad (3)$$

where: BY – biomass yield with MC 12% (t ha^{-1}); wtb – weight of bale (t); qs –quantity of string for bale (kg).

$$Qbg = \frac{\text{BYc}}{\text{wtbg}} \text{ (PE bags ha}^{-1}\text{)} \quad (4)$$

where: BYc – biomass yield with moisture content (MC) 12% including 10% loses during crushing (t ha^{-1}); wt_{bg} – weight of PE bag with briquettes (t).

Amount of electricity was calculated as electric input power of briquetting line multiplied by number of hours used for processing of 1t of material and amount of hemp biomass produced from 1ha of land (see formula 5).

$$Qe = qe * h * BY \text{ (kWh ha}^{-1}\text{)} \quad (5)$$

where: qe – input power(kW h^{-1}); h – working hours (h t^{-1}); BY – biomass yield with MC 12% (t ha^{-1}).

Cs–Ce were determined by multiplication of quantity of spent material and human labour (kg, ton, kg, PE bags, hour, l, kW) and price per single unit (CZK) (see formula 6). Prices of inputs are summarized in Table 1.

Table 1. Prices of inputs (CZK unit^{-1})

Item	Unit	Price per unit (CZK)	Source
Seeds			
Bialobrzeskie	kg	110	Agritec Sumperk (2013)
Ferimon	kg	155	
Fertilizers			
Limestone (50% CaO)	t	757	
Superphosphate (18% P_2O_2)	t	9,473	
Potassium chloride (60% K_2O)	t	10,360	Czech Statistical Office (2013)
Ammonium Nitrate (27,5% N)	t	6,604	
Farmyard manure	t	230	Own calculations
Fuel			
Diesel	1	24.6	
Electricity	kWh	2.62	Czech Statistical Office (2013)
Human labour	h	165	Own calculations (2013)
Land	ha	1,430	Ministry of Agriculture (2012)
Other material			
String	kg	60	Average market prices (2013)
PE bags	bag	1.5	

$$Cx = Qx * Px \text{ (CZK ha}^{-1}\text{)} \quad (6)$$

where: Qx – quantity of spent material or labour (kg, ton, hour, l, kW); Px – price per unit (CZK unit^{-1}).

Depreciation of machinery was calculated as a purchase price of machine divided by depreciation period of particular machine (6 years for agricultural machinery, 4 years for machines for chemical protection and fertilizing, 4 years for briquetting line) and by

recommended annual use and multiplied by hours used for production process (see formula 7).

$$D = \frac{pm \times h}{(n \times R)} \text{ (CZK ha}^{-1}\text{)} \quad (7)$$

where: Pm – purchase price of machine (CZK); n – depreciation period (years); R – recommended annual use (years); h – hours of use (h ha^{-1}).

Total revenue from briquettes production

Total revenue (TR) was determined by the quantity of hemp briquettes produced from 1 ha of land (t ha^{-1}) multiplied by respective price per ton of hemp briquettes (CZK t^{-1}) and decreased by VAT valid for 2013 – 21% (see formula 8).

$$TR = Qb * Pb * VAT \text{ (CZK ha}^{-1}\text{)} \quad (8)$$

where: *Qb* – quantity of briquettes (t ha^{-1}); *Pb* – price per unit (CZK t^{-1}); *VAT* – value added tax (21%).

Profit from briquettes production

Profit from production was calculated as total revenue minus total costs (see formula 9).

$$Pr = (TR - TC) \text{ (CZK ha}^{-1}\text{)} \quad (9)$$

where: TC – total costs (CZK ha^{-1}); TR – total revenue (CZK ha^{-1}).

Grants and Subsidies

Subsidies SAPS (Single area payment scheme) and TOP -UP were considered in the calculation. Others were not taking into account since they were not stable and change over time. In 2013 SAPS accounted for 6,069 CZK ha^{-1}. The most updated data stated complementary payment TOP-UP to be 491 CZK ha^{-1} in 2012.

RESULTS AND DISCUSSION

Hemp yield

In autumn harvests average of 22.1 t ha^{-1} of Bialobrzeskie was harvested with MC around 57%. Variety Ferimon yielded around 25.6 t ha^{-1} of green biomass with average moisture content 59.8% (see Table 1).

When harvested in spring, yield was significantly lower due to loses of leaves–with overage five years value reached 8.36 t ha^{-1} of Bialobrzeskie and 9.79 t ha^{-1} of Ferimon which accounts for loses about one quarter of yield for both varieties and corresponds to dry matter yield 7.2 and 8.2 t ha^{-1} for Bialobrzeskie and Ferimon, respectively (see Table 2).

Table 2. Biomass yield and dry matter yield for five years average

	Autumn		Spring	
	Bialobrzeskie	Ferimon	Bialobrzeskie	Ferimon
BY (t ha^{-1})	22.1	25.6	8.4	9.8
DM (t ha^{-1})	9.6	10.7	7.2	8.2

Total costs of briquettes production

Production of briquettes in autumn harvest cost 39,426 CZK ha^{-1} for B and 44,120 CZK ha^{-1} for F. Other direct costs took the highest share of TC for both scenarios including costs of fuels (21%, 20.2%), reparation of machines and buildings (7%, 6.2%), insurance against natural disasters (3.5% for both varieties), land rent (3.6%, 3.2%) and water (0.3% for both varieties), for B and F, respectively. Costs of material inputs (seeds, fertilizers and other material) accounted for 35% of TC.

TC for spring harvest were 34,566 CZK ha^{-1} and 39,116 CZK ha^{-1} for grown varieties B and F which lowered the sum by 12.3% and 11.3%, respectively in comparison with autumn harvest. Division of costs was very similar as in autumn harvest. Higher costs of briquettes production from varieties B and F in autumn harvest were caused by larger BY and thus higher labour demand, electricity consumption, etc. Although TC per hectare were higher in autumn in comparison with spring, when recalculated per tonne, they were14.7% and 13.6% lower, respectively (see Fig. 1).

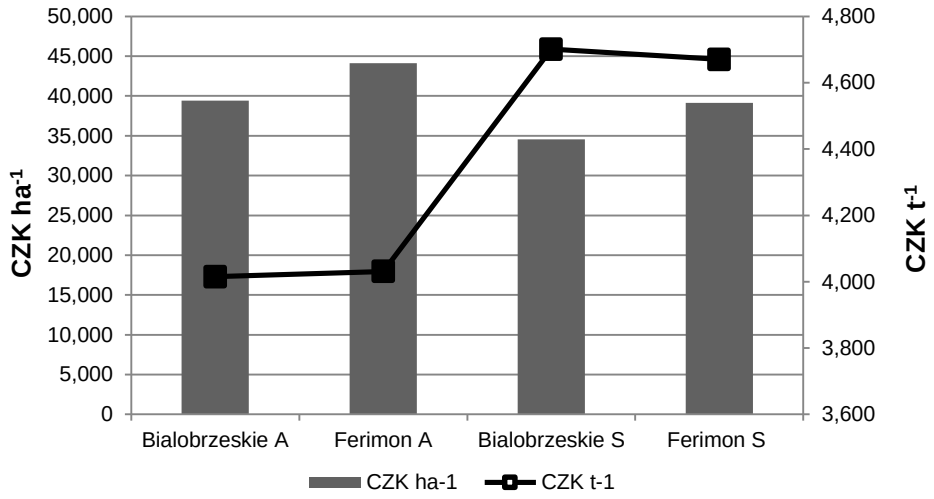

Figure 1. Total costs of briquettes production (comparison) (A – autumn harvest, S – spring harvest).

Although TC per hectare were higher in autumn harvest, when recalculated per tonne they were 15% lower for B and 14% lower for F than in spring (4,015 CZK t^{-1}, 4,031 CZK t^{-1}, respectively).

Structure of costs was very similar in all scenarios. FC made approximately one quarter of TC. Material inputs accounted for almost 40% of TC in all scenarios. Fuels made approximately one fifth of total costs; 70% of costs were made by consumption of

electricity. Labour costs represented on average 16% of TC. Share of depreciation costs was quite high; varying between 11–13%. Costs of water consumption and taxes and fees were insignificant, representing less than 1%.

Profit from briquettes production

Since production costs of hemp briquettes were higher than revenues in all scenarios, none of them made any profit. Loses varied significantly between harvesting periods, being much higher in spring. Surprisingly, in both harvests F showed to be more loss making, even though its BY was higher and thus, higher profit was expected. When subsidies SAPS and TOP –UP were taken into account, economy of production slightly improved and moderate profit was gained in autumn harvest (see Table 3).

Table 3. Costs, revenues, subsidies and profit

		Autumn harvest		Spring harvest	
		Bialobrezskie	Ferimon	Bialobrezskie	Ferimon
Total costs	CZK ha^{-1}	39,426	44,120	34,566	39,116
Total revenue	CZK ha^{-1}	36,466	40,644	27,274	31,151
Subsidies	CZK ha^{-1}	6,560	6,560	6,560	6,560
Profit	CZK ha^{-1}	3,599	3,084	-732	-1,405

All scenarios showed negative profitability without any external financial support, even if included the profitability raised up to maximum 9% in the best case (B in autumn). Assumed briquettes price 4,701 CZK t^{-1} (includingVAT) was too low. The minimum selling price of briquettes to cover total production costs would have ranged between 5,151 CZK t^{-1} to 6,070 CZK t^{-1} depending on variety and harvesting period. To reach medium profitability of 30%, the selling price of hemp briquettes would have been 30% and 40% higher for autumn and spring production, respectively than considered price. If the selling price of hemp briquettes stayed the same as it was assumed, BY in DM had to increase by 1.6–4.1 t ha^{-1} (11.2–12.3 t ha^{-1}) for investigated scenarios to become profitable.

Production of briquettes from whole hemp plant showed to be unprofitable without grants and subsidies with current market prices of competitive solid biofuels. Hemp economy slightly enhanced with subsidies in autumn scenarios, however the profitability remained still above average in comparison with other crops.

From economic point of view autumn harvest was recommended because BY was significantly higher which subsequently increased revenue from 1 ha of cultivated land by 23–25%. However, majority of authors argued that spring harvest was preferable for energy purposes due to lower MC and improved chemical properties (Honzík et al., 2012; Prade et al., 2012; Weger et al., 2012). Thus, the optimal harvesting time must be found to ensure both high BY and suitable chemical features of hemp.

Study revealed that cultivation of hemp solely for briquettes production without any subsidies was not profitable for producers in current market conditions of the Czech Republic. Panoutsou (2012) made economic analysis of hemp cultivation for stalks in Poland and Netherlands and ascertained that in both countries the cultivation was not profitable without receiving any financial help (-38% and -46%, respectively).

CONCLUSIONS

Biomass harvested in autumn produced 9.6 t ha^{-1} of variety B and 10.7 t ha^{-1} of F resulting in TC 39,426 CZK ha^{-1} (1,518 € ha^{-1}) and 44,120 CZK ha^{-1} (1,698.9 € ha^{-1}), respectively. When harvested in spring, yield was 30% lower accounting for 7.18 t ha^{-1} of B and 8.2 t ha^{-1} of F with TC 34,566 CZK ha^{-1} (1,334 € ha^{-1}) and 39,116 CZK ha^{-1} (1,506.2 € ha^{-1}). Higher TC in autumn were caused by higher BY which subsequently required more human labour and fuel for processing and higher depreciation costs due to higher use rate of briquetting line.

Although hemp did not show to be economically viable solely for briquettes production, combine production for both stem and seeds could be suggested.

Utilization of whole hemp plant for briquettes production did not show to be economically feasible due to relatively high production costs and low prices of competitive wood briquettes. The future development depends mainly on final price of product and situation on the market with other solid biofuels.

Hemp outstanding features such as high biomass yield in relatively short time, good energy characteristics, low input requirements, versatile use, etc. should be taken into consideration. Furthermore, unlike perennial crops hemp does not require any long term commitment for its cultivation.

Since higher BY positively affected hemp production economy, further research regarding improvement of hemp yield would be suggested to decrease TC and enhance hemp competitiveness on the market with solid fuels.

Based on available resources and own results hemp would be recommended rather as a break crop in fields planted with food crops than for targeted annual cultivation. Due to unfavourable situation on wholesale market with solid biofuels, hemp is not feasible as a main cash – crop for producer, but rather like complementary plant which brings additional income from sales and provides ecological biofuel for own heat consumption.

ACKNOWLEDGEMENTS. The research was supported by Internal Grant Agency of the Faculty of Tropical AgriSciences, Czech University of Life Sciences Prague (grant N°20155015).

REFERENCES

Rehman, M.S.U., Rashid, N., Saif, A., Mahmood, T., Han, J.I. 2013. Potential of bioenergy from industrial hemp (*Cannabis Sativa*): Pakistan perspective. *Renewable and Sustainable Energy Reviews* **18**, 154–164.

Mankowski, J., Kolodziej, J. 2008. Increasing Heat of Combustion of Briquettes Made of Hemp Shives. *International Conference on Flax and Other Bast Plants*. Poznan: Institute of Natural Fibres, pp. 344–352.

Honzík, R., Bjelková, M., Muňoz, J., Váňa, V. 2012. Cultivation of hemp (Cannabis sativaL.) for biogas production. Research institute of crop production, Prague. Methodology for practice.*http://www.vurv.cz/sites/File/Publications/ISBN978-80-7427-127-4.pdf.* Accessed 18.2.2015 (in Czech).

Tutt, M., Olt, J. 2011. Suitability of various plant species for bioethanol production. *Agronomy Research Biosystems Engineering* **1**, 261–267.

Prade, T., Svensson, S.E., Andersson, A. & Mattsson, J.E. 2011.Biomass and energy yield of industrial hemp for biogas and solid fuel. *Biomass & Bioenergy* **35**(7), 3040–3049.

Prade, T., Finell, M., Svensson, S.E., & Mattsson, J.E. 2012. Effect of harvest date on combustion related fuel properties of industrial hemp (Cannabis sativa L.). *Fuel* **102,** 592–604.

Kolaříková, M., Ivanova, T., Havrland, B., Amonov, K. 2014. Evaluation of sustainability aspect – energy balance of briquettes made of hemp biomass cultivated in Moldova. *Agronomy Research* **12**(2), 519–526.

Czech Statistical Office. 2013. Available at www.czso.cz: Accessed 18. 2. 2015.

MOA – Ministry of Agriculture of the Czech Republic.2012. *Outlook report –Report on Land*. Prague: Ministry of Agriculture. 101p. (in Czech).

Weger, J., Strašil, Z., Honzík, R., Bubeník, J. 2012. *Possibility of biomass cultivation as a source of energy in Ustecky region.* Výzkumný ústav Silva Taroucy pro krajinu a okrasné zahradnictví, Průhonice, 78p. ISBN: 978-80-85116-66-33 (in Czech).

Agronomy Research **13**(2), 337–347, 2015

Examination of commercial additives for biogas production

P. Kuttner[1,*], A.D. Weißböck[1], V. Leitner[2] and A. Jäger[1]

[1]University of Applied Sciences Upper Austria, 4600 Wels, Austria
[2]Energy Institute at the Johannes Kepler University Linz, 4040 Linz, Austria
[*]Correspondence: paul.kuttner@fh-wels.at

Abstract. The formation of biogas from biomass is a complex process with a multitude of variable process parameters. Stability of biogas production and production rate can be vastly improved by keeping these parameters close to their optimum. One possibility to achieve this is by use of additives. In Germany alone there currently are over 250 additives on the market which demonstrates the demand for optimisation of biogas plants. The effects of these additives are hardly investigated and can only be evaluated by costly, time consuming tests (e.g. continuous anaerobic digestion experiments). A new, fast and easy to handle method was developed to evaluate some of the effects of additives. To verify the method trace elements, organic acids, FOS/TAC, ions and cations were quantified. Three additives were tested: The addition of a commercial zeolite increased biogas production by 15%. Calcium carbonate increased performance by 8% after 16 days. No negative effect on biogas production could be observed for the addition of 0.03 and 0.06 g l^{-1} of iron(III) chloride, commonly used to reduce hydrogen sulphide concentration in biogas.

Key words: biogas, additives, zeolite, iron(III) chloride, calcium carbonate.

INTRODUCTION

Biogas production is a well-established conversion technology to obtain energy from biomass. Over 14,000 plants produce 13.4 million tons oil equivalents (toe) primary energy (52.3 TWh electricity, 432.4 ktoe heat for district heating networks and 2,010 ktoe heat consumed at the plant site) in the European Union and Switzerland (EurObserv'ER, 2014). In spite of the number of plants and the years of experience a multitude of problems still occurs. This might be due to missing monitoring instruments and equipment, the plant operator's lack of knowledge or the lack of knowledge transfer from research to application. Additives promise to enhance stability or/and performance or can be used as an emergency measure to avoid collapse of the conversion process. A study conducted by Henkelmann et al. (2012) shows that there are more than 250 additives available in Germany (Germany: 7,960 biogas plants in operation). Compared with the number of biogas plants this figure demonstrates that biogas plant operators are still facing a multitude of problems and challenges.

Additives can be classified by their main ingredients and main function: Inorganic nutrient and trace element mixtures are often prepared individually for each plant to increase stability and performance by supplying the ideal concentration of trace elements for anaerobic digestion. Since ideal concentrations depend on biocenosis and feed different optima, minima and maxima have been found by research teams, effects vary

as well (Chen et al., 2008; Demirel & Scherer, 2011). pH stabilizers are used to avoid or to reduce fluctuations of the pH which is crucial for a stable process. Additives reducing the concentration of ammonia or hydrogen sulphide are also widely in use. Both substances pose a challenge for biogas purification and can lead to corrosion in the CHP. They also can inhibit anaerobic digestion at high concentrations. Anti-foaming and anti-floating-layer agents are another large group of additives that do not affect the bacteria directly but increase the performance of the digester. Few additives based on enzymes, algae and special microorganisms are on the market.

With such a multitude of different additives on the market it is nearly impossible for the plant operators to choose, especially since effects of the additives promised by the manufacturer are hardly ever verified or in some cases not verifiable at a plant scale (e.g. process stability). To verify the effects on lab scale large scale continuous digesters fed with a variety of substrates would be needed. Thus the aim of this study is to provide a simple, cheap and fast test to quantify some effects of additives.

MATERIALS AND METHODS

Examined additives

A commercially available zeolite dotted with trace elements was used in the concentration suggested by the manufacturer (3.4 g l^{-1}). Zeolites work as a buffer, ion exchanger and provide a high surface for biofilms. To determine the amount of trace elements in the zeolite 3.4 g of the zeolite were incubated in 1 l HPLC grade water at 37.5 °C for 24 h. The liquid contained 0.54 mg l^{-1} Al, 0.18 mg l^{-1}Co, 0.26 mg l^{-1} Cu, 3.94 mg l^{-1} Fe, 0.44 mg l^{-1} Mn, 0.34 mg l^{-1} Ni, 6 mg l^{-1} Na, 10 mg l^{-1} K, 23 mg l^{-1} Mg and 84 mg l^{-1} Ca (determined as described below).

Calcium carbonate (99%, particle size 1 µm, Carl Roth) was used to differentiate the effects of the zeolite. It works as a buffer at pH 6.2 to 8.3 and could be added in excess (10 g l^{-1}) due to its low solubility to simulate the surface provided by zeolite.

Iron(III) chloride (98%, Merck) is often used to reduce the concentration of H_2S in biogas and is commercially available under many brand names from different manufacturers. Concentrations were calculated according to the sulphur contained in the samples: 30 mg l^{-1} was the amount needed to bind all sulphur in the substrate. Additionally a concentration of 60 mg l^{-1} was tested to evaluate any possible inhibition.

Substrate used for biogas tests

Unseparated material from the main digester (a 1,000 m³ horizontal digester) from a biogas plant in Upper Austria was used in this study. The substrate was stored for less than 24 h at 37.5 °C before being used. The plant was running stable during, before and after the material was taken. The main digester was fed with 80% maize silage and 20% grass silage without any additives. Dry matter (DM) content was stable at 7.19–7.43% while ash content slightly changed from 24.98% DM for the first batch to 25.95% DM for the second batch.

The biogas plant was part of an intensive monitoring program from November 2012 to August 2013 (weekly samples from main digester): 12–14.5 t (mean 13.11 t) of maize and grass silage were fed daily resulting in 135–175 m^3h^{-1} (mean 159.38 m^3 h^{-1}) biogas (45–55.9% methane; mean 49.15%). DM content of the main digester ranged from 6.4 to 11% (mean 8.71%) and ash content varied between 28.98 and 18.89% DM (mean 21.96%). pH value was between 7.03 and 8.57 (mean 7.57) and FOS/TAC between 0.208 and 1.154 (mean 0.459). Acetic acid concentration varied between 0 and 1.152 g l^{-1} (mean 0.24 g l^{-1}). Ca^{2+} concentration ranged from 72 to 468 mg l^{-1} (mean 196.95 mg l^{-1}) and Fe from 13.5 to 52.7 mg l^{-1} (mean 40.09 mg l^{-1}).

Biogas batch test

Biogas production was determined gravimetrically using 1 l plastic bottles with fermentation locks. This gravimetric method is common to determine the ethanol production during fermentation and has been established and validated for the determination of biogas potentials in the labs of the University of Applied Sciences. For standard biogas potential batch tests the separated digester material (after 10 days at 37.5 °C to reduce its gas production) would only be used as inoculum. To this inoculum a defined amount of biomass would then be added to determine its biogas potential. In this study the unseparated material of the main digester was used as both the inoculum and the substrate to simulate a biogas plant.

500 ml of the unseparated main digester content was filled into each bottle, incubated at 37.5 °C ± 0.5 in a climate chamber for 16 days and the weight was determined daily (AND GX-4000, accuracy ± 0.01 g) after shaking the bottle. Each batch consisted of 57 bottles: 18 with substrate taken from the main digester (blank), 18 for each of the two additives tested in one batch and 3 filled with water (water blank) to estimate the mass loss by evaporation. Every second day 6 bottles (2 each) were stopped and the content analysed.

Dry matter and organic dry matter

To determine the dry matter the sample was homogenized, put into crucibles (12 g per crucible; n = 3), oven dried at 40 °C for 24 h and then dried at 105 °C for 24 h. Ash content was determined by heating the crucibles to 550 °C for 24 h. Mass of the crucibles was determined using an analytical scale (Kern 770, accuracy ±0.00001 g).

FOS/TAC

The ratio of free organic acids (measured in acetic acid equivalents) to the total inorganic carbonate was determined according to the method published by Nordmann (1977). 50 ml of the sample was centrifuged at a rotational speed of 3,500 min^{-1} for 15 min, 10 g of the supernatant was then diluted to 50 g with HPLC grade water and used for titration. Amount of sulphuric acid (96%, Carl Roth, c = 0.05 mol l^{-1}) needed to reach pH 4.4 (FOS) and 5.0 (TAC) was determined using a Mettler Toledo Graphix DL50.

Free organic acids and sugars

1 ml of the supernatant from FOS/TAC determination was diluted to 2 ml with eluent (sulphuric acid, 96%, Carl Roth, c = 5 mmol l^{-1}) and analysed for free organic acids and sugars using an Agilent Technologies 1200 Series HPLC with a Varian Metacarb 87 H column (300*7.8 mm).

Anions and cations

Concentration of Ca^{2+}, Cl^{-}, K^{+}, Mg^{2+}, Na^{+}, $NH4^{+}$, PO_4^{3-} and SO_4^{2-} was determined by IC using a Dionex ICS 1000 with ASRS/CSRS suppressors. 5 ml of the sample was diluted to 20 ml with HPLC grade water and then centrifuged at a rotational speed of 3,800 min^{-1} for 15 min. The supernatant was filtered (fluted filter Macherey-Nagel 615 1/4) and then diluted 1:10 (anions) and 1:25 (cations) respectively. For anions an IonPac AS12A (4*250 mm) column with an IonPac AG12A (4*50 mm) guard and a carbonate buffer eluent (sodium carbonate, Carl Roth, 99.5%, c = 8 mmol l^{-1}, sodium hydrogen carbonate, Carl Roth, c = 1 mmol l^{-1}) was used. For cations an IonPac CS12A (4*250 mm) column with an IonPac CG12A (4*50 mm) guard and methanesulfonic acid (99% Merck, c = 20 mmol l^{-1}) as mobile phase was used.

Trace elements

Trace elements (Al, Cu, Fe, Mn, Mo, Ni, Pb and Zn) were quantified by ICP-OES: 2.5 ml of the sample were diluted to 25 ml with HPLC grade water and 0.1 ml of trace element free nitric acid (65%, Carl Roth) was added. The supernatant (after centrifugation at a rotational speed of 3,800 min^{-1} for 15 min) was filtered (fluted filter Macherey-Nagel 615 1/4) and analysed with a Horiba Jobin Yvon Ultima 2.

Data for trace elements, cations and anions is only shown where significant changes or differences were detected.

RESULTS AND DISCUSSION

Zeolite and calcium carbonate (batch 1)

An incubation time of 16 days was selected to be able to evaluate the kinetics of anaerobic digestion. Biogas production increased from 8.29 ± 0.07 g l^{-1} (blank) to 8.94 ± 0.22 g l^{-1} (increase by 8%) when calcium carbonate was added and to 9.53 ± 0.36 (increase by 15%) g l^{-1} with the addition of zeolite (see Fig. 1). These results are well within the range of values found in literature: Montalvo et al. (2006) for instance have shown an increase by 11–30% when digesting swine waste with zeolites for 10–30 days in continuous digesters.

Higher increase of biogas production (by up to 110%) has been shown for the digestion of pig and poultry manure: increase of biogas production by 109.75% (batch, 44 days, 10 g l^{-1} zeolite, 36 °C) for the codigestion of poultry and pig manure (Kougias et al., 2013), increase by 10–66% for the digestion of pig waste (batch, 15 days, 4–10 g l^{-1} natural zeolite, 55 °C, high and low organic matter content) (Kotsopoulos et al., 2008).

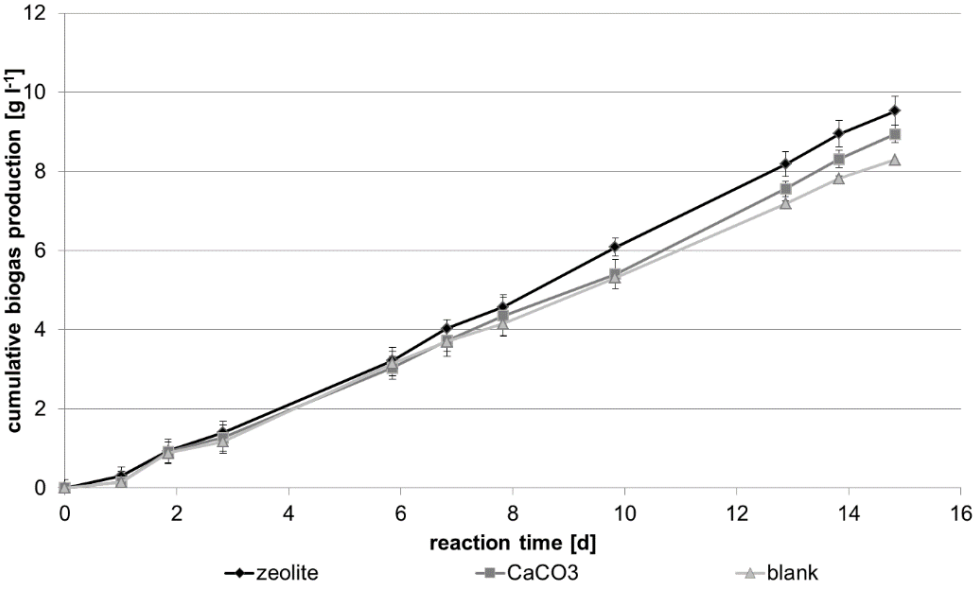

Figure 1. Cumulative biogas production for batch 1 (additives: zeolite and calcium carbonate).

Biogas results clearly show that the positive effects of zeolite exceed those of a simple buffer (calcium carbonate). The effects of zeolite as a promoter and substrate for biofilms of methanogenic archaea have been extensively studied (Milan et al., 2001, Montalvo et al., 2005, Weiß et al., 2010). It can be reasoned that the trace elements in the zeolite have a positive effect, but since the concentration is rather low (see subchapter Additives) the more likely reason is that zeolite act better as a buffer, promote biofilms and increases availability of acids and micro nutrients.

pH decreased in the first 6 days of the batch run, which is due to strong activity of hydrolysis bacteria (see Fig. 2). pH decrease is more intensive for the samples containing additives but since biogas production in this time frame is not decreased compared to the blank samples and lowest pH reached is 7.47 inhibition of methanogenisis is unlikely. pH is lower for samples containing additives during the complete batch run, which indicates a higher degradation rate of biomass. FOS/TAC confirm the strong hydrolysis in the first 6 days and indicate furthermore that degradation rate for zeolite is higher than for blank. The in comparison to zeolite and blank low value for calcium carbonat is due to the higher TAC (total inorganic carbonate) value and should be considered irrelavant for these samples.

Conversion of organic acids to acetic acid was fastest for the samples with zeolite added (see Fig. 3). Methan production rate from acetic acid was highest for zeolite and calcium carbonate while the concentration of acetic acids was stable in the blank samples between day 3 and 8 which can be an indicator for an inhibition especially since biogas production for zeolite was higher than for blank between day 6 and 8. Acetic acid concentrations are a further indicator that higher biogas yields and higher biomass throughput can be achieved by adding additives.

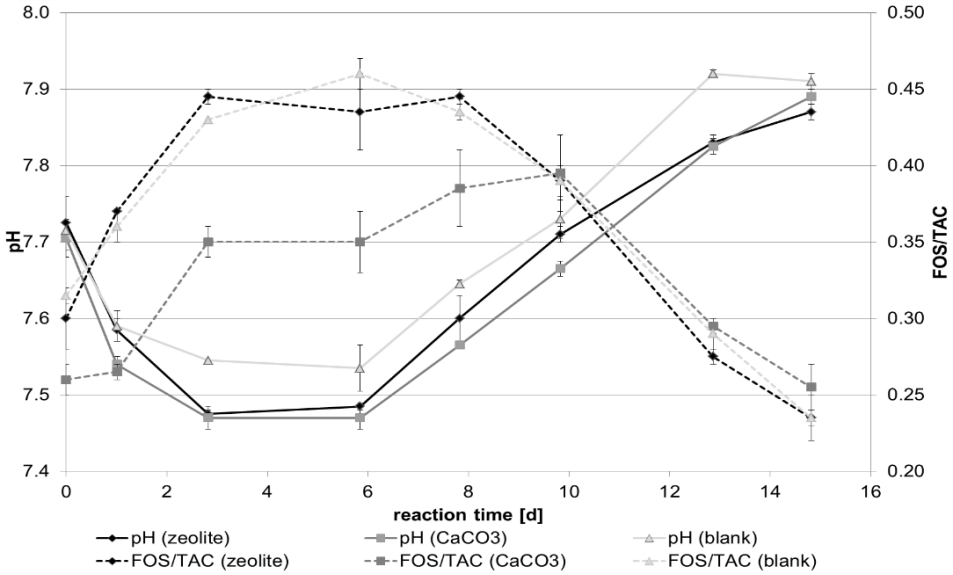

Figure 2. pH and FOS/TAC values for batch 1 (additives: zeolite and calcium carbonate).

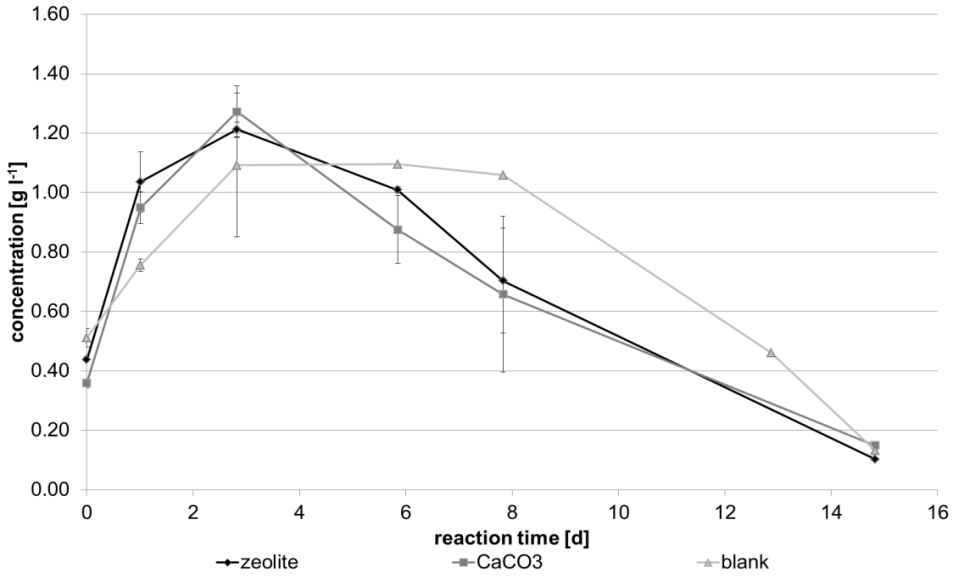

Figure 3. Concentration of acetic acid for batch 1 (additives: zeolite and calcium carbonate).

The importance and effects of trace elements have been studied extensively for numerous feedstocks on both an industrial and lab scale: Vintiloiu et al. (2012) identified concentration of Ni, Mo and S to be significant for the concentration of organic acids. Fe, Co and Na concentrations were shown to interact not directly with the concentration of organic acids but were involved in the interactions between those factors that had significant effects. Ni, Mo, S, Co and Na concentrations did not vary between blank and

additives in this test (data not shown), but iron levels were significantly higher for zeolite than for the other variations (see Fig. 4). Iron has been shown to have positive effects on methanogenic activity (Demirel & Scherer, 2011, Karlsson et al., 2012). Mn concentration is rarely studied in research, but is a cofactor for enzyms especially for hydrolysis. Concentration of Mn decreased during day 1 to 8, where hydrolysis activity was shown to be at its maximum. Concentration of heavy metals for all variations was below the detection limit. Ammonia concentration was constant between 1.3 and 1.4 g l^{-1} for all variations. None of the trace elements, anions and cations examined in this study were above or even close to a concentration, where inhibition has been reported, but concentration of nearly all trace elements was highest for zeolite, while calcium carbonat did not always have a positive effect on trace element availability (e.g. Fe). This cannot be explained by the trace elements contained in the zeolite (see subchapter Additives), but by its ability for ion exchange.

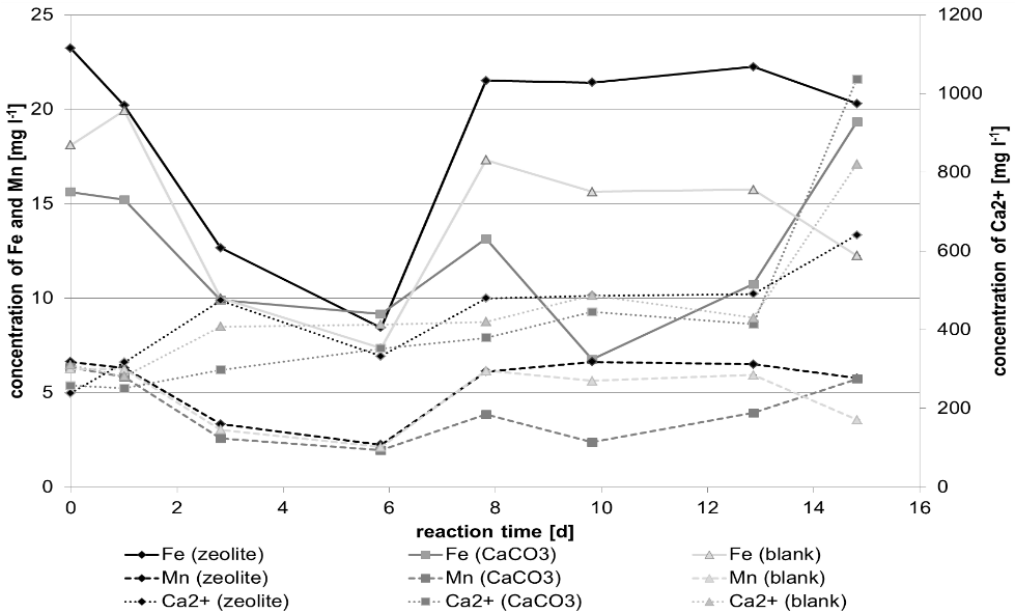

Figure 4. Concentration of iron, manganese and calcium for batch 1 (additives: zeolite and calcium carbonate).

Iron(III) chloride (batch 2)

The addition of iron(III) chloride did not result in a significant change in biogas production (see fig. 5): The blank samples produced an average of 11.06 ± 0.26 g l^{-1} biogas, addition of 0.03 g l^{-1} $FeCl_3$ led to 10.89 ± 0.37 g l^{-1} being produced and the highest biogas production (11.25 ± 0.08 g l^{-1}) was determined when 0.06 g l^{-1} $FeCl_3$ was added. Studies on the anaerobic digestion of activated sludge show a biogas reduction by 0 (Mamais et al., 1994) to 30% (Ofverstrom et al., 2011) with $FeCl_3$ doses at least 10 times higher. So the results of this study are within the expected range.

Biogas production increased by 2.77 g l^{-1} compared to batch 1 for the blank samples. This might be due to changes in feed quality and composition.

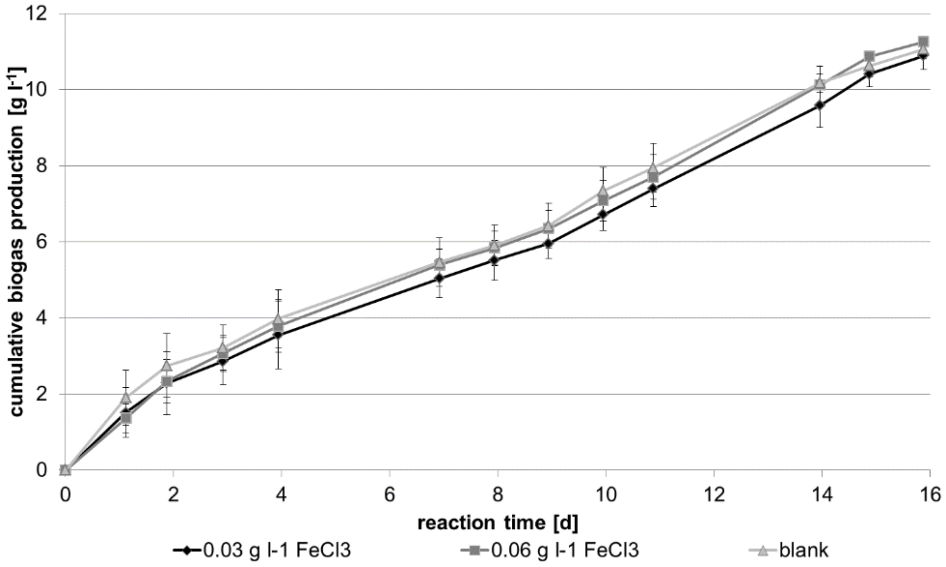

Figure 5. Cumulative biogas production for batch 2 (additive: iron(III) chloride).

Addition of $FeCl_3$ led to a slightly lower pH for days 4 to 16 and a higher pH on day 2 (see Fig. 6). $FeCO_3$ precipitation, as discussed by Mamais et al. (1994) and Ofverstrom et al. (2011), could be one reason for the lower pH. It would also explain the lower FOS/TAC values for 0.06 g l^{-1} $FeCl_3$. Addition of iron(III) chloride led to an less stable pH and FOS/TAC curve with higher minima and maxima than for the blank samples.

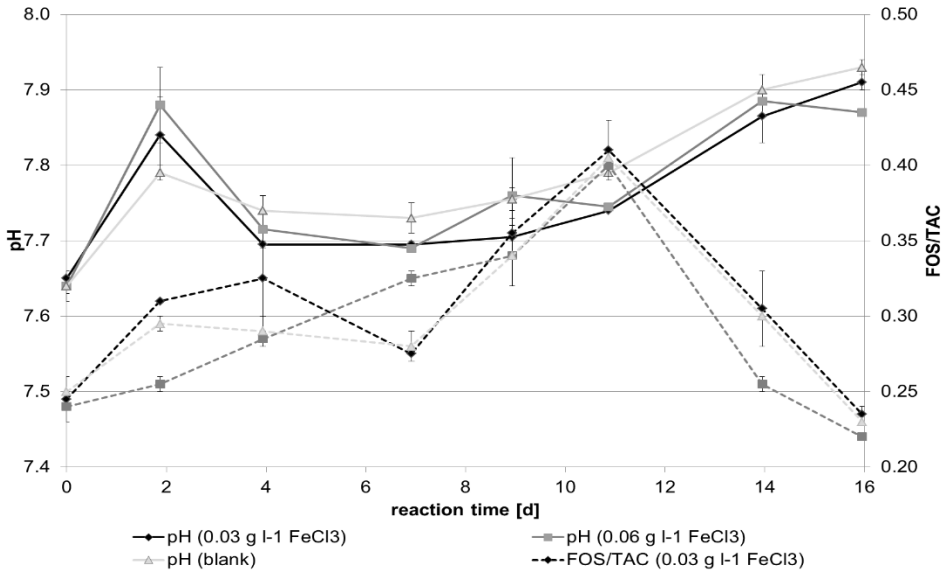

Figure 6. pH and FOS/TAC value for batch 2 (additive: iron(III) chloride).

Concentration of acetic acid was significantly higher (maximum at 1.3 ± 0.1 g l^{-1} on day 11, minimum at 0.2 on day 0) for 0.03 g l^{-1} $FeCl_3$ than for blank and 0.06 g l^{-1} $FeCl_3$ (maximum at 0.9 ± 0.1 g l^{-1} on day 11, minimum at 0.08 on day 0). The higher concentrations for 0.03 g l^{-1} $FeCl_3$ could be an indicator for a slight inhibition of methanogenesis and explain the slightly lower biogas production.

SO_4^{2-} concentration decreased over time for all variations (formation of H_2S and $Fe_2(SO_4)_3$) with an unexpected peak on day 9: blank and 0.03 g l^{-1} $FeCl_3$ samples reached a concentration of 8.6 ± 0.4 mg l^{-1} while the concentration for 0.06 g l^{-1} $FeCl_3$ was 19% lower. On day 9 FOS/TAC was at its maximum, Fe and Mn concentrations were at their minima (see Fig. 7) and biogas production was slightly lower, which indicates high hydrolytic activity. The data suggests that addition of 0.06 g l^{-1} $FeCl_3$ significantly reduced the concentration of SO_4^{2-} and therefore the concentration of H_2S in the biogas. Cl^- concentration was up to 18% higher (blank: 245–358 mg l^{-1}) for those samples with $FeCl_3$.

Concentrations of Mn and PO_4^{3-} did not vary between the variations, but Fe concentrations were slightly higher for those samples containing $FeCl_3$. Compared to batch 1 concentration of Ca^{2+} were rather frantic during batch 2 which is also reflected in a more fluctuating FOS/TAC and pH curve.

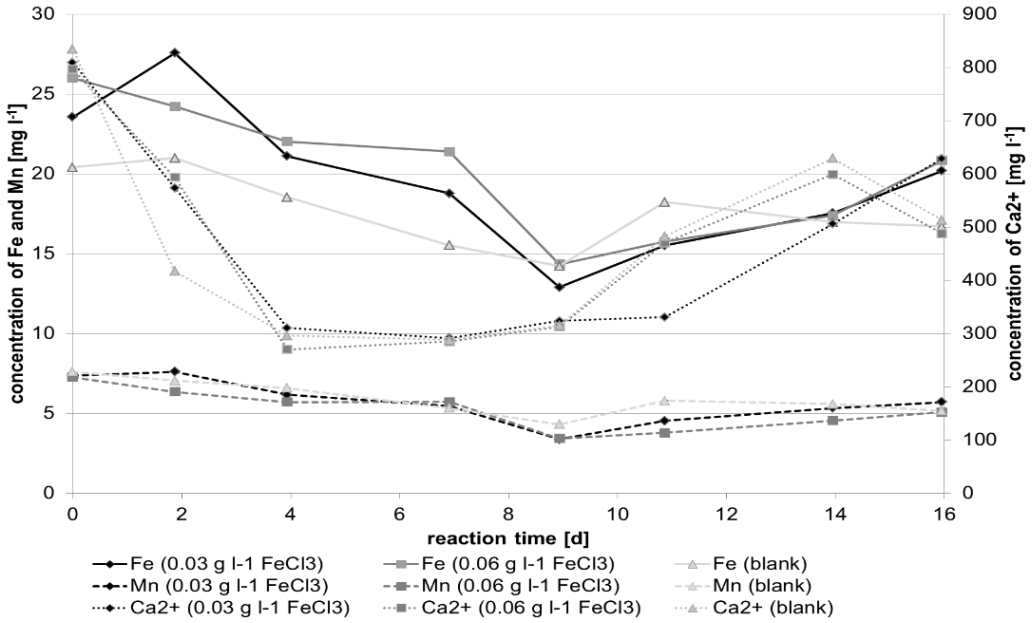

Figure 7. Concentration of iron, manganese and calcium for batch 2 (additive: iron(III) chloride).

CONCLUSIONS

The addition of a zeolite (with trace elements) significantly increased biogas production while $CaCO_3$ slightly increased it. Since biogas composition was not analysed it cannot be evaluated if the addition of $FeCl_3$ reduced the concentration of H_2S,

but results point in that direction. No negative effect of $FeCl_3$ on biogas production was found, but it can be argued that it had negative effects on pH stability.

Results are within the range of findings of other researchers using more complex and expensive biogas test systems (e.g. continuous digesters). An inexpensive test system (plastic bottles, fermentation locks, a scale, and a room with constant temperature) that could be used on site was established. To evaluate the full scale of the effects and promises of commercial additives long term continuous digestion experiments would have to be carried out. The method presented allows biogas plant operators a fast and cost-effective evaluation of an additive.

ACKNOWLEDGEMENTS. This project is financed within the scope of the European Union Program 'Regionale Wettbewerbsfähigkeit OÖ 2007-2013 (Regio 13)' from the purse of the European Fonds for Regional Development (EFRE) and the Federal State of Upper Austria, Austria. Project code: DAABAA_00477

REFERENCES

Chen, Y., Cheng, J. & Creamer, K. 2008. Inhibition of anaerobic digestion process: a review. *Bioresource technology* **99**(10), 4044–4064.

Demirel, B. & Scherer, P. 2011. Trace element requirements of agricultural biogas digesters during biological conversion of renewable biomass to methane. Biomass and Bioenergy, **35**/3, 992–998.

EurObserv'ER 2014. Biogas barometer. *http://www.energies-renouvelables.org/observer/stat_baro/observ/baro224_Biogas_en.pdf*. Accessed 19.1.2015.

Henkelmann, G., Fischer, K., Meyer zu Köck, K., Koch, K., Lebuhn, M., Effenberger, M. & Bayer, K. 2012. Marktübersicht Zusatz- und Hilfsstoffe in Biogasanlagen. Biogas Forum Bayern.

Karlsson, A., Einarsson, P., Schnürer, A., Sundberg, C., Ejlertsson, J. & Svensson, B. 2012. Impact of trace element addition on degradation efficiency of volatile fatty acids, oleic acid and phenyl acetate and on microbial populations in a biogas digester. *Journal of bioscience and bioengineering* **114**(4), 446–452.

Kotsopoulos, T., Karamanlis, X., Dotas, D. & Martzopoulos, G. 2008. The impact of different natural zeolite concentrations on the methane production in thermophilic anaerobic digestion of pig waste. *Biosystems engineering* **99**(1), 105–111.

Kougias, P., Fotidis, I., Zaganas, I., Kotsopoulos, T. & Martzopoulos, G. (2013). Zeolite and swine inoculum effect on poultry manure biomethanation. *International Agrophysics* **27**(2), 169–173.

Mamais, D., Pitt, P., Cheng, Y., Loiacono, J. & Jenkins, D. 1994. Determination of ferric chloride dose to control struvite precipitation in anaerobic sludge digesters. *Water Environment Research* **66**(7) 912–918.

Milán, Z., Sánchez, E., Borja, R., Weiland, P., & Cruz, M. 2001. Synergistic effects of natural and modified zeolites on the methanogenesis of acetate and methanol. *Biotechnology letters* **23**(7), 559–562.

Montalvo, S., Díaz, F., Guerrero, L., Sánchez, E. & Borja, R. 2005. Effect of particle size and doses of zeolite addition on anaerobic digestion processes of synthetic and piggery wastes. *Process biochemistry* **40**(3), 1475–1481.

Montalvo, S., Guerrero, L., Borja, R., Travieso, L., Sánchez, E. & Díaz, F. 2006. Use of natural zeolite at different doses and dosage procedures in batch and continuous anaerobic digestion of synthetic and swine wastes. *Resources, conservation and recycling* **47**(1), 26–41.

Nordmann, W. 1977. Die Überwachung der Schlammfaulung. KA-Informationen für das Betriebspersonal, Beilage zur Korrespondenz Abwasser **3/77**, 77.

Ofverstrom, S., Dauknys, R. & Sapkaitė, I. (2011). The Effect of Iron Salt on Anaerobic Digestion and Phosphate Release to Sludge Liquor. Science–Future of Lithuania/Mokslas–Lietuvos Ateitis, **3**/5, 123–126.

Vintiloiu, A., Lemmer, A., Oechsner, H., & Jungbluth, T. 2012. Mineral substances and macronutrients in the anaerobic conversion of biomass: An impact evaluation. *Engineering in Life Sciences*, **12**(3), 287–294.

Weiß, S., Zankel, A., Lebuhn, M., Petrak, S., Somitsch, W. & Guebitz, G. 2011. Investigation of mircroorganisms colonising activated zeolites during anaerobic biogas production from grass silage. *Bioresource techn*ology **102**(6), 4353–4359.

Agronomy Research **13**(2), 348–353, 2015

Direct and indirect energy input in the harvesting of Scots pine and Norway spruce stump-root systems from areas cleared for farmland

R. Lauhanen[1,*], J. Ahokas[2] and J. Esala[1]

[1]Seinäjoki University of Applied Sciences, School of Food and Agriculture, Ilmajoentie 525, FI60800 Ilmajoki, Finland
[2]University of Helsinki, Faculty of Agriculture and Forestry, Koetilantie 5, Helsinki, Finland
[*]Correspondence: risto.lauhanen@seamk.fi

Abstract. The aim of this study was to find the net energy and energy ratios for the recovery of Scots pine and Norway spruce stump-root systems when clearing land for cultivations. The energy analyses were carried out for direct and indirect energy under Finnish conditions. In the base study case for direct energy input; the net energy yields for stump-root system harvesting were 446–698 GJ ha^{-1}, and the energy ratios were 22–33. In the case of indirect energy input the net energy yields were 440–692 GJ ha^{-1}, and the energy ratios were 17–26. The proportion of indirect energy was low, because the amount of operating hours annually was high. When calculating indirect energy, only the energy input of machine manufacturing was used, since there was no data on the indirect energy used for repair and maintenance of the machines. The energy assessment for repairing and maintenance operations for heavy forest machines and vehicles in bioenergy procurement will need to be assessed.

Key words: agricultural land, bioenergy, clarification of forest land, energy assessment, forest machines, wood-based energy.

INTRODUCTION

New agricultural land is needed in Finland, especially for dairy farms. During 2000–2011 a total of 95,000 hectares of forest area was cleared for farmland (Niskanen & Lehtonen, 2014). In western Finland, peatlands with poor forest stands particular have been cleared for farmland, as well as clear-cut spruce stands with low stone-index (see Niskanen & Lehtonen, 2014).

The European Union aims to prevent climate change and to increase the use of renewable bioenergy (e.g. Hakkila, 2004; Laurila & Lauhanen, 2010). In Finland forest bioenergy consists of small-diameter stems from young stands and logging residues with stump-root systems from forest regeneration areas (e.g. Hakkila, 2004; Laitila et al., 2012). In addition, agro-biomass, e.g. reed canary grass and straw are also used for bioenergy in Finland (e.g. Mikkola, 2012).

In Finland, stumps are harvested for fuel for power plants with a boiler size of 5 MW or more (Laurila & Lauhanen, 2010). The energy content of stumps and roots is 130–200 MWh ha^{-1}, i.e. 468–720 GJ ha^{-1} (Hakkila, 2004; Lauhanen et al., 2014). It is

rational for the forest-owners to sell forest biomass to energy companies, and to get stumpage price for the wood (Lauhanen et al., 2014).

Stump-root system extraction is essential in clearing forest for farmland. Incomes from stumps increase the profitability of preparing new farmland (Lauhanen et al., 2014). There have been debates on the environmental effects of the utilisation of stumps and roots. The ratio of output to input energy (i.e. energy ratio) has been discussed as well. (Lauhanen et al., 2014).

The energy inputs for forest energy production and the energy contents of forest energy have also been discussed. The direct energy input of forest energy has been 2–4% of the output energy in the earlier studies (Laitila et al., 2012). The indirect energy input for forest machines in bioenergy procurement has not been published previously in Finnish conditions. The indirect energy input of machine manufacturing, repairing and maintaining the machines should also be assessed as it has been for agricultural machinery (Mikkola & Ahokas, 2010).

The hypothesis for this study is that the high amount of operating hours of forest machines will result in low indirect energy input of forest machines in stump-root system supply chain.

The objective of this study was to calculate the net energy and energy ratios for the recovery of Scots pine and Norway spruce stump-root systems under Finnish conditions.

MATERIALS AND METHODS

Energy terms and work chains

The energy content of stump-root systems were based on the earlier studies (Hakkila, 2004; Laurila & Lauhanen, 2010; Laitila et al., 2012). The direct energy input was based on the fuel consumption of forest machines, stump crushers and stump trucks (Laitila et al., 2012). The indirect energy input contained the energy input of tractor manufacturing (Hakkila, 1989; Mikkola & Ahokas, 2010).

The work chain contained: stump-root extraction by excavator, forwarder use on the work site, stump crusher use at the forest road-side storage as well as the truck transportation of crushed stumps from the forest road-side storage to the power plant. (Laurila & Lauhanen, 2007; Laitila et al., 2012). It is not rational to transport the uncrushed stumps and roots too long distances due to their low energy density in truck load (see Hakkila 1989).

Energy content of stump-root systems

The energy content of stump-root systems was assumed to be 468 GJ ha^{-1} (= 130 MWh ha^{-1}) for Scots pine mire, if all stump-root systems were harvested. (Hakkila, 2004). Timber removal from the clear cutting area was 260 m^3 ha^{-1}. The energy content of the stump-root systems was assumed to be 720 GJ ha^{-1} (= 200 MWh ha^{-1}) on mineral soil, if all of the Norway spruce stump-root systems were extracted. (Laurila & Lauhanen, 2010; Lauhanen et al., 2014). In this case, the timber removal was 400 m^3 ha^{-1}. Consequently, the energy contents of 468 GJ ha^{-1} and 720 GJ ha^{-1} for the stump-root systems were applied in the analyses.

Work site and work productivity

In the calculations, the typical work site area was 3.0 hectares. In which case the energy content of the stumps was 1,512–2,160 GJ ha^{-1} depending on the forest type. Stump-root system extraction by excavator took 3.0 days with one work shift per day; i.e. typical work productivity was 1.0 hectare per day (Fig. 1) (Laurila & Lauhanen, 2007). The same productivity rate was assumed for the forwarder on the work site (Laurila & Lauhanen, 2007). The work productivity for the stump crusher was assumed to be 100 loose cubic meters per operating hour at the forest road-side storage; based on Lauhanen et al. (2014). The crushed stumps were transported by truck from the forest road-side storage to the power plant the transportation distance being 45 kilometers (Laitila et al., 2012).

Figure 1. Excavator in stump-root system extraction on one peatland forest site (Jussi Laurila).

Direct and indirect energy

The direct energy input was calculated on the basis of the work site information and the fuel consumptions of the forest machines and vehicles (Tables 1, 2) (Laitila et al., 2012; Lauhanen et al., 2014). The energy content was 35.1 MJ per one litre of fuel. Thus, total direct energy input in the supply chain was 64.8 GJ from forest work site to power plant (Table 1).

Table 1. Fuel consumptions of the work machines and vehicles in the stump-root system supply chain. The work site was 3.0 hectares, and the transportation distance for the chip-truck was 45 kilometres. Legend: Weight = machine weight in tons, Hours = operating hours per work site of 3.0 hectares, Fuel = fuel consumption litres per an operating hour, and Energy = fuel-based direct energy input in GJ. (Laitila et al., 2012; Lauhanen et al., 2014)

Work machine	Weight	Hours	Fuel	Energy
Forwarder	10	27	12	11.4
Crusher	36	9	65	20.5
Truck	20	9	50	15.8
Total	87	72	1,845	64.8

Table 2. Fuel consumptions of the work machines in the logging residual (residual wood) supply chain. Legend: Weight = Machine weight in tons, Hours = operating hours per work site of 3.0 hectares, Fuel = fuel consumption litres per an operating hour, and Energy = fuel-based direct energy input in GJ. (Laitila et al., 2012; Lauhanen et al., 2014)

Work machine	Weight	Hours	Fuel	Energy
Harvester	10	27	0	0.00
Forwarder	10	27	12	11.37
Crusher	36	9	65	20.53
Truck	20	9	50	15.80
Total	76	72	1,359	59.10

According to Hakkila (1989), the indirect energy input of tractor manufacturing was assumed to be 158.9 MJ kg^{-1}. First, this value was multiplied with the mass of the machine or vehicle (kg). Secondly, this indirect energy input (GJ) was related to work site hours per the life-time of the machine or vehicle in hours. The technical life-time of the machinery was assumed to be 4.0 years, i.e. 12,000 hours totally (Lauhanen et al. 2014). These numbers were equal to 3,000 operation hours per one machine or one vehicle in forest energy procurement (Laitila et al., 2010; Lauhanen et al., 2014).

Energy analyses

In the calculations energy analyses were computed for stump-root system extraction from Scots pine and Norway spruce stands (cf. Mikkola & Ahokas, 2010). The net energy was the difference between the energy content of the stump-root systems and the energy inputs for the forest machines and vehicles (in GJ ha^{-1}). The energy ratio was obtained, when the energy content of the stump-root systems was divided by the energy inputs of the machines and vehicles (Mikkola & Ahokas, 2010).

The sensitivity analyses were also calculated with the varying fuel consumptions of excavators (i.e. 12 litres per an operating hour and 18 litres per operating hour) (Laitila et al. 2012; Lauhanen et al. 2014).

Before stump-root system extraction the residual wood needs to be harvested, too (Laitila et al., 2012) Additional and comparative energy analyses were also assessed (Table 2). The energy contents of the residual wood were 396–566 GJ ha^{-1} (= 110–160 MWh ha^{-1}).

One-grip harvester is a forest machine that carries out tree-felling and prepares saw logs and pulp wood for the mills. (Lauhanen et al., 2014). On clear-cutting work sites one-grip harvester also makes the small piles of saw logs and pulp wood and also the low piles for residual wood (Laitila et al., 2012; Lauhanen et al., 2014). This is conventional work for one-grip harvester, and that is why the energy input for the one-grip harvester in this work was assumed to be 0.00 GJ (Table 2) (Laitila et al., 2012). After one-grip harvester, the forest forwarder removes the small wood piles into great wood storages along the forest road sides. (Laitila et al., 2012; Lauhanen et al., 2014).

RESULTS AND DISCUSSION

In the case of direct energy input, the net energy yields for wood stump-root system harvesting were 446–698 GJ ha^{-1}. The energy ratios were 22–33. In the case of indirect energy, the yields were 440–692 GJ ha^{-1}, and energy ratios were 17–26.

The case of an excavator of 21 tons with the fuel consumption of 12.0 liters per an operation hour was also calculated in the sensitivity analysis. In which case, the net energy yields for wood stump harvesting were 448–700 GJ ha^{-1}. The energy ratios were 24–37. In the case of indirect energy input, the net energy yields were 442–694 GJ ha^{-1}, and energy ratios were 18–28.

For the harvesting of residual wood, in the case of direct energy the net energy yields were 386–566 GJ ha^{-1}. The energy ratios were 40–59. In the case of indirect energy input the net energy yields were 384–564 GJ ha^{-1}, and energy ratios were 33–47. The fuel consumption was lower for the logging of residual wood than for stump-root system logging, but also the energy content of the residues was lower than that of stumps.

This direct energy assessment produced results that were comparable with the results of Laitila et al. (2012). The energy yields and ratios for indirect energy of forest stump-root systems and residual wood however, were new.

According to Hakkila (1989), the indirect energy input of tractor manufacturing in was assumed to be 158.9 MJ kg^{-1}. Later Mikkola & Ahokas (2010) and Mikkola (2012) used the value of 86.8 MJ kg^{-1} energy input for the manufacturing energy of modern agricultural machines, but we applied the higher value given by Hakkila (1989). The share of indirect energy input for the manufacturing of forest machines was however low in this study, since the life-time of the machines was rather short and there were lots of annual technical operation hours. Thus, these energy assessment calculations confirmed the hypothesis for this study.

We had no sufficient data for the indirect energy input of the forest machines and vehicles, because the energy input data for the repair and maintenance was not available. The inventory on the energy input of the repair and maintenance of forest machines is thus needed in the further studies.

The fuel consumption of the machinery affected the results. Sensitivity analyses and the evaluation of the initial parameters were important in the calculations. However, the energy input of the forest roads and earlier forest stand operations were not included in the calculations, since it was difficult to evaluate them as Mikkola (2012) stated for the calculations in agriculture. On the other hand, the forest roads and earlier forest operations were assumed to be constant in the calculations. The modern forest energy terminals were excluded in the calculations. In which case, the indirect energy of terminals should be assessed as well. Also, the wood stump material loss was not included in the analyses.

CONCLUSIONS

Stump-root system extraction and collection of logging residues are essential in clearing of forest for farmland. The results showed that the net energy of harvesting of the stump-root systems and logging residues was clearly positive. Landowners and farmers sell stump-root systems and logging residues for energy when they clear forest for farmland. Farmers usually outsource the clearing work to contractors.

The direct energy input of the clearing work was detected to be equal as in the earlier studies. The indirect energy input of forest biomass utilization was assessed in this study for the first time in Finland. The proportion of indirect energy input was low due to the high annual number of operating hours. For indirect energy input only the energy used in machine manufacturing was used in the calculations, because there was no sufficient data on the indirect energy input of repair and maintenance of the machines.

ACKNOWLEDGEMENTS. Dr. Hannu J. Mikkola gave valuable comments for the manuscript. University of Helsinki and Seinäjoki University of Applied Sciences provided work sites and facilities for this study. Mr John Pearce checked the English text. M.Sc. Tuomas Hakonen and M. Sc. Ismo Makkonen helped in the photograph processing.

REFERENCES

Hakkila, P. 1989. Utilization of forest residual biomass. Springer-Verlag, Berlin, 568 pp.

Hakkila, P. 2004. Wood energy technology programme in 1999–2003. The production of forest chips. Loppuraportti. *Tekes. Teknologiaohjelmaraportti* **5,** 1–135. (in Finnish)

Laitila, J., Heikkilä, J. & Anttila, P. 2010. Harvesting alternatives, accumulation and procurement cost of small-diameter thinning wood for fuel in Central Finland. *Silva Fennica* **44**(3), 465–480.

Laitila, J., Asikainen, A. & Pasanen, K. 2012. The procurement technology, logistics and carbon dioxide emissions. *Metlan työraportteja* **240,** 171–184. http://www.metla.fi/julkaisut/workingpapers/2012/mwp240.htm Accessed 16.1.2015. (in Finnish)

Laurila, J. & Lauhanen, R. 2007. The productivity and operating costs for the stump-root system harvesting and forwarding. In: Lauhanen, R. & Laurila, J. (eds.) Bioenergian hankintalogistiikka. Tapaustutkimuksia Etelä-Pohjanmaalta. *Seinäjoen ammattikorkeakoulun julkaisuja* **B33,** 68–92. (in Finnish)

Laurila, J. & Lauhanen, R. 2010. Moisture content of Norway spruce (Picea abies (L.) Karst.) stump wood at clear cutting areas and roadside storage sites. *Silva Fennica* **44**(3), 427–434.

Lauhanen, R., Ahokas, J., Esala, J., Hakonen, T., Sippola, H., Viirimäki, J., Koskiniemi, E., Laurila, J. & Makkonen, I. 2014. Mathematics for B.Sc. and M.Sc. students in forestry. *Seinäjoen ammattikorkeakoulun julkaisusarja C. Oppimateriaaleja* **6,** 1–167. (in Finnish)

Mikkola, H. 2012. Finnish field crop production for energy. Potential, energy ratios and net energy. Helsingin yliopisto, Maatalous-metsätieteellinen tiedekunta. *Maataloustieteiden laitos. Julkaisuja* **10,** 1–93. (in Finnish)

Mikkola, H. J. & Ahokas, J. 2010. Indirect energy input of agricultural machinery in bioenergy production. *Renewable Energy* **35**, 23–28.

Niskanen, O. & Lehtonen, E. 2014. Maatilojen tilusrakenne ja pellonraivaus Suomessa 2000–luvulla. Development of parcel structure and clearing of new fields in Finland in the 2000s. *MTT Raportti* **150,** 1–27. http://www.mtt.fi/mttraportti/pdf/mttraportti150.pdf Accessed 2.1.2015. (in Finnish)

Agronomy Research **13**(2), 354–360, 2015

Influence of lammas shoots on productivity of Norway spruce in Latvia

U. Neimane[1,*], M. Zadina[1], L. Sisenis[2], B. Dzerina[1] and A. Pobiarzens[3]

[1]Latvian State Forest Institute 'Silava', Rigas 111, LV2169 Salaspils, Latvia
[2]Latvia University of Agriculture, Forest Faculty, Akademijas 11, LV3001 Jelgava ,Latvia
[3]Forest Competence Centre, Dzerbenes 27, LV1006 Riga, Latvia
[*]Correspondence: una.neimane@silava.lv

Abstract. The Norway spruce is widely spread in Eastern Europe and it is managed mainly for the production of sawlogs, though its logging residues are now increasingly used for the production of wood chips for bioenergy. The growth of the Norway spruce is and will be affected by climatic changes; one of the possible effects might be an increase in the frequency of trees with lammas shoots. Therefore, the aim of this study was to assess the influence of lammas shoots on the length of height increment of young Norway spruce in Latvia. Tree height and height increment was repeatedly measured and the presence of lammas shoots, bud flushing grades and frost injuries were assessed in two young (8–13 years) open-pollinated progeny tests in the central part of Latvia (56°46´N, 24°48´E). The mean portion of trees with lammas shoots in one experiment was 6% at the end of 8th growing season. In another experiment, it was 8.7%, 26.9% and 8.1% at the end of 10th, 11th and 13th growing seasons, respectively; 32.3% of trees had lammas shoots at least in one of three seasons. Faster growing and earlier flushing trees had a significantly higher frequency of lammas shoots. Lammas shoots increased the length of annual height increment by 10 to 14 cm, resulting in a 14–20% taller tree height at the age of 13 years. The reduction of height increment as a result of frost damages for very early flushing trees was less pronounced for trees with lammas shoots than without them.

Key words: height increment, tree height, open-pollinated family.

INTRODUCTION

The Norway spruce is the most important commercial tree species in Northern European countries. It occupies 18 million ha of forest land, with a total growing stock of 2,700 million m^3 – which is a third of the wood resources in the region (Rytter et al., 2013). The Norway spruce is grown mainly for sawlog production; however, its sawdust and logging residues are increasingly used for bioenergy production. For example, the amount of wood chips produced from logging residues in Latvia's state forests has increased from 3 thousand m^3 in 2006 to 380 thousand m^3 in 2013 (Latvijas valsts meži, 2012). Harvest residues from the Norway spruce, consisting of branches and tops, are an important source of biomass energy in Finland and Sweden (Rytter et al., 2013). In Latvia, it was found that the biomass of dead and living branches forms 6.4% and 17.4% of the total above-ground biomass in 40-year old Norway spruce stand, respectively (Lībiete-Zālīte & Jansons, 2011).

Due to the economic importance of coniferous trees, a substantial amount of studies have been carried out to understand the possible effects of climatic changes on their vitality and growth (Gabrilavičius & Danusevičius, 2003; Bergh et al., 2005; Jansons et al., 2013a; Jansons et al., 2013b). Long term phenological observations in Latvia and other European countries have indicated a trend towards an earlier start of the spring (–0.54 days year^{-1}) and a longer (0.96 days year^{-1}) vegetation period (Stöckli & Vidale, 2004). This trend is predicted to continue in the future and, in combination with increasing temperatures, will lead to more frequent formation of lammas growth – additional height increment in the second half of the vegetation period. Formation of lammas shoots can lead to increased frequency of frost damages (Gabrilavičius & Danusevičius, 2003; Søgaard et al., 2011) and up to a 40% higher frequency of double leaders (Søgaard et al., 2011). In contrast, a significant correlation between the proportion of trees with lammas shoots and stem quality at provenance mean level was not found for young Norway spruce in Sweden (Danusevičius & Persson, 1998). It is suggested that the formation of lammas shoots could increase height increment of the trees (Rone, 1975), however, this effect has rarely been quantified. Therefore, the aim of our study was to assess the influence of lammas shoots on height increment of young Norway spruce in Latvia.

MATERIALS AND METHODS

The study was carried out in two Norway spruce experiments, planted on fertile abandoned agricultural land (corresponding to the *Oxalidosa* forest type), hereafter referred to in this text as 'A' and 'B', at ages of 8 and 13 years, respectively. Both experiments were located in the central part of Latvia (56°46´N, 24°48´E). According to the data from the nearest meteorological station (Skriveri) of the Latvian Environment, Geology and Meteorology Centre, long-term average annual temperature was +6.1 °C, and the sum of precipitation was on average 717 mm per year. Experiment B was located in three fields of close proximity, with slightly different soil and micro-relief conditions, hereafter referred to in this text as 'trials.' Tree height, length of the last season height increment and presence of lammas shoots were assessed at the end of the 8th growing season for 3,887 trees from 60 open-pollinated families in experiment A (October 2014), and at the end of the 10th (November 2011), 11th (October 2012), and 13th (November 2014), growing seasons for 3,412 trees from 112 open-pollinated families in experiment B. Bud flushing grade was assessed in experiment B trial 2 (1930 trees) at the beginning of 11th growing season (June 2012) using a four grade scale: grade 1 = very late flushing (length of current increment < 3 cm), grade 2 = late flushing (3–6 cm), grade 3 = early flushing (7–10 cm), grade 4 = very early flushing (> 10 cm). Also the presence (or absence) of spring frost damage on shoots was noted.

Data analysis was carried out using ANOVA, correlation and χ^2 test and the mean values ± confidence intervals were calculated.

RESULTS AND DISCUSSION

Mean height at the age of 8 years in experiment A was 117 ± 1.4 cm and height increment was 27 ± 0.6 cm. During the 8th growing season, lammas shoots formed for 6% of trees. Tree height at the age of 13 years in the each of the three trials of experiment

B was 394 ± 6.8 cm, 442 ± 5.8 cm, 439 ± 10.2 cm, and the mean height increment in the last 3 years in each of the trials was 64 ± 1.1 cm, 72 ± 0.9 cm, 80 ± 1.7 cm, respectively. Differences in height increment between the trials were statistically significant ($P < 0.001$); therefore, a separate analysis of lammas shoots (characterized as the presence of them in at least one of the three years of assessment) was carried out for each of them. The proportion of trees with lammas shoots in a particular year at the end of 10th, 11th and 13th growing seasons in experiment B was 8.7%, 26.9% and 8.1%, respectively, and lammas shoots in at least one of the assessment years were found for 32.3% of trees.

The proportion of the Norway spruce trees with lammas shoots in this study was in a range of previously reported results from other countries. For example, in Sweden, in trials at the age of 5 years, 7% of spruces from Baltic State provenances had lammas shoots (Danusevičius & Persson, 1998); in Norway, in trials at the same age, 28% of spruces from Latvian provenances had lammas shoots (Søgaard et al., 2011).

In experiment A, the proportion of trees with lammas shoots was highest (reaching 20%) in classes of trees with the largest height and height increment, but was lowest (approximately 1%) in the classes of trees with slowest growth (Fig. 1); differences between the classes were statistically significant ($P < 0.001$).

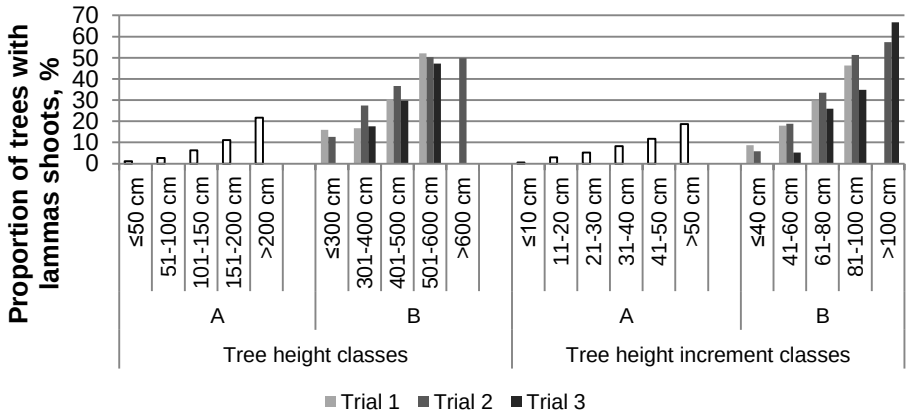

Figure 1. Proportion of trees with lammas shoots in experiment A (at the end of the 8th growing season) and B (at the end of at least one of the three assessment seasons) in different tree height and height increment classes.
In trial 1 (experiment B) trees of height increment 81–100 cm were clustered together with trees of height increment > 80 cm, and trees of height 501–600 cm were clustered together with trees of height > 500 cm.
In trial 3 (experiment B) trees of height increment 41–60 cm were clustered together with trees of height increment ≤ 60 cm, and trees of height 301–400 cm were clustered together with trees of height ≤ 400 cm.

Analyses of each of the trials in experiment B revealed a similar trend – faster growth was associated with higher frequency of lammas shoots: on average, 47–68% of the trees in the class with the largest height and mean height increment had lammas shoots, but lammas shoots were present in only 5–18% of the class with the smallest (the

slowest growing) trees. The difference in the proportion of trees with lammas shoots between the classes was statistically significant ($P < 0.001$).

A significant association between tree height and frequency of presence of lammas shoots was also previously reported in Latvia in an analysis of more than 100 stands (Neimane et al., 2015, submitted) and tree breeding trials (Rone, 1975), as well as from analysis of provenance trials in other countries (Hoffmann, 1965). Significant positive correlation ($r \approx 0.3$; $P < 0.01$) was found at provenance mean level between tree height and proportion of trees with lammas shoots in analyses of a trial including 107 Swedish and 16 Eastern European spruce provenances at the age of 5 and 9 years (Danusevičius & Persson, 1998). In experiment A of this study, the proportion of trees with lammas shoots at family mean level had significant positive correlation with height increment ($r = 0.44$; $P < 0.001$) and weaker, non-significant correlation with tree height ($r = 0.22$; $P = 0.09$). Similarly, in experiment B, the proportion of trees with lammas shoots at family mean level had statistically significant ($P < 0.01$) correlation with tree height (when all trials were analysed together ($r = 0.49$) and separately ($r = 0.41...0.71$)) and height increment ($r = 0.51$ and $r = 0.48...0.70$, respectively).

In experiment A, the height increment of the 8th growing season for trees with lammas shoots (44 ± 2.4 cm) was notably (by 68%) and significantly ($P < 0.001$) larger than for trees without them (26 ± 1.7 cm) (Fig. 2). Similarly, in experiment B, spruces with lammas shoots had significantly ($P < 0.001$) larger mean height increment of the last three years than spruces without them: mean differences in these particular trials were from 10 to 14 cm.

Figure 2. Height increment of trees with and without lammas shoots (height increment of the 8th growing season in experiment A; mean height increment of the last 3 years in experiment B).

The cumulative influence of these seemingly small differences was notable (and significant – $P < 0.001$): at the end of the 13th growing season, the height of trees with lammas shoots was on average 450 ± 11.8 cm, while those without lammas shoots averaged at 374 ± 7.8 cm in trial 1; in trial 2 – 490 ± 8.1 cm and 416 ± 7.4 cm, respectively; in trial 3 – 481 ± 16.0 cm and 420 ± 12.2 cm, respectively (Fig. 3). Thus, trees with lammas shoots were 14–20% taller than trees without them. Also, in experiment A, trees with lammas shoots were 29% taller than trees without them (148 ± 5.8 cm vs. 115 ± 1.4 cm, $P < 0.001$).

The additional height increment due to lammas shoots might be dependent on the absolute length of the height increment. To evaluate whether this was the case, in each

trial, trees with lammas shoots and trees without them were sorted according to height increments in descending order, and four groups (equal number of trees in each group) were formed. For example, in trial 2, the number of trees with lammas shoots in each group was 688/4 = 172, but without them was 1242/4 = 310. Height increment in each of the four groups was significantly ($P < 0.001$) higher for trees with lammas shoots than for trees without them in each of the trials.

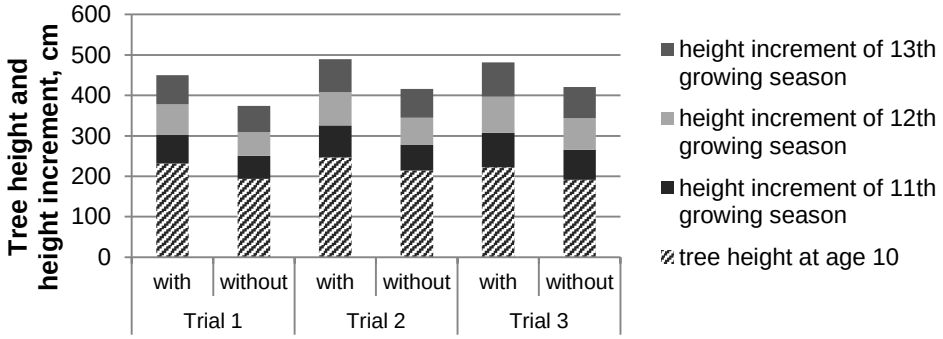

Figure 3. Height and height increment of trees with and without lammas shoots in trials 1–3 of experiment B ('with' – trees with lammas shoots; 'without' – trees without lammas shoots).

The frequency of lammas shoots was linked not only to tree height increment, but also to their bud flushing phenology: earlier flushing trees had a higher frequency of lammas shoots. For example, in trial 2, for trees with flushing grade 4 (very early), 56% of trees had lammas shoots, but in grade 1 (very late), only 22%. Within every flushing grade, the mean height increment was significantly ($P < 0.001$) higher for spruces with lammas shoots than without them (Fig. 4).

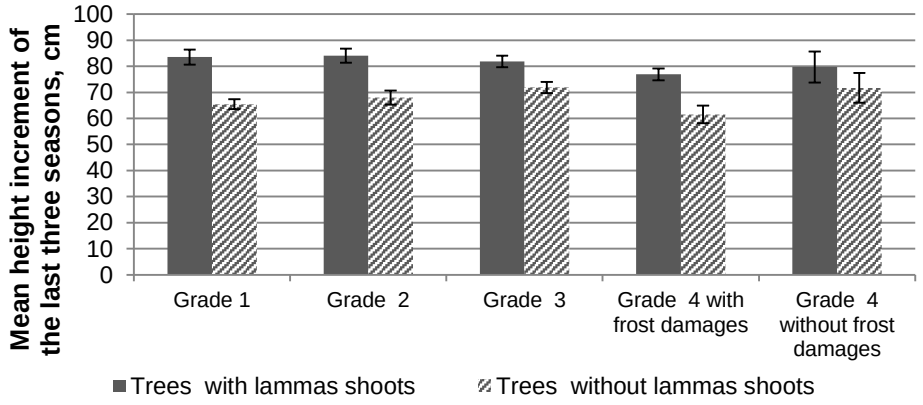

Figure 4. Height increment of the last three seasons for trees with and without lammas shoots in different bud flushing grades in trial 2 of experiment B.

This contrasts the observations by Danusevičius & Persson (1998), who found a higher proportion of trees with lammas shoots for provenances with later flushing. Frost damages were not observed for very late and late flushing trees (grades 1 and 2), but were observed for 2% of early flushing and 87% of very early flushing trees (grades 3 and 4). The reduction of height increment as a result of frost damages for very early flushing trees was less pronounced for trees with lammas shoots than for those without them (Fig. 4).

CONCLUSIONS

Results indicate that lammas shoots are linked to an increase in height increment and can reduce the impact of frost damages on the length of height increment. Increased frequency of the formation of lammas shoots due to climatic changes would raise the height increment of the Norway spruce.

ACKNOWLEDGEMENTS. The study was carried out in Forest Competence Centre's (ERAF) project 'Methods and technologies for increasing forest capital value' (No. L-KC-11-0004).

REFERENCES

Bergh, J., Linder, S. & Bergström, J. 2005. Potential production of Norway spruce in Sweden. *Forest Ecology and Management* **204**, 1–10.

Danusevičius, D. & Persson, B. 1998. Phenology of natural Swedish populations of Picea abies as compared with introduced seed sources. *Forest Genetics* **5**, 211–220.

Gabrilavičius, R. & Danusevičius, D. 2003. Genetics and Breeding of Norway Spruce in Lithuania. UAB Petro ofsetas, Vilnius, 364 pp. (in Lithuanian, English summary).

Hoffmann, K. 1965. Bedeutung des Austriebes für den Fichtenbau im Pleistozän der DDR. *Die Sozialistische Forstwirtschaft* **7**, 204–207.

Jansons, A., Matisons, R., Baumanis, I. & Purina, L. 2013b. Effect of climatic factors on height increment of Scots pine in experimental plantation in Kalsnava, Latvia. *Forest Ecology and Management* **306**, 185–191.

Jansons, A., Matisons, R., Libiete-Zālīte, Z., Baders, E. & Rieksts-Riekstiņš, J. 2013a. Relationships of height growth of Lodgepole pine (*Pinus contorta* var. latifolia) and Scots pine (*Pinus sylvestris*) with climatic factors in Zvirgzde, Latvia. *Baltic Forestry* **19**, 236–244.

Latvijas valsts meži (Latvian State Forests data). 2012. http://www.lps.lv/images/objects/committee_files/sittings/18e7853a7bd77430898021adb4f2e0e20jars_Keziks_meza_skelda.pdf. Accessed 6.12.2015.

Līviete-Zālīte, Z. & Jansons, Ā. 2011. Influence of genetic factors on Norway spruce (*Picea abies* (L.) Karst.) above-ground biomass and its distribution. In Gaile, Z. (ed): *Proceedings of the 17th international scientific conference Research for Rural Development.* LLU, Jelgava, Latvia, pp. 39–45.

Neimane, U., Zadina, M., Jansons, J. & Jansons, A. 2015. Environmental factors affecting formation of lammas shoots in young stands of Norway spruce in Latvia. *Baltic Forestry* (submitted).

Rone, V. 1975. The family and clonal selection for Norway spruce. In *Genetic Researches of Trees in Latvian SSR*. Zinatne, Riga, pp. 34–44 (in Russian, English summary).

Rytter, L., Johansson, K., Karlsson, B. & Stener, L.-G. 2013. Tree species, genetics and regeneration for bioenergy feedstock in Northern Europe. In Kellomaki, S.,

Kilpeläinen, A. & Alam, A. (eds). *Forest BioEnergy Production. Management: Carbon sequestration and adaption*. Springer, pp. 7–16.

Søgaard, G., Fløistad, I.S., Granhus, A., Hanssen, K.H., Kvaalen, H., Skrøppa, T. & Steffenrem A. 2011. Lammas shoots in spruce - occurrence, genetics and climate effects. *http://www.skogoglandskap.no/filearchive/lammas_shoots_in_spruce.pdf* Accessed 10.12.2014.

Stöckli, R. & Vidale, P.L. 2004. European plant phenology and climate as seen in a 20-year AVHRR land-surface parameter dataset. *International Journal of Remote Sensing* **25**, 3303–3330.

Agronomy Research **13**(2), 361–371, 2015

Harvest technology for short rotation coppices and costs of harvest, transport and storage

R. Pecenka* and T. Hoffmann

Leibniz Institute for Agricultural Engineering Potsdam-Bornim (ATB), Max-Eyth-Allee 100, 14469 Potsdam, Germany; *Correspondence: rpecenka@atb-potsdam.de

Abstract. The lack of knowledge regarding cost-efficient design of whole production chains as well as the availability of powerful harvest machinery are some of the main obstacles for competitive production of bioenergy from short rotation coppices (SRC) at practice. In general, two different harvest lines are available: the cut-and-chip and the cut-and-store lines. Whereas the cut-and chip line provides wood chips which have to be stored until next heating season, the product for intermediate storage of the cut-and-store line are whole trees. Both process lines have major differences not only in harvesting, but also in transport, storage and process losses leading to different costs of the end product wood chips. On basis of data from several SRC harvest campaigns, production costs for wood chips have been calculated to identify best practice solutions taking the following factors into account: chip size determined by the harvest system, storage including related costs and losses, field size and shape as well as transport to storage. According to the results, mower-chippers and forage harvesters can provide wood chips at lowest production costs (43…45 € t_{dm}^{-1}) if field shape is favourable for harvest operations. Under less favourable field conditions costs are approx. 7 to 14% higher. Highest production costs have to be accepted if whole trees are harvested with a shoot harvester (64 to 72 € t_{dm}^{-1}). The reduction in storage losses and storage costs are not sufficient to compensate higher machine costs for harvest and additional comminution with mobile chippers from forestry.

Key words: short rotation coppice, poplar, willow, harvest, costs.

INTRODUCTION

Cropping short rotation coppices (SRC) on agricultural land is a promising option for environmentally friendly production of biomass and concurrent improvement of farmer's income. Under European climate conditions fast growing trees such as poplar (*Populus sp.*), willow (*Salix viminalis*), and black locust (*Robinia pseudoacacia L.*) cultivated in SRC plantations or agroforestry systems have the potential for production of more than 10 t_{dm} $ha^{-1}yr^{-1}$ woody biomass (Scholz et al., 2011; Benetka et al., 2014; Larsen et al., 2014). Usually, the produced wood is harvested as wood chips for the production of heat in local boilers at farms or in regional heating plants. At present, approx. 50,000 ha of short rotation coppices are farmed in Europe (Pecenka et al., 2014a) respectively more than 5,000 ha in Germany (Murach et al., 2013; Wirkner, 2015). However, for the transition of cropping SRC from demonstration to agricultural practice, several problems have to be solved. Different investigations of the current situation in the management of SRC have shown that harvest costs alone represent 35 to 60% of the total costs of biomass production from SRC (Schweier & Becker, 2012a; Ehlert &

Pecenka, 2013). Several machine developments have been carried out with the target to reduce harvest costs in the last 30 year, but only few systems reached marketability (Hartsough & Spinelli 2001, Baldini & Fulvio 2009, Abrahamson et al. 2010; Berhongaray & Kasmioui 2013; Eisenbies et al. 2014).

MATERIALS AND METHODS

Analysis of harvest equipment and process lines

Harvest lines for SRC can be classified according to the level of mechanisation, the combination of process steps, the produced assortments of wood, or the rotation length (Scholz et al., 2008). With focus on the combination of process steps necessary for harvest the most successful harvest machine developments can be grouped in two different harvest lines: *1) Cut-and-Chip lines* and *2) Cut-and-Storage lines*.

Cut-and-Chip harvesting is a one-step operation converting standing biomass into wood chips using modified forage harvesters or tractor mounted respectively tractor pulled chippers. Freshly harvested wood chips have moisture contents of 50 to 60%. Therefore, wood chips have to be dried in dependence to following storage operations and later use to reduce mass losses and mould contamination (Garstang et al., 2002). Two different systems are currently used in practice for cut-and-chips lines (Fig. 1):

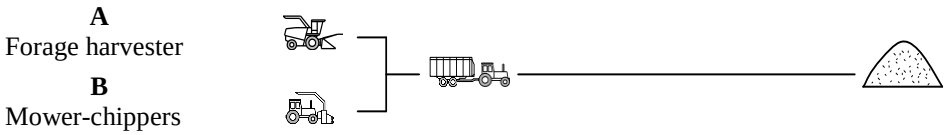

Figure 1. Cut-and-chip harvest of wood chips from SRC.

A) Forage harvesters: For harvesting SRC with self-propelled forage harvesters, these machines have to be equipped with special cutter-headers designed for cutting the trees from the stools, pushing them down to an almost horizontal position, and continuous feeding of these trees to the chipping drum of the harvester. Such machines proved to work very efficient for poplar and willow planted in single or double rows (Fig. 2). Problems have been reported from older plantations (> 3 year), bigger trees (diameter at cutting height of more than 15 cm), from very dense plantations or older plantations with naturally wider stools. The harvested material consists of wood chips with particle length between 16 to 45 mm, classified as P31S according to standard DIN EN ISO 17225-4. Several investigations regarding productivity of self-propelled forage harvesters at SRC harvest have been carried out in the last 10 years (Spinelli et al, 2009; Burger, 2010; Schweier & Becker, 2012a; Pari et al., 2013). However, it's very difficult to compare these results among each other due to the fact, that there are manifold factors influencing the productivity such as field design, age of trees and stools, rotation cycle, tree variety, location and weather conditions. In average, a productivity of 15 to 21 t_{dm} per scheduled machine hour can be expected under typical harvest conditions.

B) Mower-chippers are tractor-mounted or tractor-pulled harvest devices designed for cutting and chipping trees in a single operation comparable to harvest with forage harvesters. Several developments have been started in the last 20 year (Ehlert et al., 2013) but only very few machines have reached marketability until now. Such machines can be mounted at front- or backside of standard tractors (e.g. JENZ GMHT 140). Newer developments (e.g. ATB mower-chipper – Fig. 3 – or 'Göttinger' auger-chipper) are design for chipping trees in an upright position. Harvesting trees without pushing trees down before chipping has several major advantages: Older and very dense plantations can be harvested, damaging stools during harvest can be avoided, and in dependence to the design of the mower-chipper also trees with diameters at cutting height of 15 cm and more can be harvested. These harvesters are typically designed to produce coarse wood chips to take advantage of favourable storage and drying behaviour of bigger chips (Pecenka et al., 2014b). The harvested material consists of wood chips with length between 20–100 mm, classified as P45S according to standard DIN EN ISO 17225-4. According to investigations of Burger (2010) and Ehlert &Pecenka (2013) a productivity of 10 to 12 t_{dm} per scheduled machine hour can be expected under typical harvest conditions.

Figure 2. Modified forage harvester.

Figure 3. ATB mower-chipper.

Table 1 shows the results of different field studies in detail which have been analysed regarding costs and productivity of cut-and-chips harvest equipment used at practice.

Table 1. Productivity and costs of different machines for cut-and-chip harvest at practice (Pecenka & Schweier 2014)

A Forage harvester			
Harvest system (model/header)	Productivity (t_{dm} smh^{-1}) *	Costs (€ t_{dm}^{-1})	Reference
New Holland/FB130	10.2–21.7	12.94–27.55	Schweier & Becker 2012a
New Holland/FB130	4.2–13.2	25.19–47.30	Kern 2012
Claas/GB1	Ø 16.1	Ø 14.60	Spinelli et al. 2009
Claas/HS2	Ø 7.7	Ø 26.40	Spinelli et al. 2009
Krone/HTM	11.1–23.3	11.60–24.20	Spinelli et al. 2011
B Mower-chippers			
Auger chipper ('Göttinger')	3.4	12.27	Burger 2010
ATB Mower chipper	6.6–9.9	15.30–21.50	Pecenka & Schweier 2014

* t_{dm} … ton dry matter, smh … scheduled machine hour

Cut-and-Storage harvesting are two-step process lines which are usually known from forestry with special advantages at harvest of older trees. Commonly they are applied for trees of bigger diameter when harvest with agricultural equipment is not possible or storage of whole trees is considered as advantageous (Fig. 4).

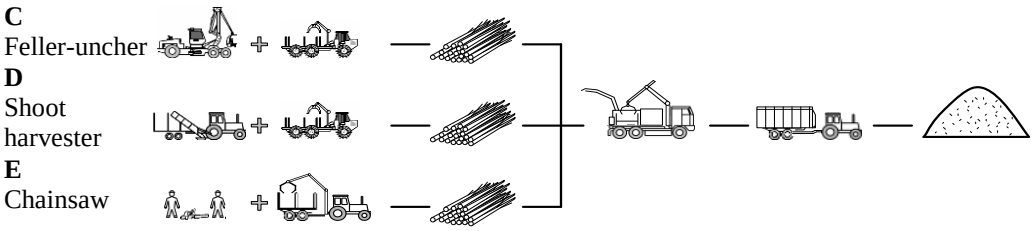

Figure 4. Cut-and-storage harvest of wood chips from SRC.

Whereas cut-and-chip lines are characterised by simultaneous mowing and comminution of the trees, cut-and-storage lines are two step harvesting with intermediate storage of trees in big piles at field site. Generally, due to the more complex process and the higher number of involved machines during harvest cut-and-storage lines have a lower productivity than cut-and-chip lines.

C) Feller-buncher / Harvest with forest equipment: Feller-bunchers (Fig. 5) are standard harvest equipment from forestry designed for harvesting smaller trees such as small or energy wood. Feller-buncher headers (e.g. Timberjack TJ 720) can be mounted on forestry harvesters to cut, collect and pile bundles of trees between the rows. Later on, a forwarder can be used to collect the tree bundles, transport them to storage place and pile them for drying by natural aeration. According to time studies from the last years (Burger, 2010; Spinelli et al., 2011) the productivity averages from 4 to 14 t_{dm} per scheduled machine hour (∅ 8.6 t_{dm}).

D) Shoot harvester are special machinery design for harvesting and collecting whole shoots (trees) from SRC (e.g. Stemster MKIII, Fig. 6). The trees are continuously cut and collected on the loading floor of the machine. If a forwarder is used for transport of trees to the storage place, the productivity of harvest can be increased. Trees with diameters of 15 to 20 cm at cutting height can be harvested. According to Schweier & Becker (2012b) a productivity of 16 to 21 t_{dm} per scheduled machine hour can be expected.

E) Manual harvest with a chainsaw: At very small fields, regional scattered fields or on very wet fields with difficult soil condition harvesting with heavy machines is not productive or often not possible. In such cases manual harvest with a chain saw is an option (Fig. 7). To increase working progress, harvest should be organised in teams of two workers – one cutting and the other pre-piling the trees for later faster collection by a forwarder. However, according to Burger (2010), Schweier & Becker (2012c) and Schneider (1995) the productivity is very low with an average of 3.6 t_{dm} per scheduled machine hour.

Table 2 shows the results of different field studies in detail which have been analysed regarding costs and productivity of cut-and-storage harvest equipment used at practice.

Table 2. Productivity and costs of different machines for cut-and-storage harvest at practice (Pecenka & Schweier 2014)

C Feller-buncher (forest harvester)			
Harvest system (model)	Productivity (t_{dm} smh^{-1}) *	Costs (€ t_{dm}^{-1})**	Reference
Valmet 921	7.7–9.6	11.50–14.30	Spinelli et al. 2011
Timberjack 1270A	Ø 5.8	Ø 12.90	Burger 2010
Hitachi EX 165	Ø 16.2	Ø 3.60	Schweier et al. 2014
D Shoot harvester			
Stemster MK III	8.1–11.3	29.23–40.78	Schweier & Becker 2012b
E Chain saw			
Stihl 026	1.6–2.3	31.80–45.50	Burger 2010
Stihl 026	0.9–1.7	43.40–81.90	Schweier & Becker 2012c
Chain saw & brush saw	0.4–0.7	105.30–184.30	Schneider 1995

* t_{dm} … ton dry matter, smh … scheduled machine hour;
** labour costs at harvest with chain saw/brush cutter 35 € h^{-1}, machine costs (chain saw) 3.73 € smh^{-1}.

Figure 5. Feller buncher.

Figure 6. Shoot harvester.

Figure 7. Manual harvest.

After storage and drying in the storage pile, the trees have to be comminuted to wood chips before transport to end user for all cut-and-storage lines. Standard mobile chipper-trucks or tractor-driven chippers from forestry can be used for this operation. According to Nahm et al. (2012), Kuptz & Hartman (2014) and Schweier et al. (2013) productivities of 40 to 110 m³ of wood chips can be reached at chipping of poplar from SRC at average costs of approx. 4 € m^{-3}.

Analysis of harvest costs

Practice experience and many time studies from different European countries have shown that powerful machinery for harvest of SRC is available. Test resp. practice conditions have been always very different at the majority of these time studies. Thus, it's difficult to compare harvest systems regarding final costs for the production of wood chips from SRC. Therefore, a cost calculation model has been developed, taking typical costs, performance data as well as different field layouts into account. For modelling typical field layouts a field model is required.

Field model: Three different typical field shapes have been used for calculation of production costs. The total size of the considered field has been kept constant (3 ha). As shown in Table 3, with increasing field length the number of necessary turnings at the end of the rows declines and the percentage of field area covered with trees (effective planting area) increases.

Table 3. Models of different 3 ha fields used for the calculation of harvest costs

	Field 1	Field 2	Field 3
Field size and shape (width x length)	3 ha (300 x 100 m)	3 ha (200 x 150 m)	3 ha (100 x 300 m)
Required headland for turning	2 x 10 m (6,000 m²)	2 x 10 m (4,000 m²)	2 x 10 m (2,000 m²)
Effective planting area	2.4 ha (80%)	2.6 ha (87%)	2.8 ha (93%)
Row length	80 m	180 m	280 m
Row distance	2.4 m	2.4 m	2.4 m
Number of rows (total)	125	63	42

Harvest performance and productivity: On the basis of own experiments and results from work times studies from literature (see Table 1 & 2) basic data for performance, productivity and costs of different harvest solutions have been compiled for calculation of production costs of wood chips from SRC. Storage and transport costs as well as losses during harvest, 6-months storage, chipping of whole trees after storage (as required for cut-and-storage lines C – E) and handling have been incorporated into the cost model (Table 4 and 5).

Table 4. Basic data for calculation of harvest costs in cut-and-chip lines

Harvest line	**A**	**B**
Cut-and-chip	Forage harvester (e.g. New Holland/FB130)	Mower-chipper (e.g. ATB mower-chipper)
Performance (ha h^{-1}) *	0.74	0.42
Productivity[1)] (t_{dm} h^{-1})	21	12
Turning time (s per row)	50	50
Machine costs (€ h^{-1})	300	150
Specific transport costs (€ t_{dm}^{-1})		
distance 5 km	10.67	10.67
10 km	15.29	15.29
Mass losses during harvest, storage and transport (%)	20	20
Planting	Poplar in single row (8,000…10,000 plants per ha) stem diameter at cutting height 6…12 cm	
Rotation cycle (years)	3	3
Annual dry matter yield/biomass growth (t_{dm} ha^{-1} yr^{-1})	10	10

* At optimum field shape conditions of field 3

Table 5. Basic data for calculation of harvest costs in cut-and-storage lines

Harvest line	**C**	**E**	**D**
Cut-and-storage	Feller-buncher (e.g. Hitachi EX 165)	Chainsaw	Shoot harvester (e.g. Stemster MKIII)
Performance (ha h^{-1}) *	0.12	0.05	0.75
Productivity[1)] (t_{dm} h^{-1})	8.6	3.6	21
Turning time (s per row)	0	0	45
Machine costs (€ h^{-1})			
Harvest machine (€ h^{-1})	95	34	300
Forwarder (€ m^{-3})	3.2	3.2	2.9…3.8
Chipper (€ m^{-3})	4	4	4
Specific transport costs (€ t_{dm}^{-1})			
distance 5 km	8.90	8.90	8.90
10 km	11.80	11.80	11.80
Mass losses during harvest, storage and transport (%)	15	15	15
Planting	Poplar in single row (4,000…5,000 plants per ha) stem diameter at cutting height 15…20 cm		Poplar in single row (8,000…10,000 plants per ha) stem diameter at cutting height 6…12 cm
Rotation cycle (years)	8	8	3
Annual dry matter yield/biomass growth (t_{dm} ha^{-1} yr^{-1})	10	10	10

* At optimum field shape conditions of field 3

RESULTS AND DISCUSSION

Results of the cost calculations including required transport of wood chips to a storage site in 5 km distance to field are shown in Table 6. For cut-and-storage lines, costs of chipping trees with a mobile chipper after storage and following transport to a storage place on farm (5 km distance) have been calculated too. Due to the fact, that wood chips from cut-and-storage lines are often transported directly to the end consumer after chipping, cost for this option are also given in Table 6.

Comparing all harvest lines, harvest of a field with optimised field shape (field 3) with a mower-chipper (line B) is connected to the lowest harvest costs (approx. 43 € t_{dm}^{-1}) at all, closely followed by harvest with a forage harvester (line A, approx. 45 € t_{dm}^{-1}). Focusing on the influence of the field shape, harvest costs under unfavourable conditions (field 1) are approx. 7% higher for the forage harvester resp. 14% for the mower-chipper.

Due to the high cost of chipping with a mobile chipper, all cut-and-storage lines (D – E) are connected to higher production costs than cut-and-storage lines (A, B). Regarding cut-and-storage, lowest costs of approx. 59 € t dm^{-1} can be realised at manual harvest with a chainsaw (line E, including transport). If the chips can be sold directly from field after chipping, these costs can be reduced to approx. 50 € t_{dm}^{-1}. Further advantages of cut-and-storage lines C and E can be seen in lower costs for cultivation due to a lower planting density and higher chip quality due to higher stem diameters at

harvest as a consequence of longer rotation cycles (8 years instead of 3 years in these scenarios – see Table 4 and 5). However, the lower planting density can reduce wood chip costs by 5 € t_{dm}^{-1} at best. If longer rotation cycles essentially improve chip quality as well as consumers are willing to pay a higher price for such chips is doubted at present. Finally, harvest with a shoot harvester (line D) is even less economic than harvest with forestry equipment due to higher machine costs and the high influence of the field layout. Harvest costs of approx. 55 € t_{dm}^{-1} have been calculated if no additional transport from field to storage is required. Due to technical limitations of available shoot harvesters a rotation cycle of 3 year has been assumed for this line. Thus, no advantages of a lower planting density or longer rotations cycles can be credited for line D.

Table 6. Production costs of wood chips from SRC

Harvest line		**Harvest costs**					
		€ t_{dm}^{-1}			€ t^{-1} (x = 30%) [2)]		
		field 1	field 2	field 3	field 1	field 2	field 3
A Forage harvester[1)]		48.1	45.1	45.1	33.6	31.6	31.6
B Mower-chipper[1)]		48.6	44.1	42.8	34.0	30.9	30.0
D Shoot harvester (Stemster)	without transport	63.5	57	55.0	44.4	39.9	38.5
	with transport[1)]	72.3	65.8	63.9	50.6	46.1	44.7
C Feller-buncher	without transport	52.4			39.9		
	with transport[1)]	61.2			46.1		
E Chainsaw	without transport	50.5			35.3		
	with transport[1)]	59.3			41.5		

All costs without travel cost for harvest equipment to field
[1)] Transport distance 5 km
[2)] x = moisture content of fresh matter

For all harvest lines no travel costs for harvest equipment have been calculated due to the fact, that service companies charge farmers very differently in dependence to travel distance from company to field. For instance, prices for distances between 100 to 200 km of 600 to 1,200 € had to be paid in Germany in the last years. If lower planting densities are chosen with the aim of using a cut-and-storage line someone should bear in mind that higher travel costs for the first harvest after 8 years alone are in the same range as possible cost reductions credited for 20 years due to optimised planting. This problem would be even more serious for cut-and-storage lines if more machinery (harvester, forwarder and mobile chipper) is required. Such disadvantages could be only partly compensated by reduced storage losses or transport operations.

In dependence to the field conditions, weather during harvest or availability of harvest equipment real harvest costs and machine performance can vary a lot. Therefore, the influence of variations of main costs factors have been taken into consideration as

well. Fig. 8 shows the influence of variations of productivity and harvest machine cost for harvest with a mower-chipper. Harvest machine costs of 150 € h^{-1} and a productivity of 0.42 ha h^{-1} have been used as basic scenario (100%). If productivity is reduced by 30%, the production costs will increase from 43 to 55 € t_{dm}^{-1}. Whereas an increase of machine costs by 30% induces an increase of production costs to 47 € t_{dm}^{-1} only.

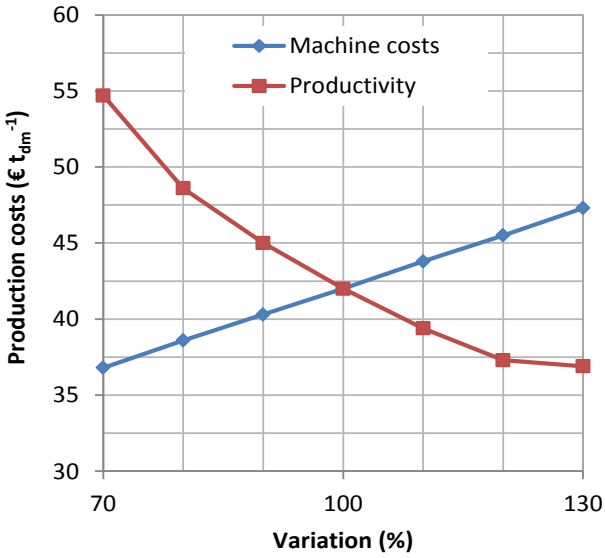

Figure 8. Influence of variations of productivity and machine costs on productions cost for harvest with mower-chippers.

CONCLUSIONS

In general, the availability of harvest equipment at farm or at least in the region where SRC's are cultivated is very important for the reduction of harvest costs. Marked prices for wood chips are a subject to high variations in dependence to the regional structure of supply from forestry and demand from heating plants or other end users. On the basis of a market price of 60 € t_{dm}^{-1} farmers can supply wood chips with profit using all harvest lines investigated in this study. However, for the calculation of sales prices for wood chips from SRC additional costs such as planting cost, rent or costs for reconversion of the plantation to conventional agricultural land (when the stools have lost its productivity) have to be taken into consideration too. According to this study, one step cut-and-chip lines are advantageous because of 20 to 40% lower costs in average compared to cut-and-storage lines. Comparing favourable cut-and-chip lines only, harvest with forage harvesters and mower-chippers are in the same cost range. But cut-and-chip lines on the basis of mower-chippers could be favourable due to lower machine investment costs connected to an improved regional availability of such inexpensive harvest equipment in future. Furthermore, travel costs for harvest with mower-chippers are much smaller because only a car trailer is required for transport and the harvest machine can be operated with standard tractors (130 to 180 KW) available on the majority of all farms. Advantages of cut-an-storage lines can be seen particularly

in longer rotation cycles and reduced costs if small fields (< 2 ha) or fields with unfavourable field shapes should be used for SRC. Among these lines, manual harvest with a chain saw showed to be best closely followed by harvest with a feller-buncher.

REFERENCES

Abrahamson, L.P., Volk, TA., Castellano, P., Foster, C. & Posselius, J. 2010. Development of a harvesting system for short rotation willow & hybrid poplar biomass crops. In: *SRWCOWG MEETING*, 18 Oct. 2010 Syracuse, USA.

Baldini, S. & Fulvio, D. 2009. Short rotation forestry: una meccanizzazione per la realiteta italiana. *Mondo Macchina* **18**, 36–43 (in Italian).

Benetka, V., Novotná, K. & Štochlová, P. 2014. Biomass production of Populus nigra L. clones grown in short rotation coppice systems in three different environments over four rotations. *IForest* **7**(4), 233–239.

Berhongaray, G., El Kasmioui, O. & Ceulemans, R. 2013. Comparative analysis of harvesting machines on an operational high-density short rotation woody crop (SRWC) culture: One-process versus two-process harvest operation. *Biomass and Bioenergy* **58**, 333–342.

Burger, FJ. 2010. Bewirtschaftung und Ökobilanzierung von Kurzumtriebsplantagen. *PhD-Thesis*. Lehrstuhl für Holzkunde und Holztechnik: Technische Universität München. 180 pp. (in German).

DIN EN ISO 17225-4 Solid biofuels – Fuel specifications and classes – Part 4: Graded wood chips. 2014.

Ehlert, D. & Pecenka, R. 2013. Harvesters for short rotation coppice: Current status and new solutions. *International Journal of Forest Engineering* **24**. 170–182.

Eisenbies, M.H., Volk, T.A., Posselius, J., Foster, C., Shi, S. & Karapetyan, S. 2014. Evaluation of a Single-Pass, Cut and Chip Harvest System on Commercial-Scale, Short-Rotation Shrub Willow Biomass Crops. *Bioenergy Research* **7**(4), 1506–1518.

Garstang, J., Weekes, A., Poulter, R. & Bartlett, D. 2002. Identification and characterization of factors affecting losses in the large-scale, non-ventilated bulk storage of wood chips and development of best storage practices. *DTI/Pub URN 02/1535*. London: First Renewables Ltd. for DTI. 119 pp.

Hartsough, B. & Spinelli, R. 2001. Recent reports on SRC harvesters in Europe. Productivities and costs of short rotation woody crops harvest technologies: projections for American plantations. *Final Report to Oak Ridge National Laboratory*. Davis, University of California, USA.

Kern, C. 2012. Untersuchung zu Produktivitäten und Kosten der Holzernte in Kurzumtriebsplantagen mit dem New Holland Feldhäcksler FR 9060 auf verschiedenen Flächen. *BSc-Thesis*. Institut für Forstbenutzung und Forstliche Arbeitswissenschaft. Albert-Ludwigs-Universität Freiburg. 85 pp. (in German).

Kuptz, D. & Hartmann, H. 2014. Throughput rate and energy consumption during wood chip production in relation to raw material, chipper type and machine setting. In: *22nd European Biomass Conference and Exhibition*, 23–26 June 2014, Hamburg, Germany.

Larsen, S.U., Jørgensen, U., Kjeldsen, J.B. & Lærke, P.E. 2014. Long-term yield effects of establishment method and weed control in willow for short rotation coppice (SRC). *Biomass & Bioenergy* **71**, 266–274.

Murach, D., Hartmann, H., Koim, N., Mollnau, C., Rademacher, P. & Schlepphorst, R. Recent experiences with agrowood in Brandenburg/Germany. In: *Intern. Agrarholz Kongress*. 19–20 Febr. 2013, Berlin, Germany. 133–144. (in German)

Nahm, M., Brodbeck, F. & Sauter, U.H. 2012. Verschiedene Erntemethoden für Kurzumtriebsplantagen, *FVA Research Report*. Forstliche Versuchs- und Forschungsanstalt Baden Württemberg. Germany. 30 pp. (in German).

Pari, L., Civitarese, V., del Giudice, A., Assirelli, A., Spinelli, R. & Santangelo, E. 2013. Influence of chipping device and storage method on the quality of SRC poplar biomass. *Biomass and Bioenergy* **51**,169–176.

Pecenka, R., Ehlert, D. & Lenz, H. 2014. Efficient harvest lines for Short Rotation Coppices (SRC) in Agriculture and Agroforestry. *Agronomy Research* **12**(1), 151–160.

Pecenka, R., Lenz, H., Idler, C., Daries, W. & Ehlert, D. 2014b. Development of bio-physical properties during storage of poplar chips from 15 ha test fields. *Biomass & Bioenergy* **65**, 13–19.

Pecenka, R. & Schweier, J. 2014. Was kostet die Ernte von KUP? Praxiserprobte Erntetechnologien im Vergleich. In: *20. Fachtagung Nutzung nachwachsender Rohstoffe*. 4–5 Sept. 2014, Dresden, Germany. (in German).

Schneider, I. 1995. Statusbericht ‚Praxisversuch Energieproduktion und –verwertung'. Bewirtschaftung, Ernte und Verwertung von Pappel- und Weiden in Kurzumtrieb. Forstliche Versuchs- und Forschungsanstalt Baden-Württemberg (Hrsg.). *Vers. Ber. AWF* **95**/1. 35 pp. (in German).

Scholz, V., Ehlert, D., Hoffmann, T., Kern, J. & Pecenka, R. 2011. Cultivation, harvest and storage of short rotation coppice – Long-term field trials, environmental effects and optimization potentials. *Journal of Agricultural Machinery Science* **7**, 205–210.

Scholz, V., Boelke, B., Burger, F., Hofmann, M., Hohm, C. & Lorbacher, F.R. 2008. Produktion von Pappeln und Weiden auf landwirtschaftlichen Flächen. *KTBL- Heft* **79**. Darmstadt: Kuratorium für Technik und Bauwesen in der Landwirtschaft. (in German).

Schweier, J. & Becker, G. 2012a. New Holland forage harvester's productivity in short rotation coppice: Evaluation of field studies from a German perspective. *International Journal of Forest Engineering* **23.** 82–88.

Schweier, J. & Becker, G. 2012b. Harvesting of Short Rotation Coppice – Harvesting Trials with a Cut and Storage System in Germany. *Silva Fennica* **46**(2), 287–299.

Schweier, J. & Becker, G. 2012c. Manuelle Ernte von Kurzumtriebsplantagen in Südwestdeutschland. *Allgemeine Forst und Jagdzeitung* **183** (7/8), 159–167 (in German).

Schweier, J., Becker, G. & Jaeger, D. 2013 Bewertung alternativer Bereitstellungsverfahren

Für Hackschnitzel aus Kurzumtriebsplantagen. In: *Intern. Agrarholz Kongress*. 19–20 Febr. 2013, Berlin, Germany. (in German).

Schweier, J., Spinelli, R., Magagnotti, N. & Becker, G. 2014. Harvesting of Hardwood with New Small-Scale Fellers and Feller-Bunchers. In: 22nd European Biomass Conference & Exhibition. 23–26 June 2014, Hamburg, Germany.

Spinelli, R., Nati, C. & Magagnotti, N. 2009. Using modified foragers to harvest short-rotation poplar plantations. *Biomass & Bioenergy* **33**(5), 817–821.

Spinelli, R., Magagnotti, N., Picchi, G., Lombardini, C. & Nati, C. 2011. Upsized harvesting technology for coping with the new trends in short-rotation coppice. *Applied Engineering in Agricultulture* **27**(4), 551–557.

Wirkner, R. 2015. Schnellwachsende Baumarten in Deutschland und deren Einsatz zur Wärmebereitstellung. In: *Anwenderseminar Ernte und Verwertung von Holz aus Kurzumtriebsplantagen*. 15 Jan. 2015 Köllitsch. Germany. (in German)

Agronomy Research **13**(2), 372–381, 2015

Environmental consequences of anaerobic digestion of manure with different co-substrates to produce bioenergy: A review of life cycle assessments

S. Pehme* and E. Veromann

Estonian University of Life Sciences, Kreutzwaldi 1, EE51014 Tartu, Estonia; *Correspondence: sirli.pehme@emu.ee

Abstract. Consequential life cycle assessment approach is needed to assess the environmental impacts of increase in biogas production. To see the full impacts of anaerobic co-digestion all possible environmental consequences caused by this change, i.e. the impacts of changed management and possible substitution impacts of substrates, should be taken into account. Generally anaerobic digestion of manure shows great environmental benefit instead of managing it conventionally, especially for the global warming potential. Environmental performance of co-digestion depends strongly on the initial use of the substrate. Co-digestion with wastes/residues has a great potential to produce bioenergy and reduce global warming potential. Co-digestion with land dependant special energy crops increases the bioenergy output but also increases the environmental impacts due to the need to substitute the substrate and thus should be avoided or limited.

Key words: life cycle assessment, biogas, anaerobic digestion, environmental impacts.

INTRODUCTION

The demand for renewable energy is continuously growing and anaerobic digestion offers a great potential to support it. Manure-biogas based energy production in the European Union (EU) is currently far below its full potential (Hamelin et al., 2014), however biogas production is planned to be increased drastically in the EU in the near future (Beurskens and Hekkenberg, 2011). Due to too low carbon (C) content of manure, the usual practice is to mix manure with C-rich co-substrate for anaerobic digestion. Environmental consequences of increased bioenergy production need to be studied comprehensively to avoid the situations where environmental impacts are higher than savings.

Life cycle assessment (LCA) is a standardised environmental assessment methodology that aims to assess the potential environmental impacts and use of resources through a product's life cycle, i.e. from raw material acquisition, via production and use phases, to waste management (ISO-14040, 2006). There are two main approaches for LCA: (i) the attributional LCA which is aimed to analyse the environmental impacts through product`s life cycle as a static system; and (ii) the consequential LCA, the aim of which is to show the environmental consequences of the decision that is assessed by the LCA. Accordingly, to assess the impact of increased biogas production, all possible environmental consequences caused by this change

should also be taken into account. If co-substrates are taken away from their initial use, it leads to environmental consequences, e.g. caused by the need to substitute them. The initial function of co-substrate may be, for example, composting, using it for animal feed or fertilizer etc. The consequences of changed management of substrates also need to be included to the analyses to see the full impacts of the change. According to the consequential approach, all impacts from taking the substrates away from their previous use, and also the consequences of substituting the marginal resources as fossil fuels, mineral fertilizers etc. should be included in the system boundaries.

However, attributional LCA is still the most commonly used LCA method and this practice can be strongly misleading for the policy-makers (Plevin et al., 2014). Attributional LCA results are often presented as comparisons of different alternatives, without accounting for the consequences each decision may cause in the real world (Plevin et al., 2014). A number of biogas LCA studies (e.g. Poechl et al., 2012; Huopana et al., 2013; Lijó et al., 2014) and some reviews have been published in recent years (e.g. Muench and Guenther, 2013; Huttunen et al., 2014), but not all the environmental consequences of changed management were considered in those studies, especially the substitution impacts of substrates was not accounted.

Based on the recent scientific literature, the goal of this study was to identify the environmental life-cycle consequences of anaerobic digestion of manure with different co-substrates, also taking into account the lost alternative of the substrates.

MATERIALS AND METHODS

LCA studies assessing environmental consequences of anaerobic digestion of manure with different co-substrates were searched from Scopus, the database of peer-reviewed scientific literature, using the key words 'biogas LCA' and 'anaerobic digestion LCA'. Selected papers were focused on full life-cycle of the anaerobic co-digestion of manure, starting from the production of substrates and the excretion of manure to application of digestate on field. Mono-digestion of manure was also included as an alternative scenario often included in co-digestion studies.

Another important criterion was that the environmental impacts of lost alternative of the substrates had to be included in to the studies. Increase in manure-based biogas production changes initial manure management chain and also the initial management of co-substrate. The consequences of lost alternatives have to be included if the goal is to measure the impacts of the change in the system. The importance of such approach in designing the system limits of biofuel LCA studies is well described in Wenzel (2009) and the general principles of consequential LCA are detailed in Ekvall and Weidema (2004).

Basic principles of system boundaries for consequential LCA of anaerobic co-digestion are visualised in Fig. 1, with an example of scenario where manure is co-digested with an energy crop.

In conclusion, the system boundaries for all the papers reviewed here (Table 1) included not only the processes directly involved in biogas production chain, but also the processes affected by the change, i.e. increased biogas production. The results of those studies are presented as net impacts, by subtracting the avoided impacts from induced impacts for each scenario. Overview of included studies in Table 1 details the studies by different co-substrates, and also specifies the country, functional unit (FU),

environmental impacts studied, and the end use of the biogas for each scenario. The FU is the reference unit for which all the environmental impacts are expressed in LCAs.

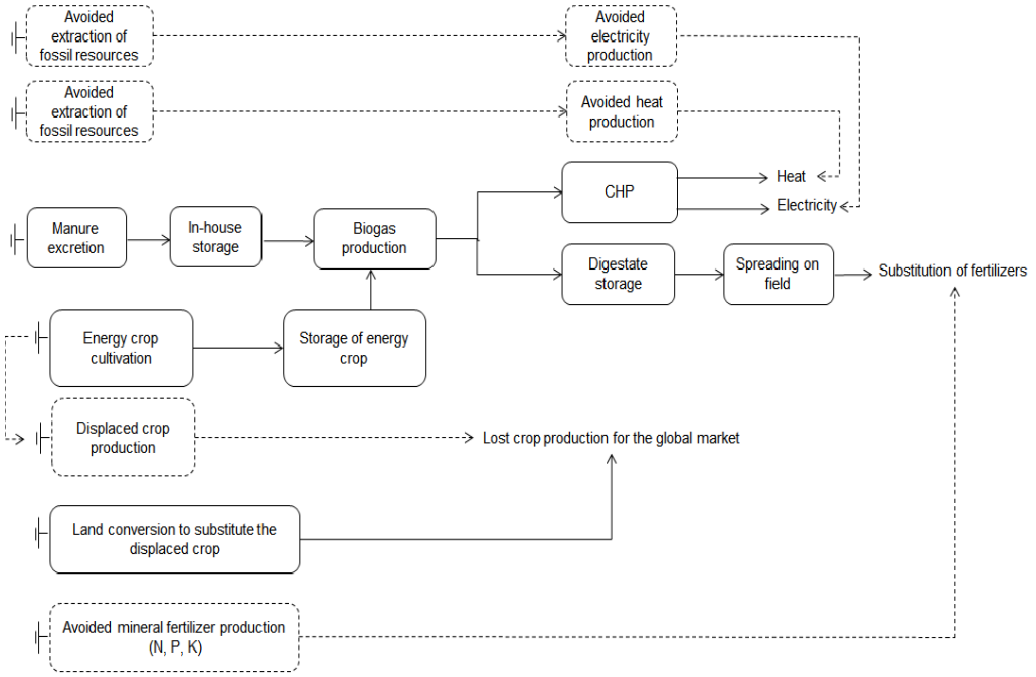

Figure 1. Example of the system boundaries for consequential LCA of the manure co-digestion with energy crop, where the produced energy is replacing the fossil electricity and heat and the energy crop production is causing additional land conversion to cropland.

RESULTS AND DISCUSSION

Environmental impact categories

Generally, the most often studied environmental impact categories of manure co-digestion LCA studies are global warming potential, acidification potential and eutrophication potential (Table 1). Also, those categories are usually investigated for agricultural LCAs (e.g. de Vries and de Boer, 2010), and reflect the main impacts of the manure management chain well. Additionally, in connection with production of co-substrates impacts, land use area and biodiversity impacts would also be relevant to include in some cases. While land occupation is rather simple to account, the biodiversity impacts are much more complex and it is not possible to do straightforward generalizations and simplifications, for that reason biodiversity is mostly excluded from LCAs. However, one of the main drivers of biodiversity loss is habitat and land use change, thus, proper methods are needed to quantify the biodiversity impacts on a global scale (De Baan et al., 2013). Using the residual grass from semi-natural grasslands for co-digestion would increase biodiversity; therefore, including biodiversity assessment would improve the environmental performance of this scenario even more than it is showed already for the global warming potential (Pehme et al., 2014).

Mono-digestion of manure

Overall mono-digestion of manure reduces environmental impacts in categories as global warming potential and resource depletion potential compared to a scenario where manure is not digested. However, for the acidification potential, eutrophication potential, and land use impacts the benefits of mono-digestion are not so clear (De Vries et al., 2012; Hamelin et al., 2014; Styles et al., 2014). Main reduction impact of mono-digestion is caused by avoided traditional manure management, and to a smaller extent, also by the fossil energy that is avoided by providing biogas-based energy.

Slurry-based biogas production has also been found to be one of the most cost-effective methods to reduce global warming potential from the life cycle perspective compared to other possible measures (Landbrug og klima, 2008), but the problem is how to assure the economical profitability of this production cycle for the companies. There are three main strategies to increase the economic feasibility of biogas (Hamelin et al., 2011): (i) to increase carbon input by using energy crops, (ii) to change housing systems to collect urine and solid manure separately to increase carbon input, (iii) to separate the slurry into a liquid and concentrated fraction and use the latter as co-substrate for slurry; (iv) to accept the lower biogas yields of mono-digestion of slurry and to compensate it with higher retention time in bigger digesters. There is also an option to use wastes/residues from other production chains but the amount of the material is limited and in some countries already in use.

Hamelin et al. (2011) compared different slurry separation technologies for biogas production and all slurry separation technologies resulted in lower or equal net impacts for all impact categories compared to traditional manure management. Environmental benefits of such practice depended strongly on the efficiency of the separation technology, as higher DM separation means higher amount of easily degradable volatile solids (VS) which leads to higher energy production and a greater displacement of fossil energy (Hamelin et al., 2011). Croxatto Vega et al. (2014) also found that slurry separation reduces the impacts for most of the categories. Slurry separation offers a good potential to reduce environmental impacts and increase biogas production, and is most likely to fit well for the countries where farmers have surplus manure and they need to transport it to longer distances.

Co-digestion with special energy crops

Maize and different grasses are the most commonly suggested energy crops for anaerobic co-digestion due to their relatively high biogas potential; accordingly they have been also included in different biogas LCAs (Table 1). One of the critical issues related to all special energy crops is their land dependency. Energy crop which is produced specifically for anaerobic digestion is most likely displacing some other crop that cannot be produced on the same land any more. Land use changes (LUC) caused by the expansion of specific crop in the area are considered as direct land use changes (DLUC) in consequential LCAs. The impacts of avoided crop production are subtracted from induced impacts of energy crop production and the result represents the net direct land use change (DLUC) impacts which can be either positive or negative, depending on the both crops and the practice. The displaced i.e. the marginal crop is the crop that will most probably be replaced by increased energy crop production. The marginal crop is for instance considered to be barley (e.g. De Vries et al., 2012; Tonini et al., 2012) or feed maize (Hamelin et al., 2014).

According to consequential rationale, the displaced production needs to be substituted and the global market will most likely react to the need by intensification, land conversion to cropland in somewhere else (Tonini et al., 2012; Hamelin et al., 2014) or the combination of both (De Vries et al., 2012). Land conversion refers to indirect land use chances (ILUC), and it has a significant climate change impact due to induced CO_2 emissions. Although co-digestion with energy crops (maize, grasses or willow) has significantly higher energy output compared to mono-digestion, this scenario results in higher climate change impact than the scenario when biogas is not produced at all, and this is caused mainly by the ILUC impact (De Vries et al., 2012; Tonini et al., 2012; Hamelin et al., 2014). Co-digestion with energy crops increases also the land use, acidification and eutrophication potential as there are more nutrients available across the flow chain (De Vries et al., 2012; Hamelin et al., 2014).

Co-digestion with substrates competing with animal feed

The environmental consequences of using the beet tails, maize silage and wheat yeast concentrate for anaerobic co-digestion instead of using the substrates for animal feed have also been studied (Table 1). All authors concluded that co-digestion with substrates with alternative use as an animal feed increased bioenergy output, but also increased most of the environmental impacts due to the need to substitute the feed. The main impact was again caused by the ILUC based on the logic described in the last section. The co-digestion with energy crops should be avoided or limited to avoid large greenhouse gas emissions due to the need to replace the fodder by more concentrate feed (Styles et al., 2014).

Co-digestion with wastes/residues

Wastes/residues considered in this study were straw, roadside grass, food wastes/household wastes and garden wastes (Table 1). Co-digestion of wastes or residues gave the best environmental performance compared to other scenarios (except the source-segregation of manure). The roadside grass co-digestion showed the best impact reduction in all categories and it was mainly caused by the avoided composting with significant amount of N_2O emissions (De Vries et al., 2012). Croxatto Vega et al. (2014) showed that the straw, which otherwise would have been left on field, has the best impact environmental reduction potential. Hamelin et al. (2014) also concluded that straw is a great option to reduce GWP, but the result was not positive for AP and EP. Food waste, bio-waste and garden waste scenarios presented GWP savings, but also higher AP and EP because of the higher nutrient content of the material (Hamelin et al., 2014; Styles et al., 2014).

Table 1. Characteristics of the studies included to review

Study	Country/context	Functional unit of the study	Environmental impacts studied*	Use of biogas
1	*2*	*3*	*4*	*4*
Mono-digestion of manure				
De Vries et al., 2012	North-Western Europe/Netherland	1 ton of substrate entering to digester	GWP, AP, EP, FFD, PMF, LU	Heat and electricity
Hamelin et al., 2014	Denmark	1 ton of manure ex-animal	GWP, AP, EP	Heat and electricity
Styles et al., 2014	UK	1 year of farm operation	GWP, AP, EP, RDP	Heat and electricity
Separated solid part of the slurry				
Hamelin et al., 2011	Denmark	1 ton of manure ex-animal	GWP, AP, EP, POF, RI	Heat and electricity, natural gas grid
Hamelin et al., 2014	Denmark	1 ton of manure ex-animal	GWP, AP, EP	Heat and electricity
Vega et al., 2014	Denmark	1 ton of manure ex-animal	GWP, AP, EP, FD	Natural gas grid
Maize				
De Vries et al., 2012 (special energy maize)	North-Western Europe/Netherland	1 ton of substrate mixture entering to digester	GWP, AP, EP, FFD, PMF, LU.	Heat and electricity
Hamelin et al., 2014 (special energy maize)	Denmark	1 ton of manure ex-animal	GWP, AP, EP	Heat and electricity
Styles et al., 2014 (fodder maize)	UK	1 year of farm operation	GWP, AP, EP, RDP	Heat and electricity
Grass				
Tonini et al., 2012 (ryegrass)	Denmark	1 ha of farmland to grow the energy crops	GWP, EP	Heat and electricity
Tonini et al., 2012 (Miscanthus giganteus)	Denmark	1 ha of farmland to grow the energy crops	GWP, EP	Heat and electricity
Styles et al., 2014 (grass silage)	UK	1 year of dairy farm operation	GWP, AP, EP, RDP	Heat and electricity

Table 1 continued

1	*2*	*3*	*4*	*5*
Straw				
Hamelin et al., 2014	Denmark	1 ton of manure ex-animal	GWP, AP, EP	Heat and electricity
Vega et al., 2014	Denmark	1 ton of manure ex-animal	GWP, AP, EP, FD	Natural gas grid
Beet tails				
De Vries et al., 2012	North-Western Europe/Netherland	1 ton of substrate mixture entering digester	GWP, AP, EP, FFD, PMF, LU	Heat and electricity
Wheat yeast concentrate				
De Vries et al., 2012	North-Western Europe/Netherland	1 ton of substrate mixture entering digester	GWP, AP, EP, FFD, PMF, LU	Heat and electricity
Roadside grass				
De Vries et al., 2012	North-Western Europe/Netherland	1 ton of substrate mixture entering digester	GWP, AP, EP, FFD, PMF, LU	Heat and electricity
Food wastes/household wastes				
Hamelin et al., 2014	Denmark	1 ton of manure ex-animal	GWP, AP, EP	Heat and electricity
Vega et al., 2014	Denmark	1 ton of manure ex-animal	GWP, AP, EP, FD	Natural gas grid
Styles et al., 2014	UK	1 year of farm operation	GWP, AP, EP, RDP	Heat and electricity
Garden waste				
Hamelin et al., 2014	Denmark	1 ton of manure ex-animal	GWP, AP, EP	Heat and electricity

*GWP – global warming potential; AP – acidification potential; EP – eutrophication potential; FFD – fossil fuel depletion; RDP – resource depletion potential; PMF – particulate matter formation; POF – photochemical ozone formation; RI – respiratory inorganics; LU – land use.

General discussion

The results of the consequential LCA depend strongly on the impacts of 'lost alternative', i.e. the initial use of the manure and co-substrate. The worse is the environmental impact of baseline situation the bigger is the possible change. If the initial use of the substrate is animal feed, there are no environmental advantages using it for biogas. Producing biogas from waste substrates, which would otherwise be composted or left on field, has a great GWP reduction potential. Still, it often does not improve the AP and EP.

If the 'lost alternative' is the food/feed crop production, then it leads to large GWP impact through ILUC, caused by the need to substitute the product. Surely, it can be argued if ILUC impact is always the case in reality, especially when there is a significant amount of unused agricultural land resource available in some countries. Also, small changes in co-substrate use will probably not affect the global market, but when planning the broader changes and long-term policies, the land use strategies need to be analysed carefully in order to have sustainable solutions for food, feed and energy production. The partial use of abandoned farmland or the restoration of opened peat-land with perennial grass would probably be an option to avoid the land competition and ILUC impacts.

Although there is no methodological consensus on how to quantify the ILUC impact (so it is rather uncertain value), it is still important to include it based on best available data.

Also the choice of the avoided marginal processes, e.g. the type of energy replaced etc. may affect the results. A consequential methodology considers the markets affected by the decisions by defining the main affected technology, e.g. the marginal technology (Ekvall & Weidema, 2004), thus the selection of the marginal energy is important as also previous LCAs have concluded (Vad Mathiesen et al., 2009). In current studies biogas is assumed to replace fossil fuels and it gives significant reduction impact, but this may not necessarily be the case in the future when more renewable alternatives might be available; this would reduce the environmental impact reduction potential of anaerobic digestion compared to present studies.

CONCLUSIONS

* Commonly anaerobic digestion of manure shows great environmental benefit instead of managing it conventionally, especially for the GWP.

* Impacts of co-digestion depend strongly on the type of the co-substrate and the initial/alternative use of the substrate. Co-digestion with wastes/residues as source-segregated solid manure, straw, garden wastes, roadside grass and food wastes is the most promising option to produce bioenergy and reduce global warming potential.

* Co-digestion with land-dependent special energy crops competing with food/feed products, e.g. maize or energy grass increases the biogas output but increases also the overall environmental impacts due to the need to substitute the substrate.

ACKNOWLEDGEMENTS. This work was supported by institutional research funding IUT36-2 of the Estonian Ministry of Education and Research.

REFERENCES

Beurskens, L.W.M. & Hekkenberg, M. 2011. *Renewable Energy Projections as Published in the National Renewable Energy Action Plans of the European Member States*.

Croxatto Vega, G.C., ten Hoeve, M., Birkved, M., Sommer, S.G. & Bruun, S. 2014. Choosing co-substrates to supplement biogas production from animal slurry-a life cycle assessment of the environmental consequences. *Bioresource Technology* **171**, 410–20.

De Baan, L., Alkemade, R. & Koellner, T. 2013. Land use impacts on biodiversity in LCA: A global approach. *International Journal of Life Cycle Assessment* **18**, 1216–1230.

De Vries, J.W., Vinken, T.M.W.J., Hamelin, L. & De Boer, I.J.M. 2012. Comparing environmental consequences of anaerobic mono- and co-digestion of pig manure to produce bio-energy--a life cycle perspective. *Bioresource Technology* **125**, 239–48.

De Vries, M. & de Boer, I.J.M. 2010. Comparing environmental impacts for livestock products: A review of life cycle assessments. *Livestock Science* **128**(1–3), 1–11.

Ekvall, T. & Weidema, B.P. 2004. System boundaries and input data in consequential life cycle inventory analysis. *The International Journal of Life Cycle Assessment* **9**(3), 161–171.

Hamelin, L., Naroznova, I. & Wenzel, H. 2014. Environmental consequences of different carbon alternatives for increased manure-based biogas. *Applied Energy* **114**, 774–782.

Hamelin, L., Wesnæs, M., Wenzel, H. & Petersen, B.M. 2011. Environmental consequences of future biogas technologies based on separated slurry. *Environmental Science & Technology* **45**(13), 5869–77.

Huopana, T., Song, H., Kolehmainen, M., Niska, H., 2013. A regional model for sustainable biogas electricity production: A case study from a Finnish province. *Applied Energy* **102,** 676–686.

Huttunen, S., Manninen, K. & Leskinen, P. 2014. Combining biogas LCA reviews with stakeholder interviews to analyse life cycle impacts at a practical level. *Journal of Cleaner Production* **80**, 5–16.

ISO-14040. 2006. Environmental management – life cycle assessment – principles and framework. International Organisation for Standardisation. Geneva, Switzerland.

Landbrug og klima. 2008. *Analyse af Landbrugets Virkemidler Til Reduktion Af Drivhusgasser og de Økonomiske Konsekvenser*. Danish Ministry of Food, Agriculture and Fisheries. Copenhagen, Denmark. http://fvm.dk/fileadmin/user_upload/FVM.dk/Dokumenter/Foedevarer/Indsatser/Klima/Rapport_Landbrug_klima_.pdf Accessed 12.01.2015.

Lijó, L., González-García, S., Bacenetti, J., Fiala, M., Feijoo, G., Lema, J. M. & Moreira, M.T. 2014. Life Cycle Assessment of electricity production in Italy from anaerobic co-digestion of pig slurry and energy crops. *Renewable Energy* **68**, 625–635.

Muench, S. & Guenther, E. 2013. A systematic review of bioenergy life cycle assessments. *Applied Energy*, **112**, 257–273.

Pehme, S., Hamelin, L., Veromann, E. 2014. Grass as a C booster for manure-biogas in Estonia: a consequential LCA. In Schenk, R. & Huizenga, D. (eds): *Proceedings of the 9th International Conference on Life Cycle Assessment in the Agri-Food Sector. American Center of Life Cycle Assessment, San Fransisco, USA, pp* 970–975.

Plevin, R.J., Delucchi, M.A. & Creutzig, F. 2014. Using Attributional Life Cycle Assessment to Estimate Climate-Change Mitigation Benefits Misleads Policy Makers. *Journal of Industrial Ecology* **18**(1), 73–83.

Poechl, M., Ward, S., Owende, P. 2012. Environmental impacts of biogas deployment – Part II: life cycle assessment of multiple production and utilization pathways. *Journal of Cleaner Production* **24**, 184–201.

Styles, D., Gibbons, J., Williams, A.P., Stichnothe, H., Chadwick, D.R., Healey, J.R. 2014. Cattle feed or bioenergy? Consequential life cycle assessment of biogas feedstock options on dairy farms. *Global Change Biology Bioenergy* (In press).

Tonini, D., Hamelin, L., Wenzel, H. & Astrup, T. 2012. Bioenergy production from perennial energy crops: a consequential LCA of 12 bioenergy scenarios including land use changes. *Environmental Science & Technology* **46**(24), 13521–30.

Vad Mathiesen, B., Münster, M., Fruergaard, T. 2009. Uncertainties related to the identification of the marginal energy technology in consequential life cycle assessments. *Journal of Cleaner Production* **17**(15), 1331–1338.

Wenzel, H. 2009. Biofuels: The good, the bad, the ugly-and the unwise policy. *Clean Technologies and Environmental Policy* **11**, 143–145.

Agronomy Research **13**(2), 382–395, 2015

Biochemical oxygen demand sensor arrays

K. Pitman, M. Raud and T. Kikas*

Estonian University of Life Sciences, Institute of Technology, Kreutzwaldi 56, EE51014 Tartu, Estonia. *Correspondence: timo.kikas@emu.ee

Abstract. Biochemical oxygen demand (BOD) is one of the most widely utilized parameters in water quality evaluation. BOD as a parameter illustrates the amount of organic compounds susceptible to biochemical degradation in the water. The BOD test lasts for at least 5–7 days or even up to 21 days. An incubation time this long is not acceptable for monitoring purposes or system control. In order to shorten the BOD measurement time, a multitude of biosensors have been proposed. Unfortunately, BOD biosensors have several limitations, such as short lifetime, limited substrate range, precision etc. Some of those limitations can be overcome by using microbial sensor-arrays. Such bioelectronic tongues can achieve the much wider substrate range usually attributed to multiculture sensors and still maintain the long lifetime of a single culture sensor. This is achieved by separating different cultures from each other in the array and using the signals of separate sensors to produce summarised information via statistical analysis. The purpose of this review is to give a short overview of BOD measurements and discuss the potential of using sensor-arrays for BOD measurements.

Key words: sensor-array, BOD sensor-array, electronic tongue, biosensor, biochemical oxygen demand.

INTRODUCTION

Water quality monitoring is an important aspect of water management with regard to pollution control. One of the most important water quality parameters is biochemical oxygen demand (BOD). This parameter was first introduced in 1917 and published in *Standard Methods* (Bourgeois, 2001). BOD is determined by means of an empirical test in which standardized laboratory procedures are used to determine the relative oxygen requirements of wastewater, effluents and polluted waters (APHA, 1985; Tan & Wu, 1999; Bourgeois, 2001). The standardized test measures the oxygen required for the biochemical degradation of organic material and the oxygen used to oxidize inorganic material, such as sulphides, ferrous iron and reduced forms of nitrogen, unless their oxidation is prevented by an inhibitor (APHA, 1985). The results of a BOD test characterize the total content of biochemically oxidizable organic substances in the water as well as the ability of the water to self-cleanse (Ponomareva, 2011).

In a standardized BOD test, a sample is placed in a full, airtight bottle and incubated under the specified conditions (20 ± 1 °C, in the dark) for a specific time (APHA, 1985). The incubation period is 5 or 7 days according to the American (APHA, 1985) or Swedish standard (Liu & Mattiasson, 2002), respectively. The BOD value is calculated based on the difference between the initial and final dissolved oxygen concentrations (APHA, 1985; Liu & Mattiasson, 2002). The BOD value is measured in milligrams of

oxygen per litre or cubic decimetre ($mgO_2\ l^{-1}$ or $mgO_2\ dm^{-3}$). The BOD_5 values in surface water layers usually fall into the range of 0.5–4 mg l^{-1} (Ponomareva, 2011), while in industrial wastewaters BOD_5 may be as high as 30,000 mg l^{-1}. The precision of the method is around 15–20% (Namour & Jaffrezic-Renault, 2010).

The BOD test has been the most widely used method to measure organic pollution in water samples because of its wide applicability to different type of samples as well as its simplicity (Liu, 2014), since it requires no expensive equipment. However, due to the prolonged incubation time, it is not suitable for the monitoring or control of wastewater treatment systems where fast feedback is necessary (Raud, 2012a).

One way to overcome the long delay between the measurements and the results is to use biosensors. Depending on the measurement method, BOD biosensors can give results within 5 to 30 minutes (Kim, 2006; Kibena, 2012). Many papers on BOD biosensors have been published and these biosensors have been developed and marketed by various manufacturers in both biofilm and bioreactor-type configurations (Rodriguez-Mozaz, 2006). The purpose of this paper is to give an overview of the biosensors used in BOD measurements and to direct more attention to the possibility of using sensor-arrays for BOD measurements.

BIOSENSORS FOR BOD

A biosensor is defined as a self-contained integrated device capable of providing specific quantitative analytical information. A biosensor consists of a biological recognition element (Luong, 2008; Lagarde & Jaffrezic-Renault, 2011; Su, 2011), which is in direct spatial contact with a transduction element (Thévenot, 2001; Xu & Ying, 2011). A variety of transducers have been used in biosensors, such as electrochemical, colorimetric, optical, acoustic, luminescence, and fluorescence transducers. Furthermore, different biological sensing materials have also been used, such as microorganisms, tissues, organelles, receptors, enzymes, antibodies, nucleic acids, aptamers, cofactors, etc. The most frequently used ones are enzymes and microorganisms (D'Souza, 2001; Kissinger, 2005; Su, 2011).

The first BOD biosensor was reported by Karube in 1977 (Karube, 1977). It consisted of a dissolved oxygen electrode and a membrane impregnated with the yeast *T. cutaneum*. Since then, many BOD biosensors based on various measurement principles and biological sensing elements have been reported. Various microorganisms, including yeasts and viable cells of bacteria such as *Arxula adeninivorans, Bacillus polymyxa, Bacillus subtilis, Candida, Escherichia coli, Hansenula anomala, Issatchenkia, Klebsiella, Pseudomonas fluorescens Pseudomonas putida, Saccharomyces cerevisiae, Serratia marcescens, Torulopsis candida, Trichosporon* etc., have been used for the construction of BOD biosensors (Liu & Mattiasson, 2002; Raud, 2010b; Lagarde & Jaffrezic-Renault, 2011; Ponomareva, 2011). Microorganisms have been used in the form of a single pure culture, mixtures of several pure cultures, or mixed cultures, such as activated sludge or the BODSEED culture (Tan & Wu, 1999; Rastogi, 2003). BOD sensors based on a single strain have relatively good stability and a long service life (Kim, 2006), but the sensor-BOD value will be limited due to the narrow substrate spectrum of one microbial strain (Liu & Mattiasson, 2002; Raud, 2012), which may lead to an underestimation of BOD. In order to construct a BOD biosensor with a wider substrate spectrum, mixtures of several microbial strains or mixed cultures have

been used (Suriyawattanakul, 2002). However, compared to single strain biosensors, mixed culture biosensors have decreased stability and a shorter service life due to the different life-spans and growth rates of various microorganisms used in consortia (Liu & Mattiasson, 2002). Thermally killed cells have been used to overcome the instability of microbial consortia and to achieve a longer service life for biosensors (Ponomareva, 2011). Thermally killed cells do not need a periodic nutrients supply. On the other hand, living cells need careful maintenance and a supply of nutrients and minerals during storage (Liu & Mattiasson, 2002).

Most of the reported BOD biosensors fall into one of two types – biofilm and respirometric (also called bioreactor-type) biosensors. Biofilm-type BOD biosensors are based on measuring the change in the dissolved oxygen concentration due to the respiration of microorganisms in the proximity of the transducer (Ponomareva, 2011). Microorganisms may be immobilized directly onto the transducer or immobilized and placed as a separate film or membrane in close proximity to the transducer. The transducer is most commonly a dissolved oxygen sensor. Respirometric or bioreactor-type biosensors, on the other hand, are biosensors where the microorganisms are not attached to the transducer but float freely in the measurement solution and the dissolved oxygen concentration is measured directly from the solution. These systems provide a constant measurement of the respiratory activity of a microbial suspension (Ponomareva, 2011).

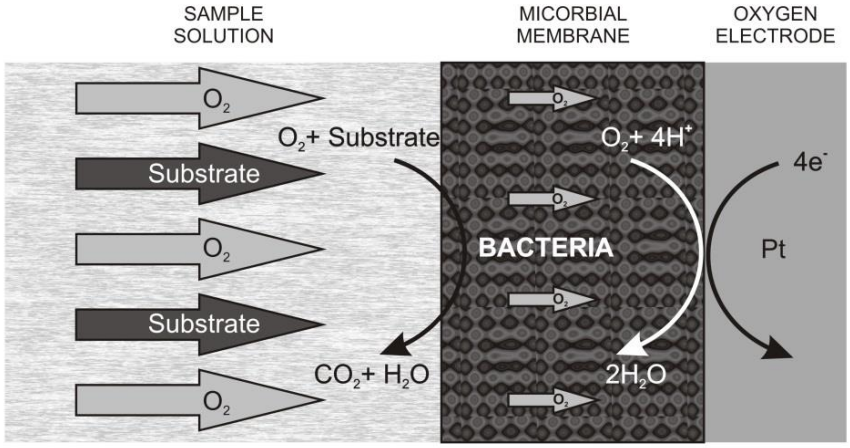

Figure 1. The basic principle of a microbial biosensor based on an amperometric transducer.

The working principle of a typical biofilm-type BOD biosensor is illustrated in Fig. 1. The microorganisms are immobilized or placed onto the oxygen electrode and the biosensor in immersed in the measurement solution. In a clean measuring solution the biosensor achieves a steady state current slightly lower than in the measurement medium, as most of the dissolved oxygen diffuses through the membrane but some is used up by microorganisms. When a sample containing biodegradable substrates is added to the measuring solution, the microorganisms start using oxygen for the assimilation of substrates at a certain rate and the measured oxygen concentration

decreases to a new and lower steady state. The decrease in the concentration of dissolved oxygen is proportional to the concentration of added biodegradable substrates. Based on the decrease in measured oxygen concentration, BOD can be calculated (Liu & Mattiasson, 2002).

With both biosensor types, the signal can be analysed using either the steady-state method or the kinetic method. The first one derives BOD from the current difference between two steady states, before and after adding the sample. It is often also called the end-point method. The kinetic method, on the other hand, uses the time derivative of the current right after the addition of the sample, and is also known as the initial rate, quasi-kinetic or dynamic transient method (Pasco, 2011).

The duration of measurement is 5–25 min in the stationary mode and 15–30 s with the initial rate method (Ponomareva, 2011). Recovery time is 15–60 min in the stationary mode and more than 10 min when using the initial rate method (Liu & Mattiasson, 2002). Hence, the initial rate method is preferable where a constant BOD monitoring is necessary, for example, when controlling a wastewater treatment plant or analysing a large number of samples (Ponomareva, 2011). The sensitivity of the initial-rate method, however, is twice as high as that of the stationary mode (Liu & Mattiasson, 2002).

The BOD values gained from BOD sensors do not always match the conventional BOD results due to differences in the measuring principles. The conventional BOD test has an incubation time of 5 or 7 days. In the course of this time the microorganisms can assimilate easily degradable compounds but also they have time to induce the necessary enzymes for the degradation of refractory compounds. However, during the short measurement time of a biosensor, the immobilized microorganisms are able to assimilate and thereby detect only easily degradable compounds, which may result in an underestimation of BOD values.

The problem with the underestimation of BOD could be overcome by choosing a suitable calibration solution. The most common calibration solutions are: a solution of equal parts of glucose and glutamic acid (GGA) (Ponomareva, 2011) and a synthetic wastewater according to the recipe established by the Organisation for Economic Cooperation and Development (OECD). Due to its simple composition, the GGA solution is unsuitable for studying samples of a more complicated composition (Liu & Mattiasson, 2002). Better results have been obtained with the OECD synthetic wastewater, as its composition closely resembles that of municipal wastewater (Liu & Mattiasson, 2002). Other artificial wastewaters have also been used for the calibration of BOD sensors (Chee, 2005; Chee, 2007). The ideal calibration solution would be as close to the composition of the wastewater to be analysed as possible (Liu, 2000; Liu & Mattiasson, 2002). Therefore, there is no universal calibration solution; rather, it must be chosen based on the composition of the sample to be later analysed.

Other ways to achieve a better match between the BOD values measured by different methods consist in preselecting microorganisms that have wide substrate spectra and are able to assimilate specific refractory compounds found in wastewater, or pre-incubating the living cells in a solution whose composition is similar to the sample to be analysed (Liu & Mattiasson, 2002). The pre-incubation helps living cells to start producing the enzymes that otherwise would not be present in the cells, thus widening their substrate spectrum.

BIOSENSOR ARRAYS

The principle of sensor-arrays is based on an analogy to the biological organization of the olfactory and taste systems of mammals, where millions of nonspecific receptors in nose and taste systems respond to different substances. The idea of artificially reproducing the natural response of a human to environmental stimuli was first published in 1943 (Vlasov, 2005); however, the first attempts to design an artificial olfactory system for smell were made in the 1960s (Vlasov, 2008), while non-specific sensor-arrays became commercially available in the mid-1990s (Bourgeois, 2003). According to the IUPAC (The International Union of Pure and Applied Chemistry) definition, 'an electronic tongue is a multisensor system, which consists of a number of low-selective sensors and uses advanced mathematical procedures for signal processing based on pattern recognition and/or multivariate data analysis' (Vlasov, 2005; del Valle, 2010). The basic principle of a sensor-array is shown in Fig. 2. Each sensor in an array produces an individual signal, which may not always correlate with the samples' composition. The summarised signal of the sensor-array is analysed using statistical multivariate analysis methods, which enable extracting qualitative and quantitative information about the samples. Arrays of gas sensors are termed 'electronic noses' while arrays of liquid sensors are referred to as 'electronic tongues' (Escuder-Gilabert & Peris, 2010).

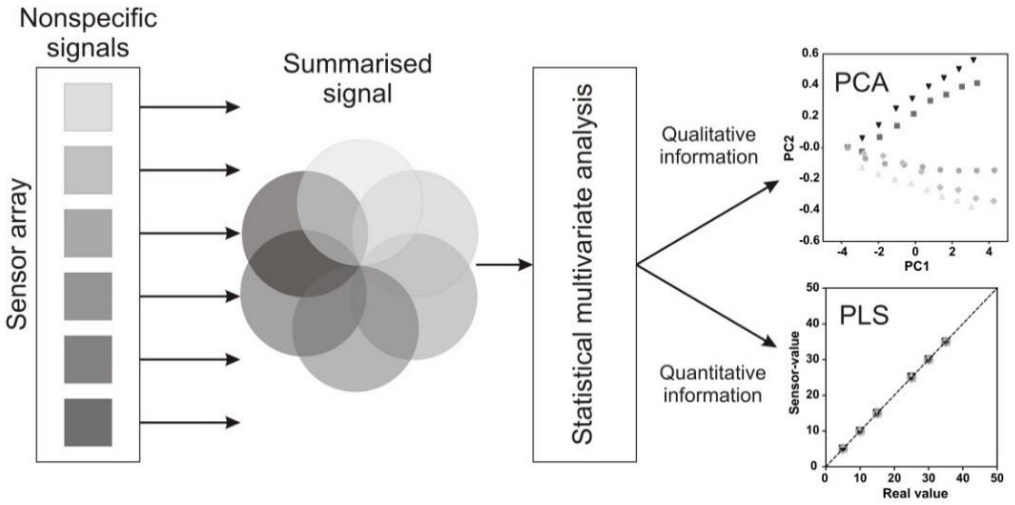

Figure 2. The working principle of a sensor array.

The most typical feature shared by electronic nose and electronic tongue systems is that an array of low selective and cross-sensitive sensors is conjugated with data processing and pattern recognition methods (Vlasov, 2008). Cross-sensitivity in this context is the ability of a sensor to respond to a number of different compounds in a solution and produce a stable response in the sample (Vlasov, 2005). Thereby, when the sensors are responding to several different substrates, the sensor-array creates a chemical image of the sample (Hruškar, 2010) or a signal pattern, which can be related to certain features or qualities of the sample (Krantz-Rülcker, 2001). In this way, the limited selectivity of each individual sensor will be compensated by the data processing, which

allows the determination of a species in the presence of its interference (del Valle, 2010). Electronic tongues are a powerful tool in the rapid assessment of information of complex solutions (Riul Jr, 2010).

Various sensing principles can be employed in sensor-arrays. The most widespread are electrochemical (del Valle, 2010) and optical sensors (Krantz-Rülcker, 2001; Vlasov, 2005; Witkowska, 2010); however, other techniques, such as surface acoustic waves (Krantz-Rülcker, 2001), piezoelectric mass sensors (del Valle, 2010) etc. have been reported. Usually, a single sensor-array consists of sensors of the same type; however, sensors based on different principles of signal transduction may be used in the same sensor-array. The number of sensors in the array may vary from 4 to 40 (Vlasov, 2005), depending on the analytical task and the number of different sensing materials available. Usually, a sensor-array consists of an excessive number of sensors compared to the analytes to be detected and is thereby applicable to different analytical tasks (Vlasov, 2005).

Various biosensor-arrays have been developed for different purposes. Several biorecognition elements can be used for biosensor-arrays, for example, microorganisms, cofactors or enzymes. The most widely used biorecognition elements are enzymes belonging to the classes of oxidoreductases and hydrolases (Solna, 2005). Enzymatic biosensor-arrays are promising pre-screening methods for rapid and simple measurements and an express analysis of many pollutants, which can function either directly as substrates or as inhibitors of the enzymes selected for the sensing array (Solna, 2005).

Multisensor electronic tongue systems are suitable for a diversity of analytical tasks, both conventional and nonconventional for chemical sensors. In recent years, much attention has been given to electronic tongue applications such as industrial and environmental monitoring, and quality control (Vlasov, 2008) (e.g. fermentation processes), as electronic tongues are capable of fast, inexpensive, automated and on-line control (Witkowska, 2010).

SENSOR-ARRAY DATA ANALYSIS

In case of a single biosensor, the linear regression model (LRM) is often used for data analysis (Badertscher & Pretsch, 2006). However, since sensors used in the array may respond to all analytes, a vast amount of multidimensional information is generated (del Valle, 2010). This complex data can be processed using multivariate analysis methods (del Valle, 2010; Vlasov, 2008). Multivariate treatment makes it possible to transform the complex responses of a sensor-array into a format that is easier to interpret. It has been shown that the use of biosensor-arrays with multivariate analysis can be a promising approach for simple, fast, reproducible, selective and sensitive detection of different compounds in various samples and provides both a qualitative and quantitative overview of sample compositions (Solna, 2005).

Qualitative information from sensor-array data is used for the classification and identification of samples. The most commonly used method for this purpose is the principal component analysis (PCA), which is widely used in statistical analysis to present the data (Riul Jr, 2010). PCA makes it possible to explore multivariate data and reduce its noise without loss of information; in addition, the significance of individual components can be assessed (Riul Jr, 2010). PCA is a linear multivariate analysis method

(Hines, 1999; Solna, 2005) whose mathematics is based on matrix algebra (Massart, 2004). PCA decomposes the initial data matrix into latent variables in such a way as to preserve as much variance as possible in the first principal components (PCs). Through this method, loading and score plots can be produced which show the relationship between the variables and the samples, respectively, as well as their influence on the system. The groupings in the score plot can be used for classification, since the more similar samples are grouped together (Krantz-Rülcker, 2001). PCA requires no prior knowledge of the samples and the data is presented in as few variables as possible.

In order to extract quantitative information from biosensor-array signals, a multivariate calibration method must be applied to connect the observed signals with the identity of an analyte and its concentration. However, for the calibration of sensor-arrays, a large amount of various samples are needed in order to divide the samples into two sets: training and test samples. There are several multivariate regression models for calibration available – these can be either linear or non-linear methods (Nascu, 1999). The most widely used methods are partial least squares (PLS) and principal component regression (PCR), which are both factor-based (Correia, 2005) linear calibration methods. PCR is conducted in a similar manner to PCA; however, when used in calibration, PCR performs a linear least squares regression of the dependent variable against the scores of the significant PCs (Hibbert, 1998). On the other hand, in PLS, a principal component analysis is performed on both the dataset and the corresponding actual values (Krantz-Rülcker, 2001). The difference between PCR and PLS is that PLS includes information about the function vector in the model while PCR does not (Hines, 1999). PLS is specially devised for quantification purposes and mainly used in multi-determination applications (del Valle, 2010). The partial least square (PLS) regression method is very useful in predicting a set of dependent variables from a large set of independent variables (Hruškar, 2010).

In case of non-linear data, other methods for data treatment are required. For non-linear data, artificial neural networks (ANNs) methods are widely used. ANN is a massively parallel computing technique, especially suited to non-linear sensor responses and very similar to human pattern recognition (del Valle, 2010). ANNs are distributed computing systems composed of processing units connected by weighted links that can be assembled in one or more layers, resembling the structure and functioning of the human brain (Hruškar, 2010; Riul Jr, 2010). Thereby, ANN creates models that are non-linear (Hibbert, 1998; Krantz-Rülcker, 2001; Hruškar, 2010) and non-parametric (Hines, 1999).

BOD SENSOR-ARRAYS

Various types of BOD sensor-arrays have been reported. Not all of them are based on biosensors but also chemical sensors have been applied. Some BOD sensor-arrays are outlined in Table 1.

Table 1. Overview of BOD sensor-arrays

Transducer	Sensor modification method	Immobilization method	Calibration solution	Application	Data analysis
Clark-type oxygen electrodes (Yang, 1997)	*Trichosporon cutaneum*	Photo-crosslinkable resin ENT-3400	GGA	BOD	Calibration graph
Polypyrrole conducting polymer sensors (Stuetz, 1999) (Bourgeois & Stuetz, 2002)	N/A	N/A	Wastewater samples	BOD	ANN, PCA
The sensor chip with four platinum containment electrodes (König, 2000)	*Sphingomonas yanoikuyae* B1, *Candida parapsilosis*,	Poly(vinyl alcohol) - PVA	Synthetic wastewater	BOD, PAH*	Calibration graph
Polypyrrole conducting polymer sensors (Onkal-Engin, 2005)	N/A	N/A	Wastewater samples	BOD	Multiple discriminant analysis, canonical correlation analysis, ANN
8 screen printed Pt and Pt-graphite electrodes (Tønning, 2005)	Enzymes: tyrosinase, horseradish peroxidase, acetyl cholinesterase and butyryl cholinesterase	cross-linking with glutaraldehyde	N/A	N/A	Drift correction, PCA
CCD camera (Sakaguchi, 2007)	*Photobacterium phosphoreum* IFO 13896	Sodium alginate gel	GGA	BOD	Linear calibration graphs
8 metal electrodes (Au, Pt, Rh, Ir, Ag, Ni, Co, Cu) (Campos, 2012)	N/A	N/A	Wastewater samples	BOD, COD*, NH_4-N, PO_4-P, SO_4-S, acetic acid, alkalinity	PLS
Clark-type oxygen electrodes (Raud & Kikas, 2013)	7 different microorganisms	Agarose	OECD synthetic wastewater	BOD	Sheffe test, PCA, PLS

*PAH – polycyclic aromatic hydrocarbons, COD – chemical oxygen demand.

Stuetz and colleagues used a non-specific electronic nose, which consisted of 12 electrodes coated with a polypyrrole-based conducting polymer doped with different dopants to monitor wastewater samples. The concentration of biodegradable organic matter as determined by BOD was measured in samples collected from different parts of the wastewater treatment facility. The BOD values were derived from the odour profiles of different samples and ANN was applied for data analysis. The results were compared to the corresponding conventional 5-day BOD values and a good correlation was obtained. However, a linear correlation between the sensor responses and BOD was only evident for up to 4 weeks (Stuetz, 1999). A similar approach of using a polypyrrole-based conducting polymer sensor-array for odour analysis was also applied later to a BOD analysis (Bourgeois & Stuetz, 2002; Onkal-Engin, 2005). In that study, a good correlation between odour and the corresponding BOD values as well as good classification accuracy were achieved. However, classification was difficult due to the large variability of wastewater, especially in facilities where domestic and industrial loads frequently alternated (Onkal-Engin, 2005).

Campos and colleagues applied a voltammetric electronic tongue, which consisted of 8 electrodes made of different metals, and PLS was used for data analysis to monitor various parameters in the influent and effluent of the wastewater treatment plant. The sensor-array showed relatively good predictive power for the determination of some parameters; therefore it might be possible to use this technology for semi-quantitative analysis (Campos, 2012).

A biosensor-array utilizing different enzymes was used to extract qualitative information, i.e. to study the quality of the wastewater treatment. However, the sensor performance was not easily characterized due to its decreasing sensitivity over time and the effect of inhibiting compounds. These problems were mitigated by using drift correction algorithms (Tønning, 2005).

One of the first biosensor-arrays with immobilized microorganisms was reported by Yang and colleagues, who used thin film technology to prepare miniaturized Clark-type oxygen electrodes. This dual-type BOD sensor consisted of two oxygen electrodes – one cathode functionalized with yeast and the other without it – and two anodes. The yeast *Trichosporon cutaneum* was immobilized onto the cathode with photo-crosslinkable resin and the GGA solution was used for sensor calibration, while the difference between the outputs of the two oxygen electrodes was used to estimate the BOD. The sensor was also used for an analysis of real samples and the results obtained were in good correlation with the conventional 5-day BOD values (Yang, 1997).

A different approach was employed by Sakaguchi, who used a biosensor-array based on immobilized luminous bacteria in arrayed holes on a microchip. Several different samples were analysed at the same time, since only one strain was used in all the micro-holes. The system used a digital CCD camera to detect the luminescence as well as a mobile PC, making on-site measurements available (Sakaguchi, 2007).

Konig and colleagues immobilized two different microbial strains, one of which was a PAH-degrading bacterium, into separate platinum electrode cavities. The biosensor chip was integrated into a flow-through system to measure the oxygen consumption of the immobilized microorganisms. Good correlations of BOD_5 and sensor-BOD results were achieved. In addition, while both strains responded to glucose, only the PAH-degrading strain gave signals with a naphthalene solution; as a result, the naphthalene concentration was successfully estimated with the sensor-array. Although

high concentrations of toxic substances were supposed to be present, none of the microbial sensors showed any decrease in sensitivity after measurements with these real samples (König, 2000).

Seven microbial cultures were used to construct a biosensor-array to measure BOD in different synthetic wastewater samples containing refractory compounds. The Scheffe test, PCA and multivariate calibration methods were applied to extract qualitative and quantitative information about the different biosensors and wastewater samples. A good correlation between sensor-array measured BOD values and BOD_7 values was obtained. In addition, PCA enabled the separation of samples according to their type and BOD_7 value, making it possible to extract qualitative information about the samples (Raud & Kikas, 2013).

DISCUSSION

Despite the fact that the first BOD biosensor was developed 38 years ago, investigation and development of new devices is still active. The majority of BOD biosensors use microorganisms or a combination of microorganisms as a biological recognition element. Therefore, one main field of study is finding the most suitable microbial cultures for any particular analytical purpose. However, a single culture does not have sufficiently wide substrate spectrum to analyse diverse samples despite the fact that a single culture is more stable than a consortium of several bacterial cultures. To overcome this problem, several sensor-arrays have been proposed for BOD measurements. The first proposed sensor-arrays did not make use of statistical analysis and were thus cast aside. The second wave of sensor-arrays did use statistical analysis, but also utilized chemical sensors with no specificity of the biorecognition element. This led to a summarised signal with no qualitative information. Only in recent years have sensor-arrays been proposed that utilize both statistical multivariate analysis and specific biorecognition elements. Biosensor-arrays utilizing a variety of microorganisms make it possible to conduct measurements with several cultures at the same time, which helps to save time, since information from several biosensors is received simultaneously and a more complex signal is obtained. Applying a multivariate statistical analysis to this kind of signal will yield both more accurate quantitative information and qualitative information.

There is a need for the development of new on-line monitoring techniques, since the standard BOD test is too time-consuming for process control in water treatment systems. On-line measurements are available when automated biosensor-arrays are used. Automated measurements, fully controlled by the computers, are noticeably less labour-intensive and thus measurement precision increases since human error is minimized.

Many new technologies, such as screen-printing and microfabrication, are available that enable the construction of miniaturized biosensor-arrays. Smaller, miniaturized biosensor-arrays lead to less chemical usage and consequently cheaper measuring technology. In addition, using smaller sensors makes it easier to develop portable devices, which enable conducting field measurements. Small but automated on-line biosensor-arrays like these can give real-time information about wastewater parameters and make it possible to operate the treatment plants over the network.

New data analysis methods provide other ways to interpret biosensor-array results. It has been shown that various multidimensional data analysis methods are making it

possible to extract more information from data than ever before. Various classification, calibration and information extraction methods are available, some of which do not require linear models and are even self-learning, such as ANN. Data analysis has become more complex, using sensor-arrays instead of a single biosensor. However, biosensor-arrays with complex data analysis provide more precise results.

Still, there are more problems to be solved. Sensor drift is a big problem with sensor-arrays. It may be caused by the ageing of a sensor, temperature or pressure changes, or the ageing of the biological recognition element (Bourgeois, 2003). Achieving a longer and more stable service life for biological recognition elements, guaranteeing easy and effective maintenance of the measurement system, and overcoming the toxic effect of samples to microorganisms are just a few of those challenges. Another problem, a political one, lies in the fact that it takes time before new devices and methods are accepted by governments and proper legislation is issued to encourage the use of biosensor-array systems.

CONCLUSIONS

Biosensors have been investigated for more than thirty years. Over that time a number of biosensors for the determination of a variety of analytes have been developed, out of which BOD biosensors are probably the most widely reported microbial biosensors. In the past decade various sensor-arrays comprising a set of different sensors and multivariate analysis methods for signal analysis have been developed. Sensor-arrays have been used for BOD measurements; however, there is still room for development. By combining several technologies, such as the application of several specific microorganisms, the miniaturization of sensors and sensor-arrays, the flow-through technology, and the complex multivariate technology for data analysis, superior results could be achieved. A biosensor-array of that kind would be small and fully automated, and precise, multifaceted information could be obtained about the samples.

ACKNOWLEDGEMENTS. Financial support for this research was partially provided by the Estonian Environmental Investment Centre and by 'Integrated Biosystems Engineering', a topic receiving base funding.

REFERENCES

APHA. 1985. *Standard methods for examination of water and wastewater*. Washington American Public Health Association.

Badertscher, M. & Pretsch, E. 2006. 'Bad results from good data'. *TrAC Trends in Analytical Chemistry* **25**(11), 1131–1138.

Bourgeois, W., Burgess, J.E. & Stuetz, R.M. 2001. 'On-line monitoring of wastewater quality: a review'. *Journal of Chemical Technology and Biotechnology* **76**(4), 337–348.

Bourgeois, W., Romain, A.-C., Nicolas, J. & Stuetz, R.M. 2003. 'The use of sensor arrays for environmental monitoring: interests and limitations'. *Journal of Environmental Monitoring* **5**(6), 852–860.

Bourgeois, W. & Stuetz, R.M. 2002. 'Use of a chemical sensor array for detecting pollutants in domestic wastewater'. *Water Research* **36**(18), 4505–4512.

Campos, I., Alcañiz, M., Aguado, D., Barat, R., Ferrer, J., Gil, L., Marrakchi, M., Martínez-Mañez, R., Soto, J. & Vivancos, J.-L. 2012. 'A voltammetric electronic tongue as tool for

water quality monitoring in wastewater treatment plants'. *Water Research* **46**(8), 2605–2614.

Chee, G.-J., Nomura, Y., Ikebukuro, K. & Karube, I. 2005. 'Development of photocatalytic biosensor for the evaluation of biochemical oxygen demand'. *Biosensors and Bioelectronics* **21**(1), 67–73.

Chee, G.-J., Nomura, Y., Ikebukuro, K. & Karube, I. 2007. 'Stopped-flow system with ozonizer for the estimation of low biochemical oxygen demand in environmental samples'. *Biosensors and Bioelectronics* **22**(12), 3092–3098.

Correia, D.P.A., Magalhães, J.M.C.S., Machado, A.A.S.C. 2005. 'Array of potentiometric sensors for simultaneous analysis of urea and potassium'. *Talanta* **67**, 773–782.

D'Souza, S.F. 2001. 'Microbial biosensors'. *Biosensors and Bioelectronics* **16**(6), 337–353.

del Valle, M. 2010). 'Electronic Tongues Employing Electrochemical Sensors'. *Electroanalysis* **22**(14), 1539–1555.

Escuder-Gilabert, L. & Peris, M. 2010. 'Review: Highlights in recent applications of electronic tongues in food analysis'. *Analytica Chimica Acta* **665**(1), 15–25.

Hibbert, D.B. 1998). 'Data Analysis of Multi-Sensor Arrays'. *Electroanalysis* **10**(16), 1077–1080.

Hines, E.L., Llobet, E. & Gardner, J.W. 1999. 'Electronic noses: a review of signal processing techniques'. *Iee Proceedings-Circuits Devices and Systems* **146**(6), 297–310.

Hruškar, M., Major, N. & Krpan, M. 2010. 'Application of a potentiometric sensor array as a technique in sensory analysis'. *Talanta* **81**(1–2), 398–403.

Karube, I., Matsunaga, T., Mitsuda, S. & Suzuki, S. 1977. 'Microbial electrode BOD sensors'. *Biotechnology and Bioengineering* **19**(10), 1535–1547.

Kibena, E., Raud, M., Jõgi, E. & Kikas, T. 2012. 'Semi-specific Microbacterium phyllosphaerae-based microbial sensor for biochemical oxygen demand measurements in dairy wastewater'. *Environmental Science and Pollution Research*, 1–7.

Kim, B.H., Chang, I.S. & Moon, H. 2006. 'Microbial Fuel Cell-Type Biochemical Oxygen Demand Sensor'. *Encyclopedia of Sensors* **X**, 1–12.

Kim, M.-N. & Kwon, H.-S. 1999. 'Biochemical oxygen demand sensor using Serratia marcescens LSY 4'. *Biosensors and Bioelectronics* **14**(1), 1–7.

Kissinger, P.T. 2005. 'Biosensors – a perspective'. *Biosensors and Bioelectronics* **20**(12), 2512–2516.

Krantz-Rülcker, C., Stenberg, M., Winquist, F. & Lundström, I. 2001. 'Electronic tongues for environmental monitoring based on sensor arrays and pattern recognition: a review'. *Analytica Chimica Acta* **426**(2), 217–226.

König, A., Reul, T., Harmeling, C., Spener, F., Knoll, M. & Zaborosch, C. 2000. 'Multimicrobial Sensor Using Microstructured Three-Dimensional Electrodes Based on Silicon Technology'. *Analytical Chemistry* **72**(9), 2022–2028.

Lagarde, F. & Jaffrezic-Renault, N. 2011. 'Cell-based electrochemical biosensors for water quality assessment'. *Analytical and Bioanalytical Chemistry* **400**(4), 947–964.

Liu, C., Zhao, H., Ma, Z., An, T., Liu, C., Zhao, L., Yong, D., Jia, J., Li, X. & Dong, S. 2014. 'Novel Environmental Analytical System based on Combined Biodegradation and Photoelectrocatalytic Detection Principles for Rapid Determination of Organic Pollutants in Wastewaters'. *Environmental Science and Technology* **48**, 1762–1768.

Liu, J., Björnsson, L. & Mattiasson, B. 2000. 'Immobilised activated sludge based biosensor for biochemical oxygen demand measurement'. *Biosensors and Bioelectronics* **14**(12), 883–893.

Liu, J. & Mattiasson, B. 2002. 'Microbial BOD sensors for wastewater analysis'. *Water Research* **36**(15), 3786–3802.

Luong, J.H.T., Male, K.B. & Glennon, J.D. 2008. 'Biosensor technology: Technology push versus market pull'. *Biotechnology Advances* **26**(5), 492–500.

Massart, D.L.H. & Vander, Y. 2004. ‘From Tables to Visuals: Principal Component Analysis, Part 1’. *LC – GC Europe* **17**(11), 586–591.

Namour, P. & Jaffrezic-Renault, N. 2010. ‘Sensors for measuring biodegradable and total organic matter in water’. *TRAC Trends in Analytical Chemistry* **29**(8), 848–857.

Nascu, H., Jantschi, L., Hodisan, T., Cimpoiu, C. & Cimpan, G. 1999. ‘Some applications of statistics in analytical chemistry’. *Reviews in Analytical Chemistry* **18**(6), 409–456.

Onkal-Engin, G., Demir, I. & Engin, S.N. 2005. ‘Determination of the relationship between sewage odour and BOD by neural networks’. *Environmental Modelling & Software* **20**(7), 843–850.

Pasco, N., Weld, R., Hay, J. & Gooneratne, R. 2011. ‘Development and applications of whole cell biosensors for ecotoxicity testing’. *Analytical and Bioanalytical Chemistry* **400**(4), 931–945.

Ponomareva, O.N.A., Alferov, V.A., Reshetilov, A.N. 2011. ‘Microbial Biosensors for Detection of Biological Oxygen Demand (a Review)’. *Applied Biochemistry and Microbiology* **47**(1), 1–11.

Rastogi, S., Kumar, A., Mehra, N.K., Makhijani, S.D., Manoharan, A., Gangal, V. & Kumar, R. 2003. ‘Development and characterization of a novel immobilized microbial membrane for rapid determination of biochemical oxygen demand load in industrial waste-waters’. *Biosensors and Bioelectronics* **18**(1), 23–29.

Raud, M. & Kikas, T. 2013. ‘Bioelectronic tongue and multivariate analysis: A next step in BOD measurements’. *Water Research* **47**(7), 2555–2562.

Raud, M., Linde, E., Kibena, E., Velling, S., Tenno, T., Talpsep, E. & Kikas, T. 2010. ‘Semi-specific biosensors for measuring BOD in dairy wastewater’. *Journal of Chemical Technology and Biotechnology* **85**(7), 957–961.

Raud, M., Tenno, T., Jõgi, E. & Kikas, T. 2012a. ‘Comparative study of semi-specific Aeromonas hydrophila and universal Pseudomonas fluorescens biosensors for BOD measurements in meat industry wastewaters’. *Enzyme and Microbial Technology* **50**(4–5), 221–226.

Raud, M., Tutt, M., Jõgi, E. & Kikas, T. 2012b. ‘BOD biosensors for pulp and paper industry wastewater analysis’. *Environmental Science and Pollution Research* **19**(7), 3039–3045.

Riul Jr, A., Dantas, C.A.R., Miyazaki, C.M. & Oliveira, Jr, O.N. (2010). ‘Recent advances in electronic tongues’. *Analyst* **135**(10), 2481–2495.

Rodriguez-Mozaz, S., Lopez De Alda, M.J. & BarcelĆ, D. 2006. ‘Biosensors as useful tools for environmental analysis and monitoring’. *Analytical and Bioanalytical Chemistry* **386**(4), 1025–1041.

Sakaguchi, T., Morioka, Y., Yamasaki, M., Iwanaga, J., Beppu, K., Maeda, H., Morita, Y. & Tamiya, E. 2007. ‘Rapid and onsite BOD sensing system using luminous bacterial cells-immobilized chip’. *Biosensors and Bioelectronics* **22**(7), 1345–1350.

Solna, R., Dock, E., Christenson, A., Winther-Nielsen, M., Carlsson, C., Emnéus, J., Ruzgas, T. & Skladal, P. 2005. ‘Amperometric screen-printed biosensor arrays with co-immobilised oxidoreductases and cholinesterases’. *Analytica Chimica Acta* **528**(1), 9–19.

Stuetz, R.M., George, S., Fenner, R.A. & Hall, S.J. 1999. ‘Monitoring wastewater BOD using a non-specific sensor array’. *Journal of Chemical Technology and Biotechnology* **74**(11), 1069–1074.

Su, L., Jia, W., Hou, C. & Lei, Y. 2011. ‘Microbial biosensors: A review’. *Biosensors and Bioelectronics* **26**(5), 1788–1799.

Suriyawattanakul, L., Surareungchai, W., Sritongkam, P., Tanticharoen, M. & Kirtikara, K. 2002. ‘The use of co-immobilization of Trichosporon cutaneum and Bacillus licheniformis for a BOD sensor’. *Applied Microbiology and Biotechnology* **59**(1), 40–44.

Tan, T.C. & Wu, C. 1999. ‘BOD sensors using multi-species living or thermally killed cells of a BODSEED microbial culture’. *Sensors and Actuators B: Chemical* **54**(3), 252–260.

Thévenot, D.R., Toth, K., Durst, R.A. & Wilson, G.S. 2001. 'Electrochemical biosensors: Recommended definitions and classification'. *Biosensors and Bioelectronics* **16**(1–2), 121–131.

Tønning, E., Sapelnikova, S., Christensen, J., Carlsson, C., Winther-Nielsen, M., Dock, E., Solna, R., Skladal, P., Nørgaard, L., Ruzgas, T. & Emnéus, J. 2005. 'Chemometric exploration of an amperometric biosensor array for fast determination of wastewater quality'. *Biosensors and Bioelectronics* **21**(4), 608–617.

Witkowska, E., Buczkowska, A., Zamojska, A., Szewczyk, K.W. & Ciosek, P. 2010. 'Monitoring of periodic anaerobic digestion with flow-through array of miniaturized ion-selective electrodes'. *Bioelectrochemistry* **80**(1), 87–93.

Vlasov, Y., Legin, A., Rudnitskaya, A., Natale, C.D. & D'Amico, A. 2005. 'Nonspecific sensor arrays ('electronic tongue') for chemical analysis of liquids (IUPAC Technical Report)'. *Pure and Applied Chemistry* **77**(11), 1965–1983.

Vlasov, Y., Legin, A. & Rudnitskaya, A. 2008. 'Electronic tongue: Chemical sensor systems for analysis of aquatic media'. *Russian Journal of General Chemistry* **78**(12), 2532–2544.

Xu, X. & Ying, Y. 2011. 'Microbial Biosensors for Environmental Monitoring and Food Analysis'. *Food Reviews International* **27**(3), 300–329.

Yang, Z., Sasaki, S., Karube, I. & Suzuki, H. 1997. 'Fabrication of oxygen electrode arrays and their incorporation into sensors for measuring biochemical oxygen demand'. *Analytica Chimica Acta* **357**(1–2), 41–49.

Agronomy Research **13**(2), 396–404, 2015

Amount of manure used for biogas production

J. Priekulis, A. Aboltins* and A. Laurs

Latvia University of Agriculture, Institute of Agricultural Machinery, Cakstes blvd. 5, LV3001 Jelgava, Latvia; *Correspondence: aivars.aboltins@inbox.lv

Abstract. Methods for calculation of the amount of manure from every agricultural animal species and subgroup for production of biogas have been developed in compliance with the 2006 IPCC Guidelines. These methods can be applied for future forecasts if the amount of biogas produced in the country increases. It has been stated that in 2013 in Latvia for production of biogas mostly chicken and pig manure was used – correspondingly 33.7% and 26.7% from the amount of manure obtained from these animals. In the forecast for 2020, in turn, it is expected that the consumption of manure will be 31.9% of chicken manure and 31.5% of pig manure, from the amount of manure obtained from the corresponding group of animals.

Key words: biogas, manure, 2006 IPCC Guidelines.

INTRODUCTION

At present there are 53 biogas plants operating in Latvia and their total capacity exceeds 54 MW. According to the renewable energy development forecasts in the country, it has been planned to build 89 plants with the total capacity 130 MW by 2030 (VARAM Infozin_Biogāze_09012013).

The most important raw material for production of biogas is animal manure, corn silage, animal feed residue and biomass of other kinds. Nevertheless, the main attention is paid to the usage of manure as it reduces emissions of methane and nitrogen in the surrounding atmosphere thus decreasing the formation of the greenhouse effect emissions in the atmosphere. Besides, in the result of manure recycling biogas and digestate are obtained. Biogas is used for production of heat and electric energy, but digestate is not smelly and can be used for fertilization of soil as it contains all main biogenic elements (N, P, K). Besides, N has obtained a form of ammonium that can be more easily used by plants (Dubrovskis & Adamovičs, 2012).

It has to be noted that reduction of greenhouse gas emissions is one of the main purposes why the state supports the development of biogas production, at the same time requiring that at least 30% of the biomass used for production of biogas is manure (Regulations of the Cabinet of Ministers, No.268).

The aim of the present research is to state the proportion of manure used for production of biogas from every corresponding agricultural animal species in Latvia. It is necessary for preparation of annual state inventory reports on greenhouse gas emissions as well as for future forecasts about the necessary consumption of biomass with production of biogas increasing.

MATERIALS AND METHODS

At present, there is information available in Latvia on the kind and amount of biomass used for production of biogas. But these data do not specifically indicate what the distribution of manure along separate farm animal groups for production of biogas is in accordance with the 2006 IPCC Guidelines (IPCC Guidelines for National Greenhouse Gas Inventories, 2006). Besides, according to these data there are problems with forecasting biomass consumption in future, especially because the kinds and amounts of definite biomass have a tendency to change.

To achieve the aim of the investigation, two methods were developed: the first – for calculation of the proportion of manure for production of biogas according to the obtained statistical data on a definite year, for example, last year; the second – for future forecasts of the used part of manure for production of biogas, i.e., for stating of the amount of this biomass in any of the future years according to the biogas production development plan.

The first method – stating of the proportion of manure used for production of biogas according to the statistical data

For production of biogas, different kinds of biomass can be used, but on animal farms for this reason the following is used: cattle manure, pig manure, poultry manure and grass (mainly corn) silage. Besides, the Rural Support Service has summarised information on the consumed amount of every kind of biomass. Nevertheless, this distribution does not comply with the 2006 IPCC Guidelines as considerably more detailed distribution of the used manure for production of biogas among the farm animal subgroups is determined in these guidelines (Table 1).

Table 1. Classification of cattle, pigs and poultry according to the animal classification determined in 2006 IPCC Guidelines

Animal groups	Animal subgroups	Explanation
Cattle	Adult milk cows	First-calvers or older cows, including dry cows
	Suckling cows, breeding bulls	Cattle reached breeding age
	Young stock	Calves, heifers, feedlot young stock
Pigs	Hogs	All kinds of sows, boars
	Young pigs	Weanings, feedlot stock, young sows, young boars
Chicken	Laying hens*	Handling in cage batteries
	Chicken and poulets	Handling in cage batteries

*for handling laying hens, chicken and poulets also other solutions can be used but in that case poultry manure is not used for production of biogas

To calculate the percentual proportion of the manure used for biogas production from every group of farm animals, the total amount of manure obtained from every corresponding group of animals used for production of biogas has to be known.

Therefore, this proportion can be calculated according to the following formulae (1)–(3):

$$\lambda_l = \frac{M_{bl}}{\sum M_l} \cdot 100 \quad (1)$$

$$\lambda_c = \frac{M_{bc}}{\sum M_c} \cdot 100 \quad (2)$$

$$\lambda_p = \frac{M_{bp}}{\sum M_p} \cdot 100 \quad (3)$$

where: λ_l, λ_c, λ_p – percentual amount of cattle, pig and poultry manure used for production of biogas, %; M_{bl}, M_{bc}, M_{bp} – amount of cattle, pig and poultry manure used for production of biogas, t/year; $\sum M_l$, $\sum M_c$, $\sum M_p$ – total amount of cattle, pig and poultry manure, t year^{-1}.

The second method – forecasting of manure proportion necessary for production of biogas

In order to forecast the consumption of manure for production of biogas in the nearest future years the amount of the planned biogas or produced electric energy as well as the number of animals the manure of which will be used for production of biogas have to be known. For this reason the calculation can be divided in several stages.

1. The necessary amount of dry matter in manure for production of biogas is calculated, tsd.t year^{-1}

$$M_{s.nep} = \frac{b_k \cdot (1 - b_{at}) \cdot Q_{b.en}}{q_{gs} \cdot E_g \cdot k_{el}} \quad (4)$$

where: b_k – proportion of manure used for production of biogas; b_{at} – coefficient showing the proportion of biogas produced from waste, b_{at} ~ 0,4 (VARAM Infozin_Biogāze); $Q_{b.en}$ – amount of electric energy to be produced from biogas per year (according to the energetics forecast data), GWh; q_{gs} – average weighed biogas output from the used biomass, m^3 t^{-1}; E_g – heat capacity of biogas.

If the content of CH_4 in biogas is ~ 60%, then E_g ~ 6 kWh m^{-3} (Dubrovskis & Adamovičs, 2012); k_{el} – coefficient showing what part of the obtained biogas heat capacity is turned into electric energy. According to literature (Dubrovskis & Adamovičs, 2012) k_{el} ~ 0,4.

According to the requirements of the Cabinet of Ministers Regulations No. 268 manure must comprise not less than 30% of the biomass for production of biogas. But it can be made more precise by calculation based on the statistical data

$$b_k = \frac{M_{bl} + M_{bc} + M_{bp}}{M_{bl} + M_{bc} + M_{bp} + M_{bsk}} \quad (5)$$

where M_{bsk} – amount of silage used for production of biogas in the corresponding year, t year^{-1}.

The average weighed biogas output q_{gs}, using the corresponding biomass can be calculated as follows

$$q_{gs} = \frac{q_l \cdot M_{bl} \cdot S_l + q_c \cdot M_{bc} \cdot S_c + q_p \cdot M_{bp} \cdot S_p + q_{sk} \cdot M_{bsk} \cdot S_{sk}}{M_{bl} \cdot S_l + M_{bc} \cdot S_c + M_{bp} \cdot S_p + M_{bsk} \cdot S_{sk}} \quad (6)$$

where: q_l, q_c, q_p – average weighed biogas output from cattle, pig and poultry manure dry matter correspondingly, m^3 t^{-1}; q_{sk} – average weighed biogas output from silage dry matter, m^3 t^{-1}; S_l, S_c, S_p – content of cattle, pig and poultry manure dry matter used for production of biogas, %; S_{sk} – average silage dry matter content used for production of biogas, %.

2. The amount of manure dry matter that is necessary for biogas production from every group of animals is calculated considering the statistical data on the amount of cattle, pig and poultry manure used in production of biogas.

$$M_{s.l} = \frac{M_{bl} \cdot S_l}{M_{bl} \cdot S_l + M_{bc} \cdot S_c + M_{bp} \cdot S_p} \cdot M_{s.nep} \quad (7)$$

$$M_{s.c} = \frac{M_{bc} \cdot S_c}{M_{bl} \cdot S_l + M_{bc} \cdot S_c + M_{bp} \cdot S_p} \cdot M_{s.nep} \quad (8)$$

$$M_{s.p} = \frac{M_{bp} \cdot S_p}{M_{bl} \cdot S_l + M_{bc} \cdot S_c + M_{bp} \cdot S_p} \cdot M_{s.nep} \quad (9)$$

where: $M_{s.l}$, $M_{s.c}$, $M_{s.p}$ – necessary amount of cattle, pig and poultry manure to be used in production of biogas, tsd. t year^{-1}.

3. The amount of manure dry matter obtained in a year from every separate group of animals is calculated: cattle

$$M_{i.s.l} = \frac{z_g \cdot S_g \cdot m_g}{100 \cdot 1000} + \frac{z_n \cdot S_n \cdot m_n}{100 \cdot 1000}, \quad (10)$$

pigs

$$M_{i.s.c} = \frac{z_c \cdot S_c \cdot m_c}{100 \cdot 1000}, \quad (11)$$

poultry

$$M_{i.s.p} = \frac{z_p \cdot S_p \cdot m_p}{100 \cdot 1000}, \quad (12)$$

where: $M_{i.s.l}$, $M_{i.s.c}$, $M_{i.s.p}$ – amount of manure dry matter obtained from cattle, pigs and poultry, tsd.t year^{-1}; z_g, z_n, z_c, z_p – planned number of milk cows, suckling cows and other adult cattle, pigs and poultry in the corresponding year, tsds; S_g, S_n – average dry matter content of milk cow, suckling cow and other adult cattle manure, %; m_g – average manure outcome from one milk cow, t year^{-1}; m_n, m_c, m_p – average weighed manure outcome from one suckling cow and all kinds of young stock, from pigs of all ages and poultry, t anim year^{-1}.

4. Proportion of the amount of manure to be used for production of biogas from every group of animals is determined: cattle

$$\lambda_l = \frac{M_{s.l}}{M_{i.s.l}} \cdot 100, \quad (13)$$

pigs

$$\lambda_c = \frac{M_{s.c}}{M_{i.s.c}} \cdot 100, \quad (14)$$

poultry

$$\lambda_v = \frac{M_{s.v}}{M_{i.s.v}} \cdot 100. \quad (15)$$

RESULTS AND DISCUSSION

To explain the procedure of calculation of the amount of manure necessary for production of biogas considering the 2006 IPCC Guidelines, the two above mentioned methods will be discussed: the first – calculating the proportion of manure for production of biogas in Latvia in 2013, the second – forecasting of this proportion for 2020.

Determination of the proportion of manure for production of biogas according to the statistical data

According to the data of the Latvian Rural Service, there were biogas production plants operating on 37 Latvian rural farms in 2013. Information on biomass used for production of biogas is summarized in Table 2.

Table 2 shows the amount of biomass of every kind of manure and the average of dry matter. Multiplying these parameters the amount of the corresponding biomass dry matter is obtained.

Table 2. Biomass used for production of biogas and proportion of manure used for this purpose considering the amount of dry matter

Raw material used	Amount, t year^{-1}	Average dry matter content,%	Amount of dry matter, t year^{-1}
Cattle manure	395,150	10	39,515
Pig manure	130,000	8	10,400
Poultry manure	27,050	30	8,115
Grass silage	1,056,600	Total	58,030
Total	1,608,800		

The next step is calculation of the manure output from separate groups of animals according to the classification in the 2006 IPCC Guidelines. For this purpose Table 3 is developed.

Table 3. Total amount of manure obtained in Latvia in 2013 from separate animal groups and subgroups

Animal group and subgroup	Number of animals *	Manure outcome, tsd. t year^{-1}				Consumption for biogas, %
		per 1 animal **	total	total in subgroup	total in group	
Cattle						
Milk cows	164,000	0.019	3,116	3116		
Suckling cows and other adult cattle	57,000	0.011	627	627	5,343.7	7,4
Calves up to the age of one year	109,300	0.005	549.5	1,603.7		
Young stock from 1 to 2 years	75,300	0.014	1,054.2			
Pigs						
Adult sows	43,300	0.0025	108.3	110		
Breeding boars	700	0.0025	1.8			
Pigs up to the age of 2 months	87,100	0.0003	26.1			
Pigs up to the age of from 2 to 4 months	108,100	0.0006	64.9	376.2	762.09	26,7
Feedlock stock and breeding young pigs	142,600	0.002	285.2			
Poultry						
Laying hens (starting from the age of 17-20 weeks)	2,430,500	0.00003	72.9	72.9	80.2	33,7
Chicken and poulets	750,000	0.00001	7.5	7.5		

Sources: *Central Statistical Bureau of the Republic of Latvia
**Regulations of the Cabinet of Ministers No.834.

In the first column of the table, more detailed classification of animal groups is given compared to the 2006 IPCC Guidelines, as it corresponds more precisely to the data on the number of agricultural animals in the corresponding year published by the Central Statistical Bureau of the Republic of Latvia. Besides, it makes it easier to calculate the amount of the obtained manure as it corresponds more precisely to the outcome of manure calculating per one animal that is determined in the Regulation No. 834 of the Cabinet of Ministers.

Calculation is started with stating the manure outcome from the animals of every subgroup mentioned in the table by multiplying the number of the corresponding animals with the corresponding manure outcome from one animal.

After that the calculated manure outcomes are summarized from the rows that correspond to one animal subgroup in accordance with the 2006 IPCC Guidelines and the total amount of the obtained manure in every animal subgroup and group is calculated.

At last, the amount of manure from every farm animal group necessary for production of biogas (second column of Table 2) is divided by the amount of manure obtained in this group of farm animals (Table 3) and the result is multiplied by 100 to get the result in per cents.

Forecast of the proportion of manure necessary for production of biogsas

In order to forecast the amount of manure necessary for production of biogas from every subgroup of agricultural animals, the manure biomass dry matter amount necessary for production of biogas has to be calculated.

Using the formula (5) the coefficient b_k of the portion of manure used for production of biogas is calculated which in the given case is 0.34. After that, using Table 2 and the information published in literature (Dubrovskis, Adamovičs, 2012) about the average biogas outcome from cattle, pig and poultry manure dry matter, the average weighed biogas output from biomass dry matter q_{gs} = 440 m^3 t^{-1} is calculated using the formula (6).

`Also the forecasts that in Latvia in 2020 the total capacity of biogas production equipment will reach 92 MW, published in the VARAM informative report, as well as the data of the Ministry of Agriculture on the number of planned agricultural animals (Table 4) are used.

Table 4. Calculation input data for 2020

Farm animal groups	Planned number	Average weighed manure outcome, t year-^{1} from one animal	Average manure dry matter content, %
Milk cows	190,000	19	10
Cattle (beef)	290,000*	6**	15
Pigs	500,000*	1.27	8
Poultry	5,200,000*	0.025	30

*including all animals up to the breeding age

**considering the pasture period

Table 4 shows the average weighed manure outcome and the content of dry matter from the animals of the corresponding groups. Using formulas (7)–(9) the manure dry matter content that in a definite year is necessary for production of biogas from every group of animals as well as the total amount of the corresponding manure to be obtained in that year can be calculated, formulas (10)–(12), and the obtained results are shown in Table 5. After that using formulas (14)–(16) the necessary proportion of manure for every corresponding subgroup of animals for production of biogas is calculated (last column of Table 5).

Table 5. Forecast results for 2020

Farm animal groups	Total obtained manure dry matter content, tsd.tons year^{-1}	Proportion of manure necessary for production of biogas from the corresponding group of animals, %
Cattle	622	9.7
Pigs	50.8	31.5
Poultry	39	31.9

The results of the calculations show that in 2020 approximately 89 thousand tons of manure dry matter are necessary for production of biogas, and the necessary amount of manure from separate animal groups to ensure it can be seen in Table 5.

The obtained results prove that based on the prognosticated data for production of biogas in 2020 mostly pig and poultry manure will be used, 31.5% and 31.9% respectively from the total obtained amount. Besides, the consumption of pig manure will increase by 18% in 2020.

In accordance with our unpublished research on the largest pig farms in Latvia, the obtained pig manure is stored mainly in anaerobic lagoons, but the amount of greenhouse gas emissions from such lagoons is almost three times higher than from the digestate obtained in biogas production plants. Therefore, expansion of biogas production using pig manure is highly important for decreasing the total greenhouse gas amount emitted by the production of animal breeding products.

CONCLUSIONS

To state the proportion of manure consumed for production of biogas from every corresponding group of farm animals in accordance with the 2006 IPCC Guidelines, statistical data on the amount of biomass used for production of biogas as well as on the number of farm animals and their classification in separate subgroups shall be obtained.

If it is necessary to forecast the consumption of manure needed for production of biogas in the nearest future, apart from the planned number of animals, data on the amount of biogas to be produced or the amount of electric energy produced from it, are required.

Applying the methods described in the article, it has been stated that in 2013 in Latvia mostly poultry manure was used – 33.7% of the total amount as well as pig manure – 26.7% of the total amount for production of biogas. The forecasts for 2020 are similar, as the planned consumption of poultry manure is 31.9% but of pig manure – 31.5% of the total amount of manure obtained from the corresponding animal subgroups.

REFERENCES

IPCC Guidelines for National Greenhouse Gas Inventories. 2006. Chapter 10: Emissions from Livestock and Manure Management, 87p.

Regulations of the Cabinet of Ministers No. 268. Procedure of granting the European Union support for the measure 'Support for Establishment and development of enterprises (including diversification of activities not related to agriculture) activity 'Production of energy from biomass of agricultural and forestry origin', hereinafter – activity. In force from March 16, 2010 (in Latvian).

Regulations of the Cabinet of Ministers No. 834. Regulations of water and soil protection from pollution with nitrate caused by agricultural activities. In force from 7.01.2015 (in Latvian).
VARAM Infozin_Biogāze_09012013; Informative report on '*Procedure of biogas production and usage development program for 2007-2011*'. [Electronic resource] 9.07.2014.
CM Regulation No.157 'Regulations on greenhouse effect gas emission unit national system'. (In force from 25.02.2009.)
Agriculture in Latvia 2014, *Collection of Statistical Data*. Rīga: Central Statistical Bureau of Latvia, 64 pp.
Dubrovskis, V. & Adamovičs, A. 2012, *Bioenergetic horizons*. Monograph. Jelgava: LLU, 352 pp.

Agronomy Research **13**(2), 405–412, 2015

Effect of lignin content of lignocellulosic material on hydrolysis efficiency

M. Raud, M. Tutt, J. Olt and T. Kikas*

Estonian University of Life Sciences, Institute of Technology, Kreutzwaldi 56, EE51014 Tartu, Estonia; *Correspondence: timo.kikas@emu.ee

Abstract. Lignocellulosic material is the most promising feedstock for bioethanol production; however, due to the varying physicochemical characteristics of different biomasses, it is necessary to select a biomass with a composition suitable for bioethanol production. For this purpose several different alternative non-food energy crops were chosen to investigate their suitability for bioethanol production, considering their cellulose, hemicellulose and lignin content. The traditional three-step bioethanol production process was used, where dilute acid was applied for biomass pre-treatment. Glucose and ethanol concentrations were measured during the process. Glucose and ethanol yields and hydrolysis efficiency were used to evaluate the suitability of different energy crops for bioethanol production. The results show that, with most biomass types, the glucose yield increases as the cellulose content in the biomass rises. However, a sharp decrease in hydrolysis efficiency was noted in the lignin content range of 7 to 9 g 100 g^{-1}. The lower hydrolysis efficiency also resulted in a lower ethanol yield in the next step of the bioethanol production process for these samples.

Key words: bioethanol, lignocellulosic biomass, lignin, biofuel, acid pre-treatment.

INTRODUCTION

Lignocellulosic biomass is considered an attractive feedstock for the production of a second-generation biofuel – bioethanol. Traditional lignocellulosic feedstocks include mainly energy crops (purpose-grown vegetative grasses, short rotation forests etc.) and agricultural residues (e.g. corn stover, wheat straw, sugar cane bagasse) (Tutt et al., 2012; Tutt et al., 2013; Cybulska et al., 2014) but also different kinds of waste (e.g. organic components of municipal solid waste) (Sims et al., 2010; Raud et al. 2014; Tutt et al., 2014). The main advantage of the production of second-generation biofuels from non-edible feedstock is that it limits the direct food versus fuel competition associated with first-generation biofuels (Naik et al., 2010; Nigam & Singh, 2011; Haghighi Mood et al., 2013).

Lignocellulosic materials are the most promising feedstock for bioethanol production, considering their great availability, low cost, and sustainable supply (Agbor et al., 2011). Plant biomass is primarily composed of plant cell walls, of which about 75% consists of polysaccharides (Phitsuwan et al., 2013), which could be used for ethanol production. The conversion of lignocellulosic biomass to alcohol traditionally requires a three-step process – the pre-treatment of biomass, acid or enzymatic hydrolysis, and fermentation/distillation (Mosier et al., 2005; Naik et al., 2010;

Demirbas, 2011). However, the complicated structure of lignocellulosic material makes it recalcitrant to chemical and biochemical reactions (Min et al., 2013; Xu et al., 2013). Due to many physical and chemical factors, such as the presence of lignin, the crystallinity of cellulose, and the presence of covalent cross-linkages between lignin and hemicelluloses in the plant cell wall, lignocellulosic biomass is naturally resistant to microbial attack (Li et al., 2011).

Different biomass pre-treatment methods have been reported to overcome the recalcitrance of lignocellulosic biomass. The goal of the pre-treatment is to enhance the conversion steps by separating the biomass components and/or by providing easier access to cellulose (Chiaramonti et al., 2012; Conde-Mejia et al., 2012). The main techniques for the selective fractionation of hemicelluloses from the biomass include the use of acids, water (liquid or steam), organic solvents and alkaline agents (Girio et al., 2010; Cybulska et al., 2014). Different pre-treatment methods have different targets. For example, acid treatment breaks down the glycosidic bonds of polysaccharides, freeing individual monosaccharides and thereby removing hemicellulose. Alkaline pre-treatment, on the other hand, alters and removes the lignin structure (Min et al., 2013; Barakat et al., 2014). Physicochemical pre-treatment methods, like steam-explosion and AFEX pre-treatment, alter the biomass structure by separating the individual fibres in combination with partial hemicellulose hydrolysis and solubilization (Alvira et al., 2010).

However, during pre-treatment, various enzyme inhibitors/deactivators and toxic substances are produced, which may also inhibit the later fermentation processes, leading to lower ethanol yields and productivities (Girio et al., 2010; Cybulska et al., 2014). These compounds are principally generated from lignocellulosic components during pre-treatment (Phitsuwan et al., 2013) and, depending on the operational conditions, degradation products are formed both from sugars (furan derivatives and organic acids) and, to a lesser extent, from lignin (phenolic compounds) (Girio et al., 2010; Cybulska et al., 2014). The type and amount of the generated toxic compounds depend on the raw material and the harshness of the pre-treatment conditions (Alvira et al., 2010). In addition, several other factors have been reported to affect the hydrolysis of cellulose, including the porosity of the biomass, cellulose fibre crystallinity, and lignin and hemicellulose content. The presence of lignin and hemicellulose makes it difficult for cellulase enzymes to access the cellulose fibres and thus reduces the efficiency of the hydrolysis process (Sun & Cheng, 2002).

It has been observed that since different lignocellulosic materials have different physicochemical characteristics, it is necessary to adopt suitable pre-treatment technologies based on the biochemical composition of the lignocellulosic biomass (Alvira et al., 2010). It has been shown that a biomass with a high cellulose content helps to gain high glucose and ethanol yields (Kikas et al., 2014) while the other major components of biomass decrease the bioethanol production potential by acting as a physical barrier, preventing the cellulose in the biomass to be hydrolysed by enzymes (Alvira et al., 2010).

The purpose of this study was to investigate the effect of biomass composition on the bioethanol production potential. Different non-food biomass types were collected and used in the traditional three-step bioethanol production process, where dilute acid was used for biomass pre-treatment. Glucose and ethanol concentrations were measured

during the process. The bioethanol production potential was evaluated on the basis of glucose and ethanol yields and hydrolysis efficiency.

MATERIALS AND METHODS

Description of the biomass

Different alternative crops were chosen to investigate their suitability for bioethanol production, considering their lignin content. The species selected were: Jerusalem artichoke (*Helianthus tuberosus L.*), fibre hemp (*Cannabis sativa L.*) cv USO-31, energy sunflower (*Helianthus annuus L.*) cv Wielkopolski, Amur silver-grass (*Miscanthus sacchariflorus*), energy grass cv Szarvasi-1, rye and reed. In addition, a sample of silage was used as a biomass. A more detailed description of the growth parameters and sampling conditions of the biomass is given in a previous paper (Kikas et al., 2014).

The percentage of lignin, Acid Detergent Fibre (ADF) and Neutral Detergent Fibre (NDF) in the dry mass (DM) of all the plant samples was determined in the Laboratory of Plant Biochemistry at the Estonian University of Life Sciences (Tecator ASN 3430). Standard methods of the Association of Official Analytical Chemists (AOAC 973.18) and the methods of the company Tecator (fibre determination using the Fibertec M&I systems) were applied in the analysis. All samples were ground up with Cutting Mill SM 100 comfort (Retsch GmbH) and then with Cutting Mill ZM 200 (Retsch GmbH).

Bioethanol production

A dilute acid pre-treatment followed by enzymatic hydrolysis was used for the degradation of cellulose into glucose. For the pre-treatment, 750 mL of a 1% (m m^{-1}) H_2SO_4 solution was added to 75 g of dried and milled biomass (moisture content < 5%, m m^{-1}). All the samples were heated for 30 minutes at a temperature of 150 ± 3 °C and at a pressure of 5 bar. The samples were cooled to below 50 °C and the pH of the mixture was neutralized with $Ca(OH)_2$ to achieve a pH between 4.5–5.5 in order to avoid enzyme inactivation at pH ranges of pH < 4 and pH > 6.

The pre-treatment was followed by enzymatic hydrolysis using the enzyme complex Accellerase 1500. The enzymes were added to the sample in a proportion of 0.2 mL per g of biomass. The hydrolysis lasted for 48 hours under constant stirring and at a temperature of 50 °C. As a result most of the biomass was dissolved and the mixture turned into a brown liquid. After the hydrolysis, the glucose concentration in all the samples was measured reflectometrically (RQflex 10 reflectometer, Reflectoquant glucose & fructose test).

Fermentation with the yeast *Saccharomyces cerevisiae* was used in order to convert the glucose to ethanol. 2.5 g of dry yeast *Saccharomyces cerevisiae* was added to all the samples and the fermentation process was carried out at room temperature in 1,000 mL glass bottles sealed with a fermentation tube and a water lock that provided low-oxygen conditions. The fermentation lasted for 168 h, after which the ethanol concentration was measured. The concentration was measured reflectometrically using the RQflex 10 reflectometer and the Reflectoquant alcohol test by Merck Inc.

RESULTS AND DISCUSSION

Biomass analysis

In this study biomass was characterized on the basis of its relative proportion of cellulose, hemicellulose, lignin, and ash as outlined in Table 1. The potential glucose and ethanol yields are directly proportional to the cellulose content of the biomass (Kikas et al., 2014); therefore, a biomass with higher cellulose content is usually preferred for ethanol production. From Table 1 it can be seen that reed and hemp exhibited the highest cellulose content of 49.40 and 53.86 g $100g^{-1}$, respectively, while Jerusalem artichoke had by far the lowest cellulose content regardless of the harvesting time. Reed together with Amur silver-grass also had high hemicellulose content. The highest lignin content was measured in energy grass and silage, 9.65 and 9.02 g 100 g^{-1}, respectively. The lowest hemicellulose and lignin content was also found in samples of Jerusalem artichoke. Furthermore, its biochemical composition depended on the harvesting time of the biomass since the biochemical composition of plants changes during the vegetation period (Tutt et al., 2013; Kikas et al., 2014). The highest ash content of 9.78 g 100 g^{-1} was found in sunflower samples.

Table 1. Hemicellulose (HC), cellulose (CEL), lignin and ash content (g 100 g^{-1}) in the biomass samples of different energy crops

Energy crop	HC	CEL	Lignin	Ash
Amur silver-grass	30.15	42.00	7.00	5.37
Energy grass cv Szarvasi-1	27.33	37.85	9.65	7.01
Hemp	10.60	53.86	8.76	5.25
Sunflower	5.18	34.06	7.72	9.78
Rye	27.86	42.83	6.51	5.21
Reed	31.50	49.40	8.74	n/a
Silage	25.96	39.27	9.02	n/a
Jerusalem artichoke (Oct)	4.50	25.99	5.70	4.56
Jerusalem artichoke (Sep)	5.48	20.95	5.05	5.15

Glucose production from biomass

Fig. 1 illustrates how the glucose yield from the selected energy crops related to the cellulose content of different types of biomass. As expected, based on previous research, the results show that the glucose yield is proportional to the cellulose content in biomass. Since cellulose is a polymer that consists of glucose monomers, glucose is the main product formed during the enzymatic hydrolysis of cellulose. As a result, when the cellulose content in the biomass rises, the glucose yield from this biomass should also increase. However, two types of biomass – sunflower and reed – showed considerably lower glucose yields than what could be expected based on the cellulose content of the biomass. The glucose yield from reed was 24% lower than expected, while the glucose yield from sunflower was nearly two times lower than what could be expected based on the cellulose content of the respective biomass.

In order to explain this deviation from the expected glucose yields, other parameters, like hemicellulose and lignin content of the biomass, were analyzed. While no correlation was found between hemicellulose content and glucose yield, there was a distinct relationship between the lignin content of the biomass and hydrolysis efficiency. Fig. 2 illustrates the change in hydrolysis efficiency of various types of biomass

depending on their lignin content. A hydrolysis efficiency of over 60% was achieved with many different biomass types that had low or high lignin content. However, a sharp decrease in hydrolysis efficiency can be seen in the lignin content range of 7–9 g 100 g^{-1}, where the lowest efficiencies were seen with sunflower and reed. These results suggest that in case of acid pre-treatment where hemicellulose is hydrolysed during the pre-treatment, the absolute value of lignin content in the biomass is less important than the range within which it lies. This points to a possibility that the efficiency of enzymatic hydrolysis is dependent not only on the presence of lignin in the biomass but also on the way the cellulose macrofibrils are wrapped in the lignin sheath. Too little or too much lignin does not provide the cellulose fibres with effective coverage and thus makes them more accessible for the enzymes after the removal of hemicellulose, which in turn results in a more efficient hydrolysis of cellulose.

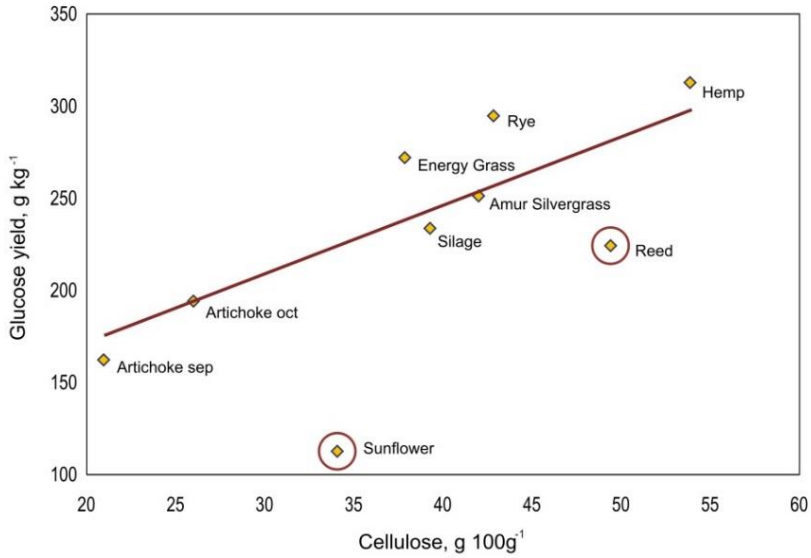

Figure 1. The dependence of glucose yield on the cellulose content of different biomass types. The red line indicates a linear dependence of the glucose yield on the cellulose content; outliers from the main linear trendline are circled.

During the conversion of biomass to ethanol it is essential to minimize sugar losses to reduce the production cost of ethanol (Alvira et al., 2010). Therefore, for an efficient bioethanol production process it is vital to achieve a high glucose yield. This could be achieved by choosing a biomass with a lignin content of below or above 7–9 g 100 g^{-1}, where the lignin coverage of the cellulose fibrils is not optimal, in combination with choosing the most suitable pre-treatment method.

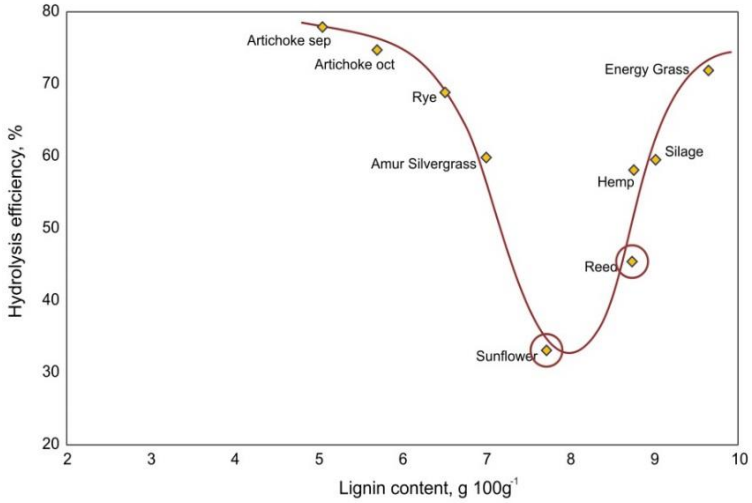

Figure 2. The dependence of the hydrolysis efficiency of different types of biomass on the lignin content. The red line indicates s dependence of hydrolysis efficiency on the lignin content; two outliers from the cellulose-glucose linear trendline are circled.

Ethanol production

As ethanol is the final product of this process, the ethanol yields from different energy crops were also analyzed. Fig. 3 describes the dependence of ethanol yield on the cellulose content of different types of biomass. The results show that ethanol yield is proportional to the cellulose content of the biomass – more ethanol was gained from biomasses with higher cellulose content. This is expected as the ethanol yield is directly proportional to the amount of glucose available for fermentation and the glucose yield was shown to be proportional to the cellulose content of the biomass.

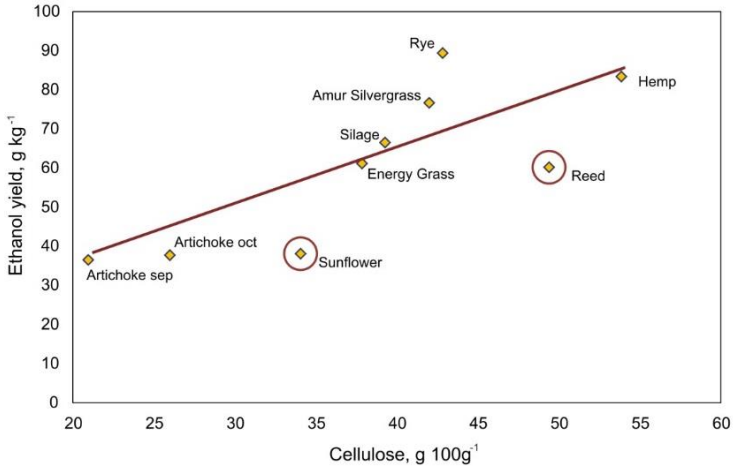

Figure 3. The dependence of ethanol yield on the cellulose contents of different types of biomass. The red line indicates a linear dependence of ethanol yield on the cellulose content; two outliers from the cellulose-glucose linear trendline are circled.

Fig. 3 also shows that the rye sample has a higher glucose yield, while sunflower and reed have lower glucose yields than assumed from the general trendline. The lower ethanol yield of reed and sunflower is expected since the glucose yield (Fig. 1) and hydrolysis efficiency (Fig. 2) of these energy crops were also lower than those of other samples with similar cellulose contents.

CONCLUSIONS

Different types of non-food biomass were collected and used in the traditional three-step bioethanol production process, where dilute acid was used for biomass pre-treatment to study the effect of biomass composition on the bioethanol production potential. In this study, glucose and ethanol yields together with hydrolysis efficiency were used to evaluate the suitability of different energy crops for bioethanol production. The results show that although glucose and ethanol yields rise when the cellulose content of biomass increases it is not the only parameter that influences the glucose and ethanol yields. Considerably lower glucose and ethanol yields were gained when the lignin content of the biomass was between 7–9 g 100 g^{-1}, which leads to lower ethanol yields. This suggests that the efficiency of enzymatic hydrolysis is dependent not only on the pre-treatment conditions and on the presence of lignin in the biomass, but also on the way the cellulose fibrils are wrapped in the lignin sheath.

REFERENCES

Agbor, V.B., Cicek, N., Sparling, R., Berlin, A. and Levin, D.B. 2011. Biomass pretreatment: Fundamentals toward application. *Biotechnology Advances* **29**(6), 675–685.

Alvira, P., Tomás-Pejó, E., Ballesteros, M. and Negro, M.J. 2010. Pretreatment technologies for an efficient bioethanol production process based on enzymatic hydrolysis: A review. *Bioresource Technology* **101**(13), 4851–4861.

Barakat, A., Chuetor, S., Monlau, F., Solhy, A. and Rouau, X. 2014. Eco-friendly dry chemo-mechanical pretreatments of lignocellulosic biomass: Impact on energy and yield of the enzymatic hydrolysis. *Applied Energy* **113**, 97–105.

Chiaramonti, D., Prussi, M., Ferrero, S., Oriani, L., Ottonello, P., Torre, P. and Cherchi, F. 2012. Review of pretreatment processes for lignocellulosic ethanol production, and development of an innovative method. *Biomass and Bioenergy* **46**, 25–35.

Conde-Mejía, C., Jiménez-Gutiérrez, A. & El-Halwagi, M. 2012. A comparison of pretreatment methods for bioethanol production from lignocellulosic materials. *Process Safety and Environmental Protection* **90**(3), 189–202.

Cybulska, I., Chaturvedi, T., Brudecki, G.P., Kádár, Z., Meyer, A.S., Baldwin, R.M. and Thomsen, M.H. 2014. Chemical characterization and hydrothermal pretreatment of *Salicornia bigelovii* straw for enhanced enzymatic hydrolysis and bioethanol potential. *Bioresource Technology* **153**, 165–172.

Demirbas, A. 2011. Competitive liquid biofuels from biomass. *Applied Energy* **88**(1), 17–28.

Gírio, F.M., Fonseca, C., Carvalheiro, F., Duarte, L.C., Marques, S. and Bogel-Łukasik, R. 2010. Hemicelluloses for fuel ethanol: A review. *Bioresource Technology* **101**(13), 4775–4800.

Haghighi Mood, S., Hossein Golfeshan, A., Tabatabaei, M., Salehi Jouzani, G., Najafi, G.H., Gholami, M. and Ardjmand, M. 2013. Lignocellulosic biomass to bioethanol, a comprehensive review with a focus on pretreatment. *Renewable and Sustainable Energy Reviews* **27**, 77–93.

Kikas, T., Tutt, M., Raud, M., Alaru, M., Lauk, R. and Olt, J. 2014. Basis of Energy Crop Selection for Biofuel Production: Cellulose vs. Lignin. *International Journal of Green Energy* DOI: 10.1080/15435075.2014.909359.

Li, C., Cheng, G., Balan, V., Kent, M.S., Ong, M., Chundawat, S.P.S., Sousa, L.d., Melnichenko, Y.B., Dale, B.E., Simmons, B.A. and Singh, S. 2011. Influence of physico-chemical changes on enzymatic digestibility of ionic liquid and AFEX pretreated corn stover. *Bioresource Technology* **102**(13), 6928–6936.

Min, D., Yang, C., Shi, R., Jameel, H., Chiang, V. and Chang, H. 2013. The elucidation of the lignin structure effect on the cellulase-mediated saccharification by genetic engineering poplars (*Populus nigra L.* × *Populus maximowiczii A.*). *Biomass and Bioenergy* **58**, 52–57.

Mosier, N., Wyman, C., Dale, B., Elander, R., Lee, Y.Y., Holtzapple, M. and Ladisch, M.2005. Features of promising technologies for pretreatment of lignocellulosic biomass. *Bioresource Technology* **96**(6), 673–686.

Naik, S.N., Goud, V.V., Rout, P.K. and Dalai, A.K. 2010. Production of first and second generation biofuels: A comprehensive review. *Renewable and Sustainable Energy Reviews* **14**(2), 578–597.

Nigam, P.S. & Singh, A. 2011. Production of liquid biofuels from renewable resources. *Progress in Energy and Combustion Science* **37**(1), 52–68.

Phitsuwan, P., Sakka, K. & Ratanakhanokchai, K. 2013. Improvement of lignocellulosic biomass in planta: A review of feedstocks, biomass recalcitrance, and strategic manipulation of ideal plants designed for ethanol production and processability. *Biomass and Bioenergy* **58**, 390–405.

Raud, M., Kesperi, R., Oja, T., Olt, J. and Kikas, T. 2014. Utilization of urban waste in bioethanol production: Potential and technical solutions. *Agronomy Research* **12**(2), 397–406.

Sims, R.E.H., Mabee, W., Saddler, J.N. and Taylor, M. 2010. An overview of second generation biofuel technologies. *Bioresource Technology* **101**(6), 1570–1580.

Sun, Y. & Cheng, J. 2002. Hydrolysis of lignocellulosic materials for ethanol production: a review. *Bioresource Technology* **83**(1), 1–11.

Tutt, M., Kikas, T. & Olt, J. 2012. Influence of different pretreatment methods on bioethanol production from wheat straw, *Agronomy Research* **10**, 269–276.

Tutt, M., Kikas, T. & Olt, J. 2013. Influence of harvesting time on biochemical composition and glucose yield from hemp, *Agronomy Research* **11**, 215–220.

Tutt, M., Kikas, T., Kahr, H., Pointner, M., Kuttner, P. & Olt, J., 2014. Using steam explosion pretreatment method for bioethanol production from floodplain meadow hay, *Agronomy Research* **12**(2), 417–424.

Xu, F., Shi, Y.-C. & Wang, D. 2013. X-ray scattering studies of lignocellulosic biomass: A review. *Carbohydrate Polymers* **94**(2), 904–917.

Agronomy Research **13**(2), 413–419, 2015

Energy use of compost pellets for small combustion plants

K. Skanderová, J. Malaťák* and J. Bradna

Czech University of Life Sciences Prague, Faculty of Engineering, Department of Technological Equipment of Buildings, Kamýcká 129, CZ16521 Prague, Czech Republic; *Correspondence: malatak@tf.czu.cz

Abstract. The purpose of this paper is to explore the thermal emission characteristics of alternative fuels gained from the composting process and intended for local energy use. The first goal is to determine the basic parameters of the examined samples (elemental analysis). The thermal emission parameters of the combustion device, such as the flue gas temperature and emission concentration of carbon monoxide, carbon dioxide and nitrogen oxides in relation to the operating conditions of the combustion device with an automatic feed fuel burner furnace are also considered. Pellets from oversized chips gained from the composting process and the pelleted mixtures of compost and spruce sawdust in the ratio 1:1 were burnt in the burner furnace.
The resulting values of the samples' individual elemental analyses indicate the optimal properties for further energy utilization. The amount of excess air generated during combustion, however, is high and this is also reflected in the great loss of flue gas sensible heat. The resulting parameters further prove that the excess air coefficient (n) depends on flue gas temperature, as well as carbon dioxide, monoxide and nitrogen oxides content in the flue gas. It was concluded during the combustion tests that the pollutants monitored in the flow did not reach the limit values. The scientific hypothesis of the author confirms that the stabilized dried mixture of plant biomass and appropriate biodegradable waste is suitable for biomass combustion. The available data suggest that the use of compost for energy purposes through combustion is possible, if biodried biomass is used, i.e., special products of composting processes are used in medium-sized and large combustion devices.

Key words: alternative fuel, elemental and stoichiometric analyses, emission concentrations.

INTRODUCTION

The available data suggest that the use of compost for energy purposes through combustion is possible if the biomass is biologically dried, i.e., a special product of the composting process (Kranert et al., 2010) is used. Compost is a stable and sanitized slow-acting organic fertilizer that does not contain soluble forms of nitrogen. It has a wide ratio of nutrients C : N; besides the basic macroelements (NPK), it contains Ca, Mg and microelements, stable humus, soil microorganisms and alkaline acting substances (Goyal et al., 2005).

Compost used for energy purposes (Raclavska et al., 2011), energy exploitable biomass, is a specific type of compost. Recently, technologies of energy compost production designed for the direct combustion, gasification or pyrolysis processing were developed in addition to traditional composting methods (Boldrin & Christensen, 2010). Generally, the end-product is so called solid fuel made from completely dried and shaped

compost (Kranert et al., 2010). So that this fuel could be used for energy, it is essential to monitor its thermal properties, such as calorific value (Ruzbarsky et al., 2014), as well as emission characteristics (Hajek et al., 2013).

The article is based on the hypothesis that the stabilized dried mixture of biomass and appropriate biodegradable waste correspond to the requirements of biomass combustion in view of combustion emissions. To confirm or refute this hypothesis, the article aims to experimentally determine the thermal emission characteristics of alternative fuels generated from composting processes and intended for local energy use. The first goal is to establish the basic parameters of examined samples (elemental analysis). Parameters such as flue gas temperature and individual emission concentration in the flue gas depending on the operating conditions of the combustion device are monitored.

MATERIALS AND METHODS

The classic composting technology of piles without forced aeration was used for measurement purposes in the composting facility at the Jarošovice, Ltd composting site. For elemental analysis, oversized components of the composting process were used. These were mainly forestry waste, sawdust, shavings, cuttings, wood, veneer, biodegradable waste paper, cardboard, wood and biodegradable waste from gardens and parks. These oversized components of the composting process were mixed with spruce sawdust in the ratio 1:1 for improving thermal emission parameters.

Elemental analysis of the samples is the primary objective of the project. Carbon, hydrogen and nitrogen were detected with the Perkin-Elmer 2400 CHN analyser. For the determination of chlorine and sulphur content, the samples were burned in an oxygen-hydrogen flame on a Wickbold apparatus. Non-combustible fuel substances, i.e., ash and total water content were determined by burning and drying the sample. The gross calorific value of the examined biofuel samples was determined by performing measurements with the calorimeter IKA 2000. Net calorific value was determined by calculations, using the elemental analysis results of individual samples.

Thermal emission measurements were carried out with the KNP hot stove made by the company KOVO NOVAK; the device incorporates automatic fuel feeding and a burner furnace. The nominal thermo-technical specifications of the hot stove are: nominal power 18 kW, controllable output 8–18 kW and fuel consumption 1.5–4.9 kg h^{-1}.

The fuel samples were burnt at the nominal thermal parameters of the combustion device, whereas a constant fuel supply was guaranteed and the combustion air supply was modified. Each sample was burnt for three hours. Emission concentration measurements were performed by measuring flue gas with Madur GA-60. The values of ambient temperature, exhaust temperature and the chemical composition of gases (O_2, CO, SO_2, NO, NO_2) were measured. The signal of transducers is proportional to the volume concentration of measured components in ppm. The record interval of the average individual components was set to one minute. The measuring device was calibrated before each measurement. Emission concentrations were converted from ppm concentrations to normal conditions and to mg m^{-3}. It was determined that reference oxygen content in the flue gas is 11%.

Next, the results of thermal emission measurements were processed with regression statistical analysis for expressing the mathematical relationship between carbon monoxide, flue gas temperature and nitrogen oxides with the excess air coefficient. The formula of excess air coefficient (n) is:

$$n = 1 + \left(\frac{CO_{2,\max}}{CO_2} - 1 \right) \cdot \frac{V_{sp,\min}}{L_{\min}} \quad (1)$$

where: $CO_{2,max}$ is the theoretical volume concentration of carbon dioxide in dry flue gases (%); CO_2 is the real (measured) volume concentration of carbon dioxide in dry flue gases (%); $V_{sp,min}$ is the theoretical mass amount of dry flue gas ($m^3_N\ kg^{-1}$); L_{min} is the theoretical amount of air necessary for complete combustion ($m^3_N\ kg^{-1}$).

RESULTS AND DISCUSSION

The values gained from the elemental analysis of selected pellet samples in their original state are shown in Table 1.

Table 1. Elemental analysis of pellet samples, diameter 6 mm

Sample	Water Content (% Wt.)	Ash (% Wt.)	Gross Calorific Value ($MJ \cdot kg^{-1}$)	Net Calorific Value ($MJ \cdot kg^{-1}$)	Carbon C (% Wt.)	Hydrogen H (% Wt.)	Nitrogen N (% Wt.)	Sulphur S (% Wt.)	Oxygen O (% Wt.)
	W	A	Q_s	Q_i	C	H	N	S	O
Compost + Spruce sawdust (1:1 ratio)	**6.37**	**22.39**	13.57	**12.66**	35.41	3.47	1.09	0.0	31.24
Oversized chips from the composting process	**6.72**	**36.85**	11.05	**10.24**	29.30	2.95	1.03	0.0	23.13

The elemental analyses reveals that the most decisive factor in terms of the thermal use of selected samples is calorific value, which depends on the water and ash content in the fuel (Ruzbarsky et al., 2014). Low water content in the samples is a positive factor because humidity affects the combustion process and exhaust gas volume produced per unit of energy (Malaťák et al., 2009). The ash content in the samples is high compared to various wood biomasses (Malatak & Kucera, 2013). The amount of ash decreases significantly after sawdust is added to the oversized chips gained from the composting process. Such a large amount of ash significantly affects the thermal properties of solid fuels under consideration and consequently affects both the selection and adjustment of the combustion device (Johansson et al., 2004).

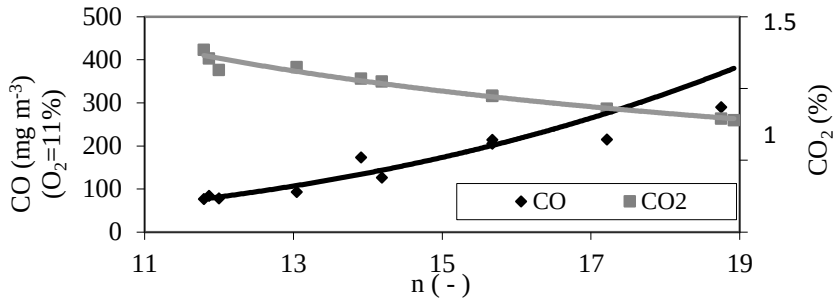

Figure 1. Dependence of carbon monoxide and carbon dioxide on the excess air coefficient – the combustion of compost and pelleted spruce sawdust mixture in the ratio 1:1.

During the combustion of the compost and pelleted spruce sawdust mixture in the ratio 1:1 (Fig. 1) the excess air coefficient *n* increased and with that, the emission concentration of carbon monoxide for *n* in the range of 12 to 19 according to the regression equation (1) at the confidence level of $R^2 = 0.90$ increased as well:

$$CO = 0.0183n^{3.3812}\ (mg \cdot m^{-3}) \qquad (2)$$

At the same time, the CO_2 concentration for *n* in the range of 12 to 19 according to the regression equation (2) gradually decreased:

$$CO_2 = 21.71n^{-1}\ (\%) \qquad (3)$$

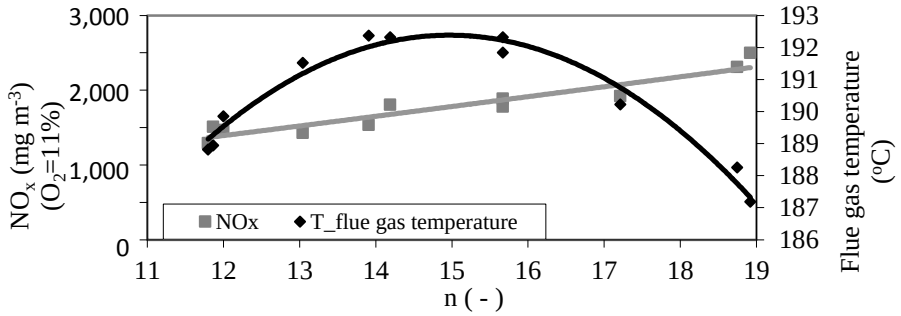

Figure 2. Dependence of nitrogen oxides and flue gas temperature on the excess air coefficient – the combustion of compost and pelleted spruce sawdust mixture in the ratio 1:1.

While the excess air coefficient (if the value of the excess air coefficient is over 21) increases, as seen in Fig. 2, the combustion process is supressed and combustion temperatures also decrease. This process can be expressed with the regression equation (3) for *n* in the range of 12 to 19 at the confidence level of $R^2 = 0.89$:

$$T_{flue\ gas} = 89.7736n^{1.1035}\ (°C) \qquad (4)$$

At the same time, it is evident that the nitrogen oxides *NOx* emission concentrations increase; while this is expressed with the regression equation (4) for *n* in the range of 12 to 19 at the confidence level of $R^2 = 0.96$:

$$NOx = -0.3235n^2 + 9{,}6916n + 119.94 \ (mg\ m^{-3}) \quad (5)$$

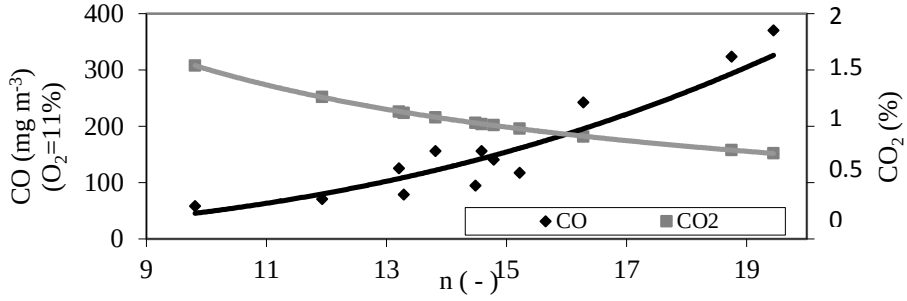

Figure 3. Dependence of carbon monoxide and carbon dioxide on the excess air coefficient – the combustion of pelleted oversized chips gained from the composting process.

The emission concentration of carbon monoxide *CO* (see Fig. 3) increases with the combustion of the compost sample, while the excess air coefficient *n* expressed with the regression equation (5) for *n* in the range of 10 to 20 at the confidence level of $R^2 = 0.84$ also increases:

$$CO = 0.0641n^{2.8756} \ (mg \cdot m^{-3}) \quad (6)$$

On the other hand, the concentration of carbon dioxide CO_2 reduces according to the regression equation (6) for *n* in the range of 10 to 20:

$$CO_2 = 20.862n^{-1.0004} \ (\%) \quad (7)$$

The ever increasing excess air coefficient, as shown in Fig. 4, leads to the attenuation of combustion processes and reduction of combustion temperatures. This process is described with the regression equation (7) at the confidence level of $R^2 = 0.86$:

$$T_{flue\ gas} = 0.2733n^2 - 11.88n + 311.6 \ (°C) \quad (8)$$

At the same time, the emission concentrations of nitrogen oxides *NOx* are constantly increasing, which is described with the regression equation (8) for *n* in the range of 10 to 20 at the confidence level of $R^2 = 0.83$:

$$NOx = 1.766n^{2.5735} \ (mg \cdot m^{-3}) \quad (9)$$

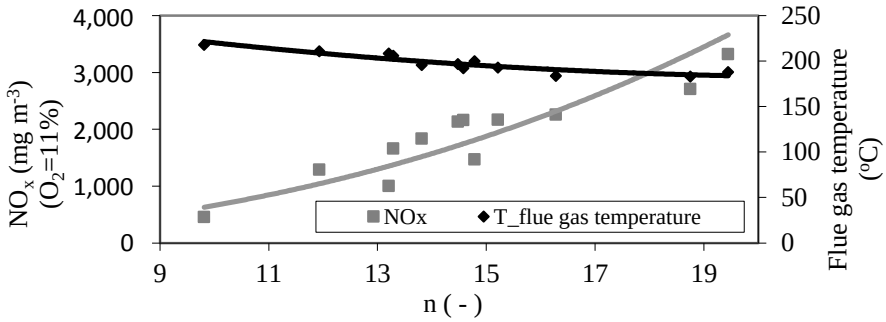

Figure 4. Dependence of nitrogen oxides and flue gas temperature on the excess air coefficient – combustion of pelleted oversized chips gained from the composting process.

The resulting values of thermal emission measurements show high concentrations of carbon monoxide *CO* and nitrogen oxides *NOx* in the areas of high excess air coefficient *n*. As shown in research works by the authors Fiedler & Persson (2009), the combustion process is the most efficient at nominal parameters, any uncontrolled change in the flow of combustion material and combustion air leads to high emissions of carbon monoxide and nitrogen oxides, and reduces the combustion temperature.

The quality (efficiency) of combustion (Johansson et al., 2003) can be determined from the content of CO_2 in the flue gas. If excess air content is low (complete combustion) and the highest possible concentration of CO_2 is achieved, the loss caused by the flue gas is minimal (flue gas at the same temperature). For each solid fuel, there is a maximum achievable stoichiometric proportion of carbon dioxide CO_2 in the flue gas, which is determined by the elemental composition of combustible fuel (Malatak & Kucera, 2013). This value is within the measurement uncertainty limits.

CONCLUSIONS

- The excess air value *n* is generally high during combustion in a burner furnace and this is also reflected in the high heat losses of the flue gas (chimney losses) and even in the carbon dioxide and nitrogen oxides' concentrations. The measurement results provide more ways for the optimal energy use of compost and separates that are not suitable for, e.g., fertilizer for various reasons.
- The increased amount of ash hinders the energy use of compost and separates for small combustion plants. These samples can be energetically used for medium-sized and large combustion devices with a controlled combustion process and exhaust gas cleaning systems.
- In terms of processing procedures, the biodrying of biomass is the most efficient for the energy use of compost. Thus, it can be used as a solid biofuel for direct combustion in medium-sized and large power plants or as feedstock for the thermochemical conversion process of carbonization, gasification or pyrolysis.

ACKNOWLEDGEMENTS. The article was financially supported by the Internal Grant Agency of the Faculty of Engineering at Czech University of Life Sciences in Prague (GA TF) No. 2014: 31170/1312/3126.

REFERENCES

Boldrin, A. & Christensen, T.H. 2010. Seasonal generation and composition of garden waste in Aarhus (Denmark). *Waste Management* **30**(4), 551–557.

Fiedler, F., & Persson, T. 2009. Carbon monoxide emissions of combined pellet and solar heating system. *Applied Energy* **86**(2), 135–143.

Goyal, S., Dhull, S.K. & Kapoor, K.K. 2005. Chemical and biological changes during composting of different organic wastes and assessment of compost maturity. *Bioresource Technology* **96**(14), 1584–1591.

Hajek, D., Malatak, J. & Hajek, P. 2013. Combustion of selected biofuels types in furnace burner. *Scientia Agriculturae Bohemica* **44**(1), 23–31.

Johansson, L.S., Leckner, B., Gustavsson, L., Cooper, D., Tullin, C. & Potter, A. 2004. Emission characteristics of modern and old-type residential boilers fired with wood logs and wood pellets. *Atmospheric Environment* **38**(25), 4183–4195.

Johansson, L.S., Tullin, C., Leckner, B., & Sjövall, P. 2003. Particle emissions from biomass combustion in small combustors. *Biomass and Bioenergy* **25**, 435–446.

Kranert, M., Gottschall, R., Bruns, C. & Hafner, G. 2010. Energy or compost from green waste? – A CO_2 - Based assessment. *Waste Management* **30**(4), 697–701.

Malaťák, J., Gurdil, G., Jevič, P. & Selvi, K.C. 2009. Biomass heat-emission characteristics of energy. *AMA – Agricultural Mechanization in Asia, Africa and Latin America* **39**(4), 9–13.

Malatak, J. & Kucera, M. 2013. Determination of some properties of solid biofuels from the pyrolysis technology. *Acta Facultatis Xylologiae* **55**(1), 119–127.

Raclavska, H., Juchelkova, D., Skrobankova, H., Wiltowski, T. & Campen, A. 2011. Conditions for energy generation as an alternative approach to compost utilization. *Environmental Technology* **32**(4), 407–417.

Ruzbarsky, J., Müller, M. & Hrabe, P. 2014. Analysis of physical and mechanical properties and of gross calorific value of Jatropha curcas seeds and waste from pressing process. *Agronomy Research* **12**(2), 603–610.

Agronomy Research **13**(2), 420–429, 2015

Green energy from different feedstock processed under anaerobic conditions

V. Skorupskaitė[1], V. Makarevičienė[1,*], G. Šiaudinis[2] and V. Zajančauskaitė[3]

[1]Aleksandras Stulginskis University, Faculty of Forest Sciences and Ecology, Institute of Environment and Ecology, Studentų Str. 11, LT53361 Akademija, Kauno district, Lithuania; [*]Correspondence: virginija.skorupskaite@asu.lt
[2]Vėžaičiai Branch of Lithuanian Research Centre for Agriculture and Forestry, Gargždų str. 29, LT96216 Vezaiciai, Klaipėda district, Lithuania
[3]Klaipėda University, Faculty of Marine Technology, Department of technological process. Herkaus Manto Str. 84, LT92294 Klaipėda, Lithuania

Abstract. The possible use of energy crops and aquaculture for bioenergy production has only recently become a research target, so there is little information on their properties and advantages. The aim of this study was to investigate the possible use of cup plant, as well as marine and freshwater algae (*Scenedesmus sp*. and *Chlorella sp*.) for biogas production. Research of a batch anaerobic digestion process at a mesophilic temperature were performed using wet wastewater sludge, cattle manure, fresh microalgae biomass and dry marine algae, cup plant biomass and mixtures of these materials. The highest biogas yield (541.28 ml g^{-1} VS) was obtained by using a new feedstock from the microalgae *Scenedesmus sp*. biomass. That yield was 1.4 times higher than the biogas yield from cattle manure and 15% lower than the biogas yield from wastewater sludge. It was found that adding microalgae biomass to a cattle manure substrate increases biogas production approx. 1.5 times. The highest methane concentration in biogas produced from microalgae ranges from 64.87% to 66.66% and exceeds the methane amount (64.26%) in biogas produced from wastewater sludge. The methane amount in biogas produced from cattle manure, cup plant and marine algae biomass is lower than 60%. In addition, it was found that it is possible to produce 5,092.3 m^3 of biogas or 113 GJ of energy from 1 ha of harvested cup plant biomass.

Key words: biogas production, microalgae, marine algae, cup plant, cattle manure, wastewater sludge.

INTRODUCTION

Decomposition of organic matter is a natural process that has happened under anaerobic conditions since time immemorial. In the absence of oxygen and at certain temperature, certain groups of bacteria break down organic materials such as carbohydrates, proteins and grease into a gas composed mainly of methane (50–85%) and carbon dioxide (20–40%) (Herout et al, 2011; Ács et al., 2015).

The beginning of biogas production and its use for energy purposes started a few decades earlier (Buswell & Mueller, 1952) than the demand for renewable energy sources. Nowadays, the most prevalent sources of biogas production are conventional raw materials, such as wastewater treatment sludge, pig, poultry and cattle manure, and maize silage, while the overall production of biomass is growing. According to a report

by the European Biogas Association, over 13,800 power plants with a more than 7,400 MW_{el} capacity were constructed in Europe in 2012.

In order to increase the quantitative and qualitative parameters of biogas, it is necessary to control some parameters, like temperature, pH, C:N ratio, substrate composition , etc.

In addition to the above-mentioned feedstocks, there are many potential candidates that could supplement or replace the raw materials of methane production. The possible use of terrestrial energy crops and aquaculture for biogas production has only recently become a research target, so there is little information on their properties and advantages.

Despite the fact that the use of crop biomass for the production of biogas has substantially increased in many European countries, maize (*Zea mays* L.) outweighs other species. The increase in maize cultivation has led to soil degradation, susceptibility to crop diseases and pests, and changes in the natural landscape (Robertson et al., 2008; Fletcher et al., 2010; Gansberg et al., 2015). One possible alternative might be the cultivation of perennial crops, which might have some superiority over the annuals due to lower amounts of energy needed for cultivation, which might substantially reduce the expenses (Jasinskas & Kryzeviciene, 2006). The most perspective are the species which can easily adapt to local agro-climatic conditions (McKendry, 2002).

Silphium species originate from North America (Huxley, 1992). In contrast, some European countries have conducted many important experiments with *Silphium* genus as a potential decorative, melliferous and fodder crop (Kowalski 2004; Kowalski 2007; Lehmkuhler, 2007).

Manu authors state that various Silphium species could produce a high annual biomass yield (Kowalski, 2004; Kowalski, 2007; Šiaudinis et al., 2012). Although there had been some suggestions that its biomass could potentially be used for biogas production, *Silphium* genus only gained attention as a potential crop for biogas production in the recent years (Voigt et al., 2012; Jasinskas et al., 2014; Mast et al., 2014). All in all, in the light of the advances in technology and the use of biomass for bioenergy purposes, this topic warrants further research (Gansberger et al., 2015).

Another source material for biofuel production could be algae. Recently, an important issue for researchers has been the investigation of possible uses of algae biomass for bioenergy production due to its advantages, such as fast growth, high carbon dioxide fixation ability, treatment of wastewater, and the lack of competition for arable land (Mata et al, 2010; Brennan & Owende, 2010; Podkuiko et al, 2014).

The goal of our study was to investigate the applicability of new non-traditional materials for biogas production, as well as to compare the quantitative and qualitative indicators of the biogas produced from these feedstocks with properties of biogas produced from conventional materials.

The aim of our research was to: 1) investigate the quantitative and qualitative parameters of new non-traditional materials (cup plant, algae) and their suitability for biogas production; 2) compare the properties of the biogas produced from new feedstock to that produced from conventional ones (manure, wastewater).

MATERIALS AND METHODS

Cup plant (*Silphium perfoliatum* L.) has been cultivated at an experimental long-term energy crops site at the Vėžaičiai branch of the Lithuanian Research Centre for Agriculture and Forestry (Western Lithuania, 55º43′N, 21º27 E) since 2008 (Fig. 1). Before the beginning of the experiment, the following characteristics of upper soil layer (0–20 cm) were determined: pH_{KCl} 4.25–4.45, mobile P_2O_5 35–120 mg kg^{-1}, mobile K_2O 140–209 mg kg^{-1}, hydrolytic acidity 21.9–62.1 mequiv kg^{-1} and mobile Al 10.7–50.9 mg kg^{-1}.

Figure 1. Cup plant at flowering stage.

The experiment was composed of two factorial designs with three levels of soil liming (not limed, limed at 3.0 t ha^{-1} and 6.0 t ha^{-1} rates) and three levels of nitrogen fertilization (0, 60 and 120 kg ha^{-1} N). Lime application was done once just before the beginning of the experiment. Nitrogen fertilization (with ammonium nitrate) was performed each year. The rates of phosphorus (with a single superphosphate) and potassium (potassium chloride) fertilizers were equal for all the treatments – 60 kg ha^{-1} P_2O_5 and 60 kg ha^{-1} K_2O.

Cup plant seedlings at 2–3 leaf stage were planted at the experimental site in 2008. From 2009 onwards, cup plant biomass yield was cut annually using a rotary reaper (Claas, Germany) at full maturity stage, which falls to the end of September. In addition, in 2014, samplings for dry mass qualitative analysis were carried out during cup plant's flowering stage (on 3 June). The biomass that was selected for analysis came from cup plants grown in the soil that had received no liming or N fertilization, as it was grown using the lowest energetic expenses, in natural soil and under natural climatic conditions.

Marine algae biomass was gathered at the coast of the Baltic Sea, at the Šventoji river mouth on 3 July 2014. It was visually estimated that red algae (Rhodophyta) was the prevailing species (Fig. 2).

Figure 2. Marine algae, air-dry mass (DM).

The mixture of primary and redundant active wastewater sludge was purchased from JSC Kauno vandenys (Kaunas).

Cattle manure was acquired from a local farmer. Before it was used for biogas production, cattle manure was stored at 5 °C temperature in a refrigerator in order to avoid biological decomposition.

Freshwater microalgae *Scenedesmus sp.* and *Chlorella sp.* were isolated from Lithuanian lakes. A laboratory stand equipped with magnetic stirrers was used for microalgae batch cultivation. Both microalgae species were cultivated under mixotrophic growth conditions at a room temperature (22 ± 2 °C) mixing, in plastic cylinders with a working volume of 3 L. The duration of microalgae cultivation was 30 days. *Scenedesmus sp*. and *Chlorella sp*. were grown under ~250 μmol photons m^{-2} s^{-1} of illumination using white fluorescent lamps for 10 h a day. Light intensity was estimated using a data logger (model LI-1400) with a LI-190SA Quantum sensor. Mixotrophic growth was carried out by growing microalgae *Scenedesmus sp*. in a modified BG11 medium (Skorupskaite et al., 2015) with adding 5 gL^{-1} of technical glycerol purchased from JSC Rapsoila (Lithuanian producer of biodiesel). *Chlorella sp*. was cultivated in a growth medium composed of modified BG11 + 2 gL^{-1} technical glycerol.

After cultivation, microalgae biomass was concentrated by centrifugation for 15 minutes at 4,700 rpm using a Thermo Scientific Heraeus Multifuge X3R centrifuge. The amount of volatile solids in microalgae biomass and other materials was measured by drying the feedstock in an oven at 105 °C to a constant weight and then by burning dry matter in a muffle oven at 550 °C for 2 hours.

Elemental composition of microalgae biomass was determined using CHNS-O Elemental Analyser (Perkin Elmer 2400 Series). Dry *Scenedesmus sp*. and *Chlorella sp*. biomass was pulverized using a mortar, weighed on thin foil (app. 2 mg), placed in an elemental furnace, combusted in a pure oxygen environment at 975 °C, analysed, and the weight of each element was calculated.

Both cup plant and marine algae green biomass were dried and recalculated to air-dry mass (DM). Chemical analyses of both crops were done based on samples dried at 105 °C for a total C and N content estimation. A dry combustion (*Dumas method*) was

used to measure organic carbon content (C). Total nitrogen content (N) was measured using the Kheldahl method.

The biogas production research was carried out using a feedstock made from wet wastewater sludge and cow manure, dry cup plant and marine algae, wet freshwater microalgae, and mixtures of these materials. Since cup plant and marine algae biomass can be stored and transported, such types of biomass was used dry for biogas production research. Wet freshwater microalgae biomass was used in the research, because drying of the biomass consisting of such type of algae requires a lot of energy and could significantly increase energy consumption during biogas production process.

Substrata containing different materials and mixtures (every species of freshwater microalgae with wastewater sludge and microalgae with cow manure 50% + 50%; marine algae with cup plant with a proportion 50% + 50% and 30% + 70% were prepared so that each of substrate should contain 0.25 g of volatile solids.

100 ml syringes (Hohenheim fermentation test) were used as small biogas reactors. Syringes were filled with a homogenized mass mixture composed of 30 ml of inoculum and substrate. The digested wastewater treatment sludge was used as an inoculum. Inoculum without substrata was used as a negative control sample. In order to keep them at the same temperature during the whole experiment, all syringes were placed on a thermostatically controlled laboratory shaker (Fig. 3). Anaerobic conditions in bioreactors were created by pushing air out of the syringes. All syringes were closed using tube clips.

Figure 3. Biogas production in syringes.

Biogas was produced at 37 °C temperature for approx. 25 days. The amount of produced biogas was measured while keeping the syringe in a vertical position. Composition of biogas was measured through gas chromatography using a Clarus 580 GC chromatograph (Perkin Elmer) equipped with a thermal conductivity detector. All experiments were performed in triplicate.

RESULTS AND DISCUSSION

The average cup plant dry mass yield per season during 2009–2014 was 13.15 t ha^{-1} (Fig. 4). In the first harvestable year (2009), cup plant yield was small. But in the following years, biomass yield was high and relatively similar. These results are in accordance with the results of other authors (Filatov et al., 1986).

Both of the investigated factors, the liming and nitrogen fertilization had a significant effect on cup plant dry mass yield.

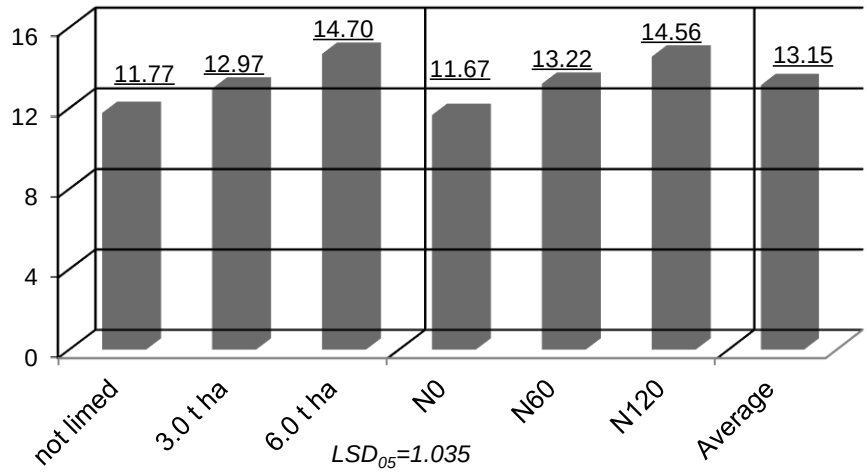

Figure 4. Cup plant dry mass yield.

The application of 6.0 t ha^{-1} $CaCO_3$ lime significantly increased cup plant productivity – the average cup plant yield was 14.70 t ha^{-1} (or 25% higher in comparison to the control sample). Similarly, the application of 120 kg ha^{-1} N rate increased dry mass yield up to 14.56 t ha^{-1} on average (or 24.80% higher in comparison to samples that had not received nitrogen treatments).

Carbon and nitrogen (C:N) ratio in the feedstock is one of the most important factors that influence biogas quality and production output. According to Schnürer & Jarvis, (2009), the maximum volume of biogas is released when the C:N ratio varies between 10 and 30. The higher the C:N ratio (from 10 to 30), the better the formation of fatty acids as well as the methanogenesis stimulation. The results of our experiments (Fig. 5) showed that the highest C:N ratio was found in cup plant biomass; meanwhile the lowest C:N ratio was found in microalgae *Chlorella sp*. biomass. It seems that C:N ratio in *Scenedesmus sp*. biomass is optimal for biogas production. Taking into consideration of these results, it could be stated that *Scenedesmus sp*. microalgae and marine algae biomass can be used for biogas production without adding of any kind of co-substratum.

This study investigated biogas production from conventional feedstock and new potential raw materials like cup plant, marine algae and freshwater microalgae. Different types of biomass and mixtures of it were used for the study.

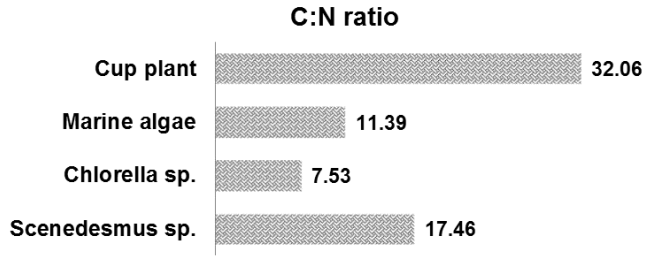

Figure 5. C:N ratio in different types of biomass.

The first experiment on biogas production was carried out using both conventional raw material like wastewater sludge and cattle manure, and new feedstock material such as microalgae and marine algae. The results of the quantitative analysis showed that potential new raw materials could be promising for biogas production (Fig. 6). Out of those, the highest biogas yield (541 ml g^{-1}VS) from new raw materials was achieved using *Scenedesmus sp*. In comparison, that is about 28% more than the biogas yield from cow manure and 16% less than the biogas yield obtained from wastewater sludge. Similar results (524 ml g^{-1}VS) were derived from *Chlorella sp*. Cup plant biogas yield was 421 ml g^{-1}VS. Results of comparatively small yields of biogas produced from cup plant and marine algae can be explained by a smaller amount of moisture, which could inhibit biocenose activity (Schnürer & Jarvis, 2009) because the cup plant and marine algae biomass was dried before use.

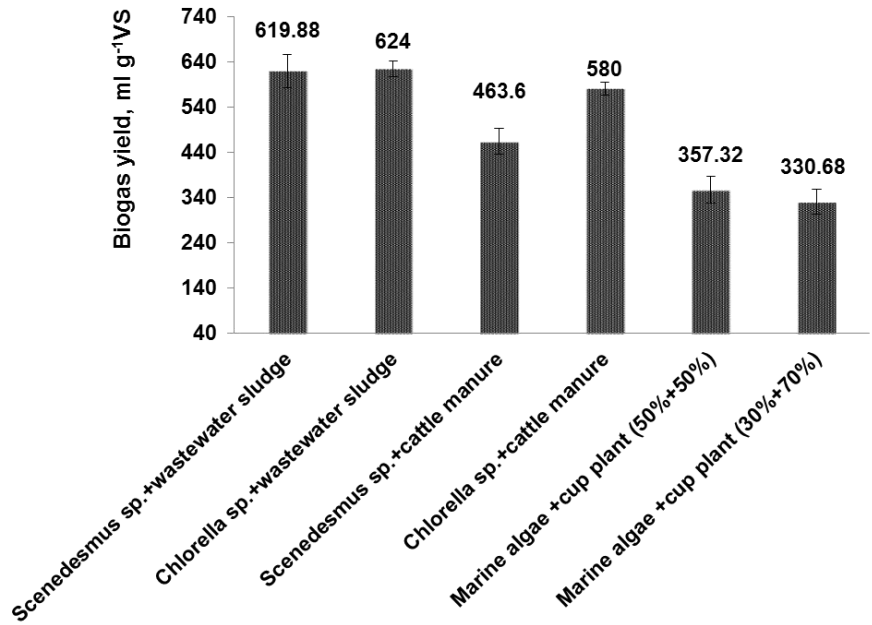

Figure 6. Biogas yield from different feedstocks.

Further analyses of biogas production were performed using mixtures of substrata (Fig. 7). Conventional raw materials were mixed with freshwater microalgae biomass, and marine algae were mixed with cup plant in different ratios. The results of the experiments reveal that aquaculture feedstock could be used for biogas production as sole substrate as well as co-substrate. A 50% of addition of freshwater microalgae to cattle manure improved the biogas yield 1.49 and 1.19 times in the case of *Chlorella sp*. and *Scenedesmus sp*., respectively. The presented results revealed that there is no big difference between the biogas yield from wastewater sludge and its mixtures with microalgae *Scenedesmus sp*. and *Chlorella sp*., therefore it can be stated that wet microalgae biomass could be used as additional feedstock to wastewater sludge substrata without adverse effects to the biogas yield.

The 50% addition of cup plant biomass to the marine algae substrate improves quantitative properties of biogas production approx. 1.4 times.

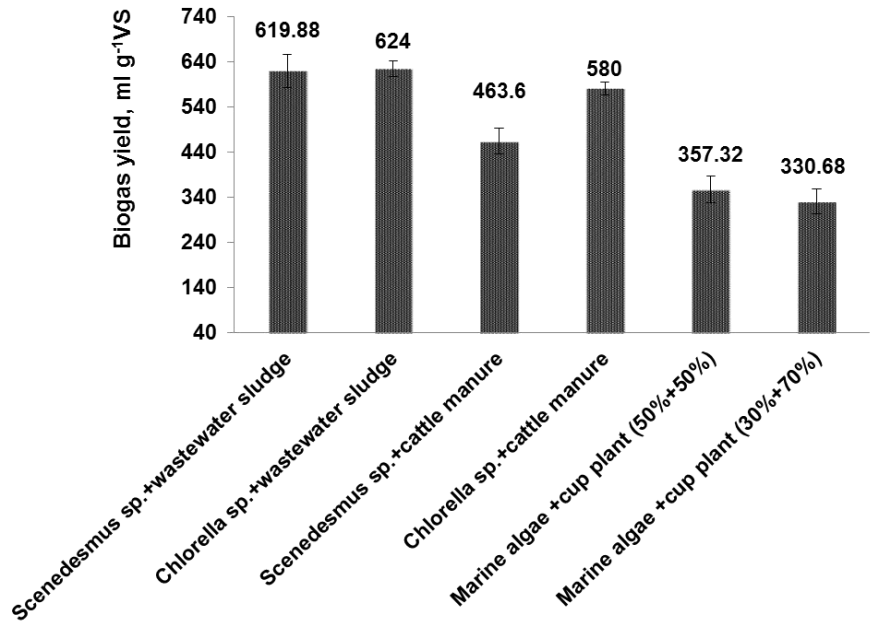

Figure 7. Dependence of biogas yield on different mixtures of substrata.

The examination of the composition of produced biogas (Fig. 8) revealed that methane content in biogas, produced from different substrata, varied between 57.53% and 66.66%. The highest methane content was found to be in the biogas produced from microalgae *Scenedesmus sp*. and *Chlorella sp*. Biogas produced from these microalgae species contain 64.87% to 66.66% of methane. The lowest methane yields (< 60%) were fixed in the biogas produced from cow manure, cup plant and marine algae. The addition of wet microalgae biomass into the wastewater sludge or cattle manure substrate increases methane content of produced biogas by approx. 2%. In this case, 1 m^3 biogas containing 2% more methane has an additional 1 kJ of energy.

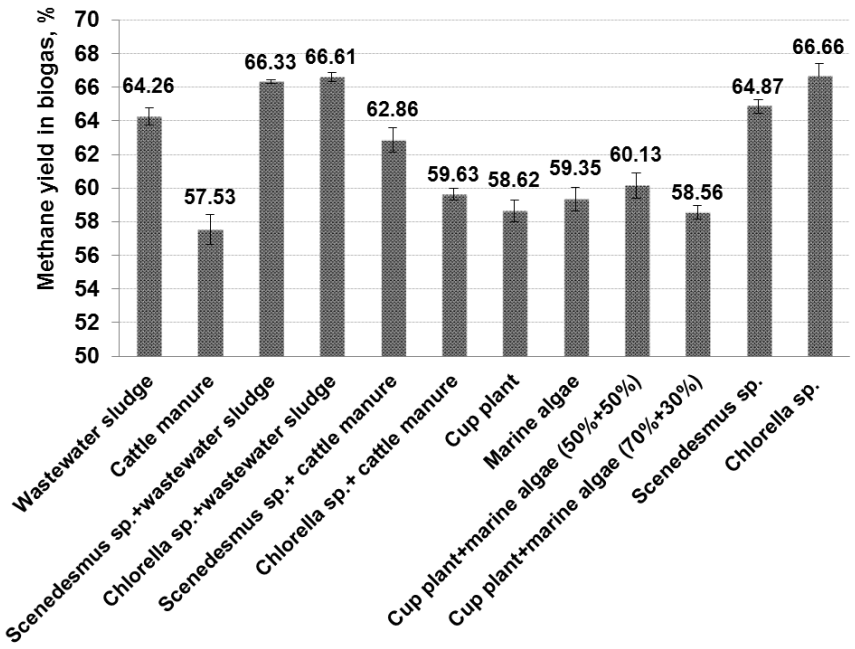

Figure 8. Methane amount in biogas produced from different types of feedstock.

According to the results of our research, 1 ha of harvested cup plant biomass could produce 5,092.3 m^3 biogas, which contains 58.62% of methane. Such amount of biogas is equal to 113 GJ of energy.

CONCLUSIONS

To summarize the results of biogas production from wastewater treatment sludge, cattle manure and cup plant, marine and freshwater algae, it has to be noted that new types of biomass sources could be added to the conventional raw materials of methane production. Fresh concentrated microalgae biomass as a supplement to cattle manure substrate helps to improve not only quantitative (approx. 1.49 times), but also qualitative (increase of methane amount from 2 to 5%) indicators in biogas production. Biogas produced from a new type of feedstock contains a relatively high concentration of methane and it could be used for co-generation systems.

REFERENCES

Ács, N., Bagi, Z., Rákhely, G., Minárovics, J., Nagy, K. & Kovác, K. L. 2015. Bioaugmentation of biogas production by a hydrogen-producing bacterium. *Bioresource technology* **186**, 286–293.

Brennan, L. & Owende, P. 2010. Biofuels from microalgae-A review of technologies for production, processing, and extractions of biofuels and co-products. *Renewable and Sustanable Energy Reviews* **14**(2), 557–577.

Buswell, A.M. & Mueller, H.F., 1952. Mechanism of Methane Fermentation. *Industrial & Engineering Chemistry* **44**(3), 550–552.

Filatov, V.I., Bakalov, A.M., Lavrov, B.V. & Komyagin, N.A. 1986. Productivity of Silphium perfoliatum as a function of agricultural technology practices on ameliorated soils. *Biological Abstracts* **82**(6): 50072. C.A.B. International Abstracts OG056-02413.

Fletcher, Jr, R.J., Robertson, B.A., Evans, J., Doran, P.J., Alavalapati, J.R. & Schemske, D.W. 2010. Biodiversity conservation in the era of biofuels: risks and opportunities. *Frontiers in Ecology and the Environment* **9**(3), 161–168.

Gansberger, M., Montgomery, L.F. & Liebhard, P. 2015. Botanical characteristics, crop management and potential of Silphium perfoliatum L. as a renewable resource for biogas production: A review. *Industrial Crops and Products* **63**, 362–372.

Herout, M., Malaťák, J., Kučera, L. & Dlabaja, T. 2011. Biogas composition depending on the type of plant biomass used. *Research in Agricultural Engineering* **57** (4), 137–143.

Huxley, A. 1992. The New RHS Dictionary of Gardening, London, UK, 3000 p.

Jasinskas, A. & Kryževičienė, A. 2006. Energetic grassland and the input of growing them and preparation for fuel. *Žemės Ūkio Inžinerija* **38**(3), 59–71.

Jasinskas, A., Simonavičiūtė, R., Šiaudinis, G., Liaudanskienė, I., Antanaitis, Š., Arak, M. & Olt, J. 2014. The assessment of common mugwort (Artemisia vulgaris L.) and cup plant (Silphium perfoliatum L.) productivity and technological preparation for solid biofuel. *Žemdirbystė (Agriculture)* **101**(1), 19–26.

Kowalski, R. 2004. Growth and development of Silphium integrifolium in the first 3 years of cultivation. *New Zealand of Crop and Horticultural Science* **32**, 389–395.

Kowalski, R. 2007. Silphium trifoliatum L. – a new alternative cultivation herbal plant? *Acta Agriculturae Scandinavica, Section B: Soil and Plant Science* **57**(2), 155–166.

Lehmkuhler, J. W., Ramos, M.H. & Albrecht, K.A. 2007. Cupplant Silage as a Replacement for Corn Silage in Growing Beef Cattle Diets. *Forage and Grazinglands*, **5**(1), [accessed 28 01 2015].

Mast, B., Lemmer, A., Oechsner, H., Reinhardt-Hanisch, A., Claupein, W. & Graeff-Hönninger, S. 2014. Methane yield potential of novel perennial biogas crops influenced by harvest date. Industrial Crops and Products, 58, 194–203.

Mata, T., Martins, A.A. & Caetano, N.S. 2010. Microalgae for biodiesel production and other applications: A review. *Renewable and Sustainable Energy Reviews* **14**(1), 217–232.

McKendry, P. 2002. Energy production from biomass (part 1): overview of biomass. Bioresource technology **83**(1), 37–46.

Podkuiko, L., Ritslaid, K., Olt, J. & Kikas, T. 2014. Review of promissing strategies for zero-waste of the third generation biofuels. *Agronomy Research* **12**(2), 373–390.

Skorupskaite, V., Makareviciene, V. & Levisauskas, D. 2015. Optimization of mixotrophic cultivation of microalgae Chlorella sp. for biofuel production using response surface methodology. *Algal Research* **7**, 45–50.

Schnürer, A. and Jarvis, Å. 2009. Microbiological handbook for biogas plants. Swedish gas centre report 207, 30–47.

Šiaudinis, G., Jasinskas, A., Šlepetienė, A. & Karčauskienė, D. 2012. The evaluation of biomass and energy productivity of common mugwort (*Artemisia vulgaris* L.) and cup plant (*Silphium perfoliatum* L.) in Albeluvisol.*Žemdirbystė (Agriculture)* **99**(4), 357–362.

Robertson, G.P., Dale, V.H., Doering, O.C., Hamburg, S.P., Melillo, J.M., Wander, M.M., Parton, W.J., Adler, P.R., Barney, J.N., Cruse, R.M., Duke, C.S., Fearnside, P.M., Follett, R.F., Gibbs, H.K., Goldemberg, J., Mladenoff, D.J., Ojima, D., Palmer, M.W., Sharpley, A., Wallace, L., Weathers, K.C., Wiens, J.A. & Wilhelm, W.W. 2008. Agriculture. Sustainable biofuels redux. *Science (New York, NY)* **322**(5898), 49.

Voigt, T.B., Lee, D.K., Klig, G.J. 2012. Perennial herbaceous crops with potential for biofuel production in the temperate regions of the USA. CAB Abstracts, **7**(15).

Agronomy Research **13**(2), 430–435, 2015

Profitability of hybrid aspen breeding in Latvia

J. Smilga[1], M. Zeps[2,*], L. Sisenis[3], J. Kalnins[2], A. Adamovics[2] and J. Donis[2]

[1]Forest Competence Centre, Dzerbenes Str. 27, LV1006 Riga, Latvia
[2]Latvian State Forest Institute 'Silava', Riga Str. 111, LV2169 Salaspils, Latvia
[3]Latvia University of Agriculture, Forestry Faculty, Akademijas Str. 11, LV3001 Jelgava, Latvia
[*]Correspondence: martins.zeps@silava.lv

Abstract. Hybrid aspen (*Populus tremuloides* × *P. tremula*) has fast growth in climatic conditions of Northern Europe and relatively high wood quality. Therefore, breeding of it has been carried out in a number of Baltic Sea Region countries. Breeding requires notable financial investment; therefore, the aim of our study was to estimate the profitability of hybrid aspen breeding in Latvia and the factors affecting it. Financial analysis was based on the differential approach, that is, only the costs and benefits that differ between two compared alternatives – planting of hybrid aspen and natural regeneration of silver birch or common aspen – were compared. Differential gain in this case included additional monetary value of the above-ground parts of trees in planted hybrid aspen stands (values obtained from trials in Latvia); differential costs were the costs of tree breeding, plants, planting, cleaning and protection against browsing damages (repeated use of browser repellents or fencing). Profitability of hybrid aspen breeding was significantly affected by the size of the area planted annually, soil fertility (site index) and length of rotation period. The differential gain from investments in tree breeding and establishment and management of plantations (r = 3%), assuming that selected clones would be used for 15 years and 500 ha are planted annually, in comparison to natural regeneration of common aspen and to silver birch, was 662 EUR ha^{-1} and 1136 EUR ha^{-1}, respectively. In contrast, if only 50 ha are planted annually, the respective figures were 588 and 756 EUR ha^{-1}. If fencing was used for protection of the hybrid aspen plantation against browsing, the differential gain was positive only on the most fertile soils (site index Ia).

Key words: differential benefits, *Populus tremuloides* × *P. tremula*, site index.

INTRODUCTION

Short rotation plantations of forest stands is an important part of a risk reduction strategy for forest (land) owners since the frequency of different disturbances (mainly storms) is predicted to rise in Europe as a result of climatic changes (Seidl et al., 2014). Trees have inherited mechanisms to adapt to environmental stresses (Voronova et al., 2014), but adaptation has its limits (capacity) and direct impact of climatic changes (rise of temperature, shift in precipitation regime) is predicted to notably affect species composition and thus, substantially reduce the economic value of European forests (Hanewinkel et al., 2013).

Hybrid aspen (*Populus tremuloides* × *P. tremula*) is suitable for short-rotation management in Northern Europe (Liesebach et al., 1999; Beuker, 2000; Rytter, 2006; Tullus et al., 2009; Tullus et al., 2012). It exceeds growth of both of its parent species, as well as other forest tree species in the region, and in 20–25 year rotations in fertile sites, it has a mean annual increment of 20 m^3 ha^{-1} y^{-1} (Rytter & Stener, 2005), which is similar or slightly lower to that of other *Populus* hybrids (Jansons et al, 2014b). In addition, modelling of climate-growth relationships has revealed a potentially beneficial effect of predicted climatic changes on the productivity of hybrid aspen (Jansons et al., 2014a).

Wood of hybrid aspen is suitable for high-quality paper production (Sable et al., 2013) and a relatively large amount of logging residues for wood chip production can be obtained from such plantations, since the stem comprises 69% of total above-ground biomass (Jansons et al., 2015, submitted). Plantations also have a notable potential to contribute to the accomplishment of the CO_2 emission reduction targets of European Union via carbon sequestration.

Notable differences in the height and radial increment amongst clones of hybrid aspen have been detected and mainly attributed to differences in the length of the growth period (Yu et al., 2001): clones with the longest growth period produce the highest increment (Zeps et al., 2012). The most reliable approach to ensure a best fit between the growth period of a particular clone and the length of the period with climatic conditions suitable for tree growth is to test the clone's performance locally. Testing is logically linked to national breeding programs of hybrid aspen, creating crosses between plus trees of native common aspen and American aspen from appropriate regions, thus increasing the likelihood of best fit to climatic conditions. Breeding requires notable financial investment; therefore, the aim of our study was to estimate profitability of hybrid aspen breeding in Latvia and the factors affecting it.

MATERIALS AND METHODS

In Latvia, the goal is to have a breeding population of hybrid aspen that consists of 120 common aspen plus trees and 30 American aspen plus trees. Crossing within the population would be carried out according to factorial design and 120 full-sib families created. Selection between full-sib families (30 unrelated crosses) and within-family (40 candidates per family) were carried out at the age of 5 years. Each of the candidates from each family was propagated (40 ramets) and clonal tests established. Based on test results at the age of 8 years, clones for industrial propagation were selected and further tested to evaluate suitability for microclonal propagation. Before a final decision, full-sib family experiments were revisited to assess the presence of diseases (especially stem canker); if susceptibility was detected, candidates from that family were not recommended for large-scale propagation.

Financial analysis of the tree breeding work according to the above-described scheme was carried out using the differential approach. In this method, only costs and benefits that differ between two compared alternatives – planting of hybrid aspen and natural regeneration of silver birch (the most common tree species of natural afforestation of abandoned fields) or common aspen – were compared. Differential gain in this case included the additional monetary value of above-ground parts of trees in

planted hybrid aspen stands; differential costs were the costs of tree breeding, plants, planting, cleaning and protection against browsing damages.

Yield of hybrid and common aspen and the parameters of trees were obtained from 9 experimental plantations in Latvia at the age of 11–41 years (unpublished data). Parameters of common aspen stands were obtained from the National Forest Inventory (NFI) database. Data from 126 sample trees did not reveal significant differences in stem form between hybrid and common aspen, therefore, an algorithm developed by Ozoliņš (2002) for common aspen was used to calculate the assortment structure of hybrid aspen. Proportion of branches in above-ground biomass were obtained using biomass equations, developed in Latvia (Jansons et al., 2015, submitted), and used to estimate the amount of wood for chipping. Mean prices of assortments and wood chips from the last 5 years, obtained from statistics collected at the Latvian State Forest Institute (Silava), were used to calculate the monetary value of the stands. Calculations did not include any premium for increased wood quality of hybrid aspen due to the lower percentage of rotten wood or any premium linked to carbon sequestration. Costs of breeding of hybrid aspen were obtained from the national tree breeding program in Latvia. Stand establishment costs included soil preparation, plants, planting, 6 cleanings (removal of competing vegetation, reducing risk of fire and vole damages) and treatment with repellents (10 applications) to deter browsing damages. The costs of these operations were obtained from JSC Latvijas valsts meži (Latvia's state forests company).

RESULTS AND DISCUSSION

Yield of hybrid aspen at the age of 20 years (325 m^3 ha^{-1}) was notably and significantly higher than that of common aspen at the same age in fertile forest types (according to the National Forest Inventory: 137 ± 29.2 m^3 ha^{-1}) and only slightly lower than that of common aspen at the age of 41 years (327 ± 54.4 m^3 ha^{-1}). Differential analysis was carried out to compare hybrid aspen at its recommended rotation age (20 years) and common aspen at the rotation age stated by legislation (41 years), assuming that the planting or natural regeneration would occur mostly on fertile sites (site index (*bonitate*) Ia) since currently, according to data of the National Forest Inventory, 55% of the total area of aspen stands are located in such conditions. With these assumptions, differential gain from investments in tree breeding and stand establishment and management with 3% interest rate was positive: 629 EUR ha^{-1}, if selected clones are used for 15 years to establish 100 ha of plantations annually, and 662 EUR ha^{-1}, if 500 ha of plantations are established annually.

Silver birch is the most common tree species in natural afforestation of abandoned agricultural lands or reforestation of forest lands on fertile soils. Its yield at the age of 71 years (cutting age stated by legislation) is 286 ± 48.5 m^3 ha^{-1} (data: NFI). Differential gain of hybrid aspen breeding and establishment of plantations, in comparison to natural regeneration of silver birch, was notably higher than that in comparison to natural regeneration of common aspen, assuming the same annual planting area. The result was affected by differences in the length of rotation period (20 years, when comparing hybrid aspen and common aspen, and 30 years, when comparing hybrid aspen and silver birch) and yield of common aspen and birch at the end of the rotation period. Differences between the two estimates increased with increasing soil fertility and increasing annual planting area. Differential gain for the comparison between breeding and planting of

hybrid aspen and natural regeneration of silver birch changed in the same way: increased with increasing soil fertility and annual planting area (Table 1). If only 50 ha of hybrid aspen plantations were established annually (as it is currently done in Latvia), on soils with high and medium fertility (site index I and II, respectively), differential gain from investments in tree breeding and plantation establishment was negative. It reached 0 with an annual planting area 75 ha in site index I and 205 ha in site index II.

Table 1. Differential gain (EUR ha^{-1}) depending on site index and area planted annually. Interest rate 3%, clones from tree breeding cycle are used for establishment of plantations in 15 years long period

Area planted annually, ha	Site index (*bonitate*) Ia	I	II
50	470	-406	-924
100	1,084	208	-310
500	1,575	699	182
1,000	1,636	761	243
1,200	1,646	771	253

Potential clear-cut area in aspen stands (with no management restrictions, i.e. 92% from all stands) at the time of use of the clones from the proposed tree breeding program was 1,270 ha annually (data: NFI). Current legislation permits the planting of hybrid aspen on forest land, however, its rotation period has to be the same as for common aspen – 41 years. Replacing all common aspen with hybrid aspen would result in a differential gain 1209 EUR ha^{-1} (interest rate 3%), but using hybrid aspen in only 40% of this potential area (500 ha) would result in a differential gain of 1,136 EUR ha^{-1}. The Internal Rate of Return (IRR) from investments in tree breeding and plantation management, if 500 ha are planted annually, was 5.2% – which is relatively high in comparison to other alternatives in forestry. Plants for such sizes of plantations can be ensured by the current capacity of the commercial propagation facility in Latvia, owned by Latvijas valsts meži.

The differential gain from breeding of hybrid aspen is higher than that reported for breeding of silver birch in a similar annual planting area (Jansons et al., 2011). For silver birch, the plants are produced from seed orchards (not vegetatively), thus reducing the selection intensity and consequently, also genetic gain expected from a particular tree breeding cycle. Also, differences in length of rotation period between planted (selected) birch and naturally regenerated birch stands reached only 10 years, further reducing the monetary gain from birch breeding. Profitability of Norway spruce breeding in Latvia has been estimated based on equivalent annual annuity (Jansons et al., 2015), but financial gains were not as high as our estimates for that of hybrid aspen, mainly for the same reasons as that of silver birch breeding.

So far, the calculation of profitability of hybrid aspen breeding has included the use of repellents as a means of protection against browsing damages. However, moose population density is increasing rapidly in Latvia: according to data from State Forest Service, it has tripled since mid-1990s. Therefore, it might be that repellents cannot provide sufficient deterrence against browsing, and consequently, fencing is needed. For the average clearcut (approximately 2 ha, approximating a rectangular shape) it would increase costs of plant protection by 2.8 times. The Internal Rate of Return from investments in tree breeding and plantation management, with the inclusion of fencing

and an area of 500 ha planted annually, was 3.5% in sites with mostly fertile soils (site index Ia), but below 3% in sites with lower soil fertility (2.6% and 1.9% in site index I and II, respectively). If only 50 ha were planted annually (as it is currently done), the differential gain was negative (internal rate of return of 2.3%) even for plantations on most fertile soils.

It is also important to note that the application of tree breeding results (i.e., establishment of plantations of faster-growing trees) to reforestation efforts can provide additional benefits which were not accounted for in the calculation:

a) increase of carbon sequestration;

b) release of the area for other uses (e.g. recreation, nature protection) without decreasing the total wood production from a particular forest massif.

CONCLUSIONS

Profitability of hybrid aspen breeding was significantly affected by the size of area planted annually, soil fertility (site index) and length of rotation period. Differential gain from investments in breeding of hybrid aspen, establishment and management of its plantations (interest rate 3%) was positive both in comparison to natural regeneration of common aspen and natural regeneration of birch (on forest land).

ACKNOWLEDGEMENTS. The study was carried out in Forest Competence Centre (ERAF) project 'Methods and technologies for increasing forest capital value' (No. L-KC-11-0004).

REFERENCES

Beuker, E. 2000. Aspen breeding in Finland, New challenges. *Baltic Forestry* **6**(2), 81–84.

Hanewinkel, M., Cullmann, D.A., Schelhaas, M.-J., Nabuurs, G-J. & Zimmermann, N.E. 2013. Climate change may cause severe loss in the economic value of European forest land. *Nature Climate Change* **3**, 203–207.

Jansons, A., Donis, J., Danusevičius, D. & Baumanis, I. 2015 Differential analysis for next breeding cycle for Norway spruce in Latvia. *Baltic Forestry* (in press).

Jansons, Ā., Gailis, A. & Donis, J. 2011. Profitability of silver birch (*Betula pendula* Roth.) breeding in Latvia. In Gaile, Z. (ed.): *Proceedings of the 17th international scientific conference Research for Rural Development.* LLU, Jelgava, Latvia, pp. 33–38.

Jansons, A., Rieksts-Riekstins, J., Zurkova, S., Katrevics, J., Lazdina, D. & Sisenis, L. 2015. Above-ground biomass equations of *Populus* hybrids in Latvia. *Baltic Forestry* (submitted).

Jansons, Ā., Zeps, M., Rieksts-Riekstiņš, J., Matisons, R. & Krišāns, O. 2014a. Height increment of hybrid aspen *Populus tremuloides* × *P. tremula* as a function of weather conditions in south-western part of Latvia. *Silva Fennica* **48**(5), 13 pp.

Jansons, A., Zurkova, S., Lazdina, D. & Zeps, M. 2014b. Productivity of poplar hybrid (*Populus balsamifera* × *P. laurifolia*) in Latvia. *Agronomy Research* **12**(1), 469–478.

Liesebach, M., Von Wuehlisch, G. & Muhs, H.J. 1999. Aspen for short-rotation coppice plantations on agricultural sites in Germany: Effect of spacing and rotation time on growth and biomass production of aspens progenies. *Forest Ecology and Management* **121**, 25–39.

Ozoliņš, R. 2002. Forest stand assortment structure analysis using mathematical modeling. *Metsanduslikud uurimused* **XXXVII**, 33–42.

Rytter, L. 2006. A management regime for hybrid aspen stands combining conventional forestry techniques with early biomass harvests to exploit their rapid early growth. *Forest Ecology and Management* **236**, 422–426.

Rytter, L. & Stener, L.G. 2005. Productivity and thinning effects in hybrid aspen (*Populus tremula* L × *P. tremuloides* Michx.) stands in southern Sweden. *Forestry* **78**, 285–295.

Sable, I., Grinfelds, U., Zeps, M., Irbe, I., Noldt, G., Jansons, A., Treimanis, A. & Koch, G. 2013. Chemistry and kraft pulping of seven hybrid aspen clones. Dimension measurements on the vessels and UMSP of the cell walls. *Holzforschung* **67**(5), 505–510.

Seidl, R., Schelhaas, M.-J., Rammer, W. & Verkerk, P.J. 2014. Increasing forest disturbances in Europe and their impact on carbon storage. *Nature Climate Change* **4**, 806–810.

Tullus, A., Rytter, L., Tullus, T., Weih, M. & Tullus, H. 2012. Short-rotation forestry with hybrid aspen (*Populus tremula* L. × *P. tremuloides* Michx.) in Northern Europe. *Scandinavian Journal of Forest Research* **27**, 10–29.

Tullus, A., Tullus, H., Soo, T. & Pärn, L. 2009. Above-ground biomass characteristics of young hybrid aspen (*Populus tremula* L. × *P. tremuloides* Michx.) plantations on former agricultural land in Estonia. *Biomass and Bioenergy* **33**, 1617–1625.

Voronova, A., Belevich, V., Jansons, A. & Rungis, D. 2014. Stress-induced transcriptional activation of retrotransposon-like sequences in the Scots pine (*Pinus sylvestris* L.) genome. *Tree Genetics & Genomes* **10**(4), 937–951.

Yu, Q., Tigerstedt, P.M.A. & Haapanen, M. 2001. Growth and phenology of hybrid aspen clones (*Populus tremula* L. × *Populus tremuloides* Michx.). *Silva Fennica* **35**(1), 15–25.

Zeps, M., Jansons, A., Smilga, J. & Purina, L. 2012. Growth intensity and height increment in a young hybrid aspen stand in Latvia. In: *Proceedings of 8th WSEAS International Conference on Energy, Environment, Ecosystems and Sustainable Development*. University of Algarve, Faro, Portugal, pp. 120–124.

Agronomy Research **13**(2), 436–441, 2015

Formation of height increment of hybrid aspen in Latvia

M. Zeps[1,*], L. Sisenis[2], S. Luguza[2], M. Purins[2], B. Dzerina[2] and J. Kalnins[3]

[1]Latvian State Forest Institute 'Silava', Riga Str. 111, LV2169 Salaspils, Latvia
[2]Latvia University of Agriculture, Forest Faculty, Akademijas Str. 11, LV3001 Jelgava, Latvia
[3]Forest Competence Centre, Dzerbenes Str. 27, LV1006 Riga, Latvia
[*]Correspondence: martins.zeps@silava.lv

Abstract. Annual increment of hybrid aspen exceeds that of other tree species (including common aspen) in Baltic States. Notable (several-fold) differences in productivity between clones have been detected and therefore tree breeding programs are established to select the best genotypes (clones) for large-scale propagation. In order to aid the selection as well as understand the potential changes in growth of hybrid aspen as a result of climatic changes, it is important to analyse the intra-annual growth dynamics. Therefore aim of our study was to assess height growth intensity of hybrid aspen and factors affecting it. Weekly measurements of height increment were carried out through the third growing season of trees in two plantations, consisting of 19 clones (10 ramets per clone), on abandoned agricultural land in western (Mazirbe, 56° 36′ N, 24° 30′ E) and central (Vecumnieki, 57° 40′ N, 22° 19′ E) part of Latvia. Mean height growth period of hybrid aspen ranged from 119 ± 8.9 days for late flushing clones to 137 ± 8.6 days for early flushing and was tightly (r = 0.69) linked to total length of height increment. Mean height growth intensity during this period for respective groups of clones ranged from 7.7 ± 3.04 mm day^{-1} to 11.7 ± 2.93 mm day^{-1}. Growth intensity (and height increment) was significantly affected by genotype (clone) and in both sites tightly (r = 0.57…0.84) linked with daily mean temperature, but not with precipitation. Increasing temperature in future might boost the productivity of hybrid aspen plantations, especially with early flushing clones.

Key words: height growth intensity, growth period, *Populus tremula* × *P. tremuloides.*

INTRODUCTION

Hybrid aspen – a cross between two geographically isolated aspen species – has higher productivity than both of its parent species, as demonstrated by number of studies in Baltic Sea region countries (Liesebach et al., 1999; Johansson, 2002; Rytter & Stener, 2005). Wood fiber properties are important in determination of its suitability for paper production (Irbe et al., 2013) and hybrid aspen has the desired properties to be used as raw material in pulp and paper industry. Demand for wood as a renewable material is raising and it is predicted to ensure the market for fast-growing trees from plantations (Schueler et al., 2013).

Hybrid aspen clones (genotypes) have notably different increment and quality (e.g. stem straightness, branch angle). Breeding programs are established to test the materials and select clones with desired properties for particular climatic conditions (Stener & Karlsson, 2004). However, rapid changes of climatic conditions are predicted within this

century: rise of temperature, increase in length of vegetation period and frequency of extreme events (e.g. longer drought periods, storms) (IPCC, 2014). To predict, how these changes could affect productivity of hybrid aspen, it is important to understand the mechanisms triggering the growth onset and cessation as well as determining the increment. It is also important to assess clonal differences in these traits. This information could potentially be used in breeding programs to boost the productivity of plantations in future.

Hybrid aspen families have different bud burst time, growth period and annual increment (Ceulemans et al., 1987; Li &Wu, 1996; Li et al., 1998; Yu et al., 2001). Observed differences could be linked to different reaction to photoperiod and temperature that are important in determination of phenological processes and development of frost hardiness for trees (Rohde et al., 2010). Most of the studies so far have analysed inter-annual differences in meteorological conditions and reaction of trees; for example, survival, proportion of trees with frost damages, radial increment (dendrochronology), but only few have addressed the intra-annual growth in relation to meteorological conditions. Therefore aim of our study was to assess height growth intensity during the vegetation period of hybrid aspen and factors affecting it.

MATERIALS AND METHODS

Fenced plantations, including 19 hybrid aspen (*Populus tremula* × *P. tremuloides*) clones were established on abandoned agricultural land in western part of Latvia, Mazirbe (~2 km from Baltic Sea, 56° 36′ N, 24° 30′ E) and central part of Latvia, Vecumnieki (57° 40′ N, 22° 19′ E), using micro-propagated, containerized one-year old plants. During the 3rd growing season height of 10 ramets per clone was measured on average every 7th day (altogether 20 measurement times in Vecumnieki and 19 in Mazirbe) and average growth intensity (mm day^{-1}) calculated. Hourly data of meteorological conditions (temperature, precipitation) were collected, using portable weather stations, located just besides each of the trials.

During the active growth period (May – August) mean temperature was by ~ 1°C higher in Vecumnieki than in Mazirbe, the highest differences were observed in August: 1.9°C. Sum of precipitation in Vecumnieki in May was higher and in June lower than in Mazirbe (76 *vs.* 42 mm and 126 *vs.* 186 mm, respectively), but the total precipitation sum of the analysed period was almost equal in both sites.

Bud development and bud-burst phases were assessed in 6 grades (based on standard developed by UPOV, 1981) visiting the sites every second day, starting from the first signs of bud spring development (0 – dormant buds completely enveloped by the scales, 1 – buds swelling with scales slightly diverging showing a narrow yellow margin; presence of one or more droplets of balsam, 2 – buds sprouting, with the tips of the small leaves emerging out of the scales, 3 – buds completely opened with leaves still clustered together; scales still present, 4 – leaves diverging with their blades still rolled up; scales may be present or absent, 5 – leaves completely unfolded (but smaller in size than mature ones); lengthening of the axis of the shoot evident; scales absent). Length of the used growth period (days) was calculated for every measured tree from the bud burst till the end of height growth.

Data analysis was carried out using ANOVA, the mean values ± confidence intervals were calculated.

RESULTS AND DISCUSSION

Hybrid aspen clones were divided into three groups based on their bud burst phenology (Ceulemans et al., 1987): early, intermediate and late flushing. Distribution of clones in groups was similar in both sites – 7 clones were early flushing and 5 late flushing. Late flushing clones in both sites were significantly ($P < 0.05$) shorter (both height and height increment) than clones from other groups (Fig. 1). Length of height increment correlated tightly ($r = 0.69$) and significantly with the length of the used growth period. It indicates that longer growth period ensures accumulation of higher amount of nutrients and therefore higher net primary production (Barbaroux & Breda, 2002; Pallardy, 2008).

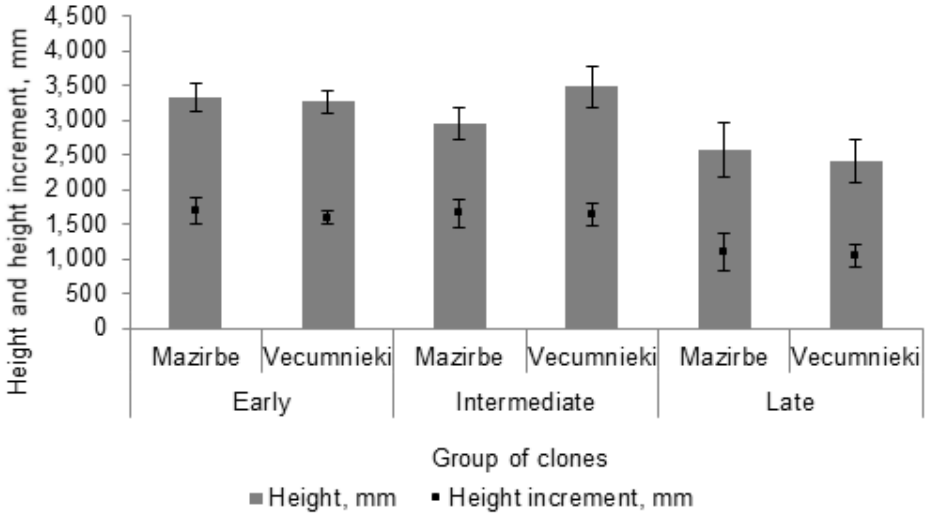

Figure 1. Height and height increment of early, intermediate and late flushing clones (mean values ± confidence interval).

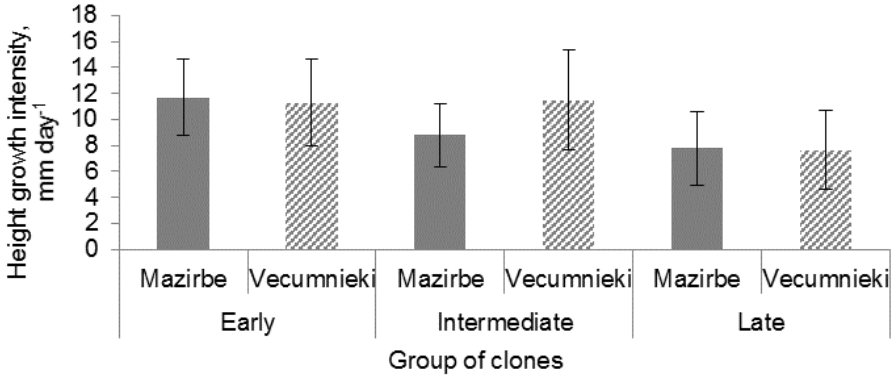

Figure 2. Mean height growth intensity of early, intermediate and late flushing clones (± confidence interval).

The longest used growth period was found for early flushing clones: 131 ± 3.60 days in Vecumnieki and 137 ± 8.6 days in Mazirbe.It was on average by 33 and 26 days shorter for intermediate and late flushing clones, respectively. Other studies have indicated, that early flushing clones might suffer from spring frost and that could negatively affect their height increment (Yu et al., 2001; Gu et al., 2008), but in our trials frost damages were not observed.

Mean growth intensity (mm day^{-1}) was slightly, but not significantly lower for late flushing clones than for clones from other two groups (Fig. 2).

Slight differences in growth intensity were found both between sites and between groups of clones within site (Fig. 3).

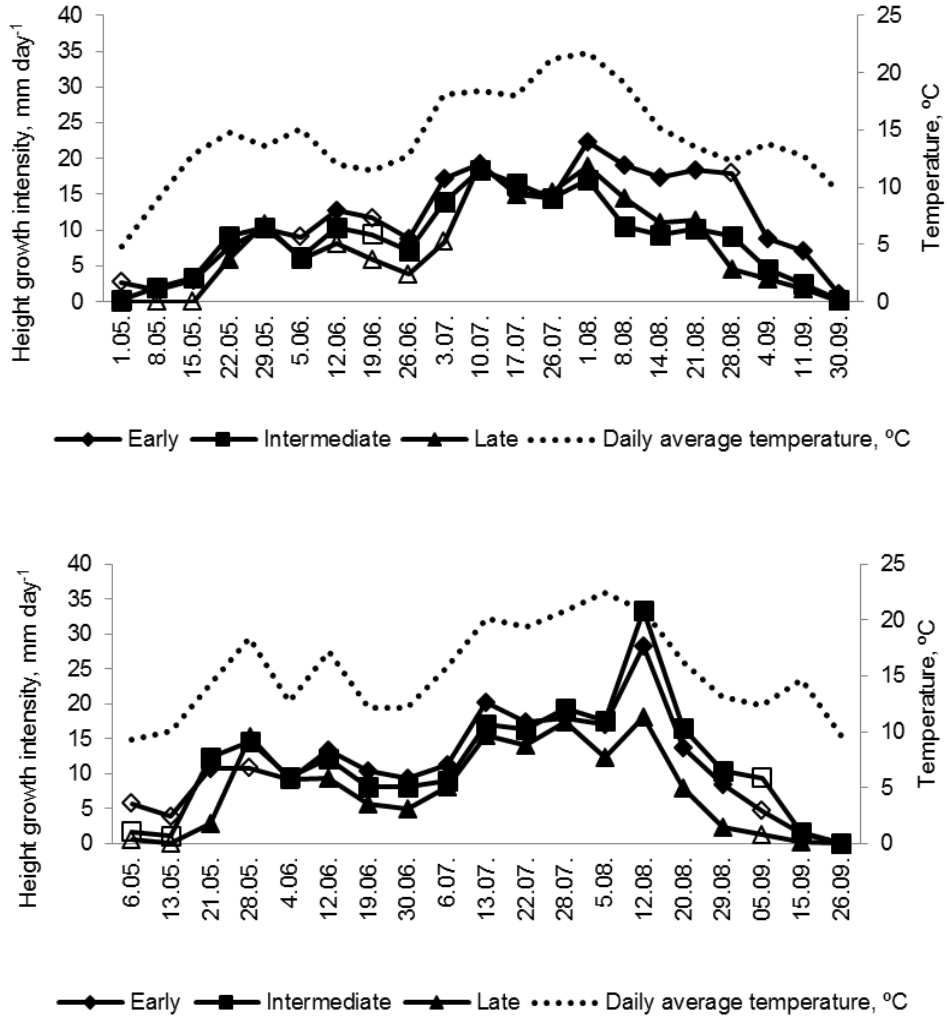

Figure 3. Height growth intensity of early, intermediate and late flushing clones in Mazirbe (a) and Vecumnieki (b).
Empty markers – growth intensity of particular group of clones in this date differs significantly ($P < 0.05$) from growth intensity of other groups of clones.

Late-flushing clones had slower start of the growth (until middle of May) and slower growth during the first part of the summer (middle of June – beginning of July). These differences were more pronounced in Mazirbe, than in Vecumnieki.

The largest (on average 7.5 mm day^{-1} in both sites) and in some of the observation periods also statistically significant differences in growth intensity between late flushing and both other groups (in Vecumnieki) or only early flushing (in Mazirbe) clones were observed at the end of growth period: from beginning of August until beginning of September.

Similar trend was observed also during previous growing seasons (Jansons et al., 2014) and indicates, that early-flushing clones in general have better ability to use the available resources effectively and produce higher increment. Influence of clone (genotype) on growth intensity and length of height increment was statistically significant. It is known from the studies of other tree species, that also meteorological conditions can have a significant influence on height increment (and growth intensity) of trees (Jansons et al., 2013 a, b). In our study in both sites tight (r = 0.57…0.84) and significant correlation between daily mean temperature and growth intensity was found. Influence of temperature on growth was higher for late flushing than for early flashing clones (in Mazirbe: r = 0.84 and r = 0.64, respectively). Lower reaction to fluctuations of meteorological conditions might be one of the reasons for better growth, observed for early flushing clones (Speer, 2010; Burton, 2012). Precipitation had no significant effect on growth intensity (r = -0.14….0.26), presumably because of sufficient water availability both from precipitation and ground water. In contrast, studies in central and southern part of Europe (in dryer conditions) have found strong influence of precipitation on both radial and height increment of trees. This influence partly depends on tree age (Carrer & Urbinati, 2006).

CONCLUSIONS

Mean height growth period of hybrid aspen ranged from 119 ± 8.9 days for late flushing clones to 137 ± 8.6 days for early flushing and was tightly (r = 0.69) linked to total length of height increment. Mean height growth intensity during this period for respective groups of clones ranged from 7.7 ± 3.04 mm day^{-1} to 11.7 ± 2.93 mm day^{-1}. It correlated significantly with daily mean temperature in a particular date.

ACKNOWLEDGEMENTS. The study was carried out in Forest Competence Centre (ERAF) project ’Methods and technologies for increasing forest capital value’ (No. L-KC-11-0004).

REFERENCES

Barbaroux, C. & Breda, N. 2002. Contrasting distribution and seasonal dynamics of carbohydrate reserves in stem wood of adult ring-porous sessile oak and diffuse-porous beech trees. *Tree Physiology* **22**, 1201–1210.

Burton, L. 2012. *Introduction to Forestry Science*. Cengage Learning, New York, 554 pp.

Carrer, M. & Urbinati, C. 2006. Long-term changes in the sensitivity of tree-ring width growth to climate forcing in *Larix decidua*. *New Phytologist* **170**, 861–872.

Ceulemans, R., Impens, I. & Steeneckers, V. 1987. Variation in photosynthetic, anatomical, and enzymatic leaf traits and correlation with growth in recently selected *Populus* hybrids. *Canadian Journal of Forest Research* **17**, 273–283.

Gu, L., Hanson, P.J., Post, W.M., Kaiser, D.P., Yang, B., Enami, R., Pallardy, S.G. & Meyers, T. 2008. The 2007 Eastern US spring freeze: increased cold damage in a warming world? *BioScience* **58**, 253–262.

IPCC, Climate Change. 2014. Synthesis Report, 35 pp.

Irbe, I., Sable, I., Treimanis, A. & Jansons, A. 2013. Variation in the tracheid dimensions of Scots pine (*Pinus sylvestris* L.) and lodgepole pine (*Pinus contorta* Dougl. var. latifolia *Engelm*) trees grown in Latvia. *Baltic Forestry* **19**, 120–127.

Jansons, A., Matisons, R., Baumanis, I. & Purina, L. 2013b. Effect of climatic factors on height increment of Scots pine in experimental plantation in Kalsnava, Latvia. *Forest Ecology and Management* **306**, 185–191.

Jansons, A., Matisons, R., Libiete-Zālīte, Z., Baders, E. & Rieksts-Riekstiņš, J. 2013a. Relationships of height growth of Lodgepole pine (*Pinus contorta* var. latifolia) and Scots pine (*Pinus sylvestris*) with climatic factors in Zvirgzde, Latvia. *Baltic Forestry* **19**, 236–244.

Jansons, Ā., Zeps, M., Rieksts-Riekstiņš, J., Matisons, R. & Krišāns, O. 2014. Height increment of hybrid aspen *Populus tremuloides* × *P. tremula* as a function of weather conditions in south-western part of Latvia. *Silva Fennica* **48**(5), 13 pp.

Johansson, T. 2002. Increment and biomass in 26- to 91-year-old European aspen and some practical implications. *Biomass and Bioenergy* **23**, 245–255.

Li, B. & Wu, R. 1996. Genetic causes of heterosis in juvenile aspen: a quantitative comparison across intra- and interspecific hybrids. *Theoretical and Applied Genetics* **93**, 380–391.

Li, B., Howe, G.T. & Wu, R. 1998. Developmental factors responsible for heterosis in aspen hybrids (*Populus tremuloides x P. tremula*). *Tree Physiology* **18**, 29–36.

Liesebach, M., Wuehlisch von, G. & Muhs, H.J. 1999. Aspen for short-rotation coppice plantations on agricultural sites in Germany: Effects of spacing and rotation time on growth and biomass production of aspen progenies. *Forest Ecology and Management* **121**, 25–39.

Pallardy, S.G. 2008. *Physiology of Woody Plants*. Elsevier, London, 454 pp.

Rohde, A., Bastien, C. & Boerjan, W. 2011. Temperature signals contribute to the timing of photoperiodic growth cessation and bud set in poplar. *Tree Physiology* **31**, 472–482.

Rytter, L. & Stener, L.-G. 2005. Productivity and thinning effects in hybrid aspen (*Populus tremula L. x P. tremuloides* Michx.) stands in southern Sweden. *Forestry* **78**, 285–295.

Schueler, V., Weddige, U., Beringer, T., Gamba, L. & Lamers, P. 2013. Global biomass potentials under sustainability restrictions defined by the European Renewable Energy Directive 2009/28/ EC. GCB *Bioenergy* **5**, 652–663.

Speer, J.H. 2010. *Fundamentals of Tree Ring Research*. University of Arizona Press, Tucson, 333 pp.

Stener, L.-G. & Karlsson, B. 2004. Improvement of *Populus tremula x P. tremuloides* by phenotypic selection and clonal testing. *Forest Genetics* **11**, 13–27.

UPOV 1981. *Guidelines for the conduct of tests for distinctness, homogeneity and stability*. International Union for the protection of new varieries of plants, 55 pp.

Yu, Q., Tigerstedt, P.M.A. & Haapanen, M. 2001. Growth and phenology of hybrid aspen clones (*Populus tremula* L. × *Populus tremuloides* Michx.). *Silva Fennica* **35**, 15–25.

IV RENEWABLE ENERGY

Agronomy Research **13**(2), 445–454, 2015

Impact of synthetic hormone 17α-ethinylestradiol on growth of microalgae *Desmodesmus communis*

K. Balina[1,*], M. Balode[2,3], L. Muzikante[2] and D. Blumberga[1]

[1]Riga Technical University, Institute of Energy Systems and Environment, Azenes Str. 12/1, LV1048 Riga, Latvia; [*]Correspondence: karina.balina@rtu.lv
[2]Latvian Institute of Aquatic Ecology, Daugavgrivas 8, LV1048 Riga, Latvia
[3]University of Latvia, Faculty of Biology, Department of Hydrobiology, Kronvalda Boulevard 4, LV1010 Riga, Latvia

Abstract. Microalgae has recently attracted much attention as a feedstock for biogas. Using wastewater as microalgae nutrition is a way how to produce algal biomass with low cost and minimum impact on environment. However, wastewater often is polluted with chemicals like pharmaceuticals which are among the commonly used chemicals in everyday life. The present study was aimed at the toxicity evaluation of a commonly used synthetic hormone, 17α-ethinylestradiol, using freshwater green algae *Desmodesmus communis* as a biotest organism. Parameters like healthy cell number and photosynthetic activity were determined and used to assess the toxicity. Lowest Observed Effect Concentration (LOEC) and 50% Effective Concentration (EC_{50}) values were calculated for the parameters at different incubation times. It was found out that 17α-ethinylestradiol affects algal cell ability to grow, inhibits cell division and reduce photosynthetic processes in algal cells. Our research shows that inhibitory effect on growth of green algae D. communis start on concentration below 10 μg L-1 (4–8 μg L-1). Concentrations in the range of concentration 80–100 reduce growth by 50%, but concentrations 100–500 μg L-1 induce 100% reduction of growth rate and even calls initial algal cell destruction. Presence of EE2 in wastewater used for algal growth can affect productivity of a microalgae aquaculture.

Key words: microalgae, 17α-ethinylestradiol, EC_{50}, carbon, photosynthesis.

INTRODUCTION

In last 50 years the world's population has more than doubled, and due to great demand of energy, amount of fossil fuel is reducing. New sources of energy are being sought (Jones & Mayfield, 2012). Microalgae cultivation can be a significant source for energy production. Comparing to other sources like forestry, agriculture and macrophytes, microalgae has higher growth rate and productivity (Blumberga et al., 2011; Daroch et al., 2013). Comparing to other crops microalgae grow highly rapidly and usually double their biomass in 24 hours. These photosynthetic microorganisms convert sunlight, water and carbon dioxide to algal biomass (Chisti, 2007). Advantage is that they can be cultivated and harvested throughout the year (Chen et al., 2011). Besides that microalgae can be grown in wastewater to remove nutrients and toxic substances (Klein-Marcuschamer, 2013; Guiry, 2014; Zhang et al., 2014).

Using wastewater as microalgae nutrition is a way how to produce algal biomass with minimal cost and low environmental impact (Park et al., 2011). Wastewaters often have high concentrations of nutrients (nitrogen and phosphorus), and range of trace elements, which are necessary for the growth and metabolism of microalgae (Aravantinou et al., 2013). Microalgal growth can effectively remove phosphates and nitrates from wastewater, thus acting as treatment for the wastewater, and creating it as a suitable substrate for microalgal cultivation (Rawat et al., 2013). *Desmodesmus communis* is one of the most widely used microalgae species for wastewater treatment (Guiry, 2014; Zhang et al., 2014). Nutrients from wastewater are increasing algal biomass growth (Guo et al., 2013).

Wastewater contains not only essential nutrients, but also a lot of pollutants, that can harm aquatic organisms including microalgae. One of the most hazardous group of toxic substances in municipal wastewaters are pharmaceuticals. They can reach aquatic environment in different ways, of which the most common are the end products of human metabolism. Wastewater treating plants are not specifically designed to attenuate pharmaceuticals. Pharmaceuticals have been widely detected in the surface, ground and coastal waters and even in drinking water. Concerns have been raised about potential toxicity of pharmaceuticals and their adverse impacts on ecological safety (Sun et al., 2014).

Pharmaceutical pollution is growing as a result of increasing use of medicine. One of the most toxic substances is synthetic hormone 17α-ethinylestradiol (EE2), which is artificial estrogen derivate and is permanent in aquatic environment. After application in humans it is excreted with metabolic end products and it can reach wastewater treatment plants (Liebig et al., 2005). Even small quantities of this hormone may cause toxic effects on aquatic organisms. Although in natural habitat EE2 occurs just in small quantities it's one of the most dangerous water pollutants and it can affect not only animals, but also decrease photosynthetic processes in plants (Perron & Juneau, 2011).

Doubt exist that endocrine disruptor may leave negative impact on photosynthetic processes in microalgae. There are studies that endocrine disruptors have a negative effect on the level of non-photochemical quenching. This process occurs in almost all photosynthetic eukaryotes and it helps to regulate and protect photosynthesis in microalgae (Yi et al., 2014). Hormones change electron transport in algal cells reducing photosynthetic activity and inducing the same effects as low light conditions (Lohr et al., 2012). Loss of biomass production caused by reduced photosynthetic processes might make algae cultivation less profitable (George et al., 2014; Han et al., 2015). Damage to the photosynthetic apparatus is not permanent and a recovery occur when there is no more contact with the toxicant (Zhou et al., 2013).

D. communis has been extensively used for evaluating the adverse effects of different toxic substances and environmental stressors. As stated before this microalgae is widely used for treating wastewater and biomass can be used as feedstock for biogas production. However, data regarding toxicity of hormonal pollution to microalgae growth ability produce biomass can hardly be found. The aim of this study was to evaluate hazard impact of this pollutant on microalgae *D. communis* growth. In order to have a picture of EE2 toxicity, growth, photosynthesis and total organic carbon were determined. Since the toxicity of chemicals vary with exposure time, the EC_{50} and Lowest Observed Effect Concentrations (LOEC) after 72 hours exposition were determined.

MATERIALS AND METHODS

Algal growth inhibition test

Algal growth inhibition test was carried out based on European standard (EN ISO 8692:2004).

Microscopic green algae *Desmodesmus communis* (DCGR-3) was used as a test organism. Culture was obtained from the Algal Culture Collection of Latvian Institute of Aquatic Ecology. Culture was pre-cultivated 3 days before test to reach exponential growth rate.

Algal growth medium BG-11 was prepared according Stanier et. al (1971). At the beginning of test, 1 mL suspended algae culture (2 10^5 cells mL^{-1}) was inoculated in 30 mL BG-11 medium and grown in Nalgene centrifuge tubes at 20 ± 2 °C, pH 8 ± 1 under the irradiance intensity of 60 µmol photon m^{-2} s^{-1}. *D. communis* was exposed to various concentrations of synthetic hormone under the defined conditions. The microalgal cultures were incubated for a period of 72 h and mixed manually once per day. Fluorometric determination was used to estimate algal biomass 0, 24, 48 and 72 h after the start of the test. Algal cell quantifying was used on the beginning of test and after 72 h.

Hormone 17α-ethinylestradiol (17α-ethinylestradiol ≥ 98%, Sigma-Aldrich, US) was initially dissolved in 96% ethanol to prepare the stock solution (100 mg EE2 in 100 ml ethanol) as EE2 in its original form is not soluble in water (Bell, 2001). In the test, the algal cultures were exposed to 10 different concentrations of the 17α-ethinylestradiol (10; 100; 500; 1,000; 1,500; 2,000; 2,500; 3,000; 4,000; 5,000 µg L^{-1}) and two different controls. First control was only algal culture with medium, second - was spiked with 96% ethanol in concentration 50 mL L^{-1} corresponding to the highest concentration of ethanol used for EE2 dissolution.

Growth measuring using algal cell counting

One mL of algal culture was aseptically sampled from each test tube and fixed with Lugol's solution. The cell number was counted with a Neubauer ruling under a light microscope (Leica ATC 2000) at magnification of 400×. Only healthy, pigmented, unbroken cells were counted.

Growth measuring using Fluorescence

Chlorophyll fluorescence was estimated using 10-AU Fluorometer (Turner Designs, Sunnyvale, CA, USA). When exposed to light, photosynthetic active organisms exhibits fluorescence radiation that originates from chlorophyll *a* (chl *a*) molecules of Photo System II (PSII). Increasing levels of fluorescence indicates for increased chl *a* concentration in algal cells. From this can be concluded algal growth rate and biomass yield. Samples were dark-acclimated for 30 min to reduce PSII to a constant fluorescence level.

Carbon quantifying

To calculate amount of carbon, fluorescence / cell number ratio was used. Ratio was established measuring fluorescence and algal cell number in different cell density levels. Total Organic Carbon (TOC) in the same cell density levels was calculated using amount of carbon in algal cell (Olguín & Sánchez-Galván, 2011). Fluorescence to TOC

ratio was established and used to calculate amount of Total Organic Carbon. Equation was derived (1), because it lets to quantify C in all cells including damaged cells.

$$TOC = (F = 390.89)/1.1588 \quad (1)$$

where *TOC* is the amount of total organic carbon in algal cells and *F* is fluorescence of chlorophyll a.

Data analysis

All the experiments were carried out in triplicates and data presented is mean values of these replicates. Data were further analysed using Microsoft Office Excel 2013 (Microsoft, USA). A statistical significance was considered at p = 0.05.

Data were processed by applying correlation and regression analysis.

The mean specific growth rate (μ) for exponentially growing cultures was calculated by using equation (2)

$$\mu = (\ln N_2 - \ln N_1)/t_2 - t_1 \quad (2)$$

where: t_1 is the time (h) of the first measurement at the start; t_2 the time of the final measurement at the end of the test; N_2 the number of cells per mL at time t_2 and N_1 the number of cells per mL at t_1. The inhibition of the growth rate was determined in the relation to the control (culture with ethanol). The same calculations were made with fluorescence measurements, replacing number of cells with fluorescence values.

The percent inhibition of growth rate for each treatment was calculated by using formula (3)

$$\%I_{\mu_i} = \frac{\mu_c - \mu_i}{\mu_c} \times 100 \quad (3)$$

where: I_{μ_i} is percent inhibition in mean specific growth rate; μ_c is value for mean specific growth rate in the control; μ_i is mean specific growth rate in concentration *i*.

Values for the mean growth inhibition were calculated for each test substance concentration (in logarithmic scale) to establish a dose-response curve.

EC_{50} and Lowest Observed Effective Concentration (LOEC) were calculated using dose-response curves for this biotest. The parameter EC_{50} expresses the effective concentration of EE2 that results in a 50% growth rate inhibition comparing to the control. LOEC is a lowest concentration, which has an impact to algal growth and reduce algal growth by 10%. EC_{50} and LOEC were determined using dose-response curves.

RESULTS AND DISCUSSION

Algal cell counting

Algal growth inhibition was determined from results of algal cell counting. The dose–response curve was designed to display inhibition in a range 10–1,000 μg L^{-1} for used concentration (Fig. 1).

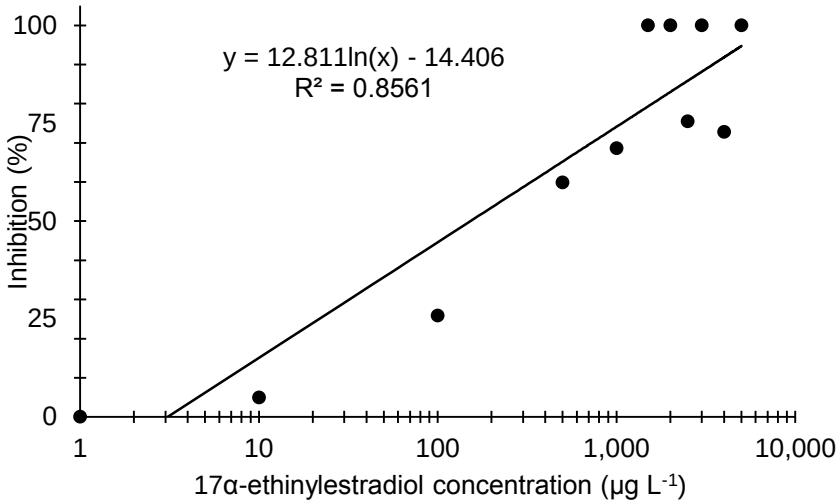

Figure 1. Dose–response curve (concentration vs. inhibition of growth rate) for 17α-ethynilestradiol, quantified with cell counting.

Strong correlation between the inhibition of growth rate of *D. communis* detected by cell counting and EE2 concentrations was detected ($R^2 = 0.8561$). Growing hormone concentrations cause increase of algal growth inhibition. Already 8μg L^{-1} of EE2 is able to reduce algal growth by 10%, but concentrations around 80 μg L^{-1} can evoke a 50% algal growth inhibition. Concentrations exceeding 1,300 μg L^{-1} are able not only completely stop cell division, but can even cause damage of initial cells. In the range of concentrations of EE2 (1,000–5,000 μg L^{-1}) there are more damaged and deformed cells observed.

Fluorescence measurements

Measurements of chlorophyll fluorescence were made to the same samples as cell counting. From measurements it is possible to assess changes of photosynthetic processes in algal cells in relation to EE2 concentrations (Fig. 2).

Statistically significant correlation between fluorescence measurements was detected ($R^2 = 0.8642$). Growing hormone concentrations decrease photosynthetic activity in algal cells. Results show that 4 μg L^{-1} of EE2 is able to reduce fluorescence of chlorophyll a by 10%, but concentrations around 100 μg L^{-1} evoke a 50% inhibition of photosynthesis. Concentrations in the range 1,000–5,000 μg L^{-1} can cause 75–100% inhibition of photosynthetic activity.

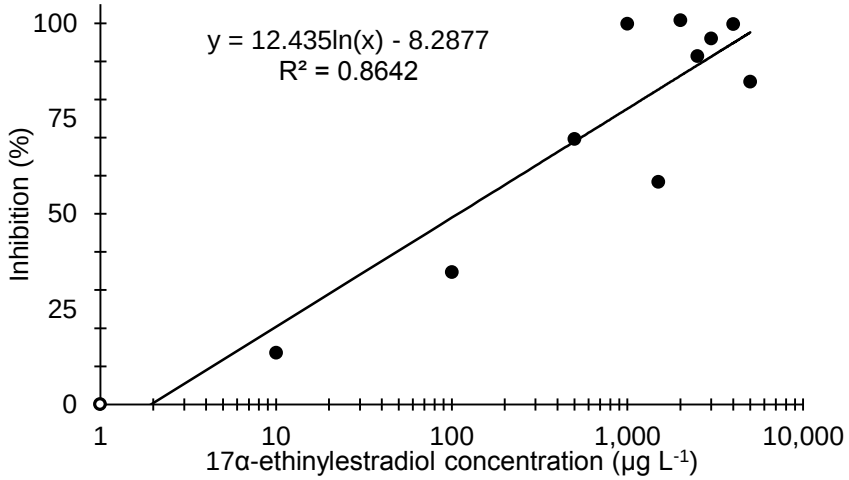

Figure 2. Dose–response curve (concentration vs. inhibition of growth rate) for 17α-ethynilestradiol, quantified with fluorescence.

Pearson's correlation was used to estimate correlation between fluorescence and cell counting. Obtained results revealed about correlation between fluorescence and cell counting results ($r^2 = 0.96$, $p = 0.019$).

Carbon quantifying

Photosynthesis fixed carbon dioxide is the main source of carbohydrates and other organic compounds containing carbon in algal cells. Quantity of carbon predicts potential amount of CH_4 and CO_2 produced by algae. Amount of Total Organic Carbon (TOC) in samples were calculated using data of fluorescence to see how algal biomass change in a time depend from concentrations. Data of fluorescence was used instead of cell counting data because fluorescence measurement show amount of carbon in all cells including damaged cells. Fig. 3 shows the results obtained for a daily changes of an amount of carbon in a range of EE2 concentration.

Graph shows that increased level of EE2 reduce production of TOC 100 µg L^{-1} of EE2 decreased production of TOC by 25%. Concentrations exceeding 500 µg L^{-1} can evoke 50% inhibition of biomass production, but over 1,500 µg L^{-1} it can stop biomass production. The most significant impact occurred in the first 24 hours. On EE2 concentration 100 µg L^{-1} small decrease of TOC was observed in 48 h, but in 72 h exposition, recovery was noticed. Higher EE2 concentrations stops carbon production. Recovery could be explained as algal ability to accumulate pollutants, and maybe some cells was not harmed and continued to divide. It is possible that recovery can happen also in higher concentrations, that 100 µg L^{-1} but it was not observed in this experiment.

Levels of pharmaceuticals in wastewaters used as nutrient source for microalgae cultivation may decrease and even stop producing biomass, thus making cultivation process inefficient.

Although EE2 is prepared to interact with human endocrine system, it is also presented in aquatic ecosystems and can reduce the development of phytoplankton (Hense et al., 2008). Even a small amount of endocrine disrupters can significantly

reduce the photosynthetic activity in algae cells (Perron & Juneau, 2011). Endocrine disruptors make damage to the algal cells leading to growth inhibition (Liu et al., 2010). Although EE2 is not soluble in water, after exposure to human body it passes in water in dissolved form and is free ingestible aquatic organisms (Feng et al., 2010). Our research shows that inhibitory effect on growth of green algae *D. communis* start on concentration below 10 µg L^{-1} (4–8 µg L^{-1}). Concentrations in the range of concentration 80-100 reduce growth by 50%, but concentrations 100–500 µg L^{-1} can reduce algal growth to minimum and even cause destruction of algal cells.

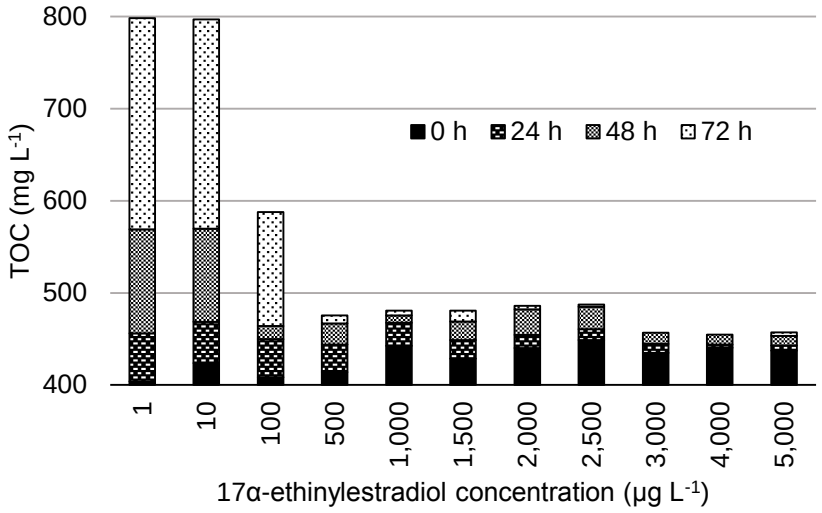

Figure 3. Effect of concentration on production of total organic carbon.

This was also demonstrated in a study, where several green algae and blue-green algae species were affected by different endocrine disruptors. Study represents reduced activity of chlorophyll in affected algal cells, showing that photosynthetic activity is reduced (Perron & Juneau, 2011). Interesting fact is that EC_{50} obtained from fluorescence is higher than EC_{50} obtained from cell counting, which can be caused by cell damage and deformation observed during cell counting.

Environmental concentrations of EE2 are 0.002 µg L^{-1} in Germany to 0.273 µg L^{-1} in North America and concentrations tend to increase (Adler et al., 2001; Daughton, 2013; Kolpin et al., 2002). Concentrations used in our experiments are much higher to predict toxic effect that may happen if there will be no improvements in wastewater treatment system. Already the smallest of the test concentrations (10 µg L^{-1}) caused above 10% algal growth inhibition as well as inhibited algal fluorescence. Consumption of endocrine disruptors is increasing due to raising living standard (Daughton, 2013). Taking into account the inflation of hormonal preparations environment and insufficient treatment of wastewater, presence of pharmaceuticals can cause significant changes on hydroecosystems.

Unfortunately EE2 is not only one pharmaceutical found in environment. There are several studies, which shows effect of pollutant mixtures on different water organisms (Silva & Kortenkamp, 2002). Different pharmaceuticals are found in environment in low

level, that are not affecting aquatic organisms, but studies show that mixture of these pharmaceuticals is affecting water organisms. Wastewaters usually contain high levels of various pharmaceuticals and other pollutants which may affect growth of microalgae and inhibit the increase of the biomass.

As current level of EE2 in nature is not affecting the algal biomass and the growth rate of cultivated microalgae, using wastewater as nutrient source is a way how to remove pharmaceuticals from water. Under natural conditions, endocrine disruptors existing in environment hinder the normal development of the phytoplankton that cause changes in phytocenosis structure, thus posing a threat to the entire hydroecosystem. In aquaculture (artificial environment) increased concentrations of hormones can reduce the practical application not only in cosmetics and pharmaceuticals, but also in energy production.

CONCLUSIONS

Endocrine disruptors have an effect on microalgae photosystem. Increased concentrations of synthetic hormone 17α-ethinylestradiol can damage phytoplankton cells and can stop algal cell division. It was observed that synthetic hormone has a negative influence on carbon production. Decreased biomass leads to smaller carbon production in this way making bioenergy production from microalgae less effective. It is suggested not to use wastewater with pharmaceutical pollution for microalgae cultivation. In further studies it is suggested to analyse carbon content changes in algal cells. Concentrations of EE2 used in experiment are above average concentrations abundant in environment, but increasing pharmaceutical pollution in long term may cause significant loss of microalgal biomass production and impede sustainable development of aquatic ecosystems.

ACKNOWLEDGEMENTS. The authors thank MSc. Ieva Putna and MSc. Mara Pfeifere for advices and Latvian Institute of Aquatic Ecology, Department of Experimental Hydrobiology for providing necessary algal cultures and laboratory devices. The work has been supported by the National Research Program ‘Energy efficient and low-carbon solutions for a secure, sustainable and climate variability reducing energy supply (LATENERGI)’.

REFERENCES

Adler, P., Steger-Hartmann, T. & Kalfbus, W. 2001. Vorkommen naturlichen und synthetisher estrogener Steroid in Wassern des sud- und mitteldeutschen Raumes. (Distribution of natural und synthetic estrogenic steroid hormones in water samples from southern and middle Germany. *Acta Hydrochim. Hydrobiol.* **29**, 227–241.

Aravantinou, A.F., Theodorakopoulos, M.A. & Manariotis, I.D. 2013. Selection of microalgae for wastewater treatment and potential lipids production. *Bioresour. Technol.* **147**, 130–4.

Bell, A.M. 2001. Effects of an endocrine disrupter on courtship and aggressive behaviour of male three-spined stickleback,Gasterosteus aculeatus. *Anim. Behav.* **62**(4), 775–780.

Blumberga, D., Veidenbergs, I., Romagnoli, F., Rochas, C. & Žandeckis, A. 2011. *Bioenerģijas tehnoloģijas* (p. 272). Rīga: RTU Vides aizsardzības un siltuma sistēmu institūts.

Chen, C.-Y., Yeh, K.-L., Aisyah, R., Lee, D.-J. & Chang, J.-S. 2011. Cultivation, photobioreactor design and harvesting of microalgae for biodiesel production: a critical review. *Bioresour. Technol.* **102**(1), 71–81.

Chisti, Y. 2007. Biodiesel from microalgae. *Biotechnol. Adv.* **25**(3), 294–306.
Daroch, M., Geng, S. & Wang, G. 2013. Recent advances in liquid biofuel production from algal feedstocks. *Appl. Energy* **102**, 1371–1381.
Daughton, C.G. 2013. *Analysis, Removal, Effects and Risk of Pharmaceuticals in the Water Cycle - Occurrence and Transformation in the Environment*. *Compr. Anal. Chem.* (Vol. 62, pp. 37–69). Elsevier.
Feng, Y., Zhang, Z., Gao, P., Su, H., Yu, Y. & Ren, N. 2010. Adsorption behavior of EE2 (17 alpha-ethinylestradiol) onto the inactivated sewage sludge: kinetics, thermodynamics and influence factors. *J. Hazard. Mater.* **175**(1–3), 970–6.
George, B., Pancha, I., Desai, C., Chokshi, K., Paliwal, C., Ghosh, T. & Mishra, S. 2014. Effects of different media composition, light intensity and photoperiod on morphology and physiology of freshwater microalgae Ankistrodesmus falcatus - A potential strain for bio-fuel production. *Bioresour. Technol.* **171**, 367–74.
Guiry, M. J. 2014. AlgaeBase. *World-wide Electron. Publ.*
Guo, Z., Liu, Y., Guo, H., Yan, S. & Mu, J. 2013. Microalgae cultivation using an aquaculture wastewater as growth medium for biomass and biofuel production. *J. Environ. Sci. (China)* **25**(Suppl 1), 85–88.
Han, F., Pei, H., Hu, W., Song, M., Ma, G. & Pei, R. 2015. Optimization and lipid production enhancement of microalgae culture by efficiently changing the conditions along with the growth-state. *Energy Convers. Manag.* **90**, 315–322.
Hense, B.A., Jaser, W., Welzl, G., Pfister, G., Wöhler-Moorhoff, G.F. & Schramm, K.-W. 2008. Impact of 17alpha-ethinylestradiol on the plankton in freshwater microcosms--II: responses of phytoplankton and the interrelation within the ecosystem. *Ecotoxicol. Environ. Saf.* **69**(3), 453–65.
Jones, C.S. & Mayfield, S.P. 2012. Algae biofuels: versatility for the future of bioenergy. *Curr. Opin. Biotechnol.* **23**(3), 346–51.
Klein-Marcuschamer, D. 2013. V IEWPOINT A Matter of Detail : Assessing the True Potential of Microalgal Biofuels. *Biotechnol. Bioeng.* **110**(9), 2317–2322.
Kolpin, D.W., Furlong, E.T., Meyer, M.T., Thurman, E.M., Zaugg, S.D., Barber, L.B., … Al., E. 2002. Pharmaceuticals, hormones, and other organic wastewater contaminants in U.S. streams, 1999 - 2000. *Environ. Sci. Technol.* **36**, 1202–1211.
Liebig, M., Egeler, P., Oehlmann, J. & Knacker, T. 2005. Bioaccumulation of 14C-17alpha-ethinylestradiol by the aquatic oligochaete Lumbriculus variegatus in spiked artificial sediment. *Chemosphere* **59**(2), 271–80.
Liu, Y., Guan, Y., Gao, Q., Tam, N.F.Y. & Zhu, W. 2010. Cellular responses, biodegradation and bioaccumulation of endocrine disrupting chemicals in marine diatom Navicula incerta. *Chemosphere* **80**(5), 592–9.
Lohr, M., Schwender, J. & Polle, J.E.W. 2012. Isoprenoid biosynthesis in eukaryotic phototrophs: a spotlight on algae. *Plant Sci.* **185-186**, 9–22.
Olguín, E.J. & Sánchez-Galván, G. 2011. *Comprehensive Biotechnology*. *Compr. Biotechnol.* (pp. 215–222). Elsevier.
Park, J.B.K., Craggs, R.J. & Shilton, A.N. 2011. Wastewater treatment high rate algal ponds for biofuel production. *Bioresour. Technol.* **102**(1), 35–42.
Perron, M.-C. & Juneau, P. 2011. Effect of endocrine disrupters on photosystem II energy fluxes of green algae and cyanobacteria. *Environ. Res.* **111**(4), 520–9.
Rawat, I., Ranjith Kumar, R., Mutanda, T. & Bux, F. 2013. Biodiesel from microalgae: A critical evaluation from laboratory to large scale production. *Appl. Energy* **103**, 444–467.
Silva, E. & Kortenkamp, A. 2002. Something from 'Nothing' – Eight Weak Estrogenic Chemicals Combined at Concentrations below NOECs Produce Significant Mixture Effects **36**(8), 1751–1756.

Stanier, R. Y., Kunisawa, R., Mandel, M. & Cohen-Bazire, G. 1971. Purification and properties of unicellular blue-green algae (order Chroococcales). *Bacteriol. Rev.* **35**(2), 171–205.

Sun, Q., Lv, M., Hu, A., Yang, X. & Yu, C.-P. 2014. Seasonal variation in the occurrence and removal of pharmaceuticals and personal care products in a wastewater treatment plant in Xiamen, China. *J. Hazard. Mater.* **277**, 69–75.

Yi, A. X., Leung, P. T. Y. & Leung, K. M. Y. 2014. Photosynthetic and molecular responses of the marine diatom Thalassiosira pseudonana to triphenyltin exposure. *Aquat. Toxicol.* **154**, 48–57.

Zhang, C., Zhang, Y., Zhuang, B. & Zhou, X. 2014. Strategic enhancement of algal biomass, nutrient uptake and lipid through statistical optimization of nutrient supplementation in coupling Scenedesmus obliquus-like microalgae cultivation and municipal wastewater treatment. *Bioresour. Technol.* **171C**, 71–79.

Zhou, G.-J., Peng, F.-Q., Yang, B. & Ying, G.-G. 2013. Cellular responses and bioremoval of nonylphenol and octylphenol in the freshwater green microalga Scenedesmus obliquus. *Ecotoxicol. Environ. Saf.* **87**, 10–6.

Agronomy Research **13**(2), 455–463, 2015

A proposition of management of the waste from biogas plant cooperating with wastewater treatment

M. Bloch-Michalik* and M. Gaworski

Department of Production Management and Engineering, Warsaw University of Life Sciences, Nowoursynowska str. 164, 02-787 Warsaw, Poland
*Correspondence: marta_michalik@sggw.pl

Abstract. The energy policy relevant to ecological aspects in all EU members since couple of years is determined by renewable energy sources (RES) development. Specific activities related to the increase of the share of RES in national energy like certificates of origin, penalties and fees all together make up a kind of enforcement that would encourage society to searching new possibilities to generate energy in accordance to respect to the natural environment. Seeking alternatives to fossil energy sources is the best option to force the approaching energy crisis.
The paper aimed at analysis of possibility in using the digestate coming from biogas plant which cooperating with wastewater treatment. In details, some aspects of underestimated energy potential of digestate was developed as well as energy flow in analysed technological solution to demonstrate that it is possible to close this balance circle. As a result of the undertaken considerations there are some suggestions how to adopt the treatment system to improve effectiveness of waste management in accordance with energy production.

Key words: biogas, pellet, waste water treatment.

INTRODUCTION

The energy policy relevant with ecological aspects in all EU members since couple of years is determined by RES (renewable energy sources) development. Specific activities related to the increase of the share of RES electricity in national energy like certificates of origin, penalties and fees all together make up a kind of enforcement that would encourage society to searching new possibilities of energy generation in accordance with respect to the natural environment. Seeking alternatives to fossil energy sources is the best option to force the approaching energy crisis. The paper presents an innovation solution as power generation from wastes called digestate. The digestate is a left-over from biogas production process. Economic viability of energy and pellet manufacturing process of undergoing anaerobic digestion of municipal sewage sludge, as a product of integrated technology of sewage sludge disposal were investigated but this paper shows only energy part of elaborations.

In Poland operates more than 4,000 municipal and industrial wastewater treatment plants. This kind of systems produce large amount of sediments. For biogas production usually goes so called biological fraction of the sludge that can be an excellent material for methane fermentation for two main reasons (Kirchmann & Bernal, 1997):

1) do not contain toxic substrates,
2) contains 4–5% dry matter, in which more over 90% is organic.

Despite this potential, they are usually disposed-off in landfills. In the light of the Council Directive 99/31/EC and Polish law (Act of 14 December 2012 on waste – Dz.U. 2013 No. 21) transparent to this document that's become an increasing problem. Since the letter of the law limits the storage of sediment, it is necessary to disseminate appropriate methods of disposal of sewage sludge and its rational management. Recycling of organic materials has essential role due to protection of the environment.

The oxygen fermentation (aka anaerobic digestion - AD) is one of the most universal methods of decreasing the quantity of organic wastes. Utilization of the organic wastes means efficient conversion to the energy and heat. In addition biogas production technic as known as destroying pathogens (Paavola & Rintala, 2008) gives ideal product for advanced research that calls digestate. Digestate quality is determined by selected technology of fermentation and character of products used in the process. However, some common stages can be found in the course of the digestion process which allows evaluating the quality of the digestate.

The most important integrands helpful with energy use of digestate are (Stinner et al., 2008):

- amount of ODM (organic dry matter) and
- the carbon content which quantity determines final energetic value of product.

MATERIALS AND METHODS

Case study

The subject described in the following paper is a sewage treatment plant designed for an average amount of treated wastewater in quantities of 38,000 m^3 per day. Sewage treatment plant is equipped with mechanical, biological and chemical purification technologies. Final waste in a shape of sludge consists organic crudes from the mechanical treatment (from primary settling tanks), and the biological sludge produced in the secondary clarifiers. Average sludge production is about 6,000 tons per day with an average hydration level of 80%.

The deposit (biological active sludge) is transferred to closed fermentation chamber (CFC) by gravity thickeners. Before entering CFC the sludge passes through the spiral heat exchanger which heats it to the correct temperature (mesophilic which amounts about 310 K). Heated sludge is pumped into open fermentation chamber, which acts as storage where deposit is subjected to the stabilization with the help of oxygen, dewatering in gravitational tank, degasification and homogenization.

Produced biogas composed mainly of methane (approx. 65%) and carbon dioxide with annual production is determined on average level of 990,000 m^3 per year ant its calorific value is 26 MJ m^{-3}.

Proposed solution

The solution of digestate management described in this paper assumes remaking the redundant substrate into valuable product – the fuel by transformation of digestate into pellets. Pellet is an increasingly popular fuel. Heating technology based on it is in

the mainstream. Competitively low price and high boilers efficiency makes this energy carrier a very cost-effective alternative to conventional fuels.

Designed technology bases on three main elements:

1. Decantation centifruge;
2. Greenhouse (solar drying);
3. Pelletizer.

Digestate is provided by conveyor belt, which transports it from the post-fermentation tank directly into decanter centrifuge and next driven by the inverter spreading on the floor of the greenhouse. Dry and shredded material goes to the store which fulfils the role of a stabilizing tank where permanent humidity standardizing the process. Chain arterial selector transfers the material to bucket elevator. The next step is material gravity pouring into the pelletizer buffer tank.

Prepared material goes into the pelletizer buffer tank where waits for granulation. Pelletizing process by-product is water vapour, which is removed from the granulation chamber by gravity through exhaust pipe system. Hot pellet is transported by feeder system to the cooler counter.

Furthermore the conception is projected to use a co-generator unit which would products:

- Electricity: used to ensure the continuity of decanter and pelletizer work and generate incomes from *green* certificates of origin.
- Heat: used as a central heating and technological process heat source.

Basis on these criteria was selected cogeneration unit VITOBLOC 200 EM 363/498 produced by VIESSMAN with the following technical data:

fuel: biogas; engine: Otto's 6-cylindder turbocharged with internal combustion; efficiency: 90.4%; electric power: 363 kW_e; heat power: 498 kW_{th}.

Theory and calculations

The main aim of the investigation is to optimize a treatment work with an usage of produced wastes. Assumed methodology based on diversified analysis. In case of it complexity this paper shows only main assumption data. More details will be approached in further articles.

At the beginning it is important to mention the calorific value of digestate pellets as an amount of 11 GJ t^{-1} which results from calculation shown in (Michalik, 2011) but scrutiny is going to be experiment soon.

First step in calculation gives amount of annual biogas production which was computing in accordance with (Curkowski et al., 2009).

By assuming that the methane average content for analysed study is equal to 65% of total biogas volume (1)

Methane capacity

$$p_{CH_4} = V_{bio} * \sigma \quad (1)$$

where: V_{bio} – biogas volume (m^3); σ – average methane content (%); the model equation for an energy balance was possible.

The value is a base for estimation energy CHP production which in final gives net heat and electricity production in monthly configuration.

Subsequently annual digestate production was estimated by process simple transformation as it is shown below.

Annual dry matter production:

$$d.m. = annual\ volume\ of\ treated\ sludge * dry\ matter\ contain \quad (2)$$

Annual digestate production:

$$d = (annual\ dry\ matter\ production * 100\%)/20\% \quad (3)$$

Wastewater treatment plant is a consumer of electricity from the local supplier in the terms of ordered capacity – declared by the customer – amounts 500 kW, by medium voltage network, with variable demand. Rely on data given from the wastewater treatment operator author elaborated consumer profile of electricity consumption which was set together with monthly electricity production from CHP unit.

All technical elements mentioned in Table 1 as electricity consumption factors are permanent elements of technological line. Biogas plant and technological line components work 8,000 hour per year. Treatment plant works incessantly. Monthly electricity production was calculated by multiply biogas plant installed capacity (according to prior computations and working time (Pieczykolan & Romańczuk, 2012).

Analyzed treatment plant is equipped with gas boiler working as an only source of heat for whole facility (biogas plant, sewage treatment plant and social buildings). To balance heat demand with its production (purchase) it was necessary to inspect the energy audit for buildings which are part of treatment plant infrastructure.

Table 1. Monthly electricity consumption

Month	Electricity consumption:			
	proposed equipment	biogas plant	treatment plant	total
	MWh			
January	21.1	22.9	200.3	244.2
February	19.0	20.7	180.9	220.6
March	21.1	22.9	200.3	244.2
April	20.4	22.2	193.8	236.4
May	21.1	22.9	200.3	244.2
June	20.4	22.2	193.8	236.4
July	21.1	22.9	200.3	244.2
August	21.1	22.9	200.3	244.2
September	20.4	22.2	193.8	236.4
October	21.1	22.9	200.3	244.2
November	20.4	22.2	193.8	236.4
December	21.1	22.9	200.3	244.2

Source: Michalik, 2013

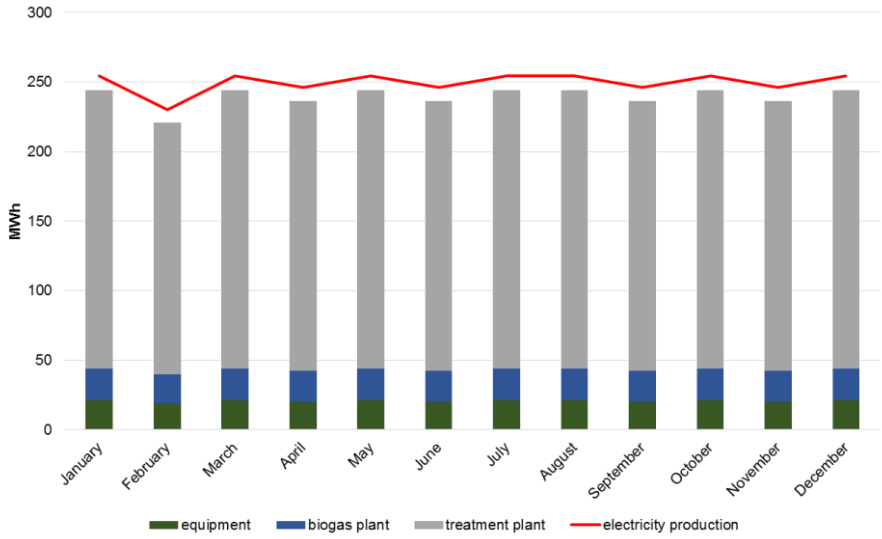

Figure 1. Monthly electricity balance (Source: own elaboration).

Whole audit procedure base on particular acts:

- Act of 19 September 2007 Building Law.
- Ministry of Transport, Construction and Maritime Economy Regulation (Dz. U. z 2008 r. Nr 17, poz. 104) of 21 January 2008 the conduct of training and examination for persons seeking permission to draw up the certificate of the energy performance of a dwelling and the building which is the independent whole technical-utilitarian.
- Ministry of Transport, Construction and Maritime Economy Regulation (Dz. U. z 2008 r. Nr 201, poz. 1240) of 6 November 2008 a methodology for calculating the energy performance of the building and an apartment building or part of a whole which is the independent technical-utilitarian and the preparation and presentation of certificates of energy performance.
- Ministry of Transport, Construction and Maritime Economy Regulation (Dz. U. z 2008 r. Nr 201, poz. 1239) of 6 November 2008 amending the Regulation on the scope and form of the building project.
- Ministry of Transport, Construction and Maritime Economy Regulation (Dz. U. z 2008 r. Nr 228, poz. 1513) of 17 December 2008 amending Regulation of the amended Regulation on the scope and form of the building project.
- Ministry of Transport, Construction and Maritime Economy Regulation (Dz. U. z 2008 r. Nr 201, poz. 1238) of 6 November 2008 amending the Regulation on technical conditions to be met by buildings and their location.
- Ministry of Transport, Construction and Maritime Economy Regulation (Dz. U. z 2008 r. Nr 228, poz. 1514) of 17 December 2008 amending Regulation of the amended the Regulation on technical conditions to be met by buildings and their location.
- Directive 2002/91/EC of the European Parliament and of the Council of 16 December 2002 on the energy performance of buildings.

Table 2. Monthly heat consumption

Month	Heat consumption:			
	social buildings	biogas plant	treatment plant	Total
	MWh			
January	20.2	81.9	170.4	272.4
February	15.9	73.9	153.9	243.7
March	4.4	81.9	170.4	256.6
April	-5.7	79.2	164.9	238.4
May	0.1	81.9	170.4	252.4
June	0.0	79.2	164.9	244.1
July	0.0	81.9	170.4	252.2
August	0.0	81.9	170.4	252.2
September	9.3	79.2	164.9	253.4
October	14.7	81.9	170.4	267.0
November	22.2	79.2	164.9	266.3
December	23.7	81.9	170.4	275.9

Source: Michalik, 2013

Apparently in November and December total heat demand exceed gross heat production (Table 2) as follows. Taking into account that heat producers should secure continuity of heat production by other fuel this little exceeds does not pose. Instead of additional fuel was proposed an installation of a buffer tank.

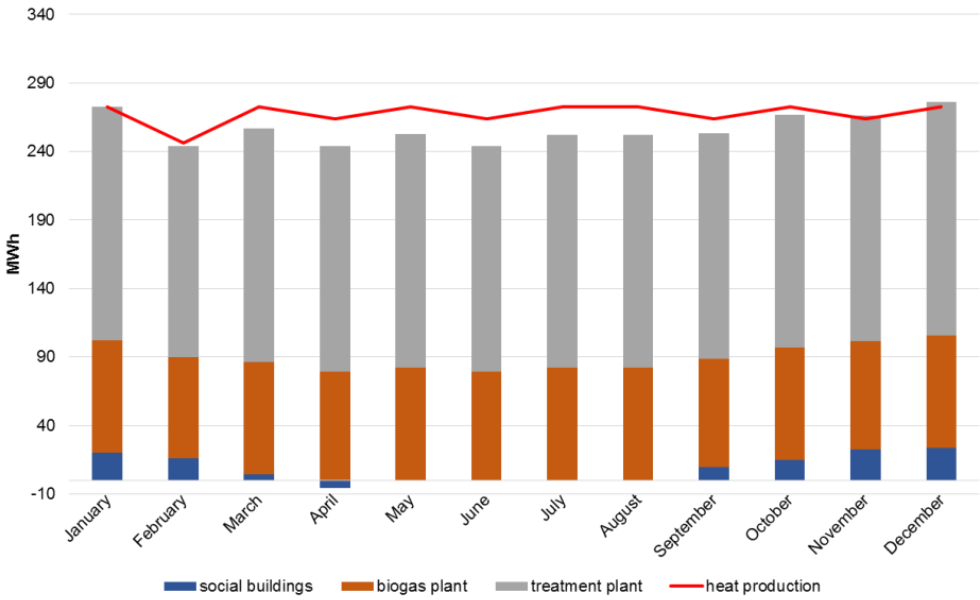

Figure 2. Monthly heat balance (Source: own elaboration).

Total heat consumption for analyzed year was calculated in assessment of biogas annual consumption which was given by treatment operator and defined as total heat

consumption in 2011 – 11,081 GJ. From case study calculation comes out biogas plant heat demand – 3,481 GJ and social building heat demand – 377 GJ. More detailed and exhaustive material are presented in (Michalik 2013) and (Michalik 2011) as well would be elaborated in further studies.

To estimate mass flow in the process it has be done a reverse operation. Annual real biogas production is 998,978 m^3 and it is known that 1 m^3 of sewage sludge delivered into the digester tank should give 20 m^3 of biogas (Gans et al., 2010).

$$\dot{m} = \frac{p_{rb}}{p_{tb}} * \rho_s \tag{4}$$

where: p_{rb} – real biogas production (t $year^{-1}$); p_{tb} – theoretical biogas production (m^3 of biogas m^{-3} of sewage sludge); ρ_s – sewage sludge density (t m^{-3}).

According to the research carried out by Michalik (2011) the hydration of digestate after 30 days of storage is 74%. When the digestate retention time ends the mass is delivery to the decantation centrifuge by conveyor belt. The device guarantees 50% decrease of hydration of the substrate. Afterwards greenhouse (solar drying) provides obligated hydration of pelletized substrate about 20%.

RESULTS AND DISCUSSION

Classic combustion of sewage sludge is well understood and mastered but in case of nitrogen oxides emission and heavy metals content could cause negative effects on environment and be a source of social objections (Werle & Wilk, 2011).

Agricultural use of sewage sludge is bothersome due to legislative connotation (Council Directive 86/278/EEC of 12 June 1986 on the protection of the environment, and in particular of the soil, when sewage sludge is used in agriculture).

Oxygen fermentation (aka anaerobic digestion – AD) is one of the most universal methods of organic wastes utilization that provides efficient transformation into electricity and heat and also helps with pathogens destroying (ENconsult Council, 2011). Product of the AD process calls digestate.

In accordance of theoretical research (Michalik, 2011) during the pelletization process substrate loses even 50% of water contains. According to formulas from (Morris, 2011) and author's data total mass of produced pellets amounts almost 17,000 tons per year which can be sell as an alternative fuel allow generating incomes.

Digestate quality (as a product of AD) is determined by fermentation technology and substrates used in the process (Paavola & Rintala, 2008). However, some common assuming can be done by the available literature.

Table 3. Typical fuel properties of digestate pellets

Net calorific value	Ash content	Water content	Softening temperature of ash	Nitrogen	Sulphur	Chlorine
GJ t^{-1}	%	%	K	%	%	%
15–18	16–20	9–10	1,373	1.5–3	0.3–1	0.3–0.9

Source: Christa & Wopienka, 2009

On account of lack of possibility of laboratory research of calorific value of produced pellets only experimented quantity was carried out base on simple calculation:

$$Q_i=Q_s-24.42*(W^a+8,94H^a) \quad (5)$$

where: Q_i – heat of combustion (MJ kg^{-1}); 24.42 – heat of water vaporization in temperature of 298.15 K corresponding to 1% water content in the fuel (MJ kg^{-1}); W^a – water content in the fuel sample (%); H^a – hydrogen content in the fuel sample (%).

The result amounts 11 MJ kg^{-1}. More exact experiment will be subject of further research.

CONCLUSIONS

This paper has investigated the reasonableness of alternative way in digester management. To do this it has to by choose suitable methodology. Obtained results gives reasonable arguments about whole conception.

Energetic results are very positive. The electricity demand for biogas plant, treatment plant and proposed pelletization line is minor than theoretical production. Also heat theoretical production is high than its demand, but only in annual depiction. Monthly analysis show that in November and December could take place the deficiency of produced heat. The proposed solution is use of a buffer tank.

The main research conclusions:

1. The production process where pellets are created from digestate resultant from anaerobic digestion is possible to carry out.
2. Thanks to small number of technologies changes in treatment plant the facility could obtains energy independence.
3. Suitable management of analysed digestate gains free fuel in a form of pellets.

Further research could be conducted to determine the effectiveness of pellet production from different types of digestate.

REFERENCES

Christa, K. & Wopienka, E. 2009. Cost analysis report. Brussels: *MixBioPell*.

Curkowski, A., Mroczkowski, P. & Oniszk-Popławska, A. 2009. Biogaz rolniczy – produkcja i wykorzystanie. Warszawa: *Mazowiecka Agencja Energii* (in Polish).

ENconsult Council; 2011. A technical feasibility study for Leicestershire. Anaerobic digestion – a renewable energy resource. Dunfermline: *Leicestershire Country Council*.

Gans, N., Mobini, S. & Zhang, X.N. 2010. Appendix E. Mass and Energy Balances at the Gaobeidian Wastewater Treatment Plant in Beijing, China. Water and Environmental Engineering, Department of Chemical Engineering, Lund Institute of Technology, *Lund University*, Sweden.

Instytut Gospodarki Surowcami Mineralnymi i Energią. 2005. Wykorzystanie biogazu w oczyszczalni ścieków w Zawierciu. Kraków: *Polska Akademia Nauk* (in Polish).

Kirchmann, H. & Bernal, M.P. 1997. Organic waste treatment and C stabilization efficiency. *Soil Biology and Biochemistry*, **11/12**(29), 1747–1753.

Michalik, M. 2011. Utilization of anaerobic digestion waste from biogas plant cooperate with sewage works. Technological resolution. Bachelor thesis, manuscript, *Warsaw University of Life Sciences*, Warsaw, Poland.

Michalik, M. 2013. Energetic and economic analysis of alternative digestate management. Master thesis, manuscript, *Warsaw University of Life Sciences*, Warsaw, Poland.

Morris, A.E. 2011. Handbook on Material and Energy Balance Calculations in Material Processing. Hoboken: *John Willey&Sons*.

Paavola, T. & Rintala, J. 2008. Effects of storage on characteristics and hygienic quality of digestates from four co-digestion concepts of manure and biowaste. *Bioresource Technology*, **15**(99), 7041–7050.

Pieczykolan, M. & Romańczuk, P. 2012. Porównanie eksploatowanych technologii. Tychy: *Regionalne Centrum Gospodarki Wodno-Ściekowej S.A.* w Tychach (in Polish).

Stinner, W., Möller, K. & Leithold, G. 2008. Effect of biogas digestion of clover/grass-leys, cover crops and crop residues on nitrogen cycle and crop yield in organic stockless farming system. *European Journal of Agronomy* **2–3**(29), 125–134.

Werle, S. & Wilk, R.K. 2011. Energetyczne wykorzystanie komunalnych osadów ściekowych – możliwość czy konieczność. VIII Ekoenergetyczna Konferencja, Gliwice, 17.06.2011. Gliwice: (b.w.), 14–25 (in Polish).

Agronomy Research **13**(2), 464–476, 2015

Modeling greenhouse gas emissions from the forestry sector – the case of Latvia

E. Dace* and I. Muizniece

Riga Technical University, Institute of Energy Systems and Environment, Azenes street 12/1, LV1048 Riga, Latvia; *Correspondence: elina.dace@rtu.lv

Abstract. A system dynamics model for assessing the greenhouse gas (GHG) emissions from forestry and forest land is presented in the paper. The model is based on the IPCC guidelines for national GHG inventories and includes the main elements of the forestry sector, i.e. changes in the living biomass, dead organic matter and soils. The developed model allows simulating various policies and measures implemented and decisions made, and their impact on change in the GHG emissions. Various scenarios of potential development in the medium-term planning were simulated till 2030 to assess their impact on the GHG emissions. It is found that the most sustainable option would be use of wood processing waste for production of e.g. wood chips or some added-value products. The case of Latvia is selected for simulations, as forests compose about 52% of the country's area. Nevertheless, by changing specific parametric values the model can be adapted and applied for estimation and analysis of GHG emissions from forestry in other countries, as well.

Key words: GHG emissions, forestry, living biomass, wood waste, system dynamics.

INTRODUCTION

Latvia is the fourth most forested country in Europe. About 52% of the country's total area is covered by forests, which is 3.5 million hectares (State Forest service). Over the last century, Latvian forest areas have nearly doubled – in 1923, the forest area accounted for only 27% of the country's territory. The forest area continues to increase, though on a slower rate (Forest sector in Latvia). The forest areas have increased mainly due to the natural and artificial afforestation of agricultural land (State Forest service). Usually, the naturally afforested land contains generally more inferior stands.

An indicator characterizing the increasing forest resources in Latvia is the fact that the annual increase in wood stock is triple of the increase of the forest areas (State Forest service). Thus, it can be stated that the forest land increases as a result of targeted forestry activities. Over the last decade, the annual amount of round wood extracted has been around 12 million m^3 (State Forest service). The amount is smaller than the natural increment, thus the Latvian forestry can be considered as sustainable.

The forestry sector is directly associated with the greenhouse gas (GHG) emissions that are released and removed simultaneously. Latvia is one of the few countries where more emissions are removed than emitted (LNIR, 2014). This is due to the comparatively large forest areas and living forest biomass that is able to remove emissions released by other sectors (agriculture, energy, industry, waste management etc.). However, in recent

years the emission amount removed has a tendency to decrease. In 2012, the net GHG emissions from the forestry sector were equal to -13,099 Gg CO_2 eq. (LNIR, 2014) being practically the lowest level since 1990. The reason for that is the increase in forest felling. As a result not only the capacity of the living biomass is reduced, but the amount of forest processing waste is increased. Therefore, it is important to assess the possibilities for increased emission removals or at least balancing them at the current level.

The Intergovernmental Panel on Climate Change (IPCC) has established a methodology for estimating GHG emissions from various sectors, including forestry (IPCC, 2006). The IPCC guidelines facilitate making an inventory of the GHG emissions generated in the past. However, the forecasting options are limited, especially when an effect of various decisions, measures and policy instruments on GHG emission dynamics has to be assessed. Thereof, the aim of this paper is to present an alternative tool for estimating the forestry's GHG emissions. The tool is developed by using the system dynamics (SD) method that allows capturing the relationship between cause and effect of a complex dynamic system as the forestry is (Dace et al., 2014). In addition, the aim of the study was to test the possibilities to limit the increase in the net GHG emissions of the forestry sector.

SD was developed by Jay Forrester in 1950's (Forrester, 1958) and has, since then, been applied to a diverse set problems (Sterman, 2000), e.g. collection of waste portable batteries (Blumberga et.al., 2015), development of a low-carbon strategy (Blumberga et.al., 2014), switching to renewable energy sources (Romagnoli et.al., 2014), etc. To our knowledge, the studies where SD has been applied to assess forestry's GHG emissions are scarce. Machado et.al. (Machado et al., 2013) have used SD to evaluate the growth and carbon stock of eucalyptus forests in Brazil. They have considered the four main flows, i.e. land use, wood stock, carbon stock and forest land increase. In addition SD has not been used to evaluate an impact on emissions from land use, land-use change and forestry (LULUCF). Though, other types of models have been created. E.g. CBM-CFS3 (Carbon Budget Model of the Canadian Forest Sector) has been developed based on the IPCC methodology to assess carbon dynamics in forestry and land-use change in Canada (Kurtz et al., 2009). Thus, we believe, that the SD model built in this study is a unique tool that can be adapted to other countries similar to Latvia, as the structure of the system remains, and only specific parametric values have to be changed.

METHODOLOGY

A SD model was developed based on the IPCC guidelines for national GHG inventories (IPCC, 2006). Thus, a static linear methodology for assessing national GHG emissions was combined with dynamic modeling of non-linear complex systems provided by SD. The model was built in two separate major blocks, i.e. agriculture and forestry (see Fig.1). GHG emissions from the processes of livestock enteric fermentation, manure management and soil cultivation were simulated in the agricultural sub-model. Whereas, modeling of the GHG emissions from the forestry sector included emission removals by the living biomass (various tree species) and emissions from decomposition of dead organic matter and organic and mineral soils.

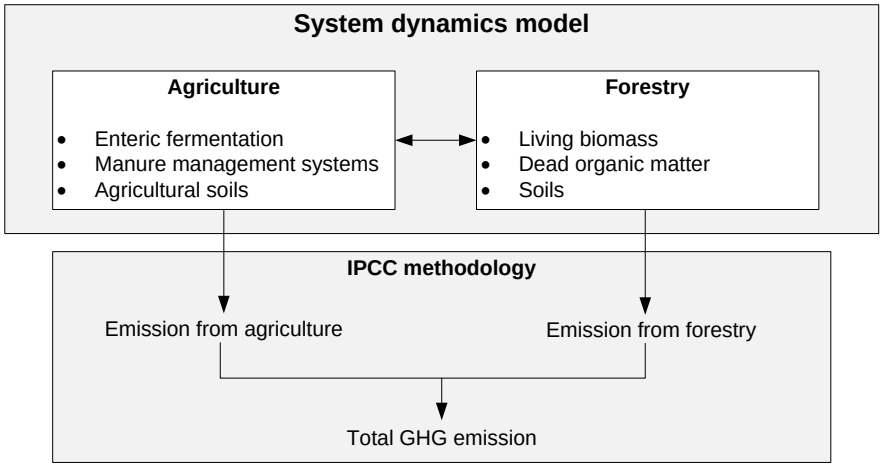

Figure 1. Logical framework of the methodology applied.

In SD, stock-and-flow diagrams are used to build the structure of the studied real-world system. That allows capturing the essential activities and accumulations of the system, as the drivers of activity are represented as information-feedback processes (Buch et al., 2008). The system's performance is determined by the system's structure which, on its turn, is created by the feedbacks.

In our study, *Powersim Studio 8* software environment was used to develop the model. Numeric values of certain quantitative parameters were estimated from the historic statistical data bases on GDP, prices, land stocks, agricultural and forestry products etc. In addition, interviews with experts were used to assess accuracy of the processes and future developments simulated. In the model, all the information reflects the situation in Latvia. Nevertheless, many of the case-specific numeric parameter values may be changed to represent the situation in some other country, as the structure of the model is similar in many countries.

In our model, the emissions were simulated for the time period from 2005 until 2030. That allowed us to compare the simulation results with the historical observed tendency (back-casting) and to analyze the future development under various policy decisions. It has to be noted, that the aim of SD modeling is to present the trend of dynamic behavior of the real system, not to give projection of exact values (Sterman, 2000). Thus, the focus is on relationships rather than on the precision of the simulated parametric values.

Agriculture is directly associated with climate change issues on environmental, economic and social dimensions. Agricultural activities emit greenhouse gases that, on their turn, influence the agricultural productivity. The GHG emissions in the agricultural sector arise from livestock farms as a result of processes of livestock enteric fermentation and management and storage of manure. Emissions arise also from cultivation and fertilization of agricultural soils. Agricultural sector is problematic with respect to GHG emissions, as within the sector options for GHG emission abatement are limited. Hence, the most efficient option is to limit agricultural activities themselves. Obviously, abandoning the idea of streaming towards increased agricultural productivity is not a solution, and mechanisms mitigating the negative environmental impacts (GHG

emissions) have to be found. Conversely, forests work as removers of the GHG emissions from the atmosphere. As 52% of the area of Latvia is covered by forests (State Forest service), all of the local agricultural emissions, theoretically, are removed. Still, in the last decades, intense felling has been carried, thus steadily reducing the amount of emissions removed. In addition, wood waste is created. Gradual decomposition of the wood waste and litter, wood burning, and also forest soils generate emissions. All these interactions are simulated with the developed model.

The model (see Fig. 2) simulates the dynamics of the forest area of each tree species and how it is split in young forest stand, mature forest and clearings. Also, the wood stock, its increment, as well as wood mortality and decomposition are simulated. In addition, the model simulates the amount of above- and below-ground wood waste generated. Thus, the results for forest land's GHG emissions and removals are estimated.

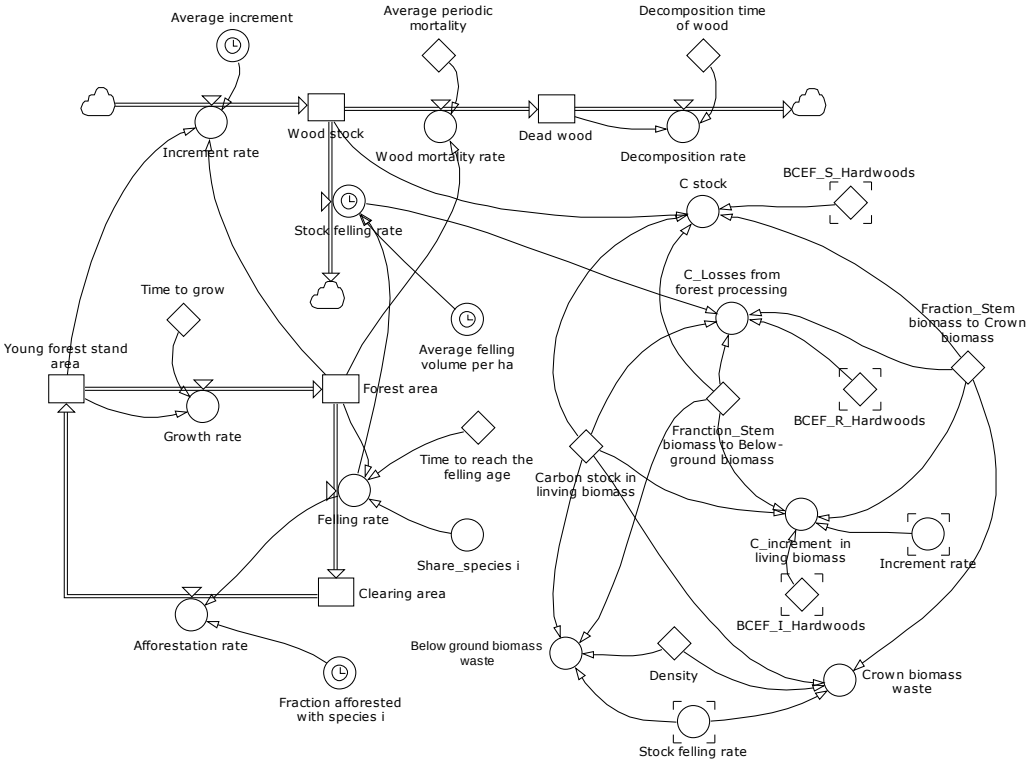

Figure 2. Stock-and-flow diagram of the wood stock and waste model.

The simulation is started in 2005. Thereof, the initial state of each stock in the model corresponds to the value reported in statistical databases for 2005. Then, the flows are defined. For each tree species, a certain amount of time necessary to grow and reach the felling age. Yet, felling largely depend on the market price of the particular wood species, as that determines the interest in cutting and selling the wood. Hence, the felling rate is determined as:

$$r_{f\,i} = \frac{A_{Fi} \cdot \left[\frac{e^{\alpha \cdot P_i}}{\sum e^{\alpha \cdot P_n}} \right]}{T_{fi}} \quad (1)$$

where: r_{fi} – felling rate of species *i*, ha yr^{-1}; A_{Fi} – forest area of species *i*, ha; e = 2.718 – the base of the natural logarithm (Euler number); α – coefficient that determines the steepness of the curve of share of wood species as a function of the market price; P_i – market price of wood of species *i*, EUR m^{-3}; P_n – market price of wood, EUR m^{-3}; T_{fi} – time to reach the felling age, yr; *n* – wood species (pine, spruce, birch, oak, ash, black alder, grey alder, aspen and other species).

Knowing the average amount of wood cut per hectare and multiplying it with the felling rate r_f, the stock felling rate is determined. The wood stock accumulates the difference between the stock increment rate flowing in and the stock felling rate and wood mortality rate flowing out of the stock (see Eq.2).

$$S_i = \int (r_{ii} - r_{sfi} - r_{mi})(t) \cdot dt + S_i' \quad (2)$$

where: S_i – stock of wood species *i*, m^3; r_{ii} – increment rate of species *i*, m^3 yr^{-1}; r_{sfi} – stock felling rate of species *i*, ha yr^{-1}; r_{mi} – wood mortality rate of species *i*, m^3 yr^{-1}; S'_i – initial stock of wood species *i*, m^3.

The estimated *S*, r_i and r_{sf} are used to calculate the annual carbon stock and carbon increment in living biomass and carbon loss from forest processing according to the IPCC guidelines for national GHG inventories (IPCC, 2006). The calculated parameters are then used to estimate removals of GHG emissions.

r_{sf} is also used to assess the wood waste generated by cutting the trees. It is assumed that 80% of wood wastes are left in forests. 5% of the wastes left in forests are burned. Whereas, the remaining part decays during a 20 year period. The annual carbon stock in forest litter is estimated assuming that the decomposition rate is 0.1% yr^{-1} (Berg, 2000). The resulting values are used to calculate the emissions from forests.

The emissions and removals from forests are affected not only by the processes happening in the forest, but also by the total area of land available for forests. Since 1990s, the area of forest land has been steadily increasing in Latvia (Forest sector in Latvia). The main reason for that was the overgrowth of agricultural land, as a result of its abandoning. Since implementation of the support payments for management of agricultural land (single area payments, direct payments and complementary national direct payments), the abandoning and overgrowth has descended, thus reducing the increase rate of the forest land area. In the model, the transition from agricultural to forest land was simulated by building two stocks – the stock of agricultural land and the stock of forest land (see Fig. 3). Agricultural land becomes the forest land when bush and trees reach 5 m height and occupy 20% of the area considering the crown projection (The Law on Forests). In addition, it is considered that 20 years are necessary to change the land-use type (IPCC, 2006). Moreover, there is an indicated maximum area that can be taken

by forests. It is assumed that the indicated area equals the sum of forest land area and 30% of the agricultural land area that was registered in 2005. Thus, the area of forests in Latvia cannot exceed 3,566,328 ha. The rate of transition is calculated as follows:

$$r_t = IF(L_F^{\max} > L_F), THEN(L_A \cdot (1 - F_m)/T_o), ELSE(0) \quad (3)$$

where: r_t – transition rate from agricultural land to forest land, ha yr^{-1}; $L_F^{\max}$ – indicated maximum area of forest land, ha; L_F – area of forest land, ha; L_A – area of agricultural land, ha; F_m – fraction of managed agricultural land; T_o – time necessary for agricultural land to overgrow and become the forest land, yr.

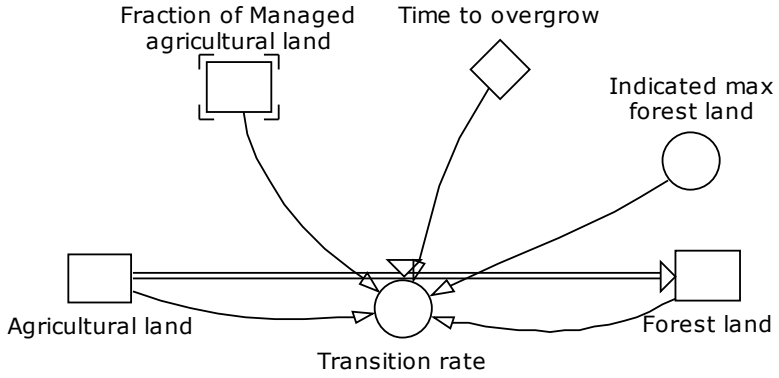

Figure 3. Stock-and-flow diagram of the overgrowth of agricultural land.

The parametric values used in the model are shown in Tables 1 and 2 (only parameters not indicated in the IPPC guidelines (IPCC, 2006) are shown).

In order to assess the dynamics of the GHG emissions and removals from forest land, several scenarios were developed. First, the base scenario (reference scenario) was developed to observe the potential dynamics of the system provided that the forestry and agricultural sectors will continue to develop following the historically observed tendency. Then, based on the results of the base scenario, various decisions and measures were tested to assess their impact on net GHG emission rates from the forest land.

In scenario I, an option of increased use of the above-ground (crown) biomass waste for production of wood chips is assessed. Currently, only small amount of forest processing wastes are used for wood chips' production. This is due to the high production costs and low market price. The wood processing wastes frequently are polluted with impurities (e.g. sand) which determines their low quality. Most of the wood chips produced in Latvia are exported, and demand exists only for high-quality wood chips.

Table 1. Wood species-specific parametric values of the model

Parameter	Unit	Value									Source
		Pine	Spruce	Birch	Aspen	Black alder	Grey alder	Oak	Ash	Other	
Average increment	$m^3\ ha^{-1}\ yr^{-1}$	8.3	11.7	7.8	10.4	9.9	8.9	5.7	5.7	12.0	LNIR, 2014
Average periodic mortality	$m^3\ ha^{-1}\ yr^{-1}$	2.4	3.3	2.3	3.1	2.6	0.8	4.6	4.6	1.2	LNIR, 2014
Wood density	$t\ m^{-3}$	0.38	0.36	0.47	0.40	0.41	0.41	0.41	0.41	0.41	LNIR, 2014
Time to grow	yr	40	40	20	20	20	10	40	40	20	The Law on Forests
Time to reach felling age	yr	70	41	31	21	51	51	61	41	41	The Law on Forests
Greenery mass	$kg\ m^{-3}$	78.0	117.7	-	-	-	-	-	-	-	Daugavietis et. at., 2012, Stibe, 1976
Initial wood stock	$m^3\ 10^6$	248.1	88.82	159.1	23.9	15.0	31.1	2.2	3.7	1.2	State Forest service
Initial dead wood amount	$m^3\ 10^6$	2.65	2.21	2.24	0.64	0.46	0.25	0.11	0.19	0.09	State Forest service
Initial young forest stand area	$ha\ 10^3$	118.0	273.3	98.2	25.5	5.9	7.6	0.7	5.8	0.9	State Forest service
Initial forest area	$ha\ 10^3$	928.4	242.0	733.6	75.1	68.6	182.2	9.3	12.5	5.8	State Forest service
Initial clearings area	$ha\ 10^3$	11.12	9.46	11.26	4.75	0.76	5.98	0.04	0.12	0.0	State Forest service

Table 2. Other parametric values of the model

Parameter	Unit	Value	Source
Technologically obtainable fraction of above-ground biomass	%	70	Adamovics et al., 2009
Technologically obtainable fraction of below-ground biomass	%	60	Adamovics et al., 2009
Average litter decomposition rate	$\%\ da^{-1}$	0.1	Berg, 2000
Initial agricultural land area	$ha\ 10^6$	2.45	CSB, 2015
Initial forest land area	$ha\ 10^6$	2.82	CSB, 2015
Indicated max forest land	$ha\ 10^6$	3.56	State Forest service

It is assumed that only 70% of the wood processing waste in clearings can be used for production purposes, as 30% are considered as the technological loss (Adamovics et al., 2009). However, should there be favorable conditions (e.g. increased demand) allowing economically feasible realization the technologically available crown biomass, the wood processing waste would be cut considerably. Thus, the emissions from the decay of the dead organic matter would be reduced. That forms the base for the scenario I.

In scenario II, a situation where also below-ground biomass wastes (stumps) are used is assessed. Technologically it is possible to extract up to 60% of the below-ground biomass (Adamovics et al., 2009). So far, in Latvia, utilization of the stumps for production of wood chips has not been practiced, as more easily collectable wood has been available. Still, stumps are valuable and hitherto undervalued resource. It should be noted that a specific extraction technology has to be applied (Silava, 2008). Besides, the stump extraction is allowed only in certain types of forests.

Another option to reduce the wood processing wastes is to use the greenery (needles and small branches) of conifers for manufacturing products. In Latvia, the greenery in small amounts is used for production of needle extract (Pollution permit, 2010). Yet, before also high-quality forage has been produced. In the recent years, use of the greenery for production of insulation materials has been intensely studied (Muizniece et al., 2015). In the last case, a large amount of the material would be required. Thereof, collection and use of the greenery (considering the technological loss of 30%) is simulated in scenario III.

In scenario IV, the dynamics in GHG emissions is assessed assuming that policy instruments are implemented and changes in legislation are made that limit forest felling by 20%. E.g. introduction of felling quota could serve as such an instrument. As a result, emissions generated during decomposition of wood waste would decrease (as there would be less waste). Moreover, removal of GHG emissions would increase as the wood stock would not be depleted on such a rate as before. Introduction of the instrument would allow slowing the rate of stock felling to prevent the stock reduction to a critical level and endangering biodiversity.

Similarly, an influence of introducing a tax on wood felling is assessed in scenario V. The tax would increase the wood price, thus decreasing the demand for wood. That would allow reduction of amount of wood processing waste and preservation of the living biomass that removes emissions. It is simulated that the prices increase by 20% as a result of tax introduction.

Changes in transition rate from agricultural land to forest land are simulated in scenario VI. In the National Development Plan of Latvia for 2014–2020 (NDP, 2012), an ambitious target for management of agricultural land is set, i.e. a more intensive, though sustainable use of each hectare of the agricultural land. According to the Plan, 95% of the agricultural land should be managed by 2020. In 2013, 85% of the agricultural land was managed. Thus, it is planned to decrease the area of land left unmanaged and overgrown with bush and natural forest. As a result, the increase rate of forest land area will lower, biodiversity will decrease, and the amount of GHG emissions from agricultural activity will rise. Therefore, it is necessary to assess how emissions from forest land would change upon realization of the target set in the Plan.

In the model, implementation of the simulated decisions and measures is started from 2016. An exception is the intensification of management of the agricultural land that should have been started in 2014, already.

RESULTS AND DISCUSSION

The results of the base scenario show that, in the forest sector, a tendency exists for emissions to increase and removals – to decrease (see Fig. 4). This is in agreement with the emission tendency reported in the Latvia's National Inventory Report (LNIR) (LNIR, 2014). However, the numerical values differ. The results depend on the choice of the database used for parameter definition, as large discrepancy exists in the data of various national databases. In addition, the choice of methodology for estimating some of the parameters might differ, thus creating the difference in the results. This is in agreement with findings of the leading forestry researchers in Latvia that conclude that diverse results are obtained when different emission calculation methods are applied (Silava, 2012).

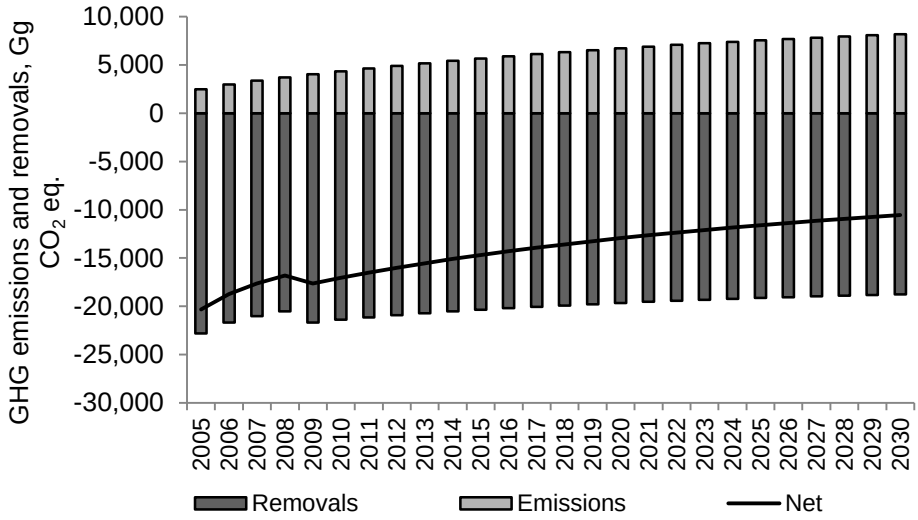

Figure 4. Results of the GHG emissions and removals in base scenario.

The results indicate that the net GHG emissions will increase as a result of the existing forestry practice (see Fig. 4). In fact, in 2030, the net GHG emissions will double. It forces reconsidering the future balance of the total national GHG emissions. Latvia has had a unique situation where all emissions generated in agricultural, energy, industrial etc. sectors were removed by the living biomass of forests. The obtained results make us conclude, that this privilege might change in the near future. Furthermore, continuation of the felling rates of the last decade will have a long-term effect, as the time necessary for trees to grow and reach the felling age takes 40 to 120 years depending on species.

The results of simulating the developed scenarios demonstrate that the largest impact on net GHG emissions would be caused by the scenario IV – considerable reduction in felling (see Fig. 5). That would cause a sharp decrease (by 34% in 2016 and 53.8% in 2030) in the net GHG emissions. As a result, in 2030, the net emissions would be 5,678 Gg CO_2 eq. less as compared to the base scenario. While the emission reduction is significant, the measure is questionable with respect to the damage caused to the

forestry and wood processing industries. Reducing the felling and forest processing rates would considerably reduce the number of working places and decrease the national income from the forestry, wood processing and export of wood resources. Thus, implementation of such a limiting policy instrument would be possible only in case of proving that the gain of GHG emission reduction is larger than the economic and social loss of the industry.

Also, the results of the scenario V where an introduction of a tax was simulated demonstrate the reduced net GHG emissions. Though the emissions would decrease by 5.2% or 549 Gg CO_2 eq. the benefits should be evaluated against the impact caused on the forestry and wood processing industries. In addition, the usefulness of such an instrument should be evaluated, as the reduction in GHG emissions would be comparatively small.

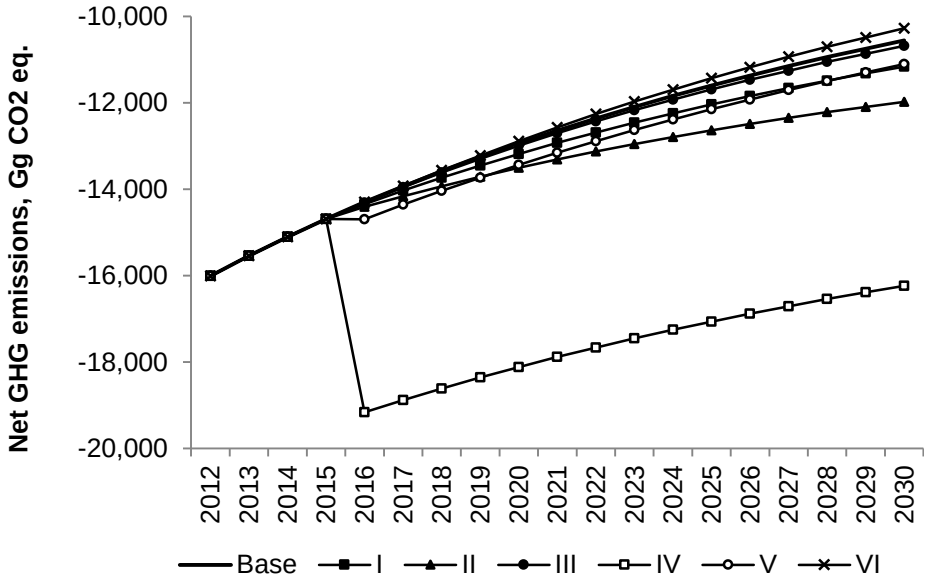

Figure 5. Results of the effects of various measures on the net GHG emission dynamics, 2012–2030.

The results of the scenarios IV and V are not reached by direct decrease of the forestry emissions, but reduction of the amount of wood processed that allows preserving the stock of the living biomass removing the emissions. The stock of living biomass has a larger impact on the total emission balance compared to the forest processing waste (see Fig. 6). The stock of stem lost in the forest processing is calculated as an immediate source of emissions, while wood processing waste left in forest would decay in a longer time, thus constantly generating small amounts of emissions. Thereof, instruments oriented towards decrease in felling rates should be implemented to achieve greater effect on the net GHG emission reduction. Still, introduction of measures reducing GHG emitted directly from the forestry sector should be considered.

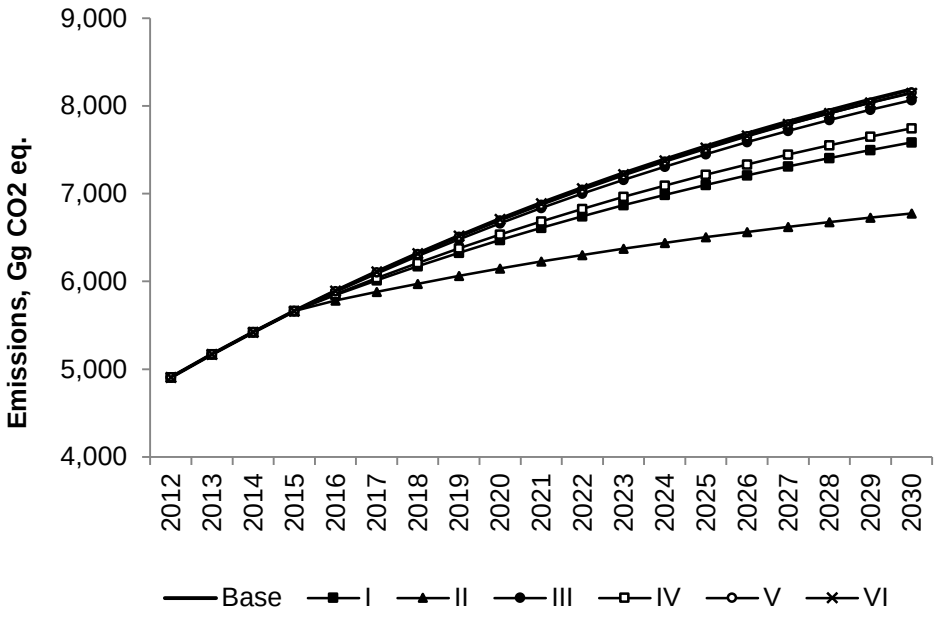

Figure 6. Results of the effects of various measures on the GHG emission dynamics, 2012–2030.

Scenarios I, II and III differed with the fraction of biomass waste used in production of products (wood chips). In scenario II, use of all technologically extractable waste was considered. Whereas, the use of the crown biomass waste only was simulated in scenario I. That way, in 2030, the emissions would be by 7.4% and 17.3% smaller in scenarios I and II, respectively, as compared to the base scenario. The least impact on GHG emission reduction would be achieved in the case of scenario III, where greenery of conifers solely would be used. In 2030, that would create emission reduction by 125 Gg CO_2 eq. or 1.5% as compared to the base scenario. While the effect on GHG emission reduction seems minor, use of conifers' greenery for manufacture of products would increase the social and economic benefits from forestry. In addition, an added value would be created for the forest processing waste turning them into a valuable resource. Moreover, use of wood processing waste would provide an option of using local renewable resources to meet the local and foreign market demand.

Reaching the target of increased fraction of the managed agricultural land will impact the forest land's emissions insignificantly (scenario VI). Comparing to the base scenario the net GHG emissions would be increased by 2.7% or 280 Gg CO_2 eq. Scenario VI is the only scenario among the simulated in our study that causes the net emissions to rise. That means that in order to reduce the emissions in the forestry sector the management of forest land and resources has to be well-considered and sustainable. Especially because options for increasing the area of forest land seem to be limited in the future.

CONCLUSIONS

A system dynamics model was developed to assess the GHG emissions from the forestry sector in Latvia. The results of the base scenario demonstrated that a tendency exists for emissions to increase and removals – to decrease. The results have confirmed that the consequence of the existing forestry practice will be an increase in the net GHG emissions that, in 2030, will reach double of the level of 2005.

Several measures that might affect the future emission generation were tested. It was found that considerable reduction (by 20%) in forest felling would reduce the net GHG emissions significantly. Yet, the implementation of such an instrument should be evaluated more thoroughly with respect to the negative economic and social effects arising from reduced activity in forestry and wood processing industries. To avoid the negative impacts on the industry, other measures that focus on the use of wood processing waste were evaluated. The results showed that it would help reducing the emissions caused by decomposition of the waste left in forests. In addition, by producing e.g. wood chips or some added-value products (as insulation materials from conifers' greenery) the forest resources would be used in a more efficient way thus providing economic and social benefits. Moreover, emission reduction in other sectors would be achieved, e.g. in energy sector by replacing the fossil fuels for wood chips.

Simulating an increase in the fraction of managed agricultural land indicated that in the future the options for increase in area of the forest land will be limited. Therefore, management of forest land and resources should be sustainable and well-considered to maintain the ability of negative net GHG emissions.

ACKNOWLEDGEMENTS. The work has been supported by the National Research Program 'Energy efficient and low-carbon solutions for a secure, sustainable and climate variability reducing energy supply (LATENERGI)'.

REFERENCES

Adamovičs, A., Dubrovskis, V., Plūme, I., Jansons, Ā., Lazdiņa, D. & Lazdiņš, A. 2009. *Biomasas izmantošanas ilgtspējības kritēriju pielietošana un pasākumu izstrāde*. SIA Vides projekti, 174 pp. (in Latvian).

Berg, B. 2000. Litter decomposition and organic matter turnover in northern forest soils. *Forest Ecology and Management* **133**, 13–22.

Blumberga, A., Timma, L., Romagnoli, F. & Blumberga, D. 2015. Dynamic modelling of a collection scheme of waste portable batteries for ecological and economic sustainability. *Journal of Cleaner Production* **88**, 224–233.

Blumberga, D., Blumberga, A., Barisa, A. & Rosa, M. 2014. System Dynamic Modeling of Low Carbon Strategy in Latvia. *Energy Procedia* **61**, 2164–2167.

Bush, B., Duffy, M., Sandor, D. & Peterson, S. 2008. Using system dynamics to model the transition to biofuels in the United States. *Third International Conference on Systems of Systems Engineering*, Monterey, California, pp. 1–6. DOI:10.1109/SYSOSE.2008.4724136

CSB. 2015. Geographical Position of the Republic of Latvia. Available at: http://data.csb.gov.lv/pxweb/en/visp/visp__ikgad__geogr/GZ010.px/?rxid=a79839fe-11ba-4ecd-8cc3-4035692c5fc8.

Dace, E., Bazbauers, G., Berzina, A. & Davidsen, P.I. 2014. System dynamics model for analyzing effects of eco-design policy on packaging waste management system. *Resources, Conservation and Recycling* **87**, 175–190.

Daugavietis, M., Polis, O., Korica, A. & Seļezņovs, J. 2012. Scotch pine – a natural raw material for high-quality biologically active substances. *Proceedings of the Latvia University of Agriculture* **5**, 59–67.

Forest sector in Latvia. Available at: http://www.lvm.lv/sabiedribai/meza-apsaimniekosana/latvijas-meza-nozare.

Forrester, J.W. 1958. Industrial dynamics: a major breakthrough for decision makers. *Harvard Business Review* **36**, 37–66.

IPCC. 2006. Eggleston H.S., Buendia L., Miwa K., Ngara T. and Tanabe K. (eds). *IPCC Guidelines for National Greenhouse Gas Inventories.* IGES, Japan.

Kurz, W.A., Dymond, C.C., White, T.M., Stinson, G., Shaw, C.H., Rampley, G.J., Smyth, C., Simpson, B.N., Neilson, E.T., Trofymow, J.A., Metsaranta, J. & Apps, M.J. 2009. CBM-CFS3: A model of carbon-dynamics in forestry and land-use change implementing IPCC standards. *Ecological Modelling* **220**(4), 480–504.

LNIR, 2014. *Latvia's National Inventory Report, Submission under UNFCCC and the Kyoto Protocol, Common Reporting Formats (CRF) 1990 – 2012.* http://unfccc.int/national_reports/annex_i_ghg_inventories/national_inventories_submissions/items/8108.php

Machado, R.R., Conceição, S.V., Leite, H.G., Souza, A.L. & Wolff, E. 2013. Evaluation of forest growth and carbon stock in forestry projects by system dynamics. *Journal of Cleaner Production* (in press).

Muizniece, I., Blumberga, D. & Ansone, A. 2015. The use of coniferous greenery for heat insulation material production. *Environmental and Climate Technologies* **14** (submitted).

Muizniece, I., Lauka, D. & Blumberga, D. 2015. Thermal Conductivity of Freely Patterned Pine and Spruce Needles. *Environmental and Climate Technologies* **14** (submitted).

NDP. 2012. Cross-Sectoral Coordination Centre. *National Development Plan of Latvia for 2014–2020*.

Pollution permit. 2010. Available at: http://www.vpvb.gov.lv/lv/piesarnojums/a-b-atlaujas/?ur=vecventa&id_ur=&search_ur_submit=Mekl%C4%93t+p%C4%93c+uz%C5%86%C4%93muma.

Romagnoli, F., Barisa, A., Dzene, I., Blumberga, A. & Blumberga, D. 2014. Implementation of different policy strategies promoting the use of wood fuel in the Latvian district heating system: Impact evaluation through a system dynamic model. *Energy* **76**, 210–222.

Silava. 2008. *Celmu izstrādes tehnoloģijas enerģētiskās koksnes ražošanai.* Salaspils, 20 pp. (in Latvian).

Silava. 2012. *Latvijas meža apsaimniekošanas radītās ogļskābās gāzes (CO_2) piesaistes un siltumnīcefekta gāzu (SEG) emisiju references līmeņa aprēķina modeļa izstrāde*. *Pārskats par projekta 1. etapa darbu izpildi*. Salaspils, 42 pp. (in Latvian).

State Forest Service statistics. Available at: http://www.vmd.gov.lv/valsts-meza-dienests/statiskas-lapas/publikacijas-un-statistika?nid=1047#jump.

Sterman J.D. 2000. *Business dynamics: Systems thinking and modeling for a complex world.* Irwin McGraw-Hill, Boston, 1008 pp.

Stibe, U. 1976. *Tree crown elements of quantitative indicators logging old–age spruce forest* (In Latvian). PhD thesis, Latvia University of Agriculture, Jelgava, Latvia.

The Law on Forests, Parliament of the Republic of Latvia, Latvijas Vēstnesis, 98/99 (2009/2010), 16.03.2000., 'Ziņotājs', 8, 20.04.2000.

Agronomy Research **13**(2), 477–484, 2015

Conceptual design of experimental solar heat accumulation system with phase change materials

M. Dzikevics*, A. Blumberga and D. Blumberga

Riga Technical University, Faculty of Power and Electrical Engineering, Institute of Energy Systems and Environment, Azenes 12/1, LV1048 Riga, Latvia;
*Correspondence: mikelis.dzikevics@rtu.lv

Abstract. The research on solar heating systems often is faced with choice of carrying out experiments in real systems with changing parameters or to use modelling software with constant parameters but many undefined parameters or assumptions. The design of experimental system for simulating solar heat accumulation is proposed in this paper. The proposed design allows testing of phase change materials which provide higher thermal density compared to water. Results from computational fluid dynamic simulations carried out by other studies have been analysed for implementation into designing of the tank. All of these factors have been taken into account to create a system that resembles real case and can simulate for a long periods of time.

Key words: thermal, energy, renewable, hot water, PCM.

INTRODUCTION

In latest years the market of the solar thermal systems in Europe has been in slow stagnation from 3.36 GW_{th} in 2008 to 2.14 GW_{th} in 2013 of annually installed power. Nevertheless the role of solar thermal heating is important since it saved 3.8 million tons of CO_2 in Europe in 2013 and 24.5 million tons of oil in 2012 globally, which is equivalent to 80 million tons of CO_2 (Mauthner & Weiss, 2014). The use of renewable energy is a necessity since in Europe 46% of the energy in residential sector is used for heating and cooling (H&C). The EU target for year 2020 is that 1.26% of energy required for H&C is supplied by solar thermal systems (ESTIF 2014).

For scientific community, in the field of solar thermal energy, to help to improve the growth of new technologies and improvements of existing ones, it is necessary to provide access to facilities where these ideas can be tested. The research on solar heating systems often is faced with choice of carrying out experiments in real systems or to use modelling software. In the first case the parameters of the system are never constant, it is impossible to recreate the conditions twice, access may be limited if the system is not solely used for experimental purposes and possibilities may be limited if the system is used as a primary supply for heating or preparation of hot water. The modelling softwares cannot be disregarded, since they provide a fast, economically liable and easily adjustable solution. However any computation is based on set amount of formulas and number of assumptions. Belessiotis et al. (2013) calculated the discrepancy between the measured energy outputs calculated using the experimental values and measured energy output. The discrepancy value in most cases is in range of 5%, but in some cases for

specific conditions it can reach 19%, therefore a real life system is integral part of a process of delivering a reliable new technology to the consumer. It becomes even more complicated when non-traditional elements are introduced in the system, for example phase change materials in heat accumulation tank.

All of the solar heating systems are faced with variable energy supply. Since all of the energy must be stored during the daytime, accumulation tank is crucial part of the system. Latent heat of fusion of phase change materials (PCMs) are used to increase heat accumulation capacity of solar system by increasing thermal density of accumulation tank. Latent heat of fusion, compared to traditional systems with sensible heat storage, is isothermal during the melting or solidification of PCM. PCM can be divided into paraffin's, fatty-acids, inorganic and organic salt hydrates and organic and inorganic eutectic compounds (Sharma & Chen, 2009).

The use PCMs in solar thermal systems have been studied mainly by use of modelling. Pielichowska & Pielichowski (2014) presented a thorough review of PCMs for thermal energy storage applications. Many of the studies have been dealing with calculating the phase change phenomena with different types of containers, types of PCM and scenarios (Karthikeyan & Velraj, 2012; Oró et al., 2013; Yaïci et al., 2013). A common outcome of the studies were that the use of PCM increased the storage capacity. However only few have gone as far as simulating annual gains from using PCM in accumulation tanks. Two studies, one followed by the other were carried out by Talmatsky & Kribus (2008) and Kousksou et al. (2011) and the conclusions were that there can be cases were use of PCM increases heat losses to the environment during night and can cancel gains made during day. Interestingly in earlier study Kousksou et al. (2007) neglected the heat losses in the mathematical model. Similarly Yang et al. (2014) have assumed that the heat losses from bottom and sides of the storage tank can be neglected. These and other studies prove that modelling always has to be backed up with experimental systems.

Similar system to the one described in this paper has been used in study of López-Navarro et al. (2014). It consists of single heating circuit from building condensation ring and a cooling circuit with evaporation chiller and was used for analysing cooling with PCMs. Most of the studies employ traditional system with addition of more sophisticated measurement apparatus or small scale set-ups (Sharma et al., 2009). In this paper the design of experimental system for simulating solar heat accumulation is proposed. It allows scientists to imitate heating load of certain real building in a laboratory environment. It allows researchers to provide solutions for an individual cases and study them in further detail without the need of setting up a solar collector system at the building under investigation.

DESIGN OF SYSTEM

The experimental solar thermal system design proposed in this paper consists of two sets of solar collectors, heat exchanger loops, two accumulation tanks, gas boiler and systems for imitating domestic hot water consumption and energy used for heating.

System have two sets of solar collectors that allow to carry out side-by-side tests for collectors, accumulation tanks and other optimization of such parameters as angle of collectors, flow speed, pipe size, heat exchanger size, insulation thickness, inlet and outlet positions for tank and other small adjustments.

Temperature can be measured before and after solar collector, before and after each side of heat exchanger, at the inlets and outlet of the storage tank. Temperature is converted into signal and sent to controller, which subsequently sends signal to pumps and or mechanical valves. Employment of sophisticated control system allows optimization of control algorithms or to create different conditions for each of the storage tanks.

Solar collector loops (SCL) for both tanks are similar and if needed can be made identical. SCL (Fig. 1) consists of elements such as solar collectors (SC), balancing valves (BV), expansion tank (EV), hydraulic blocks (HB), heat meters (HM), temperature sensors (T), solar controller connections (S,A) and electric heater (ES).

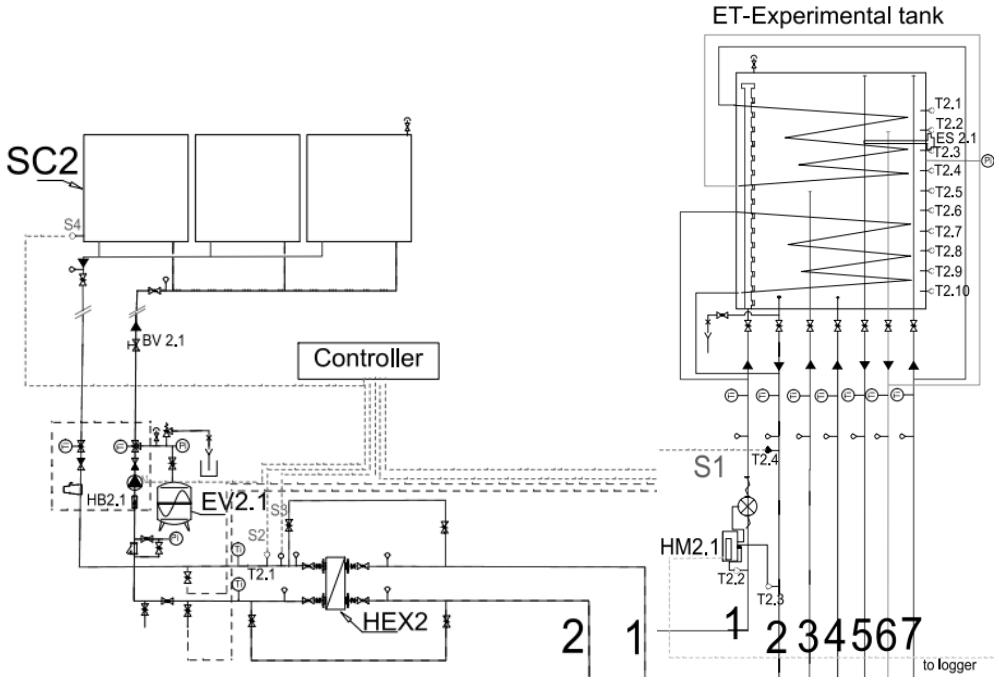

Figure 1. Solar collector loop on left; inlets and outlets in experimental tank (1 – hot water from HEX2; 2 – return to solar HEX2; 3 – return from heating; 4 – return from DHW; 5 –supply to DHW; 6 – return to gas boiler; 7 – hot water from gas boiler).

SCL with heat exchanger dividing SCL (HEX2) gives an option to use two types of working fluids – glycol and water mixture for collector side and mixture or pure water in tank side. Use of glycol is common in northern countries, however it is possible to remove HEX2 and to simulate solar collector systems that use water as only working fluid. In similar fashion immersed HEX can be used either at SCL side or at the side of load or removed if it is an open system.

There are two parameters controlling the pump – the change in the pressure or temperature difference between solar collector and inlet of HEX2 at collector side. The secondary pump is controlled by the changes in temperature between tank and temperature before the HEX2 at collector side or it can automatically turn of if the temperature in collectors are too low.

The role of heating load imitation (HLI) in Fig. 2 is to cool the fluid flowing into heat exchanger (HEX3) similarly as radiators or other heating equipment is cooled due to heat losses from building. Like in buildings, the heating power can vary depending on the outside temperature and the individual comfort levels of occupants. HLI consists of on-roof cooler (condenser) with variable cooling power (in this case 8 kW), that measures the temperature outside and before heat exchanger (HEX3) separating cooler from other parts of the system.

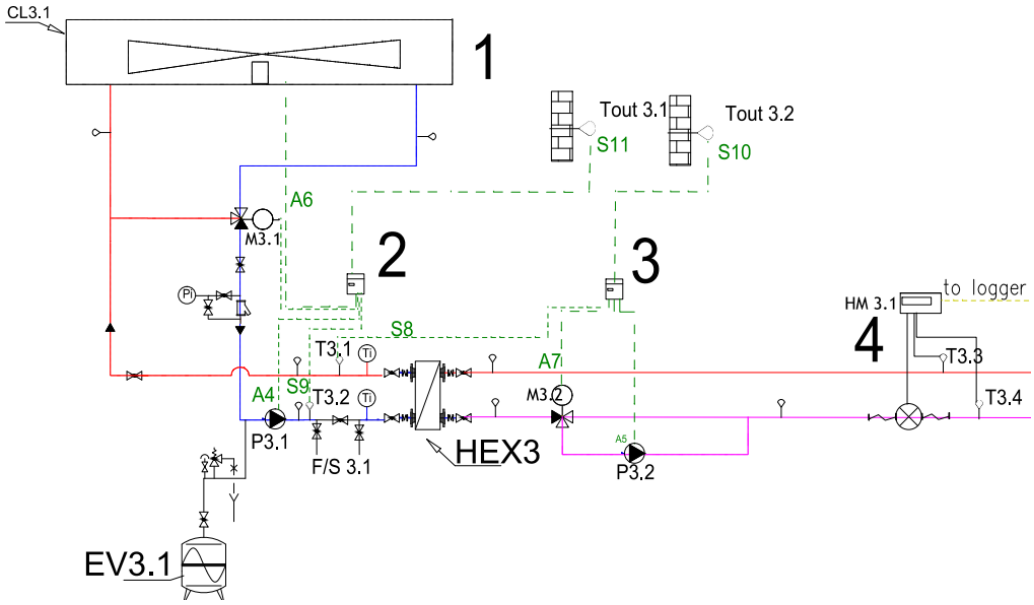

Figure 2. Heating load imitation diagram (1 – on-roof cooler; 2 – controller for imitating temperature at cooler loop; 3 – controller for valve and pump; 4 – flow rate and power meter).

For the control of HLI two controllers are used to turn on pumps depending on the temperature, regulate cooler depending on the outside temperature or heating curve and regulate motorized three-way valve depending.

The domestic hot water imitation (DHWI) is achieved by using motorized valve and a controller allowing to create consumption patterns for different types of consumers (Fig.3). Additionally backpressure regulator (PS) is required, since the water is sent to drainage at atmospheric pressure. Use of PS ensures that the HEX4 is pressurized equally in both sides. On the left side of HEX4 no pump is required, since central cold water (CW) is under pressure.

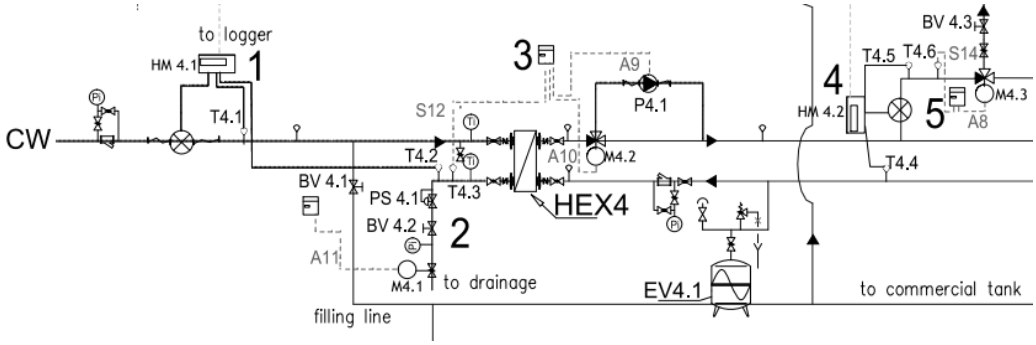

Figure 3. Domestic hot water load imitation diagram (1 – flow rate and power meter for cold side; 2 – pressure valve; 3 – controller for imitating DHW load; 4 – flow and power meter for test tank; 5 – controller for test tank return option).

The main element of the system is the experimental tank (Fig. 4). The base of design is existing commercial tanks – cylindrical, with attachments for immersed heat exchangers, filling and emptying. For the tank to work as stratification tank there are 3 options – to add immersed stratification pipes from the top or bottom, or use multiple side inlets to direct the water with higher temperatures at the higher inlets. Additionally the top of the tank can be removed, allowing to customize the elements within the tank.

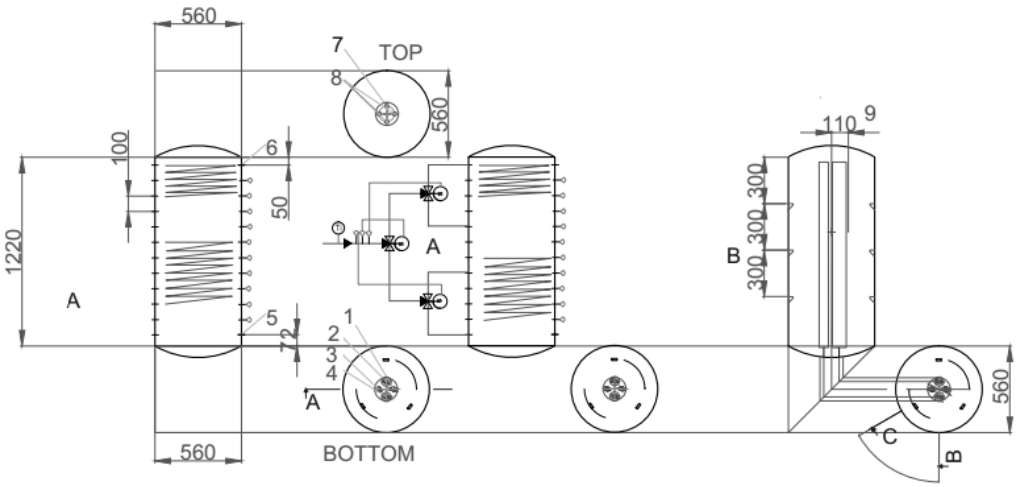

Figure 4. Experimental tank's inlet/outlet elements (1 – hot water from solar collector; 2 –supply to DHW; 3 – return to solar collector loop; 4 – return from heating load; 5 – cold water supply; 6 – supply to heating load and DHW; 7 – bleeding valve; 8 – spare fittings; 9 – stratification pipe).

In the making of the tank, stratification was looked at as an important parameter that can increase the efficiency of the solar system. Suitable height and diameter (H/D) ratio for achieving stratification has been analysed by Furbo and Shah (2005) and Yaïci et al. (2013). Former concluded that the higher the H/D ratio, the better is stratification. Lateral used computational fluid dynamics (CFD) and found that by changing the ratio

from 2 to 3.5 showed that stratification remained the same. It was found that the tanks with higher H/D ratio have advantage in cases where hot water layer becomes so thick, that the thermocline becomes too narrow to separate hot and cold water. Based on these results, the dimensions of the experimental tank was chosen to have an H/D ratio above 2. However, the experimental tank was kept at low H/D ratio (2.17) to improve the accessibility to the elements at the bottom and sides of interior of the tank.

Location of the inlet of the hot water was found to have high influence on the stratification. In the study by Yaïci et al. in Fig 5. it can be seen that after 1,000 s, the temperature distribution vary due to different jet momentum (horizontal flow) and bouyancy effect (vertical flow). Further away the inlet is from the top, lower is the jet momentum and higher bouyancy effect causing mixing of the warm water.

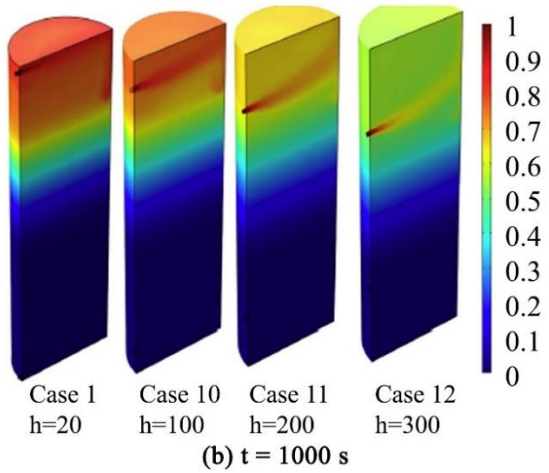

Figure 5. Effect of inlet locations on thermal stratification. X axis has a dimensionless temperature $(T-T_{ini})/(T_{in}-T_{ini})$ (Yaïci et al. 2013).

CFD can be used to analyse location of inlet, the effects of changes in mass flow rate, inlet hot water temperature and initial temperature conditions. In the mentioned study, the validation was calculated using experimental data from study of Zachar et al. (2003). However the experimental data were gathered on a tank with a different H/D ratio, different inlet position and a baffle plate at the bottom. As a result, the uncertainty is estimated to be $\leq 15\%$. It is planned that the use of experimental tank proposed in this paper will reduce uncertainty since different options can be tested experimentally.

The experimental tank can also be used to analyse performance of accumulation tank filled with multiple types of PCM with different melting temperatures. If the PCM is capsulated in the shape of spheres with a diameter around 50 mm, the solution is to employ the packed bed principle where the PCM spheres are freely placed inside tank. However to achieve separation of different types of PCM, round plates can be used. Similar system has been numerically analysed by Yang et al. (2014). Other experimental system have employed steel mesh (Reddy et al., 2012), however perforation of the plates allow many design options since different distribution and sizes of holes will have different impact on the flow of the water between the two layers divided by the plates.

The studies analysing use of baffle (buffer) plates have been review by Altuntop et al. (2005). Often small obstacle are placed in front of the inlet to reduce the jet momentum, however in some cases larger plates are used to improve stratification. The study also concluded that the use of plates provide better thermal stratification compared to the no obstacle case and that the gap in the middle performed better than having a gap closer to the tank wall. However to the knowledge of the author, no studies have been carried out to analyse different plates in combination with PCM.

CONCLUSIONS

There are many challenges in programming any system to imitate real life situations. In this system there are 12 controllable elements where some of them can be used to complement other, meaning that they have to improve each other rather than compete. For example – a pump, a motorized valve and a variable cooler. All of the elements affect the cooling power, so there is a question of prioritizing them.

As mentioned in this paper, experimental systems can favour from the use of numerical analysis, therefore creating the same design within the environment of software such as TRNSYS will increase the number of applications for the system.

The adaptability of the experimental tank allows it to be used for gathering required validation data and to reduce the uncertainty of the numerical analysis that use experimental data from the systems that differ from the one modelled.

The use of PCM in experimental systems has often been restricted to a small scale systems. By the knowledge of the authors, no experimental studies with real life consumption has been carried out where PCM was employed in solar thermal system accumulation tanks for long periods. The proposed system will provide the necessary experimental data required for quicker and safer implementation of PCM into consumer systems.

ACKNOWLEDGEMENTS. The work has been supported by the National Research Program ‘Energy efficient and low-carbon solutions for a secure, sustainable and climate variability reducing energy supply (LATENERGI)’.

REFERENCES

Altuntop, N., Arslan, M., Ozceyhan, V. & Kanoglu, M. 2005. Effect of obstacles on thermal stratification in hot water storage tanks. *Appl. Therm. Eng.* **25**, 2285–2298.

Belessiotis, V., Mathioulakis, E. & Papanicolaou, E. 2013. Experimental validation of the input–output modeling approach for large solar thermal systems − Accuracy of the test procedure. *Renew. Energy* **51**, 197–205.

ESTIF 2014. *Trends and Market Statistics 2013*.

Furbo, S. & Shah, L.J. 2005. How mixing during hot water draw-offs influence the thermal performance of small solar domestic hot water systems. In *Proceedings of the 2005 Solar world Congress*. Orlando, pp. 6.

Karthikeyan, S. & Velraj, R. 2012. Numerical investigation of packed bed storage unit filled with PCM encapsulated spherical containers – A comparison between various mathematical models. *Int. J. Therm. Sci.* **60**, 153–160.

Kousksou, T., Bruel, P., Cherreau, G., Leoussoff, V. & El Rhafiki, T. 2011. PCM storage for solar DHW: From an unfulfilled promise to a real benefit. *Sol. Energy* **85**, 2033–2040.

Kousksou, T., Strub, F., Castainglasvignottes, J., Jamil, A & Bedecarrats, J. 2007. Second law analysis of latent thermal storage for solar system. *Sol. Energy Mater. Sol. Cells* **91**, 1275–1281.

López-Navarro, A., Biosca-Taronger, J., Corberán, J.M., Peñalosa, C., Lázaro, A., Dolado, P. & Payá, J. 2014. Performance characterization of a PCM storage tank. *Appl. Energy* **119**, 151–162.

Mauthner, F. & Weiss, W. 2014. *Solar Heat Worldwide. Markets and Contribution to the Energy Supply 2012*, Gleisdorf, Austria.

Oró, E., Chiu, J., Martin, V. & Cabeza, L.F. 2013. Comparative study of different numerical models of packed bed thermal energy storage systems. *Appl. Therm. Eng.* **50**, 384–392.

Pielichowska, K. & Pielichowski, K. 2014. Phase change materials for thermal energy storage. *Prog. Mater. Sci.* **65**, 67–123.

Reddy, R.M., Nallusamy, N. & Reddy, K.H. 2012. Experimental Studies on Phase Change Material-Based Thermal Energy Storage System for Solar Water Heating Applications. *J. Fundam. Renew. Energy Appl.* **2**, 1–6.

Sharma, A. & Chen, C.R. 2009. Solar Water Heating System with Phase Change Materials **1**, 297–307.

Sharma, A., Tyagi, V.V., Chen, C.R. & Buddhi, D. 2009. Review on thermal energy storage with phase change materials and applications. *Renew. Sustain. Energy Rev.* **13**, 318–345.

Talmatsky, E. & Kribus, A. 2008. PCM storage for solar DHW: An unfulfilled promise? *Sol. Energy* **82**, 861–869.

Yaïci, W., Ghorab, M., Entchev, E. & Hayden, S. 2013. Three-dimensional unsteady CFD simulations of a thermal storage tank performance for optimum design. *Appl. Therm. Eng.* **60**, 152–163.

Yang, L., Zhang, X. & Xu, G. 2014. Thermal performance of a solar storage packed bed using spherical capsules filled with PCM having different melting points. *Energy Build.* **68**, 639–646.

Zachar, A., Farkas, I. & Szlivka, F. 2003. Numerical analyses of the impact of plates for thermal stratification inside a storage tank with upper and lower inlet flows. *Sol. Energy* **74**, 287–302.

Agronomy Research **13**(2), 485–493, 2015

Seasonal temperature variation in heat collection liquid used in renewable, carbon-free heat production from urban and rural water areas

E. Hiltunen, J.B. Martinkauppi*, A. Mäkiranta, J. Rinta-Luoma and T. Syrjälä

University of Vaasa, Faculty of Technology, Electrical Engineering and Energy Technology, Wolffintie 34, FI65200 Vaasa, Finland
*Correspondence: Birgitta.Martinkauppi@uva.fi

Abstract. A renewable energy source called sediment energy is based on heat collection with tubes similar to those used in ground energy and is installed inside a sediment layer under water body. In this paper, an investigation of temperature behaviour of heat carrier liquid is made during several years to evaluate utilization of sediment energy. This is done by evaluating temperature variations of heat carrier liquid and its correlation to air temperature. This increases advancement of knowledge how the temperature of the sediment recovers from the heat collection. The temperature variation of the liquid seems to correlate with the mean monthly air temperature. The selected methods clearly indicate that sediment energy seems to be yearly renewable because there is a clear correlation between air temperature and heat carrier liquid temperature.

Key words: renewable, energy source, carbon-free, heat energy, sediment energy.

INTRODUCTION

New methods and technologies are needed to take advantage of abundance of renewable, carbon-free energy sources existing both in urban and rural areas. This energy is collectable even with small, local distributed systems which makes them suitable even for small applications. These systems can be, for example, solar panels, solar collectors, ground heat collection pipes or wind turbines. These local, renewable systems provide energy independence as well as typically energy-savings in the long term. The initial implementation costs are usually higher than the traditional solutions but as the technology get more common, then its cost should go down. The lack of knowledge as well as a need for more suitable methods limits the utilization of renewable sources.

One of the new methods is a heat energy collection system from solid, organic sediment layers at bottoms of water bodies using pipes and heat carrier liquid (Hiltunen et al., 2014). Specially designed pipes are installed horizontally into the sediment layer, 3–4 meters under the bottom of the water body. The heat is then collected by the heat carrier liquid like it is done for other ground heat systems. A COMSOL model of the system has been implemented to study the heat extraction and behaviour of the system (Haq et al., 2014). Since the heat is extracted from a layer consisting of sediments, the approach is named as 'sediment energy'. This energy is renewable: the heat energy of sediment layer comes mainly from the Sun and only a minor part is from the Earth's own

geothermal energy. The layer gets warmer during summer and release heat during winter. Since the density of water is highest at +4 °C, the bottom of the water body is at this temperature and forms a natural limitation to heat release from sediment during winter time. The ice cover and snow over the water body may also have a significant effect especially in shallow and small lakes in arctic areas (see e.g. Tsay et al., 1992). Models for the warming and cooling cycle of lake sediments has been suggested many authors like e.g. Fang & Stefan (1998) or Golosov & Kirillin (2010).

A heat collection system should be able to operate in the long term and preferably to be able to replace the taken heat energy. Thus heat extraction from the sediment layer is a critical factor for the sediment energy system to operate. The suitable heat extraction rate needs to design correctly in order not to overuse the heat source. On the other hand, undersizing the system will increase costs of implementation. To study the heat extraction, the liquid temperature is measured for a period of several years. This will cover the natural yearly variation in air temperature and other weather conditions.

The evaluation is done in three parts. First, the minimum temperatures of the heat carrier liquid is searched as the minimum operating liquid temperature for the system should exceed -15 °C. Second, the durations of cold (temperature below 0 °C) and warm periods for liquid are evaluated. If the durations of cold periods were to get longer in the course of years then this would indicate overuse of the source. Third, the correlation between air temperature and liquid temperature is calculated with Spearson's and Pearson's coefficient (Sprinthall, 2012). This is very important for sediment energy since its renewability depends on complex interaction between air, water, sediment and sun. Of course, some investigation between air temperature and heat carrier liquid has been done for example a helical heat exchanger (Zarrella & De Carli, 2013) but not for sediment heat energy system as this is a very new invention.

The results demonstrate the suitability of sediment energy for long term use. This information is important to designing the suitable heat extraction rate as well as evaluating the available heat energy capacity. The liquid temperature information has been collected from a pilot system installed in 2008 at the Suvilahti suburb and sediment layer of seabed of Suvilahti bay, Vaasa, Finland. The pilot system supplies heat and service water for a very small district with 42 houses. The initial usability of the system has been demonstrated by measuring the sediment temperatures as well as showing the energy consumption (Hiltunen et al., 2014).

SEDIMENT ENERGY COLLECTION SYSTEM

The prototype system consists of 26 pipes shoved into the sediment layer, 2 heat collection wells at Suvilahti shore and 12 distribution wells. The pipes are designed especially for sediment layers and a sectional view is shown in Fig. 1a. Five outer chambers of the pipe will carry a cooler heat carrier liquid while the warmed liquid will return through the inner chamber.

The pipes were installed at a fan formation as displayed in Fig. 1 b. At the seaside, the pipes are approximately 3–4 meters depths from the bottom of the water layer. An optical cable was installed with a pipe for temperature measurement of sediment near the pipe. At the shore side, the pipes are connected to the heat collection wells which are then connected to distribution wells. The distributions wells then deliver warmed liquid for household use. The system has also been used for cooling in the summer time.

The carrier liquid is currently a mix of water and ethanol. The frost resistance of the mixture is -15°C which allows the operation even if the sediment freezes.

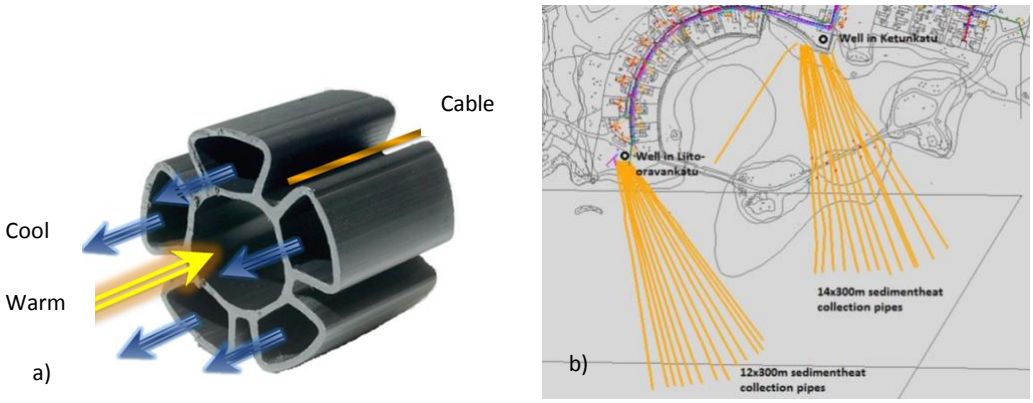

Figure 1. a) Heat collection pipe has a special structure designed for heat extraction from sediment with 5 outer and 1 inner chambers; b) Together 26 collection pipes were shoved into sediments (Mauri Lieskoski private communications; source of the figure: Vaasan Eko-lämpö Oy).

TEMPERATURE DATA OF AIR AND HEAT CARRIER LIQUID

Temperature data from sediment has been collected also earlier but their purpose has been different like for modelling (Golosov & Kirillin, 2010) or for temperature variation at different depths of surface (Banks, 2012). In our approach, we have collected temperature values of heat carrier liquid which correlates with temperatures of the sediment, to study recovery of sediment temperature. Of course, this is done during the heat collection for the district.

The temperature data for this study was obtained from Finnish Meteorological Institute. This is official, quality controlled data and it is measured according to ISO9001:2008 and WMO-No.8, CIMO Guide. The temperature was given as a monthly average as we have assumed that total heat energy matters more than a short, temporary variations like diurnal changes. Temperature of the liquid has been monthly recorded with Ouman temperature measurement device between years 2008–2013.

THEORY AND MODELLING

The suggested physical explanation for the liquid temperature is that the heat carrier liquid collects heat from the sediment inside the seabed. The sediment is warmed up directly by the conduction of the Earth's geothermal energy (small amount), and indirectly by solar energy (main cause). The Sun warms air and water, and water then conveys the heat energy to sediment. It is also possible that some solar radiation reaches the upper layer of sediment. During the winter time, the usage of sediment energy is greater and thus more heat is extracted. Since the heat energy at the sediment is limited

and its diffusion is relatively slow, the liquid gets colder. Some of the sediment heat also dissipates back to water.

To be usable energy source, sediment energy should be annually renewable and sustainable– i.e. its heat energy comes (mainly) from the Sun. The interactions between the Sun, air, water, and underwater sediments are, however, very complex and difficult to model. Therefore, the temperature variations of liquid and air are used for the evaluation as they are easy to measure. The goal is to study that enough sediment energy is available for years and it is correlated to air temperature which then depends on the solar radiation. This correlation is assumed to be due two factors: interaction between water and thus sediment, and an increased need of heating houses during winter due to crease in solar radiation. The need of hot service water is, of course, all-year.

The renewability and use of sediment energy is evaluated by inspecting the length of periods with positive and negative temperatures. This is a very simple test. If the length of periods for liquid temperatures stays approximately the same in different years, then this is very like due the annual renewal of sediment energy. It also implicates that there is no overuse. A sum over each period is calculated and this approximates an integral over the period. This evaluation method was selected because shape of periods varies and they cannot be directly compared.

The correlation between air temperature and liquid temperature may implicate that the solar radiation is the main source of heat in the sediment. Pearson product-moment correlation coefficient and Spearman's rank correlation coefficient were chosen to study this correlation. They are shortly described here; a more comprehensive overview can be found many statistical textbook (e.g. Sprinthall, 2012).

Pearson product-moment correlation coefficient (Pearson r) is used to measure linear correlation or dependence between air temperature (symbol x) and liquid temperature (symbol y). The values can be between +1 and -1 where 1 is total positive correlation, -1 total negative correlation and 0 is no correlation. The Pearson r is defined as:

$$r_{x,y} = \frac{cov(x,y)}{\sigma_x \sigma_y} = \frac{E[(x-\mu_x)(y-\mu_y)]}{\sigma_x \sigma_y}, \quad (1)$$

where: cov indicates covariance; σ is the standard deviation; μ is mean; E is expectation; subindex x indicates air data; and subindex y indicates liquid data. It is assumed here that the entire range of air and liquid data can be presented as normally distributed. The temperature values naturally belong to interval data.

The significance of Pearson r is tested against the null hypothesis: the correlation is due to change. The significance can be assessed using Pearson r table with the degree of freedom (the number of pairs of scores minus 2) (Sprinthall, 2012).

Another selected metric is Spearman's rank correlation coefficient (Spearman's r_s) which is a nonparametric measure. Both air and liquid temperature values are converted into ordinal ranks. For each month, the absolute difference d between air and liquid temperature ranks is calculated and squared. The Spearman's r_s is calculated using the following formula:

$$r_s = 1 - \frac{6\sum d^2}{N(N^2-1)}, \quad (2)$$

where: N is the number of pairs. It is used here to evaluate the statistical dependence between air and liquid temperatures: it compares their relationship to a monotonic function. The values are again between +1 and -1.

RESULTS AND DISCUSSION

The original data of mean air temperature per month and liquid temperature is plotted in Fig. 2. Both data have a seasonal, cyclical variation. The highest liquid temperature was obtained in summer 2009 (12 °C) when the system had been used in very short time. The lowest value is -2.0 °C which was obtained 2010 January and February. The liquid achieve its maximum temperature typically after one month of the peak value for air temperature. However, the minimum liquid temperature stays between 0 and -2 °C in winter time although the system is in full use. Since the minimum value stays over the critical liquid limit temperature of -15 °C, the system operates without problems.

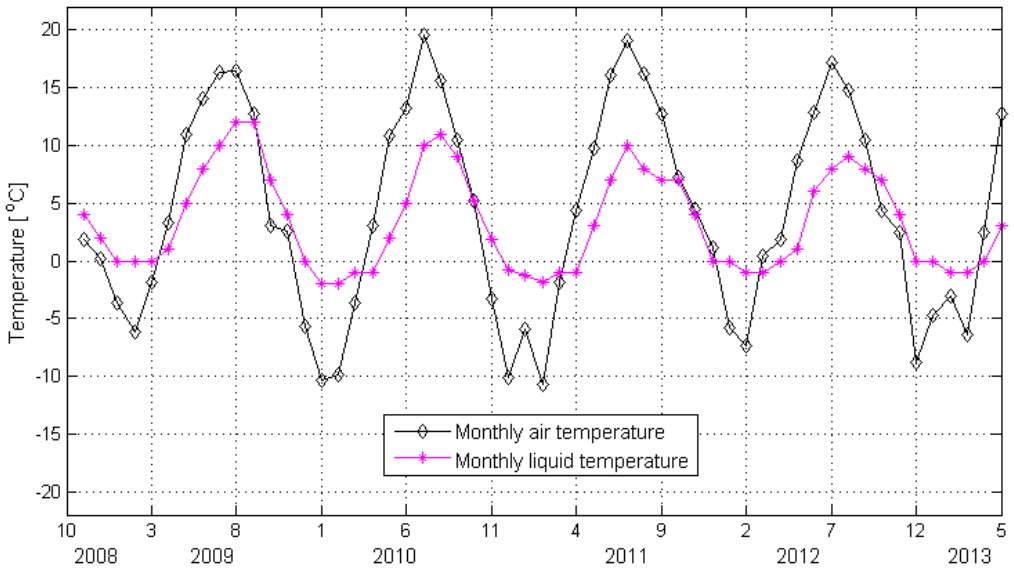

Figure 2. Both the mean air temperature as well as the temperature of heat carrier liquid show clear cyclical variation as a function of season.

Fig. 3 visualizes the length of cold and warm periods for both air and liquid. A period consists of months which mean temperature either exceeds 0 °C ('warm period') or is below 0 °C ('cold period'). The value of 0 °C was selected because it is the freezing point of water. It is of course possible to select another limit value but the goal here is look at trends existing in data. As can be seen from Fig. 3, there is clearly natural

variation in lengths of air temperature periods. The mean temperature sum for cold and warm periods is shown in Fig. 4.

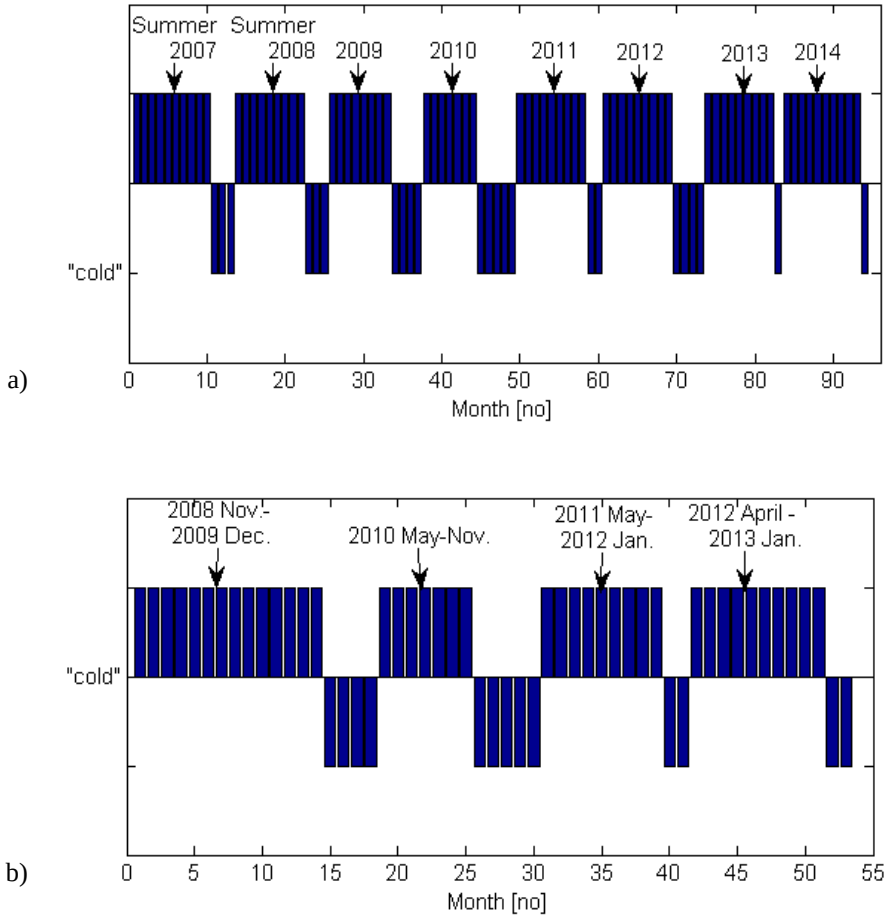

Figure 3. The length of positive and negative temperature periods is visualized for a) air temperatures and b) liquid temperature. One bar indicates one month.

The same data is in numerical format in Table 1. The mean value for warm period temperature sum is 80.4 °C and standard deviation 5.6 °C. For cold period sum, the mean value is -15.8 °C and standard deviation 11.0 °C. The sum of mean temperatures varies more between cold periods than between warm periods. This is due to natural variation between years and it probably has some effect on amount of heat energy in sediment. The length of negative period for liquid temperature has recently got shorter, only 2 month length as shown in Fig. 3b. Also the sum of negative temperatures has decreased.

a)

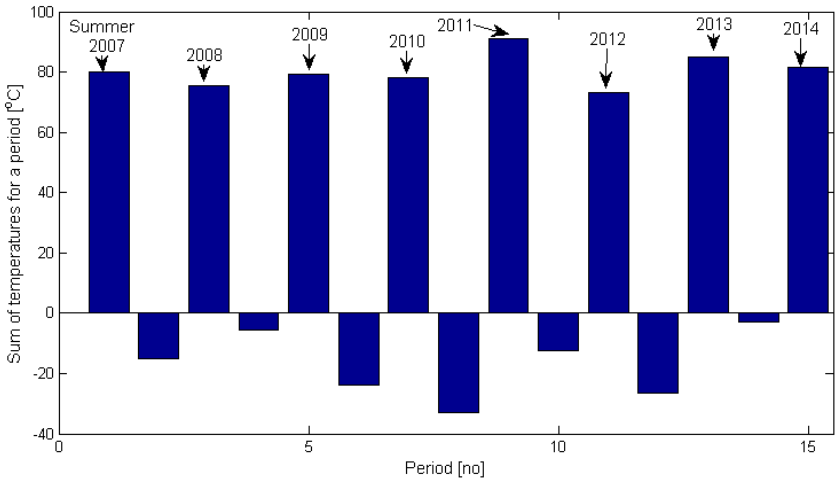

b)

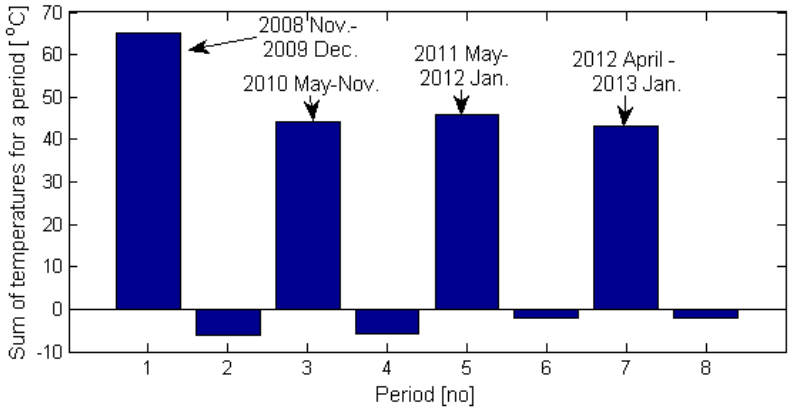

Figure 4. The sum of mean temperatures is calculated for a) air temperatures and b) liquid temperatures. The sum of mean air temperatures has a greater variation between the cold periods than the warm periods.

Table 1. Numerical values for period lengths and temperature sums

Parameter/period	Length (month)		Sum of temperatures (°C)	
	Air	Liquid	Air	Liquid
2007 warm	10	NA	79.9	NA
2007-2008 cold	3	NA	-15.1	NA
2008 warm	9	NA	75.6	NA
2008-2009 cold	3	NA	-5.6	NA
2009 warm	8	12	79.4	65.0
2009-2010 cold	4	4	-24.0	-6.0
2010 warm	7	7	78.0	44.1
2010–2011 cold	5	5	-32.8	-5.9
2011 warm	9	9	91.0	46.0
2011–2012 cold	2	3	-12.5	-2.0
2012 warm	9	10	73.1	43.0
2012–2013 cold	4	2	-26.6	-2.0

This indicates that the heat energy is renewable and available for longer term use as well as not overused in addition to the fact that the system is still currently used.

It is also possible to calculate correlation between monthly air temperature and temperature. First, the linearity between these variables is investigated by plotting them as shown in Fig. 5. Since variables seems to be linearly related. Thus, both selected statistical metrics should produce valid results. Fig. 6. shows results for Pearson's and Spearman's coefficients. When the both data is taken from the same month, Pearson value is 0.8571 (p-value 6.7744e-17) and Spearman value is 0.8640 (2.0105e-17). If the liquid data is taken from the next month, then the values are even higher: Pearson 0.9319 (1.4481e-24) and Spearman 0.9347 (5.1819e-25). Tables gives critical values (N = 55) 0.338 for Pearson coefficient (α = 0.01) and 0.346 for Spearman's coefficient (α = 0.01). This indicates are surprisingly high correlation.

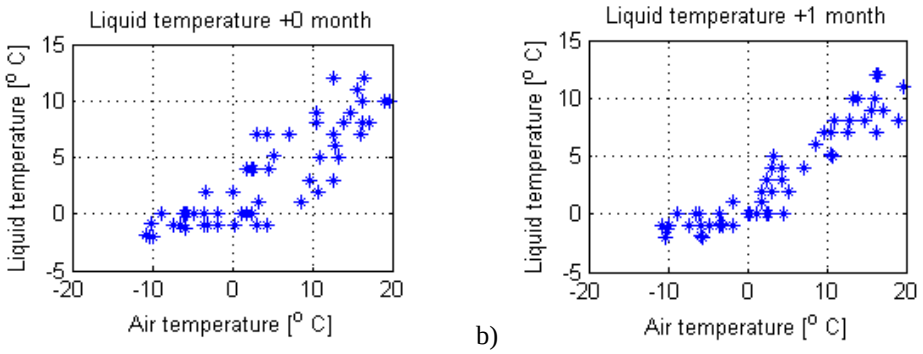

a) b)

Figure 5. Mean air temperature is plotted against liquid temperature. In a) both temperatures are measured in the same month while in b) liquid temperature of the next month is plotted against air temperature.

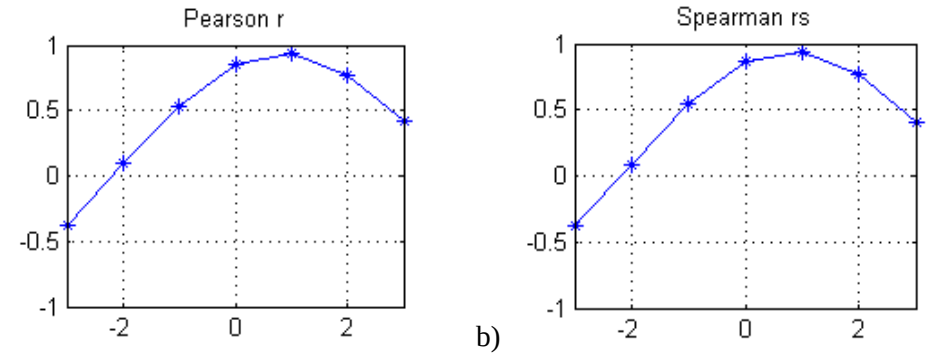

a) b)

Figure 6. a) Pearson r and b) Spearman's r_s both indicate high correlation between air temperature and liquid temperature. The correlation is highest between air temperature and next month's liquid temperature. The x-axis indicates whether the air data is correlated with liquid data value delayed or furthered. When it is zero, both liquid and air data is from the same month.

CONCLUSIONS

During the first years of the studied periods, the minimum value of the liquid temperature was -2 °C which is well above the critical system operation temperature of -15 °C. The absolute difference between these two values is over 10 °C, so there system has still a buffer for a greater heat extraction. During the last part of the periods, the minimum value of liquid temperature has been even closer to zero and the duration of periods of negative temperatures has been shorter than earlier. This all indicate that the sediment energy system is stable and renewable.

The correlation between monthly mean air temperature and liquid temperature has been studied using Pearson's and Spearman's coefficient since the temperature data seems to have a linear dependency. The both coefficient indicate a strong correlation and it is significant.

ACKNOWLEDGEMENTS. We thank Mr. Juhani Luopajärvi, Mr. Mauri Lieskoski (Geo-Pipe GP Oy), City of Vaasa and TEKES (the Finnish Funding Agency for Technology and Innovation).

REFERENCES

Banks, D. 2012. An introduction to thermogeology: ground source heating and cooling. John Wiley & Sons.

Fang, X., & Stefan, H.G. 1998. Temperature variability in lake sediments. *Water Resources Research* **34(4)**, 717–729.

Finnish Meteorological Institute, monthly mean air temperature data.

Golosov, S., & Kirillin, G. 2010. A parameterized model of heat storage by lake sediments". *Environmental Modelling & Software* **25(6)**, 793–801.

Haq, H., Martinkauppi, B. & Hiltunen, E. 2014. Thermal Response of Multiple Pipes and Liquids Using COMSOL for Geothermal Energy System Application, *International Journal of Energy and Environment* **8**, 162–170.

Hiltunen, E., Martinkauppi, B., Zhu, L., Mäkiranta, A., Lieskoski, M. & Rinta-Luoma, K. 2014. Renewable, carbon-free heat production from urban and rural water areas, submitted.

Sprinthall, R.C. 2012. Basic statistical analysis. 9th edition. Pearson.

Tsay, T.K., Ruggaber, G.J., Effler, S.W. & Driscoll, C.T. 1992. Thermal stratification modeling of lakes with sediment heat flux. *Journal of Hydraulic Engineering* **118**(3), 407–419.

Zarrella, A. & De Carli, M. 2013. Heat transfer analysis of short helical borehole heat exchangers. *Applied Energy* **102**, 1477–1491.

Agronomy Research **13**(2), 494–499, 2015

Hot-air distribution in the floor heating

P. Kic

Czech University of Life Sciences Prague, Faculty of Engineering, Kamycka 129, CZ16521 Prague 6, Czech Republic; e-mail: kic@tf.czu.cz

Abstract. The aim of this paper is to present results of measurement of hot-air floor heating system. The energy from fireplace directly heats the house near to the chimney and partly is distributed by the special ventilation under the floor in the whole heated room. The main principle is based on specially designed accumulative floors, consisting of a set of special chambers, which enable to heated air from the fireplace to flow through them. The layer of concrete floor is installed on the surface of these chambers. Hot-air can be intensively distributed around the house with time shift, but the air flow is not uniform and some places are warmer or colder. The results of measurements in the building showed that the accumulation in the floor compensates temperature differences. The result of proper application of this type of heating is a stable thermal comfort and saving of heating costs. Based on the results of measurements, practical recommendations for the design, installation and use of these types of heating were summarised in the conclusions.

Key words: energy accumulation, fireplace, floor, temperature.

INTRODUCTION

Fireplace is currently very popular equipment of newly built or modernized family or townhouses. For home owners, this investment is attractive for both aesthetic and practical reasons. Fireplace provides traditional wood heating, which is still relatively easily accessible and relatively cheap fuel. Suitable heating system is important for the human comfort in winter, but it the suitable indoor conditions can be important also for a material used for a construction, e.g. durability influenced by the air humidity of timber construction (Papez & Kic, 2013).

Current development of construction and continuously increasing prices of energy compels owners and designers of all types of houses to look for high-quality integrated solutions of buildings including the heating and to optimize the operation, in particular to reduce the energy consumption (Kic & Kadlecek, 2012).

The basic mission of a residential building is to create a healthy and pleasant environment for its residents. For a human organism is very important 'radiation comfort', which means that one should take the heat from the environment predominantly by radiation and remove excess heat from his body by convection (cooling by the flow of ambient air) (Kic, 2013).

Radiation, based on the heating surfaces, impacts the other surfaces surrounding the room and the objects that are inside the room. They are heated and they transmit the heat to people and warm the air in the room (Cihelka, 1961). Now, there are advantages

of the utilization of new modern techniques in design (Vio, 2011), but also in economical operation with automatic control, according to user requirements.

The main attention in this research was paid to the function hot air distribution through the special AKU elements, developed especially for this purpose. Another important aim of provided experiments was the control and measurement of heat accumulation in the floor during the hot air supply. There was measured the transfer of energy to the heated space after the stop of heating, and the influence of the radiant heating from the large floor area on the indoor thermal conditions.

The continued improvement of thermal properties of buildings, especially high quality thermal insulation is achieved with less and less consumption of energy for heating. Fireplace usually has a sufficiently large heat capacity, which at the time of heating relatively quickly heats the air in the room in which it is installed. In some cases, therefore, is used part of energy from a fireplace to heat the hot water for heating other rooms. These systems require a relatively large water storage tanks with complex regulatory elements.

The problem remains uneven temperatures in the large space rooms, in which is usually installed fireplace. Around the fireplace is a part of the room overheated and more distant parts of the room are, however, poorly heated. If the room has large window surfaces and more fragmented area e.g. with bay windows, this problem is even greater. More distant parts of the room also cool faster after heating interruption, e.g. during the night.

The solution of these problems can be AKU heating system, which allows the distribution of hot air from the fireplace into the floor, which also serves to accumulate heat uniformly throughout the room. Simultaneously it reduces the overheating of the room during the heating operation in the fireplace and then maintains the desired temperature in the space for a longer time.

This article is a continuation of publication (Kic, 2013), in which has been described the basic principles of the underfloor AKU heating system and the results of measurements in experimental laboratory conditions. The aim of this paper is to present some results from measurements and experience from the implementation of AKU heating system in the construction of a real family house.

MATERIALS AND METHODS

This research work and measurements of the actual values were carried out in the new construction of low-energy consumption house in the Czech Republic. This is a classic two-storeyed building constructed from thermo-insulating brick blocks, with a flat roof and a built-in garage. All the technological equipment is concentrated in the technical room on the ground floor as well.

As an unattended heating source has been selected heat pump air-water with warm water underfloor heating by pipelines inside the concrete accumulative layer. Ventilation of house is provided by recuperation unit. Air ducts are combined with the hot air distribution for heating from the fireplace and AKU floor air distribution system. This heating system that takes energy from irregular sources of heat-cold (fire, sun, cooling) should distribute the heat more uniformly in space but also in time. After the initiation of heating in the fireplace and distribution of hot air into the floor, temperature sensor of water floor heaters reacts and shut down the heating. After cooling of the floor is water

floor heating from heat pump switched on again. So the inhabitant can not recognise that something happened and has permanently pleasant warm floor.

Measurements were focused on the verification of the function of AKU floor heating from the fireplace installed in the living room located on the ground floor area of 30 m^2. The cold air is sucked by fan with an average air flow of 450 $m^3 h^{-1}$ into the air duct, by which the heated and warm air flows into the distribution system formed by distribution AKU elements in the concrete floor of a thickness 60 mm which ensures the heat accumulation. There the thermal energy is transmitted to the storage layer and the cooled air flows back into the room.

The measurement process was divided into two parts. The first part started by burning of wood in the fireplace and by the operation of AKU system and hot air distribution in the floor. The wood has been burned approximately 4.5 hours. In the second part of the measurement was a fireplace left without supply of wood and after another 2 hours burning completely finished. Basic measurements still continued for 1.5 hours, a total of 8 hours from the beginning of measurement.

Air temperatures were measured by thermocouples NiCr-Ni type K during the air flow through the whole system (in the inlet, after the heating, also in different parts of distribution systems of under-floor heating, and in the outlet from the pipeline at the end of the heating system.

Furthermore, there was measured by thermocouples the temperature at the bottom of the concrete layer (between distribution element and the concrete). Under the concrete layer was measured the heat flux passing into the accumulation mass of the floor by the heat flow plates type FQA 017C and there was measured also the heat flux on the surface transferred from the floor surface to the air by the heat flow plates type FQA 018C. The temperature of the upper surface of the concrete was measured by thermographic camera IR Flexcam Pro.

Thermal comfort in the space heated by radiant heating is necessary to evaluate by globe temperature (measured by globe thermometer FPA 805 GTS) together with air temperature. All data were measured continuously and stored at intervals of three minutes to measuring instrument ALMEMO 2590-9.

RESULTS AND DISCUSSION

Principal results of microclimate measurement and description of the AKU system function is presented in the Figs 1–5. Curves of temperatures in the Fig. 1 show gradual heating of the air and floor during the heating and cooling of the fireplace. The curves on the graph confirm significant effect of radiant heating component, which is reflected by higher globe bulb temperature (tg) than the air temperature (ta). Approximately 4.5 hours after the heating (after wood burning) has a significant effect heat accumulated in the floor and slowly transferred into the room, which results in the higher surface temperature (ts) than the air temperature (ta). The maximal surface temperature was 22.1 °C, which is below the 30 °C recommended as a maximum for floor surface temperature in literature (Cihelka, 1961).

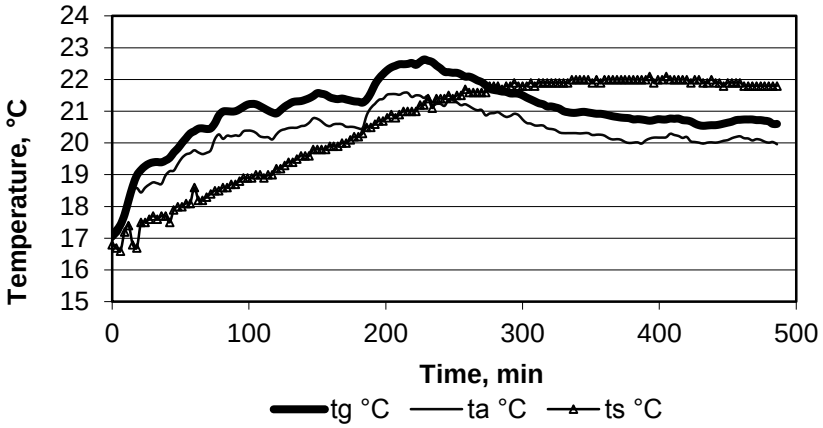

Figure 1. The course of air temperature (ta), globe temperature (tg) and surface temperature on the floor (ts).

The heating of the whole floor in the living room is gradual. It corresponds with the surface temperature measured by thermographic camera (Figs 2–4). In the first hours most rapidly warmed the floor surface near the fireplace mainly by radiation from the front surface fireplace (Fig. 2). It is obvious from the floor surface on the thermogram (Fig. 3) in the front of the fireplace after 6.5 hours since the beginning of heating (fire is completely burnt out) that the surface temperatures of the floor in different parts of the room are already balanced.

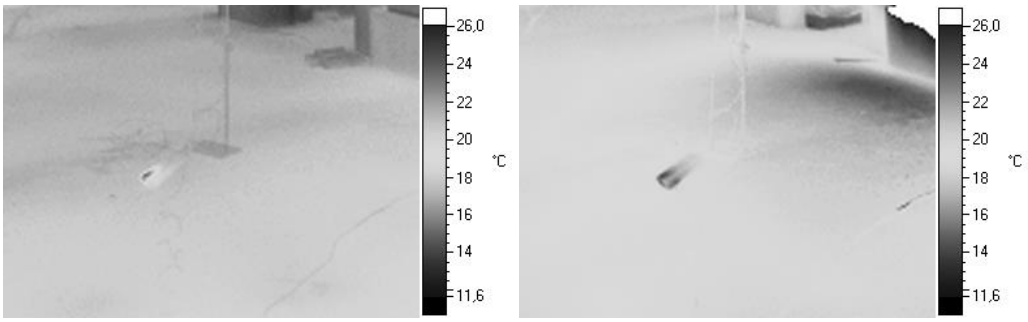

Figure 2. The thermogram of the floor surface near to the fireplace at the beginning of heating period and after 2 hours of heating.

Fig. 4 shows us thermogram of the floor surface in front of the fireplace after 8 hours from the beginning of heating; the floor still maintains a higher temperature than the air in the entire area equally thoroughly heated. There is the heat flux transferred into the concrete accumulation layer and from the surface by radiation and convection into the room. The result should is comfortable, rather stable temperature distributed uniformly in space during the longer time.

Even more apparent is the effect of heating by the floor AKU system from the course of the specific heat flow on the floor surface specific heat flux on the surface from the concrete floor to the air inside the room presented on the Fig. 5.

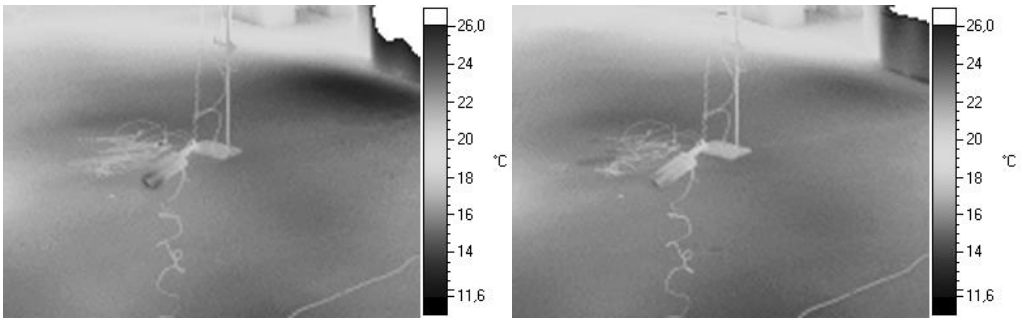

Figure 3. The thermogram of the floor surface after 4.5 hours of heating (there is finished wood stoking in the fireplace) and after 6.5 hours since the beginning of heating (fire is completely burnt out).

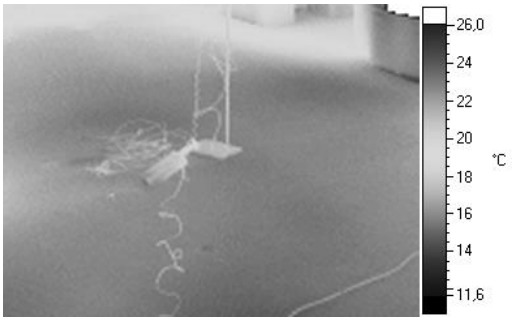

Figure 4. The thermogram of the floor surface after 8 hours since the beginning of heating. The floor still maintains a higher temperature than the air.

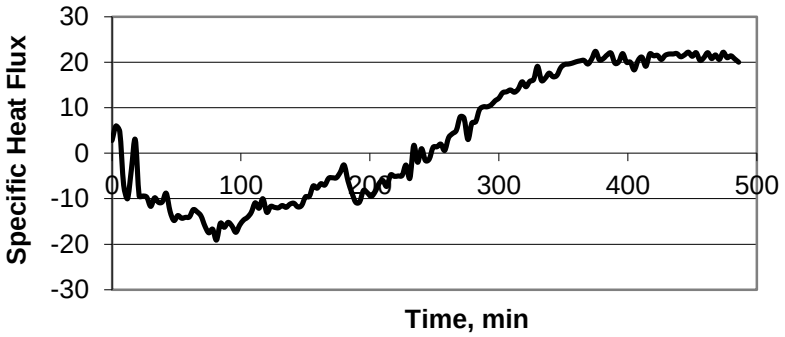

Figure 5. The specific heat flux (W m^{-2}) from the floor surface to the air.

The first 250 minutes is negative heat flux on the floor surface, which means that the massive concrete floor is gradually heated by hot air circulation inside floor as well as by shared heat from the warm air in the room near the fireplace. After 250 minutes, there is a progressive increase in a positive heat flow from the floor to the room. The accumulated heat keeps the whole floor surface for several hours warm after the end of fuel supply.

CONCLUSIONS

The results of measurements in the living room showed that the radiant heating with accumulation of energy in the floor compensates temperature differences. The accumulation of excessive heat into the floor with accumulation capacity enables the reduction of overheating during the heating period and subsequently the longer maintaining of required temperature inside the room.

Radiant component of heat transfer very favourably influences the thermal comfort of indoor environment. The heat can be intensively distributed around the house with time shift. The result is the more stable thermal comfort inside the room and savings of heating costs. This system is particularly suited for rural areas, as it is possible to use wood or other biofuels for heating. As there are not visible radiators inside the room, it is reduced the risk of injury and it allows achieving easily an aesthetically impressive interior room. It is suitable for new or modernized rural family houses.

ACKNOWLEDGEMENTS. Author is grateful and express many thanks to the company Atelier Zilvar and Mr. Lipka who permitted and enabled to author to carry out all measurements of indoor environment in room equipped by the AKU heating system.

REFERENCES

Cihelka, J. 1961. *Radiant Heating*. SNTL, Praha, 373 pp. (in Czech).

Kic, P. 2013. Hot-Air Heating of Family Houses with Accumulation of Energy in the Floor. *Agronomy Research* **11**(2), 329–334.

Kic, P. & Kadlecek, B. 2012. Improvement of heat balance of family house. In Galins, A.: *12th International Scientific Conference Engineering for Rural Development*. Latvia University of Agriculture, Jelgava, Latvia, pp. 134–138.

Papez, J. & Kic, P. 2013. Wood moisture of rural timber constructions. *Agronomy Research* **11**(2), 505–512.

Vio, M. 2011. *Climatization with Radiant Systems.* Editoriale Delfino, Milano, 264 pp. (in Italian).

Agronomy Research **13**(2), 500–510, 2015

Investigation of fuel effect on biomass gasification process using equilibrium model

V. Kirsanovs* and A. Žandeckis

[1]Riga Technical University, Faculty of Power and Electrical Engineering, Institute of Energy Systems and Environment, Azenes street 12/1, LV1048 Riga, Latvia; *Correspondence: vladimirs.kirsanovs@rtu.lv

Abstract. Gasification is one of the most promising technologies of converting biomass into energy. Different type of biomass can be used for gasification process since there are no strict limitations for parameters of used fuel. Various types of biomass are used in Latvia for production of energy. Wood fuels make up the main part of used biomass in Latvia. However, many non-wood biomass types are available as well.

This study presents the comparison of wood and non-wood biomass use in gasification process. Biomass gasification model based on thermodynamic equilibrium was used to simulate gasification process with various biomass types. All input parameters were constant in model except fuel properties. In general gasification process was simulated with seven types of biomass – draff from beer production, common reed, middling from oats and wheat sieving, straw from grain cultivation, buckwheat hulls, rapeseed by-product from biofuel production, as well as wood. These non-wood biomass types are available in Latvia.

Produced syngas calorific value and gasification process efficiency are taken as the indicators to examine the gasification performances using various biomass types. The regression model was proposed to describe relation between fuel properties and efficiency of the gasification process. Results show that non-wood biomass can be successfully used for gasification process. Ash content growth in the fuel promotes temperature decrease in the reactor. Fuel chemical composition has effect on the produced syngas composition and heating value.

Key words: biomass gasification, non-wood biomass, thermodynamic model, syngas.

INTRODUCTION

The use of fossil fuels for energy production generates the overwhelming amount of CO_2. Biomass is one of the dominant sources of alternative energy to substitute fossil energy use (Berndes et al., 2003). Wood is the most frequently used biomass type. However, there are many other non-wood biomass resources available for energy production. Different methods exist to convert biomass into energy. Nowadays rapid progress in biomass gasification technology became one of the most perspective methods. Biomass gasification is economically favourable and environmentally friendly technology. One on the advantages is that there are no strict limitations in biomass properties of its use in gasification process. Resource availability, economical substantiation and suitability for use in definite technology for biomass conversion in the energy are the main factors which should be taken into consideration choosing non-wood material.

The diversity of non-wood biomass is very high, and types of available raw material vary between world regions and countries. Rice straw is one of frequently used material for gasification process in the Southeast Asia (Suramaythangkoor & Gheewala, 2010). The amount of available rice straw and husk are notable in Japan as well. Potato, corn, sugarcane, sorghum and some other agricultural residue can be used as an energy resource in Japan, too (Matsumura et al., 2005). Some amount of energy is produced using olive and olive oil residues in Greece. Typically simple combustion technologies were used. Syngas with calorific value more than 8 MJ Nm^{-3} can be produced using olive residues as fuel (Skoulou et al., 2008).

From all energy source consumption in Latvia, 59,274 TJ or 34.6% related to the oil products, 50,269 TJ or 29.3% to the natural gas and 53,106 TJ or 31.0% to the wood fuels in year 2013 (Energy balance, 2013). It follows that the fossil fuel has determinant role in the energy production. However, the amount of used wood fuel increased by 13.9% from 45,646 TJ in 2010 up to 53,106 TJ in 2013, but fossil fuels amount decreased conversely. The fastest growth is seen in the use of wood chips from 8,596 TJ up to 14,182 TJ by 39.4% and pellets from 562 TJ up to 1,728 TJ by 67.5%. Unfortunately, no regulation to control quality of the produced pellet is available. It promotes the accessibility of pellets with various properties in the market in Latvia (Beloborodko et al., 2012).

The amount of non-wood biomass consumed in the energy production is minimal, 80 TJ produced from peat and 58 TJ from straw. The amount of non-wood biomass use for energy production can increase using herbaceous material from agricultural sector and using industrial by-products. Availability and energy potential of herbaceous and fruit biomass resources in Latvia are described in study done by Beloborodko et al (2013). Total amount of energy from straw and hogweed exceeds 3,000 TJ and can be used for the energy production.

The biomass updated technologies use before gasification process can noticeably improve produced syngas properties. The pyrolysis of the biomass is a frequently used method to produce fuel with high energy content. The torrefaction of biomass can improve gasification process as well. Torrefaction is a mild pyrolysis process at the temperature typically between 200 and 300 °C. The oxygen/carbon ration of torrefied biomass decreases, but energy content of wood increases after the torrefaction process. Hydrogen and carbon monoxide content in the syngas goes up using torrefied fuel (Couhert et al., 2009). Tar content typically is lower in the syngas produced from torrefied fuel. The growth of temperature in the gasifier reactor using torrefied fuel is one of the main reasons of it. Another reason is that torrefaction process provides partial devolatilisation and lower production of water fractions (Dudynski et al., 2015).

The biomass torrefaction and gasification can be successfully united into one combined process. Different technological methods to unite these processes are available. Oxygen-blown gasification of torrefied wood can be one of the most promising methods (Prins et al., 2006). Biomass pretreatments methods as pyrolysis and torrefaction as well as drying and dissolution were analysed in the study done by Svoboda et al. (2009) to dominate effect on the gasification process.

At the same time gasification process is considerably dependent on fuel properties. Fuel chemical composition, calorific value, ash and moisture content are prior factors which effect produced syngas properties. The calorific value of produced syngas depends on heating value of used biomass. The higher is biomass heating value the higher calorific value of syngas can be achieved (Antonopoulos et al., 2012). Tar content in the syngas typically is higher for fuel richer with ash (Wei et al., 2007). However, small-scale difference in the amount of carbon and hydrogen in fuel doesn't cause constitutive changes in produced syngas composition (Andre et al., 2005).

The moisture content of fuel has more crucial effect on the gasification process. CO content goes down sharply due to the moisture increase. It provides decrease of the heating value of the produced syngas. This tendency proves gasification process with sawdust (Altafini et al., 2003), cashew nut shell (Ramanan et al., 2008), sugarcane mills (Pellegrini & de Oliveira, 2007), paddy husk and wood (Zainal et al., 2001).

The main objective of this paper is to compare the gasification process efficiency and syngas properties produced from different wood and non-wood fuels. Only the non-wood biomass types accessible in Latvia were considered. Determination of biomass types for energy production and fossil fuel replacement is one of the goals. The second goal is to identify the independent variable parameters of the fuels that cause the highest influence on the gasification process.

MATERIALS AND METHODS

Fuel description

The gasification process was simulated using seven different biomass types available in Latvia. Draff from beer production (DR), common reed (CR), middling from oats and wheat sieving (OWM), straw from grain cultivation (ST), buckwheat hulls (BH), rapeseed by-product from biofuel production (RB) were chosen to present non-wood biomass. One wood (WO) sample was used as benchmark to compare produced syngas quality and the gasification process in general. The analysis of fuel samples was done in the Environmental Monitoring Laboratory of Riga Technical University (see Table 1). The ultimate and proximate properties of the biomass were presented in the study done by Žandeckis also (2014).

Table 1. The ultimate and proximate properties of the biomass samples

	DR	CR	OWM	ST	BH	RB	WO
Ash, w-%,dr*	4.91	4.89	3.61	4.72	2.19	11.3	0.82
C, w-%,dr af**	46.3	44.5	43.6	45.1	47.2	48.2	50.2
H, w-%, dr af	7.26	5.84	7.52	5.77	6.15	8.00	6.98
N, w-%, dr af	4.05	0.38	1.84	0.42	0.65	3.05	0.14
S, w-%, dr af	0.05	0.04	0.09	0.10	0.08	0.06	0.01
O, w-%, dr af	42.3	49.2	47.0	48.6	45.9	40.7	42.7
HHV, MJ kg^{-1}***	19.2	16.4	18.4	18.0	18.5	19.2	21.1
LHV, MJ kg^{-1}****	15.6	13.2	14.9	14.6	15.0	15.8	17.2

* – on dry basis; ** – dry and ash free basis; *** – calculated value from the model; **** – calculated value from the model at similar moisture 10% for all samples.

The gross calorific value of the fuels was calculated in model using following equation:

$$HHV_f = 339.1C_{dr} + 1178.3H_{dr} + 100.5S_{dr} - 103.4O_{dr} - 15.1N_{dr} - 21.1A_{dr} \quad (1)$$

where: HHV_f – gross calorific value of the fuel on dry basis, kJ kg^{-1}; C_{dr}, H_{dr}, O_{dr}, S_{dr}, N_{dr} – the fuel chemical composition on dry basis, %; A_{dr} – ash content in the fuel on dry basis, %.

It was decided to take the similar moisture content 10% for all biomass samples. Tipically raw material firstly undergoes the pretreatments stage before use. The fuel moisture content 10% can present real amount of water in biomass after pretreatments stage. It was done to exclude the effect of the water content and present the influence of fuel chemical properties and ash content. Lower calorific values were calculated by:

$$LHV_f = 339.1C_{af} + 1029H_{af} + 109S_{af} - 109O_{af} - 25W \quad (2)$$

where: LHV_f – lower calorific value of the fuel as fired basis kJ kg^{-1}; C_{dr}, H_{dr}, O_{dr}, S_{dr}, N_{dr} – the fuel chemical composition as fired basis, %; A_{af} – ash content in the fuel as fired basis, %.

Model description

The mathematical model of gasification process was created to determine the possibilities of non-wood biomass use for syngas production. Model was based on the thermodynamic equilibrium reactions. Model describes gasification process for the downdraft gasifier where air was used as gasifying agent. The oxygen and nitrogen make 100% of air in the model. It was decided take the constant equivalence ratio 0.25 for all biomass types to make comparison more credible. The efficiency of gasification process typically achieves maximum values when equivalence ratio lies between 0.2 and 0.3 (Pellegrini et al., 2007). Similarly the fuel and ambient temperatures were chosen as constant in the model for all biomass types. The produced syngas comprise only from CO, CO_2, H_2, CH_4, N_2 and H_2O vapour.

The model was based on the global gasification reaction:

$$CH_xO_yN_z + wH_2O + m \cdot (O_2 + 3.76N_2) = n_{H_2}H_2 + n_{CO}CO + n_{CO_2}CO_2 + n_{H_2O}H_2O + n_{CH_4}CH_4 + (\frac{z}{2} + 3.76m) \cdot N_2 \quad (3)$$

where: n_{H2}, n_{CO}, n_{CO2}, n_{H2O}, n_{CH4} and n_{N2} – the numbers of moles of H_2, CO, CO_2, H_2O, CH_4 and N_2 in the syngas; m – the air moles; w – the moisture associated with the biomass.

Based on global gasification reaction carbon, hydrogen and oxygen balances are calculated using the following equations:

$$n_{CO} + n_{CO_2} + n_{CH_4} - 1 = 0 \quad (4)$$

$$n_{H_2} + 2n_{H_2O} + 4n_{CH_4} - x - 2w = 0 \quad (5)$$

$$n_{CO} + 2n_{CO_2} + n_{H_2O} - w - 2m - y = 0 \quad (6)$$

The mass balance consists of two input and two output flows. The input flow includes biomass consumption on dry ash free basis, mass of the water and ash contained in the fuel. The produced syngas and ash are the output flows.

The fuel heating value, fuel sensible heat and sensible heat of gases form the input flow in the energy balance of the gasification process. The majority of energy is injected in the gasifier with fuel heating value. The sensible heat of fuel and air depends on fuel and air temperatures. The heat losses aren't divided into types, but are only calculated as total amount. Heat losses are basically formed by heat losses from gasifier to surrounding, heat from condensation and from energy removed with tar and char.

The model validation was created to make certain of verity of results obtained from model. Two models done by Zainal et al. (2001) and Jarungthammachote et al. (2007) and experimental study of biomass gasification (Gai & Dong, 2012) were used for validation (see Table 2). The similar biomass chemical composition, water content and equivalent ratio were used in present model for validation. Models comparison shows that acquired results were in close range with the results from others models. For this reason the created model can be used to simulate gasification process with various biomass types.

Table 2. Model validation

Model	Biomass properties				ER	Syngas composition, %				
	C, %	H, %	O, %	M, %		CO, %	CO_2, %	CH_4, %	H_2, %	N_2, %
Gao & Dong (2012)	43.0	5.83	44.1	6.17	0.32	19.8	11.6	3.70	20.8	55.7
Present						24.8	9.80	1.03	20.4	44.0
Zainal et al. (2001)	40.0	4.80	35.2	14.0	0.39	20.0	10.4	0.31	14.0	56.6
Present						22.4	9.03	0.31	18.1	50.2
Jarungthammachote et al. (2007)	43.9	5.83	33.7	14.0	0.44	18.5	11.7	1.06	16.8	51.9
Present						20.9	8.57	0.11	15.3	55.1

Model calculates such parameters as amount of produced syngas, syngas chemical composition and heating value, sensible heat of each syngas components, efficiency of gasification process and other values. The efficiency of gasification process is expressed in model as:

$$\eta = \frac{LHV_g \cdot V_g + Q_s \cdot V_g}{LHV_f \cdot m_f} \quad (7)$$

where: η – the efficiency of the gasification process, %; LHV_g – lower calorific value of the syngas, kJ Nm^{-3}; V_g – volume of the produced syngas, Nm^3; Q_s – sensible heat of syngas, kJ m^{-3}; m_f – the mass of the fuel as fired basis kg.

RESULTS AND DISCUSSION

Gasification process was simulated using the model with six non-wood and one wood biomass samples. Fig. 1 displays syngas composition for the various type of biomass. In general syngas composition is relatively similar for all biomass samples. The CH_4 content of syngas produced from rapeseed by-product is 12.2%, but average CH_4 content for all samples is 6.85%. N_2 content is high as well in comparison to other acquired syngas. However, H_2 and CO content in the syngas from rapeseed by-product is noticeably lower. Syngas produced from wood have the highest CO and H_2 content comparing with other syngas samples.

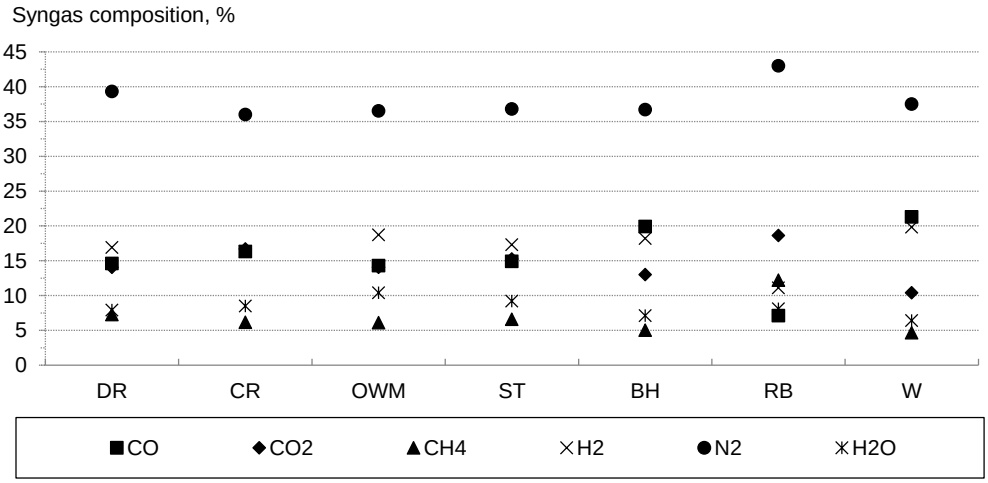

Figure 1. Syngas composition depending on the biomass types.

Gasification process efficiency and produced syngas lower calorific value changes between various biomass types have similar tendencies (see Fig. 2). Gasification efficiency is near 80% for majority of samples including wood. Only gasification process efficiency using middling from oats and wheat sieving is comparatively low about 76.4%, but the use of rapeseed by-product is contrariwise high about 87.8%. The lower calorific value of syngas produced from wood, draff and buckwheat hulls is about 5.5 MJ Nm^{-3}. The calorific value of syngas from common reed, middling from oats and wheat sieving and straw from grain cultivation is lower. The energy value of the syngas from rapeseed by-product is conversely higher and exceeds 6.0 MJ Nm^{-3}. The elevated amount of CH_4 in the syngas from rapeseed by-product is the main reason of it.

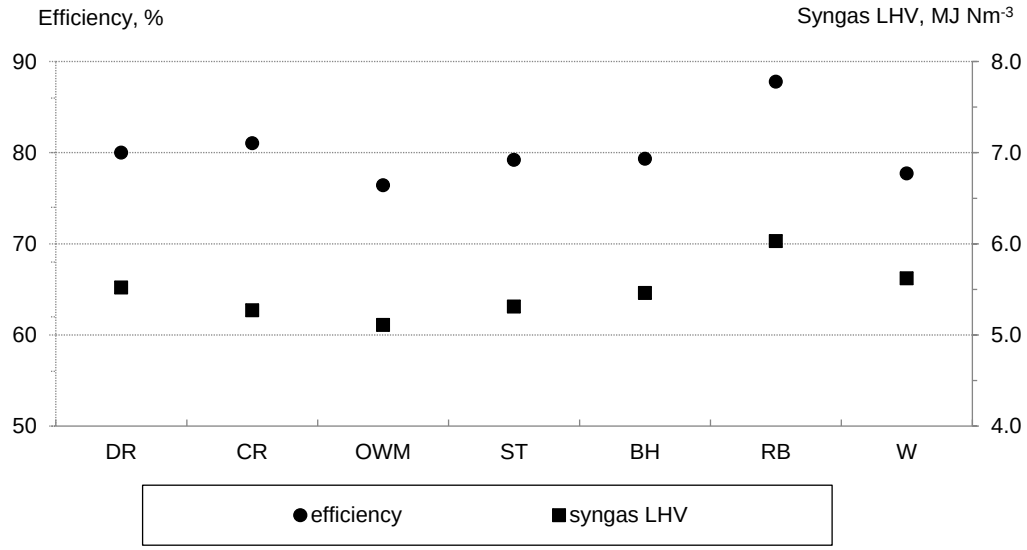

Figure 2. Syngas lower heating value and gasification efficiency depending on the biomass types.

The relations between different parameters of the gasification process were determined based on the acquired data (see Fig. 3.) Close correlation between ash content in the fuel and temperature in the gasifier reactor was discovered. The ash content growth promotes the temperature decrease. The problems of carbon and char conversion can be the main reason of it. The reduction of the temperature promotes the growth of CO and H_2 concentration in the syngas and the decrease of CH_4 content. The increase of temperature causes primary and secondary water gas reactions, secondary cracking and reforming of heavy hydrocarbons activity. The content of produced H_2 in the syngas goes up in the result. The activity of water gas and Boudouard reactions also increases due to temperature growth. Therefore, carbon reacts with CO_2 and H_2O vapour and produces higher amounts of CO. On the other hand, the temperature growth promotes combustion reactions and CH_4 amount decrease.

The lower is the content of oxygen in the fuel the higher amount of air should be injected in the gasifier to acquire the required equivalent ratio for the gasification process. Nitrogen content in the air is about 78.1%. Therefore, the N_2 content in the produced syngas increases if injected amount of air goes up. The N_2 content in the syngas is not recommended and promotes the decrease of the calorific value of produced syngas. That is why there is correlation between amount of oxygen content in the fuel and energy content of syngas.

The carbon amount in the fuel has effect on the CO content in the syngas. However, the correlation is not so strong, because some amount of carbon was converted in the CO_2, but some amount cannot be converted in general. The stronger connection is between carbon to oxygen ratio and heating value of syngas. The higher is the carbon to oxygen ratio of fuel the higher is heating value of produced syngas.

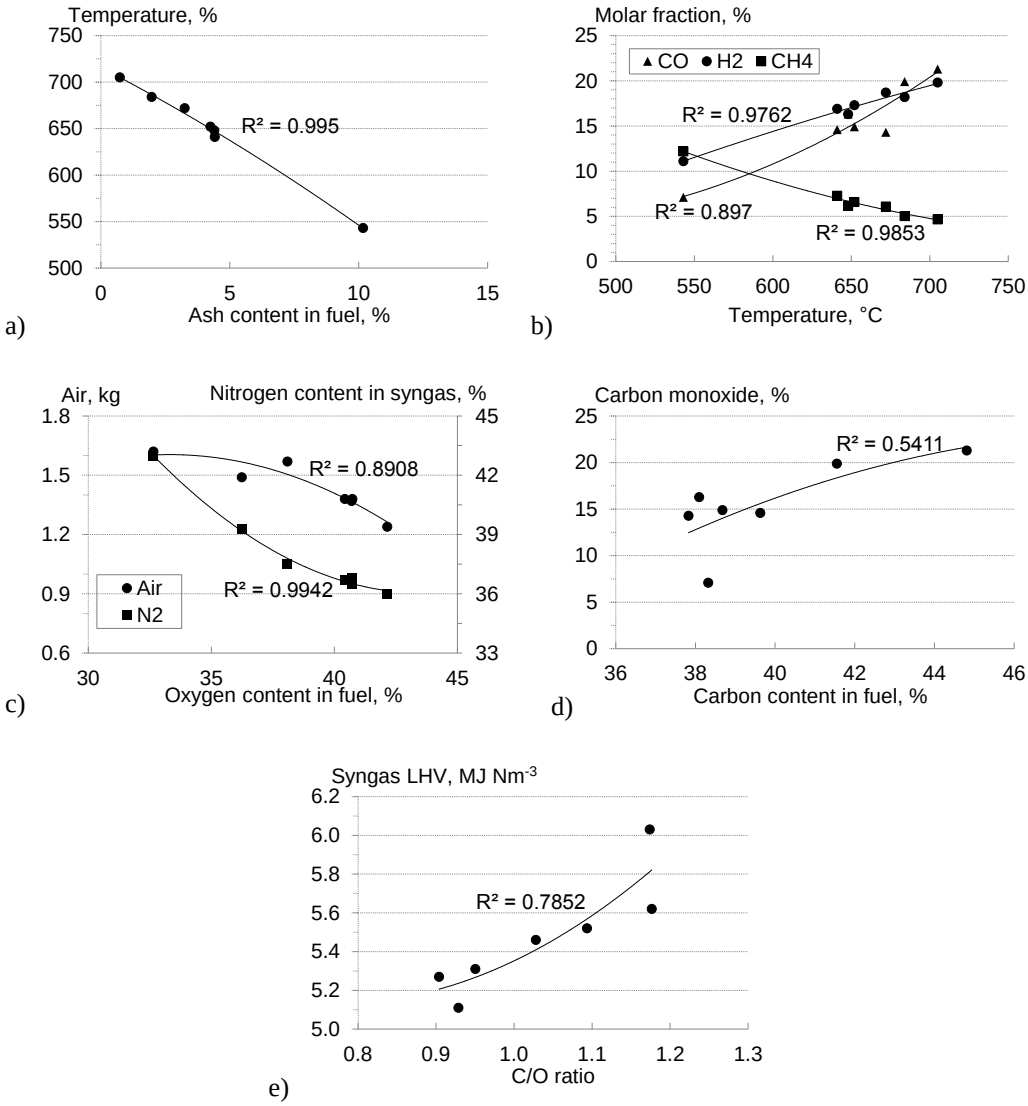

Figure 3. The relation between parameters in the gasification process: a) ash content in the fuel vs temperature in the gasifier reactor; b) temperature in the gasifier reactor vs CO, H_2 and CH_4 content in the syngas; c) oxygen content in the fuel vs required amount of air and nitrogen content in the syngas; d) carbon content in the fuel vs CO content in the syngas; e) C/O ratio of fuel vs produced syngas lower calorific value.

The regression model was elaborated where efficiency of gasification process was dependent on variable. The independent variables were ash, carbon, hydrogen, oxygen content in the fuel as fired basis. The data analysis done in STATGRAPHICS Centurion 16.1.15 environment shows that the efficiency is described by Eq.8:

$$\eta = 56.5309 + 0.711207C_f - 1.8791H_f + 1.56684A_f \quad (8)$$

Data analysis shows that in model all parameters have hight influential on the indicator (see Table 3.). Since P-value in the analysis of the variance (ANOVA) table is less than 0.05, there is statistically significant relationship between the variables. Durbin-Watson statistics is close to 3.1, therefore, there is no autocorrelation observed between independent variables. Coefficient of determination R^2 and adjusted R^2 explains 99.6% and 99.3% of data input for regression model.

Table 3. Data analysis of the regression model

Variables	P-value	P-value for the ANOVA	R^2 & adj. R^2 %[b]	Standard error	Durbin-Watson statistic
Efficiency	0.0003	0.0004	99.644 99.2879	0.3090	3.1194 P = 0.9710
Carbon content	0.0017				
Hydrogen content	0.0043				
Ash content	0.0001				

CONCLUSIONS

The comparison of wood and non-wood biomass for the use in gasification process was done. The thermochemical equilibrium model was used in the study. Produced syngas properties and gasification process efficiency were main criteria in comparison of biomass types. Gasification process was simulated with draff from beer production, common reed, middling from oats and wheat sieving, straw from grain cultivation, buckwheat hulls, rapeseed by-product from biofuel production and wood biomass types. All these herbaceous agricultural and processing industry by-products are available in Latvia.

Results show that all non-wood raw materials can be successfully used in gasification process and on the same basis as wood. Gasification efficiency was about 80% for major samples including wood, but produced syngas calorific value was around 5.5 MJ Nm^{-3}. The consumption of wood fuels for energy production is continuously increasing and non-wood material can be used to satisfy the demand for biomass. In such a way the greater amount of the fossil fuel can substitute with biomass. It is important that one non-wood biomass type can be substituted by another without altering the produced syngas quality.

It was determined that higher ash content results in the process with lower temperature. Temperature reduction promotes the growth of CO and H_2 concentration in the syngas and the decrease of CH_4 content. The lower is oxygen content in the fuel the more air must be injected in the gasifier. Therefore, the low oxygen content in the fuel favours low heating value of syngas. The correlation between carbon content in the fuel and CO content in the syngas was identified as well.

The regression model was proposed to describe the connection between used fuel properties and efficiency of the gasification process. Data analysis shows that the model had sufficient correlation between the variables that will be used to describe the actual situation. Ash and hydrogen content in the fuel is the most influential parameter in model. Coefficient of determination R^2 and adjusted R^2 explains 99.6% and 99.3% of data input for regression model at 95% confidence level.

ACKNOWLEDGMENTS. This work has been supported by the Involvement of Human Resources for Development of Integrated Renewable Energy Resources Energy Production System (No.1DP/1.1.1.2/13/APIA/026).

REFERENCES

Altafini, C.R., Wander, P.R., Barreto, R.M. 2003. Prediction of the working parameters of a wood waste gasifier through an equilibrium model. *Energy Conversion and Management* **44**, 2763–2777.

Andre, R.N., Pinto, F., Franco, C., Dias, M., Gulyurtlu, I., Matos, M.A.A., Cabrita, I. 2005. Fluidesed bed co-gasification of coal and olive oil industry wastes. *Fuel* **84**, 1635–1644.

Antonopoulos, I.-S., Karagiannidis, A., Gkouletsos, A., Perkoulidis, G. 2012. Modelling of a downdraft gasifier fed by agricultural residues. *Waste management* **32**, 710–718.

Beloborodko, A., Klavina, K., Romagnoli, F., Kenga, K., Rosa, M., Blumberga, D. 2013. Study on availability of herbaceous resources for production of solid biomass fuels in Latvia. *Agronomy research* **11**(2), 283–294.

Beloborodko, A., Timma, L., Žandeckis, A., Romagnoli, F. 2012. The Regression Model for the Evaluation of the Quality Parameters for Pellets. *Agronomy Research* **10**(1), 17–24.

Berndes, G., Hoogwijk, M., Broek, R.V.D. 2003. The contribution of biomass in the future global energy supply: a review of 17 studies. *Biomass and bioenergy* **25**, 1–28.

Couhert, C., Salvador, S., Commandre, J-M. 2009. Impact of torrefaction on syngas production from wood. **Fuel** *88*, 2286–2290.

Dudynski, M., Dyk, J.C.V., Kwiatkowski, K., Sosnowska, M. 2015. Biomass gasification: influence of torrefaction on syngas production and tar formation. *Fuel processing technology* **131**, 203–212.

Energy balance. 2013. Central Statistical Bureau of Latvia. Riga, Latvia.

Gai, C., Dong, Y. 2012. Experimental study on non-woody biomass gasification in a downdraft gasifier. *International journal of hydrogen energy* **37**, 4935–4944.

Jarungthammachote, S., Dutta, A. 2007. Thermodynamic equilibrium model and second law analysis of a downdraft waste gasifier. *Energy* **32**, 1660–1669.

Matsumura, Y., Minowa, T., Yamamoto, H. 2005. Amount, availability, and potential use of rice straw (agricultural residue) biomass as an energy resource in Japan. *Biomass and bioenergy* **29**, 347–354.

Pellegrini, L., de Oliveira, Jr.S. 2007. Exergy analysis of sugarcane bagasse gasification. *Energy* **32**, 314–327.

Prins, M.J., Ptasinski, K.J., Janssen, F.J.J.G. 2006. More efficient biomass gasification via torrefaction. *Energy* **31**, 3458–3470.

Ramanan, M.V., Lakshmanan, E., Sethumadhavan, R., Renganarayanan, S. 2008. Performance prediction and validation of equilibrium modeling for gasification of cashew nut shell char. *Brazilian Journal of Chemical Engineering* **25**, 585–601.

Skoulou, V., Zabaniotou, A., Stavropouls, G., Sakelaropoulos, G. 2008. Syngas production from olive tree cuttings and olive kernels in a downdraft fixed-bed gasifier. *International journal of hydrogen energy* **33**, 1185–1194.

Suramaythangkoor, T., Gheewala, S.H. 2010. Potential alternatives of heat and power technology application using rice straw in Thailand. *Applied energy* **87**, 128–133.

Svoboda, K., Pohorely, M., Hartman, M., Martinec, J. 2009. Pretreatment and feeding of biomass for pressurized entrained flow gasification. *Fuel processing technology* **90**, 629–635.

Wei, L., Xu, S., Zhang, L., Liu, C., Zhu, H., Liu, S. 2007. Steam gasification of biomass for hydrogen-rich gas in a free-fall reactor. *International journal of hydrogen energy* **32**, 24–31.

Zainal, Z.A., Ali, R., Lean, C.H., Seetharamu, K.N. 2001. Prediction of performance of a downdraft gasifier using equilibrium modelling for different biomass materials. *Energy conversion and management* **42**, 1499–1515.

Žandeckis, A., Romagnoli, F., Beloborodko, A., Kirsanovs, V., Menind, A., Hovi, M. 2014. Briquettes from mixtures of herbaceous biomass and wood: biofuel investigation and combustion tests. *Chemical engineering transactions* **42**, 67–72.

Agronomy Research **13**(2), 511–519, 2015

Charcoal production environmental performance

K. Kļaviņa*, K. Kārkliņa and D. Blumberga

Riga Technical University, Faculty of Power and Electrical Engineering, Institute of Energy Systems and Environment, Āzenes st. 12/1-616, LV1048 Riga, Latvia; *Correspondence: krista.klavina@rtu.lv

Abstract. Charcoal is a well-known material obtained through thermal conversion of different types of biomass in an anoxic environment. The greatest share of the overall charcoal amount is produced in inefficient batch pyrolysis chambers. Thus contribution in an in-depth charcoal production process research for process optimization is of great importance. In this study an industrial experiment of charcoal production in a continuous up-to-date retort is performed. The selected industrial object has a high level of automation and process control. The retort is connected to a continuous monitoring system that records and stores the process parameter values. Apart from the process control parameter measurements attention has to be paid to the charcoal production plant pollution as this industry often gets contradictory attention towards its environmental performance. The air pollution is evaluated by air quality measurements at the production facility site. The obtained experimental results from an industrial facility with a state-of-the-art technology give an opportunity to evaluate the potential of the charcoal industry to be a sustainable player in the renewable energy market.

Key words: industrial experiment, sustainable energy, production, emissions.

INTRODUCTION

Historically the introduction of charcoal lead to the development of energy intensive industry establishment, such as glass production and metal smelting as no other energy source at the time could produce enough heat. These industries expanded rapidly and were followed by an extensive use of biomass and wildwood clearance. Many areas met a faster growing industry than the availability of the energy resource. This lead to a rapid switching from charcoal to fossil fuels.

Since the beginning of an intensive use of fossil fuels the global greenhouse gas (GHG) emissions have grown to 49.5 giga tonnes of carbon dioxide equivalents in the year 2010 (Victor et al., 2014). GHG emission regulations, programs and policies have taken place and are further expected in order to mitigate the climate change caused by the elevated GHG levels in the atmosphere. The most significant actions have taken place in the past two to three years (Bhander et al., 2014). The Intergovernmental Panel on Climate Change (IPCC) in its Fifth Assessment Report has included the use of biochar as one of the tools for GHG emission reduction. Biochar is charcoal when specifically used as a soil amendment. Using biochar as a soil amendment increases biomass productivity and isolates carbon dioxide from the atmosphere by locking it in the soil (Smith et al., 2014). Some promising research has been done in relation to the use of charcoal as a feasible replacement of fossil fuels by creating fuel blends with an addition

of hardwood derived charcoal to coke in iron-ore sintering thus decreasing the GHG emissions from this industry (Ooi et al., 2011).

The charcoal production feed can be a wide range of materials. Different types of biomass feed lead to the production of different charcoal grades – basic grade biochar, premium grade biochar and charcoal. The used biomass can be starting from biodegradable waste from local waste collection services to hardwood (Schmidt et al., 2012). The use of biodegradable waste for production of valuable materials and energy is highly recommendable in order to reach the EU targets for minimization of the share of landfilled biodegradable waste as well as to avoid resource scarcity (Pubule et al., 2014).

Charcoal is produced in slow pyrolysis carbonisation process. The charcoal yield being dependent on such process parameters as the final temperature, the biomass particle size, the heating rate and the reaction atmosphere (Elyounssi et al., 2012). Traditionally charcoal is made in small, simple batch-type kilns where the parameter management and control is very limited. In the early 1940's the most successful charcoal production technologies were developed - the Lambiotte and SIFIC process. This is a continuous carbonization process where the retort is filled continuously with wood from the top, while downstream simultaneously carbonisation takes place. The cooled charcoal is removed from the bottom. The process is energy autonomous gaining the necessary heat from burning gases attained from pyrolysis. The gases go through a condenser and afterwards are blown in the bottom of the retort where it cools the fresh charcoal while preheating the gases (Vertes et al., 2010). This technology has much higher process control and it offers the possibility of producing charcoal more efficiently and with higher increased yields then the traditional batch methods. This leads to the conclusion that with an increased interest of charcoal production this kind of technologies have to be evaluated form the environmental performance aspects.

This case study is carried out for a Lambiotte type retort producing charcoal from hardwood in Latvia. The hardwood (roundwood) in the form of firewood is prepared on the production facility premises, it includes log sawing, cleaving and drying. The drying of the firewood is crucial for proper functioning of the retort torch, where the excess pyrolysis gases are burnt before emitting to the atmosphere. The fresh wood is received with around 55% moisture content, while the technological process requires the moisture content of the input fuel to be below 25%. The drying takes place in four chamber dryers heated with wood-fuelled water boilers.

The retort is operated under experimental conditions in order to carry out the relevant measurements that describe the production facilities' environmental performance regarding the emissions. The discovered results can be used to evaluate whether there is place for charcoal production in an economically developed country where the environmental performance is of high importance, and it is strictly regulated.

MATERIALS AND METHODS

Evaluating the whole production process stages the main emission sources are distinguished. The technological scheme of the charcoal production process in the studied facility is illustrated in Fig. 1.

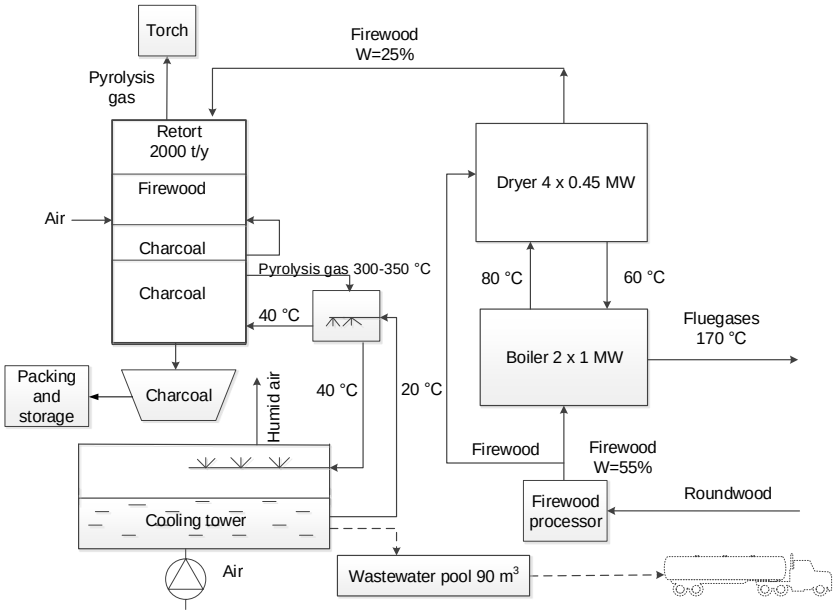

Figure 1. Technological scheme of the production facility using Lambiotte SIFIC retort.

The measurements at the production facility are conducted according to the corresponding Standard Method. The distinguished emission sources, emission types and the selected methods for the emission evaluation measurements are summarized in Table 1.

Table 1. The main emission types, sources and the measurement procedures

Emission type	Emission source	Method
wastewater (oil product hydrocarbons index)	cooling tower	LVS EN ISO 9377-2:2001
noise	firewood processor, fans, aspiration system, vibrating screener, firewood conveyor	LVS ISO 1996/2-2008
odours	boiler stack, retort	LVS EN 13725:2004
particulate matter (in stack gases; surrounding area)	boiler stack, retort, packing and forwarding of charcoal	LVS ISO 9096:2004/TC1:2007 РД 52.04.186-89 (5.2.6.): 1989
NO_x	boiler stack, retort	LVS ISO 10849:2001
CO	boiler stack, retort	LVS EN 15058:2006
CO_2	boiler stack, retort	ISO 12039:2001
volatiles organic compounds VOC (total; qualitative analysis)	boiler stack, retort	LVS EN 12619:2013 NIST 2008 MS LIB cat.NrG1033A Revision Jun 2010

The measurements are made during the period when the manufacturing process has reached a steady operating mode and the settings are adjusted. The measurements are carried out by an accredited laboratory according the research plan. The measurement location is described in Fig. 2.

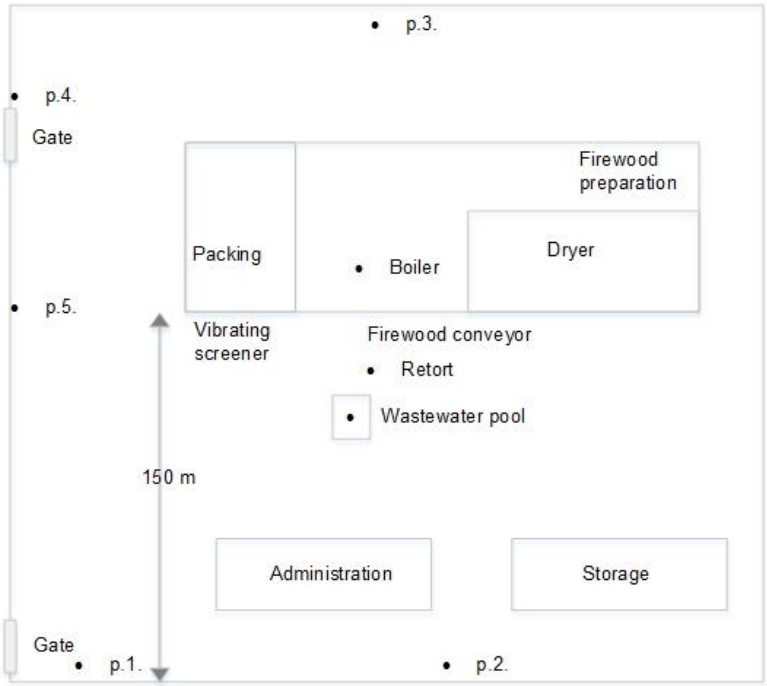

Figure 2. Measurement locations in the factory territory.

The measurement locations in Fig. 1 are marked with a dot. The locations p.1 to 5 mark the places where the samples for the particulate matter in the surrounding area, odour and noise determination are taken.

RESULTS AND DISCUSSION

The industrial experiment at the charcoal production facility took place for 22 days, including the material preparation, process set-up and maintenance. The environmental pollution monitoring was carried out in two separate takes. The obtained results are discussed regarding the legislation requirements and the set thresholds in Latvia. Subdivision according to the specific emission output is used.

Wastewater

There are several types of wastewater created in the facility – domestic wastewater from the administrative buildings, rainwater and the wastewater that is formed in the cooling circuit. The cooling waters are used repeatedly and have to be utilised rarely.

The hydrocarbon index is determined for a sample of the cooling wastewater, returning the value of 3.6 ±1.4 mg L^{-1}. The result characterizes the water after around

twenty days of operation. According to UNEP (2000) the hydrocarbon oil index environmental limit is 0.01 mg L^{-1}while for the Offshore petroleum activities it is 40 mg L^{-1} (Department of Energy & Climate Change, 2014) but for example in Massachusett the upper concentration limit in groundwater is 50 mg L^{-1}. These wastewaters have to be either handled by an appropriate authority or the production facility have to ensure an appropriate industrial wastewater pre-treatment meeting the centralized wastewater operator requirements before transition (Cabinet of Ministers, 2002).

Noise

The noise measurements are carried out in three different charcoal factory production states in a steady operation mode. The ongoing processes and active noise sources while taking the measurements, and the measurement results are described in the Table 2.

Table 2. Operation modes and the sound pressure levels

	System operation mode			
	1	2	3	L_{day}, dB(A)
firewood processor	☒	☒	☒	
dryer fans	☒	☒	☒	
packing	☒	☒	☒	
retort fans	☒	☒	☒	
vibrating screener	☒	☒	☐	
firewood conveyor	☒	☐	☐	
$L_{Aeq,\,T}$ measurement location p.1., dB(A)	50.1	47.5	45.2	47.2 ± 3.8
$L_{Aeq,\,T}$ measurement location p.2., dB(A)	53.4	53.0	49.5	51.8 ± 3.8

$L_{Aeq,T}$ – weighted measured continuous sound pressure level during the time period T,dB(A)
L_{day} – weighted estimated continuous sound pressure level, taking into account all the days of the year (as a daily share), dB(A).

The measurement locations mentioned in Table 2 correspond to those depicted in Fig. 2. These locations are chosen because of the sound corridors formed by the buildings in the sound transmission route. The direction of the measurements from the sound sources is selected towards the closest noise recipient – a residential homestead immediately after the factory border.

The national noise limit for individual residential house building areas in Latvia for the day (7.00 to 19.00) period is 55 dB(A), for the evening (19.00 to 23.00) period 50 dB(A), and the night (23.00 to 7.00) period 45 dB(A) (Cabinet of Ministers, 2014a). Thus it can be observed that during the day period the charcoal production facility under different operation modes does not exceed the thresholds. The given measurements do not give a definite assessment for the evening and night periods though, because during these times the firewood processor is not operated and gives an unknown noise reduction. Anyway even if the factory would work at the same operation modes during the night period the sound levels would be just slightly elevated and could be easily reduced by introducing simple cost-effective sound barriers.

Odours

The odours are measured in the factory surroundings where the measurement includes both odour sources – the stack gases from the boiler and the effluents from the charcoal production retort. The odour measurement methods detection limit is 11 OU_E m^{-3}. In the territory measurement does not register a result – meaning that the odour is less than 11 OU_E/m^3. A disagreement with the legislation is faced, where the odour target value for an hour is 5 OU_E m^{-3} since 17/12/2014 (Cabinet of Ministers, 2014b) but the available monitoring technologies do not offer measurements with an appropriate measurement range.

Emissions to air

The main emission sources are the retort, the boiler and the charcoal transportation and packaging processes. Three separate measurements are carried out, one in the factory surroundings, another at the boiler stack, and the third at the retort torch.

The point source emission measurements from the boiler stack include the concentration of nitrogen oxides (NO_x), carbon monoxide (CO) and PM in the flue gases. The measured values and the corresponding legislative limits (Cabinet of Ministers, 2013) are gathered in Table 3.

Table 3. Boiler emission review

	NO_x, mg m^{-3}	CO, mg m^{-3}	PM, mg m^{-3}
Emission limits for average combustion plants up to 10 MW, solid fuels (biomass)*	600	2,000	1,000
Measurement results	12 ± 2	2,260 ± 300	76 ± 8

* the values are indicative as the regulations govern biomass boilers starting from 5 MW. The nominal capacity of the boiler used in the charcoal factory is 1 MW.

The boiler emission evaluation indicates that while its environmental performance is tolerable the high concentration of CO in the stack gasses indicate high losses of energy content as it could still be further reduced to carbon dioxide (CO_2) and return valuable heat. General boiler efficiency improvements are strongly advisable.

The point source emissions measured from the charcoal production retort include CO_2, CO, NO_x, and the total VOS's. The measurements at the retort presented several significant obstacles. First of all the construction of the technology does not offer a place for a proper measurement (considering the pipe diameters before and after the measurement point with a stabilised gas flow), secondly the effluent gases before ignition in the torch contain different tars and water droplets that can be harmful for the measurement equipment, and thirdly some of the measured parameter values do not match the equipment measurement ranges (the gas flow rate is detected to be smaller than the minimum value of the equipment measurement range, the total VOC concentration exceeds the concentration accepted by the qualitative analysis of the VOC). This leads to the measurements being made 0.1 m from the top of the torch. Thus the measurement values characterise partly burnt effluent gasses. After the measurement point a complete combustion takes place, as the combustion process is well oxygenated. The measurement values are presented in Table 4.

Table 4. The measured parameter values at the retort

Parameter	Value and the uncertainty
CO_2, vol.%	2.8
CO, mg m^{-3}	1,940 ± 600
NO_x, mg m^{-3}	82 ± 14
total VOC, mg_C m^{-3}	650 ± 20

The emissions from the point source of the retort are not directly regulated, but are subjected to the Natural resource tax according to (The Saeima, 2005). According to EPA (1995) the combustion of the effluent pyrolysis gases reduces the emissions for at least 80%.

The air quality measurement samples at the surrounding area that characterises the influence of the point sources to the surrounding areas are taken in a 2 m height at the measurement locations from p.3. to p.5. The emissions from charcoal handling and packing are included in the overall surrounding emissions and are not measured separately. The measured parameters are the particulate matter (PM), and the qualitative and quantitative analysis of the VOC. The measurements are carried out according to the wind direction. The meteorological conditions during the measurements: air temperature +2 °C, wind velocity 0.8 m s^{-1}, air relative humidity 60%, atmospheric pressure 763 mmHg. The measurement period includes the loading of the firewood in to the trolley and retort, product handling, screening and conveying to the packing line.

The PM measurement results according to the particulate size are described in Table 5.

Table 5. Measurement results for the PM in air

Measurement No	PM_{10}, μg m^{-3}	$PM_{2.5}$, μg m^{-3}	PM_{total}, μg m^{-3}
1	-	-	650
2	-	11	665
3	22	21	78

A similar disagreement as in the odour measurements is met here, because the accredited laboratory offers only the measurement of the total PM while the legislation regulates the permissible levels of PM_{10} and $PM_{2.5}$ with the according values of 40 (for the annual calculation period) and 25 μg m^{-3} (Cabinet of Ministers, 2009). Thus additional measurements (No 2 and 3) are carried out by the authors to evaluate the regulated sphere. The results fall within the regulatory limits.

The qualitative analysis of VOC's in the surrounding air indicates the presence of the following elements:

- ✓ acetone
- ✓ benzene
- ✓ toluene
- ✓ p-Xylene
- ✓ 1,3,5- trimethyl-benzene
- ✓ naphthalene
- ✓ nonanal
- ✓ decanal

The quantitative VOC analysis report a total concentration of 0.3 mg m^{-3} with a 0.2 mg m^{-3} uncertainty (Cabinet of Ministers, 2009). From the above list the Latvian legislation regulates only the weekly concentration of toluene with the value of 0.26 mg m^{-3}. It can be assessed that this threshold is not exceeded as the total concentration includes additional seven elements and it is doubtful that toluene would compile the largest share. Though some improvements should be introduced to the measurement uncertainty boundaries to indorse this statement.

CONCLUSIONS

The study carried out for experimental operation of a real life charcoal factory gives a great example of a successful collaboration of a private company and a scientific institution. An accredited laboratory was involved as a third party, on the one hand attracting an independent third party to perform the measurements give more credible results while on the other hand poses some difficulties in the compliance with the experimental design.

The discussed results indicate that a modern charcoal production facility can be sustainable and without a significant environmental impact in sense of its emissions. However some deeper environmental performance evaluation could take place with the availability of measurement equipment with a wider measurement range, higher precision and more suitable for measurements in a charcoal factory. Also additional research could be performed with a wider perspective evaluating the sustainability impact from biomass use for carbonisation, as the historical charcoal use lead to an extensive reduction of forest area and is still connected with deforestation in some locations. Introduction of a lower grade biomass for charcoal production and the consequent changes in the environmental performance of the factory should be studied.

This far the research gives a good perspective for the development of a sustainable charcoal production sector in Latvia. It is important to remember though that the overall environmental performance of every specific facility is highly influenced by the individual management of the company, but the available technology offers a possibility for a production that can fulfil the environmental requirements. The results were also presented to the Ministry of Environmental Protection and Regional Development of the Republic of Latvia in order to provide a scientific background for decision-making.

ACKNOWLEDGEMENTS. The work has been supported by the National Research Program ‘Energy efficient and low-carbon solutions for a secure, sustainable and climate variability reducing energy supply (LATENERGI)’.

REFERENCES

Bhander, G., Hutson, N., Rosati, J., Princiotta, F., Pelt, K., Staudt, J., Petrusa, J. 2014. GHG mitigation options database (GMOD) and analysis tool. *International Journal of Greenhouse Gas Control* **26**, 1–8.

Cabinet of Ministers 2002. No.34 Terms of emissions of pollutants in water. *Latvijas Vēstnesis* **16** (2591).

Cabinet of Ministers 2009. No.1290 Air Quality Regulations. *detection methods as well as the procedures for restricting the spread of odors* **182**(4168).

Cabinet of Ministers 2013. No.187 Procedures for preventing, limiting and controlling air pollutant emissions from incinerators. *Latvijas Vēstensis* **73**(4879).

Cabinet of Ministers 2014a. No.16 Noise Assessment and Management Procedures. *Latvijas Vēstnesis* **16**(5075).

Cabinet of Ministers 2014b. No.724 Regulations on detection methods as well as the procedures for restricting the spread of odours caused by a polluting activity. *Latvijas Vēstensis* **250** (5310).

Department of Energy & Climate Change 2014. *Methodology for the Sampling and Analysis of Produced Water and Other Hydrocarbon Discharges*, London, 97 pp.

Elyounssi, K., Collard, F.-X., Mateke, J.N., Blin, J. 2012. Improvement of charcoal yield by two-step pyrolysis on eucalyptus wood: A thermogravimetric study. *Fuel* **96**, 161–167.

EPA Environmental Protection Agency 1995. *Emissions Factor Documentation for AP–42 Section 10.7 Charcoal*, 29 pp.

Ooi, T.C., Thompson, D., Anderson, D.R., Fisher, R., Fray, T., Zandi, M. 2011. The effect of charcoal combustion on iron-ore sintering performance and emission of persistent organic pollutants. *Combustion and Flame* **158**, 979–987.

Pubule, J., Kamenders, A., Valtere, S., Blumberga, D. 2014. Cleaner production in biowaste management. *Agronomy Research* **12**(2), 575–588.

Schmidt, H. P., Abiven, S., Kammann, C., Glaser, B., Bucheli, T., Leifeld J. 2012. *European Biochar Certificate, Guidelines for biochar production*. 18 pp.

Smith, P., Bustamante, M., Ahammad, H., Clark, H., Dong, H., Elsiddig, E.A., Haberl, H., Harper, R., House, J., Jafari, M., Masera, O., Mbow, C., Ravindranath, N.H., Rice, C.W., Robledo Abad, C., Romanovskaya, A., Sperling, F., and Tubiello, F. 2014. Agriculture, Forestry and Other Land Use (AFOLU). In Edenhofer O., Pichs-Madruga R., Sokona Y., Farahani E., Kadner S. et al. (eds): *Climate Change 2014: Mitigation of Climate Change. Contribution of Working Group III to the Fifth Assessment Report of the Intergovernmental Panel on Climate Change*, Cambridge University Press, Cambridge, UK and NY.

The Saeima 2005. Natural Resources Tax Law. *Latvijas Vēstnesis* **209** (3367).

UNEP 2000. *Update report by the technology and economic assessment panel on alternatives for ozone-depleting substances used to extract oil and grease from water*. Ouagadougou.

Vertes, A.A., Qureshi, N., Blaschek, H.P. Yukawa, H. 2010. *Biomass to Biofuels: Strategies for Global Industries*. John Wiley & Sons, Hoboken, 559 pp.

Victor, D.G., Zhou, D., Ahmed, E.H.M., Dadhich, P.K., Olivier, J.G.J., Rogner, H-H., Sheikho K., and Yamaguchi M. 2014. Introductory Chapter. In Edenhofer, O., Pichs-Madruga R., Sokona Y., Farahani E., Kadner S. et al. (eds.): *Climate Change 2014: Mitigation of Climate Change. Contribution of Working Group III to the Fifth Assessment Report of the Intergovernmental Panel on Climate Change.* Cambridge University Press, Cambridge, UK and NY.

Agronomy Research **13**(2), 520–525, 2015

Methodology of demand side management Study course. experience of case studies

T. Prodanuks* and D. Blumberga

Riga Technical University, Faculty of Power and Electrical Engineering, Institute of Energy Systems and Environment, Azenes street 12-K1, LV1043 Riga, Latvia; *Correspondence: toms.prodanuks_1@rtu.lv

Abstract. The role of environmental and energy security issues due to political issues are increasing and this stimulates governments to review sustainable energy strategies. One of the ways to reach the targets set by many countries for cuts in greenhouse-gas emissions, free competition and security of supply is energy efficiency. Energy efficiency can be achieved by demand side management (DSM) programs. DMS requires regular and intensive work with energy users and it makes a platform for introduction of DSM strategies in engineering education. The paper discusses the integration models of DSM in the engineering education, analyses the components significant for ensurance of sustainable engineering education and energy efficiency and climate change targets. Based on analysis a methodology for of integration of DSM is developed.

Methodology shows how to introduce environmental specialists, students and municipality employees with demand side management in public buildings and how to evaluate efficiency of such integration. Methodology is analysed through several case studies and conclusions and recommendations developed.

Key words: energy efficiency, energy audits, study program.

INTRODUCTION

Environmental and energy security issues are becoming more and more actual for politicians. Governments are looking for solutions to develop energy policies that can help reduce carbon emissions and increase energy security. One of the ways to reach targets is energy efficiency (Bergaentzlé et al., 2014).

Energy efficiency directive (2012/27/EU) determines that in 2020 there should be 20% increase in energy efficiency. (European Parliament, 2012) This means that member states have to look for solutions. One of the solution is demand side management (DSM) programs.

The term ‘demand side management’ (DSM) was first minted by Clark Gellings (Electrical Power Research Institute, USA) in 1894, where he gives the definition. ‘Demandside management (DSM) is the planning and implementation of those electric utility activities designed to influence customer uses of electricity in ways that will produce desired changes in the utility’s load shape. While the objective of any DSM activity is to produce a loadshape change, the art of successful implementation and the

ultimate success of the program rests within the balancing of utility and customer needs' (Gellings, 1985).

DSM consists of three main categories: DSM policies, DSM implementers and DSM categories. DSM Categories includes energy efficiency (efficiency, conservation), demand side response (price-based, incentive payment-based) and on-site buck-up (generation, storage). DSM policies can be regulatory, market-based, voluntary and financial. DSM implementers are utility, customer, network operator, aggregator and government (Strbac, 2008; Warren, 2014).

Energy Efficiency Plan 2011 reports that the greatest potential for energy savings are energy intensive buildings, especially in public buildings. Higher energy efficiency can be achieved by overlooking public spending, renovation of public buildings, energy performance contracting and implementing energy efficiency on the ground (European Commission, 2011; Annunziata et al., 2014).

To use DSM for increasing energy efficiency to reach Energy Efficiency directives' (2012/27/EU) goals needs specialists with knowledge in DSM. In this paper a new methodology of practical work in DSM study course is developed and tested in Riga Technical University, Institute of Energy Systems and Environment.

METHODOLOGY

Algorithm of methodology for course paper includes 10 modules, see Fig. 1, from which the most important are selection of object, electricity data collection and processing as well as analysis of results and suggestions reduction of energy consumption in the object.

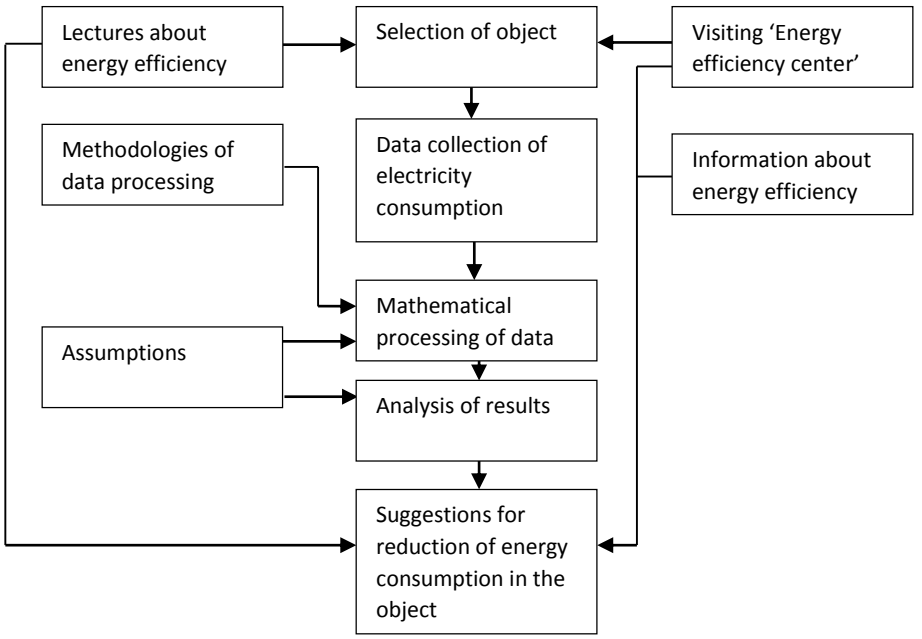

Figure 1. Methodology of practical work in DSM study course.

At the beginning, it is important to give basic knowledge about energy, energy efficiency, energy consumers and consumer's habits. In European Union energy consumption is distributed in five sectors, which are transport, household, industry, service and agriculture (Eurostat, 2014). Based on these sectors, draw up topics in lectures. After lectures students must have understanding about the existing situation, problems and possible solutions for increasing energy efficiency in each sector. Lectures about consumer's habits and equipment, that measures electricity consumption, need to be given too, so students are fully ready for practical part of course and they can give suggestions to reduce energy consumption.

To get better understanding about energy efficiency students visit 'Energy Efficiency Center'. There is possible to get to know energy efficient appliances and get practical advices from specialists about their usage. The resulting information from Energy Efficiency Center also can help in the end of practical work, where suggestions have to be given to increase energy efficiency.

To choose an object need to consider how easy will be data collecting. That is why it is recommended to choose an object that student knows. Students was obligated to choose a public building, because it there is the biggest potential to increase energy efficiency (European Commission, 2011). Students were recommended to choose the school where student studied before. It is a building, which student knows well enough and also knows people who work there, what can make course paper easier to write, because data will be easier to collect.

Data collection is a part of practical work, when students go to an object and do research. The object must been visited at least twice or even more. Data collection is divided in two parts. In the first visitation goal is to collect electric energy bills for last three years, so energy consumption is clear. As well in the first visitation form needs to be given to teachers and administrative staff to know time of every device and light system usage. Questions about usage time must be divided in summer time and winter time, work days and holidays. The second visitation is about collecting forms, measuring power of every device in the object and counting lighting units. Lighting units have to be subdivided by their power. Power of devices can be measured by plug-in power meter that shows momentary power.

Collected data must be mathematical processed. Power and time usage data of device need to be processed by simple formula.

$$Q_{el} = P \cdot t \tag{1}$$

where: Q_{el} – electrical energy consumption, kWh; P – power, kW; t – time, h.

To get electric energy consumption of device or lighting unit, its power and usage time must be multiplied. Usage time must be given in hours per year, so it is possible to compare consumption later. Choosing data for theoretical energy consumption, it is necessary to consider the most trustable data for calculation of year consumption. In some month there can be reconstruction works or different condition that increases electric energy consumption that is why they should not be considered.

To analyze results of theoretical and practical electric energy consumption, data must be compered. The result of electric energy consumption in both data collecting ways must be close, divergence about 5%. It shows that practical work has been done

well. If there is bigger divergence, collected data chosen in calculation must be reconsider. Very important part of analyzing results is trend line empirical model. It is necessary to choose independent and dependent variables, and analyze correlation between them.

After analyzing results students give suggestions for reduction of electric energy consumption. Lectures, visitation to 'Energy efficiency center' and information about electric efficiency from other sources should help them offer some DSM programs.

TESTING OF METHODOLOGY

Methodology was tested in Riga Technical University in Institute of Energy Systems and Environment. During study course of DSM, students were obligated to draft practical work. In this chapter one specific case study is examined.

Methodology was verified in Kandava Karlis Milenbahs Secondary School (Fig. 2). It is located in small town in Latvia. The school was built in 1978 and it is has not been renovated, except replacing all windows from 2001 to 2005. In October 2013, there were working 41 teachers, 13 administrative staff and studying 432 students. The building is made of four floors, basement and gym. It is made of white and red bricks and consists of classrooms, rooms for teachers and staff, dining room, workroom, assembly hall and shooting gallery. Rooms can be divided in two groups, which have undergone refurbishment work and which have not. Refurbishment work includes new lighting system and classroom equipment.

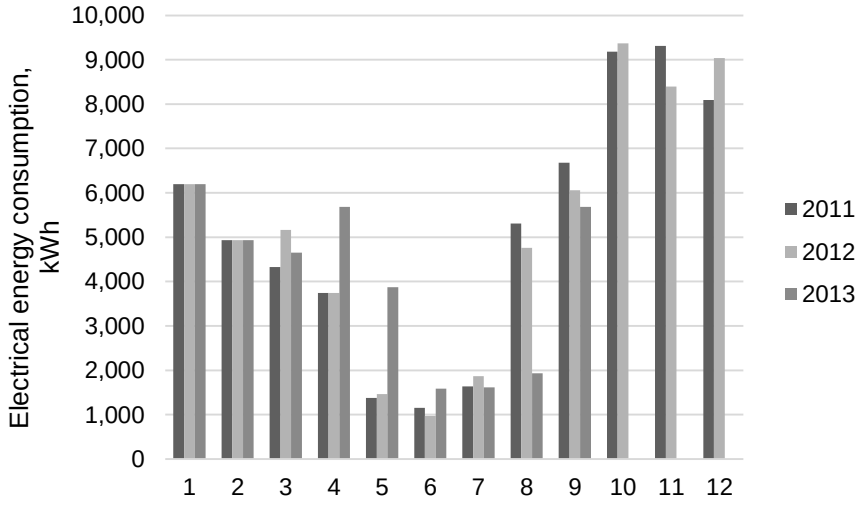

Figure 2. Electrical energy consumption in Kandava K. Milenbahs Secondary School.

To collect data there were three visitations in the object. In the first visit, energy consumption data for three past years were collected. In the building there are three energy meters, but for data processing were used two energy meters, because one shows energy consumption only in dining room. DSM in dining room was not included in practical work tasks. Month data from two energy meters were counted together and

compared with other month. Some month data were not available; therefore these data were assumed the same with energy consumption data in specific month, previously year. There were no data for last three month in 2013, because practical work was taking place in October 2013.

The first part of the second and third visitation was about counting every electric device in the building measuring its power and counting every lighting unit and defining its power. The second part of this visitation was about to survey the habits of people that uses devices. The aim was to get information about how many hours they use definite electric device and lights. There is one responsible person in the each room, who knows how long each device or light unit is used per day.

RESULTS

After getting all data from the second part, it was possible to calculate practical energy consumption per year, which was 59,212 kWh. To get this number there had to multiply each electric device's power and usage time in hours per year and had to do the same with lighting units.

Analysing results of energy consumption per month, on April and May there is big difference between 2013, 2011 and 2012. Interviewing the responsible person for reasons, it was told, that in 2013 on April and May there have been refurbishment works. After analysing all aspects of collected data, it was decided to compare theoretical energy consumption per year in 2012, which was 61,983 kWh with practical data which have been calculated after the second part of visitations. Difference between practical and theoretical energy consumption is 2,771 kWh (per year)$^{-1}$. Mistake could be occurred because of incorrect usage time or incorrect assumed power of device which was not measureable. To see how lighting system affects electrical energy consumption night-time in workdays and energy consumption per month were analysed with correlation. Results show that correlation is big in this Case.

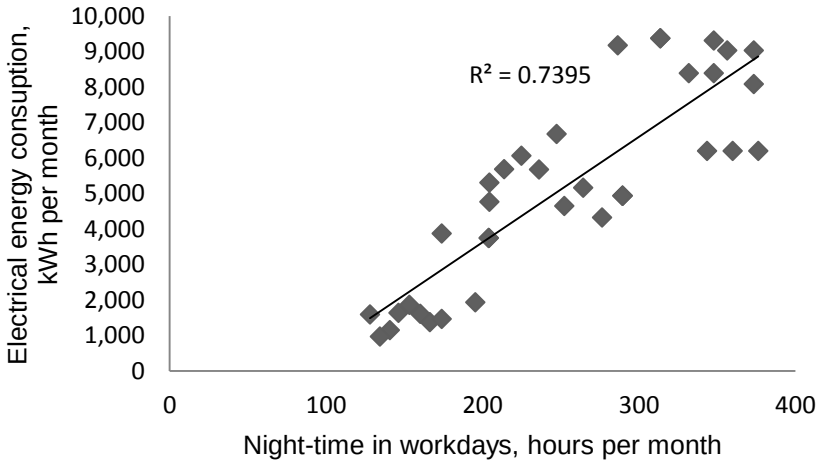

Figure 3. Energy consumption trend line of school.

Lights take 67% of all energy consumption and correlation between energy consumption and night-time in workdays is $R^2 = 0.7395$ in this building that is why necessary to draw a biggest attention to this part to save energy (Fig. 3). The first suggestion is to change all light bulbs to more energy efficient ones. The second suggestion is to buy desk lamps for class rooms, because part of the time when all lamps are on in the class room, teacher is there alone, without students. There is no need to turn on all lights in room, only to be comfortable around working place. The third suggestion is to inform students, teachers and administrative staff about the energy efficiency and plans in DSM.

CONCLUSIONS AND DISCUSSION

Results after testing methodology shows, that following given methodology student is able to choose an object, collect data, analyze them and give useful suggestions to increase energy efficiency. Practical duties allow to forecast the usefulness of the energy efficiency activities and to define the possible acquisitions, not only to analyze the existing situation. The methodology of the established course can be used by various range of municipality and industrial companies' specialists and engineering.

Looking to advantages of this methodology, going through all modules gives broad knowledge. This methodology doesn't require very deep knowledge in mathematics, but it is based on data analyze.

ACKNOWLEDGEMENTS. The work has been supported by the National Research Program 'Energy efficient and low-carbon solutions for a secure, sustainable and climate variability reducing energy supply (LATENERGI)'.

REFERENCES

Annunziata, E., Rizzi, F., & Frey, M. 2014). Enhancing energy efficiency in public buildings: The role of local energy audit programmes. *Energy Policy* **69**, 364–373.

Bergaentzlé, C., Clastres, C., & Khalfallah, H. 2014. Demand-side management and European environmental and energy goals: An optimal complementary approach. *Energy Policy* **67**, 858–869.

European Commission 2011. Energy Efficiency Plan, Brussels, pp 16.

European Parliament 2012. Directive 2012/27/EU of the European Parliament and of the Council of 25 October 2012 on energy efficiency. *Official Journal of the European Union Directive*, pp. 1–56.

Eurostat 2014. Consumption of energy *2012*, *pp.* 1–8.

Gellings, C.W. 1985, The concept of demand-side management for electric utilities. *Proceedings of the IEEE* **73**(10), 1468–1470.

Strbac, G. 2008.Demand side management: Benefits and challenges. *Energy Policy* **36**, 4419–4426.

Warren, P. 2014. A review of demand-side management policy in the UK. *Renewable and Sustainable Energy Reviews* **29**, 941–951.

Agronomy Research **13**(2), 526–532, 2015

Application of industrial wastes in renewable energy production

K. Rugele[1,2,*], G. Bumanis[3], L. Mezule[1], T. Juhna[1] and D. Bajare[3]

[1]Riga Technical University, Faculty of Civil Engineering, Department of Water Engineering and Technology, Kalku 1, LV1047 Riga, Latvia
[2]Riga Technical University, Faculty of Materials Science and Applied Chemistry, Institute of General Chemical Engineering, Kalku 1, LV1047 Riga, Latvia,
[3]Riga Technical University, Faculty of Civil Engineering, Department of Building Materials and Products, Kalku 1, LV1047 Riga, Latvia
[*]Correspondence: kristine.rugele@rtu.lv

Abstract. This research focuses on the industrial waste application as raw materials to create composite material and its characterisation for their possible application in anaerobic digestion. As the limitation of effective biogas digestion process is associated with inhibition of the some elements and acidification of biodegradable organic matter, therefore a highly porous alkaline composite material was evaluated in this research as buffer capacity increasing material. Batch experiments were provided with composite material additive in anaerobic digesters. Results indicate that alkaline composite materials in anaerobic digesters treated acidic whey could increase BMP up to 22%, but pH value could be kept in the optimal range (7.2–7.4) to ensure the effective digestion process.

Key words: biogas, anaerobic digestion, alkaline composite material.

INTRODUCTION

The use of industrial waste to produce energy and reduce environmental pollution is a very attractive topic. Whey is the most important waste and pollutant in dairy industry. Despite the high potential for waste reduction and energy production, anaerobic digestion is not widespread in the dairy industry (Chatzipaschali et al., 2012). This is largely due to the problem of slow reaction rates which require long hydraulic retention time (HRT) and poor process stability (Rugele et al., 2013). However, the treatment of whey by anaerobic digestion is a solution to minimise the environmental impact and, at the same time, convert waste into energy, which could be further consumed in production process (Siso, 1996).

The amount of industrial waste is growing, which makes recycling possibility a very significant challenge nowadays. More than 3,760 t of glass fibre waste and 100 t of metal manufacturing waste were disposed in landfills in Latvia in 2012. However, diverting non-hazardous industrial and manufacturing by-products to recycling saves disposal costs and preserves natural resources by decreasing the demand for virgin materials. Alkali activated composite matrices (CM) or geopolymers could be created from wide group of alumina and silica contained waste. Geopolymers are similar to zeolites in chemical composition, but they reveal an amorphous microstructure, which

are forming by the co-polymerisation of individual alumino and silicate species, which originate from the dissolution of silicon and aluminium containing source materials at a high pH in the presence of soluble alkali metal silicates. It has been shown before that geopolymerisation can transform a wide range of waste alumino-silicate materials into building and mining materials with excellent chemical and physical properties (Xu et al., 2000). During the production of CM, reutilization of industrial waste materials takes place, thus, making the technology environmentally friendly.

The use of industrial waste and food industry residues to produce energy is a new challenge in our recycling society and creates a novel point of view in 'waste to energy' topic. The potential use of alkali-releasing composite materials from industrial wastes for pH control within the anaerobic treatment process of whey was evaluated in this study. The alkali-releasing material was produced from aluminium and glass fibre production waste since it has the potential for long term pH stabilization and can act as a support for microorganism immobilisation (Ruģele et al., 2014).

MATERIALS AND METHODS

Composite matrices (CM)

CM consisted of alumina and silica rich materials and was activated by modified sodium silicate solution. Porous composite matrices used for stabilization of pH during anaerobic digestion process was created from aluminium scrap recycling waste (ASRW), silicate glass (SG) and metakaolin (MK). MK and aluminium scrap recycling waste was used as alumina source in CM. MK, SG and sodium silicate solution was the silica source. The alkali source was sodium silicate solution and SG. The chemical composition of raw materials is given in Table 1 and it was determined according to LVS EN-196-2 with sensibility ±0.5 w%.

Table 1. Chemical composition of raw materials

Chemical component	ASRW (w%)	MK (w%)	SG (w%)
Al_2O_3	63.19	51.7	1.03
SiO_2	7.92	34.4	68.07
CaO	2.57	0.09	1.39
SO_3	0.36	–	–
TiO_2	0.53	0.55	–
MgO	4.43	0.13	–
Fe_2O_3	4.54	0.53	0.19

The metakaolin (MK) was generated in the Material research laboratory of Institute of Materials and Structures (RTU) by calcination of commercial kaolin clay containing minor quartz impurities. Calcination of kaolin clay was carried out at 800 °C in an air atmosphere rotary furnace for approximately 30 min in maximum temperature. MK was ground in the laboratory planetary ball mill Retsch PM 400 for 30 min with speed 300 rpm. Specific surface area of ground MK was 15.86 $m^2 g^{-1}$ (detected by BET method, Nova 1200 E-Series, Quantachrome Instruments), but effective diameter of MK particles was 743.1 nm (detected by Zeta potential, 90 Plus and MAS ZetaPALS Brookhaven Instruments). The crystalline layer structure, which is a common characteristic of clay

minerals, had a fine particle size (1–3 μm) and plate like morphology (detected by SEM, TESCAN Mira\LMU Field-Emission-Gun). According to XRD analyses (Rigaku Ultima+) the produced MK was largely amorphous, with a small quantity of quartz (SiO_2) as an impurity phase and low amount of kaolin.

The sodium silicate solution was created from sodium silicate solution ($Na_2SiO_3 + nH_2O$) and sodium hydroxide (NaOH, purity 97%) to increase alkalinity of solution.

Mixture design of CM was calculated with the SiO_2/Al_2O_3 mass ratio 1.8 and SiO_2/Na_2O – 3.67, Na_2O/Al_2O_3 – 0.5 respectively. The porous structure of CM develops from gasses which are released from aluminium scrap recycling wastes mixed with sodium silicate solution. Material was moulded in 40 x 40 x 160 mm moulds. After expansion of the green material it was cured at temperature 80 °C for 24 h.

After demoulding physical properties, such as density, water absorption, open and total porosity were determined for CM in accordance with EN 1097-6 and EN 1097-7. Mechanical properties were determined according to LVS EN 1015-11.

Alkalinity is defined as a measure of the buffering capacity of water to neutralize acid. High alkalinity in water indicates increased buffering capacity. Buffer capacity was tested for 3 days old CM by immersing cubical specimens (weight 3.5 ± 0.5 g) in deionized water and measuring the alkalinity dynamics within 30 days. Samples were moved to a new bath with deionized water (100 ml) each 24 h. pH of water solution was determined and alkalinity was calculated with strong acid-strong base titration method. The pH at the equivalence point for this titration was 7.0.

For anaerobic digestion in batch experimental setup CM granules with size 2/4 mm and 4/8 mm were prepared.

Cheese whey and inoculum

The cheese whey was supplied by a dairy product manufacturer 'Vecsiljani Ltd' (Latvia). The inoculum was supplied by a municipal waste water treatment plant. Prior experiments the inoculum was kept at 37 °C for 2 days to stabilize the microorganisms. The characteristic values of chemical analysis of the cheese whey and inoculum used are presented in Table 2. Whey sample had a high level of TS (total solids – 6.48%) and VS (volatile solids – 5.89%). Whey at the same time showed to be a high strength organic substrate – COD (chemical oxygen demand) value was as high as 58.8 g O_2 L^{-1}, whereas the main organic component was lactose contributing to 4.2% of the total mass.

Table 2. Chemical composition of raw materials

Parameter	Inoculum	Whey
pH (20°C)	–	6.48
total solids (% w w^{-1})	5.78	5.89
volatile solids (% w w^{-1})	4.35	5.25
COD_{total} (g O_2 L^{-1})	–	58.8
ash (%w w^{-1})	0.87	0.69
protein (% w w^{-1})	–	0.5
lactose (%w w^{-1})	–	4.2
fat (% w w^{-1})	–	0.05

Experimental setup

Batch experiments were carried out in glass reactors with working volume of 100 mL. Prepared CM granules were added at the beginning of the experiment without any previous pH correction. Whey concentration was 15%. The reactors were incubated at 37 ± 0.5 °C. The mass ratio between CM granules and VS of substrate were constant 0.6 (g_{AAM} g^{-1} $_{VS}$).

Dilution process or any other pre-treatment of whey was not used. During the experiments the biogas production and gas content was controlled after each 12 hours.

The TS and VS solids were measured both for the whey and inoculum at the beginning and at the end of the fermentation for each reactor. pH was measured every 48 hours.

For the analysis of anaerobic digestion tests volatile organic fatty acids (VOA) content were measured by titration (FOS/TAC measurements according to Nordmann method) method with 0.1 M H_2SO_4. TS were determined by drying a sample at 105 °C for 24 hours. VS and ash were analyzed at 550 °C in muffle furnace for 150 minutes. COD was analyzed with Hach Lange cuvettes test. The pH was measured using pH-meter Lutron pH-208. Produced methane was measured with syringes contained 3M NaOH. Each sample average of three measurments was performed.

RESULTS AND DISCUSSION

CM characterisation

The most leachable species in CM during titration test are the Na+ and OH- ions from (alkaline) pore water transfer to leachates, and framework dissolution by alkali/H_3O^+ ion exchange (Aly et al., 2008). Under optimal conditions the rate of alkali release would reflect the mobility of the alkalis in the paste. The migration of ions affects pore volume and pore solution composition, both of which affect the amount of alkali being released from the MC.

The initial pH level of water solution with CM granules was 12.5. During the first day immersion 35 to 40% of total OH- amount leached therefore high initial buffer capacity can be ensured. This can be explained by the rapid solution of free alkali layer based on pore walls. After dissolution of basic layer, further OH- leaching decreased and after 16 days it reached a maximum of 0.0108 mol L^{-1} kg^{-1} CM (Fig. 1). Slow alkali leaching after first days can be contributed to the solution of alkalis trapped in micropores and inside the structure of material. The leaching from deeper layers of material was retarded due to closed material structure in the deeper layers. The pH level decreased continuously and at the day 20 it dropped down to pH 10.2. Although the pH level of water solution was still high, the buffer capacity of leachate was low. Thus, to ensure prolonged and effective pH control, the proper dosage of CM must be provided. This value could be defined by the pH decrease in the biogas reactors and, to ensure optional pH level in reactor, proper calculations must be provided.

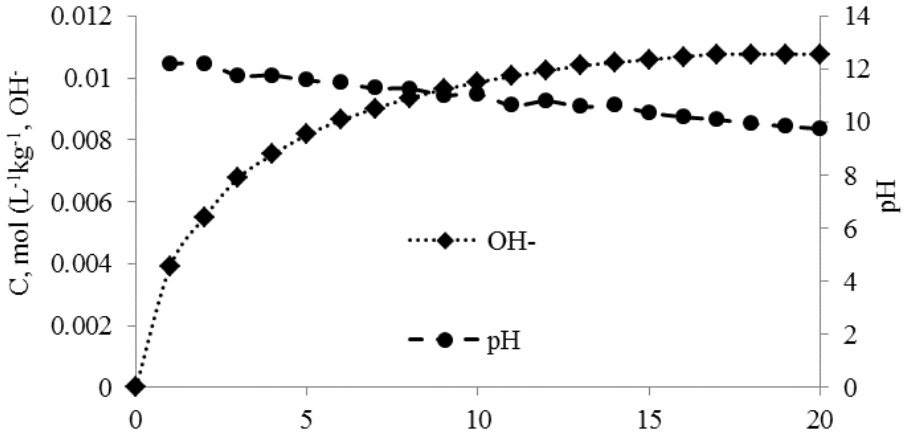

Figure 1. OH^- leaching in water and pH after CM removal.

To confirm that the leachate comes from alkaline crystals on pore surface microstructure analyses of granules were performed (Fig. 2). The granule pore surface was free of alkali layer and confirmed the assumption. SEM micrographs indicated that the CM structure was with more micropores and less solid when compared to granule structure before leaching test and no crystals on CM granule surface was present (Fig. 2B). SEM micrograph after leaching test confirmed the increase of BET surface area by revealing highly porous microstructure of CM after leaching test.

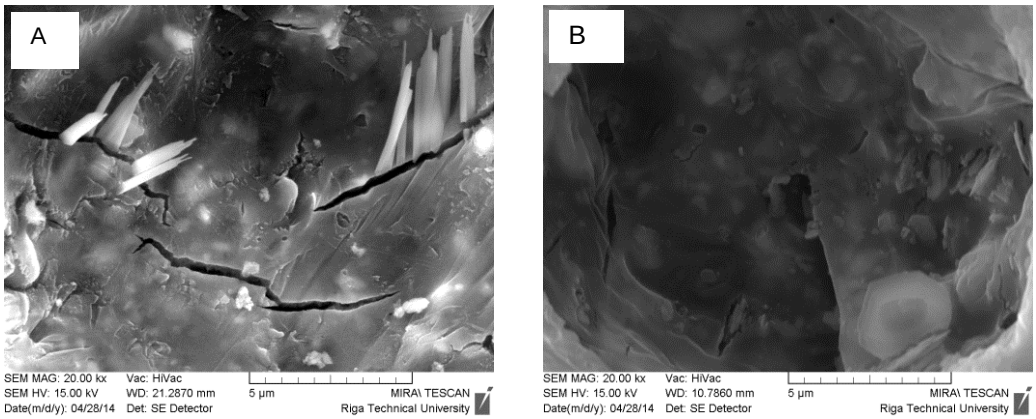

Figure 2. Microphotography of porous CM before (A) and after leaching test (B).

pH level in anaerobic digesters with CM addition

The pH level of batch experiments was analyzed during digestion. Results are showed in Fig. 3. The initial batch pH level at the beginning of test was pH 7.20 ± 0.12. The initial pH level was mainly determined by the amount of whey added to the inoculum. The effect of CM granules on batch pH level was determined. The study showed, that the addition of 0.6g CM g^{-1} VS decreased the pH level to 6.82 ± 0.04 after 24 hours. The digester without CM had a pH of 6.50 ± 0.05. After 3 days pH increased

in the digesters with CM, reaching value 7.58 on the 5th day, later stable pH around 7.20 was observed. At the end of test pH increased till 7.68 ± 0.15. pH not increase higher than 6.80 for the digesters without CM.

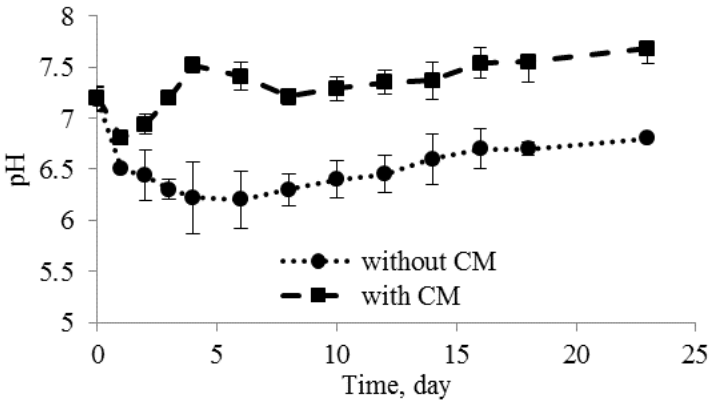

Figure 3. pH values in anaerobic digesters with 15% acid whey and CM addition.

Biochemical methane potential test

According to the methane production cumulative curves it shows that the addition of the CM improves biogas production (Fig. 4). The curve indicates that anaerobic digestion process was not inhibited by the addition of CM and high concentration of whey. In anaerobic digestion without CM added system inhibition was observed for the first ten days and BMP value was 22% lower.

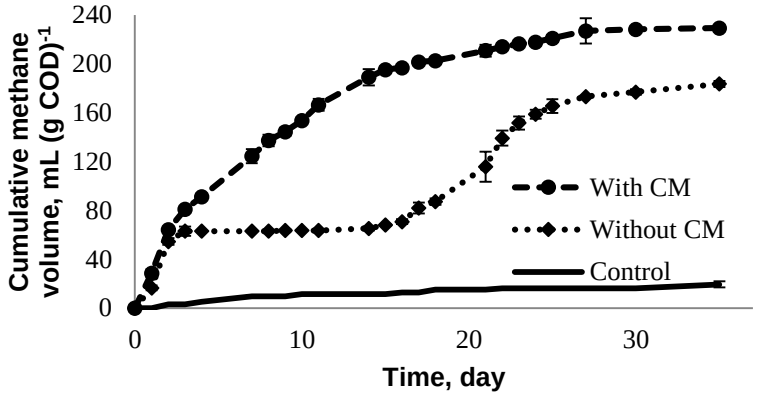

Figure 4. Cumulative methane curves with and without CM addition.

At the end of the experiment much higher VOA amount was observed in the reactors without CM addition, what indicated on process inhibition. Soluble COD showed better substrate degradation rate in reactors with material additive.

Table 3. Results in the end of batch experiment with CM and acidic whey

Sample	BMP, $ml_{CH4}\ g^{-1}$	pH	VOA, g kg^{-1}	VS, g kg^{-1}	COD reduction, %
with CM	328±12	7.68±0.05	1.81±0.07	4.11 ± 1.13	89.8±2.1
without CM	256±32	6.80±0.12	4.37±0.19	4.65 ± 0.44	54.5±3.9
control	15±3	8.20±0.23	0.02±0.003	0.43 ± 0.03	-

Much higher COD reduction (about 35% more) was observed in reactors with added CM, what characterizes a more stable and favourable conditions for the anaerobic microorganisms.

CONCLUSIONS

Effective waste management could be achieved by using alkali activation technology to create alkali activated porous composite matrices, which could be used in anaerobic digestion process to provide conversion of cheese whey into biogas. Highly porous material with alkaline crystals on the pore surface could be obtained and it can be regarded as potential passive pH controlling system in biotechnologies. It was shown that material from recycled wastes could be used as a new progressive material for enhancement of the anaerobic process. The passive pH controlling system increased pH value and ensured active digestion process up to day 15.

ACKNOWLEDGEMENTS. This work has been supported by ESF project 'Involvement of Human Resources for Development of Integrated Renewable Energy Resources Energy Production System', No. 2013/0014/1DP/1.1.1.2.0/13/APIA/VIAA/026.

REFERENCES

Aly, Z., Vance, E.R., Perera, D.S., Hanna, J.V., Griffith, C.S., Davis, J. & Durce, D. 2008. Aqueous leachability of metakaolin-based geopolymers with molar ratios of Si/Al=1.5–4. *J. Nucl. Mater.*, **378**(2), 172–179.

Chatzipaschali, A. & Stamatis, A.G., 2012. Biotechnological Utilization with a Focus on Anaerobic Treatment of Cheese Whey: Current Status and Prospects. *Energies*, **5**(12), 3492–3525.

Rugele, K., Mezule, L., Dalecka, B., Larsson, S., Vanags, J., & Rubulis, J., 2013. Application of fluorescent in situ hybridisation for monitoring methanogenic archaea in acid whey anaerobic digestion. *Agronomy Research* **11**(2), 373–380.

Rugele, K., Bumanis, G., Erina, L. & Erdmane, D., 2014. Composite Material for Effective Cheese Whey Anaerobic Digestion. *Key Eng. Mat.*, **604**, 236–239.

Siso, M.I.G., 1996. The biotechnological utilization of cheese whey: a review. *Bioresour. Technol.*, **57**(1), 1–11.

Xu, H. & Van Deventer, J., 2000. The geopolymerisation of alumino-silicate minerals. *Int. J. Miner. Process.* **59**(3), 247–266.

Agronomy Research **13**(2), 533–538, 2015

Measurement and analysis of temperature changes of ground massif with Slinky heat exchanger

M. Šeďová*, P. Neuberger and R. Adamovský

Czech University of Life Sciences Prague, Faculty of Engineering, Department of Mechanical Engineering, Kamýcká 129, CZ16521 Prague – Suchdol, Czech Republic; *Correspondence: sedova@tf.czu.cz

Abstract. The article is describing temperature changes in the ground massif with Slinky heat exchanger. The exchanger serves as a heat source for a heat pump which is used for cold water warming and a heating of the administration building. The aim of the research is to analyse the influence of the Slinky heat exchanger to the temperature of the ground massif while extracting heat energy at the beginning and during the heating season, as well as beyond it. The temperature process of the ground massif is described near the exchanger, on a reference lot in burial depth of the heat exchanger and also in a depth of 0.2 m. The energy potential of the ground massif was evaluated using the temperature differences of ground massif in the area of the Slinky heat exchanger at the beginning and at the end of the heating season.

Key words: ground massif, heat source, heating season, Slinky heat exchanger.

INTRODUCTION

We live in a time when the use of alternative energy sources gets more and more into the foreground. Heat pumps are devices that can effectively use these resources. It can draw a heat from land, air and water, but it can also utilize a secondary heat. These heat sources for heat pump evaporators are used in both residential and civil construction and in agriculture. They can be used for heating of stables for breeding sows with piglets, fattening of broiler chickens to heat water for technological purposes, drying crops, etc.

In South Korea at the Seoul National University the cost of heating greenhouses was solved (Ha et al., 2011). At the Saint Mary's University in Canada and at the Hokkaido University in Japan the issue of heating water in production ponds, grain drying and pasteurization of milk has been addressed (Tarnawski et al., 2009). At the Geriz University and at the Ege University in Turkey a usage of gas engine driven heat pump during drying of medicinal and aromatic plants was verified (Gungor et al., 2011).

Heat pumps ground – water use two sources of low potential heat energy which is drawn by heat exchangers. There are called rock massif and ground massif (ground massif is the rock to a depth of 2 m). Exchangers are installed vertically or horizontally. It consists of polyethylene pipes of different diameters and lengths. This depends mainly on the required performance.

Vertical heat exchangers are using the internal performance of the Earth using polyethylene pipe in the shape of 'U' in which a cooling medium is flowing (Petráš, 2008). The space in the borehole around the pipes is filled with a suitable material to

provide good contact between the pipe and the massif and to reduce thermal resistance (Florides & Kalorigou, 2007).

Horizontal heat exchangers are mainly using thermal energy that is naturally accumulated in the surface ground massif as a result of the incident solar radiation (Petráš, 2008). With horizontal exchanger the flow of heat is used. Heat comes from above and it is received by upper layer of the Earth from direct and indirect solar energy (radiation, rain, etc.). 98% of the energy draws horizontal heat exchanger from a layer of ground massif that is above it. Only 2% of the energy is taken from the ground massif under the exchanger. This heat exchanger can be considered as a sizable solar collector with low efficiency, which is complemented by a huge heat accumulator (surface) with an annual cycle of charging and discharging.

MATERIALS AND METHODS

Experimental measurements were carried out in Prague - Dolní Měcholupy within the company Veskom spol. s r.o. The altitude of Prague is 258 m. In this area the average temperature during the heating season is 4°C and the outside temperature for calculation is considered -12°C. The measurement of 5 vertical heat exchangers is taking place there, as well as 1 horizontal exchanger and 1 Slinky exchanger. Overall 9 vertical heat exchangers, 2 horizontal exchangers and 2 Slinky heat exchangers are the heat source for heat pumps which are used for water heating and heating of administration building with floor age of 1,480 m^2. Exchangers were put into operation in August 2008.

Slinky heat exchanger was made of polyethylene pipes PE 100RC 32 x 2.9 mm. Slinky with a total length of 200 m is installed at a depth of 1.5 m, 53 coils rolled in a circle. It is not stored in the bed of sand. The ground massif to a depth of 2 m is dark brown sandy-clay loam. In the heat exchanger a cooling liquid mixture of 33% ethanol and 67% water is used. Fig. 1 shows in placement scheme of sensors that measure the temperature of the ground massif.

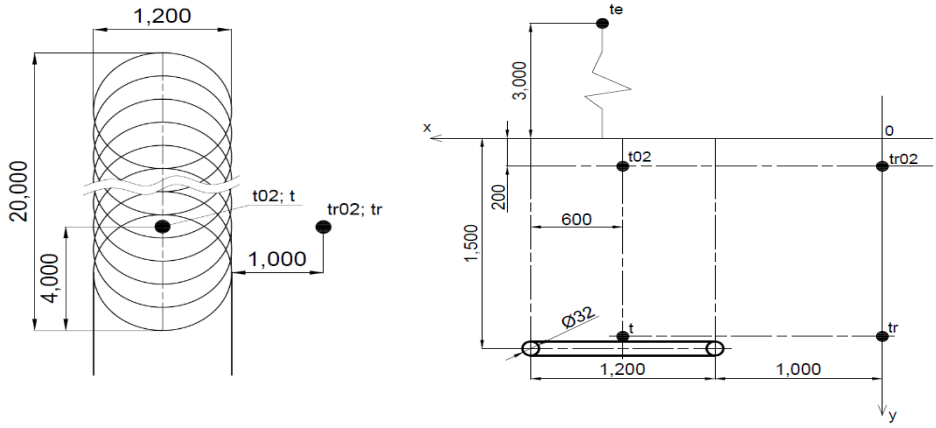

Figure 1. Scheme of Slinky heat exchanger and location of the temperature sensors.

Designation of the temperature sensors is as follows:
t – temperature sensor located at a depth of 1.5 m in the vicinity of the heat exchanger ([°C); t_r – reference temperature sensor located 1.0 m from the heat exchanger

at a depth of 1.5 m (°C); t_{02} – temperature sensor located at a depth of 0.2 m above the heat exchanger (°C); t_{r02} – reference temperature sensor located 1.0 m from the heat exchanger at a depth of 0.2 m (°C); t_e – sensor ambient temperature located at a height of 3.0 m above the surface (°C).

Temperatures of the ground massif and the ambient air are recorded from 1 March 2011 every 15 minutes.

RESULTS AND DISCUSSION

According to Czech legislation heating season lasts from 1 September to 31 May of the following year. Supply of thermal energy is initiated in heating season, when the average daily temperature of outside air in the relevant locality is below 13 °C in two consecutive days and the evolution of the weather cannot be expected to increase the temperature above 13 °C for the following day.

The average daily air temperature t_{ed} is calculated by the Eq. 1:

$$t_{ed} = 0.25 \cdot (t_7 + t_{14} + 2 \cdot t_{21}). \qquad (°C) \qquad (1)$$

where: t_7 – temperature at 7:00 a.m. (°C); t_{14} – temperature at 2:00 p.m. (°C); t_{21} – temperature at 9:00 p.m. (°C).

Fig. 2 shows temperatures of the ground massif at about 3 p.m. and the average daily air temperature in the period from 1 September 2013 to 31 May 2014.

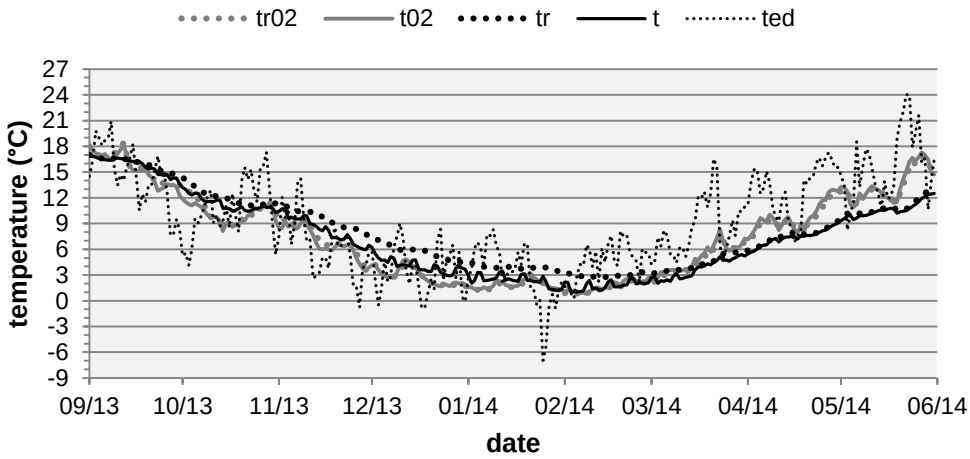

Figure 2. Temperatures of the heating season 2013/2014.

There is only a slight delay of the temperature course of t_{02} at the depth of 0.2 m with respect to air temperatures above the ground massif. A higher delay and a slight reaction to the ambient air temperature were seen for the temperature t at a depth

of 1.5 m. The generally known fact that due to a low value of the coefficient of thermal conductivity of the ground massif and a high specific heat capacity, the amplitudes of temperature changes of the ground massif decrease with the depth of the ground massif when compared to the air temperature above its surface, is valid even during the transfer of the heat flow from the ground massif by the installed heat exchanger. The temperature of the ground massif t_{02} at a depth of 0.2 m above the heat exchanger is influenced particularly by the temperature and speed of the surrounding air, the intensity of incident solar radiation, and falls of rain and snow (Neuberger et al., 2014).

The temperature course of t_{ed} shows that the heating season 2013–2014 lasted from 19 September 2013 to 20 April 2014. In this time period the temperature of the ground massif t gradually decreased from 16.07°C to the minimum value of 0.65°C. This minimum temperature was recorded at 10 a.m. on 5 February 2014. The Eq. 2 in this period is as follows:

$$t = 3 \cdot 10^{-6} \cdot d^{3} - 2 \cdot 10^{-4} \cdot d^{2} - 12.47 \cdot 10^{-2} \cdot d + 15.23. \, (R^2 = 0.979) \quad (°C) \qquad (2)$$

where d – number of days from the beginning of the heating season 2013–2014, i.e. from 19 September 2013.

The minimum temperature difference between the temperature t_r which was measured 1.0 m from the heat exchanger at a depth of 1.5 m and the temperature at a depth of 1.5 m in the vicinity of the heat exchanger t was 0.04 K. The maximum temperature difference was recorded 4 December 2013 with a value of 3.17 K. During the heating season 2011–2012 the lowest temperature of the ground massif t was measured 13 February 2012 (Neuberger et al., 2014). In the season 2012–2013 was this temperature recorded 29 March 2013.

The Eq. 3 of the reference temperature of the ground massif at a depth of 1.5 m t_r has following forms:

$$t_r = 3 \cdot 10^{-6} \cdot d^{3} - 4 \cdot 10^{-4} \cdot d^{2} - 9.79 \cdot 10^{-2} \cdot d + 15.47. \, (R^2 = 0.989) \quad (°C) \qquad (3)$$

where d – number of days from the beginning of the heating season 2013–2014, i.e. from 19 September 2013.

Fig. 2 shows a gradual increase of the temperature of the ground massif t and the reference temperature t_r in the period from 21 April to 31 May 2014. Eq. 4 and Eq. 5 in this time period are as follows:

$$t = 2 \cdot 10^{-4} \cdot d^{3} - 13.4 \cdot 10^{-3} \cdot d^{2} + 34.62 \cdot 10^{-2} \cdot d + 6.87. \qquad (R^2 = 0.969) \quad (°C) \qquad (4)$$

$$t_r = 2 \cdot 10^{-4} \cdot d^{3} - 15.5 \cdot 10^{-3} \cdot d^{2} + 38.11 \cdot 10^{-2} \cdot d + 6.96. \qquad (R^2 = 0.969) \quad (°C) \qquad (5)$$

where d – number of days from 21 April 2014.

In this time period the temperature of the ground massif t gradually increased from 7.58°C to 12.73 °C.

The energy potential of the ground massif was evaluated from temperature differences of the ground massif in the vicinity of the Slinky heat exchanger Δt at the beginning and at the end of the heating season. Table 1. shows temperature differences at the beginning and at the end of four consecutive heating seasons.

Table 1. Temperature differences of the ground massif at the beginning and at the end of heating season

Start of heating season	Date	t(°C)	Δt(K)
2010–2011	30 August 2010	18.40	
			-0.94
2011–2012	30 August 2011	17.46	
			0.2
2012–2013	30 August 2012	17.66	
2013–2014	30 August 2013	16.87	**-0.72**
End of heating season	Date	T(°C)	Δt(K)
2010–2011	1 May 2011	9.8	
			-1.04
2011–2012	1 May 2012	8.4	
			-0.37
2012–2013	1 May 2013	7.67	
2013–2014	1 May 2014	9.36	**1.69**

Temperature differences of the ground massif at the beginning and at the end of heating seasons are within the range of measurement accuracy. These temperature differences shows that ground massif with Slinky heat exchanger, under the climatic conditions and the quantity of heat, can be considered as a stable energy source for heat pumps.

CONCLUSIONS

The course of temperature ted shows that the heating season 2013–2014 lasted from 19 September 2013 to 20 April 2014.

During this time period temperatures of the ground massif at a depth of 1.5 m were higher than temperatures of the ground massif at a depth of 0.2 m. After this time period the situation is reversed. Temperatures of the ground massif at the depth of 0.2 m react to changes of air temperatures.

The temperature of the ground massif t and the reference temperature of the ground massif t_r are described by Eqs. (2) to (5).

The temperature of the ground massif at a depth of 1.5 m in the vicinity of the Slinky heat exchanger during the heating season didn't achieve negative values. The minimum measured value was 0.65 °C.

Temperature differences Δt at the beginning and at the end of heating seasons (Table 1.) did not exceed 2 K.

From results of temperature in the ground massif t at the beginning and at the end of each heating season the ground massif has sufficient potential energy and can be considered as a stable energy source for heat pumps.

ACKNOWLEDGEMENTS. It is the project supported by the IGA 2013 ‘The University Internal Grant Agency’ (Regenerační schopnosti horninového masivu a jejich využití jako zdroje nízkopotenciálního tepla pro tepelné čerpadlo s vertikálním výměníkem).

REFERENCES

Florides, G. & Kalorigou, S. 2007. Ground Heat Exchangers: A Review of Systems, Models and Applications. *Renewable Energy* **32**, 2461–2478.

Gungor, A., Erbay, Z. & Hepbasli, A. 2011. Exergoeconomic Analyses of a Gas Engine Driven Heat Pump Drier and Food Drying Process. *Applied Energy* **88**, 2677–2684.

Ha, T., Lee, I., Hwang, H., Hong, S., Seo, I. & Bitog, J. P. 2011, Development of an Assessment Model for Greenhouse Using Geothermal Heat Pump System. In: *American Society of Agricultural and Biological Engineers Annual International Meeting 2011*. Louisville, pp. 2105–2114.

Neuberger, P., Adamovský, R. & Šeďová, M. 2014. Temperatures and Heat Flows in a Soil Enclosing a Slinky Horizontal Heat Exchanger. *Energies* **7**, 972–987.

Petráš, D. 2008. *Low-temperature heating and renewable energy*. JAGA group, Bratislava, 216 pp. (in Czech)

Tarnawski, V., Leong, W.H., Momose, T. & Hamada, Y. 2009. Analysis of Ground Source Heat Pumps with Horizontal Ground Heat Exchangers for Northern Japan. *Renewable Energy* **34**, 127–134.

V VEHICLES and FUELS

Agronomy Research **13**(2), 541–549, 2015

Influence of butanol and FAME blends on operational characteristics of compression ignition engine

J. Čedík[1,*], M. Pexa[1], J. Mařík[1], V. Hönig[2], Š. Horníčková[2] and K. Kubín[3]

[1]Czech University of Life Sciences Prague, Faculty of Engineering, Department for Quality and Dependability of Machines, Kamýcká 129, CZ16521 Prague 6, Czech Republic; [*]Correspondence cedikj@tf.czu.cz
[2]Czech University of Life Sciences Prague, Faculty of Agrobiology, Food and Natural Resources, Department of Chemistry, Kamýcká 129, CZ16521 Prague 6, Czech Republic
[3]Research Institute of Agricultural Engineering, p.r.i., Drnovská 507, CZ16101 Prague 6, Czech Republic

Abstract. The issue of the use of alternative fuels in diesel engines is discussed in this paper. The purpose is to reduce the dependence of EU Member States on fuels of petroleum origin. One of the possibilities is the use of butanol produced from organic products. The use of pure butanol in diesel engines is not possible. However, it may be used as an additive for fuels of petroleum origin or adding to oil for improving the operating conditions of the engine. Successively 10, 30 and 50% n-butanol was used as an additive. Turbocharged combustion engine of the tractor Zetor 8641 Foretrra was used to the test. This engine was burdened using a dynamometer to the PTO. Performance parameters and fuel consumption of the engine were monitored during measurements. Performance parameters of the engine decreases and fuel consumption increases due to the properties of butanol. Cleansing properties of butanol which restrict carbonization on functional surfaces of the engine seems advantageous.

Key words: Biofuels, power, fuel consumption, combustion engine, butanol, FAME.

INTRODUCTION

According to European Directive 2009/28/EC the target in the field of renewable sources is substitution of 10% energy in transport by energy derived from renewable sources by 2020. In order to reach this target the liquid biofuels are used.

For diesel engines the fatty acid methyl esters are most frequently used. Fatty acid methyl ester (FAME) has a lower mass calorific value, higher density and higher viscosity than diesel (Kučera & Rousek, 2008; Hromádko et al., 2011; Pexa & Mařík, 2014). FAME can be made from vegetable oil and animal fat (Sirviö et al., 2014). The inferior storage and oxidative stability are the main disadvantages of FAME. Another disadvantage of FAME is a high feedstock cost, especially when the vegetable oil is used as a raw material. Using of animal fat, which is currently a waste product, can override this disadvantage (Barrios et al., 2014). Studies show that the internal combustion engine operating on rapeseed methyl ester (RME) achieves lower power by approx. 5–10%, higher fuel consumption and a lower average thermal efficiency by approx. 3.5%, but a

higher thermal efficiency by 3% at maximum load (Hromádko et al. 2011; Soo-Young, 2011; Pexa & Kubín, 2012; Imran et al., 2013; Pexa et al., 2013).

Other biofuels are fuels based on alcohol. Ethanol is the most used alcohol fuel. Ethanol as a fuel for diesel engines is not frequently used due to low cetane number, decreased flash point, worsened lubricity, low energy content, worse miscibility and higher volatility (Kleinová et al., 2011). Butanol is an alternative to the use of ethanol. Butanol has a lower auto-ignition temperature, it is less evaporative and releases more energy per unit of mass. It also has a higher cetane number, higher energy content and better lubricating ability than ethanol and methanol. It is also less corrosive and better miscible with vegetable oils, diesel and FAME. When mixed with diesel or FAME slightly increases specific fuel consumption and lowers the temperature of the exhaust gases because of its lower calorific value in comparison with diesel (Bhattacharya et al., 2003; Doğan, 2011; Yilmaz et al., 2014).

It was found, that butanol/FAME/diesel blends decreases the cetane number and viscosity of the fuel with increasing share of butanol (Wadumesthrige et al., 2010), ,furthermore, these blends increases the specific fuel consumption and reduces harmful emissions (CO, PM, soot) (Sukjit et al., 2012; Zhang & Balasubramanian, 2014). FAME/Butanol blends can lower the combustion temperature and thereby lower the emissions of NO_X and soot (Soloiu et al., 2013).

The purpose of the measurements was to determine the effect of butanol mixed with FAME based on animal fats, to a torque, power and specific fuel consumption of supercharged diesel engine. Due to the characteristics of butanol such as the lower heating value and a lower cetane number the decrease of performance parameters and increase of specific fuel consumption with increasing share of butanol can be expected.

MATERIALS AND METHODS

The measurement was done using the tractor engine Zetor 1204 prefilled by means of turbocharger and placed in the tractor Zetor Forterra 8641. It is in-line 4 cylinder engine, its volume is 4.156 and rated power 60 kW (it is 53.4 kW on PTO according to the measurement made by Deutsche Landwirtschafts-Gesellschaft), the maximum torque is 35l Nm, the nominal specific fuel consumption is 253 g kWh^{-1} and the rated speed is 2200 min^{-1}. The fuel is delivered to the engine by means of mechanical in-line injection pump, injecting is done by one injection with pressure 22 MPa, 12° before top dead center. The operating time of the mentioned engine does not exceed 100 operating hours.

The engine was loaded by the dynamometer AW NEB 400 connected to PTO, torque was recorded by the torque sensor MANNER Mfi 2,500 Nm_2000U min^{-1} with accuracy 0.25%. The torque values recorded by the sensor placed on PTO are converted to the engine torque by means of appropriate gear ratio (3.543). The losses in the gearbox have no effect on the comparative measuring of the influence of fuel on the external speed characteristics of the engine and therefore they are not taken into consideration. The fuel consumption was recorded by means of the flowmeter AIC VERITAS 4004 with measurement error 1%. Data were saved on the hard disk of the measuring computer (netbook), with the use of A/D converter LabJack U6 with frequency 2 Hz, in the form of text file. The programmes MS Excel and Mathcad were used for data evaluation.

As a test fuels 10, 30 and 50%$_{vol}$. mixtures of n-butanol (BUT) and FAME from animal fat were selected. Basic features of both components are shown in Table 1. The density and viscosity of mixed fuels are in Table 2. As a reference fuel the conventional diesel was used (ČSN EN 590).

Table 1. Basic parameters of the fuel components

Fuel	Density (kg m^{-3})	Heating value (MJ kg^{-1})	Viscosity at 40 °C (mm^2 s^{-1})	Cetane number
n-Butanol	810[1] (at 28 °C)	32.5[1]	2.63[3] (3.64 at 20 °C)[2]	17.0[3]
FAME	877[2] (at 17 °C)	39.86[2]	5.07[2]	58.8[2]

[1](Honig et al., 2014), [2](Mařík et al., 2014), [3](Öner & Altun, 2009), [4](Lujaji et al., 2011)

Table 2. Basic parameters of the measured fuels

Fuel	Density at 15 °C (kg m^{-3})	Viscosity at 40 °C (mm^2 s^{-1})
10% BUT 90% FAME	869.9	3.88
30% BUT 70% FAME	860.9	3.28
50% BUT 50% FAME	844.5	2.68

The external speed characteristics of the engine were measured for tested fuels at full engine load. Based on these characteristics, the measuring points were determined for the complete characteristic of specific fuel consumption. The points were selected to cover the whole range of engine load and speed. Subsequently, these points were connected by the polynomial function of the third degree with two unknown variables, using the method of least square error using Mathcad. Then the measuring points of the eight-point NRSC (Non-Road Steady Cycle) test were determined according to ISO 8178-4 (type C1). The test was used for measuring the specific fuel consumption. Specific fuel consumption for the whole NRSC test was calculated according to the equation (1). In every predetermined measurement point the measured parameters were stabilized.

$$m_{NRSC} = \frac{\sum_{i=1}^{8} \left(M_{Pi} \cdot WF_i \right)}{\sum_{i=1}^{8} \left(P_{PTO,i} \cdot WF_i \right)} \quad (1)$$

where: m_{NRSC} – Specific fuel consumption for whole NRSC test (g kWh^{-1}); $M_{P,i}$ – hourly fuel consumption (g h^{-1}); WF_i – weight factor (–); $P_{PTO,i}$ – power on the PTO (kW).

RESULTS AND DISCUSSION

External rotation speed characteristic measured for mixed fuels was created (Fig. 1). It can be seen that the highest performance parameters from mixed fuels achieves fuel containing only 10% butanol which caused 16.4% decrease of maximum torque and 18.6% decrease of maximum engine power compared to the diesel. Higher concentrations of butanol (30 and 50%) cause a noticeable decrease in maximum power and torque compared with 10% BUT. Loss of maximum engine power for 30% BUT is approximately 8.6% and for 50% BUT approximately 10% compared with 10% BUT. The decrease of the maximum engine torque was 11.1% for 30% BUT and 13.6% for 50% BUT compared with 10% BUT.

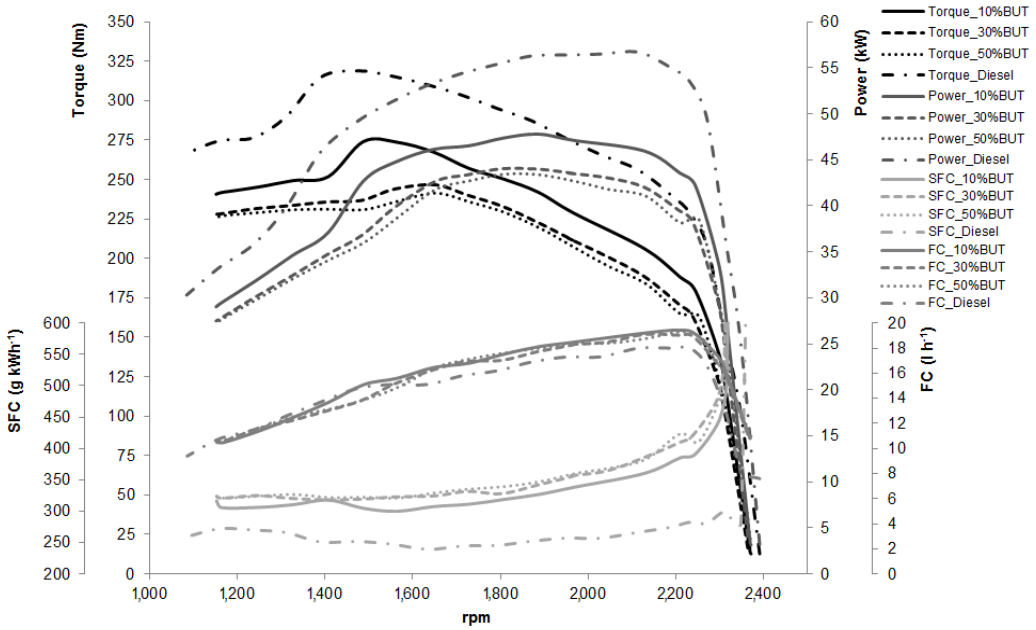

Figure 1. The external rotation speed characteristics for measured fuels (SFC – specific fuel consumption, FC – fuel consumption).

The large decrease of the maximum torque and the engine power (Table 3) is caused on the one hand by the low calorific value of n-butanol an FAME and on the other hand by the low cetane number of butanol (Table 1).

Complete characteristics of specific fuel consumption for each variant were created (Figs 2, 3, 4). From the complete and external rotation speed characteristics the minimums of the specific fuel consumption were determined. Compared with the diesel an 25.3% increase of min. specific fuel consumption can be seen for fuel containing 10% BUT. In comparison with 10% BUT the minimum specific fuel consumption for 30% BUT was higher by approx. 5.7% and for 50% BUT by approx. 6.5% (Table 3).

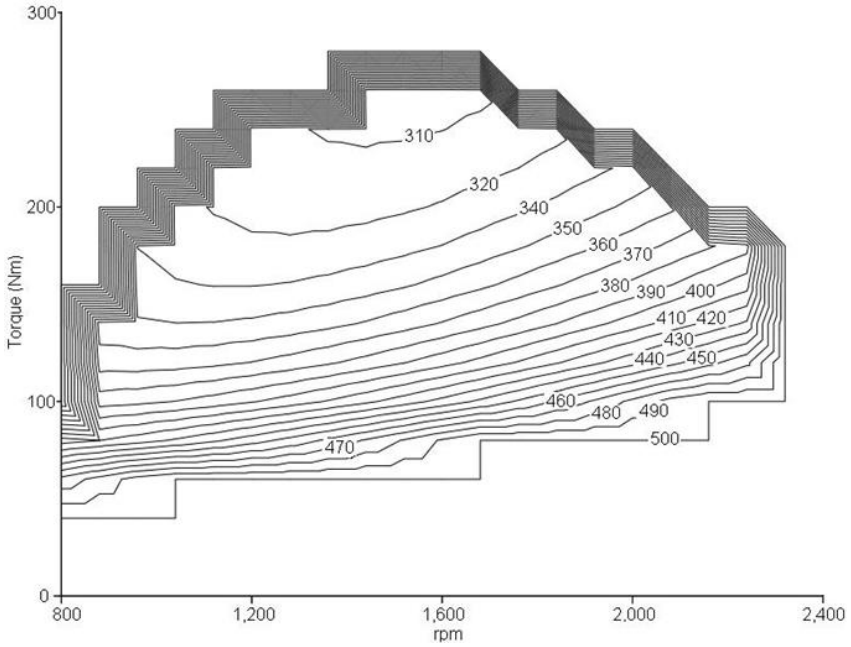

Figure 2. Full characteristic of specific fuel consumption for 10% BUT (g kWh^{-1}).

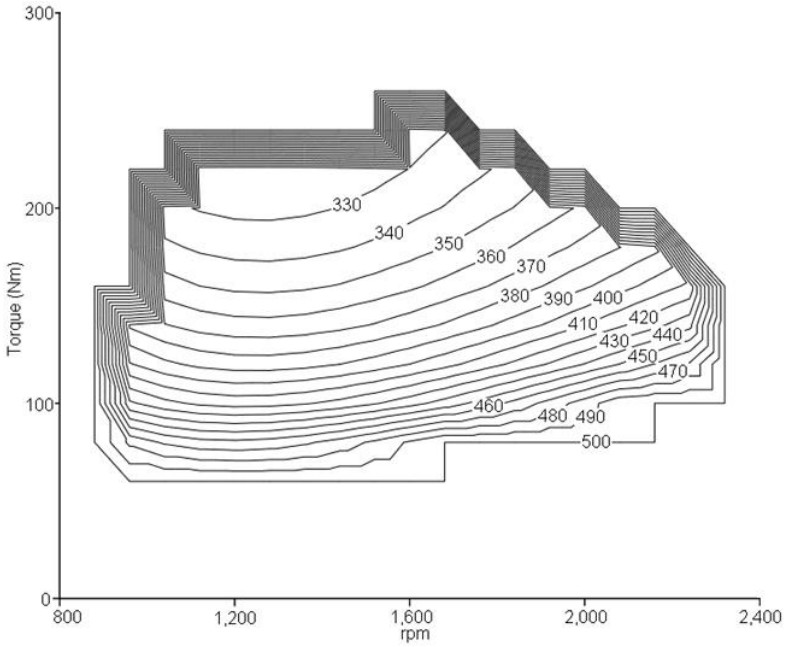

Figure 3. Full characteristic of specific fuel consumption for 30% BUT (g kWh^{-1}).

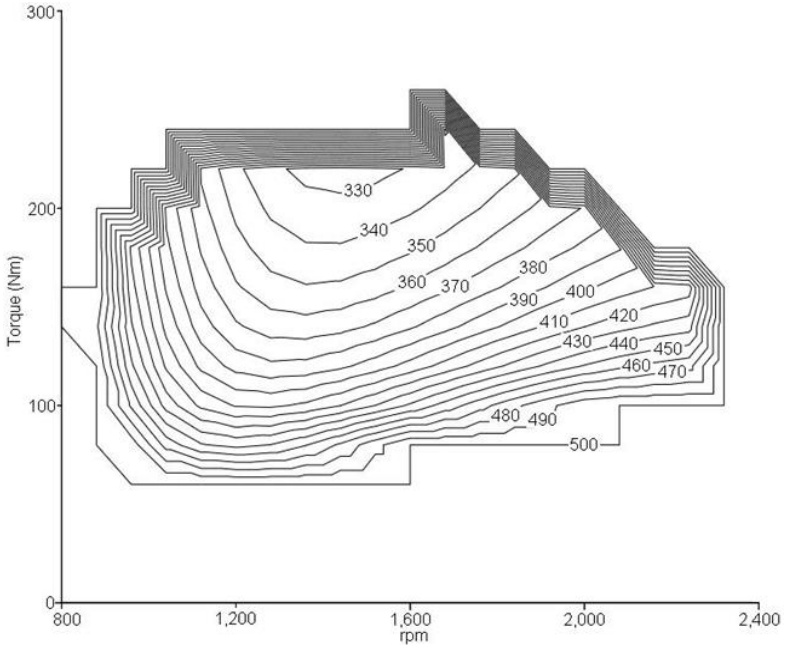

Figure 4. Full characteristic of specific fuel consumption for 50% BUT (g kWh^{-1}).

Table 3. Results of the measurement (SFC – specific fuel consumption)

Fuel	Max. Torque (Nm) rpm	Max. Power (kW) rpm	Min. SFC (g kWh^{-1}) rpm	Rated Torque (Nm)	Rated Power (kW)	Rated SFC (g kWh^{-1})	Torque backup (%)
10% BUT 90% FAME	274.1 1,488	47.8 1,886	300.04 1564	190.4	43.9	382.2	44
30% BUT 70% FAME	246.67 1,652	44.03 1,801	318.4 1405	172.5	39.7	407	43
50% BUT 50% FAME	241.4 1,652	43.4 1811	321.2 1,568	167.4	38.6	418.1	44.2
Diesel	319 1,474	56.7 2,115	239.4 1,633	237.4	54.7	276.6	34.4

From the results of the external rotation speed characteristics and from the complete characteristics it is evident that the increase of specific fuel consumption for all variants of mixed fuels is higher with increasing speed and share of butanol in comparison with diesel. At rated speed the specific fuel consumption for 10% BUT increased by 38.2% compared with the diesel. For 30% BUT there is an increase of specific fuel consumption in rated speed by 6.1% and for 50% BUT by 8.5% in comparison with 10% BUT. Further, the results of the specific fuel consumption measured using the NRSC test were evaluated (Table 4). The table shows that the NRSC specific fuel consumption is higher for 10% BUT by 26.8% compared with diesel. For 30% BUT the NRSC specific fuel

consumption is higher by 5% and for 50% BUT approximately by 8% compared with 10% BUT. It can be seen that with increasing concentration of butanol the specific fuel consumption increases.

Table 4. Results of the NRSC test for specific fuel consumption

Fuel	SFC (g kWh^{-1})	SFC (%)
10% BUT 90% FAME	424.3	100
30% BUT 70% FAME	445.7	105
50% BUT 50% FAME	457.9	107.9
Diesel	310.5	73.2

CONCLUSIONS

From the obtained results it can be seen that a high share of butanol in the fuel significantly reduces torque and engine performance. From the mixed fuels the highest difference is between 10% and 30% concentrations of butanol. The decrease of performance for 30% and 50% BUT is primarily due to lower heating value and cetane number of butanol compared with FAME, which confirms the assumptions mentioned in the introduction. Also it was proven the increase of specific fuel consumption at higher concentrations of butanol (30 and 50%) compared with 10% BUT at all measured cases (external rotation speed characteristic, complete characteristics and NRSC), especially at higher speeds, which is primarily caused by low cetane number of butanol. In this case the assumptions mentioned in the introduction were also confirmed.

During measurement the butanol showed its good miscibility with FAME by significantly reducing the viscosity of the fuel. The reduce of viscosity is most significant at 10% BUT, as shown in Tables 1 and 2. Further advantages of butanol can be seen in its ability to dissolve the deposits in the fuel system and thereby prolonging its durability.

In conclusion it can be recommended the use of butanol as an additive to FAME up to concentration of 10% BUT, primarily to reduce the viscosity of the fuel. At higher concentrations the other properties of butanol such as low cetane number and calorific value have already quite negatively impacts.

ACKNOWLEDGEMENTS. The paper was created with the grant support project CIGA CULS Prague 20153001 – Utilization of butanol in internal combustion engines of generators and with institutional support for long-term conceptual development VÚZT, v.v.i. RO0614.

REFERENCES

Barrios, C.C., Domínguez-Sáez, A., Martín, C. & Álvarez, P. 2014. Effects of animal fat based biodiesel on a TDI diesel engine performance, combustion characteristics and particle number and size distribution emissions. *Fuel* **117**, 618–623.

Bhattacharya, T.K., Mishra, T.N. & Chatterjee, S. 2003. Studies on suitability of lower ethanol proofs for alcohol – Diesel microemulsions, *AMA, Agricultural Mechanization in Asia, Africa and Latin America* **34**(1), 55–58.

Commission of the European Communities. 2009. Directive 2009/28/EC of the European Parliament and of the Council of 23 April 2009 on the promotion of the use of energy from renewable sources and amending and subsequently repealing Directives 2001/77/EC and 2003/30/EC. *Official journal of the European Union L series* **140**(52), pp. 16–62.

ČSN EN 590 Automotive fuels – Diesel – Requirements and test methods. 2004

Doğan, O. 2011. The influence of n-butanol/diesel fuel blends utilization on a small diesel engine performance and emissions. *Fuel* **90**(7), 2467–2472.

Hönig, V., Kotek, M. & Mařík, J. 2014. Use of butanol as a fuel for internal combustion engines. *Agronomy Research* **12**(2), 333–340

Hromádko, J. Hromádko, J., Hönig, V. & Miler, P. 2011. *Combustion engines.* Grada Publishing, Prague, pp. 296 (in Czech)

Imran, S., Emberson, D.R., Wen, D.S., Diez, A., Crookes, R.J. & Korakianitis, T. 2013. Performance and specific emissions contours of a diesel and RME fueled compression-ignition engine throughout its operating speed and power range. *Applied Energy* **111**, 771–777.

ISO 8178-4 Reciprocating internal combustion engines-Exhaust emission measurement-Part 4: Steady-state test cycles for different engine applications. 2007

Kleinová, A., Vailing, I., Lábaj J., Mikulec J. & Cvengroš J. 2011. Vegetable oils and animal fats as alternative fuels for diesel engines with dual fuel operation. *Fuel Processing Technology* **92**(10), 1980–1986.

Kučera M. & Rousek M. 2008. Evaluation of thermooxidation stability of biodegradable recycled rapeseed-based oil NAPRO-HO 2003. *Research in Agricultural Engineering* **54**(4), 163–169.

Lujaji F., Kristóf L., Bereczky A. & Mbarawa M. 2011. Experimental investigation of fuel properties, engine performance, combustion and emissions of blends containing croton oil, butanol, and diesel on a CI engine. *Fuel* **90**(2), 505–510.

Mařík J., Pexa M., Kotek M. & Hönig V. 2014. Comparison of the effect of gasoline – ethanol E85 – butanol on the performance and emission characteristics of the engine Saab 9-5 2.3 l turbo. *Agronomy Research* **12**(2), 359–366.

Öner C. & Altun Ş. 2009. Biodiesel production from inedible animal tallow and an experimental investigation of its use as alternative fuel in a direct injection diesel engine. *Applied Energy* **86**(10), 2114–2120.

Pexa, M. & Kubín, K. 2012. Effect of rapeseed methyl ester on fuel consumption and engine power. *Research in Agricultural Engineering* **58**(2), 37–45.

Pexa M. & Mařík J. 2014. The Impact of biofuels and technical condition to its smoke – Zetor 8641 Forterra. *Agronomy Research* **12**(2), 367–372.

Pexa M., Mařík J., Čedík J., Aleš Z. & Valášek, P. 2014. Mixture of oil and diesel as fuel for internal combustion engine. In: *2nd International Conference on Materials, Transportation and Environmental Engineering*. CMTEE, Kunming, pp. 1197–1200.

Pexa, M., Mařík, J., Kubín, K. & Veselá, K. 2013. Impact of biofuels on characteristics of the engine tractor Zetor 8641 Forterra. *Agronomy Research* **11**(1), 197–204.

Sirviö, K., Niemi, S., Vauhkonen, V. & Hiltunen, E. 2014. Antioxidant studies for animal-based fat methyl ester. *Agronomy Research* **12**(2), 407–416.

Soloiu, V., Duggan, M., Harp, S., Vlcek, B., Williams, D. 2013. PFI (port fuel injection) of n-butanol and direct injection of biodiesel to attain LTC (low-temperature combustion) for low-emissions idling in a compression engine. *Energy* **52**, 143–154.

Soo-Young N. 2011. Inedible vegetace oils and thein derivatives for alternative diesel fuels in CI engines: A review. *Renewable and Sustainable Energy Review* **15**(1), 131–149.

Sukjit E., Herreros J.M., Dearn K.D., García-Contreras, R. & Tsolakis, A. 2012. The effect of the addition of individual methyl esters on the combustion and emissions of ethanol and butanol -diesel blends. *Energy* **42**(1), 364–374.

Wadumesthrige, K., Simon Ng, K.Y. & Salley, S.O. 2010. Properties of butanol-biodiesel-ULSD ternary mixtures. *SAE International Journal of Fuels and Lubricants* **3**(2), 660–670.

Yilmaz, N., Vigil, F.M., Benalil, K., Davis, S.M. & Calva, A. 2014. Effect of biodiesel–butanol fuel blends on emissions and performance characteristics of a diesel engine. *Fuel* **135,** 46–50.

Zhang, Z.-H. & Balasubramanian, R. 2014. Influence of butanol addition to diesel–biodiesel blend on engine performance and particulate emissions of a stationary diesel engine. *Applied Energy* **119**, 530–536.

Agronomy Research **13**(2), 550–557, 2015

Determination of the phase separation temperature and the water solubility in the mixtures of gasoline with biobutanol and bioethanol

V. Hönig[1,*], Z. Linhart[2], J. Táborský[1] and J. Mařík[3]

[1]Czech University of Life Sciences Prague, Faculty of Agrobiology, Food and Natural Resources, Department of Chemistry, Kamycka 129, CZ16521, Prague 6, Czech Republic; [*]Correspondence: honig@af.czu.cz
[2]Czech University of Life Sciences Prague, Faculty of Economics and Management, Department of Management, Kamycka 129, CZ16521, Prague 6, Czech Republic
[3]Czech University of Life Sciences Prague, Faculty of Engineering, Department for Quality and Dependability of Machines, Kamycka 129, CZ16521, Prague 6, Czech Republic

Abstract. Original hydrocarbon composition, volatility, compatibility with materials, calorific value and stability of the mixture in the presence of water are monitored usually. This paper deals with the stability of gasoline-biobutanol and gasoline-bioethanol mixtures in the presence of water. Biobutanol is better biofuel than bioethanol using the same raw materials. Different contents of alcohol and oxygenated cosolvents are evaluated. Experimental analysis are focused on the water solubility and phase stability. Solubility in water of butanol and ethanol mixtures is very similar. Butanol-gasoline mixture provides better phase stability upon contact with water or atmospheric moisture oppose to ethanol mixtures. Butanol also does not enter to the aqueous layer and fuel properties remain in phase separation preserved. Further, it was found that crystals occur at low temperatures after exclusion of water was seen. Moreover, the temperature of phase separation can affect the content of alcohol, water, hydrocarbon composition and cosolvents added. The only difference found between more beneficial butanol and less beneficial ethanol was ABE (Aceton–Butanol–Ethanol) fermentation with *Clostridium Acetobutylicum* allowing to ferment also saccharidic cellulose to biobutanol according to standard of second generation biofuels.

Key words: BioEthanol, BioButanol, Water, MTBE, ETBE.

INTRODUCTION

Raw materials for bioethanol and biobutanol production are identical (Lipovský et al., 2009).

1) starchy (potatoes, corn, wheat, rice);
2) sugary (sugar beet molasses, whey);
3) lignocellulosic (straw, wood).

Traditional materials for the production of butanol are starchy crops (cereals, maize, potatoes) and molasses from sugar cane or sugar beet show that starch is also fermentable if proper technology is used. Other alternative materials such as whey, waste glycerol or unicellular algae accumulating starch in their cells need also advanced processing technology (Groot et al., 1992; Hönig et al., 2014; Pointner et al., 2014). Second generation biofuels (especially ethanol but also butanol) are sourced by saccharidic cellulose of different materials, e.g. straw or waste paper waste and energy crops (Tutt & Olt, 2011; Tutt et al., 2012; Raud et al., 2014). ABE (Aceton-Butanol-Ethanol) fermentation with *Clostridium Acetobutylicum* is able to ferment also saccharidic cellulose to biobutanol.

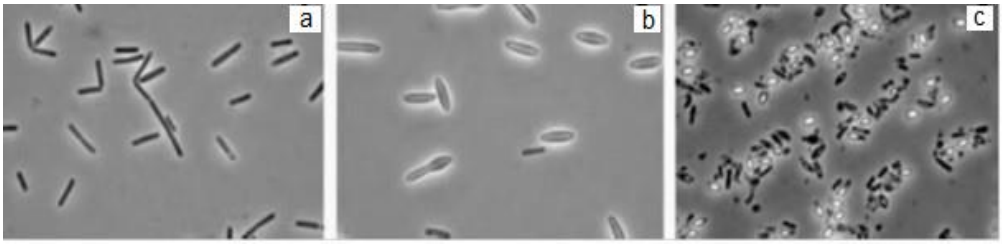

Figure 1. Solvent-generating bacteria of the genus *Clostridium*: acidifying (a), solvent–generating (b) and inactive (c) life cycle stages; magnification 2000x.

Smaller inner–ppapers in Fig. 1c spores are released from the cells of raw material. By adding alcohol to gasoline a certain physico-chemical properties of the fuel are changed, primarily:

1) volatility (vapor pressure and distillation curve);
2) octane number;
3) water solubility;
4) compatability with materials
5) calorific value.

Characteristics of bioethanol are significantly different oppose to hydrocarbons of gasoline. Polar nature and strong affinity to water makes ethanol completely miscible. Ethanol significantly increases the solubility of water in the hydrocarbon fuel, which can be useful (for example, for preventing freezing of the fuel system). But, this ability to retain water in some form in the gasoline-ethanol mixture is greatly affected by temperature. Miscibility of gasoline and water is in ppm low. Ethanol is part of this water layer, which decrease the fuel quality. When the temperature drops below a certain level the water layer is separated from fuel. Octane value is decreased, volatility is changed and oxygen lost. The aqueous phase can also cause corrosion of metallic materials in the tanks or the fuel system of the vehicle. Extraction of ethanol to the aqueous layer is an irreversible process usually. It is also possible, under certain conditions that it will dissolve back to the whole volume of water-ethanol layer into the hydrocarbon base (Patáková et al., 2010; Wang et al., 2011; Tutt et al., 2013).

After separation of aqueous phase the water content dissolved in the hydrocarbon layer is lower. Volume of water–ethanol phase is decreasing water content in gasoline layer continuesly.

Gasoline containing bioethanol can in this regard cause much more serious problems in distribution network and for consumer than gasoline without bioethanol, where the collected water does not represent a significant risk of changes in fuel quality (Beran, 2011; Küüt et al., 2011; Eisenhuber et al., 2013).

The amount of ethanol extracted into the aqueous phase is generally influenced by:

1) alcohol content in gasoline;
2) hydrocarbon composition of gasoline;
3) ratio of the amounts of aqueous and hydrocarbon phases;
4) the presence of cosolvents;
5) temperature (to some extent).

Polar character of ethanol and its ability to form hydrogen bonds increases solubility of water in ethanol–gasoline mixtures. Ethanol intended for fuel purposes must meet standard of maximum allowable water content of 0.39% vol. to be called waterless.

Ethanol is highly hygroscopic. If it is in free contact with the atmosphere it absorbs very readily the water from air humidity (Melzoch & Rychtera, 2014). Therefore, in storage or vehicle tanks volume of fuel is changing with temperature. This effect is called 'breathing fuel'.

Solubility of water in gasoline-ethanol mixture depends on:

1) temperature;
2) ethanol content;
3) hydrocarbon composition of gasoline containing aromatics and olefins;
4) other oxygenates (so–called cosolvents) content.

The separation of water from fuel is caused by temperature, temperature fluctuations during the day and at night, or by changed content of ethanol when different types of gasoline are mixed. Another possible cause of water and fuel separation may occur in mixture of gasoline with waterless ethanol or in mixtures of different gasolines of different compositions (Kamimura & Sauer, 2008; Hromádko, 2011; Pirs & Gailis, 2013).

Water solubility can be influenced to a certain extent also by hydrocarbon composition of gasoline. Aromatics and olefins are due to the presence of π –bonds easier miscible with water than saturated hydrocarbons.

Solubility continues to increase with the addition of other oxygenates (cosolvents) which can be added to the gasoline together with alcohols up to the limit of oxygen content of 2.7% wt. according to EN 228 (Yuksel & Yuksel, 2004; Mužíkova et al., 2010; Pospíšil et al., 2014).

The ability of fuel to maintain a certain amount of water in single phase system depends on temperature. Such temperature is called phase separation. Phase separation precedes usually visible turbidity at so–called cloud point. The sample with a given amount of water is gradually cooled. Cloud and consequent exclusion of the aqueous phase (possibly ice crystals) is observed. Cloud point identifies better the two formed phases (upper and lower water filling).

The cosolvent effects of oxygenates

Also other oxygenates – cosolvents (stabilizers) with respect to the maximum permitted content of oxygen in gasoline according to standard EN 228 (max. 2.7% wt.)

can be added. Cosolvents are added into ethanol–gasoline mixtures from the following reasons:

1) solubility of water in gasoline-ethanol mixture is improved;
2) the amount of ethanol extracted into the aqueous phase is reduced;
3) the increase of vapor pressure is reduced;
4) the temperature of phase separation is decreased.

As cosolvents are used following matters:

1) branched higher alcohols (TBA tertbutylalcohol, IBA isobutylalchohol, IPA isopropylalkohol) in usual ratio of 1:1 volume with ethanol;
2) higher aliphatic alcohols (1–hexanol, decanol);
3) ethers (DIPE diisopropylether, TAME tert–amyl–methylether, MTBE methyl tert–butylether, ETBE (ethyl tert–butyl ether).

To 5% vol. of ethanol in gasoline is possible to add maximally permitted oxygen content about 5% vol. of MTBE or ETBE or about 4% vol. of TBA or 3% vol. of IPA. The cosolvent effects have also aromatic hydrocarbons.

Added cosolvents must meet the following requirements:

1) oxygen cosolvents should primarily meet EN 228 standard;
2) good miscibility with all components of fuel;
3) very low water solubility and minimal tendency to pass into the aqueous layer;
4) minimum of azeotrope in hydrocarbons minimizing boiling point and increasing the vapor pressure.

The experiments deals with possibilities of application of biobutanol as an alternative to bioethanol and its low temperature properties. Gasoline–ethanol and gasoline–butanol mixtures at low temperatures behave differently with respect to hygroscopicity of ethanol.

MATERIALS AND METHODS

The experimental part of the paper focuses on phase equilibria of butanol-gasoline mixtures in presence of water. Performed procedure according to ASTM D 6422 standard has identified cloud point, which represents a temperature when emulsion in fuel mixture of homogeneous sample appears. Separation into two phases – upper hydrocarbon and lower water occurs if the sample is cooled further.

A sample of pure gasoline that meets the requirements of the standard EN 228 for the winter season (class F1) was analyzed. It contained 32.21% vol. aromatic hydrocarbons, 10.29% vol. olefins, and 0.52% vol. benzene. The water content was 48.00 mg kg^{-1} and oxidation stability exceeded 360.0 minutes.

Further, the MTBE (methyl tert–butyl ether) and ETBE (ethyl tert–butyl ether) produced by Czech refinery joint stock company, n–butanol p.a. (Lachner, Ltd) and distilled water were used. The tested bioethanol has fully met requirements of prEN15376:2013 standard.

The tested samples were labeled with working names

1. ETH for bioethanol;
2. BUT for n–butanol.

RESULTS AND DISCUSSION

The solubility of water in pure hydrocarbon gasoline varies depending on the content of aromatics between 60 and 100 mg kg^{-1}. With increasing ethanol content in gasoline the solubility of water increases nonlinearly.

Tested mixtures with concentration of 2, 4, 5, 6, 8 and 10% vol. of butanol (Figs 2, 3, 4 and 5) were further enriched by ethers in quantities of 5 and 10% vol. to study influence phase stability of mixtures.

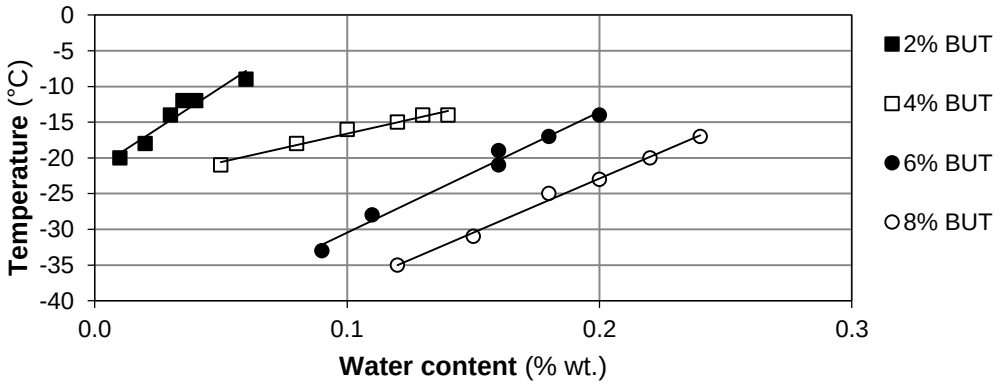

Figure 2. Water solubility according to temperature in gasoline–butanol mixture.

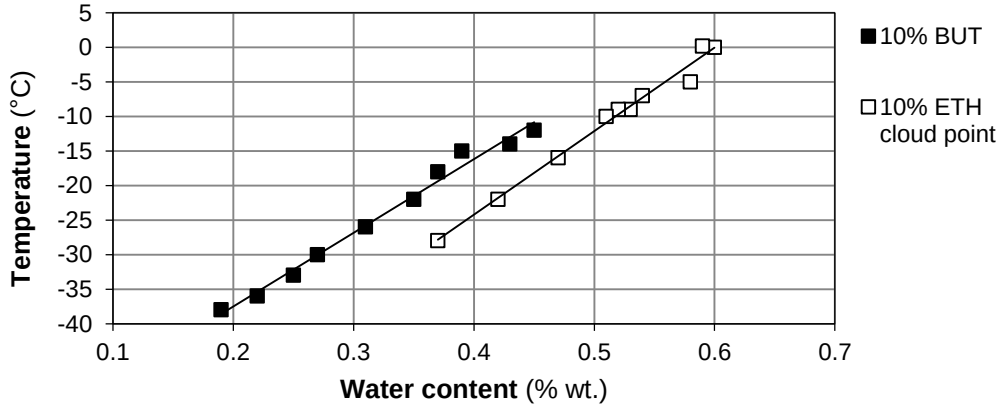

Figure 3. Water solubility expressed as the temperature of crystallization of gasoline–butanol mixtures and cloud point of gasoline-ethanol mixtures.

Freezing point of water below 0 °C is proving alcohol in aqueous phase.

Gasoline comprising 10% vol. of ethanol is very sensitive to temperature changes. Therefore, the safe content of water in gasoline containing up to 10% vol. of ethanol should have up to 0.02% wt. or (2,000 ppm) for both summer and winter conditions.

The cloud point of butanol fuel mixture during cooling couldn't be reliably determined as separation of liquid water phase was not clearly visible oppose to ethanol–gasoline mixtures. Crystals of water in the fuel mixture have emerged as soon as temperature has decreased below freezing point. This makes butanol-gasoline mixture more favorable oppose to ethanol–gasoline mixture (Fig. 3). The fuel distribution system and engines are less damaged by crystals of ice in the fuel than by ethanol-water. Properties of butanol fuel mixtures are not changed because water layer doesn't appear at all under low temperatures oppose to ethanol–gasoline mixtures. Such mixtures of butanol and gasoline needn't cosolvents.

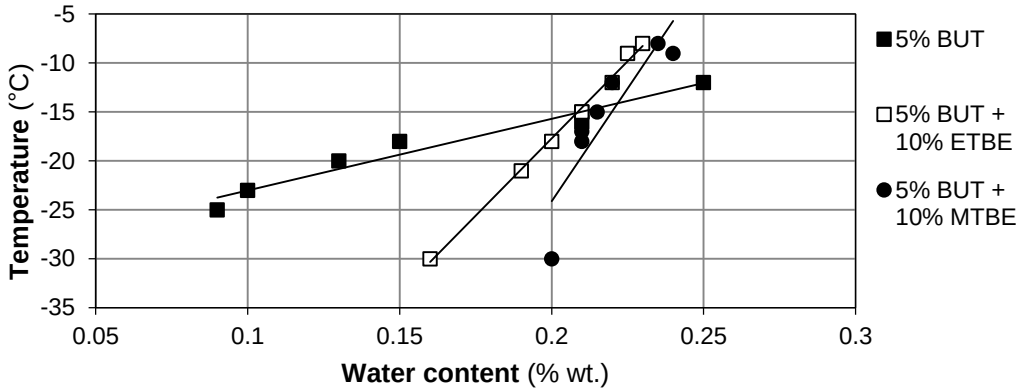

Figure 4. Water solubility expressed as the temperature of crystallization of gasoline–butanol, MTBE and ETBE mixtures.

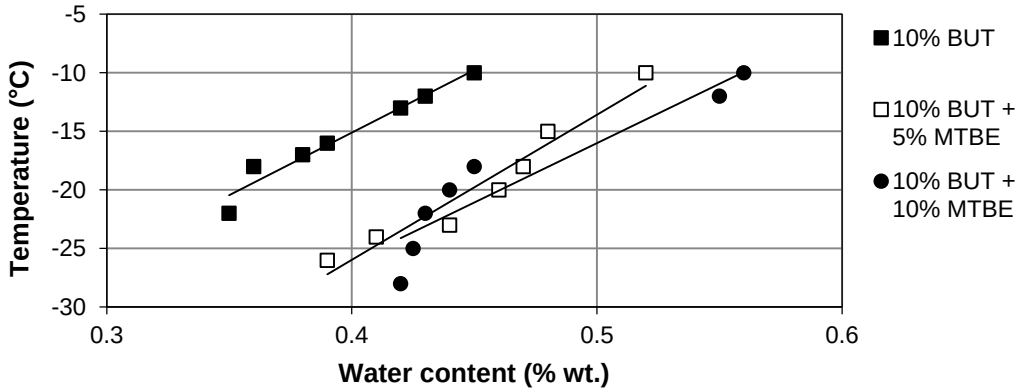

Figure 5. Water solubility expressed as the temperature of crystallization of gasoline– butanol and MTBE mixtures.

Added MTBE and ETBE affect only a little the solubility of water in fuel mixture. Gasoline containing both ether and butanol mixture (Figs 4 and 5) acts in terms of phase stability similarly as butanol-gasoline mixture. There is no visible cloud, followed by phase separation. Water is eliminated directly as ice crystals. Butanol, MTBE or ETBE

in gasoline was found temperature of crystallization, which corresponds qualitativelly to tempreature of separation of aqueous phase. Butanol remains dissolved in the hydrocarbon phase also at very low temperatures without being transferred to aqueous phase opposed to ethanol. This feature butanol is ultimately far more acceptable than the transition of ethanol to the aqueous phase as fuel properties doesn't endanger engines.

We may deduce from butanol properties that if both butanol and ethanol are present in gasoline mixtures the phase stability is significantly influenced. Water doesn't appear only in shape of ice crystals, but cloud and phase separation occurs. From this we can conclude that such a phenomenon always occurs in the presence of both alcohols if their presence in the fuel volume will be comparable. Gasoline mixture containing 5% vol. ethanol and 5% vol. butanol shows in terms of phase behavior very similar properties to characteristics of pure gasoline-ethanol mixture with 10% vol. ethanol.

The measured values of water solubility show that the mixture with 10% vol. of butanol at 0 °C is about 5,400 mg kg^{-1}. In the case of a mixture with 10% vol. of ethanol it is about 5,900 mg kg^{-1}.

CONCLUSIONS

Solubility of water in butanol and an ethanol mixtures is very similar. Ethanol is completely miscible with water, butanol is watermiscible only to limited extent. Water in MTBE and ETBE is poorly soluble in tens of units of $mg.kg^{-1}$ being similarly soluble as hydrocarbons. Butanol in gasoline fuel mixture in contact with water or atmospheric moisture improves its phase stability at low temperatures oppose to ethanol. Low temperatures exclude water crystals from fuel mixture. Butanol does not transit to aqueous phase as ethanol does. Parameters of gasoline–butanol mixture remain preserved during separation phases. Such mixtures of butanol and gasoline needn't cosolvents neither special treatment in storage. Mixtures of both ethanol and butanol with gasoline require cosolvents and special treatment in storage due to above described reactions with water.

More beneficial butanol fuel mixtures, opposed to ethanol, opens also possibility for second generation biofuels if ABE (Aceton–Butanol–Ethanol) fermentation with *Clostridium Acetobutylicum* is used for fermentation of saccharidic cellulose.

ACKNOWLEDGMENTS. The paper was created with the grant support project CIGA CULS Prague 20153001 – Utilization of butanol in internal combustion engines of generators.

REFERENCES

Beran, O. 2011. In this year the Earth's production of bioethanol will be over 88 billion litters. Biom.cz: *http://biom.cz/cz-kapalnabiopaliva/odborne-clanky/v-tomto-roce-se-na-zemi-vyrobiuz-pres-88-miliard-litrubioethanolu*. Acessed 2.12.2014. (in Czech)

Eisenhuber, K., Jager, A., Wimberger, J. & Kahr, H. 2013. Comparison of different pretreatment methods for straw for lignocellulosic bioethanol production. *Agronomy research* **11**, 173–182.

EN 228. 2009. Automotive fuels – Unleaded petrol – Requirements and test methods, ČSNI, 16 pp. (in Czech).

Groot W.J., Lans, R.G.J.M. & Luyben, K.Ch.A.M. 1992. Technologies for Butanol Recovery Integrated with Fermentations, *Process Biochemistry* **27**, 61–75.

Hönig, V. Kotek, M. & Mařík, J. 2014. Use of butanol as a fuel for internal combustion engines. *Agronomy Research* **12**(2), 333–340.

Hromádko, J. Hromádko, J., Miler, P., Hönig, V. & Štěrba, P. 2011. The use of bioethanol in internal combustion engines. *Chemické listy* **105**(2), 122–128 (in Czech).

Kamimura, A. & Sauer, I.L. 2008. The effect of flex fuel vehicles in the Brazilian light road transportation. *Energy Pol.* **36**(2), 1574–1576.

Küüt, A., Ritslaid, K. & Olt, J. 2011. Study of potential uses for farmstead ethanol as motor fuel. *Agronomy Research* **9**(1), 125–134.

Lipovský, J., Patáková, P., Rychtera, M., Čížková, H. & Melzoch, K. 2009. Prospects of Butanol Production from Starch and Cellulose Materials, *Chemické listy* **103**, 479–483 (in Czech).

Melzoch, K. & Rychtera, M. Distillery and production of spirits: *http://www.vscht.cz.* Acessed 5.12.2014.

Mužíkova, Z., Pospíšil, M. & Šebor, G. 2010. The use of bioethanol as a fuel in the form of E85 fuel. *Chemické listy* **104**(7), 678–683 (in Czech).

Patáková, P., Pospíšil, J., Lipovský, J, Fribert, P., Linhová, M, Toure, S.S.M., Rychtera, M., Melzoch, K. & Šebor G. 2010. Prospects for biobutanol production and the use in the Czech republic, *Chemagazín* **20**(5), 13–15.

Pirs, V. & Gailis, M. 2013. Research in use of fuel conversion adapters in automobiles running on bioethanol and gasoline mixtures, *Agronomy Research* **11**(1), 205–214.

Pointner, M., Kuttner, P., Obrlik, T., Jager, A. & Kahr, H. 2014. Composition of corncobs as a substrate for fermentation of biofuels. *Agronomy Research* **12**(2), 391–396.

Pospíšil, M., Šiška, J. & Šebor, G.: BioButanol as fuel in transport, Biom.cz: *www: biom.cz*. Acessed 5.7.2014.

Raud, M., Kesperi, R., Oja, T., Olt, J. & Kikas, T. 2014. Utilization of urban waste in bioethanol production: potential and technical solutions. *Agronomy Research* **12**(2), 397–406.

Tutt, M. & Olt, J. 2011. Suitability of various plant species for bioethanol production, *Agronomy Research* Biosystem Engineering Special Issue 1, 261–267.

Tutt, M., Kikas, T. & Olt, J. 2012. Influence of different pretreatment methods on bioethanol production from wheat straw. *Agronomy Research* **10**, 269–276.

Tutt, M., Kikas, T. & Olt, J. 2013. Influence of harvesting time on biochemical composition and glucose yield from hemp. *Agronomy Research* **11**, 215–220.

Wang, L., Yang, M., Fan, X., Zhu, X., Xu, T. & Yuan, Q. 2011. An environmentally friendly and efficient method for xylitol bioconversion with high-temperature-steaming corncob hydrolysate by adapted Candida tropicalis. *Process Biochemistry* **46**(8), 1619–1626.

Yuksel, F. & Yuksel, B. 2004. The use of ethanol-gasoline mixture as a fuel in an SI engine. Renewable Energy **29**, 1181–1191.

Agronomy Research **13**(2), 558–567, 2015

The distillation characteristics of automotive gasoline containing biobutanol, bioethanol and the influence of the oxygenates

V. Hönig[1,*], M. Orsák[1], M. Pexa[2] and Z. Linhart[3]

[1]Czech University of Life Sciences Prague, Faculty of Agrobiology, Food and Natural Resources, Department of Chemistry, Kamycka 129, CZ16521, Prague 6, Czech Republic; [*]Correspondence: honig@af.czu.cz
[2]Czech University of Life Sciences Prague, Faculty of Engineering, Department for Quality and Dependability of Machines, Kamycka 129, CZ16521, Prague 6, Czech Republic
[3]Czech University of Life Sciences Prague, Faculty of Economics and Management, Department of Management, Kamycka 129, CZ16521, Prague 6, Czech Republic

Abstract. Bioethanol and fatty acid methyl esters are a regular part of the production of gasoline and diesel fuels, although in limited quantities. Introduction of bioethanol as part of automobile gasoline was associated with high production costs, technical and logistical problems. This article analyses changes of distillation curve of biobutanol and isobutanol as an alternative to bioethanol. Added alcohol to gasoline causes reduction of boiling point due to the formation of azeotrope. This phenomena of distillation curve are called Plato effect. Therefore, ethers (MTBE and ETBE) are added to fuel to affect the most central part of distillation curve. Especially, to decrease the distillation temperature oppose to gasoline without oxygenates of wide range of distilled volume. This article replaces simple universal models predicting properties of alcohol-gasoline mixtures. It was found that mixture of ETBE with bioethanol in gasoline the distillation curve summarise its effects. Butanol and MTBE influence distillation curve of gasoline only in values of its boiling points. Therefore, butanol is mixable with all listed fuel components without any additional addaptations.

Key words: BioEthanol, n-Butanol, IsoButanol, MTBE, ETBE.

INTRODUCTION

EU cooperates internationally in fight against climate change according to Kyoto Protocol reducing greenhouse gas emissions (GHG). Rationalisation of energy consumption and use of renewable energy sources are main sources of GHG reduction. The transport sector may reduce GHG emissions if share of biofuels is increased (Hromádko et al., 2011).

Commercialised biofuels are bioethanol and methyl ester of rapeseed oil already. Bioethanol is used for gasoline engines and rapeseed oil methyl ester for diesel engines. Methyl esters of various oils (often referred as biodiesel) represent 85% of all produced biofuels on European scale (Hönig & Hromádko, 2014). Bioethanol was introduced to diversify biofuels and increase its share in fossil fuels. Biofuels with a higher proportion of bioethanol decrease emissions (CO, HC, NOx or PM) more than methyl esters of

vegetable oils. Methyl esters are decreasing in CO_2 emissions more than bioethanol produced from sugars or starch (Pirs & Gailis, 2013; Ilves at al., 2014).

Biofuels may be divided according to method of obtaining biofuels to first and second generations. Ethanol, methyl esters of fatty acids of vegetable oils belong to first generation biofuels (Kotus et al., 2013). Ethanol is produced from wheat or sugar beet and methyl esters are obtained mainly from oilseed rape in European conditions (Sun & Cheng, 2002; Sims et al., 2010).

Second generation biofuels are produced differently. Second generation ethanol (or other alcohols) is obtained from lignocellulose of plants which are not intended for processing into food, or from lignocellulose which constitute waste substances (Groot et al., 1992; Tutt & Olt, 2011).

Table 1. Parameters of biobutanol, bioethanol and gasoline fuel

Parameter	Gasoline C_4-C_{12}	Butanol	Ethanol
Chemical formula	$CH_{1,87}$	C_4H_9OH	C_2H_5OH
Density at 15 °C(kg dm^{-3})	~ 0.73	0.81	0.79
Kinematic viscosity at 20 °C(mm^2 s^{-1})	0.4–0.8	3.64	1.52
Calorific value (MJ kg^{-1})	42.9	32.5	26.8
Heat of vaporization (MJ kg^{-1})	0.36	0.43	0.92
Mixed octane number RON	95	94	106–130
MON	85	80–81	89–103
Oxygen content (% wt.)	< 2.7	21.6	34.7

The technology of second generation biofuels has significantly improved sustainability due to reduction of carbon dioxide emissions if bioethanol is produced from lignocellulosic materials (Yang et al., 2009; Raud et al., 2014).

Biobutanol (n-butanol, butan-1-ol) is an alternative to currently widely manufactured and used bioethanol as component of gasoline. The basic raw materials for biotechnological production of butanol are the same as for the production of ethanol (Tutt et al., 2012).

Butanol can be produced by fermentation from all lignocellulosic materials, starch and simple sugars using microorganisms, e.g. *Clostridium acetobutylicum*. Currently, researchers focus their attention on blue-green algae strain of *cyanobacteria* that produce biobutanol as isobutanol (Dien et al., 2006; Patáková et al., 2010; Pointner et al., 2014).

Table 1 lists parameters of suitability of butanol, ethanol and gasoline for engines with internal combustion. An important parameter is the oxygen content, which is limited according to the standard EN 228 up to 2.7% wt. (Hönig et al., 2014). Oxygen content is kept in accordance with this norm if 12.5% vol. of butanol is mixed with fuel.

The higher percentage of alcohols in fuel mixtures the more adaptations of engine are needed. The so–called FFV = Flexible Fuel Vehicles are vehicles adapted to fuel with an ethanol content of various content. They are equipped with a sensor recording the ethanol content in gasoline and consequently regulates combustion (Wakker et al., 2005; Küüt et al., 2012; Mařík et al., 2014).

The transition from liquid to gas is called boiling. It takes place only at boiling point in entire volume of boiled liquid. Boiling occurs when the saturated vapour pressure equals the ambient pressure. Boiling point is dependent on the atmospheric pressure, this means that the normal boiling points shows the boiling points at normal pressure (Mužíková et al., 2010).

It is relatively simple to divide components of liquid mixture by distillation. The principle of distillation is based on the different boiling points of distilled components. The degree with which component start to evaporate is called volatility. The distillation curve characterizes the volatility of gasoline along the entire boiling range (Melzoch & Rychtera, 2012).

The easiest evaporating component is the most volatile one - the lightest. Component evaporating after reaching the highest temperature is reached is the least volatile one – the hardest.

If the mixture reaches boiling point of the lightest component and it begins evaporating the heaviest component remains still in liquid phase. Vapours of volatile components are leaving the distillation column leaving its heat in condenser, where subsequently condense back to liquid phase. These are then further processed as distillation product (Dwivedi et al., 2009; Talebnia et al., 2010; Pschorn, 2012).

The distillation process is highly energy-intensive. Almost all supplied heat of distillation is removed in condenser. Distillation curve obtained as a result of distillation tests that we carry out in order to assess fractional composition of gasoline. The percentage or volume of fuel, which distils at one temperature is expressed.

Gasoline must contain light vaporizable fraction securing good start ability of cold engine without contain fractions whose boiling points are above 200°C, which would vaporize and could dilute oil in engine (Yuksel & Yuksel, 2004; Dukulis et al., 2009; Küüt et al., 2011).

For quality of gasoline according to European standard EN 228 the value of E70, E100 and E150 (evaporated at temperatures of 70, 100 and 150°C) are determining the standard range. Following values determining the fuel quality were measured and evaluated:

1. Beginning temperature of distillation varies in the range of 30–35 °C to minimise losses during fuel handling and improve work safety simultaneously.
2. T10 is temperature of 10% of distilled volume. It affects the ability to cool the engine. The tendency is to reduce T10 below 65 °C. At 37.8 °C a saturated vapour pressure is measured, which also characterizes the evaporating ability of fuel. For summer such pressure is 40–70 kPa, in winter the saturated vapour pressure of gasoline is adjusted to 60–90 kPa).
3. T50 is temperature of 50% of distilled volume. This point determines the speed of warming the engine up after a cold start, operating temperature and acceleration characteristics. Modern gasolines have this temperature close to 80 °C.
4. T95 is temperature of 95% of distilled volume. This point affects the combustion efficiency of fuel in cylinder. The hydrocarbons boiling point above 200 °C if sparks appears the engine starts, but burns incompletely. T95 is therefore is about 180 °C. Refineries try to move T95 for gasoline at temperatures 160–170 °C in future.

MATERIALS AND METHODS

A sample of pure gasoline that meets the requirements of standard EN 228 for the winter season (class F1) was analyzed. The tested gasoline contained 32.21% vol. of aromatic hydrocarbons, 10.29% vol. of olefins, and 0.52% vol. of benzene. The water content was 48.00 mg kg^{-1} and oxidation stability exceeded 360.0 minutes.

MTBE (methyl tert–butyl ether) and ETBE (ethyl tert–butyl ether) produced by Czech refinery joint stock company, n–butanol pa (Lachner, Ltd) and isobutanol pa (Lachner, Ltd) were used. The tested bioethanol has fully met requirements of prEN15376:2013 standard. Distillation curve of mixtures was determined in accordance with ASTM D86.

The test samples were labeled by working names:

1. ETH for bioethanol;
2. nBUT for n–butanol;
3. iBUT for isobutanol.

RESULTS AND DISCUSSION

The indicated amounts at distillation curves in Figs 1, 3 and 5 correspond to volume of alcohols in mixture. Curve of pure gasoline without oxygenates is marked ‘G’. Figs 2, 4 and 6 show changes in distillation curves compared to pure gasoline. Gasoline is represented as the horizontal axis.

Adding alcohol to gasoline causes reduction of boiling point due to formation of azeotrope. It appears at distillation curve as Plato effect. Bioethanol affects mainly the first half of the distillation curve (Figs 1 and 2) and in particular the temperature T50.

The course of distillation curve may records folowing changes – distillation curve decreases in a wide interval of distilled content (10–70% vol.), respectively in a wide interval of temperatures (50–150 °Cvol.) in comparison to gasoline base without oxygenates.

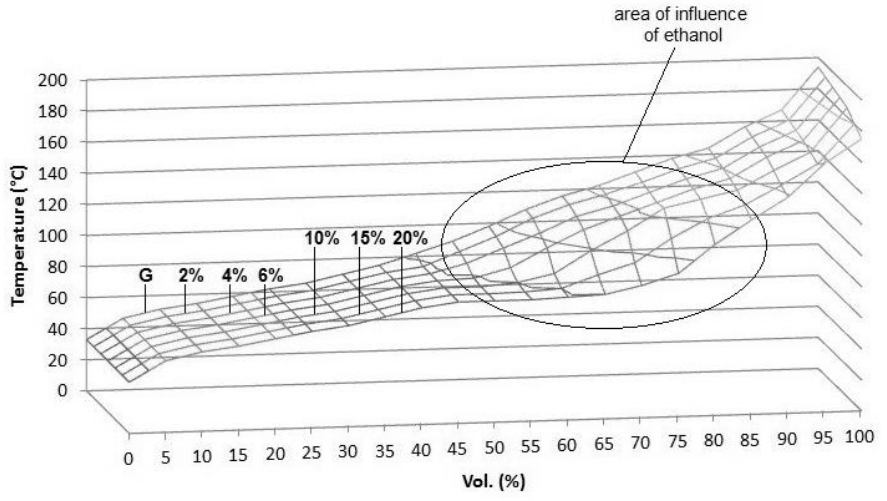

Figure 1. The distillation curve of gasoline containing bioethanol.

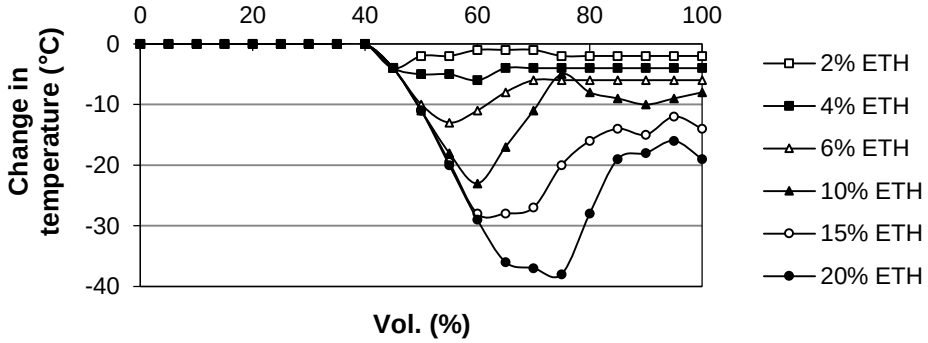

Figure 2. Changes in temperature distillation of gasoline containing bioethanol compared to gasoline base without oxygenate content.

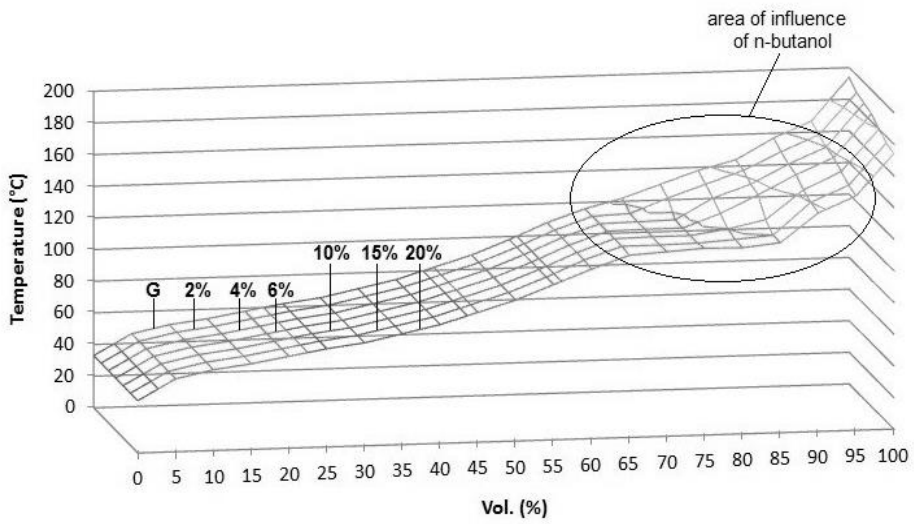

Figure 3. The distillation curve of gasoline containing n–butanol.

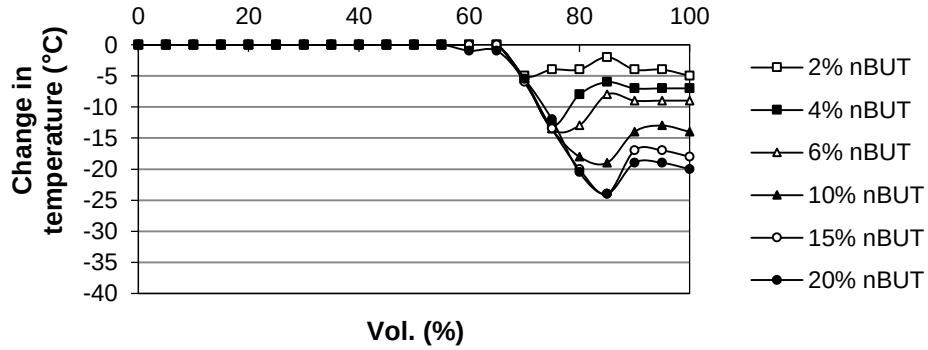

Figure 4. Changes in temperature distillation of gasoline containing n–butanol compared to gasoline base without oxygenate content.

Butanol fuels affect only the second half of distillation curve, which is considered positively. The difference in boiling points of n–butanol and isobutanol is distinctly seen on shape of distillation curves of Figs 3 and 5.

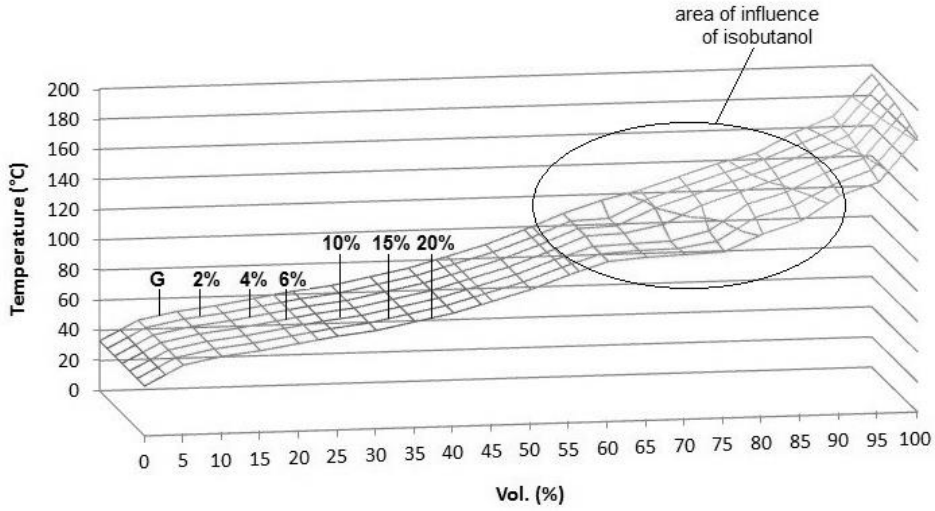

Figure 5. The distillation curve of gasoline containing isobutanol.

Decrease of temperatures of gasoline containing butanol is seen at Figs 4 and 6. Insignificant differences in boiling points of n-butanol and isobutanol are shown in different tendencies of distillation curves.

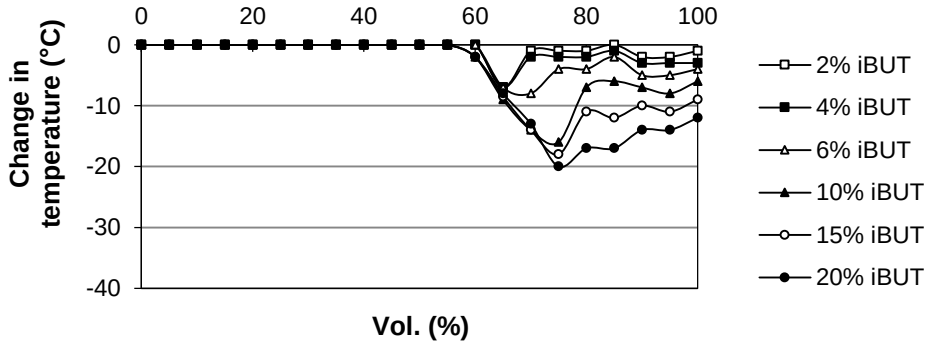

Figure 6. Changes in temperature distillation of gasoline containing isobutanol compared to gasoline base without oxygenate content.

Figs 7 and 8 are showing effect of ETBE and MTBE on analyzed mixtures. These ethers influence the course of distillation curve being well recognizable. Ethers MTBE and ETBE affect the most central part of distillation curve.

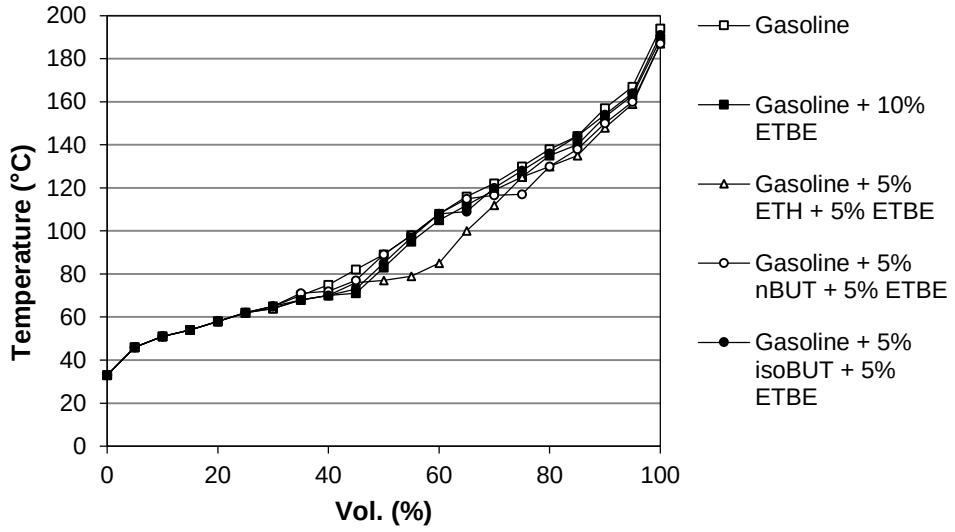

Figure 7. The distillation curves of automobile gasoline containing bioethanol, n–butanol, isobutanol and ETBE.

In case of equal representation of 5% vol. for both ethanol and ETBE the effects of these oxygenates are summarised while changing the profile of distillation curve (Fig. 7). Effect of equal representation of both ethanol and ETBE is identical as if 10% vol. of bioethanol is added to gasoline (Fig. 1).

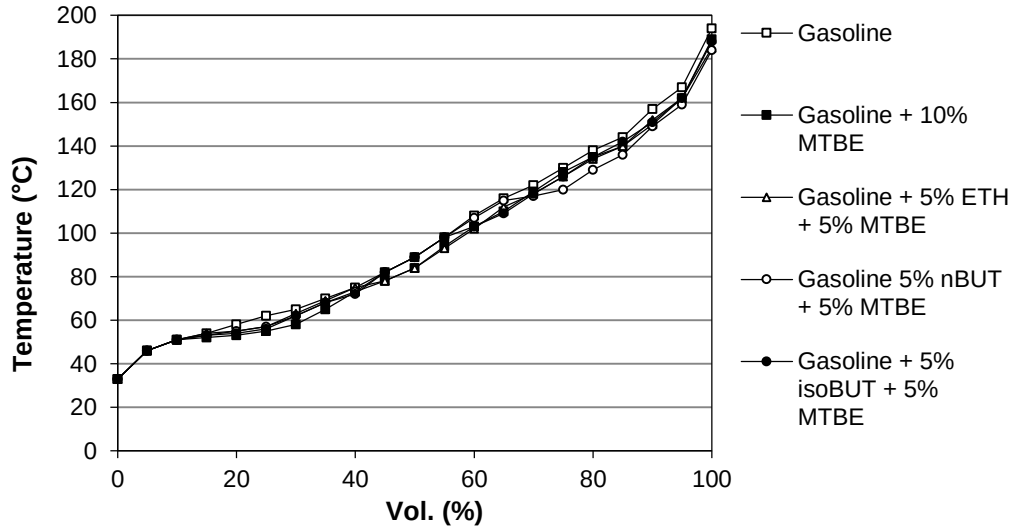

Figure 8. The distillation curves of automobile gasoline containing bioethanol, n–butanol, isobutanol and MTBE.

Figs 9 and 10 are showing change of quantity of evaporated volume at 100 °C and 150 °C (E100 and E150 according to standard EN 228) depending on addition of alcohol. These values have important implications in terms of quality parameters and also in terms of engine operation.

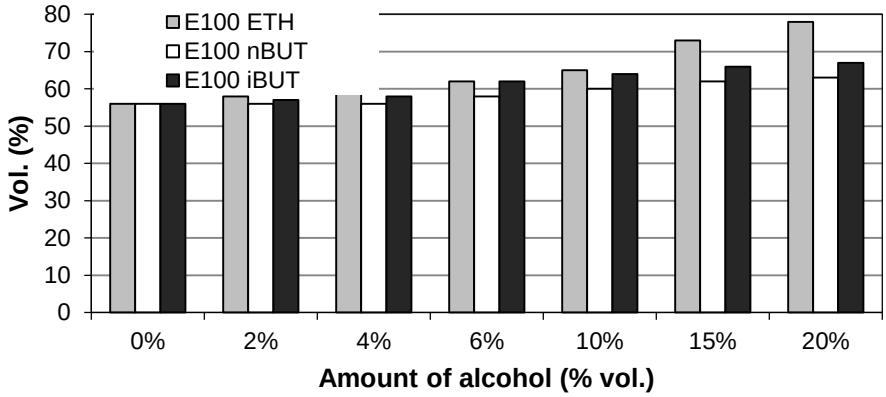

Figure 9. Effect of alcohol to E100 of gasoline.

From Fig. 9 it is seen that n–butanol value affects E100 much less than isobutanol. The boiling point of n–butanol is significantly effected by value of E150 (Fig. 10).

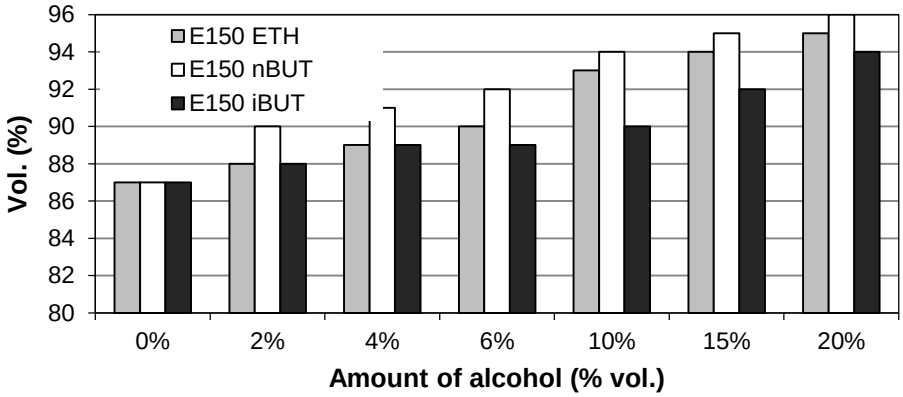

Figure 10. Effect of alcohol to E150 of gasoline.

For present oxygenates significant decrease of gasoline boiling point temperatures to min. 5 °C in wide range of distillation is necessary to expect.

Higher concentrations of alcohols and ethers (more than 10% vol. of each) cause significant changes in second half of distillation curve. If bioethanol is added to gasoline the increase of distilled volume at temperatures around 70 °C should be expected during production. Application of n–butanol and isobutanol increases distilled volume above 100 °C. This effect is seen at Fig. 9 and 10 and on values E100 and E150.

CONCLUSIONS

Changes of distillation curve of gasolines with alcohols are associated with changes of other parameters. The first part of distillation curve and temperature T50 is influenced by bioethanol if mixed with gasoline. The rest of this distillation curve follows shape of pure gasoline. Biobutanol may alternate bioethanol mixtures with gasoline but, parameters differ again. Gasoline mixtures with biobutanol either in form of n-butanol or in form of isobutanol affect only second part of distillation curve with values of E100 and E150 according to EN 228. Shape of distillation affects also performance of engine. Up to 20% of alcohols (bioethanol, n-butanol or isobutanol) in gasoline mixture shouldn't have any significant impact on combustion. But selection of gasoline, ETBE and MTBE cosolvents matters. Combination of gasoline with ETBE and ethanol summarizes its impacts on distillation curve of gasoline. Shape of distillation curve of gasoline with n-butanol or isobutanol and ethers MTBE and ETBE is according to boiling points of these components.

ACKNOWLEDGMENTS. The paper was created with the grant support project CIGA CULS Prague 20153001 – Utilization of butanol in internal combustion engines of generators.

REFERENCES

Dukulis, I., Pirs, V., Jesko, Z., Birkavs, A. & Birzietis, G. 2009. Development of Methodics for Testing Automobiles Operating on Biofuels. In: *Proceedings of the 8th International Scientific Conference 'Engineering for Rural Development'*. Latvia University of Agriculture, Jelgava, pp. 148–155.

Dien, B., Jung, H., Vogel, K., Casler, M., Lamb, J., Iten, L., Mitchell, R. & Sarath, G. 2006. Chemical composition and response to dilute-acid pretreatment and enzymatic saccharification of alfaalfa, reed canarygrass and switchgrass, *Biomass Bioenergy* **30**, 880–891.

Dwivedi, P., Alavalapati, J.R.R. & Lal, P. 2009. Cellulosic ethanol production in the United States: Conversion technologies, current production status, economics and emerging developments, *Energy for Sustainable Development* **13**, 174–182.

EN 228. 2009. Automotive fuels – *Unleaded petrol* – Requirements and test methods, ČSNI, 16 pp. (in Czech).

Groot W.J., Lans, R.G.J.M. & Luyben, K.Ch.A.M. 1992. Technologies for Butanol Recovery Integrated with Fermentations, *Process Biochemistry* **27**, 61–75.

Hönig, V. & Hromádko, J. 2014. Possibilities of using vegetable oil to power diesel engines as well as their impact on engine oil. *Agronomy Research* **12**(2), 323–332.

Hönig, V., Kotek, M. & Mařík, J. 2014. Use of butanol as a fuel for internal combustion engines. *Agronomy Research* **12**(2), 333–340.

Hromádko, J. Hromádko, J., Miler, P., Hönig, V. & Štěrba, P. 2011. The use of bioethanol in internal combustion engines. *Chemické listy* **105**(2), 122–128 (in Czech).

Ilves, R., Kuut, A., Kikas, T. & Olt J. 2014. Influence of the drop size of bioethanol fuel in airfuel mixture on combustion process of spark ignition engine. *Agronomy Research* **12**(2), 341–350.

Kotus, M., Pexa, M. & Kubín, K. 2013. Modelling of non-road transient cycle. *Journal Central European Agriculture* **14**(4), 1281–1294.

Küüt, A.,Panova, O. & Olt, J. 2012. Characteristics describing the price formation of bioethanol used as the fuel for an internal combustion engine, *Agronomy Research* **1**(Special Issue), 139–148.

Küüt, A., Ritslaid, K. & Olt, J. 2011. Study of potential uses for farmstead ethanol as motor fuel. *Agronomy Research* **9**(1), 125–134.

Mařík, J., Pexa, M., Kotek, M. & Hönig, V. 2014. Comparison of the effect of gasoline - ethanol E85 - butanol on the performance and emission characteristics of the engine Saab 9-5 2.3 l turbo. *Agronomy Research* **12**(2), 359–366.

Melzoch, K. & Rychtera, M. Distillery and production of spirits. *http://www.vscht.cz.* Acessed 2.11.2014.

Mužíkova, Z., Pospíšil, M. & Šebor, G. 2010. The use of bioethanol as a fuel in the form of E85 fuel. *Chemické listy* **104**(7), 678–683 (in Czech).

Patáková, P., Pospíšil, J., Lipovský, J, Fribert, P., Linhová, M, Toure, S.S.M., Rychtera, M., Melzoch, K. & Šebor G. 2010. Prospects for biobutanol production and the use in the Czech republic, *Chemagazín.* **20**(5), 13–15.

Pirs, V. & Gailis, M. 2013. Research in use of fuel conversion adapters in automobiles running on bioethanol and gasoline mixtures, *Agronomy Research* **11**(1), 205–214.

Pointner, M., Kuttner, P., Obrlik, T., Jager, A. & Kahr, H. 2014. Composition of corncobs as a substrate for fermentation of biofuels. *Agronomy Research* **12**(2), pp. 391–396.

Pschorn, T. 2012. Andritz providing commercial scale pretreatment systems for advanced cellulosic biofuels based on our expertise in Pulp & Paper. *Proceedigs of the IEA Bioernergy conference* 2012, pp. 499–508.

Raud, M., Kesperi, R., Oja, T., Olt, J. & Kikas, T. 2014. Utilization of urban waste in bioethanol production: potential and technical solutions. *Agronomy Research* **12**(2), pp. 397–406.

Sims, R.E.H., Mabee, W., Saddler, J.N. & Taylor, M. 2010. An overview of second generation biofuel technologies. *Bioresource Technology* **101**(6), 1570–1580.

Sun, Y. & Cheng, J. 2002. Hydrolysis of lignocellulosic materials for ethanol production: a review. *Bioresource Technology* **83**(1), 1–11.

Talebnia, F., Karakashev, D. & Angelidaki, I. 2010.Production of bioethanol from wheat straw: An overview on pretreatment, hydrolysis and fermentation. *Bioresource Technology* **101**, 4744–4753.

Tutt, M., Kikas, T. & Olt, J. 2012b. Influence of different pretreatment methods on bioethanol production from wheat straw. *Agronomy Research* **10**(1), 269–276.

Tutt, M. & Olt, J. 2011. Suitability of various plant species for bioethanol production, *Agronomy Research* **1**(Special Issue), 261–267.

Wakker, A., Egging, R., Van Thuijl, E., Van Tilburg, X., Deurwaarder, E.P., De Lange, T.J., Berndes, G. & Hansson, J. 2005. Biofuel and bioenergy implementation scenarios. Final report of VIEWLS WP5 modelling studies. Energieonderzoek Centrum, Netherland, 104 p.

Yang, Y., Sharma–Shivappa, R., Burns, J.C. & Cheng, J.J. 2009. Dilute Acid Pretreatment of Oven-dried Switchgrass Germplasms for Bioethanol Production, *Energy & Fuels* **23**, 3759–3766.

Yuksel, F. & Yuksel, B. 2004. The use of ethanol-gasoline blend as a fuel in an SI engine. *Renewable Energy* **29**, 1181–1191.

Agronomy Research **13**(2), 568–576, 2015

The analysis of the influence of biobutanol and bioethanol mixture with ethers on the vapour pressure of gasoline

V. Hönig*, M. Orsák and J. Táborský

Czech University of Life Sciences Prague, Faculty of Agrobiology, Food and Natural Resources, Department of Chemistry, Kamycka 129, CZ16521 Prague 6, Czech Republic; *Correspondence: honig@af.czu.cz

Abstract. In addition to widely known species automotive fuels that are currently on the market, there are many other chemicals which are used or can be used as fuels or fuel components for current automotive internal combustion engines. Implementation of such ingredients car brings a number of technical problems. The vapour pressure is the pressure in the system in which they are at a certain temperature gaseous and liquid phases in equilibrium. The addition of alcohols such as gasoline constituents significantly affects the volatility of the resulting mixture. The article is focused on assessing the addition of biobutanol as n–butanol or isobutanol vapour pressure compared to the already commonly used in bioethanol. Also included is the possibility to use ethers for influencing the vapour pressure of the resulting mixture. Part of the experiment is to assess the influence of the quantity and type of oxygenates and composition of gasoline. Based on the measured data it is clear that addition of alcohol to gasoline create complications. Effect biobutanol as possible alternatives is different than bioethanol. It is therefore necessary to take into account the influence of alcohol, even at low concentrations corresponding to the limit according to standard EN 228. Biobutanol compared bioethanol can be used as 100% fuel. For the low vapour pressure of the fuel experiment also aims to increase its value using pentane.

Key words: BioEthanol, n–Butanol, IsoButanol, MTBE, ETBE.

INTRODUCTION

Process of liquefying gases is opposite to evaporating liquids. When the liquid is in a closed container only partly filled it evaporates. Evaporation represents the transition from the liquid to gaseous phase. It progress at any temperature but only from the free surface.

The evaporation speed depends on:

1. surface of area;
2. temperature;
3. removal of vapour from surface.

The pressure above the liquid is increasing, some molecules are passing again into liquid phase. Bidirectional transition is still in progress between liquid and gas (evaporation and condensation). The same rate of evaporation and condensation leads to the equilibrium state in which the vapour pressure of the solvent doesn't change (Pirs & Gailis, 2013).

Vapour pressure (equilibrium vapour pressure or the pressure of saturated or saturated vapour pressure) is pressure of single component system, when a given temperature gaseous phase is in equilibrium of liquid and solid phase. Vapour pressure is the highest pressure at which the substance can exist in equilibrium gaseous state at a given temperature. It is also the lowest pressure at which the substance can exist in liquid or solid state at a given temperature (Dukulis et al., 2009; Hromádko et al., 2011; Küüt et al., 2011).

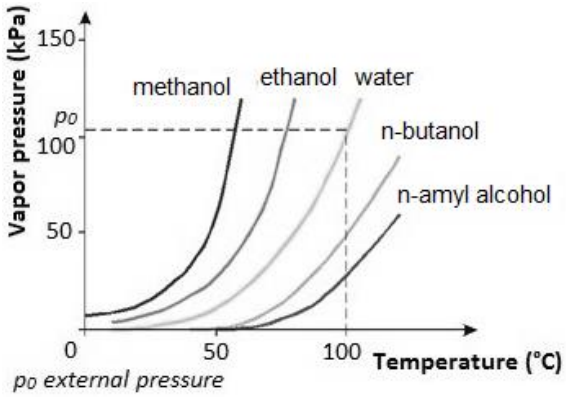

Figure 1. The dependence of vapour pressure on temperature.

Equilibrium of vapour pressure at constant temperature stabilizes without being dependent on quantity of liquid. As soon as pressure of saturated vapour reaches gas pressure in surroundings a liquid is boiling (Campos et al., 2002; Ezeji et al., 2007; De Wit & Faai, 2010).

The corresponding temperature is called the boiling point. Both boiling and also boiling point depends on the external pressure being described by vapour pressure curve (Fig. 1).

The socalled normal boiling point means temperature by which the pressure is equal to saturated vapour pressure of 101.325 kPa. Liquid can be warmed up to temperature by which pressure of saturated steam is equal to outside pressure if it is maintained at a constant value. This pair of values of the temperature–pressure is called the boiling point of liquid (Patáková et al., 2010).

The normal boiling point (T_N) is temperature of liquid with given composition in phase equilibrium with its vapour at normal atmospheric pressure (101.325 kPa). We may say, that the vapour pressure at the normal boiling point of all substances is equal to 101.325 kPa.

Liquid–vapour system receives heat from outside to maintain isothermal conditions during evapouration (Hendrich et al., 2005). A molar heat of vaporization is heat consumed during vaporization of amount of liquid substance. This is equal to molar vaporization enthalpy (ΔH_M). The dependence of vapour pressure on temperature may be expressed by the following equations.

Augustus equation

$$\log p = A - \frac{B}{T} \tag{1}$$

where: p – saturated vapour tension of the liquid; T – temperature; A,B – empirical constants.

Antoine equation

$$\log p = A - \frac{B}{C + t} \tag{2}$$

where: p – saturated vapour tension of the liquid; t – temperature; A,B,C – empirical constants

Result of Antoine equation is based on pressure unit [torr]. Therefore, it must be converted to pressure in units (Pa) after calculation.

$$torr = 133.3kPa \tag{3}$$

This calculation method has only limited accuracy. Therefore, it is suitable for lower pressures not being applicable for all substances. This is only a mathematical approximation of equilibrium of real situation.

Clausius – Clapeyron equation

$$\frac{d \ln p^o}{dT} = \frac{\Delta H_M}{RT^2} \tag{4}$$

where: p^0 – saturated vapour tension of the liquid; T – temperature; ΔH_M – molar vaporization enthalpy; R – universal gas constant (8.314 J $K^{-1}mol^{-1}$).

Assuming that the molar vaporization enthalpy of measured temperature range is constant the relationship is obtained by integration of equation (1):

$$\ln p^o = A - \frac{\Delta H_M}{R} \cdot \frac{1}{T} \tag{5}$$

which can be rewritten as:

$$\ln p^o = A + \frac{B}{T} \tag{6}$$

where A,B – are equation constants, which are usually assessed on basis of experimental data.

Vapour pressure above liquid

The release of particles from the liquid surface (evaporation) is process, which more or less intensively occurs at each temperature. Vapour pressure (vapour pressure) above the liquid is function of temperature. The higher temperature the higher pressure tendency occurs (Fig. 1). The temperature at which the saturated vapour tension reaches the external pressure is called the temperature of boiling point. The boiling point is important physical parameter of substance. It depends on relative molecular weight, polarity of substance and possibility of formation of hydrogen bridges. The socalled volatility of substance is related to boiling point (Groot et al., 1992; Moiser et al., 2005; Melzoch et al., 2010).

Vapour pressure is equilibrium of vapour and liquid phases at given temperature. Interval of vapour pressure is set by standard EN 228 according to climatic conditions during the year. Summer gasoline has lower vapour pressure (45–60 kPa) to prevent loss of fuel by increased evaporation and also to decrease emergence of vapour cushions. Vapour pressure of winter gasoline ranges from 60 to 90 kPa. Higher vapour pressure are necessary for sufficient fuel evaporation and reliable start at low temperatures (Hromádko et al., 2009; Hromádko et al., 2010).

The vapour pressure of fuel is closely related to boiling point. In purely hydrocarbon gasoline the highest vapour pressure have low boiling butanes (350–390 kPa) and pentanes (i–pentan 115 kPa). Its content can reliably regulate the resulting vapour pressure of gasoline directly during manufacturing. Biofuels, especially bioethanol, is becoming more important in recent years. Adding ethanol and other oxygenates in gasoline is causing change of vapour pressure (Mužíková et al., 2010; Hönig et al., 2014; Pointner et al., 2014).

An objective of this paper is to test if biobutanol can compete with bioethanol. Bioethanol is currently commercially produced and used as a component of gasoline or as E85. Selection of raw material for production of alcohols depends on the enzymatic equipment of microorganisms. Cultures of *Clostridium acetobutylicum* are used to produce biobutanol in shape of n–butanol (butan–1–ol). Researchers focus their attention also on blue–green algae strain of *cyanobacteria* that produce biobutanol as isobutanol (Mosier et al., 2005; Patáková et al., 2010; Pointner et al., 2014).

Effect of commonly used MTBE and ETBE on vapour pressure of mixture is also analysed. MTBE and ETBE are current cosolvents added to gasoline. Therefore, its influence on gasoline–butanol mixtures is necessary to know (Mužíková et al., 2012).

MATERIALS AND METHODS

Standard procedure determines the vapour pressure according to method of Reid (RVP). The measurement is performed at temperature of 37.8 °C in a sealed vessel with a volume about 500 ml, which is equipped with manometer. The ratio of the volume of air chamber to volume of fuel chamber is exactly 4:1. The sample in fuel chamber is saturated with air at 0–1 °C.

The vapour pressure of mixtures of pure gasoline without added oxygen and additives are used according to standard EN 228 for winter (labelled with W) and summer period (labelled with S).

Further, MTBE (methyl tert–butyl ether) and ETBE (ethyl tert–butyl ether) produced by Czech refinery joint stock company, n–butanol p.a. (Lachner, Ltd),

isobutanol p.a. (Lachner, Ltd), n–pentante p.a. (Lachner, Ltd) and anhydrous ethanol were used.

Standard of Reid according to ASTM D323 the vapour pressure of gasoline mixtures and influence of alcohols and ethers was used.

The test samples are labelled as follows:

1. ETH for bioethanol;
2. nBUT for n–butanol;
3. isoBUT for isobutanol.

RESULTS AND DISCUSSION

Fig. 2 shows that the vapor pressure of gasoline containing 10% vol. of ethanol corresponds to vapour pressure without presence of ethanol. Surprisingly, emerged mixture of 5% vol. has higher vapour pressure than original gasolines. This phenomena is seen at peak of W – gasoline curve in interval 0–10% vol. of alcohol volume (Fig. 2). This negative commingling (mixing) effect is called by vapour pressure of ethanol in gasoline.

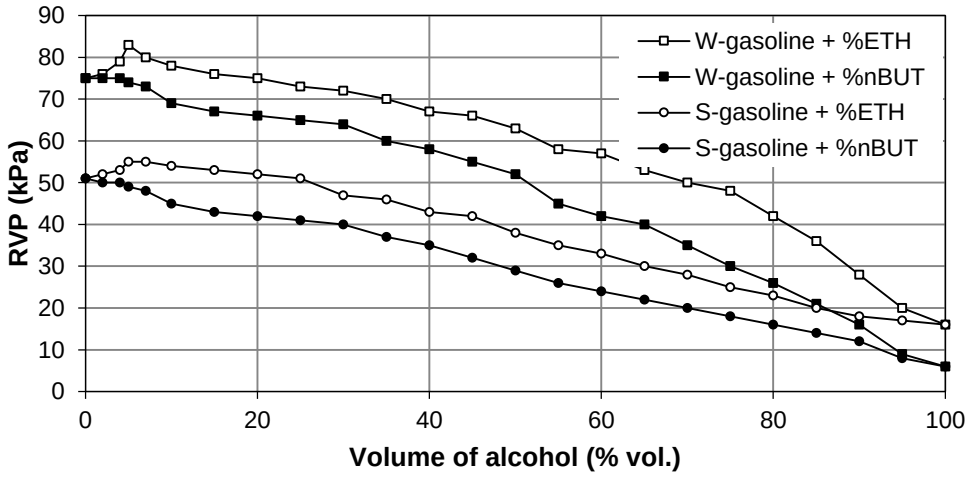

Figure 2. Vapour pressure of winter (W) and summer (S) gasoline mixtures depending on amount of added alcohol.

Ethanol actually creates new azeotrope with minimum boiling point, while the pressure of the newly formed mixture is increased. The amount of change of the vapour pressure depends on proportion of both gasolines and ethanol in the resulting mixture (Fig. 2).

Added ethanol to gasoline up to 8% vol. has maximum increase of vapour pressure. Further increasing of ethanol content in mixture decreases vapour pressure. The mixture comprising about 20% vol. of ethanol has the same vapour pressure as without ethanol being present.

The vapour pressure of E85 (85% vol. of ethanol) mixture is moving below the lower limit (45 kPa) for summer automotive gasoline. When preparing a 5% vol. mixture

of ethanol in summer gasoline is necessary to have sufficient vapour pressure up to 8 kPa, and simultaneously reduce C_4 fraction. Vapour pressure of gasoline mixed with biobutanol can be attributed to sum of both components and its points of vapour pressure.

The courses of influence of n–butanol and isobutanol on vapour pressures of gasoline are very similar. Therefore, the influence of isobutanol is shown separately in Fig. 3. Vapour pressure of mixtures containing up to 5% vol. n–butanol and isobutanol is insignificant opposed to ethanol. Higher concentrations of alcohols in gasoline lead to lower vapour pressure of resulting mixtures (Figs 2 and 3).

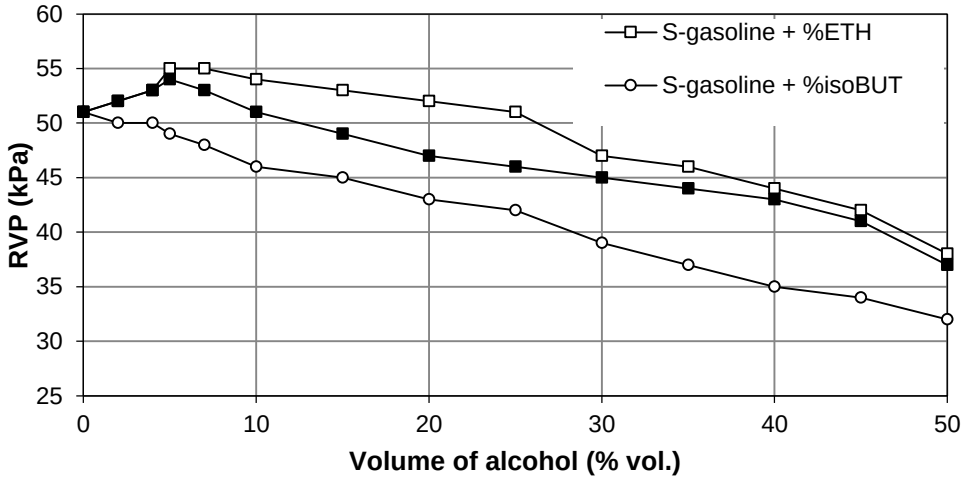

Figure 3. Vapour pressure of summer (S) mixtures of gasoline depending on added isobutanol.

With increasing boiling point of hydrocarbon the boiling point of the azeotrope increases. Alkanes n–C_4 n–C_5 have lower boiling point than ethanol. Decreased boiling point of the azeotrope of ethanol is lower opposed to e.g. n–octane. Formed azeotrope with ethanol alkanes increases vapour pressure of azeotrope more than ethanol with aromatics.

Vapour pressure of mixture of gasoline with ethanol may be positively influenced by presence of n–butanol and isobutanol (Figs 3 and 4). The growth of vapour pressure with added 5% vol. of ethanol in the mixture, which already contains 2% vol. butanol, causes a pressure increase up to 6 kPa (Fig. 4). Increasing pressure may be observed at other compositions of both alcohols.

Fig. 4 shows that in case of 5/10% vol. (ethanol/n–butanol) and 10/5% vol. is vapour pressure theoretically the same. The vapour pressure of gasoline containing 5% vol. of ethanol is characterized by formation of a new azeotrope with higher vapour pressure. The presence of n–butanol (also isobutanol Fig. 3) reduces vapour pressure of this gasoline–ethanol mixture. Vapour pressure of mixture containing 10% vol. ethanol is less than mixture containing 5% vol. of ethanol. To reduce the vapour pressure according to mixture 5/10% vol. is required smaller amount of n-butanol 10/5% vol. Differences of vapour pressures of mixtures containing 5 and 10% vol. of ethanol is also seen in mixtures 5/2% vol. and 10/2% vol.

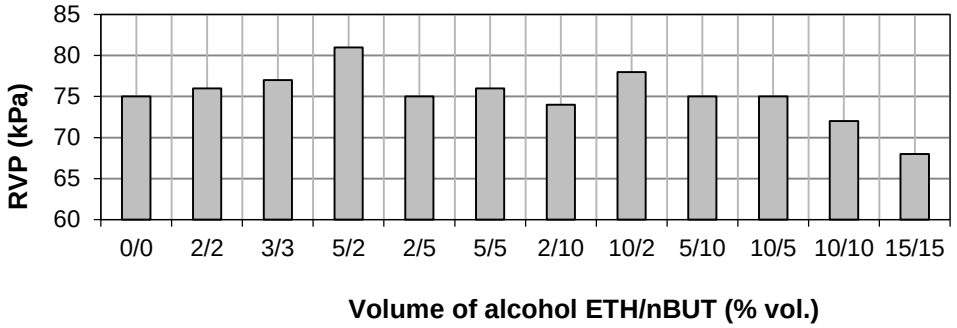

Figure 4. Vapour pressure at 37.8 °C for winter mixture of ethanol/n–butanol with gasoline.

Ethers (MTBE, ETBE) may significantly reduce increase of vapour pressure ethanol is added while azeotrope is emerging. Fig. 5 shows how a smaller amount of ether added to mixture could decrease vapour pressure of low mixtures of ethanol.

ETBE has more favourable effects opposed to both ethanol and butanol as vapour pressure of mixtures is less affected. ETBE is decreasing vapour pressure in interval of 45–90 kPa. Effect of MTBE depends on initial vapour pressure of hydrocarbon base. Vapour pressure of mixture of gasoline, n–butanol and MTBE below 55 kPa increases but, above this limit decreases. Therefore, this lower vapour pressure of summer gasoline was sample selection criteria.

The bottom axis on Fig. 5 shows the amount of n–butanol/MTBE and n–butanol/ETBE.

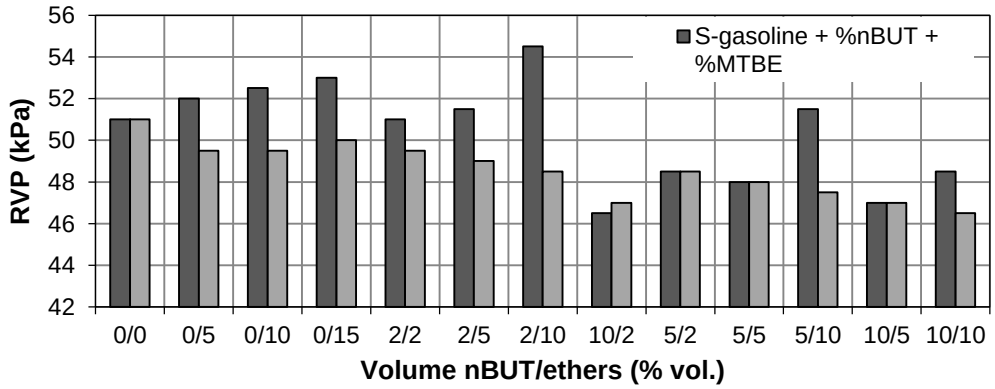

Figure 5. The vapour pressure at 37.8 °C of summer mixtures of gasoline with n–butanol, MTBE and ETBE.

The very low vapour pressure of pure biobutanol requires to know temperature of gasoline mixtures with butanol. Otherwise, cold start of engine a minimum volatility of gasoline with a minimum vapour pressure of 5 kPa is needed. This is the lowest limit allowing start of engine.

The vapour pressure of gasoline containing high percentages of ethanol, n–butanol and isobutanol must be increased by hydrocarbon component with sufficiently high

volatility. Requirement of minimum fuel volatility for starting of engine at low temperatures is fulfilled in this case. Low boiling components (hydrocarbons C_3–C_5) of gasoline allow starting of engine well, for example. Use of these hydrocarbons in commercial gasoline is due to its high vapour pressure limited. Resulting balance of refinery without watching C_3–C_5 gasoline components is also suitable enhancement.

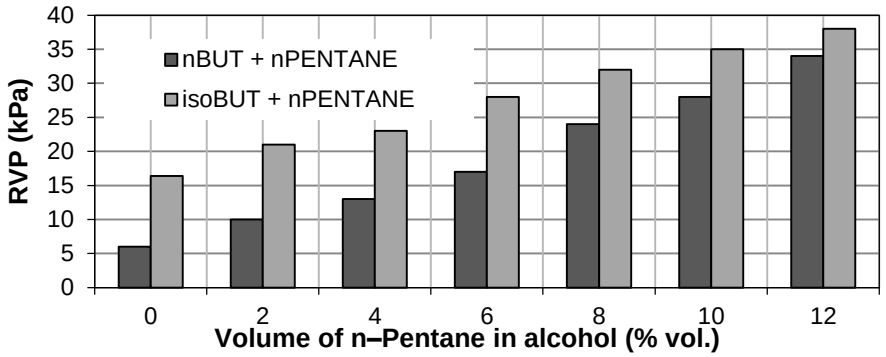

Figure 6. Vapour pressure at 37.8 °C of n–butanol and isobutanol depending on the added pentane.

The vapour pressure of biobutanol can be increased if n–pentane is added. This method may be applied for 100% biobutanol (n–butanol or isobutanol) biofuel (Fig. 6). If applied pure n–butanol or isobutanol without added volatile component (or special equipment) it would be very difficult to start engine even at temperature 37.8 °C according to method of Reid.

CONCLUSIONS

Application of renewable biofuels brings a number of technical problems. Alcohol fuel and ether mixtures affect the volatility both up and down significantly. Bioethanol and biobutanol in gasoline need adjustments of either engine or fuel according to vehicle specifications. Vapour pressure and distillation curve affect driveability of engine and fuel leaks into air during distribution.

Gasoline mixture with ethanol up to 10% vol. creates a new azeotrope with minimum boiling point, which increases vapour pressure. Gasoline mixture with butanol (n–butanol and isobutanol) a reserve of vapour pressure of gasoline needn't be created as emerging azeotrope has no impact.

Vapour pressure of gasoline containing high percentages of ethanol (for example E85), n–butanol and isobutanol needs to be increased by low–boiling gasoline components C_3–C_5. Butanol can also be administered as a pure fuel in comparison with bioethanol if n–pentan is added, for example.

Ethers (MTBE, ETBE) in gasoline with alcohols may cause unpredictable phenomena as vapour pressure of winter and summer gasoline differ and its effect is not easily predictable. The vapour pressure of the resulting mixtures must be monitored to prevent negative impact on engine starting and for fuel distribution and storage. Mixtures with a higher content of bioethanol or biobutanol require optimizing of fuel/air ratio, which is influenced by oxygen content in gasoline.

REFERENCES

Campos, E.J., Qureshi, N. & Blashek, H.P. 2002. Production of acetone Butanol ethanol from degermed corn using Clostridium beijerinckii BA 101, *Applied Biochemistry and Microbiology*, pp. 553–556.

De Wit, M. & Faai, A. 2010. European biomass resource potential and costs. *Biomass Bioenerg.* **34**, pp. 188–202.

Dukulis, I., Pirs, V., Jesko, Z., Birkavs, A. & Birzietis, G. 2009. Development of Methodics for Testing Automobiles Operating on Biofuels. In: *Proceedings of the 8th International Scientific Conference 'Engineering for Rural Development'*. Latvia University of Agriculture, Jelgava, pp. 148–155.

EN 228. 2009. Automotive fuels – Unleaded petrol – Requirements and test methods, ČSNI, 16 pp. (in Czech).

Ezeji, T., Qureshi, N. & Blashek, H.P. 2007. Butanol production from agricultural residues: impact of degradation product on Clostridium beijerinckii growth and Butanol fermentation. *Biotechnology & Bioengineering*, Wiley, 1460–1469.

Groot W.J., Lans, R.G.J.M. & Luyben, K.Ch.A.M. 1992. Technologies for Butanol Recovery Integrated with Fermentations, *Process Biochemistry* **27**, 61–75.

Hendrich, L., Hynek, V. & Šípek, M. 2005. Differential Measurement of Permeability of Gases and Organic Vapours through Flat Polymer Membranes, *Chemické listy* **99**, 345–350 (in Czech).

Hönig, V. Kotek, M. & Mařík, J. 2014. Use of butanol as a fuel for internal combustion engines. *Agronomy Research* **12**(2), 333–340.

Hromádko, J. Hromádko, J., Miler, P., Hönig, V. & Štěrba, P. 2011. The use of bioethanol in internal combustion engines. *Chemické listy* **105**(2), 122–128. (in Czech)

Hromádko, J. Hromádko, J. Miler, P. Hönig, V. & Štěrba, P. 2009. The lifecycle assessment of fossil fuels and bioethanol. *Listy cukrovarnicke a reparske* **125**, 320–323 (in Czech).

Hromádko, J. Hromádko, J. Miler, P. Hönig, V. & Štěrba, P. 2010. Production of bioethanol. *Listy cukrovarnicke a reparske* **126**, 267–270 (in Czech).

Küüt, A., Ritslaid, K. & Olt, J. 2011. Study of potential uses for farmstead ethanol as motor fuel. *Agronomy Research* **9**(1), 125–134.

Melzoch, K., Patáková, Petr., Lipovský, J., Fořtová, J., Rychtera, M. & Čížková, H. 2010. Exploitation of food feedstock and waste for production of biobutanol, *Czech Journal of Food Science* **27**(4), 276–283.

Mosier, N., Wyman, C., Dale, B., Elander, R., Lee, Y.Y., Holtzapple, M. & Ladisch, M. (2005). Features of promising technologies for pretreatment of lignocellulosic biomass. *Bioresource Technology* **96**(6), 673–686.

Mužíková, Z., Káňa, J., Pospíšil, M. & Šebor, G. 2012. Physicochemical Properties of Butanol–Gasoline Blends. *Chemické listy* **106**, 1049–1053 (in Czech).

Mužíková, Z., Pospíšil, M. & Šebor, G. 2010. The use of bioethanol as a fuel in the form of E85 fuel. *Chemické listy* **104**(7), pp. 678–683 (in Czech).

Patáková, P., Pospíšil, J., Lipovský, J, Fribert, P., Linhová, M, Toure, S.S.M., Rychtera, M., Melzoch, K. & Šebor G. 2010. Prospects for biobutanol production and the use in the Czech republic, *Chemagazín.* **20**(5), 13–15 (in Czech).

Pirs, V. & Gailis, M. 2013. Research in use of fuel conversion adapters in automobiles running on bioethanol and gasoline mixtures, *Agronomy Research* **11**(1), 205–214.

Pointner, M., Kuttner, P., Obrlik, T., Jager, A. & Kahr, H. 2014. Composition of corncobs as a substrate for fermentation of biofuels. *Agronomy Research* **12**(2), 391–396.

Agronomy Research **13**(2), 577–584, 2015

Determination of the optimal injection time for adaptation SI engine on E85 fuel using self-designed auxiliary control unit

T. Kotek[1,*], M. Kotek[2], P. Jindra[2] and M. Pexa[1]

[1]Czech University of Life Science Prague, Faculty of Engineering, Department for Quality and Dependability of Machines, Kamýcká 129, CZ16521 Prague, Czech republic; [*]Correspondence: kotek@oikt.czu.cz
[2]Czech University of Life Science Prague, Faculty of Engineering, Department of Vehicles and Ground Transport, Kamýcká 129, CZ16521 Prague, Czech republic

Abstract. Article deals with problems of the operation of spark ignition combustion engine on high-percentage of blend bioethanol. The aim of the experiment was to find the optimal value of injection time of the engine injection valves with respect to the adaptive ability of the original engine control unit (ECU) when using a special auxiliary control unit (ACU) was adjusted injection time. Special dynamic driving cycle has been designed to assess the effects of prolonged injection time on the adaptive abilities of the ECU that stemmed from a real recording vehicle's rides with the same engine as was used in conducted experiments. The results proved that by changing the extension of the period of injection occurs a gradual adaptation of the original ECU, but this adaptation is gradual and underway predominantly in modes functional closed-loop control, thus in modes of low to medium of loads. Results of the experiment provide determination of the efficient frontier of the percentage extension injection time with regard to adaptive abilities of original ECU.

Key words: E85, bioethanol, emission, power, control unit.

INTRODUCTION

Nowadays issue of bio-fuels has been becoming more and more actual topic. The whole world is keep raising the usage of fossils fuels and growth of greenhouse gases (GHG) production. Estimation supposes that approximately 80% of primary energy comes from fossil fuels and almost 60% of this energy is used in transport section (Escobar et al., 2009). The various legislative measures are introduced in various parts of the world to support usage of the biofuels which have potential to reduce GHG production. The common targets of these measures are to reduce dependency on expendable fossils fuels with their growing and unstable prices.

The first measure of EU which led to using biofuels was European parliament and Council acceptance of directive 2003/30/EC about promotion of the use of biofuels or other renewable fuels for transport. According to the directive EU states should ensure that biofuels part will be 5.75% in the fuel market by the end of 2010 (EU Directive 2003/30/EC). This directive was replaced in 2009 by directive 2009/28/EC that demands to increase the renewable fuels part to 20% in 2020, 10% of this part is set up for transport section (EU Directive 2009/28/EC; Hromádko et al., 2009). Also the directive

2009/30/EC was accepted with directive 2009/28/EC. This new directive defines environmental specifications of engine fuel (acceptable part of added bio component to fuel) (EU Directive 2009/30/EC). Both directives clearly show that to meet desired goals in renewable sources is not possible by only required adding of low-percentage biofuels to the gasoline. It is necessary to add bio-fuels with high-percentage of bio component to meet desired goals.

One of the options to meet required goals is to use bio-ethanol as a high-percentage mixed biofuel in the E85 form (85% ethanol, 15% gasoline). In comparison with standard fuel the ethanol has lower energy density than gasoline (ethanol 23.5 MJ litre^{-1}, gasoline 34.8 MJ litre^{-1}). It causes higher consumption of fuel to keep the same operational values. Advantage of ethanol is its higher octane number (ethanol 104, gasoline 95) and also quicker combustion (Roberts, 2007; Park et al., 2010; Čedík et al, 2014a).

The disadvantages of ethanol are above mentioned lower energy density, often stated corrosion of gasoline pump and fuel line or diminished ability to start engine at lower temperatures (Rovai et al., 2005).

Researched ethanol influences on emissions production often present different results. Lower productions of carbon monoxide (CO) is very often mentioned, other emissions reach different results in comparison with used gasoline according to specific construction of combustion engine (Graham et al, 2008; Winther et al., 2012; Čedík et al, 2014b).

For the operation of internal combustion engines on a high-percentage alcohol fuel mixture is required certain engine modifications. The stoichiometric ratio for a specific mixture of alcohol and gasoline must be respected. In our case, for the fuel E85 mixing ratio 9:1 (air:fuel) must be observed. In comparison with gasoline (mixing ratio 14.7:1) it is necessary make richer mixture. According to the system of fuel management more modifications of engine are possible (Irimescu, 2012).

The aim is to increase the fuel dose, which can be done in the following ways: increase the system fuel pressure (Merola et al., 2010), using injectors with higher flow rate (Vancoillie et al., 2013) or extension injection time. Injection time can be changed by reprogramming the original ECU (Hsieh et al., 2002), or using additional control unit (ACU) (Irimescu, 2012).

Modern electronic fuel injection systems use the closed-loop control (it mean the ECU fuel injection strategy with feedback signal from the oxygen sensor placed in the exhaust pipe) for adaptation to different fuels by increasing fuel dose. This regulation has limits and is often necessary to use ACU to optimize the adaptive ability of ECU. These ACU extend the injection time thereby enrich the mixture. The question is, how much is necessary extend the injection time to adaptation ECU without errors (Hsieh et al., 2002).

In case of open-loop regulations, which occurs e.g. at cold starts or at higher engine loads, the mixture control is regulated by preprogrammed fuel maps for the initial fuel, ie gasoline. When E85 is used the air-fuel equivalence ratio (λ) moved toward lean mixtures (Irimescu, 2011).

The aim of this article was to analyse the operational parameters of the internal combustion engine and adaptability of the original ECU for various extension injection times. The special additional control unit (ACU) has been constructed for this purpose. ACU's task was to change the extension opening time of injection valves' according to

programme. The majority of commercially offered additional units in Czech Republic provides only two adjustment possibilities of extension period e.g. for fuel E0-E50 or E50-E85. This paper's authors proposed design of ACU that can adjust the injection time extension gradually in steps of 5% (from 0% to 35%). The article presents a unique solution of ACU and points out the issues of ECU adaptive ability.

MATERIALS AND METHODS

The whole experiment was conducted on the test bed at the Department of Vehicles and Ground transport, CULS in Prague.

The measurement was carried out with a four-stroke inline three-cylinder engine Skoda Fabia 1.2 HTP (see Table 1 for detailed parameters) with multipoint injection system with close-loop control mode at part engine loads to keep the engine operating near stoichiometric air–fuel ratio (AFR) and open-loop control mode at full engine loads to produce maximum power.

Table 1. Technical parameters of tested engine

Engine code	AWY
Construction	3-cylinders, row, 6 valves
Volume	1198 cm^3
Compression ratio	10,3 : 1
Power	40 kW at 4,750 rpm
Torque	106 Nm at 3,000 rpm
ECU	Simos 3PD (multipoint injection)
Fuel	unleaded N95
emission standard	EU4

The tested engine was loaded with whirl dynamometer, the torque and engine speed were captured during measure. Whirl dynamometer V125 was used during experiment. Dynamometer reactions were captured with tensometric sensor with nominal load of 2 kN and with accuracy of 0.5% of the nominal load. Next values were also captured: ECU's instantaneous values, exhaust emissions and fuel consumption.

Special mobile five-component analyser VMK (technical specifications in Table 2) was used to measure emission. This analyser was constructed to measure emission under real operational conditions. The emissions of CO, CO_2, HC, NO_X and λ with a frequency of 1 Hz were continuously evaluated and stored.

The Flowmeter WF005 was used to measure fuel consumption. Technical specifications are shown in Table 3. System DataLab was used to record data from flowmeter. The development environment ControlWeb was used to create application for continuous data recording and visualising.

Diagnostic system VAG-COM was used for communication with ECU. This system was primary used to read values from control unit as engine speed, engine load and to check errors.

The engine was researched with the E85 fuel and with help of additional control unit (ACU) was gradually extended times of injection from 0, 5, 10, 15, 20, 25, 30 to 35%. The our-designed ACU was used to extend the time of injection. The ACU was connected between ECU and injectors. Inputs for this ACU were impulses from injectors

emitted by ECU. These impulses were extended by ACU for a pre-set time in percentages.

Table 2. Technical parameters of the emission analyser

Measured component	Scope	Resolution	Accuracy
CO	0–10% vol.	0.001% vol.	0–0.67%: 0.02% 0.67–10%: 3% from measured value
CO_2	0–16% vol.	0.1% vol.	0–10%: 0.3% 10–16%: 3% from measured value
HC	0–20,000 ppm	1 ppm	10 ppm or 5% from measured value
NO_X	0–5,000 ppm	1 ppm	0–1,000 ppm: 25 ppm 1,000–4,000 ppm: 4% from measured value
O_2	0–22% vol.	0.1% vol.	0–3%: 0.1% 3–21%: 3% from measured value

Table 3. Technical parameters of the flowmeter WF005

Measuring principle	hall sonde
flow range	0.005–1.5 l min^{-1}
output	1,800 imp l^{-1}
viscosity	0–2,000 mPas
accuracy	+– 0.5%

Special dynamic drive cycle (Fig. 1) was designed to assess the impact of extended opening of the injectors. This cycle was designed in accordance to the real replay of the vehicle drive (also Skoda Fabia 1.2. HTP). Recorded values from real drive were used to set up throttle setting, engine speed and load on the testing engine for our measurement. Target was to operate the engine as much similar as in real traffic conditions.

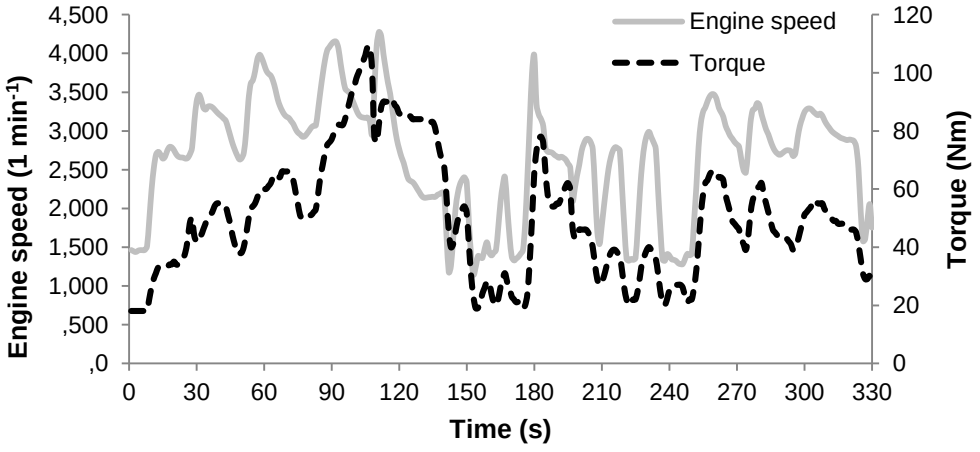

Figure 1. Test cycle.

RESULTS AND DISCUSSION

As can be seen in Table 4, there is a negligible impact on the engine's performance parameters. Fuel consumption is also essentially unchanged; the difference between the zero and maximum extension is average 4%. The emissions of CO increased when the injection time was extended. On the other hand emissions of CO_2 and NO_X were decreased. As seen the λ, the mixture was got richer when the time of extension increased. Results proved reaction of original ECU, where can be seen gradual decreasing of basic injection time with increasing extension. This is caused by mixture's correction based on the signal obtained from the exhaust oxygen senzor. Ignition advance shows no major impact on the extending time of the injection.

Table 4. Summary results of the operating parameters of the engine in driving cycle

Extension	CO	CO_2	NO_X	HC	Avg. λ	Avg. Torque	Avg. Power	Avg. Injection time	Avg. Ignition advance	Fuel consumption
(%)	(g)	(g)	(g)	(g)	(1)	(Nm)	(kW)	(ms)	(°)	(l)
0	1.6	1,204	34.34	0.2	1.057	50	15	8.79	29.62	0.642
5	10.1	1,250	19.39	0.24	1.034	50	16	7.9	30.38	0.653
10	10.1	1,247	17.98	0.2	1.021	51	16	7.28	29.75	0.658
15	36.97	1,225	1.3	0.35	1.026	51	16	6.8	29.85	0.66
20	25.27	1,216	1.04	0.2	1.032	51	15	6.24	29.81	0.652
25	25.57	1,210	1.76	0.15	1.032	50	15	5.83	29.49	0.651
30	46.68	1,202	0.5	0.36	1.021	50	15	5.46	29.51	0.662
35	59.67	1,184	0.17	0.46	1.017	50	15	5.28	29.62	0.668

Situation becomes less plausible when the on-going check of errors memory is observed. The original ECU logs errors when the extension is zero or higher than 25%. This error was called 'too lean or too rich mixture – regulation out of range'. The Table 5 shows the gradual adaptation of original ECU after repeating the driving cycle.

Table 5. Adaptation of the original ECU on 15% extension in driving cycle

Meas. num.	CO	CO_2	NO_X	HC	Avg. λ	Avg. Torque	Avg. Power	Avg. Injection time	Avg. Ignition advance	Fuel consumption
(-)	(g)	(g)	(g)	(g)	(1)	(Nm)	(kW)	(ms)	(°)	(l)
1	57.1	1,210	2.34	0.413	1.021	50.7	15.66	6.83	29.96	0.678
2	47.5	1,216	0.31	0.406	1.024	51.1	15.58	6.83	29.89	0.669
3	34.8	1,223	0.56	0.349	1.026	51.9	15.58	6.81	29.91	0.656
4	26.1	1,237	0.72	0.317	1.028	52.1	15.64	6.80	29.58	0.649
5	19.1	1,239	2.56	0.257	1.031	51.8	15.56	6.73	29.92	0.647

Adaptation is reflected by gradual modification of the fuel mixture settings which reacts to the closed-loop control. As it can be seen on the Fig. 2, the CO emission is gradually decreased with a cycle's repetition. This corresponds with Fig. 3 that shows the gradual reduction of the average injection time.

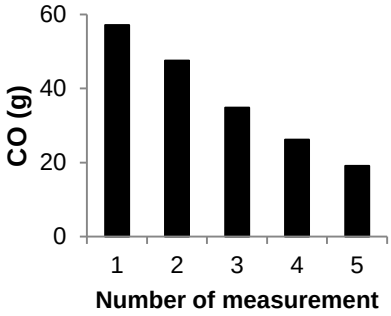

Figure 2. Process of CO emission on 15% prolong in repeat driving cycle.

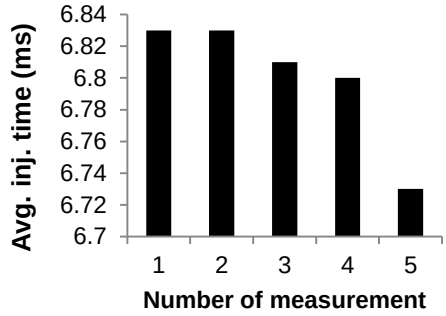

Figure 3. Process of avg. inj. time on 15% prolong in repeat driving cycle.

We can conclude, that ECU gradually adapts to a new fuel (by changing the basic injection time) after repeating the testing cycle. However the ECU cannot adapt according to the new fuel with injection extension less than 5% or more than 25%. When the extension time is set up lower than 5% then the ECU cannot adapt to the new fuel by increasing the dose of fuel enough to compensate too lean mixture. This situation was logged during testing cycle by ECU as too lean mixture error. This fact was also confirmed by the lowest CO emissions, the highest NO_X and the highest average λ during the driving cycle. This situation happens by combustion of lean mixture.

The similar situation happened when the extension of injection time was set on more than 25%. ECU was getting information from exhaust oxygen senzor that the mixture is too rich. However the ECU cannot sufficiently reduce base injection time which results in logging error 'too rich mixture' by ECU. These extreme states correspond with measured values of CO emission. As shown by above results, the optimal injection time is set by ECU according to signal from the exhaust oxygen senzor. ECU is able to regulate mixture in a specific range. This range is not sufficient for high-percentage ethanol mixture and it is necessary to adjust the injection time using ACU. This way causes the move of the ECU's adaptive range to ensure optimal injection time.

CONCLUSIONS

The tested engine has demonstrated the ability to operate on E85, however, ECU could not regulate the mixture without error. It has been shown, that without additional control unit ECU was not able to determine the optimal time of injection. Although ECU received from the exhaust oxygen senzor information about lean mixture, ECU has not been able to extend the time of injection, due to exceeding the adaptation range. By using the ACU can be moved ECU adaptation range.

These first carried out experiments have shown that there is mismatch between ACU and original ECU. Respectively: How much is extended time of injection by ACU, so much time is shortened on the basic injection time by ECU depending on the signal from exhaust oxygen sensor. Everything is depended on the adaptive abilities of the ECU. It was proved that original ECU has its own limits of adaptation abilities and in case those limits are exceeded, another adaptation does not take place and the error of

wrong mixture of the fuel is logged in the error memory (too lean or too rich mixture errors).

Experiments determined the optimal interval of injection time extension from the measured values. This interval can be set up as extreme values, which was not recognized as bad mixture errors. In this case we can define the extreme values as 5% extension as minimal value (original ECU can adapt to this value). The maximal value can be set as 20%. Control unit is able to adapt even to this state of tested fuel.

The emission results show that increasing extension time of injection causes higher CO production, while NO_X emissions are lower. CO_2 emissions and fuel consumption do not show any significant changes. As shown in above emission results, the optimal extension value is 20% when the original ECU is able to adjust the optimal injection time.

ACKNOWLEDGEMENTS. This work has been realized with the contribution of Czech University of Life Sciences in Prague Internal Grant Agency, project 2014:31150/1312/3116 'Evaluation of the environmental benefits of bioethanol blending into motor fuels'.

REFERENCES

Čedík, J., Pexa, M., Kotek, M., Hromádko, J. 2014, Effect of E85 fuel on performance parameters, fuel consumption and engine efficiency – Škoda Fabia 1.2 HTP. *Agronomy Research* **12**(2), 307–314.

Čedík, J., Pexa, M., Kotek, M., Hromádko, J.2014, Effect of E85 Fuel on Harmful Emissions – Škoda Fabia 1.2 HTP. *Agronomy Research* **12**(2), 315–322.

Escobar, J.C., Lora, E.S., Venturini, O.J., Yanez, E.E., Castillo, E.F., Almazan, O. 2009. Biofuels: environment, technology and food security, *Renew. Sustain. Energy Rev.* **13**, 1275–1287.

Graham, L.A., Belisle, S.L., Baas, C.-L. 2008. Emissions from light duty gasoline vehicles operating on low blend ethanol gasoline and E85, *Atmospheric Environment* **42**, 4498–4516.

Hromádko, J., Hromádko, J., Miler, P., Hönig, V., Schwarzkopf, M. 2009. Economic analyse of using bioethanol in positive ignition engine, *Listy cukrovar. a řep.* **125**(3), 101–103. (in Czech)

Hsieh, W.-D., Chen, R.-H., Wu, T.-L., Lin, T.-H. 2002, Engine performance and pollutant emission of an SI engine using ethanol–gasoline blended fuels, *Atmospheric Environment* **36**, 403–410.

Irimescu, A., 2011, Fuel conversion efficiency of a port injection engine fueled with gasoline-isobutanol blends, *Energy* **36**, 3030–3035.

Irimescu, A., 2012, Performance and fuel conversion efficiency of a spark ignition engine fueled with iso-butanol, *Applied Energy* **96**, 477–483.

Merola, S.S., Sementa, P., Tornatore, C., Vaglieco, B.M. 2010, Effect of the fuel injection strategy on the combustion process in a PFI boosted spark-ignition engine, *Energy* **35**, 1094–1100.

Park, C., Choi, Y., Kim, Ch., Oh, S., Lim, G., Moriyoshi, Y. 2010. Performance and exhaust emission characteristics of a spark ignition engine using ethanol and ethanol-reformed gas, *Fuel* **89**, 2118–2125.

Roberts, M.C. 2008. E85 and fuel efficiency: An empirical analysis of 2007 EPA test data, *Energy Policy* **36**, 1233–1235.

Rovai, F., Tanaka, D., Sinatora, A. 2005. Wear and corrosion evaluation of electric fuel pumps with ethanol/gasoline blends. *SAE Technical Paper* 2005-01-2196.

Vancoillie, J Demuynck, J., Sileghem, L., Ven De Ginste, M., Verhelst, S., Brabant, L., Van Hoorebeke, L. 2013, The potential of methanol as a fuel for flex-fuel and dedicated spark-ignition engines, *Applied Energy* **102**, 140–149.

Winther, M. Møller, F., Jensen, T.C. 2012. Emission consequences of introducing bio ethanol as a fuel for gasoline cars, *Atmospheric Environment* **55**, 144–153.

Agronomy Research **13**(2), 585–595, 2015

The energy consumption of public transit under rural and suburban conditions

M. Lukeš*, M. Kotek and M. Růžička

[1]Czech University of Life Sciences Prague, Faculty of Engineering, Kamýcká 129, CZ16521 Prague, Czech Republic; *Correspondence: lukesm@tf.czu.cz

Abstract. The aim of paper is to investigate an energy consumption of public transit focused on regular commuting from suburban locations. Surveyed suburban settlements have become a part of 'urban sprawl' process in the suburbanized hinterland of Prague's city. The transport links are strongly influenced by the catchment area of Prague's city that has a dominant position in surveyed region and the most of the existing transport links are carried out in relation to the Prague's city on radially oriented roads. The traffic intensities are often on a roads' full capacity during peak hours or the roads are even congested alongside a ride to the city. The 10 suburban settlements were selected for the purpose of the fuel consumption investigation. Authors have focused on the journeys carried out during the morning peak hours of the ordinary working days when the transport demands are saturated. The fuel consumption investigation has involved the journeys by public transit (commuter bus) and by passenger car. Obtained results have proved possibilities of significant fuel consumption savings under condition that the bus transit preference would be effectively used. The energy efficiency of bus public transit allows to achieve the similar energy consumption per passenger as an ordinary passenger car has at a low occupancy rate of bus.

Key words: transit, passenger car, fuel consumption, peak hours, suburbanization.

INTRODUCTION

The paper points out the interplay between the transport energy consumption and the tasks of spatial planning with regards to support sustainable transport behaviour. The papers attempts to answer these questions: 'What is the actual energy consumption during the commuting from suburban settlements to the core city?' and 'Are there any possibilities to increase the energy efficiency during the daily commuting?'.

Nowadays, the society must pay attention to the issue of energy consumption, because this topic is important in the context of the sustainable development principles of land use and spatial planning, especially at the field of suburbanization. The process of suburbanization is one of the most significant phenomena in Europe and the extensive research and public debate are focused on that issue from the perspective of architectural and urban design. Suburbanization as a process can be perceived from the different perspectives that highlight the problematic factors in this process. Some authors point out the reduced availability of public amenities for residents within suburbanized area (Zolnik et al., 2010) and the consequences of the lack of public amenities in increased mobility needs of inhabitants.

Suburbanization has a sociological aspect, since there is a mix of the population between the natives (the original inhabitants of the former rural areas) and newcomers. (Špačková & Ouředníček, 2012). While original inhabitants retain their own lifestyle, the newcomers–inhabitants keep a high dependence on the core city (the dominant city of the region) in their every day's life. Demographic issues of their coexistence are discussed by Musil & Müller (2008), where the diverse population groups and their personal preferences are taken into account.

The changes of transport behaviour occur in connection with the previously mentioned factor. The newly built suburban settlements have a high private car dependency at modal split (Lukeš et al., 2014) to compare with the municipalities without suburbanization development. Transport demands of suburban settlement residents are carried out in relation to the core city. This situation contributes to the occurrence of traffic congestion and it increases the fuel consumption during the commuting from suburban settlements. Therefore, it is possible to observe increased energy consumption concerned with the suburban transport in comparison with the regional transport in rural areas (Marique & Reiter, 2012).

The legislative effort of the European Union was focused on the energy efficiency of buildings, until nowadays. The issued directive requires the construction of houses with energy consumption close to zero since 2020 (Directive of the European Parliament and of the Council, 2010). Energy efficiency of buildings has been taken into the strategic targets of energy savings at European level, but this effort is devalued in the context of fuel consumption in relation to commuting from the suburban settlement to the core city. The expended resources are devalued through energy demands associated with the location of suburbanized area.

Increased population mobility and transport accessibility have allowed factual development of suburbanization. The increased availability of private car transport and the passenger's demands to increased travel speed have caused the growth of traffic volume and an increase of travel distance (Boussauw et al., 2011). This kind of development has led to the preference of private car transport. On the other hand, this fact is also valid in the opposite meaning. Suburbanization and diffused forms of settlement have caused the need of increased mobility demands of inhabitants, and it creates a dependency on the accessible and cheap energy (da Silva et al., 2007). This fact creates interdependence of these factors.

The relationship between the affordable mobility of inhabitants and the character of settlements is evident from the spatial urban development in historical context. Muller (2004) points out an influence of transportation to the city's development in the example of American cities. There was implemented an urban tram and a suburban commuter train as an important elements of the population's mobility at the beginning of the 20th century. Development of settlements occurred alongside the corridor of tramway tracks and of commuter train tracks. Later (in the 30's during the advent of motorization), the settlements were located alongside the highway's or motorway's corridors (Newman & Kenworthy, 1992). There was a typical massive development of residential buildings and houses with the low population density (urban sprawl), during this period.

The similar development started in the Czech Republic, although a bit later. Residential suburbanization has been developed in relation to the radially oriented railways from the core city during the period between the World Wars (Hampl et al., 2007). After the 2nd World War, the residential suburbanization associated to the

development of the automotive industry did not occur, as it was apparent in the U.S. (Pucher, 1999). Mainly it was caused by political and social changes during the period 1948–1989. The residential and commercial suburbanization has occurred since the 90's of the 20th century and the residential suburbanization is linked to the private car transport usage in the hinterland of large cities. The settlements were developed alongside the major road's corridors and also in a closer hinterland of large cities without adequate transport infrastructure. The first problems of increased traffic intensities have occurred with regards to the roads' capacity or the roads are even congested alongside the journey to the city centre. The competitiveness of public transport has been lost with the expansion of private car transport in the suburbanized city's hinterland.

The process of suburbanization and desurbanization is described as the most difficult stage of the residential development with regards to the public transport service (van den Berg et al., 1982). The transport demands are realized for a long travel distance and the passengers demand high accuracy of transit connections and sufficient transport capacity during peak hours. Public transport provides the population mobility in relation to the core city (radially oriented journeys) and also within micro–regions, where the intensity of transport demands is usually significantly higher in relation to the city to compare with micro–region relations. The scope of the public transport system is expanding further into the regional area due to growth of city's catchment area, as it is shown in example from the state of Maryland, USA (Chakraborty & Mishra, 2013). The commuter trains are needed to cover the most important transport links as a backbone of the transport system. Therefore, it is appropriate to integrate the commuter trains into an integrated transport system with including common tariff rules. It is appropriate to establish the tariff system on the base of travel distances instead of travel times, because the travel time is different for the same journey during peak hours and off–peak period. The off–peak tickets are offered in some transport systems at a reduced price as incentive to spread the peak hours onto longer period, but this kind of fare is not so useful for suburban residents and their daily commuting (Holmgren et al., 2008).

MATERIALS AND METHODS

The 10 localities of suburban settlements were chosen with the aim to describe suburban residents´ energy consumption during their commuting. The surveyed settlements are situated in newly built suburban localities with specific built up area also known as urban sprawl (or suburban sprawl) and these settlements are the only part of the original municipality. Some settlements are listed only administratively as part of municipality and they are built as a separate settlement far away from the original centre. The most of these settlements were built after the 2001 and the construction of new houses has gone on there up to nowadays. These surveyed settlements are influenced by catchment area of Prague's city that is dominant city of the region. The chosen settlements are localised by to 25 km from the Prague's city centre and up to 19 km from the nearest public transport terminal. These suburbs were chosen evenly in different directions from Prague's centre without direct commuter train connection, thus public transit is implemented as suburban bus transport only. Suburban settlements represent different type of buildings, level of public facilities etc.

Experimental fuel consumption investigation of the journey (the fuel consumption survey) was carried out during morning peak hours (from 6 to 9 am) on ordinary working days in May. The survey's time covered uniformly the morning peak hours in all of surveyed settlements. The fuel consumption survey included an investigation of commuter bus fuel consumption and of passenger car fuel consumption. On base of these fuel consumption surveys, authors found out the total fuel consumption of the bus and of the passenger car to the journey from surveyed settlements to the nearest available underground station (public transit terminal), where the 'Park and Ride' parking lot is located as well. There was considered the journey to the best reachable public transit terminal with the 'Park and Ride' parking lot. The location of some surveyed settlements allowed to reach 2 equivalent public transit terminals, therefore it was distinguished at the 'Code of the bus journey'; for instance the journeys 'J 6a' and 'J 6b' (see Table 1) There was carried out at least 2 journeys for each of the 10 surveyed suburban settlements during the morning peak hour. An exception is the journey 'J 10' (Chýně–Zličín, see Table 1), there was found as a sufficient to carry out only 1 journey (short journey with no influence by surrounding traffic conditions). The journeys were carried out through the concurrent ride of the measuring bus and of the bus under the ordinary operation with passengers. Thus, the ride and the bus stops of the measuring bus were maintained under real conditions.

Table 1. The energy consumption related to 1 kilometre and to 1 passenger (bus and passenger car)

Code of the bus journey	Surveyed transport relation	Energy consumption per kilometre and per passenger			
		bus peak hours (kWh km^{-1})	bus off–peak hours (kWh km^{-1})	ordinary car peak hours (kWh km^{-1})	economy car peak hours (kWh km^{-1})
J 1a	Říčany–Depo Hostivař	0.07	0.06	0.49	0.51
J 1b	Říčany–Háje	0.11	0.06	0.59	0.64
J 2	Psáry–Budějovická	0.11	0.08	0.53	0.52
J 3	Sulice–Budějovická	0.09	0.07	0.56	0.56
J 4	Hostivice–Zličín	0.14	0.11	0.62	0.59
J 5	Bašť–Ládví	0.13	0.11	0.52	0.51
J 6a	Jenštejn–Letňany	0.11	0.10	0.61	0.57
J 6b	Jenštejn–Černý Most	0.11	0.09	0.58	0.55
J 7	Velké Přílepy 1–Dejvická	0.11	0.09	0.46	0.48
J 8	Velké Přílepy 2–Dejvická	0.11	0.09	0.46	0.47
J 9	Holubice–Dejvická	0.11	0.09	0.46	0.46
J 10	Chýně–Zličín	0.09	0.09	0.51	0.49

The investigation of the public transit fuel consumption was carried out to the off–peak journeys for the purpose of comprehensive comparison to the peak/off–peak journeys. Since many of the peak journeys were affected by traffic congestion, It was carried a fuel consumption survey of journeys during off–peak period. The off–peak journey was carried out during night hours (from 10 pm to 4 am). The similar time of the bus stops (the time spent on the bus stop during the journey) were kept for the peak journeys and for the off–peak journeys. Thus authors gained a comparable data to the peak/off–peak journeys. The authors get an overview of the real fuel consumption related

to the transportation and the obtained data was not affected through surrounding traffic conditions. The emphasis was placed on traffic fluency during the off–peak journeys.

The measuring bus was not possible to occupy by ordinary passengers, therefore it was necessary to simulate the vehicle occupancy by ballast weight. The total weight (the ballast weight and the measuring equipment) corresponded to the occupancy by 31 passengers (all seats occupied).

Karosa B951E.1713 was used as a measuring bus; the engine: Iveco Cursor 8 F2B; the power of engine: 180 kW; the engine displacement: 7.8 litres; complying with Euro 3 emission standard; the fuel: diesel; fully automatic transmission Voith D 851.3. This type of bus is commonly deployed on the suburban bus lines nowadays.

Škoda Fabia 1.2 HTP was used as a measuring car (economy car); the engine: HTP (High Torque Performance); the power of engine: 40 kW; the engine displacement: 1.198 litres; complying with Euro 4 emission standard; the fuel: gasoline; manual transmission.

Škoda Octavia 2.0 TDI was also used as a measuring car (ordinary car); the engine: TDI (Turbo Direct Injection); the power of engine: 103 kW; the engine displacement: 1.968 litres; the fuel: diesel; manual transmission.

The measuring bus was equipped with differential flowmeter DWF as a fuel gauge with two independent measuring sections. This type of fuel gauge works on the principle of flowmeter with oval gear wheels including Hall sensor as a speed encoder of oval gear wheels. The fuel gauge was connected to the suction pipe (from the tank to the unit injector) and to the return pipe of bus fuel system from the unit injector back to the tank (Fig. 1).

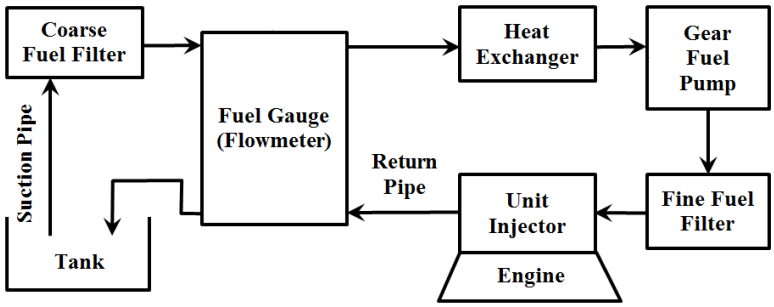

Figure 1. The schema of the bus fuel system including fuel gauge, Ed. the arrows indicate direction of the fuel flow.

The output signal of fuel gauge was a pulse with the transmission through the Hall sensor. Each pulse obtained from Hall sensor represented 0.0025 litre of fuel. This volume is determined by the flowmeter construction that provides a resolution of 400 pulses per litre. The instantaneous fuel consumption was represented as a difference between the number of pulses on the suction pipe and the number of pulses on the return pipe of fuel system. Fuel gauge provided data continuously, because it was fully implemented into the fuel system of the bus and cannot be so easily installed or removed before/after the measurement period. Fuel gauge was connected to the datalogger (see Fig. 2) that recorded each pulse of fuel gauge, for the purpose of data evaluation. These data was transmitted further to the processing device (notebook). The external GPS

receiver was also connected to the processing device. The GPS receiver was fixed by a magnet on the measuring bus roof and it provided data about position, speed, azimuth, number of available satellites and the magnetic declination.

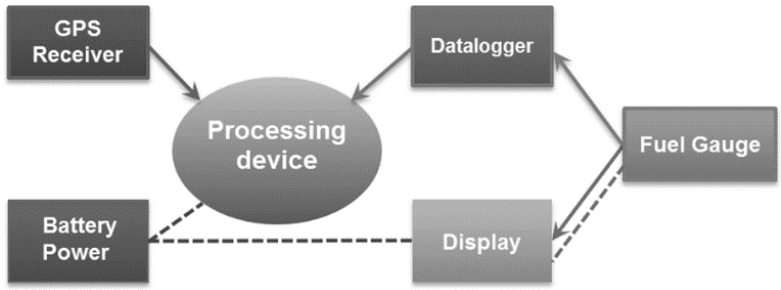

Figure 2. The schema of the measuring system, Ed. the arrow of solid lines indicate the directions of data flow, the dashed lines indicate power supply.

The processing software was implemented to the notebook and all of measured data were converted into database file (*.dbf). Thus, it was possible to process the data in any spreadsheet. The data was aggregated and synchronized in the frequency of one second. The database record included time data, data of fuel gauge (fuel flow to the suction pipe and to the return pipe) and information about the position and speed provided by GPS receiver. The battery power was used as a source of electrical supply for the fuel gauge through the display.

The data of passenger cars fuel consumptions was gained in standardized way through the OBD connector (On–Board Diagnostics) during the surveyed journey.

RESULTS AND DISCUSSION

Overall, the fuel consumption investigation was carried out to the suburban bus lines (422 km of measured journeys) and to the passenger cars (304 km of measured journeys). Another overview represents a comparison of the involved journeys during the peak hours (240 km) and during the off–peak hours (182 km). The off–peak journeys were not affected significantly by the surrounding traffic conditions and therefore the variation of fuel consumption was lower than during peak journeys. Thus the range of fuel consumption investigation might be smaller during off–peak journeys.

The summary of the distribution of speed intervals into the travel time (see Fig. 3) points out the fact that the most of the congested journeys have the highest proportion of low speeds during 7–8 am. It is mainly caused by the saturation of the transport demands linked to home–to–school journeys (pupils and students) during this period. These transport demands are complemented by transport demands of the ordinary commuters (home–to–work journeys). Therefore, the total transport demands are saturated during this period. There is evident that the most congested transport relations come from the southeast of Prague (the journeys ‘J 1’, ‘J 2’ and ‘J 3’) – the strongly influenced area through the uncoordinated development of suburbanization as it is presented in Ouředníček (2007). The position of public transit is hardly competitive in these journeys. For instance, the passengers of public transit have to spend app. 56% of travel time under

the travel speed 10 km h^{-1} (see journey 'J 1b'). It is equivalent to spend app. 56% of travel time by walk. On the other hand, there were included the fast and comfortable journeys ('J 6b' see Fig. 3) as well.

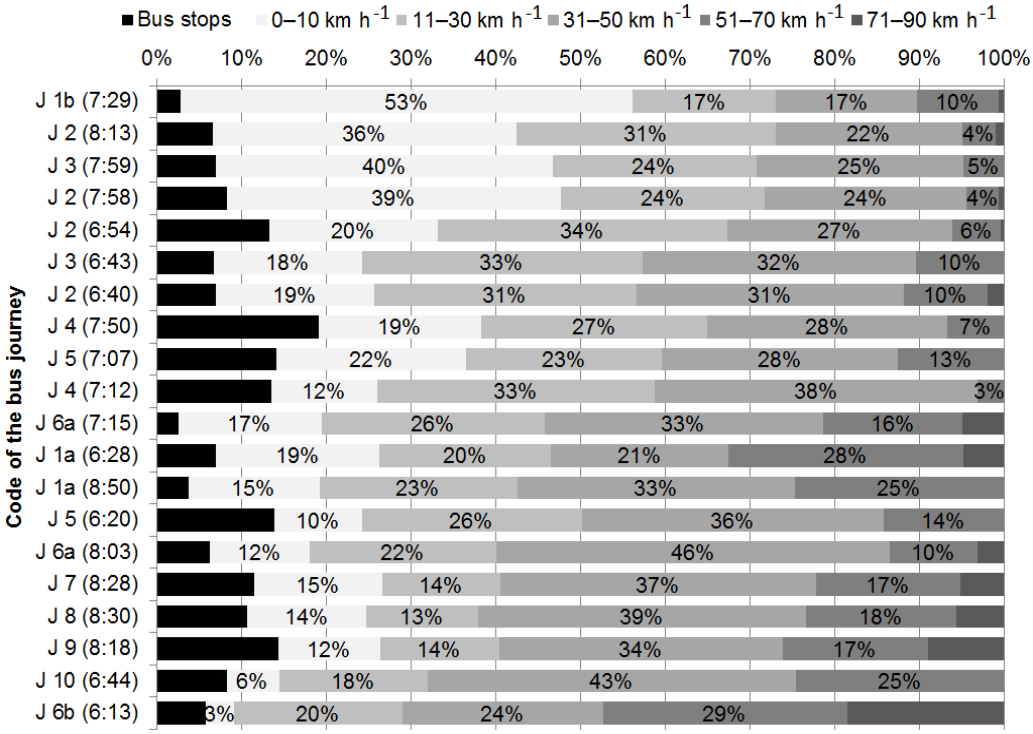

Figure 3. The distribution of speed intervals into the travel time of bus journeys during the peak hours, Ed.: the time in the brackets indicates the time of departure from the bus stop of surveyed settlements.

The peak journeys by commuter bus were taken into compared with the off–peak journeys with a fluent ride (see Table 2). There was statistically proven the difference of energy consumption between peak journeys of public transit and off–peak journeys of public transit (*t*–test, $n = 12$, $P > 0.05$). The energy consumptions savings of bus operation varies from 0% to 41% of energy consumption or fuel consumption consequently (0% = no difference between peak and off–peak consumption of bus). The off–peak journeys have represented conditions under which the bus transit is not negatively influenced by passenger car transport. The variety of energy saving provides the awareness of energy consumption impacts if effort would have been focused on traffic fluent flows and congested parts of the journey would be preferred to bus transit operation (bus lanes, bus turning lane at intersections, traffic lights preference, etc.). These practical results have shown the potential benefits of bus service traffic fluency in energy consumption context and there is shown here that the benefit could be found not only at the field of travel time reductions. This approach is in accordance with the transport policy principles concluded by Stopher (2004) 'busways represent probably a much more efficient way for buses to serve their optimum markets–suburb to downtown

movements of workers'. But these principles are often not practically implemented into reality of suburbanized area and it is only implicitly declared in transport policy released by administrative authority. The journeys that are congested during the peak hours have shown a higher energy consumption savings than others. On the other hand, there was not statistically proved the difference of energy consumption between the economy car and the ordinary car (*t*–test, $n = 12$, $P > 0.05$). The economy car usage has proved higher energy consumption than ordinary car under congested journeys, but the economy car has shown lower energy consumption than ordinary car under fluent traffic conditions (see Table 1). This fact points out that the benefit of economy car is not unambiguous at the field of fuel consumption during daily commuting. These practical results provide a different perspective to fuel consumption of cars with the lower engine displacement and it offers a complementary view on the issue that has been studied by Ntziachristos et al. (2014). The public transit usage has proved to be an important element of reducing energy consumption of the transportation.

The difference between the energy consumption of public transit and the passenger car varies in a range from 74% to 86%, as it is presented in Table 2 (0% = energy consumption of bus; data are related per one passenger and to one kilometre).

Table 2. The energy consumption savings and energy consumption equilibrium

Code of the bus journey	Travel distance of bus journey	Travel distance of passenger car journey	Energy savings		Energy consumption equilibrium	
			bus (P hours) vs. bus (OP hours)	bus vs. passenger car (P hours)	bus vs. passenger car (P hours)	bus (OP hours) vs. passenger car (P hours)
	(km)	(km)	(%)	(%)	(passengers)	(passengers)
J 1a	16,6	16,6	13%	86%	4	3
J 1b	14,4	14,4	41%	82%	5	3
J 2	15,2	15,0	25%	79%	6	4
J 3	15,1	14,7	26%	84%	4	3
J 4	7,8	8,4	21%	77%	6	5
J 5	11,8	12,6	16%	74%	7	6
J 6a	9,4	9,2	7%	81%	5	5
J 6b	7,7	7,6	16%	80%	5	4
J 7	12,5	12,2	16%	77%	6	5
J 8	11,8	11,3	17%	77%	6	5
J 9	18,5	17,2	17%	76%	6	5
J 10	6,9	7,0	0%	82%	5	5

Note: P hours – peak hours; OP hours – off–peak hours.

The energy density of fuels was considered as 32.18 MJ per litre of gasoline and as 35.86 MJ per litre of diesel (Kubička & Kubičková, 2007) for the purpose of energy consumption calculation.

As was mentioned above, passenger car transport has caused delays by itself as well as it has induced delays on a bus public transit. The position of bus public transit is different. Due to the delays it is perceived as an uncompetitive, because there is no offer of higher travel speed and even the price level of fare is not sufficiently motivating factor

(Lukeš et al., 2014). These facts probably have led to the domination of private car transport at the modal split. On the other hand the low energy efficiency of passenger car transport in comparison with public transit is often caused by low rate of car occupancy.

The average vehicle occupancy rate was found out 1.41 persons per ordinary car and 1.35 per economy car during the journeys from surveyed settlements (Lukeš et al., 2014). Thus, the presented values – see Table 1 and Table 2 where the occupancy of passenger car was considered as a 1 passenger (driver) – occur at the most cases of all journeys made from the surveyed settlements. The weighted arithmetic mean of bus occupancy was found out 21 passengers (the travel time was considered as a weighted value) across all investigated journeys, but this value differs under surveyed transport relation. For instance, the transport relation 'J 10' is used by passengers quite weakly to compare with another transport relations.

Of course, the energy efficiency of public transit declines with the decreasing of bus occupancy. The energy consumption equilibrium between passenger car and public transit occurred when the both surveyed transport modes have the similar energy consumption per one passenger under the same traffic conditions. The energy consumption equilibrium has occurred when the occupancy of bus varies from 4 to 7 of bus passengers, while the passenger car stays occupied by driver only (see Table 2). The decrease of fuel consumption linked with the lower occupancy rate of bus was included into calculations. The occupancy level of energy consumption equilibrium is even lower in case of off–peak journeys by bus (from 3 to 6 of bus passengers) and it confirm a presumption of better public transit profitability under fluent traffic flow of bus operation. This equilibrium depends on the journey from surveyed settlements, as it is presented in Table 2, regardless if the economy car or ordinary car was used, because there is no difference between those kinds of car at the surveyed journeys (*t*–test, $n = 12$, $P > 0.05$). Any higher occupancy of the bus has had energy consumption benefit on the side of public transit to compare with passenger car transport. There should be pointed out, that this statement is valid for used type of bus. It is possible to assume that newer buses or low–capacity vehicles (minibuses or midibuses) have a better economical operation. Therefore, the energy consumption equilibrium between passenger car and transit could be expected at the lower end of occupancy interval from 3 to 7 passengers.

The offered capacity of bus transit was recognized as a sufficient to cover public transit demands as for a long–travel journeys as the short–travel ones. Furthermore it was possible to travel as passenger with his own seat from all surveyed suburbs during morning peak. According to the above mentioned conclusions, there is no assumption that the next increasing of transit offer should lead to increase of transit ridership as well. This statement is suggested by determination coefficients and it was not found any statistical relation between a transit offer (represented as a number of bus departures per peak hour) and a transit ridership or total number of outgoing persons ($R^2 = 0.020$ respectively $R^2 = 0.202$) in surveyed settlements. This declaration points out the limits of transit demands in suburbanized area (Næss, 2006) and it is possible to assume that the modal split is saturated in a favour of transit under current conditions which are determined by distribution of travel time, reliability of transit, fare, etc.

Usually, the energy efficiency of transportation is not taken into account by passengers. It is a task for the concerned administrative authorities to set up the appropriate transport policy and for the organisers and designers of public transit to ensure the fulfilment of this transport policy practically.

CONCLUSIONS

The analyses have proved that the potential of energy consumption savings are not fully exploited in public transit. It is possible to save more than 40% of fuel consumption during the congested journeys, if the tools of bus transit preference would be effectively used. As it is evident, there is another way to streamline the operation of public transit in the context of energy consumptions savings, among of commonly accepted decreasing of travel time. The public transit has no likelihood perspective that the railroads could be implemented into surveyed settlements. Therefore the alternative variant of public transit system is the Bus Rapid Transit system (BRT system) or Metrobus system. The energy efficiency of bus public transit allows achieve the similar energy consumption per passenger as an ordinary passenger car has at a low occupancy rate of bus (from 3 to 7 passengers). This finding suggests that the endeavour to 'overcrowd' buses, to increase of economic profitability, is not justified in the energy consumption context.

Conclusions have proven the meaningfulness of efforts to improve the fluency of public transport in suburbanized area. The presented approach has shown that the discussion with the responsible authorities could be supported by exact data of fuel consumption and possibility of fuel savings that are often neglected.

ACKNOWLEDGEMENTS. This paper and obtained results were supported by Internal Grant Agency 2014, project IGA 2014: 31150/1312/3117 'The energy demands of transport systems in an urban and suburban conditions' (Energetická náročnost dopravních systémů v městských a suburbánních podmínkách).

REFERENCES

Boussauw, K., Derudder, B. & Witlox, F. 2011. Measuring Spatial Separation Processes through the Minimum Commute: the Case of Flanders. *European Journal of Transport and Infrastructure Research* **11**, 42–60.

Chakraborty, A. & Mishra, S. 2013. Land Use and Transit Ridership Connections: Implications for State–Level Planning Agencies. *Land Use Policy* **30**, 458–469.

da Silva, A.N.R., Costa, G.C.F. & Brondino, N.C.M. 2007. Urban sprawl and energy use for transportation in the largest Brazilian cities. *Energy for sustainable development* **11,** 44–50.

Directive of the European Parliament and of the Council 2010/31/EU. Energy Performance of Buildings (revised version). Acceessed 19/05/2010

Hampl, P., Dostál, P. & Drbohlav, D. 2007. Social and cultural geography in the Czech Republic: under pressures of globalization and post–totalitarian transformation. *Social & Cultural Geography* **8**, 473–495.

Holmgren, J., Jansson, J. & Ljungberg, A. 2008. Public transport in towns–Inevitably on the Decline. *Research in Transportation Economics* **23**, 65–74.

Kubička, D. & Kubičková, I. 2007. The Influence of motor fuels containing bio–components on operation and emissions of diesel and gasoline engines in the fleet of the Czech Republic. Research report of the project FT–TA4/066 VZ–S–1791. Litvínov (in Czech)

Lukeš, M., Kotek, M. & Růžička, M. 2014. Transport Demands in Suburbanized Locations. *Agronomy Research* **12**, 351–358.

Marique, A.–F. & Reiter, S. 2012. A method for evaluating transport energy consumption in suburban areas. *Environmental Impact Assessment Review* **33**, 1–6.

Muller, P.O. 2004.Transportation and Urban Form: Stages in the Spatial Evolution of the American Metropolis. *The Geography of Urban Transportation*. Third Edition. The Guilford Press New York. 59–85.

Musil, J. & Müller, J. 2008. Inner Peripheries of the Czech Republic as a Mechanism of Social Exclusion. *Czech Sociological Review* **44**, 321–348. (in Czech)

Næss, P. 2006. *Urban Structure Matters. Residential location, car dependence and travel behaviour*. Routledge. London. 344 pp.

Newman, P. & Kenworthy, J.R. 1992. Cities and Automobile Dependence: A Sourcebook. Avebury Technical. Avebury. 388 pp.

Ntziachristos, L., Mellios, G., Tsokolis, D., Keller, M., Hausberger, S., Ligterink, N.E. & Dilara, P. 2014. In-use vs. type-approval fuel consumption of current passenger cars in Europe. *Energy Policy* **67**, 403–411.

Ouředníček, M. 2007. Differential Suburban Development in the Prague Urban Region. *Geografiska Annaler: Series B, Human Geography* **89**, 111–126.

Pucher, J. 1999. The Transformation of Urban Transport in the Czech Republic, 1988–1998. *Transport Policy*, **6**, 225–236.

Stopher, P.R. 2004. Reducing road congestion: a reality check. *Transport Policy* **11**, 117–131.

Špačková, P. & Ouředníček, M. 2012. Spinning the web: New social contacts of Prague's suburbanites. *Cities* **29**, 341–349.

van den Berg, L, Drewett, R., Klaasen, L.H., Rossi, A. & Vijverberg, CH.T. 1982: Study of Growth and Decline. *Urban Europe*. Pergamon Press England, 162 p.

Zolnik, E., Minde, J., Das D.G. & Turner, S. 2010. Supporting planning to co–locate public facilities: A case study from Loudoun County, Virginia. *Applied Geography* **30**, 687–696.

Agronomy Research **13**(2), 596–603, 2015

Energy consumption of commuting from suburban areas

D. Marčev*, M. Růžička, M. Lukeš and M. Kotek

[1]University of Life Sciences Prague, Faculty of Engineering, Department of Vehicles ang ground transport, Kamýcká 129, CZ16521 Prague, Czech Republic; *Correspondence: marcev@tf.czu.cz

Abstract. The process of suburbanization begun half a century later in the Czech Republic in comparison to Western Europe. It has given rise to similar changes in the individual behaviour of potential residents, resulting in different land use and the emergence of new requirements involving technical and transport infrastructures. Many factors that characterize suburban land use, e.g., density of population (households), free access to public facilities, availability of transport modes, etc., are closely associated with energy consumption, specifically in transport. Suburban development affects not only transportation inside expanding suburban municipalities but also their surroundings, e.g., the cumulative effect of traffic intensity increasing on roads radially oriented towards the city centre has been observed in recent years. The construction of manufacturing facilities, logistic and commercial complexes, entertainment centres, etc. continues within the suburban areas and it tends to significantly increase traffic movements (e.g., in tangential directions towards the core of the city). The current capacity of transport infrastructures does not correspond to the increased vehicle intensity (even not only during peak hours) and it does not guarantee an adequate quality for transport operation. The results of performed traffic surveys proved that morning traffic intensity (during peak hours) on the roads (of 2nd. or 3rd. class) leading to the city centre has doubled in the last five years. These results mean that transport energy consumption has increased enormously. Transport energy consumption is higher than usually expected in these cases. The energy consumption (fuel consumption) determined according to a vehicle's homologation does not take into account the conditions that may affect driving style in a negative manner, e.g., slow driving, traffic congestions road, vertical alignment and tortuous roads. The mean consumption was 9.2 (l 100 km^{-1}) on the selected trail sections –that is 1.66 more than the combined consumption figure presented by car producers. The selected sections make up 54% of the total trail length. This 'local consumption' is linked with higher emission production, details are available below. The author compared specific fuel consumption per 100 km and found that real consumption is evidently always higher than the quantities claimed to be correct by car producers in view of mixed modes. The same has been found by, e.g. Marique & Reiter, 2012 and other authors.
The conclusions of the research are potentially relevant and should be used in a spatial planning or decision making processes to prevent 'urban sprawl' and the accompanying high energy consumption. Suburban development should go hand in hand with the construction of new transport infrastructures and high-quality public transport.

Key words: energy, transport, commuting, suburban settlements, fuel consumption.

INTRODUCTION

The process of suburbanisation (urban sprawl), which commonly describes physically (unfortunately often insufficiently controlled) expanding urban areas, is a major issue for sustainable development (European Environment Agency, 2006). As Hall Breheny quoted Banister (2005), decentralization has been a consistent and powerful force in Western Europe already since 1945. Although there is evidence that the power of this force has diminished in some countries by today, it remains a major determinant of urban structure.

Research dealing with transport energy consumption is firstly focused on urban area population (or job opportunities) densities, secondly on relationships between transport energy consumption and building density. It is still unclear how densification strategies affect the reduction of transport consumption. Maïzia et al. (2009) and Steemers (2003) argue that more compact urban forms would significantly reduce energy consumption both in the building and transport sectors. Based on data from 32 big cities located all over the world, Newman & Kenworthy (1989; 1999) have highlighted a strong inverse relationship between urban density and transport consumption, but their work is only valid for certain conditions and has been often criticized by others (Mindali et al., 2004; Owens, 1995), mainly for methodological reasons. Banister (1992) applied the same kind of approach to British cities and highlighted, on the basis of statistical data obtained from a national survey, that transport energy consumption is slightly higher in London than in smaller cities, which refutes Newman & Kenworthy's observations. Boarnet & Crane (2001) are also sceptical about the relationship between urban design and transport behaviours. On the basis of several case studies, they estimate that if land use and urban form have an impact on transport behaviours, it is through the price of travel (public transport prices are reduced in dense areas).

Marique & Reiter (2012) proposed that it is necessary to evaluate the sustainability of these suburban neighbourhoods, while it requires appropriate methods and tools, especially as far as private transport is concerned. In fact, transport energy consumption is rarely taken into account when the sustainability of these suburban structures is studied, even if sharp fluctuations in oil prices and efforts to reduce greenhouse gas emissions play an important role in contemporary discussions and policies. Marique & Reiter's study is based on input data from national censuses carried out every 10 years in Belgium, and consumption factors taking into account the mean consumption of vehicles (litre per km), the passenger rate and characteristics of fuel (these values are used in the paper; see discussion on methods).

The process of suburbanisation was delayed in Central and Eastern Europe due to the long-standing dependency on public transport means (mass transit) and reduced usage of private passenger cars in comparison with Western Europe (Ouředníček, 2002). Nevertheless, one of the most important results of contemporary suburbanisation processes is the enormous increase in traffic intensity (mainly caused by passenger cars) that is linked with congestion and other negative impacts on the environment and human health.

MATERIALS AND METHODS

Locations of the traffic survey points (R1 to R5) from Kralupy n/V city to Prague (nearest Metro terminal parking lot), alongside the road II/240 and connected with the road II/241 are shown in Fig. 1. The total length of the drive was 17 km. A traffic survey was performed during morning traffic peak hours (6.00 to 9.00) on working days (Tue, Wed, Thu), and the survey was repeated to obtain statistically plausible values. The surveys have been repeated every year in October since 2009. The surveyed radially oriented road is specific –it does not facilitate eastern tangential drives. This north-western suburban segment is bordered by the river (bridges were not built yet) from the north-eastern part of Prague's suburb. Two tangential directions (R22, R32) were surveyed there. Tangential roads are linked with motorways and Prague's ring. The surveys were compiled manually; data were collected by people, who filled in the prepared forms (number of vehicles and occupancy, modal split during time intervals) and processed in MS Excel. A survey questionnaire issued to the members of the public in the city of origin formed a part of the research.

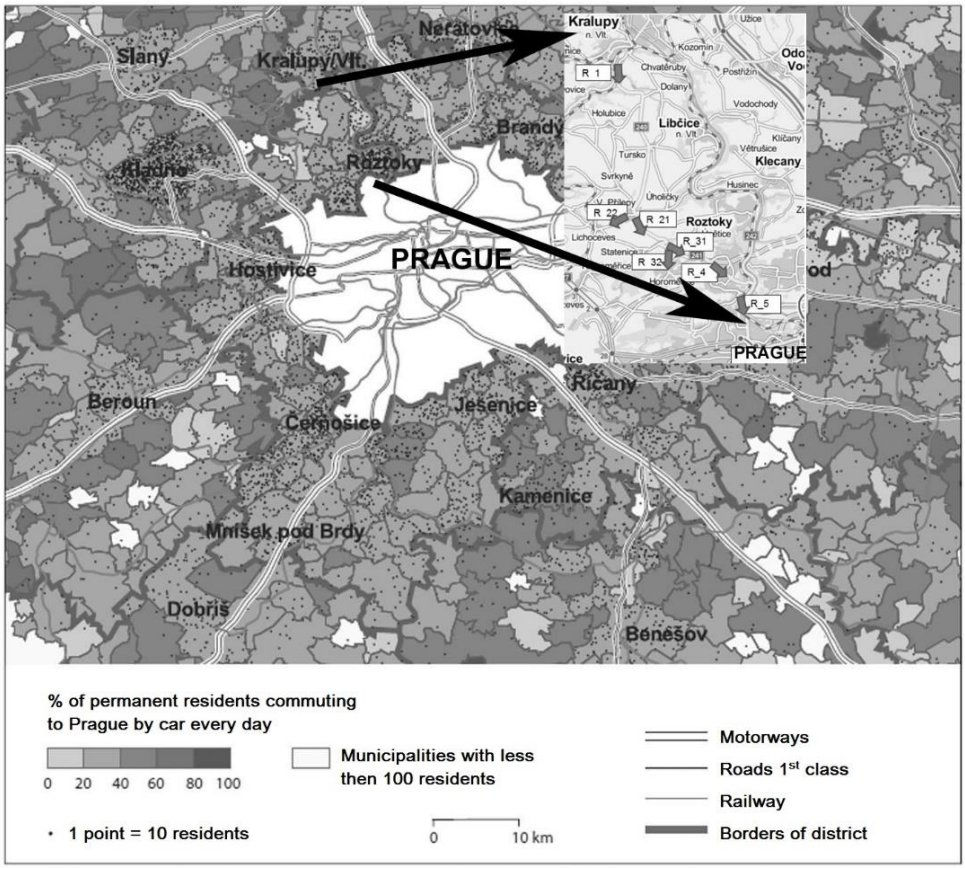

Figure 1. Map of measurement –radially oriented road from Kralupy n/V to Prague (Source: Proudy 2001 in Ouředníček–Urbánková, 2006 modifications regarding this research have been added).

A Skoda Octavia was used as a FDC (floating data car) and its basic parameters are: engine 2.0 (litre) 103 $(kW)^{-1}$ TDI PD – EU4, diesel fuel consumption declared by producer in l for 100 km^{-1}: city 7.0; outside city 4.7; combination 5.5.

The diagnostic system VAG-COM was used for communication with the vehicle's engine control unit and it enabled to collect and save instantaneous quantities (packets). The system consists of a data cable-interface connection (a standardized diagnostic plug OBD-II) on the one side and USB interface on the other side. The system software also features the program VCDS (Vag-com diagnostic system).

The FDC was equipped with the exhaust gas analyser VMK 5 – a special component emission analyser designed for mobile measurements. The device scans at 1 Hz frequency and stores the instantaneous values of CO, CO_2, HC, NO_X and O_2. The emission of carbon components is evaluated with the NDIR method. For sensing, NO_x and O_2 are used in electrochemical cells. The mobile measuring device is also equipped with an integrated Garmin GPS that stores information about the vehicle's instantaneous position and velocity at 5 Hz frequency.

All the detailed parameters of the equipment have not been listed in this paper due to limited space. The complete configuration of measuring equipment is shown in Fig. 2. Drives were repeated during the surveyed hours.

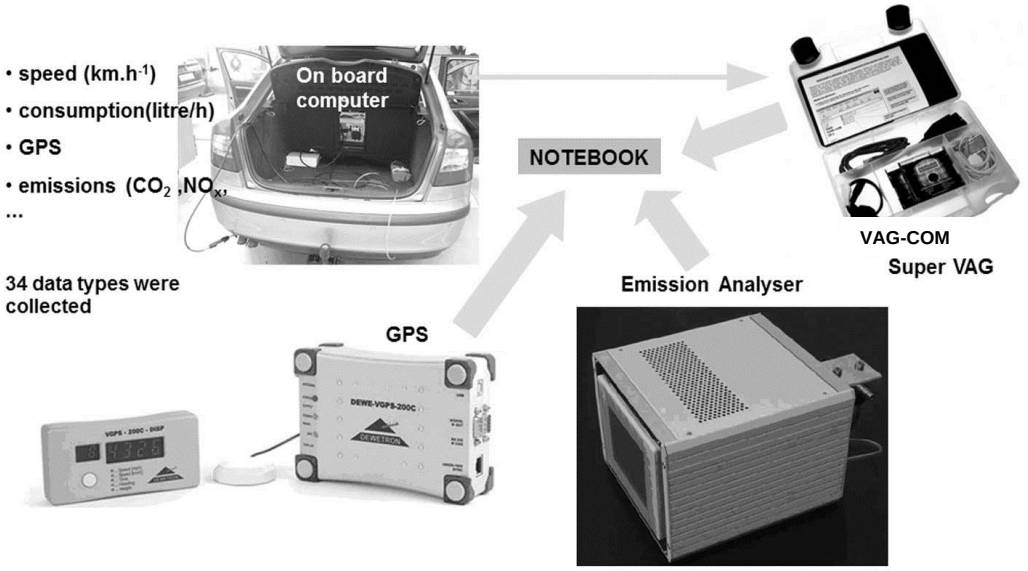

Figure 2. Configuration of measuring equipment.

The next step of data processing involves comparing consumption and occupation rates in real conditions with vehicles (diesel car, fuel car) as presented in Table 1.

Table 1. Consumption and occupation rate based on regional mean values (Source: Marique & Reiter, 2012)

	Type of vehicles			
Characteristics	Diesel car	Fuel car	Bus	Train
Consumption per kilometre	0.068 litre	0.080 litre	0.46 litre	-
Occupation rate	1.2	1.2	10	-

RESULTS AND DISCUSSION

Fig. 3 shows the results of the traffic surveys, i.e., intensities of passenger cars during three hours of morning peak traffic and the maximal one hour intensity within this time interval. Intensities at surveyed points R1 and R5 of the radial road, in other words, the 'entrance and exit' from the suburban area to the city centre, are also analysed. The generally accepted supposition is that the development of the suburban area and Kralupy n/V generates higher intensities within years. This supposition is somewhat supported by the data collected from point R1 but the results were not as definite for point R5 (see Fig. 3) – the coefficient of determination for the three hour intensity at point R1 is 0.5972, and 0.2753 at R5. This shows the differences in intensity between the two points might increase. If the supposition were completely proved, increase at point R5 should be higher (owing to the suburban area and new settlements built there).

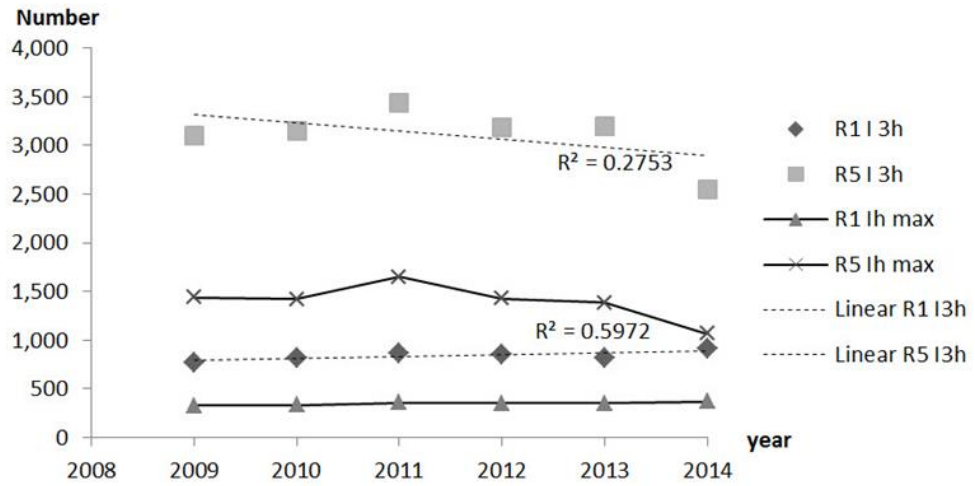

Figure 3. Intensities of passenger cars at points R1 and R5 (direction towards the city of Prague).

The explanation for these unexpected results can be found at points R22 and R32, i.e., the location where tangential movements developed an increasing trend (see Fig. 4). The increasing trends of tangential movements are proved by the coefficients of determinations, which are 0.9544 at R22; and 0.8005 at R32.

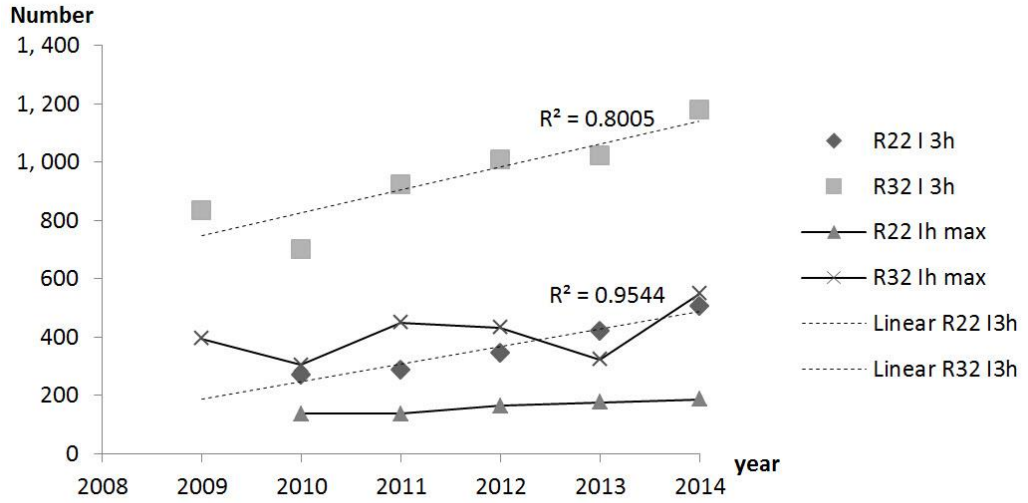

Figure 4. Intensities of passenger cars at points R22 and R32 (tangential direction).

Four sections (parts 1–4) alongside the trail were selected to represent specific driving conditions (see Table 2). Part 1 is located at the beginning of the trail and has a low hourly intensity but its terrain configuration is uphill with the average slope of +5%; the road is straight. Part 2 represents descending and ascending terrain with several curves (tortuous road). Part 3 represents a straight road inside a suburban district with a higher intensity. The traffic flow is interrupted by several pedestrian crosses. Part 4 has the highest intensities, with congestion during morning peaks. The road has traffic lights and it narrows from two lanes into one, which causes problems there.

Table 2. Results of measurements

	dist. (km)	mean velocity (km h^{-1})	mean consumption (litre 100 km^{-1})	CO (g km^{-1})	CO_2 (g km^{-1})	NO_x (g km^{-1})	HC (g km^{-1})	intensity (p.cars h^{-1})
part1	2.6	49	10.3	2.7	239	3.0	0.031	352
part 2	1.3	46	8.7	2.4	206	3.9	0.032	546
part 3	2.4	43	6.0	1.6	144	1.6	0.019	618
part 4	2.9	14	11.6	4.9	278	2.6	0.058	1,386

Analysis results prove the initial hypothesis that fuel consumption is influenced the most by traffic flow in comparison to a road's vertical alignment and tortuousness. The mean consumption of fuel on these selected trail sections was 9.2 (l 100 km^{-1}) that 1.66 higher than the combined consumption declared by the car producer. The selected sections make up 54% of total trail length. Local consumption is linked with higher emission production as shown in Table as well. The surroundings of these sections face stronger negative impact on the environment and human health due to higher fuel consumption and consequently higher emission production.

Results of the survey questionnaire show that nearly 80% of the 423 people addressed commute to Prague regularly. This high proportion might be caused by the specific time and place the survey was conducted at, age structure of respondents, etc. Nearly 41% of respondents use passenger cars for driving to Prague and the distribution of diesel and fuel (petrol) cars is approximately equal. The respondents use cars with the following engine volumes: 26% under 1.5 litres, 40% from 1.5 to 2 litres and 21% above 2 litres, 6% unknown, 7% refused to answer.

CONCLUSIONS

On the basis of the performed surveys it can be concluded that within the surveyed Prague suburban area the total number of passenger cars is on the increase. Nevertheless, this increase has not been significant in the previous six years. The average number of passenger cars leaving the surveyed area during the three hours of morning peak traffic is 4,355 vehicles. The maximal difference in this figure was recorded between the years 2009 and 2010. The question is whether the six-year surveillance period is plausible for the assessment of transport quantities within a suburban area. Regardless of this objection, the increasing number of vehicles in Prague means constantly increasing energy consumption – mostly fossil fuel obtained from non-renewable sources is used.

The comparison of specific fuel consumption per 100 (km) revealed that real consumption is always higher as opposed to the quantities claimed to be consumed by the producer in mixed mode, as also claimed by, e.g., Marique & Reiter, 2012 and other authors. The total regional (suburban) fuel consumption can be quantified according to the structure of the vehicle fleet (diesel or petrol, engine volumes, etc.) and real specific fuel consumption values per 100 km can be obtained. According to performed measurements, the traffic operation (traffic flow character) and local conditions (vertical alignment and tortuousness) can strongly influence required limits. That should be taken into account in environmental impact assessments.

ACKNOWLEDGEMENTS. This paper and the obtained results were supported by the Internal Grant Agency 2014, project IGA 2014: 31150/1312/3117 ‘Energetická náročnost dopravních systémů v městských a suburbánních podmínkách’ (The energy demands of transport systems in urban and suburban conditions).

REFERENCES

Bafna. 2013. Factors Influencing Hardness and Compression Set Measurements on O-rings *Polymer – Plastics Technology and Engineering* **52**(11), 1069–1073.

Barrios, C.C., Domínguez-Sáez, A., Martín, C. & Álvarez, P. 2014. Effects of animal fat based biodiesel on a TDI diesel engine performance, combustion characteristics and particle number and size distribution emissions. *Fuel* **117**, 618–623.

Imran, S., Emberson, D.R., Wen, D.S., Diez, A., Crookes, R.J. & Korakianitis, T. 2013. Performance and specific emissions contours of a diesel and RME fueled compression-ignition engine throughout its operating speed and power range. *Applied Energy* **111**, 771–777.

Pexa, M. & Mařík, J. 2014. The Impact of biofuels and technical condition to its smoke – Zetor 8641 Forterra. *Agronomy Research* **12**(2), 367–372.

Pexa, M., Mařík, J., Kubín, K. & Veselá, K. 2013. Impact of biofuels on characteristics of the engine tractor Zetor 8641 Forterra. *Agronomy Research* **11**(1), 197–204.

Richter, B. 2014 Evaluation of stability tests for elastomeric materials and seals. *International Polymer Science and Technology* **41**(5), 1–5.

Ružbarský, J. Müller, M., Hrabě, P. 2014a. Analysis of physical and mechanical properties and of gross calorific value of Jatropha curcas seeds and waste from pressing process. *Agronomy Research* **12**(2), 603–610.

Ružbarský, R. Müller, M. Mareček, J. Grešl, M. 2014b. Jatropha Curcas – Analysis of Gross calorific value. *Acta Universitatis Agriculturae at silviculturae mendelianae brunensis* **62**(6), 1381–1384.

Soo-Young, N. 2011. Inedible vegetace oils and thein derivatives for alternative diesel fuels in CI engines: A review. *Renewable and Sustainable Energy Review* **15**(1), 131–149.

Agronomy Research **13**(2), 604–612, 2015

Evaluation of stability of elastomer packing exposed to influence of various biofuels

M. Müller[1], V. Šleger[2], M. Pexa[3,*], J. Mařík[3] and Č. Mizera[2]

[1]Czech University of Life Sciences Prague, Faculty of Engineering, Department of Material Science and Manufacturing Technology, Kamýcká 129, CZ16521 Prague 6, Czech Republic
[2]Czech University of Life Sciences Prague, Faculty of Engineering, Department of Mechanical Engineering, Kamýcká 129, CZ16521 Prague 6, Czech Republic
[3]Czech University of Life Sciences Prague, Faculty of Engineering, Department for Quality and Dependability of Machines, Kamýcká 129, CZ16521 Prague 6, Czech Republic; [*]Correspondence: pexa@tf.czu.cz

Abstract. The aim of the European Union Member States is to reduce dependence on fuels derived from oil. For this reason, significant attention is paid to the use of organic products as a substitute or an additive in the fuel of petroleum origin. The usage of biofuels in conventional combustion engines is not easy due to the different properties of the products. The aim of the research was to determine the effect of biofuels on mechanical properties of O-rings type ACM (polyacrylate elastomer). The research was evaluated by the change of density, Shore A hardness, permanent deformation CS, tensile strength and deformation after exposure in the test environment for a period of 15 months. Comparing the O-rings immersed in standard diesel fuel it is clear that similar behaviour of the hardness shows are sunflower oil and canola oil. RME – Rapeseed Methyl Ester 20% and oil from Jatropha has a negative effect on the increase in hardness. Comparing the O-rings immersed in standard diesel fuel it is evident that except RME – Rapeseed Methyl Ester 20% other fuels have negative influence on permanent deformation CS.

Key words: biofuels, O-ring, compression and tensile properties.

INTRODUCTION

To reduce the dependence of the Member States on fuels derived from oil is an effort of the European Union. Significant attention is devoted to the use of organic products as substitutes or as an additive to petroleum based fuel for this reason. The usage of biofuels in conventional internal combustion engines is not easy due to the different properties of the products. It is necessary to deal in particular with a lower calorific value, the higher the density and viscosity of these biofuels and reflect their effect on components of combustion engines, especially sealing elements. (Soo-Young, 2011; Imran et al., 2013; Pexa et al., 2013; Barrios et al., 2014; Pexa & Mařík, 2014).

One of the main groups of materials used for manufacturing gaskets are elastomers. Elastomers exhibit good flexibility and chemical resistance.

The decisive factor is reliability - to reduce maintenance costs. One of the basic and most commonly used sealing elements is an O-ring (Bafna, 2013). An appropriate proposal of a suitable material to be used for this application is a very important issue.

The O-ring is a double-acting sealing element. The compression during installation acting in the radial or axial direction of the O-ring provides the initial sealing capability. This force increased by the power of imparting a pressure in the system represents the final sealing force. This capability can be eliminated by the liquid contaminants e.g. biofuels.

In the automotive industry, the O-rings of the type ACM (polyacrylate elastomer) are mainly used. It is a durable elastomer. Essential characteristics of the long-term ability to meet the sealing function are compression and hardness (Richter, 2014; Bafna, 2013). It is problematic to reproduce operating conditions in the case of the O-rings testing. O-rings have different sizes (Richter, 2014). When testing. Different results might be achieved (Bafna, 2013). As examples can be used the results of hardness tests at which Bafna (Bafna, 2013) demonstrates the significance of the shape factor of the test samples.

The aim of the research was to determine the effect of biofuels on mechanical properties of the sealing O-rings of the type ACM. The particular object of the experiments was the O-ring 13 x 1.9 mm (this dimension of O-rings was chosen on the base of the requirements of prominent Czech manufacturer of agricultural equipment within the grant support). There are sealing rings under the injectors of a diesel engine.

MATERIALS AND METHODS

Sealing O-rings of the ACM type (polyacrylate elastomer) were used in the study. O-rings of the ACM type are resistant to fuels, lubricants and various other ingredients. The research focused on assessing the impact of various types of biofuels on behavioural change of the O-rings used as sealing elements in the fuel system of cars. O-rings were deposited in the environment for a period of 15 months.

The gaskets provided by a manufacturer that were not exposed to the environment degradation (ethalon, marked 1) were also tested. The following fuels and biofuels were tested (Table 1):

Table 1. Tested variants – ethalon, fuels and biofuels

Tested variants	Marked
Ethalon	1
Rapeseed Methyl Ester 20% – RME	2
Sunfloweroil	3
Diesel fuel	4
Jatropha oil	5
Rapeseed oil	6

The oil from jatropha was extracted by pressing ripe seeds, imported from Indonesia (Ružbarský, J. et al., 2014a; Ružbarský, R. et al., 2014b). Within the frame of the research the changes in density, Shore A hardness, permanent deformation CS, tensile strength and deformation were evaluated.

An important parameter for determining the sealing properties is the permanent deformation CS (Compression Set). The reason for this is the fact that it doesn't only cause the compression of the elastic deformation but also plastic deformation. Permanent deformation CS was measured with respect to a modified standard ISO 815. The modification of the standard considered the use of standard real sealing rings as well as the time of loading.

Measurements were performed on electromechanical testing machine MPTest 5,050 manufactured by the Czech company LaborTech. The equipment complies with the EN 7500-1 requirements for Class 0.1. The precision the heightof the load cell used is 0.1 N, the crosshead position is detected with an accuracy of 0.001 mm. The experiment was carried out as follows:

The O-ring 13 x 1.9 was firstly compressed by a speed of 0.03 mm s^{-1}, the height of h_1 = 1.425 mm. This compression corresponds to about 25% of strain. During this deformation of the O-ring was left loaded for 30 min and then again the load was relieved by a speed of 0.03 mm s^{-1}.

The height h0 O-ring was determined by crosshead position before the steep increase of the deformation force. The speed of the deformation force was 1 $N.mm^{-1}$. The reason for this was more moderate force increase, which appeared in some O-rings when a touch of the platen did appear. This situation was caused by a non-planar shape of O-rings which was caused by exposure biofuels to O-rings. The height h_2 was determined by crosshead position when the loading force has fallen to zero. Then it is possible to calculate the value CS (1):

$$CS = \frac{h_0 - h_2}{h_0 - h_1}.100\% \qquad (1)$$

where: *CS* – permanent deformation – compression set (%); h_0 – initial height of the O ring (mm); h_1 – the height in the state of compression (mm); h_2 – the height after release (mm).

Measurement of the compression set of the O-rings is shown in Fig. 1.

Measurement of the density

Density was determined by determining the proportion of the weight and volume. The weight was determined by weighting on an analytical balance (Analytical balance BBC-22 from the German company BOEC) with a resolution of 0.01 mg which was rounded to the units of milligrams. To determine the volume, a container with an exact volume (pycnometer) was used. Measurements of mass and volume were carried out in line with CSN 621405: 1992 Rubber – Determination Standard for density.

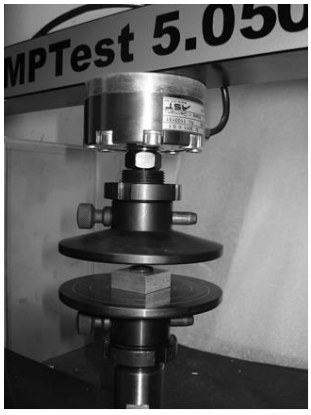

Figure 1. Measurement Compression set.

The tensile properties of rubber were determined by a modified standard ISO 37: 2012 Rubber, vulcanized or thermoplastic – Determination of Tensile Properties. The modification consisted in testing of already produced O-rings.

The tensile strength TS was calculated according to the formula (2). The maximum tensile strength Fm was detected from the record tensile tests performed on the test machine MPTest 5050. The feed speed crosshead was 100 mm min^{-1}. For clamping of the O-rings the wire hooks with a diameter of 2.9 mm were used.

$$TS = \frac{F_m}{(\frac{2\pi \cdot h_0^2}{4})} \tag{2}$$

where: TS – Tensile strength (MPa); F_m – the maximum tensile force (N); h_0 – initial height of the O ring (mm).

The Elongation E_b was calculated by the formula (3):

$$E_b = \frac{(C_b - C_{j)}}{C_j}.100\% \tag{3}$$

where: E_b – elongation (%); C_b – end inner circumference of the O-ring (mm); C_j – initial internal perimeter of the O-ring (mm).

The initial inner circumference of the O-ring was calculated from the inner diameter of the O-ring, which was determined from a distance of the hooks in a tensile test in the moment when the measured force began to grow. The final inner circumference of the O-ring C_b may be calculated using the formula (4), where the diameter of the wire hook is 2.9 mm:

$$C_b = \pi \cdot 2.9 + 2 \cdot 2.9 + 2 \cdot L_b \tag{4}$$

where: C_b – end inner circumference of the O-ring (mm); L_b – distance of the hooks when breaking the O-ring (mm).

Measurement of the tensile properties of the O-rings is shown in Fig. 2. The hardness SHORE A was measured according to the standard CSN EN ISO 868. Material hardness was measured by the Shore A i.e. by pressing the tip of the instrument durometer Shito HT. Hardness measurements according to the EN ISO 868 Shore A method requires the test specimens at least 4 mm high. The O-rings failed to meet this size limit. The height of the O-ring was measured 1.91 ± 0.02 mm. This fact led to the composition of four O-rings in a special fixture for hardness measurement (Fig. 3). This procedure is allowed by the standard.

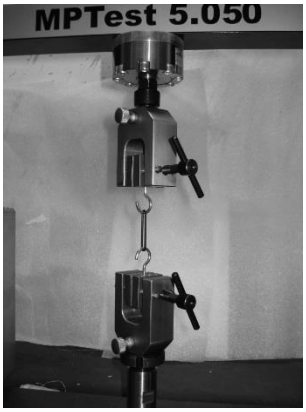

Figure 2. Measurement of tensile properties.

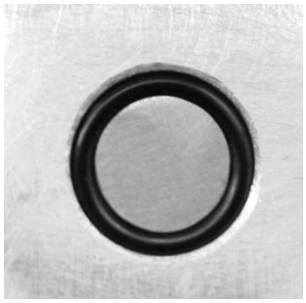

Figure 3. Preparation for measurement of Shore A hardness of O-rings.

For statistical comparison of the measured data the F-test was used. The zero hypothesis H_0 presents the state when there is no statistically significant difference in their mean values ($p > 0.05$) among tested sets of data.

RESULTS AND DISCUSSION

The results of tests aimed at assessing the density are shown in Fig. 4. It is evident that different fuels do change the density of O-rings. Different proportion of variance of results is alos obvious. The coefficient of variation was in the interval 0.45 to 4.67%. From the viewpoint of the impact of the various fuels on the density of the O-rings the F-test results can be summarized as follows: H_0 hypothesis was not confirmed ($p = 0.0158$), i.e. the difference in the 0.05 level of significance among the tested variants can be detected.

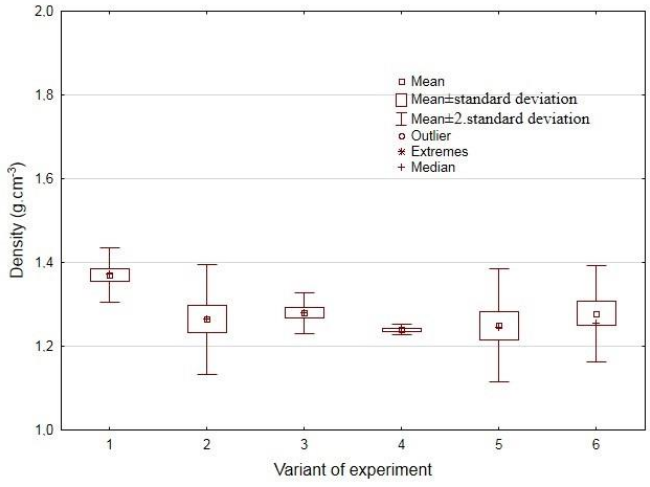

Figure 4. Results of density measurements: 1 – Ethalon; 2 – Rapeseed Methyl Ester 20%; 3 – Sunfloweroil; 4 – Diesel fuel; 5 – Jatropha oil; 6 – Rapeseed oil.

The results of tests aimed at assessing the Shore A hardness are shown in Fig. 5. From the results it is evident that the variants no. 2 (RME - Rapeseed Methyl Ester 20%) and no. 5 (Jatropha oil) do increase the hardness Shore A Hardness by 32.6 to 36.2%. The other variants are characterized by hardness stagnation with respect to the Comparative ethalon (variant no. 1).

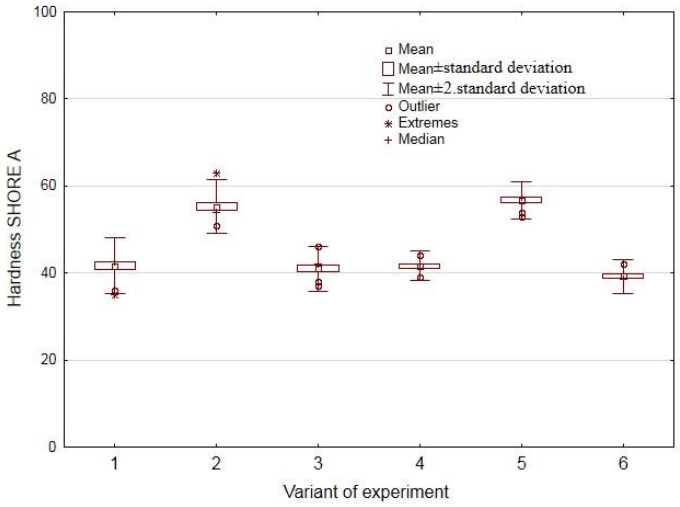

Figure 5. Results of hardness Shore A: 1 – Ethalon; 2 – Rapeseed Methyl Ester 20%; 3 – Sunfloweroil; 4 – Diesel fuel; 5 – Jatropha oil; 6 – Rapeseed oil.

From the viewpoint of the impact of the various fuels on the Shore A hardness of the O-rings the results of the F-test can be summarized as follows: H_0 hypothesis was not confirmed (p = 0.0000), i.e. the difference in the 0.05 level of significance among the tested variants was experimentally detected. When considering the F-tests of the variants 1, 3, 4 and 6 the hypothesis H_0 (p = 0.0591) was confirmed, i.e. there is no difference at the 0.05 significance level among the experimentally tested variants.

The results of the tests aimed at assessing the compression set are shown in Fig. 6. From the results it is evident that different fuels do change the compression set of O-rings.

The results show that the variant no. 3 (sunflower oil), no. 5 (Jatropha oil) and no. 6 (rapeseed oil) do increase the compression set. The higher values of the compression set are negative.

The compression set did increase by 16.7 to 29.4%. Other variants are characterized by the compression set to decrease in comparison to the Comparative etalon (variant no. 1). In variant no. 2 (RME - Rapeseed Methyl Ester 20%), the decrease was 41.5% and in the variants no. 4 (diesel) was 11.3%. From the viewpoint of the impact of the various fuels on the Compression set of the O-rings are the F-test results as follows: H_0 hypothesis was not confirmed (p = 0.0000), i.e. the difference in the 0.05 level of significance among the tested variants can be identified.

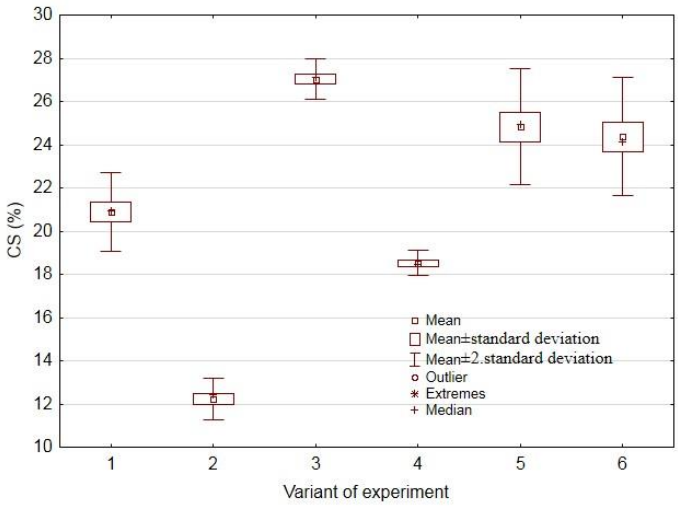

Figure 6. Results of compression set: 1 – Ethalon; 2 – Rapeseed Methyl Ester 20%; 3 – Sunfloweroil; 4 – Diesel fuel; 5 – Jatropha oil; 6 – Rapeseed oil.

The results of tests aimed at assessing the tensile strength are shown in Fig. 7. From the results it is evident that the variant no. 3 (sunflower oil) did increase the strength by about 15%. The decrease in strength was found in the variant no. 4 (diesel) by about 9%. From the viewpoint of the impact of various fuels on the tensile of the O-rings are as follows: H_0 hypothesis was not confirmed (p = 0.0033), i.e. the difference in the 0.05 level of significance of the experimentally tested variants can be identified.

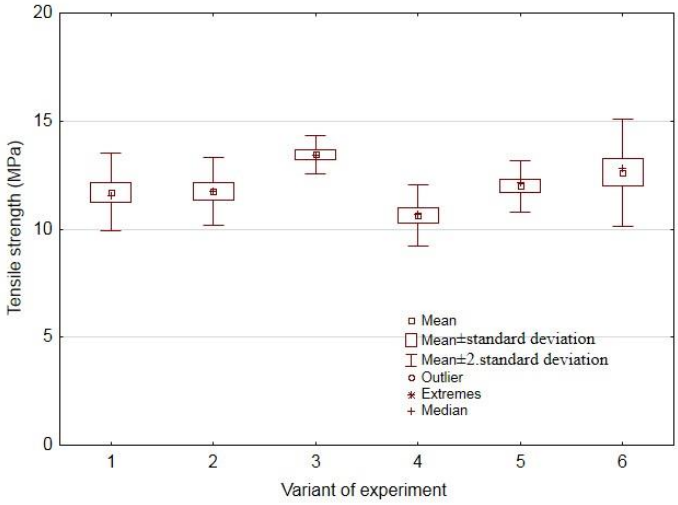

Figure 7. Results of tensile strength measurements: 1 – Ethalon; 2 – Rapeseed Methyl Ester 20%; 3 – Sunfloweroil; 4 – Diesel fuel; 5 – Jatropha oil; 6 – Rapeseed oil.

The results of tests aimed at assessing the deformation can be seen in Fig. 8. From the results it is evident that the variants 2–6 did decrease the deformation. The decrease was in the interval from 5.9 to 16.6%. From the viewpoint of the impact of various fuels on the tensile elongation of the O-rings the F-test results can be formulated as follows: H_0 hypothesis was not confirmed (p = 0.0076), i.e. the difference in the 0.05 level of significance among the tested variants can be found.

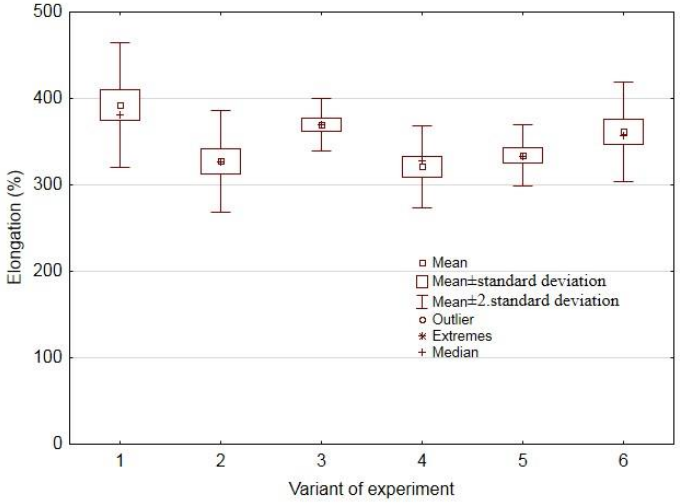

Figure 8. Results of elongation: 1 – Ethalon; 2 – Rapeseed Methyl Ester 20%; 3 – Sunfloweroil; 4 – Diesel fuel; 5 – Jatropha oil; 6 – Rapeseed oil.

Experiments results confirmed the influence of various tested fuels and biofuels (Richter 2014). Second significant parameter is the tested material of O-rings. Results of Bafna (2013) confirmed the significance of the factor. O-rings of the ACM (polyacrylate elastomer) type were used for the experiments.

CONCLUSIONS

From the results of experiments aimed at determining the changes in mechanical properties of the sealing O-rings of the ACM type influenced by various media (fuels) can lead to the following conclusions:

- Reduction in the density in the interval of about 6–9%. Test variants 2-6 cause the reduction in density of the tested O-rings.
- The increase in hardness was observed in two variants, namely no. 2 (RME – Rapeseed Methyl Ester 20%) and no. 5 (Jatropha oil). The increased hardness is negative. Other variants are characterized by hardness stagnation in comparison with the Comparative etalon (variant no. 1 – ethalon). Similar influence on hardness of the O-rings as by the standard diesel fuel were recognized by the variant 3 (sunflower oil), and variant 6 (rapeseed oil). The variants no. 2 and 5 do influence negatively the increase in hardness.
- The increase of the compression set occurred in three variants tested – no. 3 (Sunfloweroil), 5 (Jatropha oil) and 6 (Rapeseed oil). Increase in the compression

set is negative. The positive decrease in the compression set was detected in the variants 2 and 4. As a result of the comparison of the O-rings exposed to the standard diesel fuel and to other fuels became evident that variants – except no. 2 (RME – Rapeseed Methyl Ester 20%) – do negatively affect the Compression set.

- The tensile strength was increased only in the case of the variant no. 3 – Sunfloweroil (15%) and variant no. 6 – Rapeseed oil (7%). The variants no. 2–6 (2 – Rapeseed Methyl Ester 20%, 3 – Sunfloweroil, 4 – Diesel fuel, 5 – Jatropha oil, 6 – Rapeseed oil) demonstrated the decrease of deformation.

If the properties of the rubber elements change, a change of engine operating parameters (leak fuel system, in our case) occurs.

ACKNOWLEDGEMENTS. The paper was prepared under the support of the project CULS 2014:31190/1312/3127 – Utilization of Biobutanol as a Fuel for Diesel Engines.

REFERENCES

Bafna. 2013. Factors Influencing Hardness and Compression Set Measurements on O-rings *Polymer – Plastics Technology and Engineering* **52**(11), 1069–1073.

Barrios, C.C., Domínguez-Sáez, A., Martín, C. & Álvarez, P. 2014. Effects of animal fat based biodiesel on a TDI diesel engine performance, combustion characteristics and particle number and size distribution emissions. *Fuel* **117**, 618–623.

Imran, S., Emberson, D.R., Wen, D.S., Diez, A., Crookes, R.J. & Korakianitis, T. 2013. Performance and specific emissions contours of a diesel and RME fueled compression-ignition engine throughout its operating speed and power range. *Applied Energy* **111**, 771–777.

Pexa, M. & Mařík, J. 2014. The Impact of biofuels and technical condition to its smoke – Zetor 8641 Forterra. *Agronomy Research* **12**(2), 367–372.

Pexa, M., Mařík, J., Kubín, K. & Veselá, K. 2013. Impact of biofuels on characteristics of the engine tractor Zetor 8641 Forterra. *Agronomy Research* **11**(1), 197–204.

Richter, B. 2014 Evaluation of stability tests for elastomeric materials and seals. *International Polymer Science and Technology*. **41**(5), 1–5.

Ružbarský, J. Müller, M., Hrabě, P. 2014a. Analysis of physical and mechanical properties and of gross calorific value of Jatropha curcas seeds and waste from pressing process. *Agronomy Research*, **12**(2), 603–610.

Ružbarský, R. Müller, M. Mareček, J. Grešl, M. 2014b. Jatropha Curcas – Analysis of Gross calorific value. *Acta Universitatis Agriculturae at silviculturae mendelianae brunensis* **62**(6), 1381–1384.

Soo-Young, N. 2011. Inedible vegetace oils and thein derivatives for alternative diesel fuels in CI engines: A review. *Renewable and Sustainable Energy Review* **15**(1), 131–149.

Agronomy Research **13**(2), 613–620, 2015

Comparison of the operating characteristics of the internal combustion engine using rapeseed oil methyl ester and hydrogenated oil

M. Pexa[1], J. Čedík[1,*], J. Mařík[1], V. Hönig[2], Š. Horníčková[2] and K. Kubín[3]

[1]Czech University of Life Sciences Prague, Faculty of Engineering, Department for Quality and Dependability of Machines, Kamýcká 129, CZ16521 Prague 6, Czech Republic; [*]Correspondence: cedikj@tf.czu.cz
[2]Czech University of Life Sciences Prague, Faculty of Agrobiology, Food and Natural Resources, Department of Chemistry, Kamýcká 129, CZ16521 Prague 6, Czech Republic
[3]Research Institute of Agricultural Engineering, p.r.i., Drnovská 507, CZ16101 Prague 6, Czech Republic

Abstract. The issue of the use of alternative fuels in diesel engines is discussed in this paper. The purpose is to reduce the dependence of EU Member States on fuels of petroleum origin. One of the possibilities is the use of oils from biological materials. The use of the oil in standard engines is not usually possible. The engine modification or the fuel modification is necessary. Esterification or hydrogenation of oils can be used as the fuel modification. Impact of these changes on the operational characteristics of a turbocharged internal combustion engine is observed in the paper. The internal combustion engine of the tractor Zetor Foretrra 8641 was used for testing. This engine was burdened using a dynamometer to the PTO. Performance and fuel consumption of the engine were monitored during measurement. As fuels the 100% rapeseed methyl ester and 100% hydrogenated oil was elected. Based on the results we can say that the operating parameters of the internal combustion engine does not change significantly when using these fuels.

Key words: biofuels, power, fuel consumption, combustion engine, vegetable oil, RME, HVO.

INTRODUCTION

In an effort to reduce the amount of the greenhouse gases emitted into the atmosphere, to reduce the dependency on the fossil products and their import and to support local production, the liquid biofuels are used, such as vegetable oils and their products. Oil from a variety of plants with suitable oil characteristics can be used (Vanichseni et al., 2003; Sidibé et al., 2010; No, 2011).

Vegetable oil may be used in several ways while the modification of fuel or the fuel system is always required. Raw vegetable oil can be added into the diesel oil in ratio 20% oil and 80% diesel oil and it can be burned without modification of the engine (Yilmaz & Morton, 2011), some sources state 30% of oil (Masjuki et al., 2001). Another possibility is to use pure vegetable oil but it requires modification of the fuel system because it is necessary to preheat the oil to reduce viscosity (Pexa et al., 2014). The

recommended heating temperature varies significantly, the values range from 70 °C (Kumar et al., 2005) to 135 °C (Pugazhvadivu & Jeyachandran, 2005).

Another possible use of vegetable oil is its chemical processing such as transesterification, micro-emulsions, cracking or hydrogenation (No, 2011; Shambhu et al., 2012; Pexa et al., 2013a).

FAME (Fatty Acid Methyl Ester) is produced by transesterification and it may be produced from the vegetable and animal fat (Sirviö et al., 2014). The main disadvantages of FAME are high price of the input feedstock and low storage and oxidation stability. In comparison with diesel oil, generally FAME has lower mass calorific value, higher density and higher viscosity (Hönig & Hromádko, 2014; Rahman et al., 2014). Rapeseed methyl ester (RME) is currently the most widely used substitute for the diesel oil in Europe (Jokiniemi & Ahokas, 2013; Pexa & Mařík, 2014). Concerning RME the studies revealed approx. 5–10% lower engine performance and higher fuel consumption and approx. 3.5% lower average thermal efficiency, yet approx. 3% higher thermal efficiency at maximum load (No, 2011; Imran et al., 2013; Pexa et al., 2013b).

HVO (Hydrotreated Vegetable Oil), also called renewable diesel or green diesel, is fuel obtained by hydrodeoxygenation of vegetable oil. It consists of paraffinic hydrocarbons with a linear chain, it is free from aromatics, oxygen and sulphur, it has a high cetane number, lower density than diesel oil and comparable calorific value. Thus there are no problems usually connected with bio diesel (FAME), such as increased NO_X emission, deposit formation, storage stability problems, faster aging of engine oil or high cloud point (Aatola et al., 2008; Kučera & Rousek, 2008; No, 2014; Knothe, 2010; Naik et al., 2010; Hartikka et al., 2012). HVO has lower fuel consumption, lower loss of power and higher motor efficiency than conventional bio diesel (Duckhan et al., 2014; Kim et al., 2014).

The goal of the measurement was to compare performance parameters of the engine and specific fuel consumption of two differently processed fuels based on vegetable oil (HVO, RME). On the basis of the previous scientific work it is possible to assume that HVO will have better performance parameters of the engine as well as specific fuel consumption.

MATERIALS AND METHODS

The measurement was done using the tractor engine Zetor 1204 prefilled by means of turbocharger and placed in the tractor Zetor Forterra 8641. It is in-line 4 cylinder engine, its volume is 4.156 and rated power 60 kW (it is 53.4 kW on PTO according to the measurement made by Deutsche Landwirtschafts-Gesellschaft), the maximum torque is 35l Nm, the nominal specific fuel consumption is 253 g kWh^{-1} and the rated speed is 2,200 min^{-1}. The fuel is delivered to the engine by means of mechanical in-line injection pump, injecting is done by one injection with pressure 22 MPa, 12° before top dead center. The operating time of the mentioned engine does not exceed 100 operating hours.

The engine was loaded by the dynamometer AW NEB 400 connected to PTO, torque was recorded by the torque sensor MANNER Mfi 2500Nm_2000U/min with accuracy 0.25%. The torque values recorded by the sensor placed on PTO are converted to the engine torque by means of appropriate gear ratio (3.543). The losses in the gearbox have no effect on the comparative measuring of the influence of fuel on the external

speed characteristics of the engine and therefore they are not taken into consideration. The fuel consumption was recorded by means of the flowmeter AIC VERITAS 4004 with measurement error 1%. Data were saved on the hard disk of the measuring computer (netbook), with the use of A/D converter LabJack U6 with frequency 2 Hz, in the form of text file. The programmes MS Excel and Mathcad were used for data evaluation.

The following fuels were chosen for the test: rapeseed methyl ester and hydrotreated vegetable oil. Their basic characteristics are presented (Table 1).

Table 4. Basic parameters of the measured fuels

Fuel	Density at 15 °C (kg m^{-3})	Heating value (MJ kg^{-1})	Viscosity at 40 °C (mm^2 s^{-1})	Cetane number
HVO	750	44*	2.5–3.5*	80–99*
RME	880	37.5*	4.5*	51*

*(Aatola et al., 2008)

The external speed characteristics of the engine were measured for both tested fuels. Based on these characteristics, the measuring points were determined for the complete characteristic of specific fuel consumption. Subsequently, these points were connected by the polynomial function of the third degree with two unknown variables, using the method of least square error. Then the measuring points of the eight-point NRSC (Non-Road Steady Cycle) test were determined according to ISO 8178-4 (type C1) (Fig. 1). The points of the test are defined by rotation speed (idle, at max. torque and rated) and load in percentage (0, 10, 50, 75 and 100%). The test was used for measuring the specific fuel consumption. Specific fuel consumption for the whole NRSC test was calculated according to the equation (1). In every predetermined measurement point the measured parameters were stabilized.

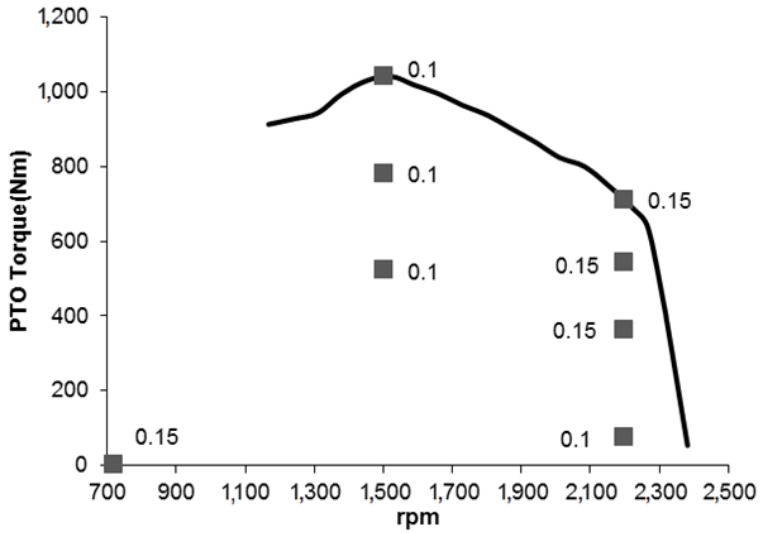

Figure 6. Measurements points for the NRSC test for HVO with weight factors.

$$m_{NRSC} = \frac{\sum_{i=1}^{8}\left(M_{Pi} \cdot WF_i\right)}{\sum_{i=1}^{8}\left(P_{PTO,i} \cdot WF_i\right)} \quad (1)$$

where: m_{NRSC} – Specific fuel consumption for whole NRSC test (g kWh^{-1}); $M_{P,i}$ –hourly fuel consumption (g h^{-1}); WF_i – weight factor (–); $P_{PTO,i}$ – power on the PTO (kW).

RESULTS AND DISCUSSION

The external speed characteristic for both tested fuels was created (Fig. 2). It is obvious that during the operation of the HVO engine, the maximum torque is reduced by approx. 0.9% and the maximum performance is reduced by approx. 6%. The specific fuel consumption of the HVO fuel is reduced in comparison to the RME fuel almost in the whole speed range. This is caused mainly by lower density of HVO in comparison with RME (Table 1). Increase of the specific fuel consumption of HVO from approx. 2,000 min^{-1} is caused by decrease of the torque or rather by performance in this speed range in comparison with RME.

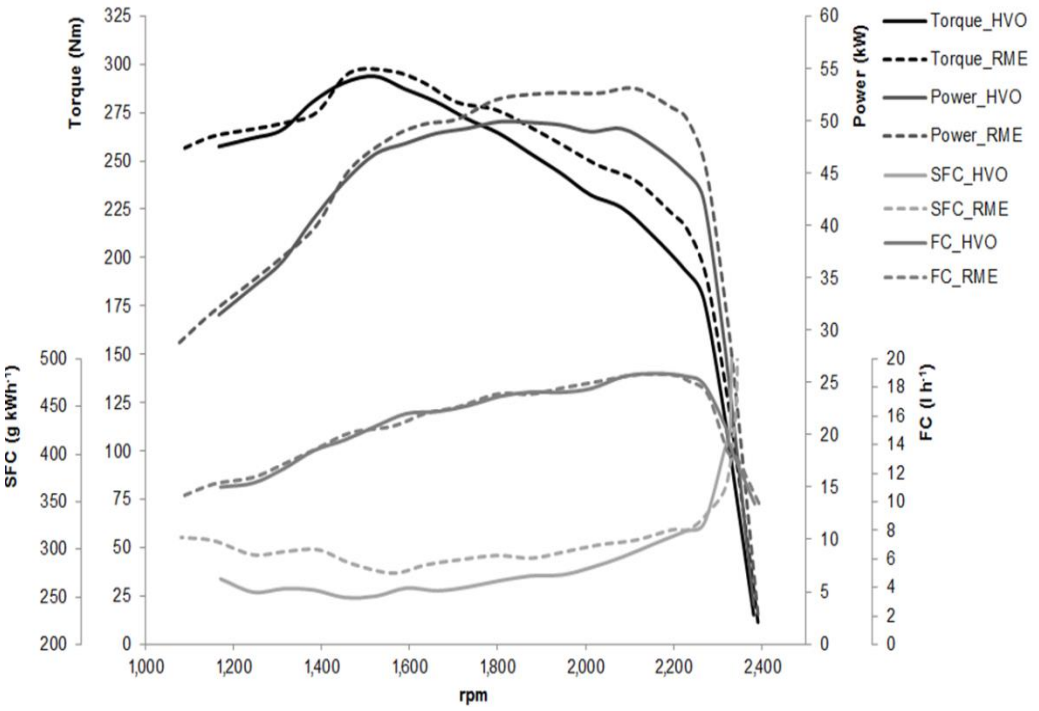

Figure 2. The external rotation speed characteristics for HVO and RME (SFC – specific fuel consumption, FC – fuel consumption).

From the presented results (Table 2, Fig. 2) it is obvious that the torque and performance are reduced by approx. 9.9% during rated speed of the engine. It is also obvious that the specific fuel consumption of HVO fuel is reduced by 1.9% during the rated speed. This is caused by lower engine performance during use of this fuel.

Table 5. Results of the measurement

Fuel	Max. Torque (Nm) rpm	Max. Power (kW) rpm	Min. SFC (g kWh^{-1}) rpm	Rated Torque (Nm)	Rated Power (kW)	Rated SFC (g kWh^{-1})	Torque Backup (%)
HVO	293.8 1,521	49.9 1,803	247.4 1,516	199.9	46	314.7	47
RME	296.5 1,559	53.1 2112	275.1 1,559	221.8	51.1	320.9	33.7

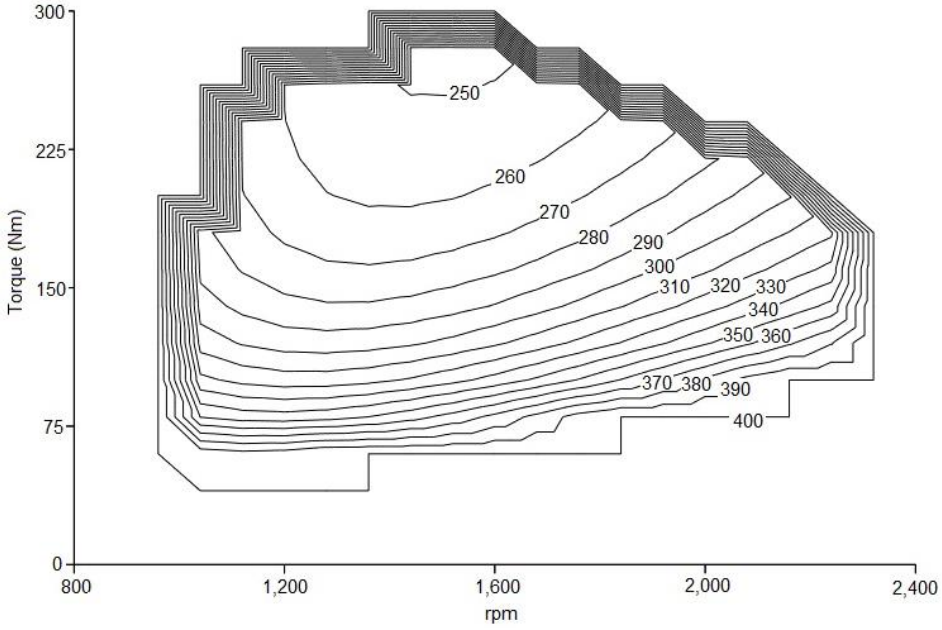

Figure 3. Complete characteristic of specific fuel consumption for HVO (g kWh^{-1}).

The complete characteristics of specific fuel consumption for HVO and RME were created (Figs 3, 4). For both variants minimums of specific fuel consumption were assessed from the complete and the external rotation speed characteristics. From the obtained results (Table 2, Figs 3, 4) it is evident that minimum of the specific fuel consumption of HVO fuel is approx. by 10.1% lower in comparison with the RME fuel and it is located at the similar rotation speed. It is also obvious that in case of HVO the specific fuel consumption is lower within the speed and load range than in case of RME.

The specific fuel consumption measured by means of NRSC test was 328.69 g kWh^{-1} for HVO fuel and 366.3 g kWh^{-1} for RME fuel, which is approx. 11% more.

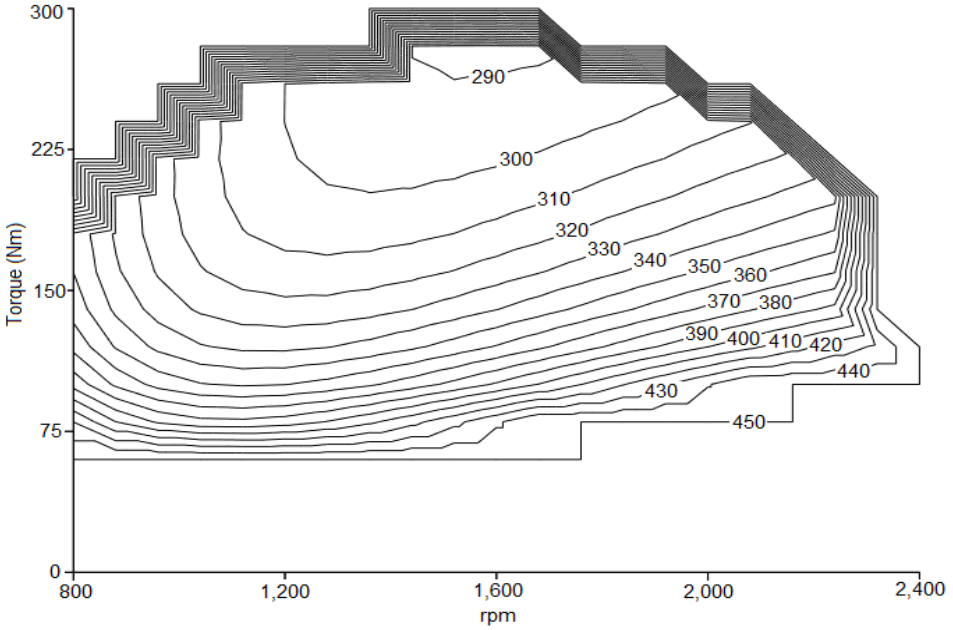

Figure 4. Complete characteristic of specific fuel consumption for RME (g kWh^{-1}).

CONCLUSIONS

Both tested fuels are based on vegetable oil and they differ only in production technology. Decrease of torque and performance during higher speed in case of use of HVO fuel can be attributed mainly to low density of this fuel because both the mass calorific value and the cetane number are higher than in case of RME. Therefore it can be assumed that if the amount of fuel is increased it would be possible to reach similar maximum performance as in case of RME.

Based on the results it is possible to state that the engine reached lower performance parameters when using HVO fuel than in case of RME, so the above mentioned assumptions were not confirmed. However, decrease of maximum performance was only 6.4% and the maximum torque was almost identical when accuracy of performance parameters was included.

The results also indicate that in comparison with RME the specific fuel consumption of HVO was lower. This proved to be the case within all measurements (external speed characteristics, complete characteristics and NRSC), which confirms the above mentioned assumptions and makes this oil modification interesting.

ACKNOWLEDGEMENTS. The paper was created with the grant support project CIGA CULS Prague 20153001 – Utilization of butanol in internal combustion engines of generators and with institutional support for long-term conceptual development VÚZT, v.v.i. RO0614.

REFERENCES

Aatola, H., Larmi, M., Sarjovaara, T. & Mikkonen, S. 2008. Hydrotreated vegetable oil (HVO) as a renewable diesel fuel: trade-off between NO_X, particulate emission, and fuel consumption of a heavy duty engine. *SAE paper*, 2008–01–2500.

Duckhan, K., Seonghwan, K., Sehun, O. & No, S.-Y. 2014.Engine performance and emission characteristics of hydrotreated vegetable oil in light duty diesel engines. *Fuel* **125**, 36–43.

Hartikka, T., Kuronen, M. & Kiiski, U. 2012. Technical performance of HVO (hydrotreated vegetable oil) in diesel engines. *SAE Technical Papers* **9**.

Hönig, V. & Hromádko, J. 2014. Possibilities of using vegetable oil to power diesel engines as well as their impact on engine oil. *Agronomy Research* **12**(2), 323–332.

Imran, S., Emberson, D.R., Wen, D.S., Diez, A., Crookes, R.J. & Korakianitis, T. 2013. Performance and specific emissions contours of a diesel and RME fueled compression-ignition engine throughout its operating speed and power range. *Applied Energy* **111**, 771–777.

ISO 8178-4 Reciprocating internal combustion engines-Exhaust emission measurement-Part 4: Steady-state test cycles for different engine applications. 2007

Jokiniemi, T. & Ahokas, J. 2013. A review of production and use of first generation biodiesel in Agriculture. *Agronomy Research* **11**(1), 239–248.

Kim, D. Kim, S., Oh, S. No, S.-Y. 2014. Engine performance and emission characteristics of hydrotreated vegetable oil in light duty diesel engines. *Fuel* **125**, 36–43.

Knothe, G. 2010. Biodiesel and renewable diesel: A comparison. *Progress in Energy and Combustion Science* **36**(3), 364–373.

Kučera, M. & Rousek, M. 2008. Evaluation of thermooxidation stability of biodegradable recycled rapeseed-based oil NAPRO-HO 2003. *Research in Agricultural Engineering* **54**(4), 163–169.

Kumar, M.S., Kerihuel, A., Bellettre, J. & Tazerout, M. 2005. Experimental investigations on the use of preheated animal fat as fuel in a compression ignition engine. *Renewable Energy* **30**(9), 1443–1456.

Masjuki, H.H., Kalam, M.A., Maleque, M.A., Kubo, A. & Nonaka, T. 2001. Performance, emissions and wear characteristics of an indirect injection diesel engine using coconut oil blended fuel. In: *Proceedings of the Institution of Mechanical Engineers, Part D: Journal of Automobile Engineering* **215**(3), 393–404.

Naik, S.N., Goud, V.V., Rout, P.K. & Dalai, A.K. 2010. Production of first and second generation biofuels: A comprehensive review. *Renewable and Sustainable Energy Reviews* **14**(2), 578–597.

No, S.-Y. 2011. Inedible vegetable oils and their derivatives for alternative diesel fuels in CI engines: A review. *Renewable and Sustainable Energy Review* **15**(1), 131–149.

No, S.-Y. 2014. Application of hydrotreated vegetable oil from triglyceride based biomass to CI engines - A review. *Fuel* **115**, 88–96.

Pexa, M. & Mařík, J. 2014. The Impact of biofuels and technical condition to its smoke – Zetor 8641 Forterra. *Agronomy Research* **12**(2), 367–372.

Pexa, M., Mařík, J., Čedík, J., Aleš, Z. & Valášek, P. 2014. Mixture of oil and diesel as fuel for internal combustion engine. In: *2nd International Conference on Materials, Transportation and Environmental Engineering*. CMTEE, Kunming, pp. 1197–1200.

Pexa, M., Mařík, J., Kubín, K. 2013a. Impact of biofuels on performance and emission characteristics combustion engine - Zetor 8641 forterra. In: *5th International Conference on Trends in Agricultural Engineering 2013.* TAE 2013, Prague, pp. 523–528.

Pexa, M., Mařík, J., Kubín, K. & Veselá, K. 2013b. Impact of biofuels on characteristics of the engine tractor Zetor 8641 Forterra. *Agronomy Research* **11**(1), 197–204.

Pugazhvadivu, M. & Jeyachandran, K. 2005. Investigations on the performance and exhaust emissions of a diesel engine using preheated waste frying oil as fuel. *Renewable Energy* **30**(14), 2189–2202.

Rahman, M.M., Hassan, M.H., Kalam, M.A., Atabani, A.E., Memon, L.A. & Rahman, S.M.A. 2014. Performance and emission analysis of Jatropha curcas and Moringa oleifera methyl ester fuel blends in a multi-cylinder diesel engine. *Journal of Cleaner Production* **65**, 304–310.

Shambhu, V.B., Chaudhary, S.K. & Bhattacharya, T.K. 2012.Compatibility of jatropha oil bio-diesel and petro diesel as an engine fuel based on their characteristic fuel properties. AMA, *Agricultural Mechanization in Asia, Africa and Latin America* **43(**2), 43–49.

Sidibé, S.S., Blin, J., Vaitilingom, G., Azoumah, Y. Use of crude filtered vegetable oil as a fuel in diesel engines state of the art: Literature review. *Renewable and Sustainable Energy Reviews* **14**(9), 2748–2759.

Sirviö, K., Niemi, S., Vauhkonen, V. & Hiltunen, E. 2014. Antioxidant studies for animal-based fat methyl ester. *Agronomy Research* **12(**2), 407–416.

Vanichseni, T., Saitthiti, B., Intaravichai, S., Kiatiwat, T. 2003. An Energy Modeling Analysis of the Integrated Commercial Biodiesel Production from Palm Oil for Thailand. *AMA, Agricultural Mechanization in Asia, Africa and Latin America* **34**(3), 67–74.

Yilmaz, N. & Morton, B. 2011. Effects of preheating vegetable oils on performance and emission characteristics of two diesel engines. *Biomass and Bioenergy* **35(**5), 2028–2033.

INSTRUCTIONS TO AUTHORS

Papers must be in English (British spelling). English will be revised by a proofreader, but authors are strongly urged to have their manuscripts reviewed linguistically prior to submission. Contributions should be sent electronically. Papers are considered by referees before acceptance. The manuscript should follow the instructions below.

Structure: Title, Authors (initials & surname; an asterisk indicates the corresponding author), Authors' affiliation with postal address (each on a separate line) and e-mail of the corresponding author, Abstract (up to 250 words), Key words (not repeating words in the title), Introduction, Materials and methods, Results and discussion, Conclusions, Acknowledgements (optional), References.

Layout, page size and font

- Use preferably the latest version of **Microsoft Word**, doc., docx. format.
- Set page size to **B5 Envelope or ISO B5 (17.6 x 25 cm)**, all margins at 2 cm.
- Use single line spacing and justify the text. Do not use page numbering. Use indent 0.8 cm (do not use tab or spaces instead).
- Use font Times New Roman, point size for the title of article **14 (Bold)**, author's names 12, core text 11; Abstract, Key words, Acknowledgements, References, tables and figure captions 10.
- Use *italics* for Latin biological names, mathematical variables and statistical terms.
- Use single ('…') instead of double quotation marks ("…").

Tables

- All tables must be referred to in the text (Table 1; Tables 1, 3; Tables 2–3).
- Use font Times New Roman, regular, 10 pt. Insert tables by Word's 'Insert' menu.
- Do not use vertical lines as dividers; only horizontal lines (1/2 pt) are allowed. Primary column and row headings should start with an initial capital.

Figures

- All figures must be referred to in the text (Fig. 1; Fig. 1 A; Figs 1, 3; Figs 1–3). Use only black and white or greyscale for figures. Avoid 3D charts, background shading, gridlines and excessive symbols. Use font **Arial** within the figures. Make sure that thickness of the lines is greater than 0.3 pt.
- Do not put caption in the frame of the figure.
- The preferred graphic format is EPS; for half-tones please use TIFF. MS Office files are also acceptable. Please include these files in your submission.
- Check and double-check spelling in figures and graphs. Proof-readers may not be able to change mistakes in a different program.

References

- **Within the text**

In case of two authors, use '&', if more than two authors, provide first author 'et al.':

Smith & Jones (1996); (Smith & Jones, 1996);
Brown et al. (1997); (Brown et al., 1997)

When referring to more than one publication, arrange them by following keys: 1. year of publication (ascending), 2. alphabetical order for the same year of publication:

(Smith & Jones, 1996; Brown et al., 1997; Adams, 1998; Smith, 1998)

- **For whole books**

Name(s) and initials of the author(s). Year of publication. *Title of the book* (*in italics*). Publisher, place of publication, number of pages.

Shiyatov, S.G. 1986. *Dendrochronology of the upper timberline in the Urals*. Nauka, Moscow, 350 pp. (in Russian).

- **For articles in a journal**

Name(s) and initials of the author(s). Year of publication. Title of the article. *Abbreviated journal title* (*in italic*) volume (in bold), page numbers.

Titles of papers published in languages other than English, German, French, Italian, Spanish, and Portuguese should be replaced by an English translation, with an explanatory note at the end, e.g., (in Russian, English abstr.).

Karube, I. & Tamiyra, M.Y. 1987. Biosensors for environmental control. *Pure Appl. Chem.* **59**, 545–554.

Frey, R. 1958. Zur Kenntnis der Diptera brachycera p.p. der Kapverdischen Inseln. *Commentat.Biol.* **18**(4), 1–61.

Danielyan, S.G. & Nabaldiyan, K.M. 1971. The causal agents of meloids in bees. *Veterinariya* **8**, 64–65 (in Russian).

- **For articles in collections:**

Name(s) and initials of the author(s). Year of publication. Title of the article. Name(s) and initials of the editor(s) (preceded by In:) *Title of the collection (in italics)*, publisher, place of publication, page numbers.

Yurtsev, B.A., Tolmachev, A.I. & Rebristaya, O.V. 1978. The floristic delimitation and subdivisions of the Arctic. In: Yurtsev, B. A. (ed.) *The Arctic Floristic Region*. Nauka, Leningrad, pp. 9–104 (in Russian).

- **For conference proceedings:**

Name(s) and initials of the author(s). Year of publication. Name(s) and initials of the editor(s) (preceded by In:) *Proceedings name (in italics)*, publisher, place of publishing, page numbers.

Ritchie, M.E. & Olff, H. 1999. Herbivore diversity and plant dynamics: compensatory and additive effects. In: Olff, H., Brown, V.K. & Drent R.H. (eds) *Herbivores between plants and predators. Proc. Int. Conf. The 38th Symposium of the British Ecological Society*, Blackwell Science, Oxford, UK, pp. 175–204.

.....……

Please note

- Use '.' (not ',') for decimal point: 0.6 ± 0.2; Use ',' for thousands – 1,230.4;
- Use '–' (not '-') and without space: pp. 27–36, 1998–2000, 4–6 min, 3–5 kg
- With spaces: 5 h, 5 kg, 5 m, 5°C, C : D = 0.6 ± 0.2; $p < 0.001$
- Without space: 55°, 5% (not 55 °, 5 %)
- Use 'kg ha^{-1}' (not 'kg/ha');
- Use degree sign ' ° ' : 5 °C (not 5 ^{O} C).